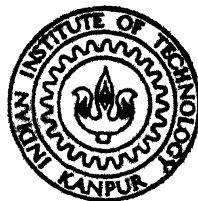


# **DIRECT STABILITY EVALUATION AND ON-LINE DYNAMIC SECURITY ASSESSMENT OF POWER SYSTEMS USING STRUCTURE PRESERVING ENERGY FUNCTIONS**

*by*

**K. K. GHOSH**



**DEPARTMENT OF ELECTRICAL ENGINEERING**

**INDIAN INSTITUTE OF TECHNOLOGY, KANPUR**

**FEBRUARY, 1987**

# **DIRECT STABILITY EVALUATION AND ON-LINE DYNAMIC SECURITY ASSESSMENT OF POWER SYSTEMS USING STRUCTURE PRESERVING ENERGY FUNCTIONS**

**A Thesis Submitted  
In Partial Fulfilment of the Requirements  
for the Degree of**

**DOCTOR OF PHILOSOPHY**

*by*

**K. K. GHOSH**

*to the*

**DEPARTMENT OF ELECTRICAL ENGINEERING**

**INDIAN INSTITUTE OF TECHNOLOGY, KANPUR**

**FEBRUARY, 1987**

CENTRAL LIBRARY  
KAMPUR  
Acc. No. 106240

62

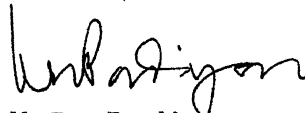
EE-1987-D-GHD-DIR

RECEIVED

TO  
MY PARENTS, TEACHERS  
AND  
FAMILY  
KABITA  
AND  
KRISHN 'NDU, KASTURI AND KAUSTABH

## CERTIFICATE

It is certified that this work entitled 'DIRECT STABILITY EVALUATION AND ON-LINE DYNAMIC SECURITY ASSESSMENT OF POWER SYSTEMS USING STRUCTURE PRESERVING ENERGY FUNCTIONS' by K.K. Ghosh has been carried out under my supervision and that this work has not been submitted elsewhere for a degree.



K.R. Padiyar  
Professor  
Department of Electrical Engineering  
Indian Institute of Technology  
Kanpur.

## ACKNOWLEDGEMENTS

It is with a deep sense of gratitude that I express my indebtedness to Dr. K.R. Padiyar for his valuable guidance and encouragement throughout the course of this work. I feel highly obliged to him for his thought-provoking discussions, patience and keen interest in the work.

It gives me pleasure to express my gratitude to Dr. M.A. Pai who alongwith Dr. K.R. Padiyar initiated me into the research in direct power system transient stability analysis.

I am thankful to Dr. P.K. Chatterjee, Dr. M.M. Hasan, Dr. R. Raghuram and Dr. A. Mahanta for their help in various ways at various stages of the research work. I sincerely express my gratefulness to Dr. L.P. Singh for valuable suggestions and constant encouragement throughout the course of this program.

I thank my senior colleagues Dr. C. Radhakrishna, Dr. Sachchidanand, Dr. H.S.Y. Sastry, Dr. A. Anwar and Dr. A.G. Kothari for fruitful discussions.

It is my pleasure to acknowledge the splendid company and moral support of my fellow research scholars M/s R.L. Verma, J. Senthil, P.N. Sridhar, V.N. Rajurkar, K.K. Islam, P.G. Poonacha, E.G. Rajan and A. Gogoi. The help rendered by M/s. R.L. Verma, J. Senthil and P.N. Sridhar in the final preparation of this thesis is gratefully acknowledged.

I thank the authorities of I.I.T., Kanpur for providing me the necessary facilities for the research. I sincerely thank Mr. C.M. Abraham for his patient and skillful typing.

I am indebted to the authorities of H.B. Technological Institute, Kanpur for initially according the permission to pursue the research work as a part-time scholar and then granting me leave for the completion of the research.

I am indebted to my mother, Mrs. G. Ghosh and elder brother Mr. S.K. Ghosh for their constant interest, care, affection and blessings. My success is the sole outcome of their selfless sacrifices during the formative years of my career. My indebtedness is also due to all my brothers, the only sister and numerous relatives who have so happily shouldered the responsibilities of medical care and nursing of my old ailing mother during my busy schedule. The heptahalenean Herculean services and sacrifices of my second elder brother, Mr. P.K. Ghosh, under whose constant persuasion and encouragement this program was initiated against personal difficulties and who is no more with us to see the completion of the work, are acknowledged with a deep sense of indebtedness and sorrow for his becoming an untimely victim of the Killer disease 'cancer'.

It is my divine duty to put on record the meritorious and selfless support of the highest order, both moral and material, rendered by the great and pious soul, Mr. R.G. Ghosh, M.A., WBCS (Retd.), my revered father-in-law and the noble members of his family. I have greatly benefitted from his prudent counselling and his rich personal experiences in both rationalising and consolidating my thoughts and actions in a much better and meaningful fashion. His divine blessings which have so profusely been showered on me and my family all these years, have stood, on the whole, like a solid rock behind me in accepting the challenges thrown by some hard realities in my not so long a career till date. Also, I highly appreciate the silent prayer of Mohuya, my sister-in-law, for the success of this scientific venture.

Finally, words are insufficient to express my gratitude to my wife Kabita and children Krishnendu, Kasturi and Kaustabh who encouraged me to continue my work inspite of many hardships to them.

K.K. Ghosh

## CONTENTS

	Page
LIST OF FIGURES	xii
LIST OF TABLES	xv
LIST OF PRINCIPAL SYMBOLS	xviii
SYNOPSIS	
Chapter 1 INTRODUCTION	1
1.1 General	1
1.2 Direct Methods	5
1.3 Literature Survey	7
1.3.1 General	7
1.3.2 Lyapunov or energy functions	8
1.3.3 Computation of stability regions	14
1.3.4 Application to on-line dynamic security assessment	15
1.4 Objectives and Scope of the Thesis	17
1.5 Outline of the Thesis	18
Chapter 2 POWER SYSTEM DYNAMIC SIMULATION INCORPORATING COMPUTATION OF STRUCTURE PRESERVING ENERGY FUNCTION	23
2.1 Introduction	23
2.2 Power System Dynamic Simulation	25
2.2.1 General	25
2.2.2 Details of existing simulation program	26
2.3 Modification of the Dynamic Simulation Program	29
2.3.1 General	29
2.3.2 Structure preserving energy function (SPEF)	32
2.3.3 Computation of SPEF	35

	2.4 Direct Evaluation of Transient Stability	37
	2.5 Numerical Examples	41
	2.5.1 Description	41
	2.5.2 Results	42
	2.5.3 Discussion	46
	2.6 Conclusions	64
Chapter 3	A STRUCTURE PRESERVING ENERGY FUNCTION WITH KNOWN MODES OF INSTABILITY	65
	3.1 Introduction	65
	3.2 System Model	67
	3.2.1 Assumptions	67
	3.2.2 Generator model	68
	3.2.2.1 General	68
	3.2.2.2 Aggregation of generators in coherent groups	71
	3.2.3 Load model	75
	3.2.4 Power flow equations	75
	3.3 Structure Preserving Energy Function (SPEF)	77
	3.4 Computation of Stability Region	85
	3.4.1 General	85
	3.4.2 Computational procedure	88
	3.5 Numerical Examples	89
	3.5.1 Description	89
	3.5.2 Results	90
	3.5.3 Discussion	106
	3.6 Conclusions	138

Chapter 4	DYNAMIC SECURITY ASSESSMENT USING STRUCTURE PRESERVING ENERGY FUNCTIONS	140
4.1	Introduction	140
4.2	Transient Stability Measures	142
4.2.1	General	142
4.2.2	Transient energy margin (TEM)	142
4.3	Dynamic Security Assessment	143
4.3.1	General	143
4.3.2	Mathematical formulation	144
4.3.2.1	Computation of $\Theta_k^*$ and critical energy	145
4.3.2.2	Computation of energy at clearing	148
4.3.3	Computational procedure	150
4.4	Numerical Examples	153
4.4.1	Description	153
4.4.2	Results	154
4.4.3	Discussion	159
4.5	Conclusions	164
Chapter 5	A STRUCTURE PRESERVING ENERGY FUNCTION INCORPORATING TRANSMISSION LINE RESISTANCES	165
5.1	Introduction	165
5.2	Network Transformation	166
5.3	System Model	167
5.3.1	Generator equations	167
5.3.2	Load model	170
5.3.3	Power flow equations	170
5.4	Structure Preserving Energy Function (SPEF)	171
5.5	Numerical Examples	176
5.5.1	Description	176
5.5.2	Results	177
5.5.3	Discussion	185
5.6	Conclusions	208

Chapter 6	A STRUCTURE PRESERVING ENERGY FUNCTION WITH DETAILED GENERATOR MODELS	209
	6.1 Introduction	209
	6.2 System Model	210
	6.2.1 Generator model	210
	6.2.2 Excitation system and voltage regulator model	212
	6.2.3 Load model	214
	6.2.4 Power flow equations	214
	6.3 Structure Preserving Energy Functions	215
	6.4 Numerical Examples	224
	6.4.1 Description	224
	6.4.2 Results and discussion	226
	6.5 Conclusions	253
Chapter 7	CONCLUSIONS	255
	7.1 General	255
	7.2 Computation of SPEF in Dynamic Simulation Program	256
	7.3 Structure Preserving Energy Functions with Known Modes of Instability	257
	7.4 Dynamic Security Assessment	259
	7.5 Structure Preserving Energy Functions with Detailed System Models	261
	7.6 Suggestions for Further Work	263
APPENDIX A	DERIVATION OF SYNCHRONOUS GENERATOR EQUATIONS	264
APPENDIX B	NETWORK SOLUTION WITH NONLINEAR VOLTAGE DEPENDENT LOADS	271
APPENDIX C	TIME DERIVATIVE OF ENERGY FUNCTION WITH NON- CONSTANT MECHANICAL POWER	274
APPENDIX D	PEBS METHOD OF DETERMINING STABILITY REGION	277

APPENDIX E	DATA FOR THE 7-MACHINE (CIGRE) TEST SYSTEM	281
APPENDIX F	DATA FOR THE 10-MACHINE (NEW ENGLAND) TEST SYSTEM	285
APPENDIX G	DATA FOR THE 13-MACHINE SYSTEM	294
APPENDIX H	ELEMENTS OF $[\partial \underline{g} / \partial \underline{x}]$ AND $[\partial \underline{g} / \partial \underline{u}]$ IN EQ.(4.34)	303
APPENDIX I	RELATIONSHIP BETWEEN POWER INJECTIONS IN LOSSY AND LOSSLESS NETWORKS	309
APPENDIX J	ENERGY STORED IN MACHINE REACTANCES AND TRANSMISSION LINES	311
APPENDIX K	DATA FOR 4-MACHINE SYSTEM	317
REFERENCES		320
CURRICULUM VITAE		

## LIST OF FIGURES

Figure No.		Page
2.1	Relationship of subroutine variables for calculating initial conditions	30
2.2	Relationship of subroutine variables during step-by-step simulation	30
2.3	Relationship of subroutine variables for calculating SPEF	36
2.4	Overall program flow diagram	38-39
2.5-2.6	Swing curves for 7-machine system, stable and unstable cases	48
2.7-2.8	Variation of total energy and its components for 7-machine system, stable and unstable cases	49
2.9-2.10	Variation of the components of potential energy for 7-machine system, stable and unstable cases	50
2.11-2.16	Swing curves for 10-machine system, stable and unstable cases	51-56
2.17-2.28	Variation of total energy, its components and the components of potential energy for 10-machine system, stable and unstable cases	57-62
3.1	A system of 'm' machines supplying power to 'n' nonlinear voltage dependent loads	69
3.2-3.3	Swing curves for 7-machine system, stable and unstable cases	107
3.4-3.7	Variation of total energy, its components and the components of potential energy for 7-machine system, stable and unstable cases	108-109
3.8-3.21	Swing curves for 10-machine system, stable and unstable cases	110-123
3.22-3.41	Variation of total energy, its components and the components of potential energy for 10-machine system, stable and unstable cases	124-133
3.42	Kinetic energy correction for 10-machine system, stable case	136

5.1	A system of $m$ generators supplying power to $n$ nonlinear voltage dependent loads (a) Original network (b) Transformed network	168
5.2-5.11	Swing curves for 10-machine system, stable and unstable cases	186-195
5.12-5.31	Variation of total energy, its components and the components of $W_2$ for 10-machine system, stable and unstable cases	196-205
5.32	Variation of the components of $W_{26}$ for 10-machine system, stable case	206
6.1	Block diagram of IEEE type 1 Excitation system	213
6.2-6.3	Swing curves for 4-machine system, stable and unstable cases	233
6.4-6.5	Variation of $E_{fd}$ for 4-machine system, stable and unstable cases	234
6.6-6.7	Variation of $E'_q$ for 4-machine system, stable and unstable cases	235
6.8-6.9	Variation of $E'_d$ for 4-machine system, stable and unstable cases	236
6.10-6.11	Variation of total energy and its components for 4-machine system, stable and unstable cases	237
6.12-6.13	Variation of some components of $W_2$ for 4-machine system, stable and unstable cases	238
6.14-6.15	Variation of $W'_{24}$ and its components for 4-machine system, stable and unstable cases	239
6.16-6.17	Variation of $W'_{25}$ and its components for 4-machine system, stable and unstable case	240
6.18-6.19	Variation of $W'_{26}$ and its components for 4-machine system, stable and unstable cases	241
6.20-6.21	Swing curves for 10-machine system, stable and unstable cases	243-244

6.22-6.23	Variation of $E_{fd}$ for 10-machine system, stable and unstable cases	245
6.24-6.25	Variation of $E'_q$ for 10-machine system, stable and unstable cases	246
6.26-6.27	Variation of $E'_d$ for 10-machine system, stable and unstable cases	247
6.28-6.29	Variation of total energy and its components for 10-machine system, stable and unstable cases	248
6.30-6.31	Variation of some components of $W_2$ for 10-machine system, stable and unstable cases	249
6.32-6.33	Variation of $W'_{24}$ and its components for 10-machine system, stable and unstable cases	250
6.34-6.35	Variation of $W'_{25}$ and its components for 10-machine system, stable and unstable cases	251
6.36-6.37	Variation of $W'_{26}$ and its components for 10-machine system, stable and unstable cases	252
A.1	Steady state synchronous generator vector diagram	269
B.1	Network for obtaining $[Y]$	272
E.1	One-line diagram of 7-machine (CIGRE) test system	284
F.1	One-line diagram of 10-machine (NEW ENGLAND) test system	293
G.1	Single line diagram of 13-machine system	302
K.1	Single line diagram of 4-machine system	319

## LIST OF TABLES

Table No.		Page
2.1	Critical energy, $W_{cr}$ and critical clearing time, $t_{cr}$ for 7-machine system	43
2.2	Critical energy, $W_{cr}$ and critical clearing time, $t_{cr}$ for 10-machine system	44
2.3	Critical energy, $W_{cr}$ and critical clearing time, $t_{cr}$ for 13-machine system	45
3.1	Effect of known modes of instability on the predicted critical clearing time, $t_{cr}$ for 7-machine system	91
3.2	Effect of known modes of instability on the predicted critical clearing time, $t_{cr}$ for 10-machine system	92
3.3	Effect of known modes of instability on the predicted critical clearing time, $t_{cr}$ for 10-machine system	93
3.4	Effect of known modes of instability on the predicted critical clearing time, $t_{cr}$ for 13-machine system	94
3.5	Variables corresponding to the critical energy, $W_{cr}$ for 7-machine system (by trajectory simulation)	97-98
3.6	Variables corresponding to the critical energy, $W_{cr}$ for 10-machine system (by trajectory simulation)	99-105
4.1	Comparison of critical energy, $W_{cr}$ for 7-machine system	155
4.2	Comparison of critical energy, $W_{cr}$ for 10-machine system	156
4.3	Comparison of critical energy, $W_{cr}$ for 13-machine system	157

4.4	$\omega_{kcl}$ and $\theta_{kcl}$ at clearing ( $t_{cl}=0.20$ sec) for 10-machine system	158
4.5	$\Delta W$ and $\Delta W_n$ by the proposed method and ranking of three phase faults for 10-machine system	160
4.6	$\Delta W$ and $\Delta W_n$ by trajectory simulation and ranking of three phase faults for 10-machine system	161
5.1	Effect of transmission line resistance on critical energy, $W_{cr}$ and predicted critical clearing time, $t_{cr}$ for 7-machine system( $\alpha=0.1$ )	178
5.2	Effect of transmission line resistance on critical energy, $W_{cr}$ and predicted critical clearing time, $t_{cr}$ for 7-machine system( $\alpha=0.2$ )	179
5.3	Comparison of critical clearing time, $t_{cr}$ by digital simulation for 7-machine system	180
5.4	Effect of transmission line resistance on critical energy, $W_{cr}$ and predicted critical clearing time, $t_{cr}$ for 10-machine system ( $\alpha = 0.1$ )	181
5.5	Effect of transmission line resistance on critical energy, $W_{cr}$ and critical clearing time, $t_{cr}$ for 10-machine system ( $\alpha = 0.2$ )	182
5.6	Effect of transmission line resistance on critical energy, $W_{cr}$ and predicted critical clearing time, $t_{cr}$ for average value of $\alpha$ for 10-machine system (av, value of $\alpha = 0.07$ )	183
5.7	Comparison of critical clearing time, $t_{cr}$ by digital simulation for 10-machine system	184
6.1	Comparison of critical energy, $W_{cr}$ and critical clearing time, $t_{cr}$ for 4-machine system using proposed SPEF	227
6.2	Comparison of critical energy, $W_{cr}$ and critical clearing time, $t_{cr}$ for 10-machine system using proposed SPEF	228-22
6.3	Comparison of critical energy, $W_{cr}$ and critical clearing time, $t_{cr}$ for 10-machine system using modified $W_{22}$ in SPEF	230

6.4	Comparison of critical energy, $W_{cr}$ and critical clearing time, $t_{cr}$ for 10-machine system using modified $W_{22}$ in the SPEF	231
E.1	Machine constants	281
E.2	Line data	282
E.3	Operating data	283
F.1	Machine constants	285
F.2	Line data	286
F.3	Transformer data	288
F.4	Operating data (including line resistance)	289
F.5	Operating data (neglecting line resistance)	291
G.1	Machine constants	294
G.2	Line data	294
G.3	Shunt capacitor data	298
G.4	Operating data	299
K.1	Machine constants	317
K.2	Line data	318
K.3	Operating data	318

## LIST OF PRINCIPAL SYMBOLS

$M_i$	Inertia constant of generator $i$ in pu-sec <sup>2</sup> /rad.
$\omega_i^{\text{syn}}$	Rotor angular velocity of generator $i$ w.r.t. arbitrary synchronous rotating reference frame (asrf)
$\delta_i$	Rotor angle of generator $i$ w.r.t. asrf
$P_{mi}$	Constant mechanical power input to generator $i$
$P_{ei}$	Active power generated by machine $i$
$Q_{ei}$	Reactive power generated by machine $i$
$P_i$	Active power injection at bus $i$
$Q_i$	Reactive power injection at bus $i$
$V_i$	Magnitude of voltage at bus $i$
$\psi_i$	Angle at bus $i$ w.r.t. asrf
$E_i$	Magnitude of internal voltage of generator $i$
$m$	Number of machines in the system
$m_\alpha$	Number of machines in area $\alpha$
$n$	Number of buses in the system excluding the internal buses of generators
$L$	Total number of elements in the system including the machine reactances
COI	Centre of inertia
$\delta_0$	System centre of inertia (global COI)
$\omega_0$	Angular velocity of global COI
$\omega_i$	Rotor angular velocity of generator $i$ w.r.t. global COI
$\theta_i$	Rotor angle of the $i$ th machine w.r.t. global COI
$\phi_i$	Angle at bus $i$ w.r.t. global COI
$\theta_0^\alpha$	COI of area $\alpha$
$\omega_0^\alpha$	Angular velocity of the COI of area $\alpha$

$\theta_{T-k}$	COI of group T-k
$\omega_{T-k}$	Angular velocity of the COI of group T-k
$\bar{\theta}_i$	Rotor angle of $i$ th machine in the group T-k w.r.t. $\theta_{T-k}$
$\bar{\omega}_i$	Rotor angular velocity of generator $i$ in the group T-k w.r.t. $\omega_{T-k}$
$\theta_i^\alpha$	Rotor angle of machine $i$ in area $\alpha$ w.r.t. $\theta_0^\alpha$
$\bar{\omega}_i^\alpha$	Rotor angular velocity of machine $i$ in area $\alpha$ w.r.t. $\omega_0^\alpha$
$P_{Li}$	Active power load at bus $i$
$Q_{Li}$	Reactive power load at bus $i$
$[Y]$	Admittance matrix of the system network excluding machine reactances
$G_{ij}, B_{ij}$	Real and imaginary parts of $[Y_{ij}]$
$f_{pi}(V_i)$	Function of voltage dependent active power at bus $i$
$f_{qi}(V_i)$	Function of voltage dependent reactive power at bus $i$
$\alpha$	G/B ratio
SPEF	Structure preserving energy function
$W$	Total transient energy
$W_1$	Kinetic energy
$W_2$	Potential energy
$W_{cr}$	Critical energy
$\Delta W$	Transient energy margin
$\Delta W_n$	Normalised transient energy margin
$W_{cl}$	Total transient energy at clearing
$W_{1cl}$	Kinetic energy at clearing
$W_{2cl}$	Potential energy at clearing
$\omega_{kcl}$	Rotor angular velocity of generator $k$ at clearing

$\theta_{kcl}$	Rotor angle of generator k at clearing
$P_{ak}$	Accelerating power of generator k
$t_{cr}$	Critical clearing time
$t_{cl}$	Clearing time
$\Delta t$	Time step
H	Step of rotor angle of generator k
$\theta_k^*$	Rotor angle of generator k corresponding to the critical energy
$k_1, k_2$	Load coefficient
sep	Stable equilibrium point
uep	Unstable equilibrium point
PEBS	Potential energy boundary surface
AVR	Automatic voltage regulator
PSS	Power system stabilizer
$x_d, x_q$	d and q axes synchronous reactances
$x'_d, x'_q$	d and q axes transient reactances
$E'_d, E'_q$	Magnitudes of d and q axes components of voltage behind d and q axes transient reactances respectively of i
$i_d, i_q$	d and q axes components of armature current
$V_d, V_q$	d and q axes components of terminal voltage
$E_{fd}$	Field applied voltage
$V_{ref}$	Exciter reference voltage

Subscript 'o' indicates the quantities evaluated at sep. Other symbols used in the text are explained as and when they are introduced.

## SYNOPSIS

### DIRECT STABILITY EVALUATION AND ON-LINE DYNAMIC SECURITY ASSESSMENT OF POWER SYSTEMS USING STRUCTURE PRESERVING ENERGY FUNCTIONS

A Thesis Submitted  
In Partial Fulfilment of the Requirements  
for the Degree of  
DOCTOR OF PHILOSOPHY

by  
K.K. GHOSH  
to the  
Department of Electrical Engineering  
Indian Institute of Technology  
Kanpur, India  
October, 1986

Successful operation of modern interconnected power systems depends largely on its ability to maintain stability during the transients. Transient stability evaluation assumes, therefore, greater significance in the planning, design and operation of large scale power systems. Power system stability is, in essence, a single concept; but for the purpose of analysis, it is classified as 'transient stability' and 'steady state stability'. The former refers to the stability of the system under large disturbances such as faults on transmission network. Steady state stability refers to the ability of the system to remain in synchronism under small perturbations caused by random changes in the load.

System security may be considered as the ability of a power system in normal state to undergo a disturbance without

going into emergency condition. The static security assessment is widely used in modern energy control centres to predict the system security when subjected to a set of contingencies. It is assumed here that the system remains stable following a contingency. This assumption is relaxed in considering dynamic security. While the objectives and methodologies of dynamic security assessment are yet to be clearly defined, there is a general consensus that the system model is similar to that used in transient stability studies just as static security assessment employs models used in load flow studies.

The transient stability analysis deals with nonlinear mathematical models describing the dynamic behaviour of the system. Digital simulation involving explicit evaluation of swing curves, is a versatile tool for stability assessment, but the method is time consuming and hence unsuitable for on-line applications. Direct methods based on transient energy calculations are recognised to be useful as screening tools in evaluating critical situations in the system. The transient energy margin (TEM) which is defined as the difference between the critical energy and the energy at the clearing time has been suggested as an index for checking the stability of the system following a disturbance. This index also serves to indicate the severity of the disturbance. [

The energy-integral criterion, first proposed by Aylett, was later generalised in the use of Lyapunov functions by a number of researchers. The application of the Lyapunov method for transient stability analysis led to conservative results in the computation of the regions of stability. Later efforts using the energy function in the centre of inertia (COI) variables and the concept of controlling unstable equilibrium point (u.e.p) have removed much of the conservativeness of the results. Approximations in evaluating the uep's and the application of the Potential Energy Boundary Surface (PEBS) technique have greatly simplified the computation of stability regions.

Hitherto, the application of direct methods using energy functions is based on reduced model of the system eliminating load buses. This is possible for constant impedance type loads. Even if such a load representation is accurate, it will be desirable to preserve the structure of the network for on-line dynamic security assessment. The recent work on the structure preserving energy function (SPEF) (defined on structure preserving models) has removed this limitation and made it possible to consider arbitrary voltage dependent load models [1-3]. The problem of transfer conductances is also overcome by the use of structure preserving models. Some attempts have been made to include detailed machine models [4] where the results are conservative.

While the concept of SPEF is undoubtedly appealing, its application to on-line dynamic security assessment requires further developments. First of all, the computational requirements with nonlinear load models are much more than with reduced models. This can be a severe limitation for on-line applications. Secondly, there is a need to improve the system models used. Finally, the user must have the tools for the stability evaluation (both in planning and operation) that can be readily used for large systems.

Another drawback of the present state of direct methods is the problem of accurate determination of the critical energy. While the PEBS method has overcome the computation of u.e.p, the accuracy of the method in multi-machine systems is governed by the fact that not all the kinetic energy (even with respect to centre of inertia) is responsible for system separation. The kinetic energy that is responsible for the system separation depends on the mode of instability and can be approximately calculated based on heuristic arguments [5]. However, an exact derivation of the energy function to be used in such cases is not available in the literature.

This thesis is aimed at trying to overcome some of the limitations mentioned above. Specifically the objectives are :

- 1) incorporation of the computation of SPEF in transient stability program to simplify the stability evaluation.

- 2) development of methods and efficient algorithms for the fast and accurate evaluation of transient stability of power systems thereby making the application of direct methods to on-line dynamic security analysis much more promising.
- 3) development of SPEF for more realistic power system models for the evaluation of system stability.

The major contributions of the thesis are listed below :

- i) An existing dynamic simulation program [6] is modified to include the computation of SPEF. The use of SPEF can speed up the calculation of critical clearing time ( $T_{cr}$ ) or the stability limit thereby avoiding the time consuming simulation runs. Both classical and detailed machine models alongwith voltage dependent loads are used in the computation of SPEF.
- ii) A new SPEF is derived considering the mode of instability where a single or a group of machines separate from the rest. This energy function differs from the previously derived energy function [3] in the kinetic energy term. The new energy function gives more accurate results.
- iii) Utilising the information on the mode of instability an algorithm is presented to speed up the computation of TEM by solving algebraic equations. This procedure eliminates the need for determining the faulted trajectory and can make the on-line assessment of dynamic security using the energy function much more attractive.

- iv) A SPEF is derived to include the resistance of transmission lines which has not been done so far. Derivation is based on the assumption that conductance to susceptance ratios ( $G/B$ ) of all the network elements are equal which permits network to be transformed into a lossless network [7]. This assumption is not found to be restricting as the numerical examples show that the use of an average value for  $G/B$  gives reasonably accurate results.
- v) A new SPEF is derived with realistic model of generators considering flux decay, transient saliency, AVR, exciter and damper winding on the quadrature axis. This is an extension of the work reported in [4]. However, the energy function derived here is constant on the post-fault trajectory with the time derivative as zero. This leads to more accurate results than that reported in [4] in the computation of stability region using PEBS method. A simplified and general method for the calculation of SPEF is also presented where the use of classical model becomes a special case.

The following is an outline of the work reported in this thesis :

- 1) Chapter 1 introduces the various aspects of energy based direct methods for stability analysis of power systems and the application of these methods to on-line dynamic security assessment. The state of the art in this area is presented and the scope and objective of the thesis are outlined alongwith the chapterwise summary.

- 2) Chapter 2 deals with the modification of a dynamic simulation program by Podmore [6] to include the computation of SPEF. The existing program provides time domain simulation of reduced power system networks. It is written in FORTRAN and is composed of a MAIN routine and a number of sub-routines beside two supporting programs for base case load flow and network reduction eliminating the load buses. The following modifications are incorporated in the existing program to develop the new transient stability program :
- A. The structure of the original network is retained to enable arbitrary voltage dependent load representation. This is done by
    - i) replacing the supporting program for network reduction by the program YMAT to construct the network bus admittance matrix.
    - ii) modifying the subroutine NWSOL used for the network solution to include voltage dependent nonlinear loads.
  - B. The program is augmented to compute SPEF. This is done by adding two new subroutines :
    - i) PFSOL for solving the post-fault network equations at the end of each integration step to obtain voltages and their angles at all the buses to be used in the computation of the energy function. Internal voltages of the generators to be used in the network solution are the same as that obtained by the integration of the machine equations.

ii) TEF to evaluate the SPEF and its components for each time step of the network solution.

The modified program can thus handle the power system stability problem using i) time domain simulation and ii) direct assessment via the SPEF. The analysis of the program output during the faulted period can be used to predict the critical energy and the critical clearing time. After the initial development, the transient stability program was tested with three realistic power system examples. The validation test confirms that direct methods provide results comparable to that of simulation.

3) Chapter 3 is devoted to the systematic development of a mathematical model for the direct stability evaluation of multi-machine power systems based on the assumptions that i) instability results from a single machine or a group of machines separating from the rest and ii) the generators in each group swing together. A new energy function is then derived and it is shown that the function has a time derivative which is zero. Structure preserving model of the system is used and the generators are represented by the classical model. Loads are modelled as arbitrary functions of respective bus voltage. The system equations and the energy function are formulated in COI variables. Critical energy is evaluated using the PEBS method. The procedure has been applied to three system examples considered in Chapter 2. The results indicate that i) the inclusion of the

mode of instability in the energy function gives consistently a better estimate of the critical clearing time compared to that obtained using the energy function of ref. [3] which does not consider the mode of instability and ii) the effect of voltage dependent active power loads on the region of stability is quite significant and thus cannot be ignored. The voltage dependent active power loads introduce path dependent term in the energy function which is computed by numerical integration using trapezoidal rule.

4) An efficient method for assessing the dynamic security of power systems on-line based on the concept of TEM, is presented in Chapter 4. The system model and the energy function of Chapter 3 are again used for the development of the method. A deterministic estimation of the transient energy margin involves the computation of the energy function i) at criticality and ii) at clearing.

It is shown that for a given mode of instability (as described in Chapter 3), the potential energy reduces to a function of single independent variable corresponding to the rotor angle(s) of the machine(s) going out-of-step with respect to the remaining machines. It is also shown that the critical and the clearing energies can be obtained by the solution of algebraic equations thereby completely eliminating the simulation of the faulted system. This leads to a substantial reduction in the computation required for stability evaluation using SPEF.

The proposed method is illustrated by considering the three system examples given in Chapters 2 and 3. The predicted value of the critical energy and that at clearing are in close agreement with those obtained using the faulted trajectory simulation. The proposed method can also be used for accurate ranking of the contingencies as illustrated in 10-machine system example.

5) Structure preserving energy functions have so far been developed without accounting for the transmission line resistances. An attempt is made in Chapter 5 to develop a valid energy function including the line resistances. The method is based on a network property which states that a network having the same  $G/B$  ratio for all its elements is equivalent to a lossless network with a new set of power injections [7]. The use of the proposed energy function is illustrated with numerical examples. Results indicate that i) inclusion of line resistances improves transient stability in terms of a larger region of stability and a higher value of critical clearing time and ii) predicted critical clearing time obtained using the average value of  $G/B$  for the network elements compares well with that obtained by digital simulation using the actual resistance of these elements. The component of the energy function accounting for the transmission line resistances is path dependent and is evaluated by trapezoidal rule.

6) The principal aim of Chapter 6 is to extend the work reported in ref. [4] considering more detailed models of the generators. The topological energy function of ref. [4] has a time derivative which is negative semi-definite. Considering the same model as in [4], a new SPEF is developed, the time derivative of which is zero. Moreover, this model is improved upon by the addition of a damper winding on the quadrature axis and a new energy function is derived. The time derivative of the energy function is again shown to be zero. Simpler expressions for the energy functions are then derived thereby increasing the speed of calculation. Investigations are carried out on a 4-machine, and a 10-machine system examples. Critical clearing times obtained by direct method and by simulation are compared and are found to be in close agreement. The results show that i) the variation of the field and the generator voltages have predominant effects on the system energy during a transient and ii) the inclusion of transient saliency, AVR and damper winding is beneficial in improving the transient stability.

7) A brief review of the major contributions of this thesis and the suggestion for further work form the seventh and the concluding chapter.

## REFERENCES

- [1] N. Narasimha Murthy and M.T. Musavi, 'A Generalised Energy Function for Transient Stability Analysis of Power Systems', IEEE Trans., CAS, vol.CAS-31, No.7, July 1984, pp 637-645.
- [2] N. Tsolas, A. Araposthasis and P. Varaiya, 'A Structure Preserving Energy Function for Power System Transient Stability Analysis', IEEE Trans. CAS, vol. CAS-32, No.10, Oct.1985, pp.1041-1049.
- [3] K.R. Padiyar and H.S.Y. Sastry, 'A Topological Energy Function Analysis of Stability of Power Systems', To be published in Int. Jr. of Electric Power and Energy Systems.
- [4] K.R. Padiyar and H.S.Y. Sastry, 'Direct Stability Analysis of Power Systems with Realistic Generator Models using Topological Energy Function', Paper presented at the IFAC Symposium, Beijing, China, Aug. 1986.
- [5] A.A. Fouad and S.E. Stanton, 'Transient Stability of a Multi-machine Power System, Part II : Critical Transient Energy', IEEE Trans. PAS, vol.PAS-100, No.7, July 1981, pp 3417-3424.
- [6] R. Podmore, 'Power System Dynamic Simulation Program - Users' Manual', University of Saskatchewan, January, 1974.
- [7] K.R. Padiyar, 'On the Nature of Power Flow Equations', Electric Machines and Power Systems, No.9, 1984, pp 297-306.

## CHAPTER 1

### INTRODUCTION

#### 1.1 GENERAL

There has been a phenomenal growth, in size and complexity, of electric power systems to match the increasing demand for electric energy. Successful operation of these modern interconnected systems depends largely on their ability to maintain stability during transients. Transient stability analysis, therefore, assumes greater significance in the planning, design and operation of large scale power systems. Power system stability may be defined as that property of the system which enables it to respond to a perturbation from a normal operating point so as to return to a condition where its operation is again normal [1-8]. The main criterion for stability is that the system maintains synchronism at the end of the transient period.

Power system stability is, in essence, a single concept; but for the purpose of analysis, it is classified as 'transient stability' and 'steady state stability' depending upon the nature and the magnitude of the disturbance. Transient stability studies are aimed at determining system stability following major disturbances. These disturbances may be due to

transmission system faults, sudden injection or rejection of a large load, tripping of a large generating unit or line switching. Three phase short circuits followed by line clearing are the most severe of all these disturbances. Usually, disturbances alter the system at least temporarily so that subsequent steady state operation will be different from that prior to the disturbance. There is then the necessity for that altered system to be stable in its new steady state.

Steady state stability refers to the ability of the system to remain in synchronism under small perturbation caused by random changes in load. Decrease in transmission system capabilities or inadequately designed regulating devices (such as AVR's) can cause steady state instability.

System security may be considered as the ability of a power system in normal state to undergo a disturbance without going into emergency condition. The static security assessment is widely used in modern energy control centres to predict the system security when subjected to a set of contingencies. It is assumed here that the system remains stable following a contingency. This assumption is relaxed in considering dynamic security. While the objectives and methodologies of dynamic security assessment are yet to be clearly defined, there is a general consensus that the system model is similar to that used in transient stability studies just as static security assessment employs models used in load flow studies.

## Methods of Analysis

The transient stability analysis of power systems deals with nonlinear mathematical models describing the dynamic behaviour of the systems. These models consist of a set of differential equations representing the dynamics of generating units (synchronous machines and their controls) and a set of algebraic equations describing the interconnections through the transmission network. Various approaches to the stability problem are :

- i) Digital simulation
- ii) Direct methods
- iii) Pattern recognition

Digital simulation techniques involve the numerical integration of the system differential equations to obtain explicit time domain solutions. The numerical integration methods used for stability analysis, although very effective in handling sophisticated models, are time consuming and hence unsuitable for on-line applications.

To overcome this limitation, energy-based direct methods for stability analysis have been developed. Computational effort is significantly reduced since only the faulted system is integrated for a short time till the clearing of the fault. As a result of continuous research and the progress made, these methods are now recognised to be useful as screening tools in assessing critical situations in the system [9].

Pattern recognition [10-12] is another approach aimed at overcoming the high computational requirements of on-line transient stability studies. A large number of off-line stability studies are performed to form a 'training set' and certain important features are selected. A classifier compares the actual operating conditions with the training set and, on the basis of this comparison, classifies the existing state as either secure or insecure.

Direct methods for stability evaluation involve the comparison of the energy attained by the system during the fault-on period with the critical energy. The transient energy margin (TEM) which is defined as the difference between the critical energy and the energy at the clearing time, has been suggested as an index for checking the stability of the system following a disturbance. This index also serves to indicate the severity of the disturbance. Normalised transient energy margin which may be defined as the excess potential energy capability (difference between the critical energy and the potential energy at fault clearing) of the system, expressed as the ratio of the kinetic energy at the instant the fault is cleared, also serves as an alternative measure for inferring system stability or instability.

The application of direct methods to transient stability evaluation and on-line dynamic security assessment of power

systems using structure preserving energy functions (SPEF) is investigated in this thesis.

## 1.2 DIRECT METHODS

As stated earlier, transient stability analysis is concerned with the system's ability to remain in synchronism following major disturbance such as a three phase fault at the terminals of generators. During transients the dynamics of the system can be described by the following set of differential-algebraic equations which are functions of the system variables

$$\dot{\underline{x}} = \underline{f}(\underline{x}, \underline{y}) \quad (1.1a)$$

$$\underline{0} = \underline{g}(\underline{x}, \underline{y}) \quad (1.1b)$$

The functions  $\underline{f}$  and  $\underline{g}$  will be different for the faulted and the post-fault networks because of change in network configuration.

Transient stability study using numerical integration methods involves explicit time domain solutions of Eqs. (1.1). These methods are, therefore, expensive in terms of computation requirement. For this reason, search for direct methods, that is, methods to determine stability independently of the time solution of Eqs. (1.1), has continued. The classical equal area criterion is such a direct method for single- or two-machine systems.

The post-fault system has an initial state decided by the state at the end of the fault period. Also, the post-fault system has a stable equilibrium point (sep) which can be obtained by solving the set of equations in (1.1) corresponding to the post-fault network. The fundamental problem of transient stability is to decide whether the post-fault system, starting in the initial state, will converge to the sep

There is a region of initial conditions in the state space from which trajectories converge to the sep. This region is called the region of stability. If the initial post fault state lies within this region, then the system is stable. Direct methods attempt to compute this region through the computation of a Lyapunov or energy function which is a positive definite function of the system variables as shown below :

$$W = W(\underline{x}, \underline{y}) \quad (1.2)$$

and whose time derivative along the post-fault trajectory is negative (semi-) definite. The region of stability surrounding the sep can be defined by

$$W(\underline{x}, \underline{y}) < W_{cr} \quad (1.3)$$

where  $W_{cr}$  is the critical value of  $W$ . In testing transient stability following a fault, the value of  $W$  is monitored at the time of clearing ( $t_{cl}$ ) and compared with  $W_{cr}$ . If

$$W(t_{cl}) < W_{cr} \quad (1.4)$$

then the system is considered stable. The evaluation of  $W(t_{cl})$  requires the solution of Eqs. (1.1) corresponding to the faulted system configuration. This is usually obtained by simulation.

The critical clearing time ( $t_{cr}$ ) which is of interest in stability studies, is defined by

$$W(t_{cr}) = W_{cr} \quad (1.5)$$

### 1.3 LITERATURE SURVEY

#### 1.3.1 General

The use of equal area criterion is the first application of Lyapunov's direct method to power system transient analysis. However, the systematic application of this method to the stability problem of realistic power systems is due to Gless [13] and El-Abiad and Nagappan [14]. Since then there has been growing interest in the application of direct methods to transient stability analysis. A summary of the research efforts is well documented in the survey papers by Ribbens-Pavella [15,16], Fouad [17], Pai [18], Varaiya [19] and in a recent monograph on the subject by Pai [1]. These investigations have essentially been directed along two distinct, although related lines :

- i) the construction of suitable Lyapunov functions with improved system models to allow for flux decay and regulating devices such as AVR, governor, etc. [20-26],

- ii) development of fast and accurate algorithms for implementation of the method to on-line transient stability studies [1, 27-33].

### 1.3.2 Lyapunov or Energy Functions

The systematic construction of Lyapunov functions was attempted by Willems [20, 21] and Pai et al [22]. Detailed models of machines were considered by Pai and Rai [23] for stability analysis of synchronous machines using Lyapunov Popov criterion. Results obtained with models higher than the second order representation of machines appear to be conservative in addition to the difficulties involved in the construction of an effective Lyapunov function. This motivated Sasaki [24] to approximately include the field flux decay in the transient stability analysis. A Lyapunov function based on Moore-Anderson Theorem considering flux decay in generators was constructed in ref. [25]. In their recent work, Kakimoto et al [26] have incorporated more realistic model for generators including AVR and PSS in investigating transient stability by direct methods. However, the Lyapunov function in [25] does not include the effect of AVR and gives inconsistent results for the predicted regions of stability.

Energy functions are possible Lyapunov functions for conservative systems. The various components of the energy function can be given a physical interpretation. Energy based

concepts for power system transient stability analysis was first proposed by Magnusson [34] and then by Aylett [35]. The energy-integral criterion was later generalised in the use of Lyapunov functions. However, for about last one decade, there has been renewed interest in the use of energy function for stability analysis, particularly dynamic security assessment.

The centre of inertia (COI) is an important variable in power system analysis. It is defined as the inertia weighted average of all the rotor angles [36, 37]. Reference [36] shows that for transient stability evaluations, the kinetic energy of the system must be calculated by utilising the relative velocities with respect to COI. In ref. [30], COI variables are used to formulate the system equations and to develop an energy function with reduced systems.

In their recent work, Pai et al [38, 39] have exploited a physically based decomposition technique to perform direct stability analysis of power systems using energy functions. Formulating the system equations in a singularly perturbed form, they use the slow coherency based grouping technique [40,41] to decompose the system into  $r$  areas. This grouping is then used to develop i) slow energies associated with the centres of inertia of the areas, ii) fast energies associated with inter-generator oscillations within an area and iii) slow-fast energies associated with both the slow and the fast variables. It

has been shown that depending on the fault location, only a few areas are disturbed and it is possible to approximate the system energy function by the fast energies of the disturbed areas, global slow energy and the slow-fast energy.

Winkelman et al [42] have proposed a Hamiltonian based approach to study the transient stability problem including flux decay and voltage regulation. They have developed a generalised potential energy function including the effects of non-conservative forces acting on the system during transients. The total energy of the post-fault system has been shown to remain constant.

### Transfer Conductances

Hitherto, the application of direct methods using energy functions is based on reduced model of the system eliminating the load buses. This is possible for constant impedance type loads. Such a load representation introduces transfer conductances in the nodal admittance matrix (corresponding to the internal nodes of the generators). Aylett [35] has shown that the presence of transfer conductances makes some of the terms in the Lyapunov function path dependent. He, therefore, suggested the omission of these terms or for the sake of consistency, the omission of all the transfer conductance terms. Later, Ribbens-Pavella [43] successfully developed two valid Lyapunov functions following the procedure of Aylett.

Uemura et al [44] handled the problem of transfer conductances by making approximations in the integrand which was once considered as a constant and another time as a linear function. Pai et al [45] succeeded in constructing valid Lyapunov functions with transfer conductances for a two-machine system. They claimed that the generalisation of their approach to multi-machine systems was straightforward. This prompted Gudarú [46] to derive a Lure type Lyapunov function for the multi-machine systems with transfer conductances following the Anderson procedure. Henner [47] and Willems [48] have, however, shown that the generalised Lyapunov function derived by him is not valid since he fails to satisfy the positive real matrix criterion.

Later, Pai and Varwandkar [49] used the same non-linearities as Gudarú and the Lyapunov function of Pai and Murthy [45] neglecting the transfer conductances and succeeded in generating the Lyapunov function by introducing approximations in the model for the multi-machine case.

Kakimoto et al [26] considered the effect of transfer conductances by adding numerical correction to the Lure type Lyapunov function under the assumption that the system trajectories are not so much different in the relative angular space between a sustained fault and the critically cleared fault and obtained two modified Lyapunov functions.

Athay et al [30] computed the critical value of the energy function using a linear path of integration while for evaluating the energy function along the faulted trajectory, they used the actual path to integrate the non-integrable terms via the trapezoidal rule.

Guindi and Mansour [50] approximated the relative velocity by a constant factor and succeeded in constructing a valid Lyapunov function.

### Structure Preserving Energy Functions (SPEF)

Another disadvantage of using the reduced system model is that it masks the topology of the system network to be investigated. Beside, it does not allow one to understand and interpret the energy shifts among system components during a disturbance. The problem of transfer conductances due to loads can be avoided by an approach suggested by Pai et al [51], using distribution factors to reflect the effect of loads as current injections at the generator internal buses. Later efforts using structure preserving energy functions (SPEF) have greatly helped in removing this limitation and made it possible to consider more realistic load models.

The concept of structure preserving energy functions to be used for transient stability evaluation is due to Bergen and Hill [52] who first proposed a system model retaining the identity of the load buses. They model the load buses as P-V type

buses and allow the active powers of load to be frequency dependent; but their 'topological' energy function does not depend on frequency dependence. In addition, the assumption of constant bus voltages is not valid, since these voltages fluctuate considerably during a fault. Their approach has been improved upon by Narasinghamurthy and Musavi [53] by considering voltage dependent reactive power loads in developing the SPEF. However, the real power at each load bus is assumed to be constant. An improved load model has been proposed by Padiyar and Sastry [54] and Ribbens-Pavella et al [55] by considering the real and the reactive power of load to be arbitrary functions of respective bus voltage. In their recent work, Ribbens-Pavella et al [56] have presented an unified approach for modelling the loads by allowing the real power load at each bus to be both voltage and frequency dependent and the reactive power load to be voltage dependent. Attempts have also been made to include detailed machine models in the development of SPEF. Tsolas et al [57] developed the structure preserving energy function considering flux decay and transient saliency in machines using constant active and reactive power loads. In ref. [58], Padiyar and Sastry developed a 'topological' energy function considering flux decay, transient saliency, exciter and AVR allowing the loads to be voltage dependent. However, their energy function has a time derivative which is negative semi-definite and the results obtained appear to be conservative.

### 1.3.3 Computation of Stability Regions

Direct methods for power system transient stability evaluation involve an accurate determination of the region of stability or the critical energy. In the past, the minimum value of the Lyapunov function evaluated at all possible unstable equilibrium points (uep) was chosen [1]. This procedure yields very conservative results for the regions of stability. Besides, the computational burden increases prohibitively for large systems. This prompted Prabhakara et al [27] to suggest simplifications in the determination of these points. Ribbens-Pavella [31] has shown with various numerical examples that consideration of the common modes of instability reduces the number of uep's to be evaluated to  $2m$ ,  $m$  is the number of machines. In ref. [30], Athay et al have shown that consideration of the controlling or the relevant uep substantially eliminates the limitations of the method due to conservativeness of results.

The Potential Energy Boundary Surface (PEBS) method has overcome the need for the computation of uep's [29,30]. PEBS is defined as the surface formed in angle space by the points corresponding to the first maxima of the potential energy with respect to the stable equilibrium point, where its directional derivative is zero. The uep's (where the gradient of potential energy is zero) lie on the PEBS. The critical energy is determined as the potential energy at the instant when the faulted

trajectory crosses the PEBS. It is assumed that the critically cleared trajectory passes very close to the controlling ucp. The results obtained using the PEBS method are, usually, in good agreement with those obtained by the controlling ucp method.

Although the PEBS method succeeds in avoiding the need to compute the ucp's, the accuracy of the method in multi-machine system is governed by the fact that not all the kinetic energy is responsible for system separation. The kinetic energy that is responsible for system separation depends on the mode of instability and can be approximately calculated based on heuristic arguments [59]. The concept of generalising the equal area criterion for multi-machine systems, is proposed in ref. [32] by Fouad and Vittal. This is used to determine the controlling ucp and the critical energy for the disturbance under investigation [33]. Michel et al [60] have used the transient energy of individual machines to study the stability problem. They claim that the use of individual machine energy functions rather than the overall system energy helps in correctly predicting the mode of instability and the critical clearing time.

#### 1.3.4 Application to on-line Dynamic Security Assessment

The problem of dynamic security assessment in an on-line environment remains largely unsolved and there is not much literature available. In refs. [32, 61], Fouad et al attempt

to assess the transient stability of power systems through the application of transient energy margin (TEM). With the help of numerical examples, they demonstrate that the use of TEM provides information on the weak links in the system and helps in ranking three phase and single line-to-ground faults. Ribbens-Pavella et al [62] derive a transient stability index (TSI) based on the maximum initial relative acceleration of the system. They then use this index to assess the robustness of a power system subject to a disturbance, without performing any disturbance simulation. However, their approach is heuristic in nature. Pai et al [63, 64] propose the use of energy margins for economic load dispatch with dynamic security constraints. They exploit the sensitivity of the energy margins to determine maximum load capability or simultaneous interchange capability. In their recent work, Fouad et al [65] suggest a technique incorporating the sensitivities of the unnormalised transient energy margin to speed up the transient energy function method in on-line dynamic security assessment of power systems.

There have been no attempts for the application of SPEF for on-line dynamic security assessment, reported in the literature.

#### 1.4 OBJECTIVES AND SCOPE OF THE THESIS

While the concept of structure preserving energy function is undoubtedly appealing, its on-line application to dynamic security assessment requires further developments. First of all, the computational requirements with nonlinear load models are much more than with reduced models. This can be a severe limitation for on-line applications. Secondly, there is a need to improve the system models used. Finally, the user must have the tools for stability evaluation (both in planning and operation) that can be readily used for large systems.

This thesis is aimed at trying to overcome some of the limitations mentioned above. Specifically, the objectives are:

- i) incorporation of the computation of SPEF in transient stability program to simplify the stability evaluation.
- ii) development of methods and efficient algorithms for the fast and accurate evaluation of transient stability of power systems thereby making the application of direct methods to on-line dynamic security analysis much more promising.
- iii) development of SPEF for more realistic power system models for evaluation of system stability.

## 1.5 OUTLINE OF THE THESIS

The chapterwise summary of the work done in this thesis is given below :

1) Chapter 2 deals with the modification of a dynamic simulation program by Podmore [66] to include the computation of SPEF. The existing program provides time domain simulation of reduced power system networks. It is written in FORTRAN and is composed of a MAIN routine and a number of subroutines beside two supporting programs for base case load flow and network reduction eliminating the load buses. The following modifications are incorporated in the existing program to develop the new transient stability program :

- A. The structure of the original network is retained to enable arbitrary voltage dependent load representation. This is done by
  - i) replacing the supporting program for network reduction by the program YMAT to construct the network bus admittance matrix
  - ii) modifying the subroutine NWSOL used for network solution to include voltage dependent nonlinear loads.
- B. The program is augmented to compute SPEF. This is done by adding two new subroutines :

- i) PFSOL for solving the post-fault network equations at the end of each integration step to obtain voltages and their angles at all the buses to be used in the computation of the energy function. Internal voltages of the generators, to be used in the network solution are the same as that obtained by the integration of the faulted system equations.
- ii) TEF to evaluate SPEF and its components for each time step of the network solution.

The modified program can thus handle the study of the power system transient stability problem using a) time domain simulation and b) direct assessment via the SPEF. The analysis of the program output during the faulted period can be used to predict the critical energy and the critical clearing time. After the initial development, the transient stability program is tested with three realistic power system examples. The validation test confirms that direct methods provide results comparable to that of simulation.

2) Chapter 3 is devoted to the systematic development of a mathematical model for the direct stability evaluation of multi-machine power systems based on the assumptions that i) instability results from a single machine or a group of machines separating from the rest and ii) the generating units in each group swing together. A new energy function is then derived and it

is shown that the function has a time derivative which is zero along the post-fault trajectory. The generators are represented by the classical model. The machine damping and transmission line losses are ignored. Loads are modelled as arbitrary functions of respective bus voltage. The system equations and the energy function are formulated in COI variables. Critical energy is evaluated using the PEBS method.

3) An efficient method for assessing the dynamic security of power systems on-line, based on the concept of TEM, is presented in Chapter 4. The system model and the energy function of Chapter 3 are again used for the development of the method. A deterministic estimation of the transient energy margin involves the computation of the energy function i) at criticality and ii) at clearing.

It is shown that for a given mode of instability (as described in Chapter 3), the potential energy reduces to a function of single independent variable corresponding to the rotor angle of the machine going out-of-step with respect to the remaining machines. It is also shown that the critical and the clearing energies can be obtained by the solution of algebraic equations thereby completely eliminating the simulation of the faulted system. This leads to a substantial reduction in the computation required for stability evaluation using SPEF.

The proposed method is illustrated by considering the three system examples given in Chapters 2 and 3.

4) Transmission lines have so far been considered to be lossless in the derivation of structure preserving energy functions. An attempt is made in Chapter 5 to include the line resistances in the development of a valid energy function. The method is based on the network property that a network, all the elements of which have the same  $G/B$  ratio, is equivalent to a lossless network with a new set of power injections [67]. An energy function is derived based on the transformed network. It is shown that the time derivative of the function on the post-fault trajectory vanishes. The use of the proposed energy function is illustrated with numerical examples.

5) The principal aim in Chapter 6 is to develop a structure preserving energy function including detailed generator models. This work is based on an earlier work by Padiyar et al [58] wherein they have derived a 'topological' energy function incorporating the effect of flux decay, transient saliency, exciter and AVR. The function in [58] has a time derivative which is negative semi-definite along the post-fault trajectory and gives pessimistic estimates of the region of stability. An attempt has been made in this chapter to remove these limitations. The generator model used in [58] is augmented by the addition of a damper winding on the quadrature axis. A new SPEF corresponding to the improved model is then derived. The

time derivative of the energy function is shown to be zero along the post-fault trajectory. A simpler and yet general expression for the energy function is then derived where the use of the classical model becomes a special case. The new energy function is tested on a 4-machine and a 10-machine system examples.

6) The summary of the research results in this thesis and suggestions for further work form the seventh and the concluding chapter.

## CHAPTER 2

# POWER SYSTEM DYNAMIC SIMULATION INCORPORATING COMPUTATION OF STRUCTURE PRESERVING ENERGY FUNCTION

### 2.1 INTRODUCTION

Transient stability evaluation using digital simulation is well developed. There are efficient transient stability programs which incorporate detailed generator models and voltage dependent load models. These programs are usually used for planning studies.

The use of direct methods can permit on-line evaluation of transient stability for security analysis. Even for off-line planning studies, direct methods can help in reducing the time of computation by reducing the number of cases that need to be studied in detail, in other words, acting as screening tools [9]. This is applicable even though simplistic models (classical models) of generators are used in direct stability analysis.

A major factor that has prevented the extensive use of direct methods by system planners is the nonavailability of effective computer programs for the computation of energy functions. Actually, modifying the existing programs can

result in a transient stability program which can help a user to apply direct methods or simulation for studying a particular case. The importance of this aspect has been appreciated by researchers [68]. It is also possible to use energy functions to provide fast information on the system stability characteristics, particularly in large systems where the handling of voluminous results, even in the form of swing curves, can be cumbersome.

Structure preserving energy function (SPEF) has the advantage of handling voltage dependent loads and even detailed generator models [57,58]. The objective of this chapter is to incorporate the computation of SPEF in an existing stability program and report on the results obtained using the augmented program. Power system dynamic simulation program by Podmore [66] is available and is well suited for research applications. This program enables detailed representation of generators with their controllers. The only restriction is the representation of load as constant impedances which permits network reduction. This limitation of the program is removed by rewriting some of the subroutines used in the program. The revised program can handle any arbitrary voltage dependent load models.

The augmented program gives additional output in terms of the energy function and its various components. By simulating

the power system only during the faulted period, it is possible to predict the critical energy using the potential energy boundary surface (PEBS) method, from the analysis of energy function. The application of the augmented program for stability evaluation is presented using case studies on three different systems (7-machine, 10-machine and 13-machine systems). These results are also validated by simulations using the same program.

## 2.2 POWER SYSTEM DYNAMIC SIMULATION

### 2.2.1 General

The equations representing the dynamic behaviour of a power system can be conveniently divided into two groups :

i) Equations describing the dynamic behaviour of the machines and their controllers. These consist of a set of differential equations of the form :

$$\dot{\underline{x}} = \underline{f}(\underline{x}, \underline{y}) \quad (2.1)$$

ii) Equations describing the steady state behaviour of the network and generator armature circuits. These consist of algebraic equations of the form :

$$\underline{g}(\underline{x}, \underline{y}) = \underline{0} \quad (2.2)$$

Variables  $\underline{x}$  are defined as the system state variables.

Variables  $\underline{y}$  are referred to as auxiliary variables and are associated with the network. Generator speed and angular position are examples of state variables, whereas bus voltages and bus angles are examples of auxiliary variables.

The structure of the network equations (2.2) may change in time due to network changes such as fault inception, fault clearing, line switching etc.

Any dynamic simulation program has to solve Eqs. (2.1) and (2.2). Numerical integration is generally used to solve the nonlinear differential equations (2.1). The network equations (2.2) reduces to a linear equation if the loads are assumed to be constant impedances. In this case,  $\underline{y}$  can be solved explicitly in terms of  $\underline{x}$  and substituted in Eq. (2.1).

### 2.2.2 Details of Existing Simulation Program [66]

This program is written in FORTRAN and is composed of a MAIN routine and a number of subroutines. The program requires the support of two other programs :

- i) A power system load flow program
- ii) A program for network reduction eliminating the load buses.

In the simulation program, loads are assumed to be constant impedances, which enables the load buses to be eliminated using network reduction. Only the generator buses are retained and one generator is assumed to be connected to each bus.

The simulation program is structured as follows :

- i) MAIN routine - for data initialization, input and providing overall control of the program.
- ii) NWSOL - a subroutine for solving the armature and the network equations. This subroutine calculates the terminal voltages and the bus current injections (generator outputs) of the network.
- iii) Equipment Subroutines - a library of subroutines for modelling various types of excitation systems and turbine-governor systems. Each equipment subroutine consists of two parts; one part calculates the initial values of the state variables and is executed once at the start of the program, the other calculates the time derivatives of the state variables for each integration time step.

The various synchronous generator representations are modelled with a single subroutine GEN1. The routine receives the terminal voltage and current as input and provides the initial conditions of the generator state variables. The synchronous machine model includes flux decay, AVR, transient saliency and a damper winding on the quadrature axis. By choosing the parameters appropriately, it is possible to represent simpler models of the machine (say, classical model). The machine model is presented in APPENDIX A.

The excitation system is modelled using three subroutines:

- AVR1 : IEEE Type 1 representation of rotating excitation system
- AVR2 : IEEE Type 1S representation of static excitation system
- AVR3 : Rotating excitation system with an auxiliary stabiliser.

The turbine governor modelling is done by the following subroutines :

- TUR1 : Three stage steam turbine (HP, IP and LP) and governor
- TUR2 : Hydraulic turbine and governor.

- iv) INT - an integration subroutine which calculates the state variables for a new time interval as a function of the state variables and state variable derivatives for the present and the preceeding intervals. The integration routine is based on the formula :

$$\underline{x}_{t+\Delta t} = \underline{\dot{x}}_t \Delta t + (\underline{\dot{x}}_t - \underline{\dot{x}}_{t-\Delta t}) \Delta t/2 + \underline{x}_t \quad (2.3)$$

where  $\underline{x}_t$  and  $\underline{\dot{x}}_t$  are the state variables and their time derivatives at time indicated by the subscript.  $\Delta t$  is the time step.

- v) OUTPUT and PLOT - these subroutines respectively give printouts and plots of the variables calculated during the simulation.

During the calculation it is necessary to account for the interconnections between the generator, excitation system and turbine governor models. Fig. 2.1 shows the relationship between the various subroutines for the calculation of the initial conditions. In this case, the field voltage and the mechanical power are calculated by the generator subroutine and consequently, this is executed before the excitation system and turbine-governor subroutines. The relationship which exists between the subroutine input and output variables during the step by step simulation is shown in Fig. 2.2. In this case, the new values of field voltage and mechanical power are respectively calculated by the excitation system and turbine-governor subroutines. Consequently, the generator subroutine is now executed after the excitation system and turbine-governor subroutines.

## 2.3 MODIFICATION OF THE DYNAMIC SIMULATION PROGRAM

### 2.3.1 General

The following modifications are incorporated in the existing program to develop the new transient stability program :

#### Inclusion of Voltage Dependent Loads

Topology of the original network is preserved to enable loads to be modelled as arbitrary functions of respective bus

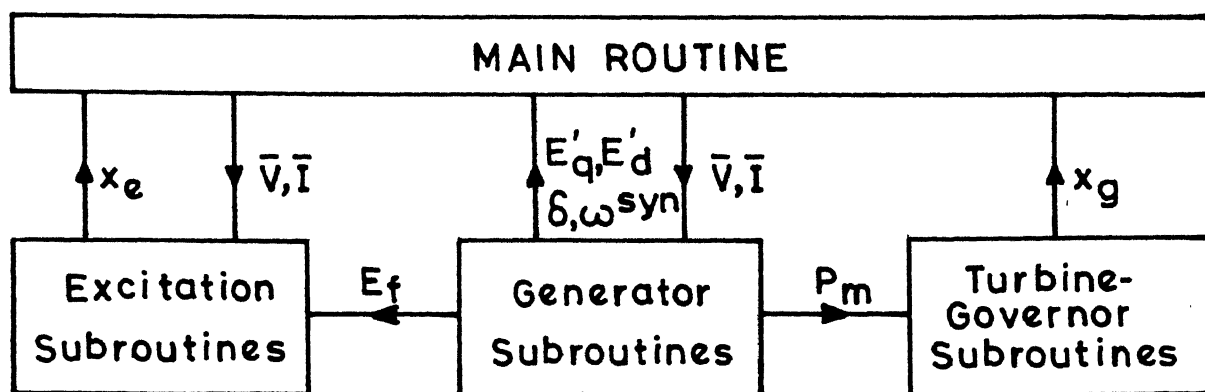


FIG. 2.1 RELATIONSHIP OF SUBROUTINE VARIABLES FOR CALCULATING INITIAL CONDITIONS.

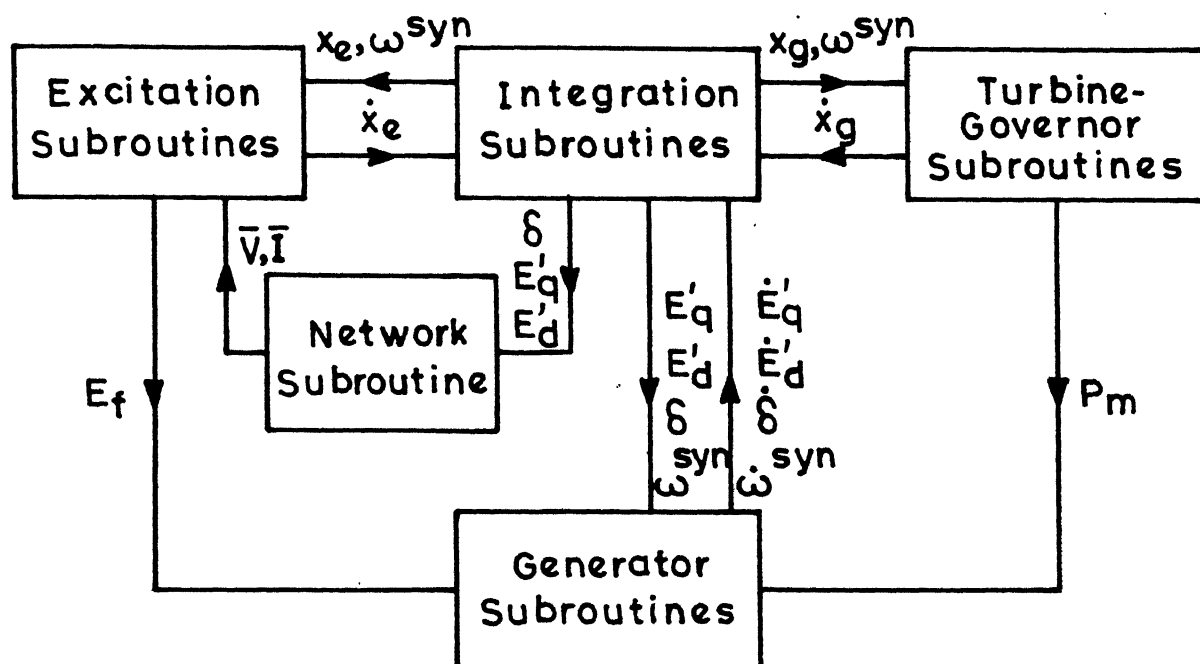


FIG. 2.2 RELATIONSHIP OF SUBROUTINE VARIABLES DURING STEP-BY-STEP SIMULATION.

voltage. This is done by

- i) replacing the supporting program for network reduction by the program YMAT to construct the network bus admittance matrix
- ii) modifying the subroutine NWSOL used for the network solution to include voltage dependent nonlinear loads.

An algorithm given in ref. [69] is used for solving the combined network and generator armature equations. This handles both saliency and nonlinear loads. The method requires iteration at each integration time step. The details of the algorithm are given in APPENDIX B.

#### Inclusion of SPEF

The program is augmented to include the computation of SPEF. This is done by adding two new subroutines :

- i) PFSOL for solving the post-fault network equations at the end of each integration step to obtain voltages and their angles at all the buses to be used in the computation of the energy function. Internal voltages of the generators to be used in the network solution are the same as that obtained by the integration of the machine equations. This routine is to be used only during the faulted period.
- ii) TEF to evaluate the SPEF and its components for each time step of the network solution.

### 2.3.2 Structure Preserving Energy Function (SPEF)

For classical model of generators, the following energy function has been defined [54] for the post-fault network :

$$W = W_1 + W_2 = W_1 + \sum_{i=1}^5 W_{2i} \quad (2.4)$$

where  $W_1$  is the kinetic energy given by

$$W_1 = \frac{1}{2} \sum_{i=1}^m M_i \omega_i^2 \quad (2.5)$$

and the components of the potential energy,  $W_2$  are

$$W_{21} = - \sum_{i=1}^m P_{mi} (\theta_i - \theta_{i0}) \quad (2.6)$$

$$W_{22} = \sum_{i=1}^n \int_{t_0}^t f_{pi}(V_i) \frac{d\varphi_i}{dt} dt \quad (2.7)$$

$$W_{23} = \sum_{i=1}^n \int_{V_{i0}}^{V_i} \frac{f_{qi}(V_i)}{V_i} dV_i \quad (2.8)$$

$$W_{24} = \sum_{i=1}^m [E_i^2 + V_i^2 - 2E_i V_i \cos(\theta_i - \varphi_i) - (E_i^2 + V_{i0}^2 - 2E_i V_{i0} \cos(\theta_{i0} - \varphi_{i0}))] \frac{1}{2x'_{di}} \quad (2.9)$$

$$W_{25} = - \frac{1}{2} \sum_{i=1}^n \sum_{j=1}^n B_{ij} (V_i V_j \cos \varphi_{ij} - V_{i0} V_{j0} \cos \varphi_{ij0}) \quad (2.10)$$

In the above expressions, the quantities with the subscript 'o' indicate their initial estimates.  $B_{ij}$  is the imaginary part

of  $Y_{ij}$ , the element of network admittance matrix  $[Y]$  (excluding machine reactances).  $\theta_i$  and  $\varphi_i$  are the COI referenced rotor angles of generator  $i$  and the voltage angles at bus  $i$  respectively. It has been shown in [54] that the time derivative of  $W$  on the post-fault trajectory is zero.

### Comments

1) It has been shown by Padiyar et al [70] that the last two components of the potential energy can be expressed as half the changes in the sum of reactive power losses in all elements of the network (including machine reactances). Thus,

$$W_{24} + W_{25} = \sum_{k=1}^L \frac{1}{2} Q_k = \frac{1}{2} \left[ \sum_{i=1}^m (Q_{Gi} - Q_{Gio}) - \sum_{j=1}^n (Q_{Lj} - Q_{Ljo}) \right] \quad (2.11)$$

where  $Q_{Gi}$  = reactive power generation (at the internal bus) of generator  $i$

$Q_{Lj}$  = reactive power load at bus  $j$  .

$L$  = total number of elements in the network including machine reactances

$Q_{Gi}$  in Eq. (2.11) can be calculated using the expression :

$$Q_{Gi} = -E_i^i d_i \quad (2.12)$$

2) The governor and prime mover system usually has little effect on stability. However, if the prime mover system is

included, mechanical power will not be constant. This can be included in the structure preserving energy function by modifying  $W_{21}$  to

$$- \sum_{i=1}^m \int_{t_0}^t P_{mi}(t) \frac{d\theta_i}{dt} dt \quad (2.13)$$

Just as with non-constant active power loads, the above term can be numerically integrated.

It is shown in APPENDIX C that the time derivative of the energy function  $W$  including the non-constant mechanical input term is zero.

3)  $W_{22}$ , the component of potential energy due to active power loads, is in general path dependent. Integrating, by parts,  $W_{22}$  can be resolved into two components, i) path independent and ii) path dependent, as follows :

$$\begin{aligned} W_{22} &= \sum_{i=1}^n [f_{pi}(V_i) \varphi_i]_{t_0}^t - \int_{t_0}^t \varphi_i f'_{pi}(V_i) dt \\ &= \sum_{i=1}^n [(f_{pi}(V_i) \varphi_i - f_{pi}(V_{i0}) \varphi_{i0}) - \int_{t_0}^t \varphi_i f'_{pi}(V_i) dt] \end{aligned} \quad (2.14)$$

It is observed that the path dependent term is zero for constant active power load characteristics. For simplicity, the path dependent term can be neglected even for the general case. With this approximation, the energy function is modified

and can be used for prediction of region of stability. It is shown in [71] that the approximation is acceptable and give accurate results.

### 2.3.3 Computation of SPEF

The total energy and its kinetic and potential energy components are calculated using a single subroutine TEF. The various input variables to the subroutine are indicated in Fig. 2.3.  $\omega^{\text{syn}}$  and  $\delta$ , obtained as output of the subroutine INT, are synchronous referenced variables. The corresponding COI referenced variables are obtained using the relations :

$$\theta_i = \delta_i - \delta_o, \quad \omega_i = \omega_i^{\text{syn}} - \omega_o, \quad i = 1, 2, \dots, m \quad (2.15)$$

Here  $\delta_o$  and  $\omega_o$  are respectively the position and the speed of COI defined as

$$\delta_o = \frac{1}{M_T} \sum_{i=1}^m M_i \delta_i, \quad \omega_o = \frac{1}{M_T} \sum_{i=1}^m M_i \omega_i^{\text{syn}} \quad (2.16)$$

$$M_T = \sum_{i=1}^m M_i$$

where  $m$  = no. of machines

$M_i$  = moment of inertia of the  $i$ th machine

The voltage  $E_i$  behind transient reactance  $x'_{di}$  is obtained as

$$E_i^2 = E_{di}'^2 + E_{qi}'^2 \quad (2.17)$$

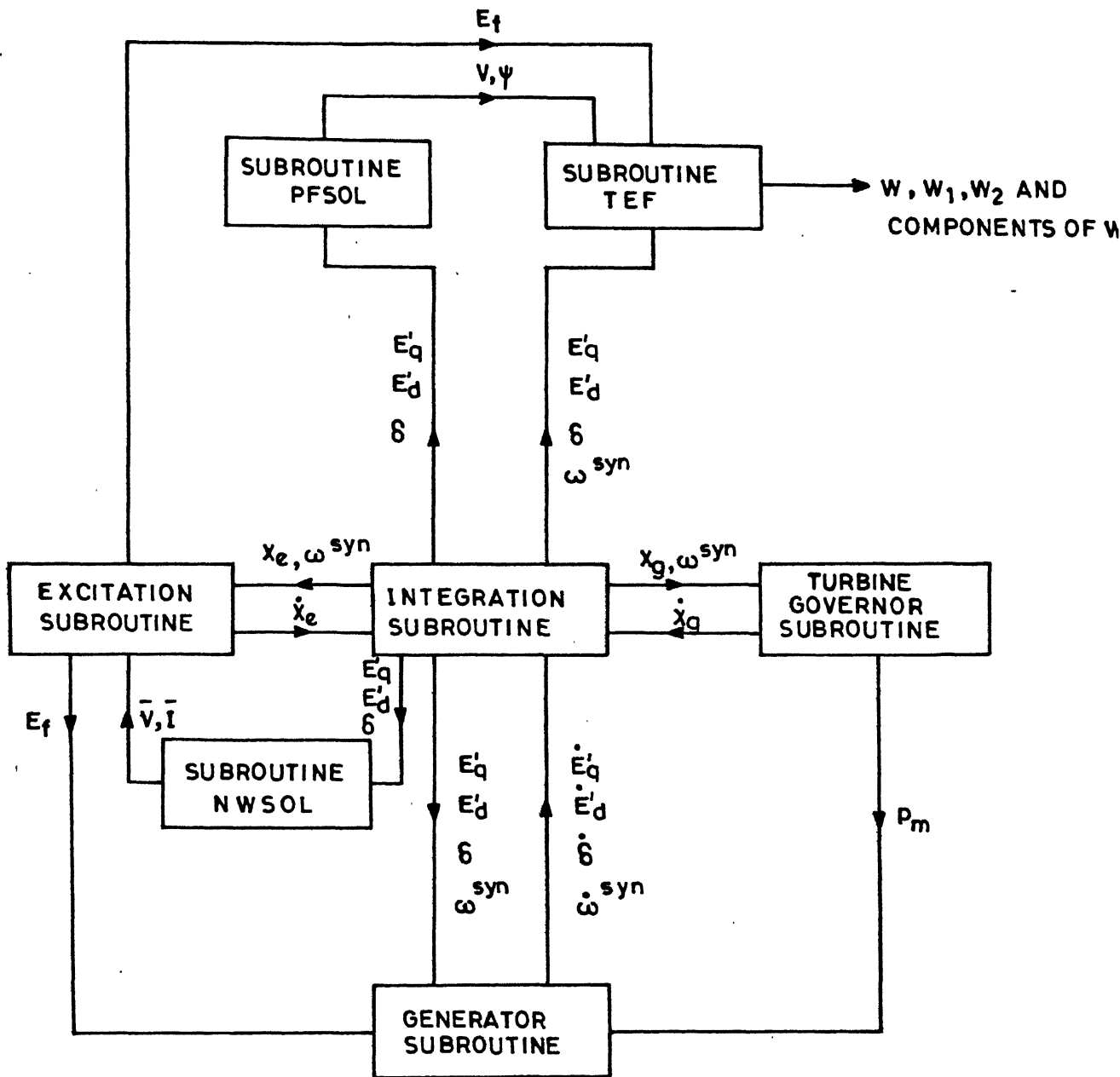


FIG.2.3 RELATIONSHIP OF SUBROUTINE VARIABLES FOR CALCULATING SPEF

It is to be noted that the classical model generator can be obtained by choosing large values of  $T'_{d0}$  and  $T'_{q0}$ . Also  $x_{qi}$  is made equal to  $x'_{di}$  to eliminate transient saliency.

The bus voltages and their angles to be used in the computation of SPEF are obtained as output of subroutine PFSOL which solves the algebraic equations of the network. COI referenced bus angles are calculated from the synchronous referenced output angles using the relation :

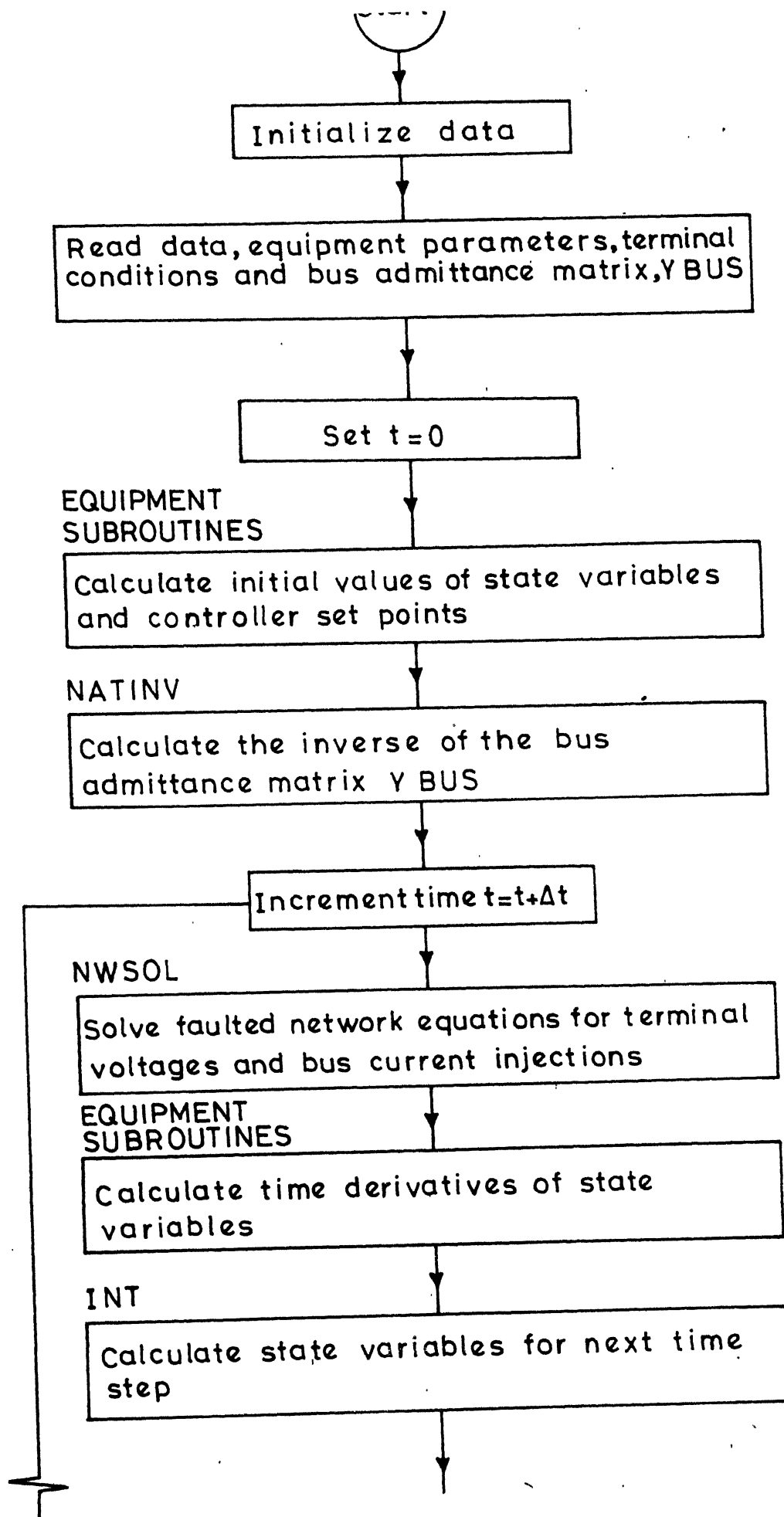
$$\varphi_i = \Psi_i - \delta_0 \quad ; \quad i = 1, 2, \dots, n \quad (2.18)$$

where  $\Psi_i$  is the bus angle with reference to a synchronous reference frame (calculated in PFSOL).

A flow-chart of the overall program for direct transient stability evaluation using SPEF is shown in Fig. 2.4.

## 2.4 DIRECT EVALUATION OF TRANSIENT STABILITY

Whenever a fault occurs in a power system, the total energy of the post-fault system, whose stability is being examined, increases with respect to its initial value (which is customarily made zero). If the fault is cleared after some time, the total energy is non-increasing. The key idea of the direct method is that the transient stability can, for a given contingency, be determined directly by comparing the total system energy which is gained during the fault-on period with a



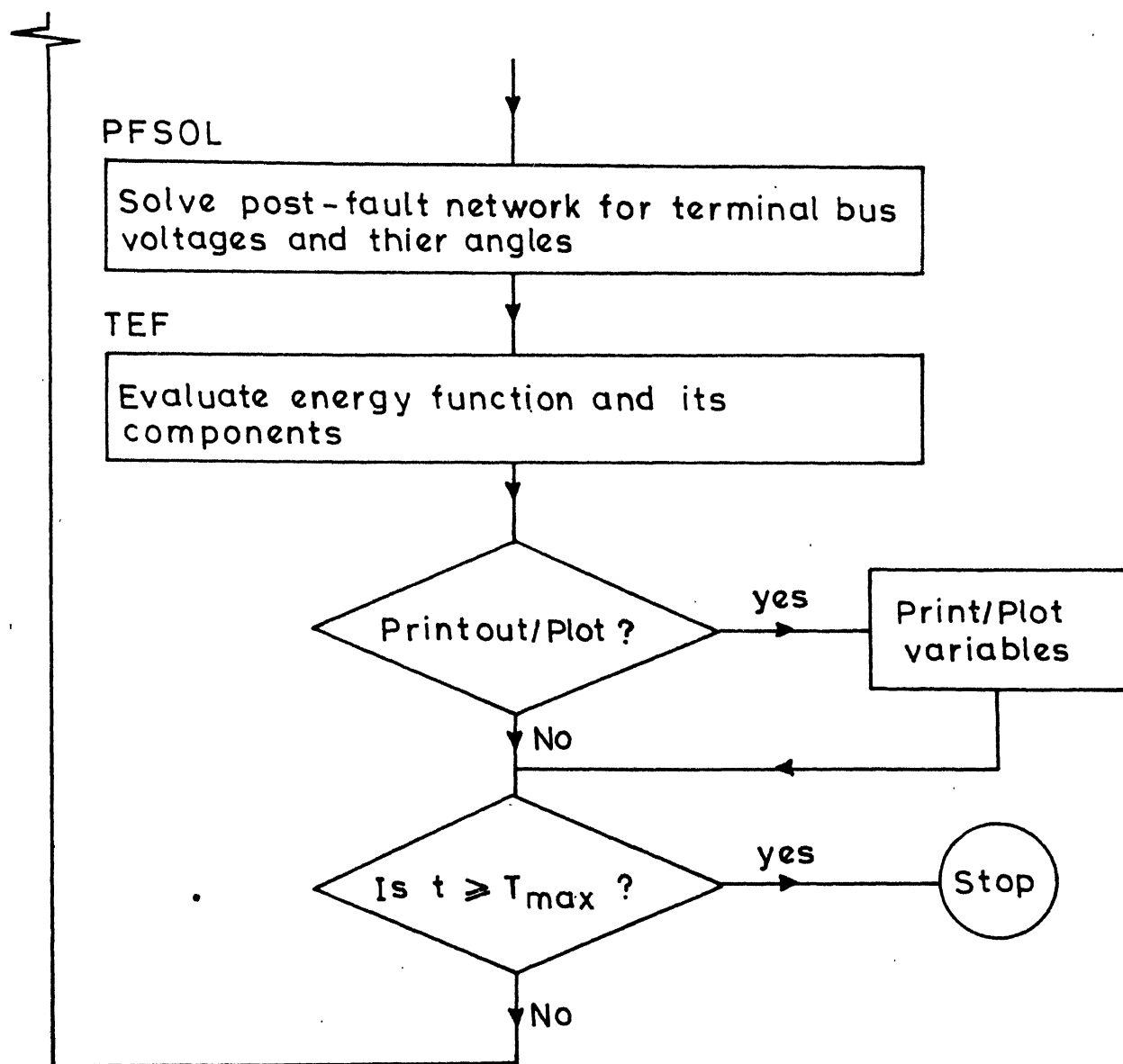


FIG.2.4 OVERALL PROGAM FLOW DIAGRAM

certain 'critical energy'. The potential energy evaluated at the unstable equilibrium point (uep) closest (in terms of energy) to the post-fault stable equilibrium point (sep) [21] gives conservative estimate of the critical energy and the region of stability. Recently, the concept of controlling uep in determining the critical energy has removed much of the conservativeness in the results [30]. Computational simplifications are possible with the use of PEBS method [29,30] in evaluating the critical energy (see APPENDIX D for a description of the PEBS method).

PEBS method is particularly attractive as it avoids the need to evaluate the uep's. In this method, it is assumed that the critically cleared trajectory goes near the uep corresponding to the fault location. PEBS is defined as the surface formed in the angle space by the points corresponding to the first maxima of the potential energy (with respect to sep) where its time derivative is zero. Inside this region, the potential energy increases and in the immediate vicinity outside this region, it decreases. Thus, the instant at which the time derivative of the potential energy function changes its sign from positive to negative, can be interpreted to be the instant when the trajectory crosses the PEBS [29,30]. The value of the potential energy at this time is the critical energy.

## 2.5 NUMERICAL EXAMPLES

### 2.5.1 Description

Three realistic power system examples have been considered for testing the transient stability program. The first system considered is a 7-machine (CIGRE) test system [72]. The second system is the 10-machine (NEW ENGLAND) test system [73]. The third system investigated is a 13-machine (UPSEB) system [74]. The single line diagram of the systems are given in Figs. E.1 , F.1 and G.1 alongwith system and operating data in APPENDICES E, F and G respectively.

It is assumed that a three phase fault occurs at the terminal of a generator, the fault is cleared and the line is instantaneously reclosed. Thus, the prefault and the post-fault system configurations are assumed to be the same. Two different load characteristics are considered. For simplicity, loads at all the buses are assumed to have identical characteristics. Critical energy is determined using PEBS technique. The following cases are considered :

Example 1 : 7-machine 10-bus (CIGRE) test system

- a) Fault at bus 1;      b) Fault at bus 2; c) Fault at bus 3;
- d) Fault at bus 5;      e) Fault at bus 6; f) Fault at bus 7.

Types of load characteristics :

$$(i) \quad k_1 V^2 + j k_2 V^2 \quad ; \quad (ii) \quad k_1 + j k_2 V^2$$

Example 2 : 10-machine 39-bus (NEW ENGLAND) test system

- a) Fault at bus 1 ; b) Fault at bus 3 ; c) Fault at bus 4 ;  
 d) Fault at bus 5 ; e) Fault at bus 6 ; f) Fault at bus 7 ;  
 g) Fault at bus 8 ; h) Fault at bus 9 ; i) Fault at bus 10 .

Types of load characteristics :

$$\text{i) } k_1 V^2 + jk_2 V^2 \quad ; \quad \text{ii) } k_1 + jk_2 V^2$$

Example 3 : 13-machine 71-bus (UPSEB) system

- a) Fault at bus 1 ; b) Fault at bus 3 ; c) Fault at bus 6 ;  
 d) Fault at bus 8 ; e) Fault at bus 15 ; f) Fault at bus 27 ;  
 g) Fault at bus 29 ; h) Fault at bus 39 ; i) Fault at bus 44 ;  
 j) Fault at bus 48 ; k) Fault at bus 64 ; l) Fault at bus 66 ;  
 m) Fault at bus 68 .

Types of load characteristics :

$$\text{(i) } k_1 V^2 + jk_2 V^2 \quad ; \quad \text{(ii) } k_1 + jk_2 V^2$$

## 2.5.2 Results

In all the cases, critical clearing time,  $t_{cr}$  is obtained both by prediction and digital simulation and the results are compared. This is shown in Tables 2.1 - 2.3 for 7-machine, 10-machine and 13-machine systems respectively for load types i) and ii) alongwith the corresponding value of the critical energy,  $W_{cr}$ .

Table 2.1 Critical Energy,  $W_{cr}$  and Critical Clearing Time,  $t_{cr}$  for 7-machine system

Fault Location	Gen. No. $k$	Load Model : $k_1 V^2 + jk_2 V^2$		Load Model : $k_1 + jk_2 V^2$	
		Critical Energy $W_{cr}$ (pu)	$t_{cr}$ (sec) obtained by Energy Function Method (proposed SPEF)	Critical Energy $W_{cr}$ (pu)	$t_{cr}$ (sec) obtained by Energy Function Method (proposed SPEF) Digital Simulation
Bus 1	1	15.8257	0.389	12.1921	0.409 0.415-0.420
Bus 2	2	15.3988	0.446	11.9425	0.394 0.400-0.405
Bus 3	3	18.4630	0.485	- *	- *
Bus 5	5	10.0852	0.437	- *	- *
Bus 6	6	14.9212	0.649	13.3835	0.593 0.595-0.600
Bus 7	7	5.8959	0.349	- *	- *

\* = Network solution does not converge

Table 2.2 Critical Energy,  $W_{cr}$  and Critical Clearing time,  $t_{cr}$  for 10-machine System

Fault Location	Gen. No. k	Load Model: $k_1 V^2 + jk_2 V^2$			Load Model: $k_1 + jk_2 V^2$		
		Critical $t_{cr}$ (sec) obtained by		Critical Energy $W_{cr}$ (pu)	$t_{cr}$ (sec) obtained by		
		Energy Function Method (Proposed SPEF)	Digital Simulation		Energy Function Method (Proposed SPEF)	Digital Simulation	
Bus 1	1	7.5771	0.248	0.260-0.265	6.4175	0.231	0.230-0.235
Bus 3	3	7.3153	0.218	0.230-0.235	6.0197*	0.200*	0.200-0.205*
Bus 4	4	9.8640	0.215	0.210-0.215	-	-	-
Bus 5	5	2.8465	0.161	0.175-0.180	2.4043*	0.149*	0.160-0.165*
Bus 6	6	9.9969	0.236	0.240-0.245	-	-	-
Bus 7	7	8.8263	0.222	0.235-0.240	7.5624	0.207	0.210-0.215
Bus 8	8	8.9164	0.220	0.230-0.235	8.0419*	0.214*	0.215-0.220*
Bus 9	9	2.3473	0.109	0.120-0.125	-	-	-
Bus 10	10	24.7726	0.647	0.570-0.575	-	-	-

\* = Network solution does not converge

Table 2.3 Critical Energy,  $W_{cr}$  and Critical Clearing Time,  $t_{cr}$  for 13-machine System

Fault Location	Gen. No. k	Load Model: $k_1 V^2 + jk_2 V^2$		Load Model: $k_1 + jk_2 V^2$	
		Critical Energy, $W_{cr}$ (pu)	$t_{cr}$ (sec) obtained by Energy Function Method (Modified SPEF)	Critical Energy, $W_{cr}$ (pu)	$t_{cr}$ (sec) obtained by Energy Function Method (Modified SPEF)
			Digital Simulation		Digital Simulation
Bus 1	1	10.7046	0.454	9.3842	0.420
Bus 3	2	8.2446	0.298	7.1736	0.264
Bus 6	3	1.8425	0.277	1.5588	0.241
Bus 8	4	2.9905	0.275	2.5816	0.242
Bus 15	5	1.9470	0.207	1.6458	0.182
Bus 27	6	2.5799	0.150	*	*
Bus 29	7	3.6178	0.192	3.0493	0.176
Bus 39	8	0.8694	0.449	0.7374	0.413
Bus 44	9	2.2569	0.331	*	*
Bus 48	10	9.0933	0.382	7.8972	0.306
Bus 64	11	3.5106	0.304	2.9683	0.268
Bus 66	12	1.5585	0.291	1.2836	0.265
Bus 68	13	1.0263	0.226	0.8825	0.201

\* = Network solution does not converge

The swing curves, the variation of the total energy and its components and that of the components of the potential energy function for the stable and unstable conditions are presented as follows :

Figs. 2.5 to 2.10	For example 1-d) (i)
Figs. 2.11 to 2.28	For examples 2-c) (i), 2-g) (i) and 2-h) (i)

### 2.5.3 Discussion

It is observed that the predicted critical clearing time from structure preserving energy function is in good agreement with that obtained from digital simulation. It is further observed from Table 2.3 that using the modified energy function where the path dependent terms are neglected, gives more accurate prediction of critical clearing time. It is to be noted that the path dependent terms are identically equal to zero for constant active power loads. The results given in Table 2.3 are based only on the modified energy function.

It is observed from the Tables that in all the cases considered for the three systems, the critical clearing time (both by prediction and digital simulation) is less for the constant active power loads compared to constant impedance type loads. This observation tallies with that made in [71] and indicates the importance of considering the voltage

dependent loads. In the case of nonlinear loads, there could be problems of convergence in network solution for some cases, indicating that the solution may not exist. These cases are indicated in the Tables. The problems of convergence with nonlinear loads can be avoided by dynamic representation of loads which is more close to the reality. However, this aspect is not investigated in this thesis.

From the swing curves it is possible to predict the mode of instability. Invariably, the generator at the terminals of which the fault occurs, accelerates and goes out-of-step. In addition, there are other generators which may also accelerate and some generators which decelerate. In general, it is not possible to predict, in advance, which of the remaining generators (excluding the faulted one) accelerate or decelerate.

In all the cases considered, the total energy increases during the fault-on period and remains constant after the fault is cleared. This is as expected and confirms the validity of the results. It is interesting to observe that the system stability can be predicted from the variation of potential and kinetic energy components. After the clearing of the fault, the kinetic energy and the potential energy oscillate and the magnitude of these oscillations are limited when the system is stable. When the system is unstable, the kinetic

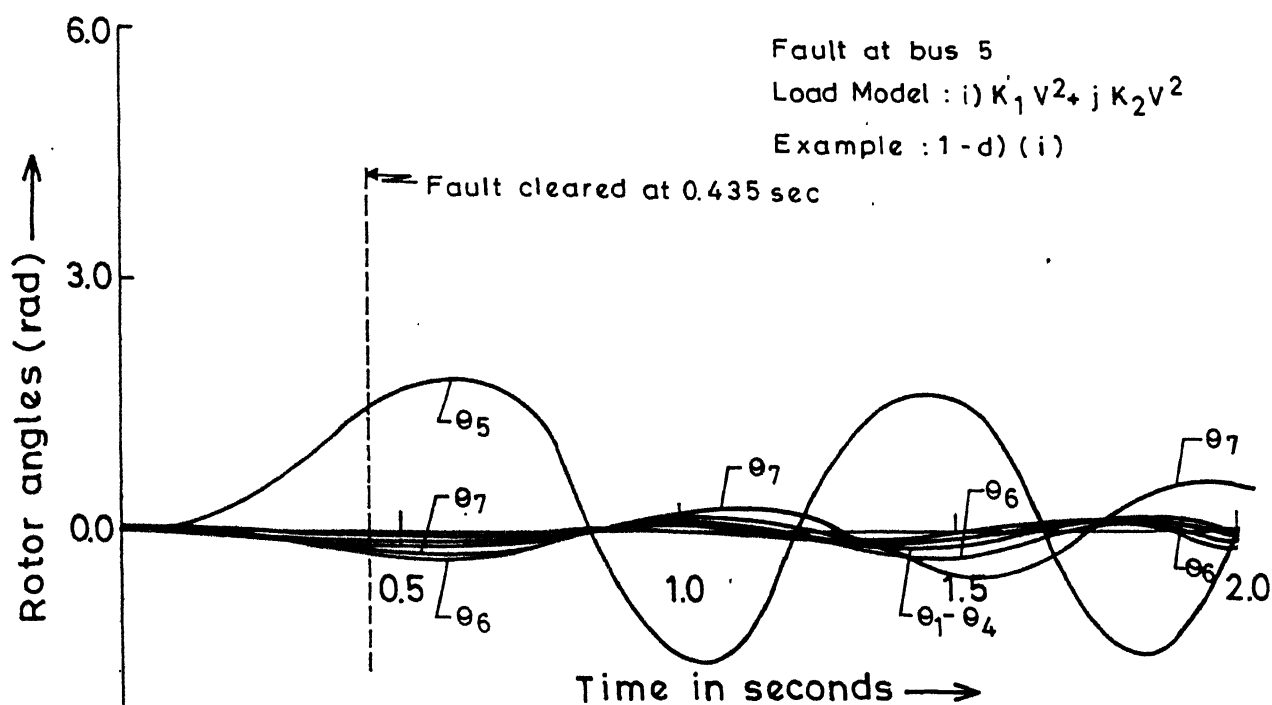


FIG.2.5 SWING CURVES FOR 7-MACHINE SYSTEM, STABLE CASE

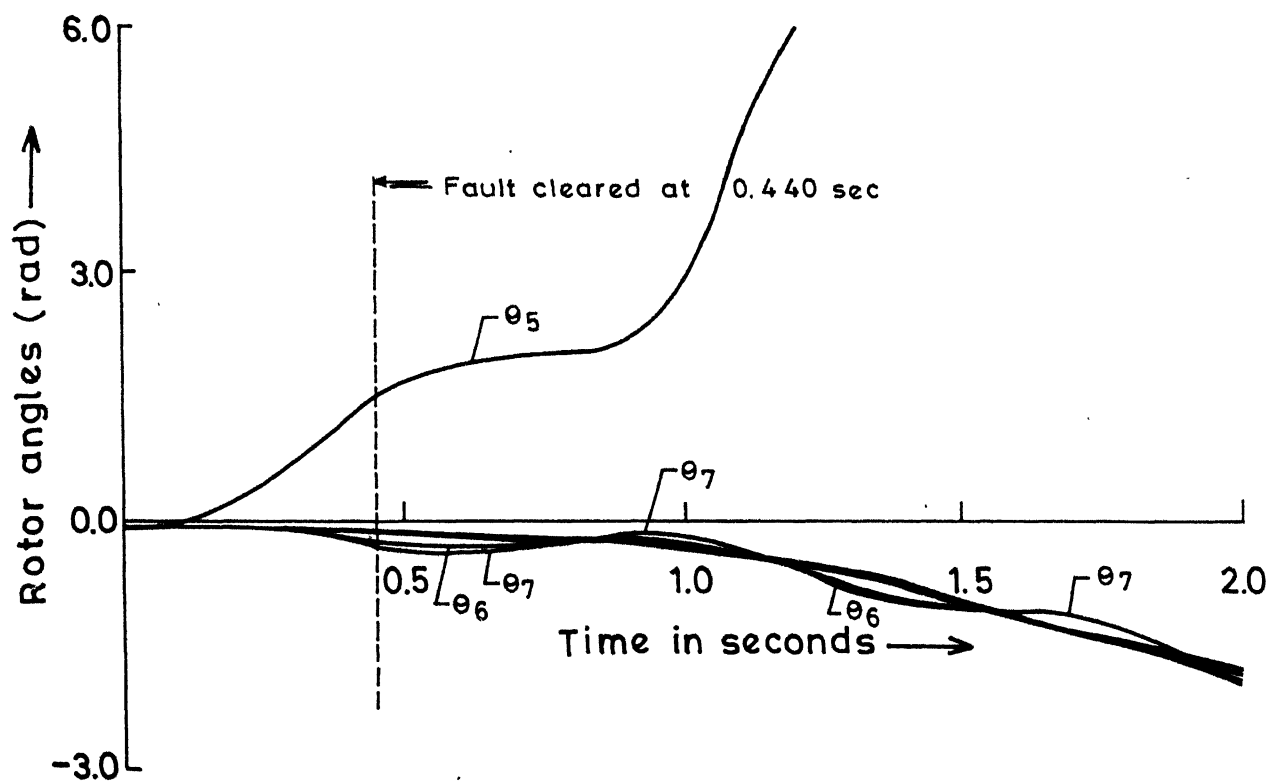


FIG.2.6 SWING CURVES FOR 7-MACHINE SYSTEM, UNSTABLE CASE

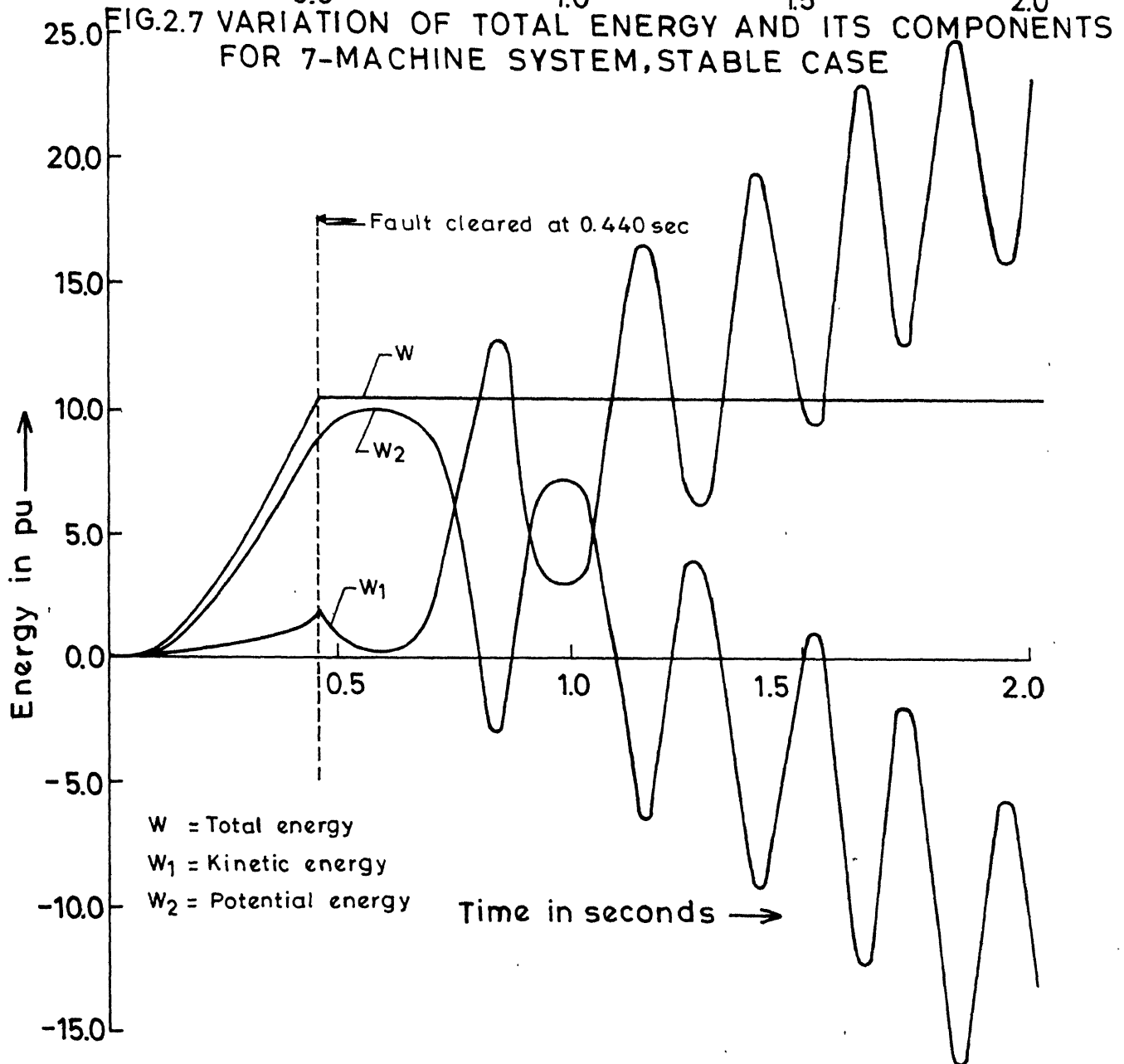
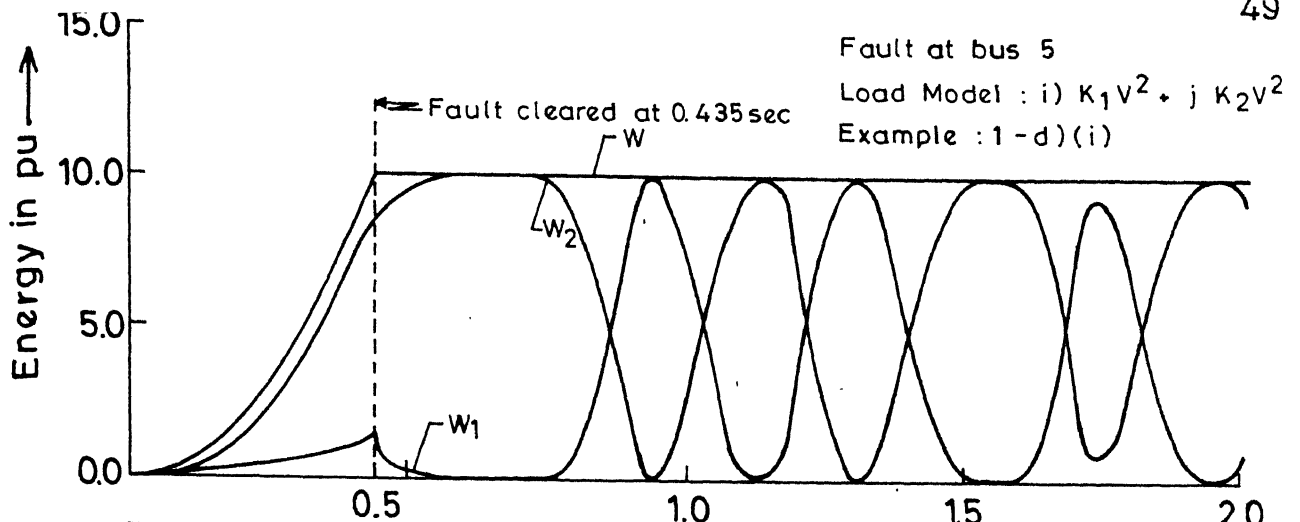


FIG.2.8 VARIATION OF TOTAL ENERGY AND ITS COMPONENT FOR 7-MACHINE SYSTEM, UNSTABLE CASE

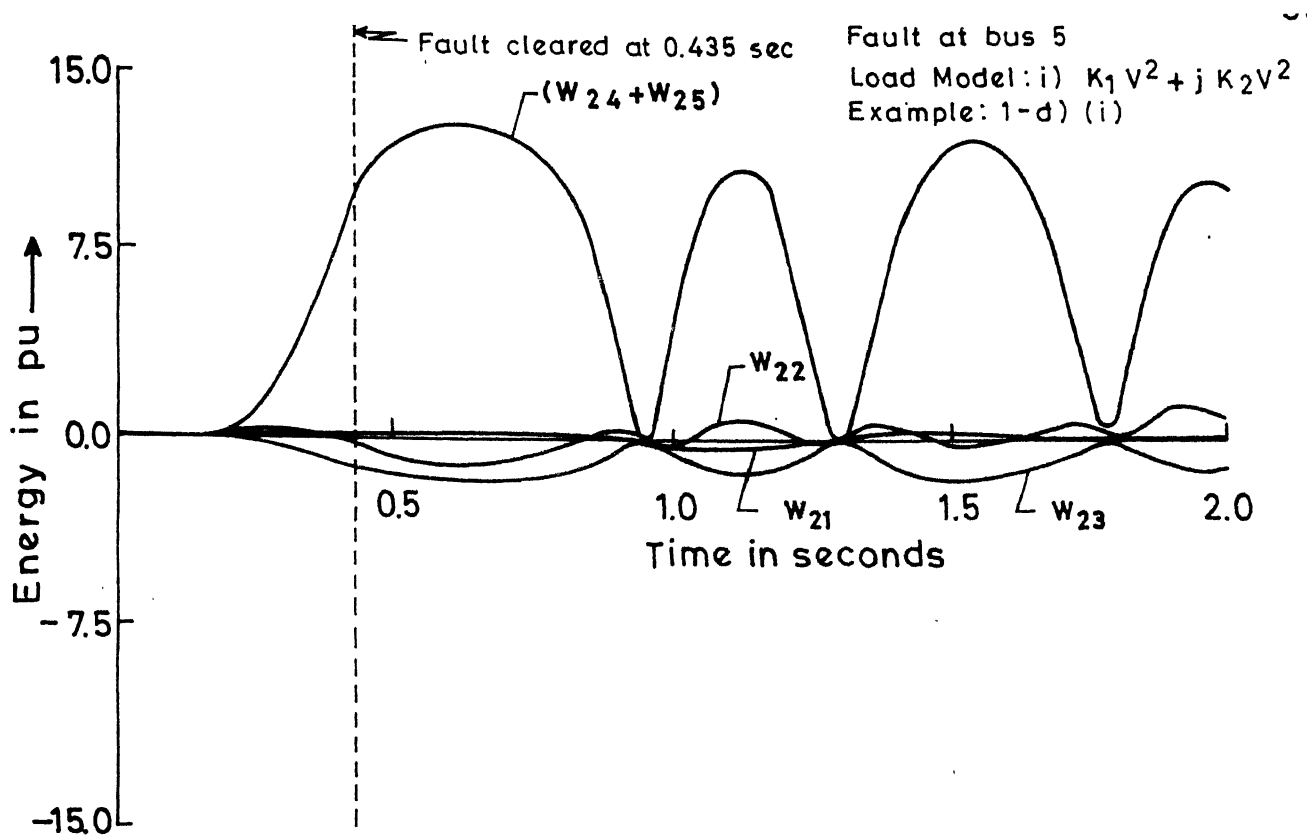


FIG. 2.9 VARIATION OF THE COMPONENTS OF POTENTIAL ENERGY FOR 7-MACHINE SYSTEM, STABLE CASE.

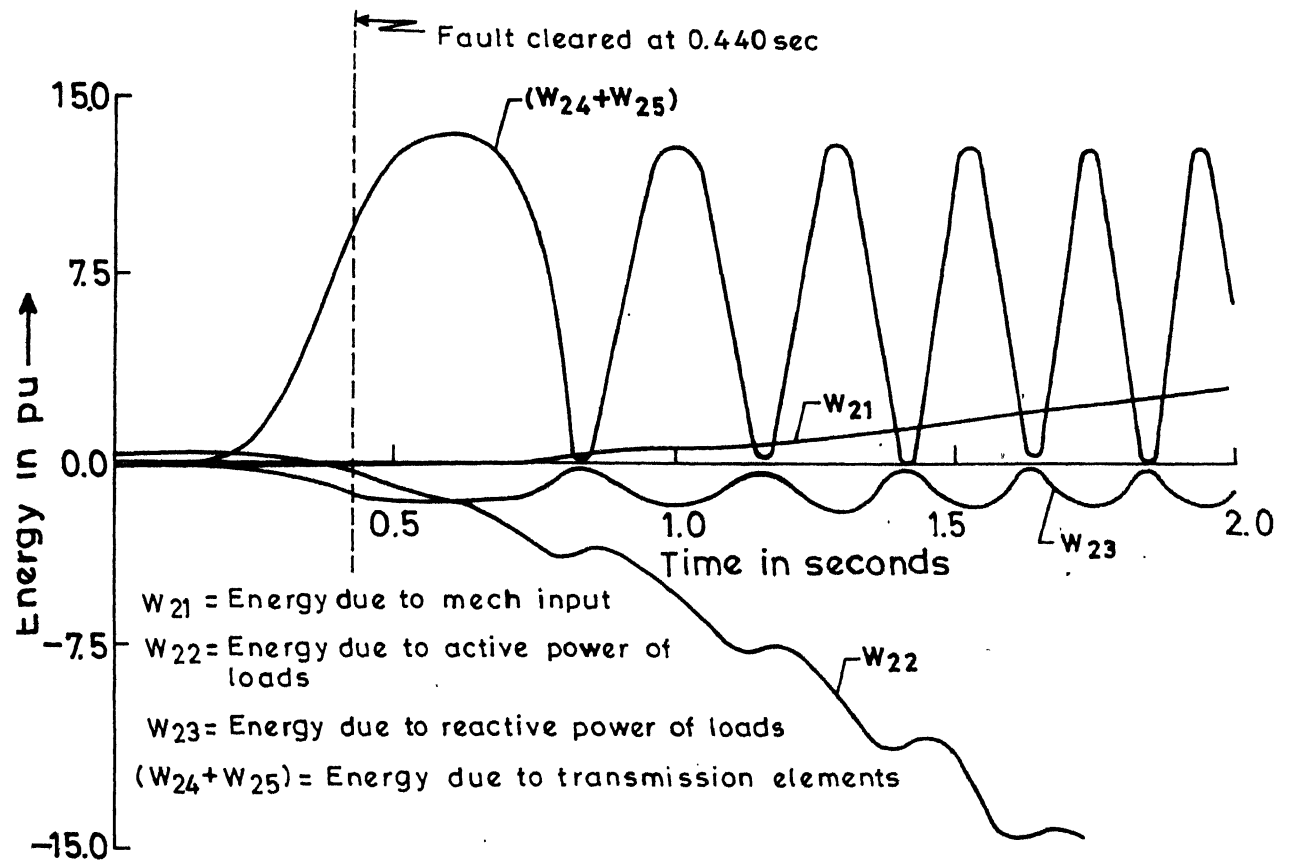


FIG. 2.10 VARIATION OF THE COMPONENTS OF POTENTIAL ENERGY FOR 7-MACHINE SYSTEM, UNSTABLE CASE.

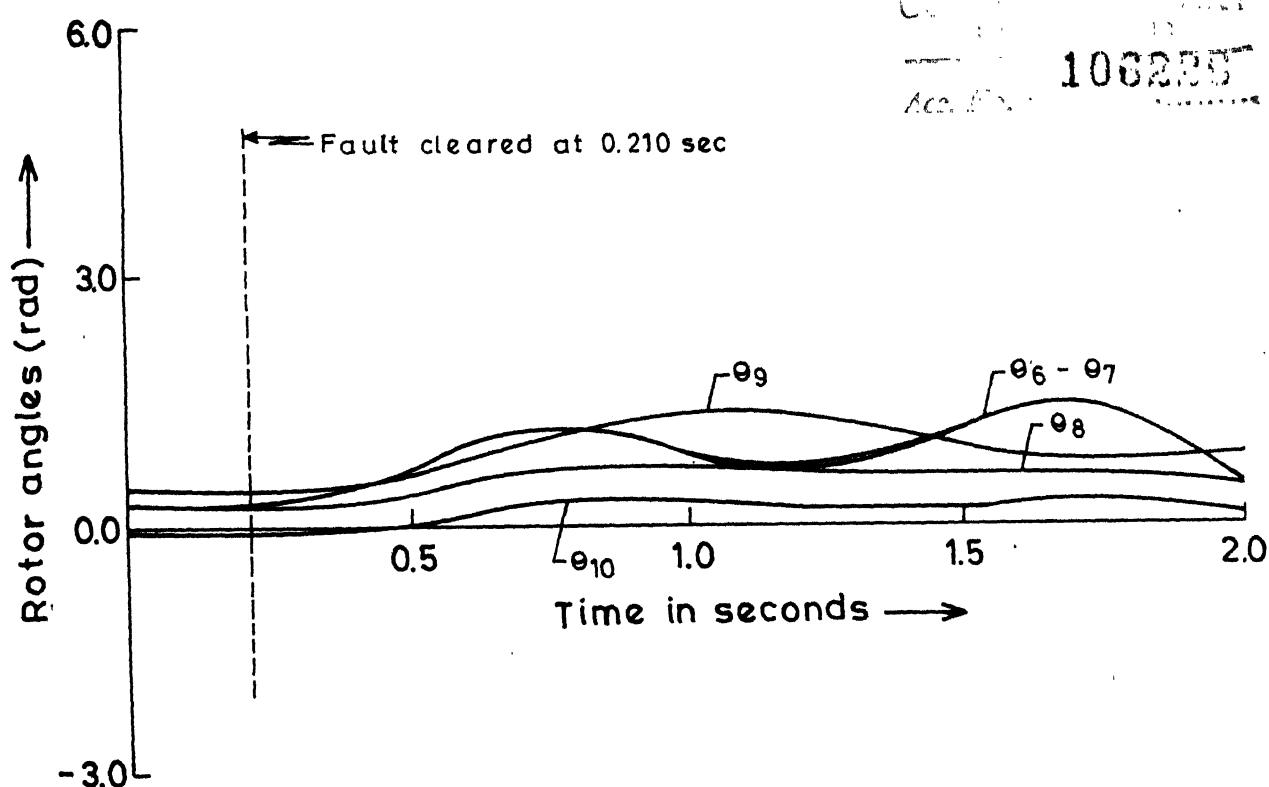
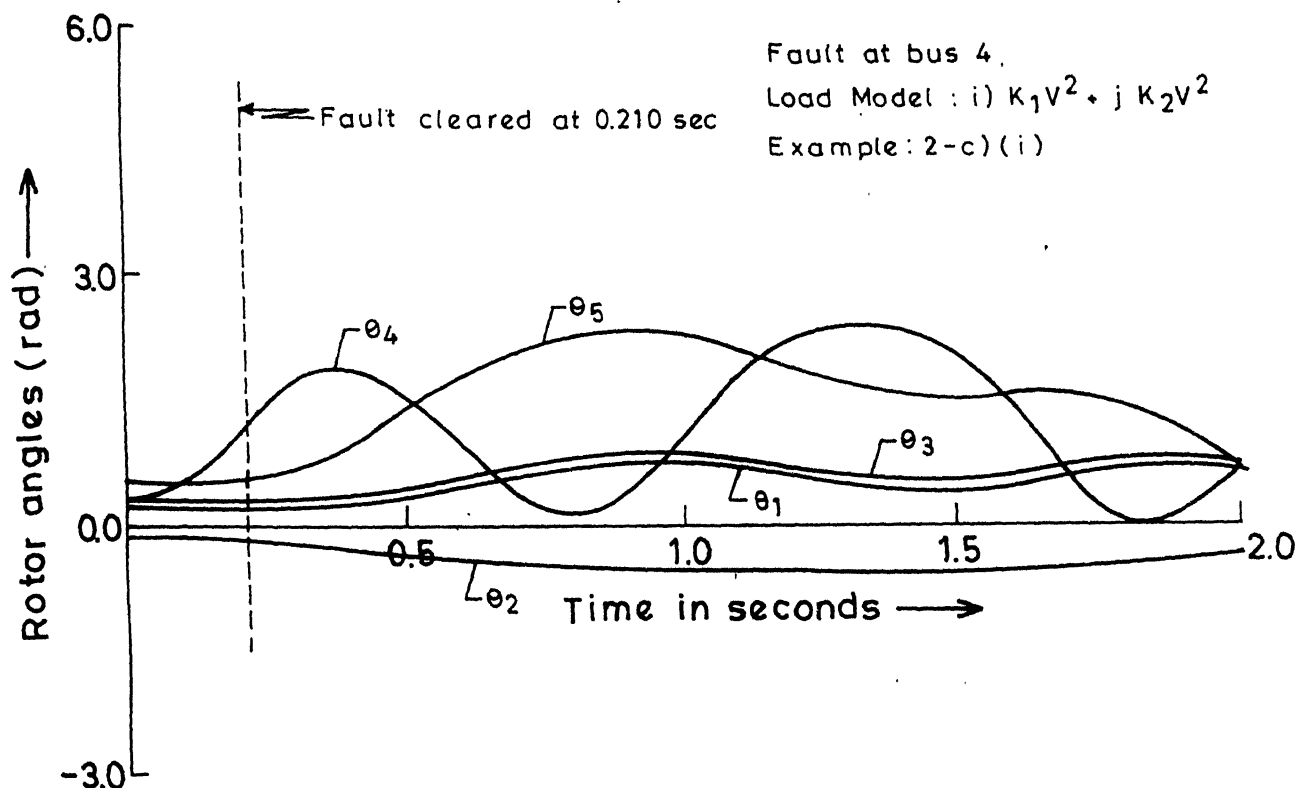


FIG.2.11 SWING CURVES FOR 10-MACHINE SYSTEM, STABLE CASE

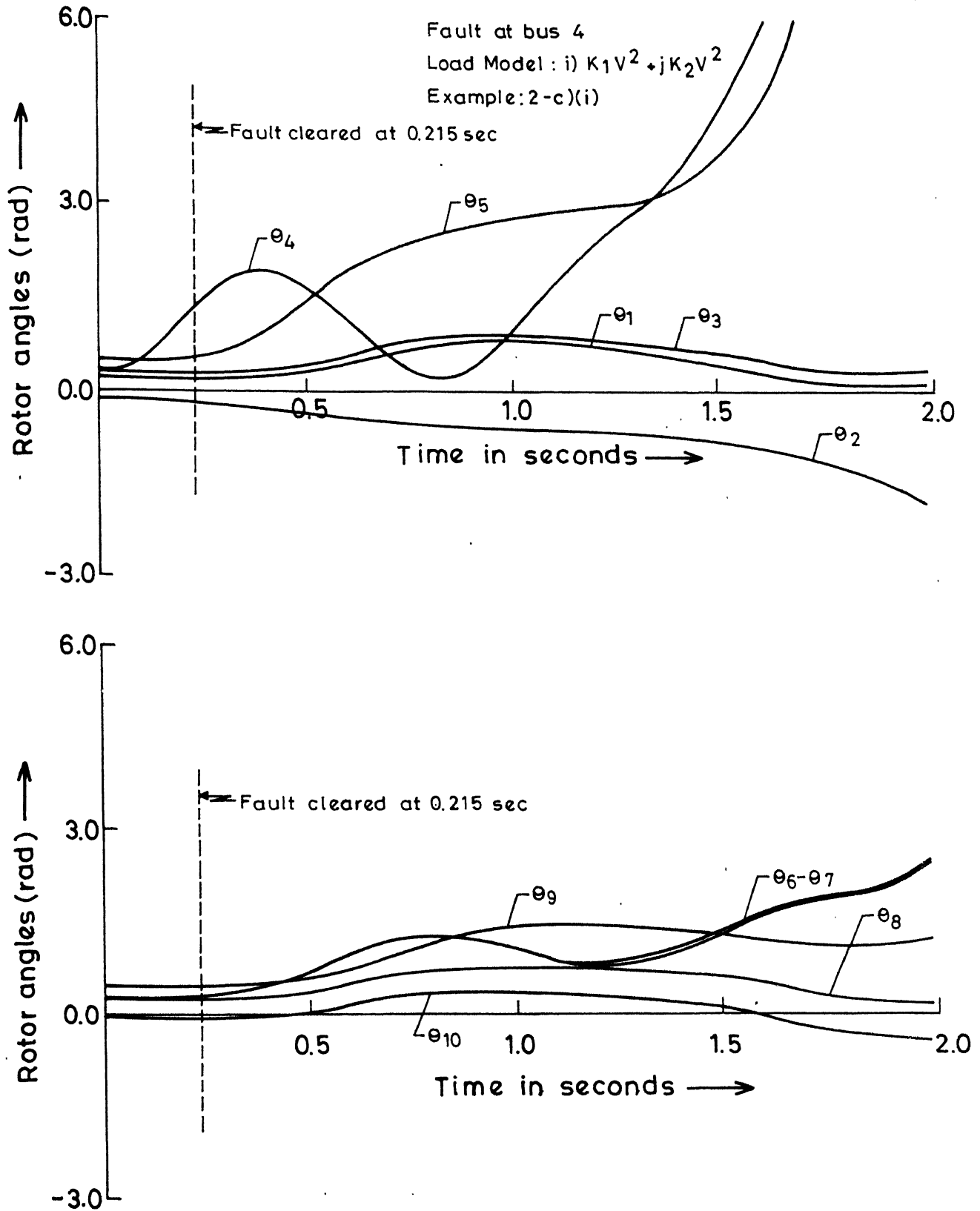


FIG.2.12 SWING CURVES FOR 10-MACHINE SYSTEM, UNSTABLE CASE

Fault at bus 8

Load Model : i)  $K_1 V^2 + j K_2 V^2$

Example : 2-g)(i)

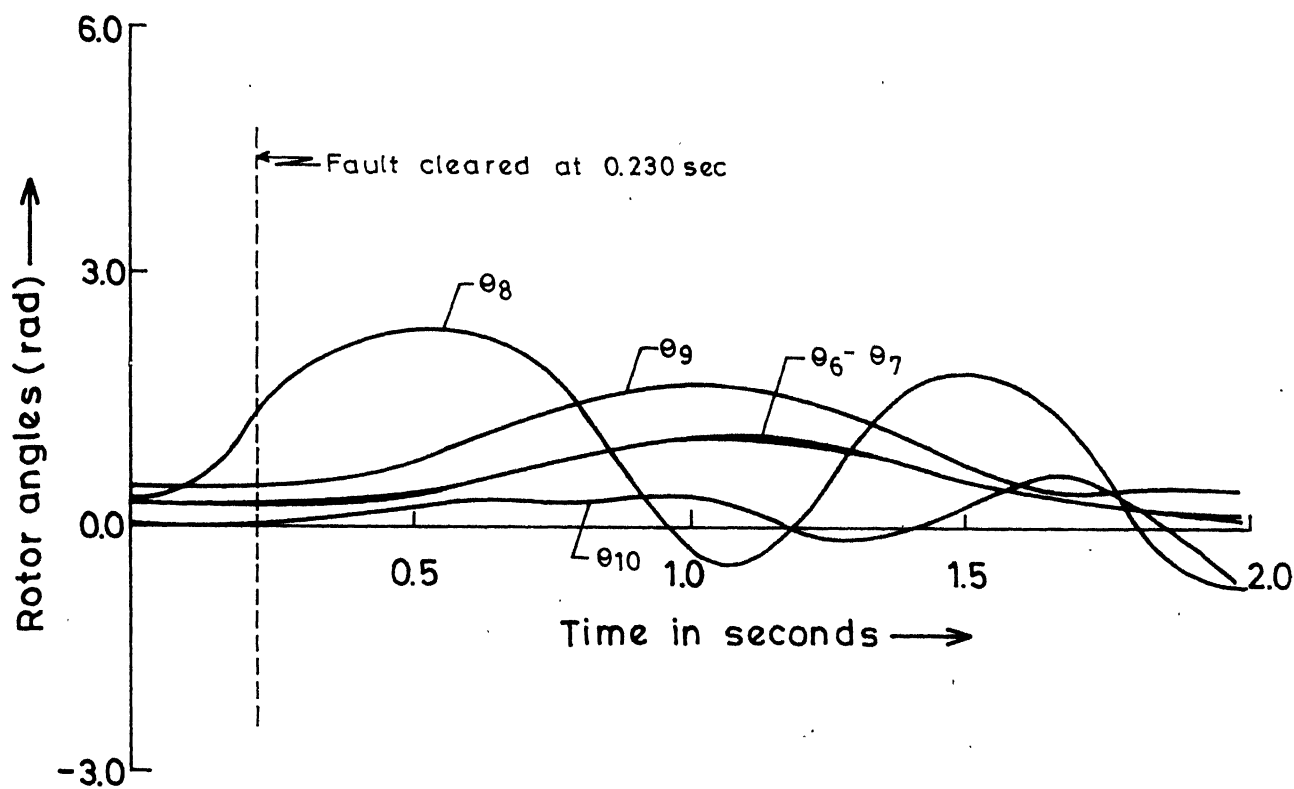
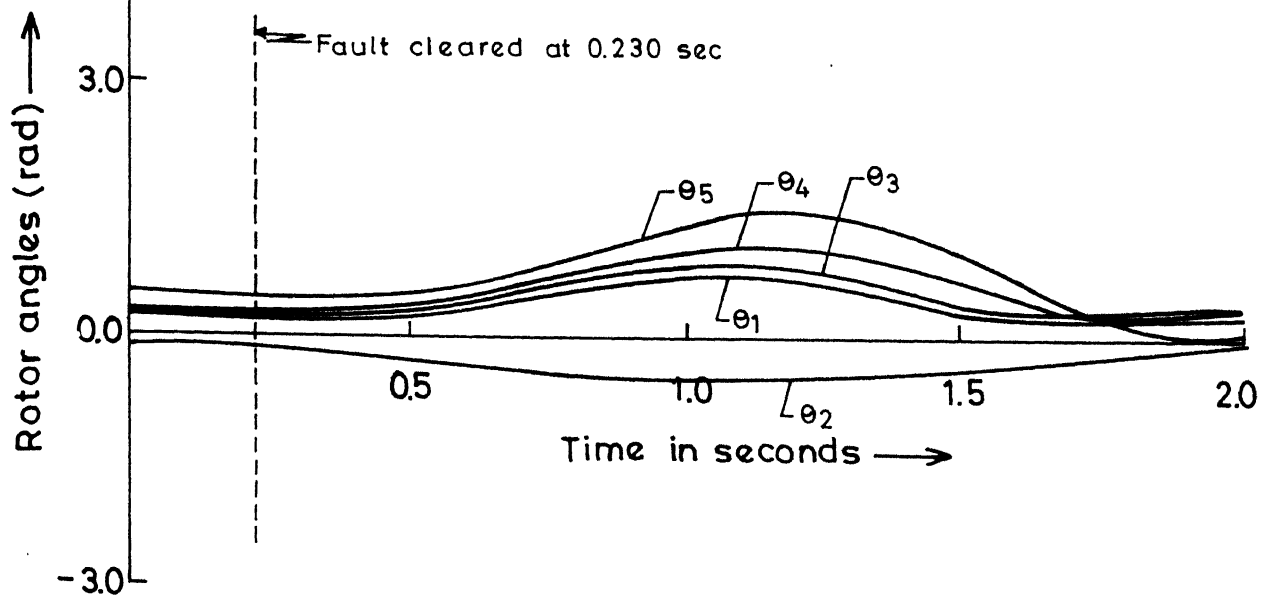


FIG.2.13 SWING CURVES FOR 10- MACHINE SYSTEM, STABLE CASE

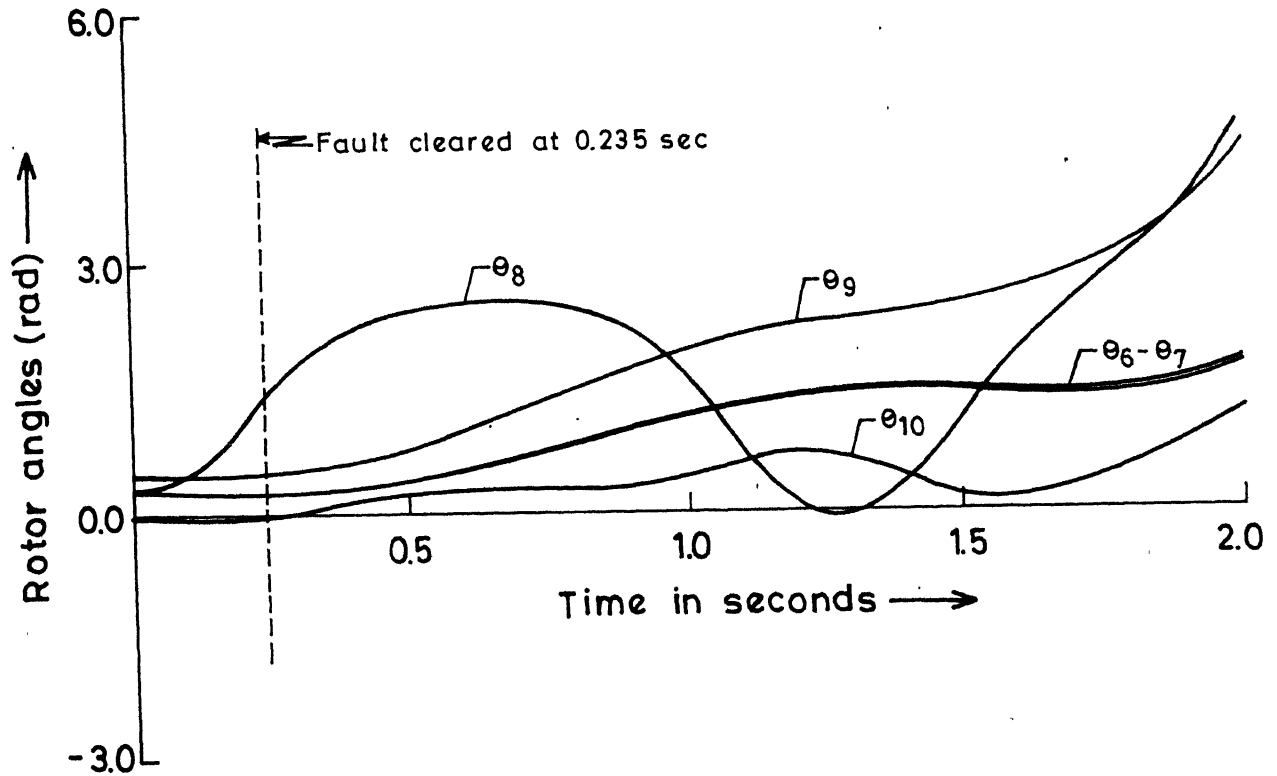
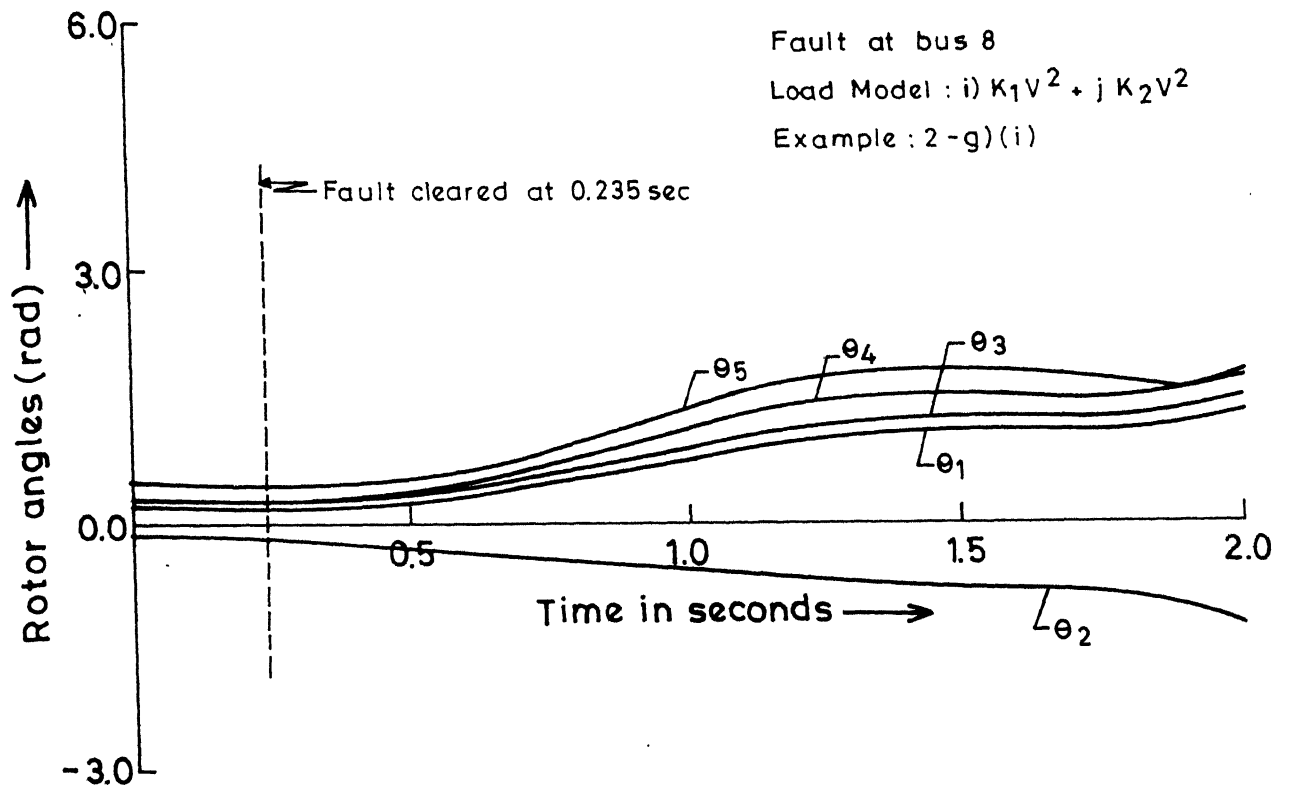


FIG.2.14 SWING CURVES FOR 10-MACHINE SYSTEM, UNSTABLE CASE

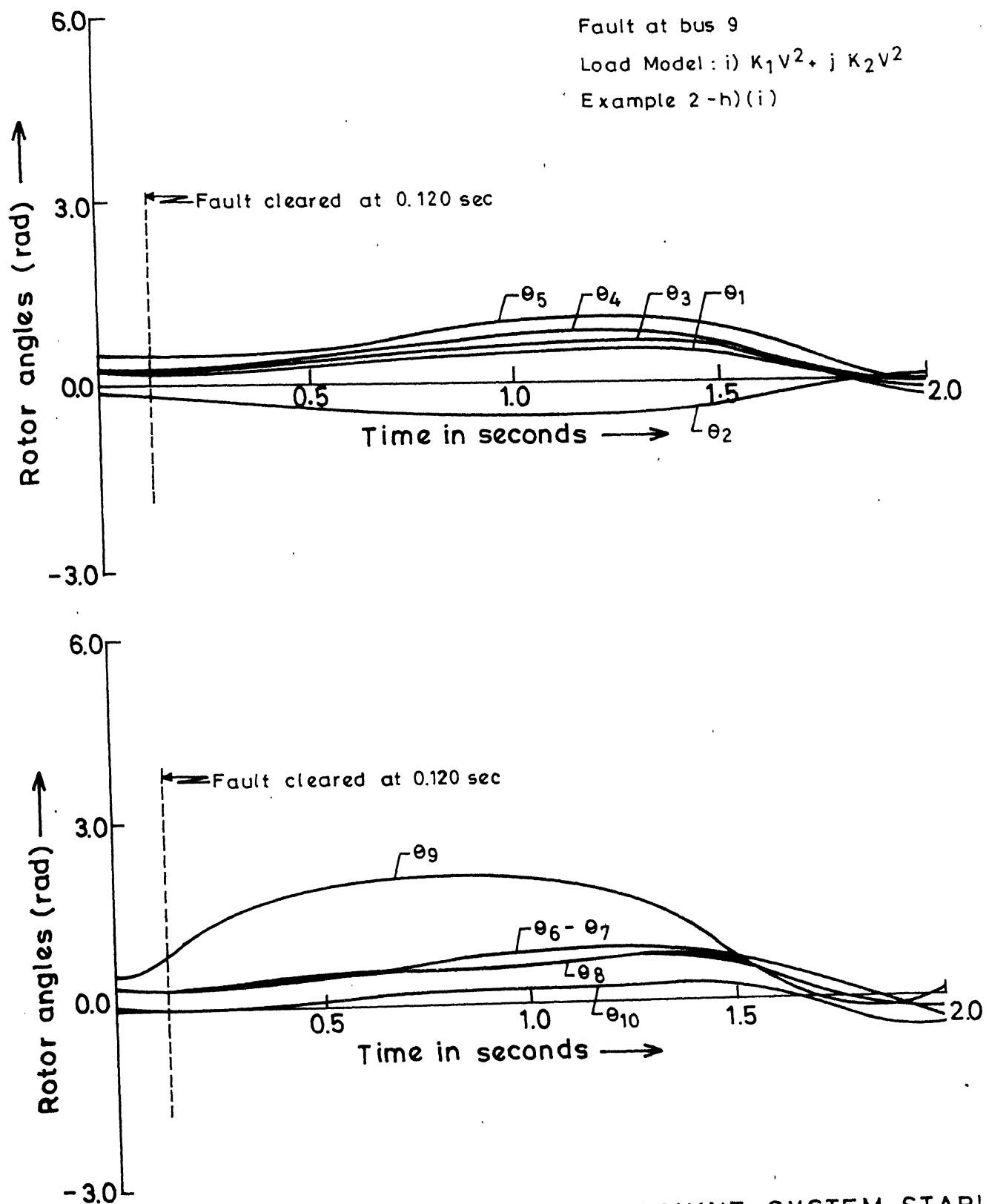


FIG.2.15 SWING CURVES FOR 10-MACHINE SYSTEM, STABLE CASE

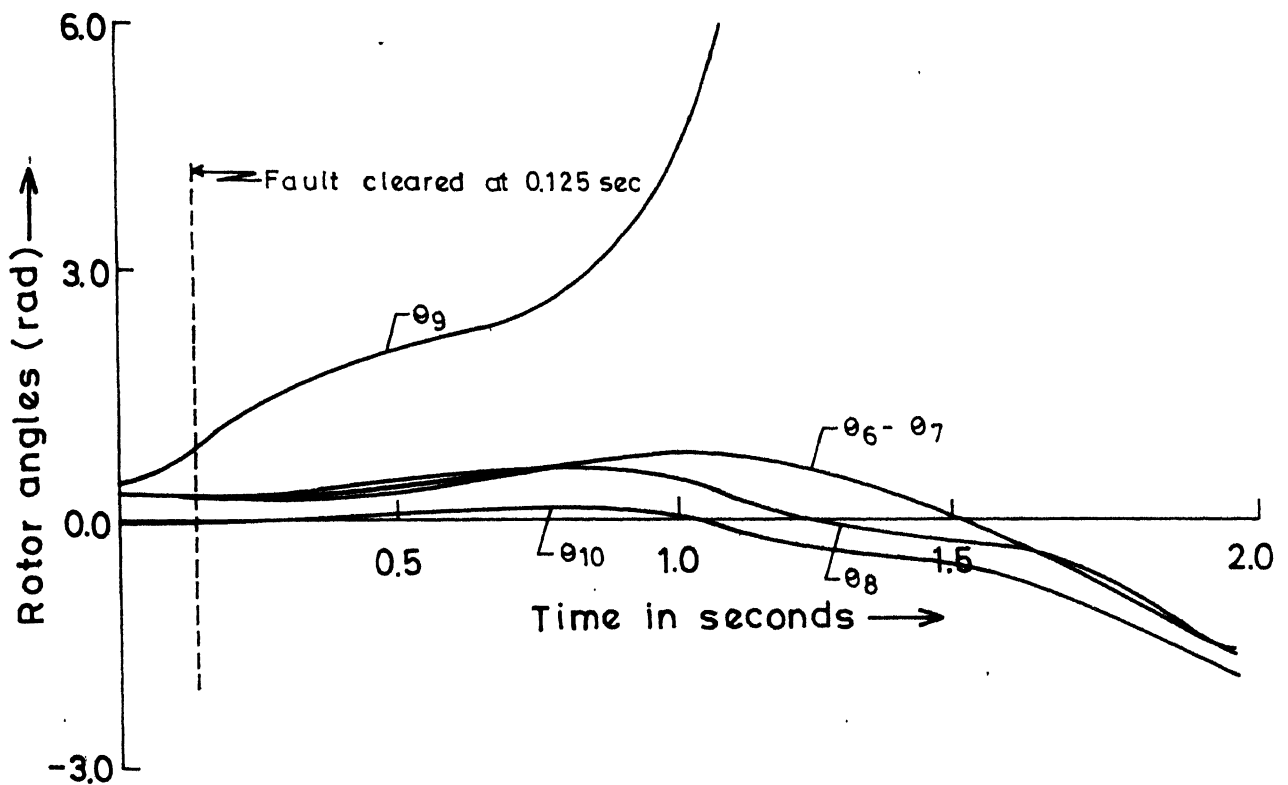
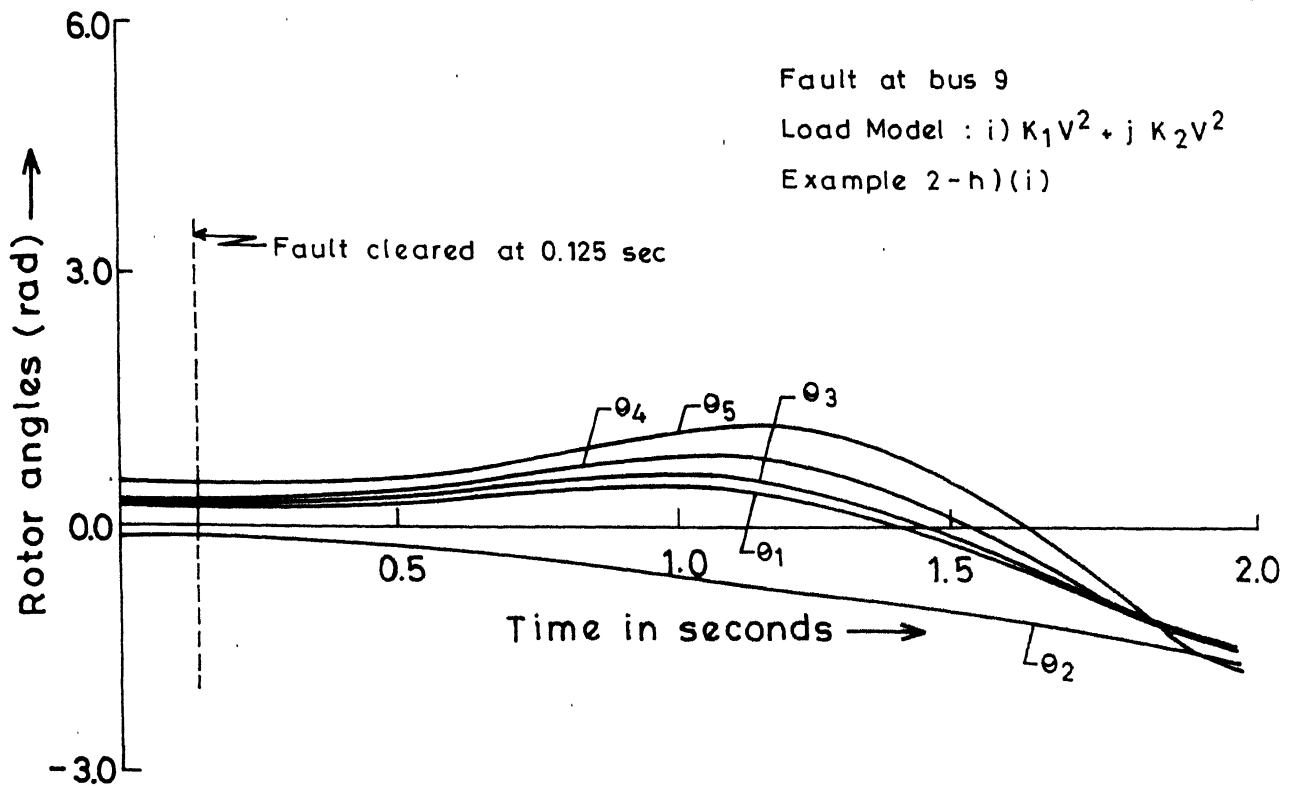


FIG. 2.16 SWING CURVES FOR 10-MACHINE SYSTEM, UNSTABLE CASE

Fault at bus 4

Load Model : i)  $K_1 V^2 + j K_2 V^2$

Example : 2c)(i)

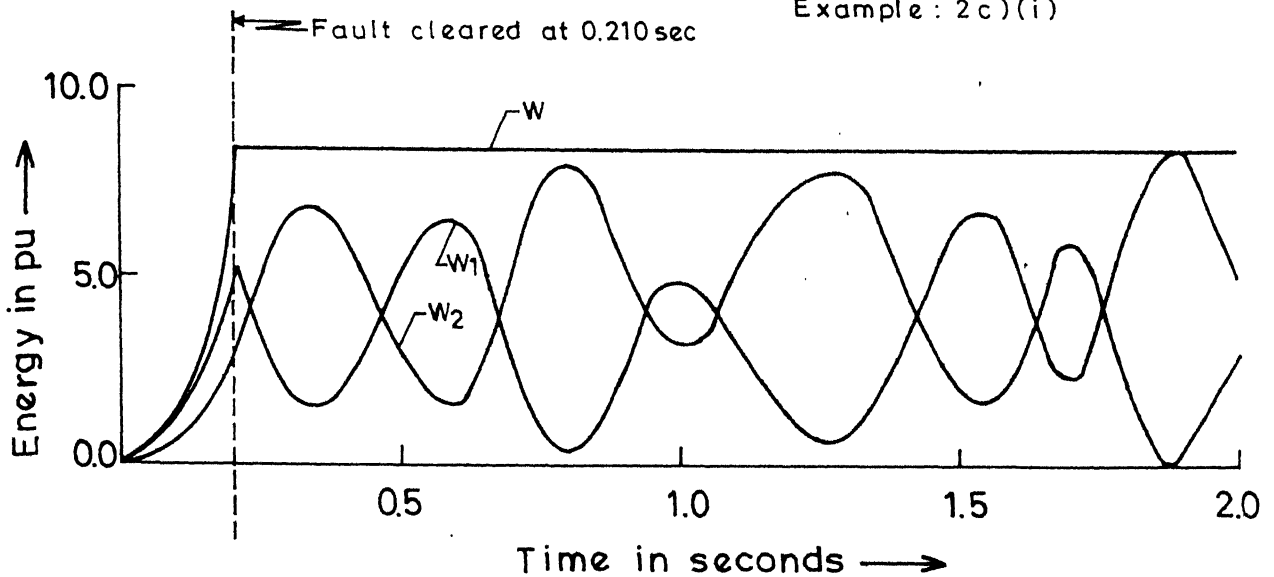


FIG. 2.17 VARIATION OF TOTAL ENERGY AND ITS COMPONENTS FOR 10-MACHINE SYSTEM, STABLE CASE

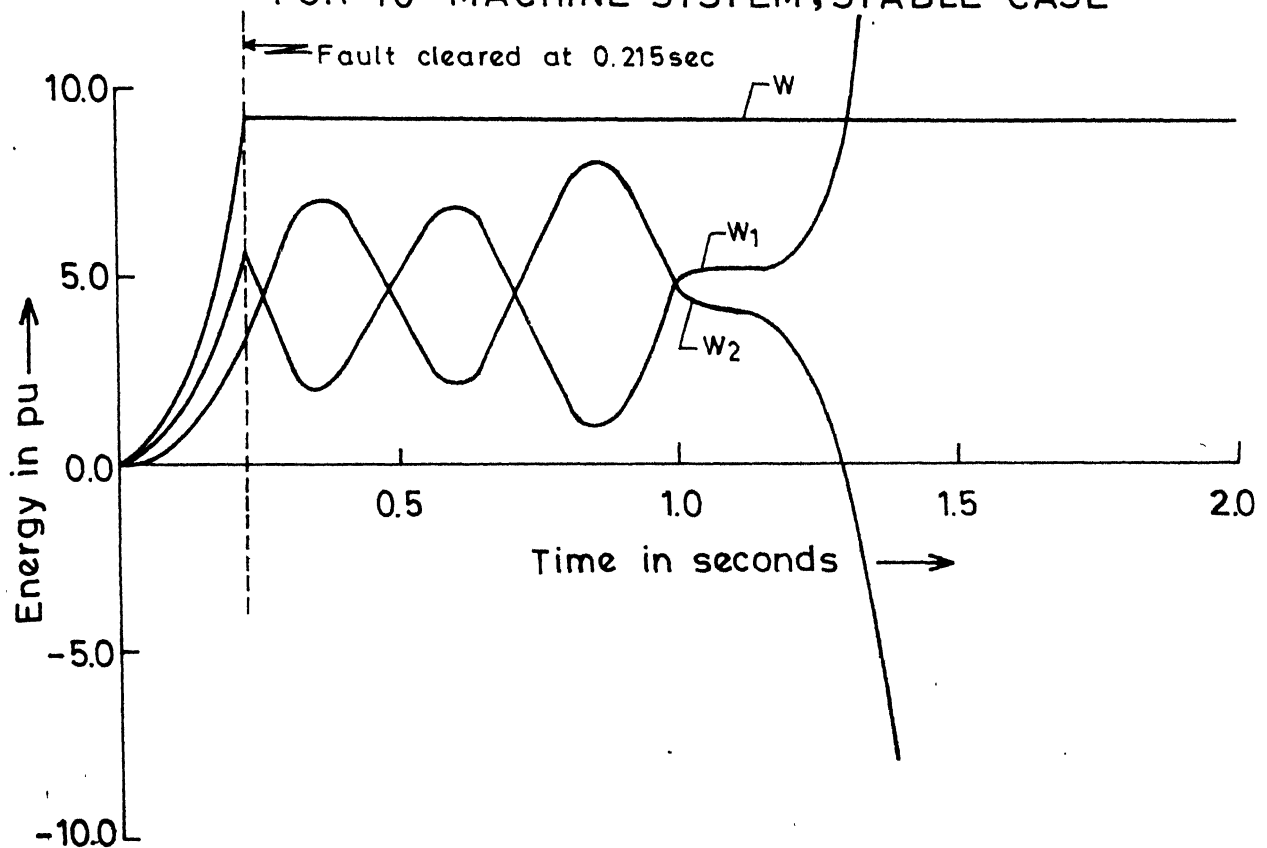


FIG. 2.18 VARIATION OF TOTAL ENERGY AND ITS COMPONENTS FOR 10-MACHINE SYSTEM, UNSTABLE CASE

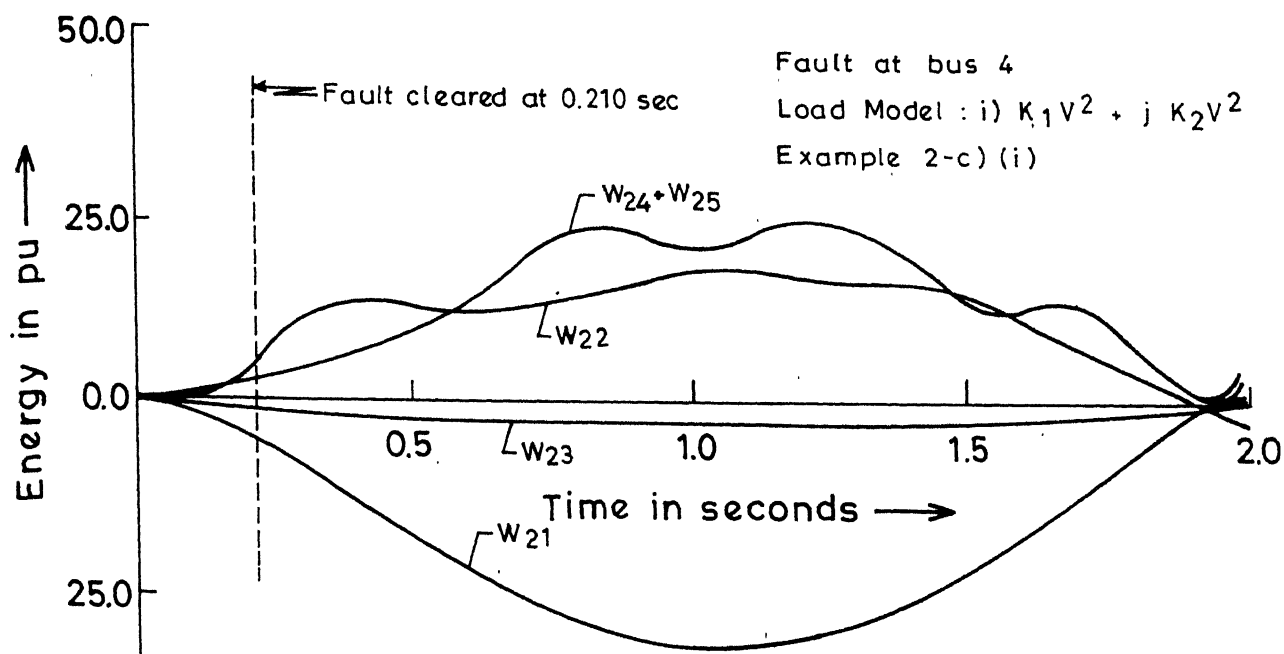


FIG.2.19 VARIATION OF THE COMPONENTS OF POTENTIAL ENERGY FOR 10-MACHINE SYSTEM, STABLE CASE

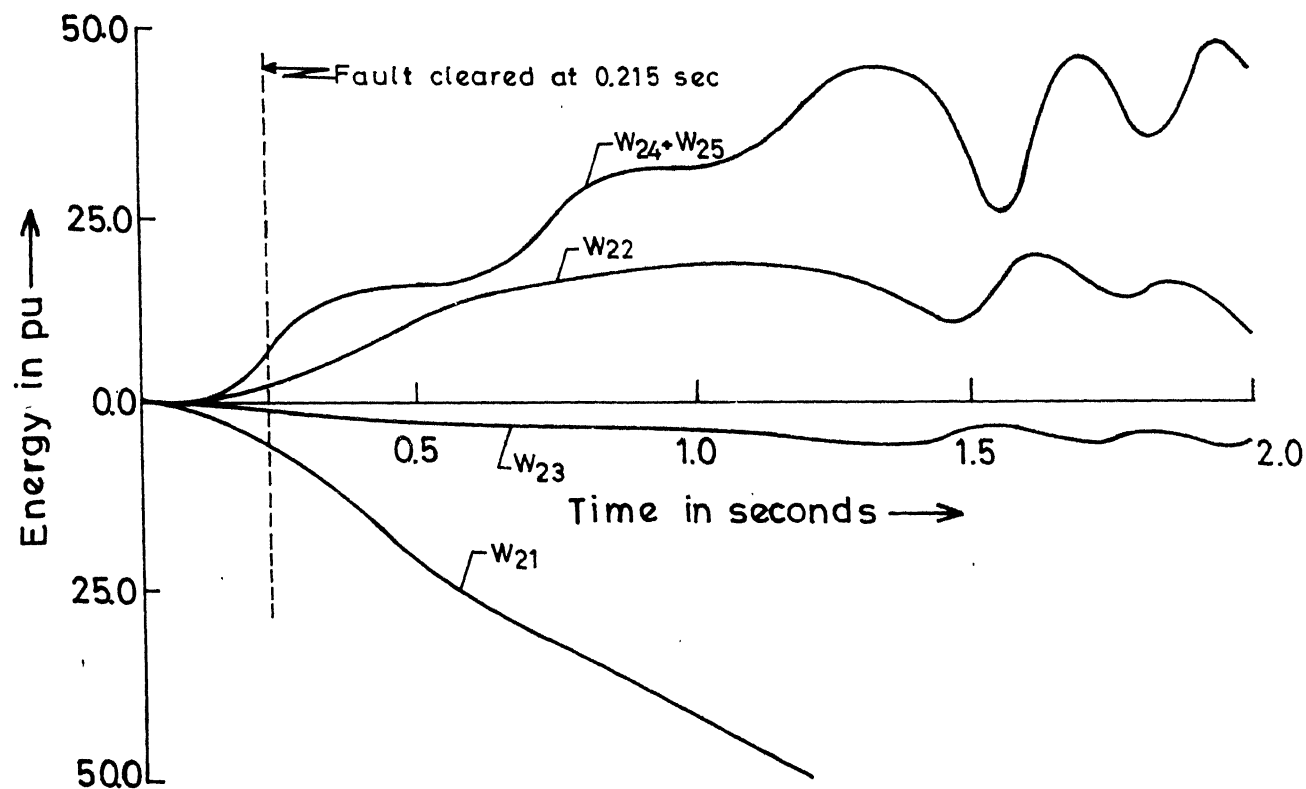


FIG.2.20 VARIATION OF THE COMPONENTS OF POTENTIAL ENERGY FOR 10-MACHINE SYSTEM, UNSTABLE CASE

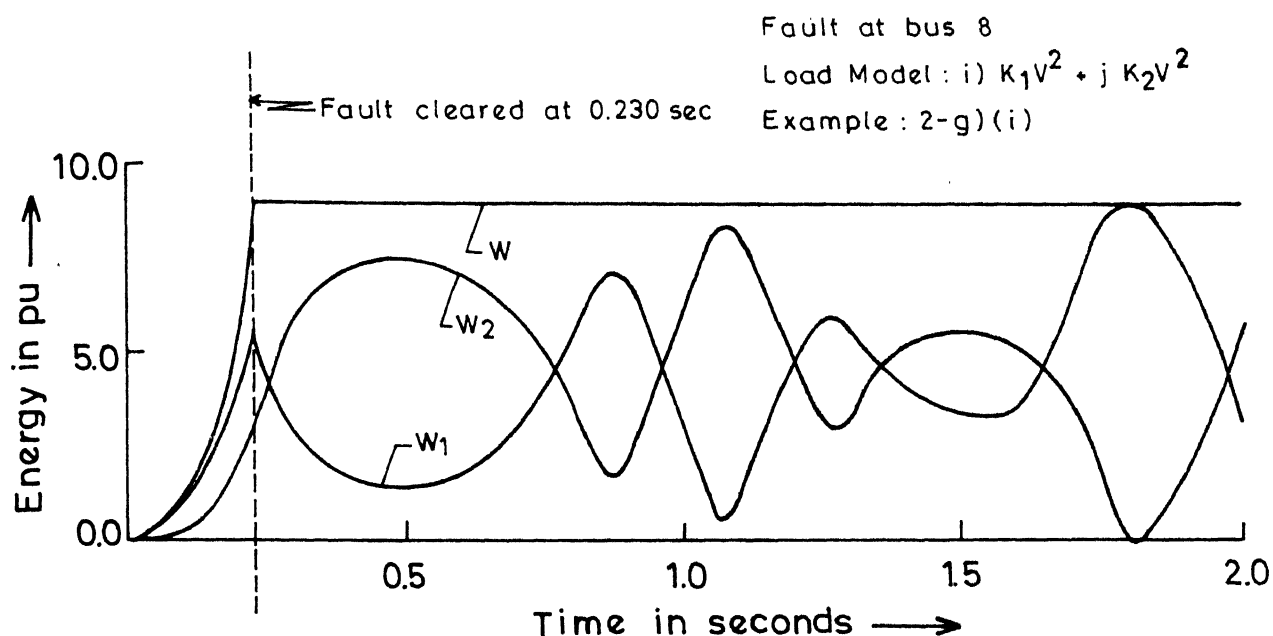


FIG.2.21 VARIATION OF TOTAL ENERGY AND ITS COMPONENTS FOR 10-MACHINE SYSTEM, UNSTABLE CASE

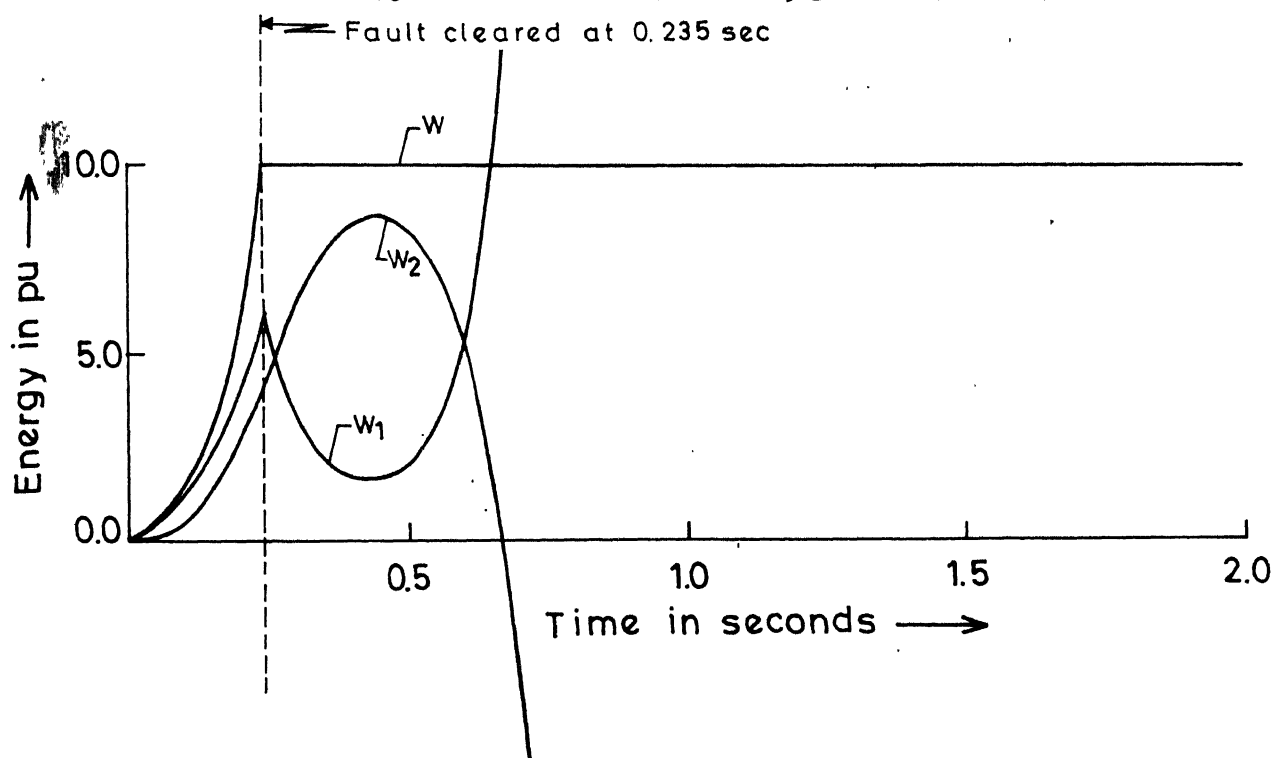
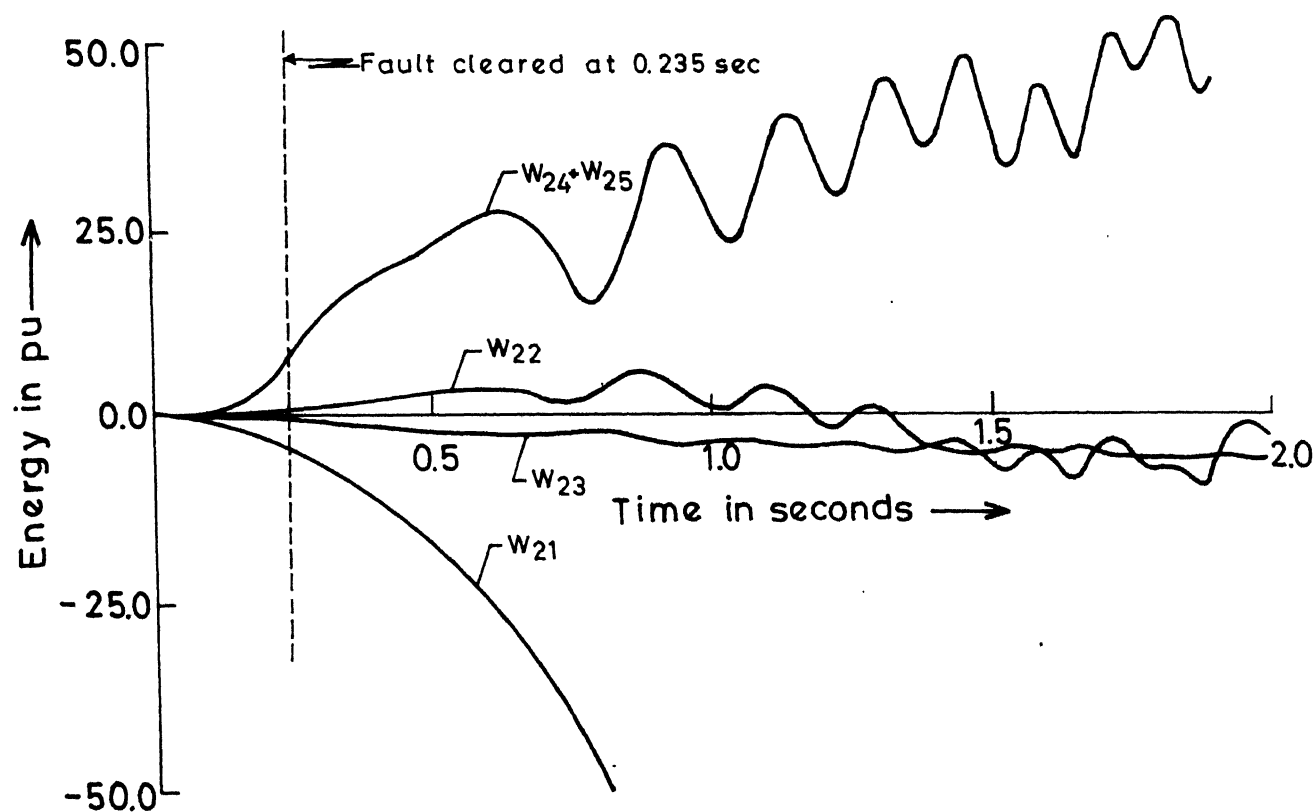
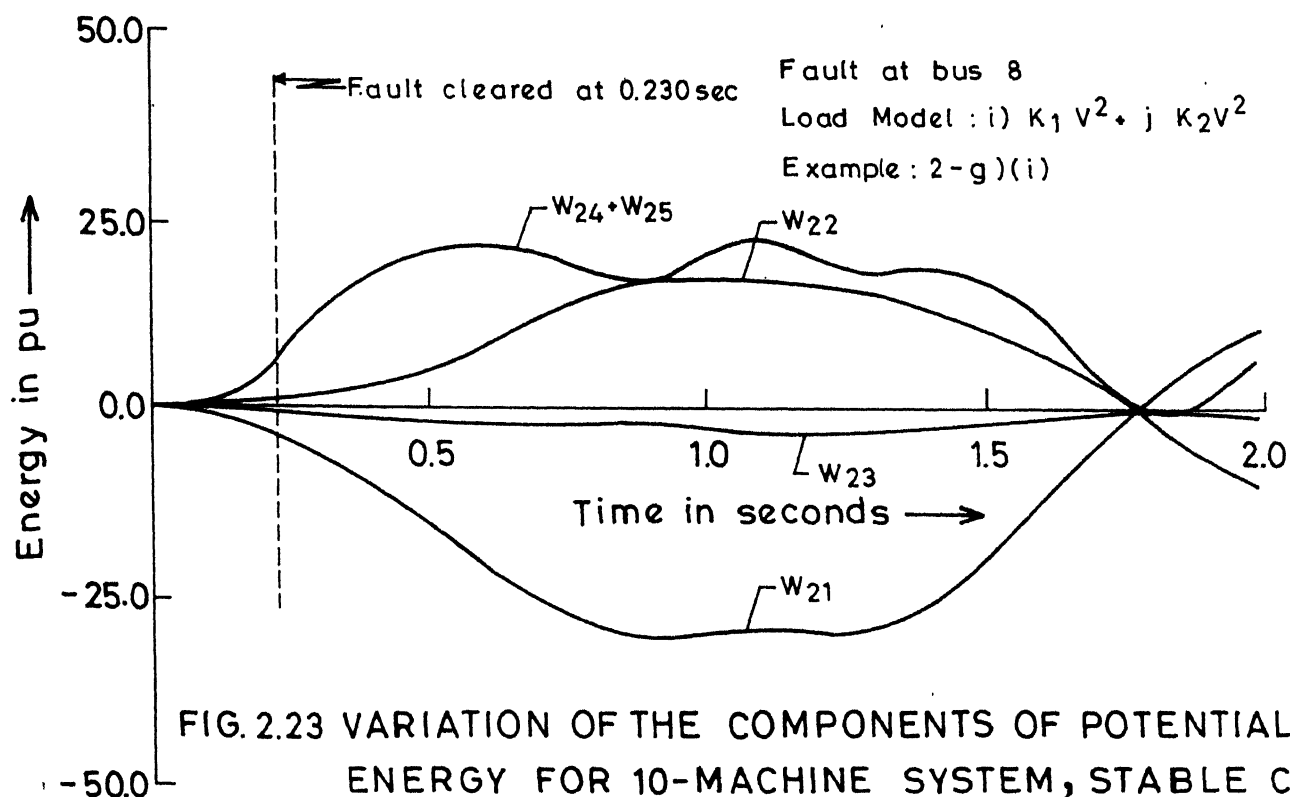


FIG.2.22 VARIATION OF TOTAL ENERGY AND ITS COMPONENTS FOR 10 MACHINE SYSTEM, UNSTABLE CASE



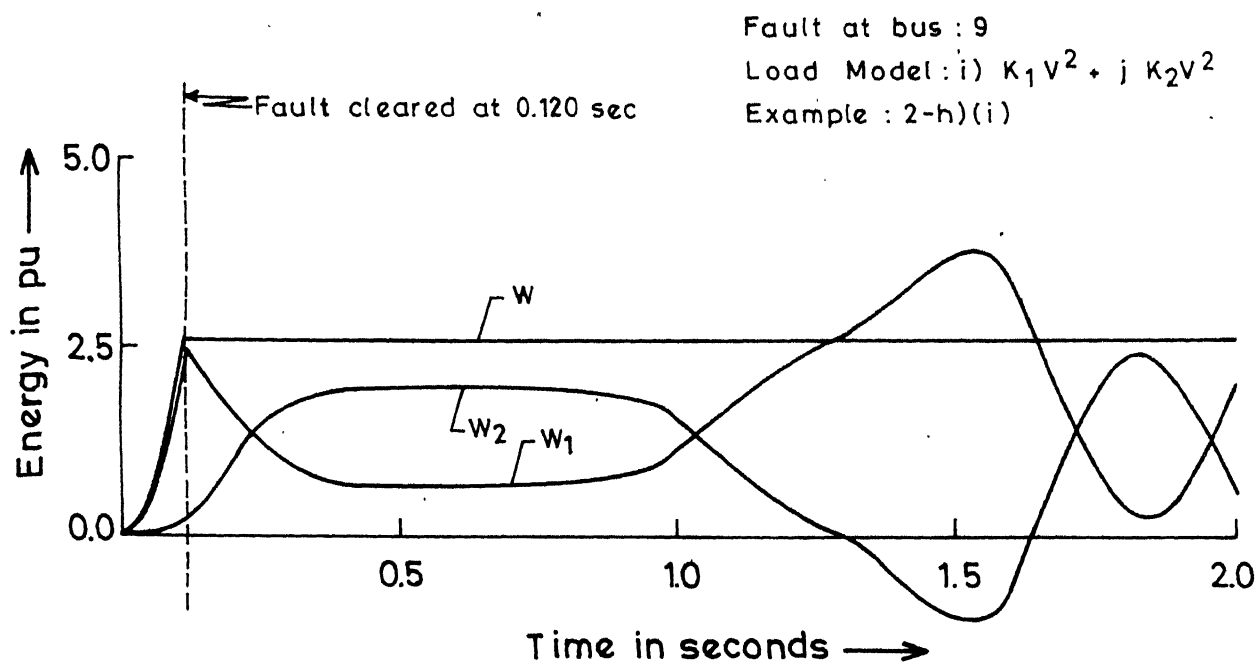


FIG.2.25 VARIATION OF TOTAL ENERGY AND ITS COMPONENTS FOR 10-MACHINE SYSTEM, STABLE CASE

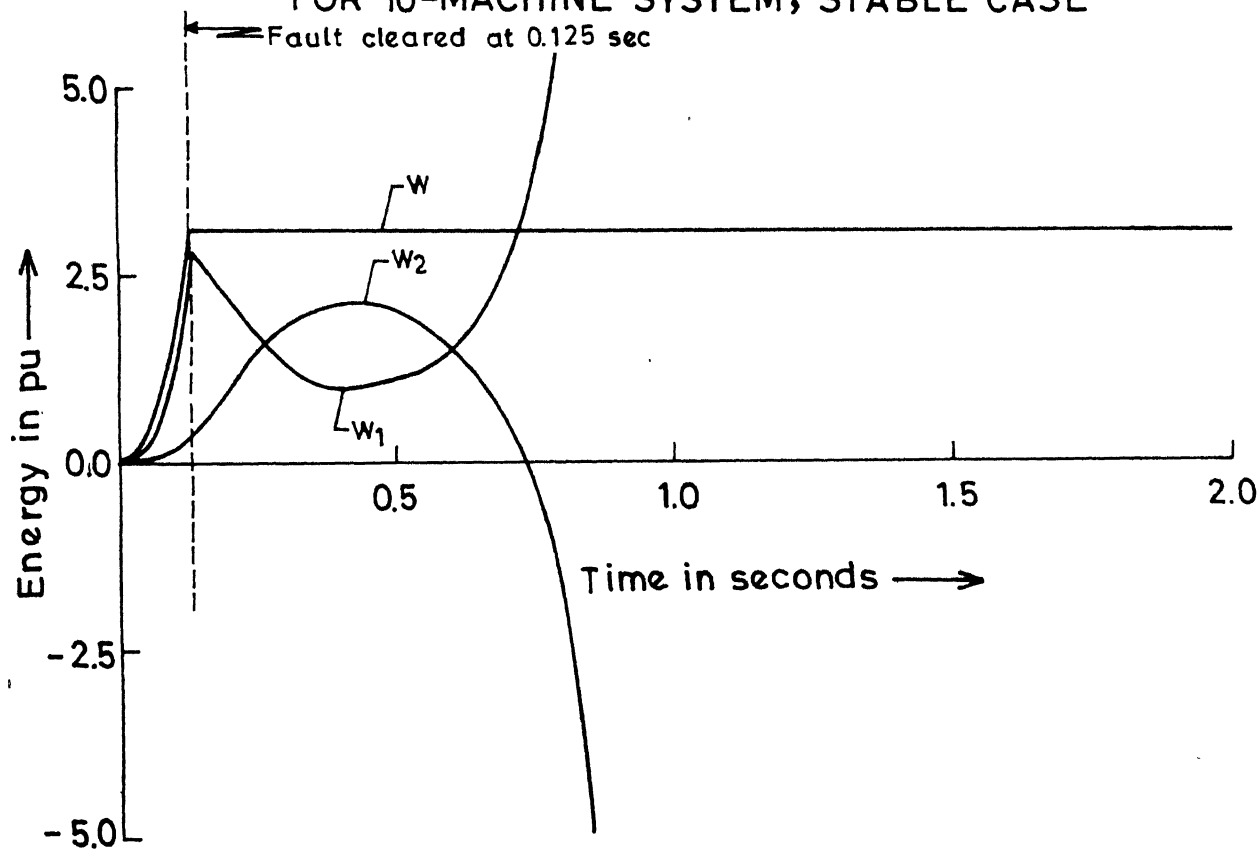


FIG.2.26 VARIATION OF TOTAL ENERGY AND ITS COMPONENTS FOR 10-MACHINE SYSTEM, UNSTABLE CASE

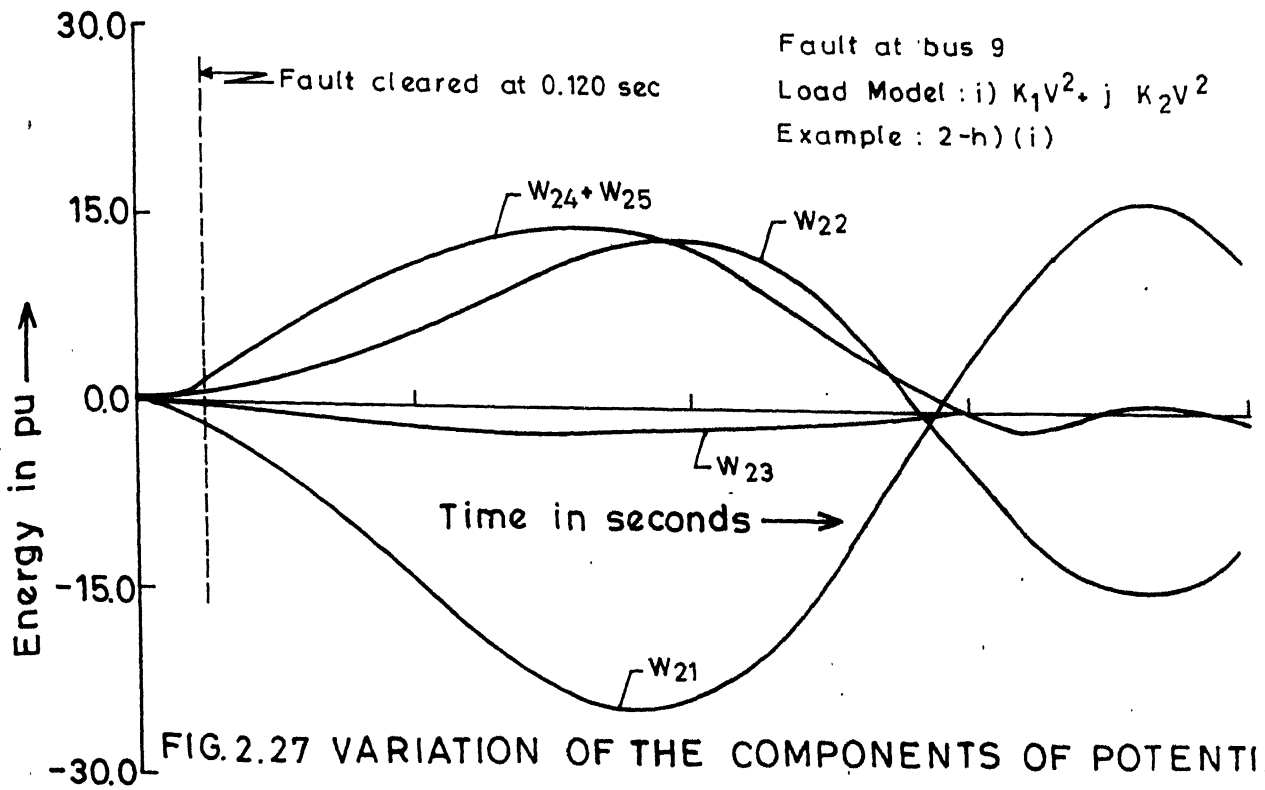


FIG. 2.27 VARIATION OF THE COMPONENTS OF POTENTIAL ENERGY FOR 10-MACHINE SYSTEM, STABLE CASE

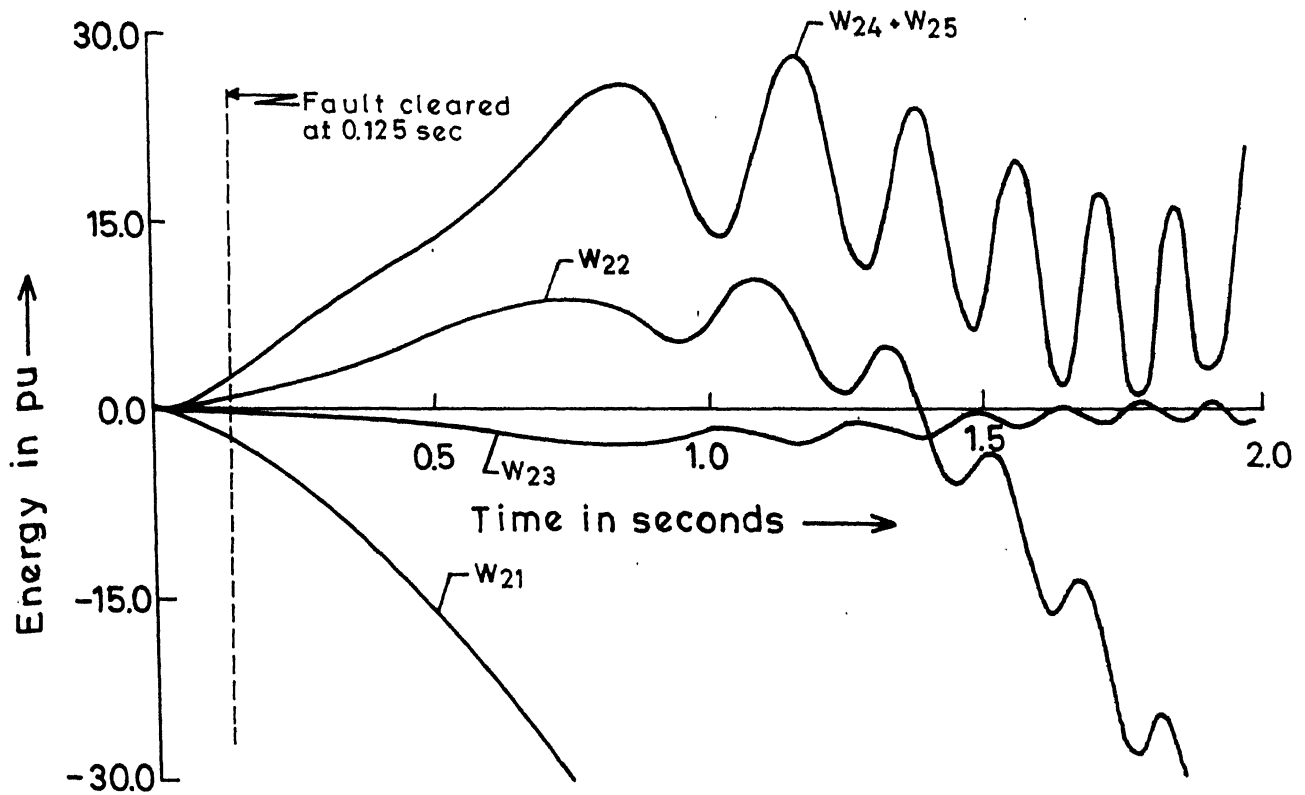


FIG. 2.28 VARIATION OF THE COMPONENTS OF POTENTIAL ENERGY FOR 10-MACHINE SYSTEM, UNSTABLE CASE

energy has a component that increases with time, while the potential energy has a component that decreases with time. Examination of the various components of potential energy shows that  $W_{21}$  or  $W_{22}$  or both can diverge.  $-W_{21}$  is the energy supplied from the generator rotors, while  $W_{22}$  is the energy consumed in the loads. The difference between the two energies is responsible for the increase in kinetic energy. It is also observed that  $W_{21}$  is negative if the generators tend to accelerate and positive if they tend to decelerate.

$W_{23}$ , the energy component due to the reactive power in the loads, is not appreciable compared to other components. However,  $W_{24} + W_{25}$  which corresponds to the energy stored in the machine reactances and transmission lines is a significant component of the potential energy. This component is always non-negative and oscillates in response to the swings of the generator rotors. It is interesting to observe that all the components of the potential energy go through the minimum at the same instant of time when the system is stable. At these instants of time, the rotor angles are close to their equilibrium values. It is also interesting to observe that the frequency of oscillations in the magnetic energy ( $W_{24} + W_{25}$ ) increases when the system becomes unstable. Also, for a large system, the peak magnitude of this energy for the unstable case is usually higher than that for the stable case.

## 2.6 CONCLUSIONS

In this chapter, an existing dynamic simulation program [66] is modified to include structure preserving model of the system enabling detailed load representation in transient stability analysis. The program is then augmented by the addition of two new subroutines to incorporate the computation of SPEF. The resultant program can, thus, be conveniently employed to evaluate the transient stability of power systems by i) digital simulation method and ii) direct methods using the SPEF. The transient stability program is tested on three realistic power systems. The following conclusions are drawn :

- 1) Program output during the fault-on period can be analysed to determine the critical energy,  $W_{cr}$  and the critical clearing time  $t_{cr}$ .
- 2) The predicted value of  $t_{cr}$  using SPEF agrees closely with that obtained by digital simulation in, practically, all the cases considered.
- 3) The variation of energy components can give significant information about the system behaviour. In particular, the stability can be inferred from this instead of swing curves.

## CHAPTER 3

### A STRUCTURE PRESERVING ENERGY FUNCTION WITH KNOWN MODES OF INSTABILITY

#### 3.1 INTRODUCTION

In Chapter 2, the application of structure preserving energy function to predict the critical clearing time was presented. This was based upon the computation of critical energy using PEBS method. The advantage of using PEBS method was that it avoids the calculation of controlling ucp which can be quite complex [32].

The application of PEBS is based upon the assumption that the system is stable if the kinetic energy at the time of clearing gets converted into potential energy. However, in multi-machine systems, it is observed that the total kinetic energy need not be fully converted into potential energy [59]. This is because of the relative motion among the generators that remain in synchronism. An iterative PEBS method has been suggested to account for this effect by modifying the critical energy or subtracting the component of the kinetic energy from the total kinetic energy at clearing, that does not lead to system separation [73]. The kinetic energy correction is equal to the minimum of the kinetic energy after the fault

is critically cleared. Implementing this correction, adds to the computational burden in predicting the region of stability.

It has been suggested [32,59] that the kinetic energy responsible for system separation can be obtained by considering the mode of instability. For example, a three phase fault at the generator terminals can lead to the separation of the faulted generator from the rest of the generators which remain in synchronism. In this case, it is the kinetic energy component corresponding to the relative velocity between the generator going out-of-step and the remaining generators, that is contributing to system separation. This is an intuitive concept that has been utilised in providing the kinetic energy correction in [59]. In [32] a two machine equivalent has been proposed to analyse this mode of instability.

An exact derivation of the energy function based on mode of instability has not been presented so far. In this chapter, a novel structure preserving energy function is derived assuming that instability occurs due to the separation of the generators into  $r$  coherent groups where,  $r$  is greater than or equal to 2. However, in practice, it is not possible to know the mode of instability a priori, yet if the fault is assumed to be at the terminals of a generator, then it is reasonable to conclude that the faulted generator separates from the rest at the

onset of instability. This is a valid assumption in predicting 'first swing' stability using PEBS method.

The application of the new SPEF for direct stability evaluation to three realistic system examples is also presented.

## 3.2 SYSTEM MODEL

### 3.2.1 Assumptions

In transient stability evaluation by direct methods using SPEF, the following assumptions are usually made :

- i) The generator is represented by a constant voltage behind the direct axis transient reactance (constant flux linkage).
- ii) The governor action is neglected which implies that the power output from generator and turbine remains essentially constant during the transient.
- iii) Damping is ignored.
- iv) Transient saliency of the generators is neglected.
- v) Transmission lines are assumed to be lossless. This is generally true as the extra high voltage lines in a power system have high  $X/R$  ratio.

The above assumptions are useful in the study of transient stability for only the 'first swing' or for periods of the order of one second [ 2 ] and the error introduced by them are

small. However, the above assumptions can be relaxed without complicating the analysis. Assumption (v) has been relaxed in Chapter 5 for the development of system model and energy function to consider the transmission line resistances in stability study, while assumptions (i) and (iv) are relaxed in Chapter 6 for detailed modelling of machines.

### 3.2.2 Generator Model

#### 3.2.2.1 General

Consider a 'm' machine system supplying 'n' nonlinear voltage dependent loads as shown in Fig. 3.1. Under the assumptions mentioned in Section 3.2.1, the motion of the *i*th machine can be described by the following differential equations :

$$\dot{\delta}_i = \omega_i^{\text{syn}} \quad (3.1)$$

$$M_i \dot{\omega}_i^{\text{syn}} = P_{mi} - P_{ei}$$

$$\text{where } P_{ei} = \frac{E_i V_i \sin(\delta_i - \Psi_i)}{x'_{di}} ; i = 1, 2, \dots, m \quad (3.2)$$

Eq. (3.1) is written with respect to an arbitrary synchronous reference frame. The coordinates of the rotational elements relative to COI of the system (global COI) describes exactly the synchronous behaviour of the system [36,37]. Global COI is defined as the inertia weighted average of all the rotor angles, i.e.,

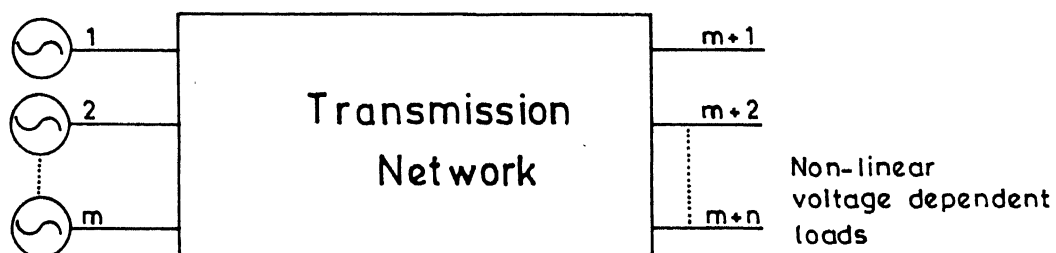


FIG. 3.1 A SYSTEM OF  $m$  MACHINES SUPPLYING POWER TO  $n$  NON-LINEAR VOLTAGE DEPENDENT LOADS.

$$\delta_o = \frac{1}{M_T} \sum_{i=1}^m M_i \delta_i, \quad \omega_o = \frac{1}{M_T} \sum_{i=1}^m M_i \omega_i^{\text{syn}}, \quad M_T = \sum_{i=1}^m M_i \quad (3.3)$$

Following the formulation procedure outlined in ref. [30], we get,

$$\begin{aligned} \dot{\delta}_o &= \omega_o \\ M_T \dot{\omega}_o &= \sum_{i=1}^m (P_{mi} - P_{ei}) = P_{\text{COI}} \end{aligned} \quad (3.4)$$

The dynamics of the global COI reference are governed by the equations (3.4). By defining new angles and speeds relative to this reference

$$\theta_i = \delta_i - \delta_o, \quad \omega_i = \omega_i^{\text{syn}} - \omega_o, \quad i = 1, 2, \dots, m \quad (3.5)$$

the system equations of motions become

$$\begin{aligned} \dot{\theta}_i &= \omega_i \\ M_i \dot{\omega}_i &= P_{mi} - P_{ei} - \frac{M_i}{M_T} P_{\text{COI}}, \quad i = 1, 2, \dots, m \end{aligned} \quad (3.6)$$

In view of the definitions in (3.3) and (3.5), the COI variables satisfy the following relations :

$$\sum_{i=1}^m M_i \theta_i = \sum_{i=1}^m M_i \omega_i = 0 \quad (3.7)$$

### 3.2.2.2 Aggregation of Generators in Coherent Groups

When a disturbance occurs in the system, the generators in a coherent group swing together. Generally, the total number of coherent groups will be much less than  $m$ . In this case, it is possible to represent a coherent group by an equivalent generator and the order of the system dynamics is reduced. The equations describing a group  $\alpha$  are derived below :

The local COI of a group  $\alpha$  can be defined as

$$\theta_o^\alpha = \frac{1}{M_T^\alpha} \sum_{i=1}^{m_\alpha} M_i \theta_i, \quad \omega_o^\alpha = \frac{1}{M_T^\alpha} \sum_{i=1}^{m_\alpha} M_i \omega_i, \quad M_T^\alpha = \sum_{i=1}^{m_\alpha} M_i, \quad \alpha = 1, 2, \dots, r \quad (3.8)$$

where  $m_\alpha$  = number of machines in group  $\alpha$ .

Dynamics of group  $\alpha$  can be described by

$$\dot{\theta}_o^\alpha = \omega_o^\alpha$$

$$M_T^\alpha \dot{\omega}_o^\alpha = \sum_{i=1}^{m_\alpha} (P_{mi} - P_{ei}) - \frac{M_T^\alpha}{M_T} P_{COI}, \quad \alpha = 1, 2, \dots, r \quad (3.9)$$

Define new rotor angles and speeds of the machines in group  $\alpha$  as

$$\bar{\theta}_i^\alpha = \theta_i - \theta_o^\alpha, \quad \bar{\omega}_i^\alpha = \omega_i - \omega_o^\alpha, \quad i = 1, 2, \dots, m_\alpha \quad (3.10)$$

$$\alpha = 1, 2, \dots, r.$$

Variables  $\bar{\theta}_i^\alpha$  and  $\bar{\omega}_i^\alpha$  satisfy the relations :

$$\sum_{i=1}^{m_\alpha} M_i \bar{\theta}_i^\alpha = \sum_{i=1}^{m_\alpha} M_i \bar{\omega}_i^\alpha = 0, \quad \alpha = 1, 2, \dots, r \quad (3.11)$$

Substituting for  $\omega_i$  in Eq. (3.6) from Eq. (3.10), the equation of motion of the  $i$ th machine in group  $\alpha$  in the new variables  $\bar{\theta}_i^\alpha$  and  $\bar{\omega}_i^\alpha$  can be written as

$$\begin{aligned} M_i \dot{\bar{\omega}}_i^\alpha &= -M_i \dot{\bar{\omega}}_0^\alpha + P_{mi} - P_{ei} - \frac{M_i}{M_T} P_{COI} \\ &= -\frac{M_i}{M_T^\alpha} \left[ \sum_{i=1}^{m_\alpha} (P_{mi} - P_{ei}) - \frac{M_T^\alpha}{M_T} P_{COI} \right] + P_{mi} - P_{ei} - \frac{M_i}{M_T} P_{COI} \end{aligned} \quad (3.12)$$

substituting for  $\dot{\bar{\omega}}_0^\alpha$  from Eq. (3.9)

Simplifying the R.H.S. of Eq. (3.12), finally we have,

$$M_i \dot{\bar{\omega}}_i^\alpha = P_{mi} - P_{ei} - \frac{M_i}{M_T^\alpha} P_{COI}^\alpha, \quad i = 1, 2, \dots, m_\alpha \quad (3.13)$$

$$\alpha = 1, 2, \dots, r$$

where,

$$P_{COI}^\alpha = \sum_{i=1}^{m_\alpha} (P_{mi} - P_{ei}), \quad \alpha = 1, 2, \dots, r \quad (3.14)$$

Since the machines in group  $\alpha$  are assumed to swing together, their angular rates are zero, i.e.,  $\dot{\bar{\omega}}_i^\alpha = 0$  ( $i = 1, 2, \dots, m_\alpha$ ). Thus, Eq. (3.13) can be written as

$$0 = P_{mi} - P_{ei} - \frac{M_i}{M_T^\alpha} P_{COI}^\alpha, \quad i = 1, 2, \dots, m_\alpha \quad (3.15)$$

$$\alpha = 1, 2, \dots, r$$

Group  $\alpha$  is described by the dynamical equations (3.9) and the algebraic equations (3.15). It is to be noted that there are  $(m_\alpha - 1)$  independent algebraic equations which can be used to solve for  $(m_\alpha - 1)$  independent angle variables  $\bar{\theta}_i^\alpha$ . It can be shown that the variables corresponding to the local COI's of  $r$  groups satisfy the relations :

$$\sum_{\alpha=1}^r M_T^\alpha \theta_o^\alpha = \sum_{i=1}^m M_i \theta_i = 0 \quad (3.16)$$

$$\sum_{\alpha=1}^r M_T^\alpha \omega_o^\alpha = \sum_{i=1}^m M_i \omega_i = 0 \quad (3.17)$$

### Case of Two Groups

This is a special case with  $r = 2$ . It is an important case as most of the times, at the onset of instability, one group (which may consist of a single generator with fault at its terminals) separates from the rest of the generators which may be clubbed into a single group. The dynamics of the COI's of the two groups are described by

$$\begin{aligned} \dot{\theta}_o^1 &= \omega_o^1 \\ M_T^1 \dot{\omega}_o^1 &= \sum_{i=1}^{m_1} (P_{mi} - P_{ei}) - \frac{M_T^1}{M_T} P_{COI} \end{aligned} \quad (3.18)$$

$$\begin{aligned} \dot{\theta}_o^2 &= \omega_o^2 \\ M_T^2 \dot{\omega}_o^2 &= \sum_{i=1}^{m_2} (P_{mi} - P_{ei}) - \frac{M_T^2}{M_T} P_{COI} \end{aligned} \quad (3.19)$$

If the machines in groups 1 and 2 are assumed to swing together, the equations of motion of the machines in each group can be written as

$$0 = P_{mi} - P_{ei} - \frac{M_i}{M_T} P_{COI}^1, \quad i = 1, 2, \dots, m_1 \quad (3.20)$$

$$0 = P_{mi} - P_{ei} - \frac{M_i}{M_T} P_{COI}^2, \quad i = 1, 2, \dots, m_2 \quad (3.21)$$

If group 1 consists of only a single machine (say, k), then Eqs. (3.18) and (3.19) reduce to

$$\begin{aligned} \dot{\theta}_k &= \omega_k \\ M_k \dot{\omega}_k &= P_{mk} - P_{ek} - \frac{M_k}{M_T} P_{COI} \end{aligned} \quad (3.22)$$

$$\begin{aligned} \dot{\theta}_{T-k} &= \omega_{T-k} \\ M_{T-k} \dot{\omega}_{T-k} &= \sum_{\substack{i=1 \\ \neq k}}^m (P_{mi} - P_{ei}) - \frac{M_{T-k}}{M_T} P_{COI} \end{aligned} \quad (3.23)$$

Here group 2 is labelled as (T-k). Based on the assumption that the machines of this group swing together, their equations of motion can be written as

$$0 = P_{mi} - P_{ei} - \frac{M_i}{M_{T-k}} P_{COI, T-k}, \quad i = 1, 2, \dots, m \quad (3.24)$$

$\neq k$

$$\text{where } P_{COI, T-k} = \sum_{\substack{i=1 \\ \neq k}}^m (P_{mi} - P_{ei}) \quad (3.25)$$

### 3.2.3 Load Model

The real and the reactive power demands are modelled as arbitrary functions of respective bus voltage. Thus,

$$P_{Li} = f_{pi}(V_i) \quad , \quad i = 1, 2, \dots, n \quad (3.26)$$

$$Q_{Li} = f_{qi}(V_i) \quad , \quad i = 1, 2, \dots, n \quad (3.27)$$

### 3.2.4 Power Flow Equations

At a node  $i$  corresponding to the terminals of a generator, the complex power injection can be written as (neglecting resistance)

$$\begin{aligned} S_i = \bar{V}_i \bar{I}_i^* &= \bar{V}_i \left[ \frac{\bar{V}_i^* - \bar{E}_i^*}{-jx'_{di}} \right] + (\bar{V}_i \left[ \sum_{j=1}^n \bar{V}_j^* (-j B_{ij}) \right]), \quad i = 1, 2, \dots, m \\ &= S_1 + S_2 \end{aligned} \quad (3.28)$$

The first term  $S_1$  on the R.H.S. of Eq. (3.28) corresponds to power flow through the reactance of machine  $i$  connected to node  $i$  and the second term  $S_2$  corresponds to the power flow in the lines connecting node  $i$  to node  $j$  (excludes the internal nodes of generators). In the above expression,  $B_{ij} = \text{Im} [Y_{ij}]$  where  $[Y]$  is the admittance matrix of the network (excluding machine reactances).

The term  $S_1$  can be written as

$$\begin{aligned}
S_1 &= V_i e^{j\varphi_i} \left[ \frac{V_i e^{-j\varphi_i} - E_i e^{-j\theta_i}}{-j x'_{di}} \right] \\
&= j \frac{V_i^2}{x'_{di}} - j \frac{E_i V_i e^{j(\varphi_i - \theta_i)}}{x'_{di}} \\
&= \frac{E_i V_i \sin(\varphi_i - \theta_i)}{x'_{di}} + j \left[ \frac{V_i^2}{x'_{di}} - \frac{E_i V_i \cos(\varphi_i - \theta_i)}{x'_{di}} \right] \quad (3.29)
\end{aligned}$$

The term  $S_2$  can also be written as

$$\begin{aligned}
S_2 &= V_i e^{j\varphi_i} \left[ \sum_{j=1}^n V_j e^{-j\varphi_j} (-j B_{ij}) \right] \\
&= j \left[ \sum_{j=1}^n B_{ij} V_i V_j e^{j(\varphi_i - \varphi_j)} \right] \\
&= \sum_{j=1}^n B_{ij} V_i V_j \sin \varphi_{ij} - j \sum_{j=1}^n B_{ij} V_i V_j \cos \varphi_{ij} \quad (3.30)
\end{aligned}$$

where  $\varphi_{ij} = \varphi_i - \varphi_j$

If there are no machines connected to node  $i$ , the complex power injection is given by

$$\begin{aligned}
S_i &= \bar{V}_i \bar{I}_i^* = \bar{V}_i \left[ \sum_{j=1}^n V_j^* (-j B_{ij}) \right] \\
&= \sum_{j=1}^n B_{ij} V_i V_j \sin \varphi_{ij} - j \sum_{j=1}^n B_{ij} V_i V_j \cos \varphi_{ij}, \\
&\quad i = m+1, \dots, n \quad (3.31)
\end{aligned}$$

Thus, in view of Eqs. (3.28) to (3.31), the real and the reactive power injections at bus  $i$  of a lossless system can be written as

$$P_i = \frac{E_i V_i \sin(\varphi_i - \theta_i)}{x'_{di}} + \sum_{j=1}^n B_{ij} V_i V_j \sin \varphi_{ij}, \quad i = 1, 2, \dots, m \quad (3.32a)$$

$$= \sum_{j=1}^n B_{ij} V_i V_j \sin \varphi_{ij}, \quad i = m+1, m+2, \dots, n \quad (3.32b)$$

$$Q_i = \frac{V_i^2}{x'_{di}} - \frac{E_i V_i \cos(\theta_i - \varphi_i)}{x'_{di}} - \sum_{j=1}^n B_{ij} V_i V_j \cos \varphi_{ij}, \quad i = 1, 2, \dots, m \quad (3.33a)$$

$$= - \sum_{j=1}^n B_{ij} V_i V_j \cos \varphi_{ij}, \quad i = m+1, m+2, \dots, n \quad (3.33b)$$

Since the net real and reactive power at bus  $i$  is zero, we get from Eqs. (3.26) to (3.33) the following power flow equations :

$$P_i + f_{pi}(V_i) = 0, \quad i = 1, 2, \dots, n \quad (3.34)$$

$$Q_i + f_{qi}(V_i) = 0, \quad i = 1, 2, \dots, n \quad (3.35)$$

### 3.3 STRUCTURE PRESERVING ENERGY FUNCTION (SPEF)

Consider the energy function, defined for the post-fault system, as

$$W = W_{11} + W_2 = W_{11} + \sum_{i=1}^5 W_{2i} \quad (3.36)$$

$$\text{where } W_{11} = \text{kinetic energy} = \frac{1}{2} \sum_{\alpha=1}^r M_T^{\alpha} (\omega_o^{\alpha})^2 \quad (3.37)$$

The components of the potential energy,  $W_2$  are

$$W_{21} = - \sum_{i=1}^m P_{mi} (\theta_i - \theta_{i0}) \quad (3.38)$$

$$W_{22} = \sum_{i=1}^n \int_{t_0}^t P_{Li} \frac{d\varphi_i}{dt} dt \quad (3.39)$$

$$W_{23} = \sum_{i=1}^n \int_{V_{i0}}^{V_i} \frac{f_{qi}(x_i)}{x_i} dx_i \quad (3.40)$$

$$W_{24} = \sum_{i=1}^m [E_i^2 + V_i^2 - 2E_i V_i \cos(\theta_i - \varphi_i) - (E_{i0}^2 + V_{i0}^2 - 2E_{i0} V_{i0} \cos(\theta_{i0} - \varphi_{i0}))] \frac{1}{2x'_{di}} \quad (3.41)$$

$$W_{25} = - \frac{1}{2} \sum_{i=1}^n \sum_{j=1}^n B_{ij} (V_i V_j \cos \varphi_{ij} - V_{i0} V_{j0} \cos \varphi_{ij0}) \quad (3.42)$$

The subscript 'o' in the above expressions indicates the quantities at the initial equilibrium.

The time derivative of the energy function  $W$  in Eq. (3.36) can be shown to be zero as follows :

Taking partial derivative of  $W_{11}$  w.r.t.  $\omega_o^\alpha$ , we get,

$$\frac{\partial W_{11}}{\partial \omega_o^\alpha} = M_I^\alpha \omega_o^\alpha, \quad \alpha = 1, 2, \dots, r \quad (3.43)$$

Partial derivatives of  $W_2$  w.r.t.  $\theta_i$ ,  $V_i$ ,  $\varphi_i$  and  $t$  are

$$\frac{\partial W_2}{\partial \theta_i} = -P_{mi} + \frac{E_i V_i \sin(\theta_i - \varphi_i)}{x'_{di}} = -P_{mi} + P_{ei}, \quad i = 1, 2, \dots, m \quad (3.44)$$

$$\frac{\partial W_2}{\partial V_i} = \frac{1}{V_i} \left[ \frac{V_i^2}{x'_{di}} - \frac{E_i V_i \cos(\theta_i - \varphi_i)}{x'_{di}} + f_{qi}(V_i) - \sum_{j=1}^n B_{ij} V_i V_j \cos \varphi_{ij} \right],$$

$$i = 1, 2, \dots, m$$

$$= \frac{1}{V_i} [f_{qi}(V_i) - \sum_{j=1}^n B_{ij} V_i V_j \cos \varphi_{ij}], \quad i = m+1, m+2, \dots, n$$

$$= \frac{1}{V_i} [Q_{Li} + Q_i], \quad i = 1, 2, \dots, n$$

$$= 0, \quad \text{in view of Eqs. (3.27) and (3.35).} \quad (3.45)$$

$$\frac{\partial W_2}{\partial \varphi_i} = - \frac{E_i V_i \sin(\theta_i - \varphi_i)}{x'_{di}} + \sum_{j=1}^n B_{ij} V_i V_j \sin \varphi_{ij}, \quad i = 1, 2, \dots, m$$

$$= \sum_{j=1}^n B_{ij} V_i V_j \sin \varphi_{ij}, \quad i = m+1, m+2, \dots, n$$

$$= P_i, \quad \text{in view of Eqs. (3.32)} \quad (3.46)$$

$$\frac{\partial W_2}{\partial t} = \sum_{i=1}^n P_{Li} \frac{d\varphi_i}{dt} \quad (3.47)$$

From Eqs. (3.43) and (3.44), we get,

$$\begin{aligned} \frac{dW_{11}}{dt} + \sum_{i=1}^m \frac{\partial W_2}{\partial \theta_i} \frac{d\theta_i}{dt} &= \sum_{\alpha=1}^r \frac{\partial W_{11}}{\partial \omega_\alpha} \frac{d\omega_\alpha}{dt} + \sum_{\alpha=1}^r \sum_{i=1}^{m_\alpha} \frac{\partial W_2}{\partial \theta_i} \frac{d\theta_i}{dt} \\ &= \sum_{\alpha=1}^r [M_I^\alpha \omega_\alpha^\alpha \dot{\omega}_\alpha^\alpha + \sum_{i=1}^{m_\alpha} (-P_{mi} + P_{ei}) \omega_i] \end{aligned}$$

$$= \sum_{\alpha=1}^r [M_T^\alpha \omega_o^\alpha \dot{\omega}_o^\alpha + \sum_{i=1}^{m_\alpha} (-P_{mi} + P_{ei})(\bar{\omega}_i^\alpha + \omega_o^\alpha)], \text{ in view of Eq. (3.10)}$$

$$= \sum_{\alpha=1}^r \left( [M_T^\alpha \dot{\omega}_o^\alpha - \sum_{i=1}^{m_\alpha} (P_{mi} - P_{ei})] \omega_o^\alpha + \sum_{i=1}^{m_\alpha} (-P_{mi} + P_{ei}) \bar{\omega}_i^\alpha \right)$$

$$= - \sum_{\alpha=1}^r \left[ \frac{M_T^\alpha \omega_o^\alpha}{M_T} P_{COI} - \sum_{i=1}^{m_\alpha} \frac{M_i \bar{\omega}_i^\alpha}{M_T^\alpha} P_{COI}^\alpha \right], \text{ in view of Eqs. (3.9) and (3.15)}$$

$$= 0, \text{ on substituting from Eqs. (3.11) and (3.17)} \quad (3.48)$$

From Eqs. (3.46) and (3.47), we have,

$$\left( \sum_{i=1}^n \frac{\partial W_2}{\partial \varphi_i} \frac{d\varphi_i}{dt} \right) + \frac{\partial W_2}{\partial t} = \sum_{i=1}^n (P_i + P_{Li}) \frac{d\varphi_i}{dt}$$

$$= 0, \text{ in view of Eqs. (3.26) and (3.34)} \quad (3.49)$$

$$\text{Hence, } \frac{dW}{dt} = \frac{d}{dt} (W_{11} + W_2)$$

$$= \left[ \frac{dW_{11}}{dt} + \sum_{i=1}^m \frac{\partial W_2}{\partial \theta_i} \frac{d\theta_i}{dt} \right] + \sum_{i=1}^n \frac{\partial W_2}{\partial V_i} \frac{dV_i}{dt}$$

$$+ \left[ \left( \sum_{i=1}^n \frac{\partial W_2}{\partial \varphi_i} \frac{d\varphi_i}{dt} \right) + \frac{\partial W_2}{\partial t} \right]$$

$$= 0, \text{ in view of Eqs. (3.45), (3.48) and (3.49)} \quad (3.50)$$

### Comments

1) The terms in Eqs. (3.38) to (3.42) of the potential energy function,  $W_2$  in Eq. (3.36) may be physically interpreted in the following way :

$W_{21}$  = change in potential energy due to mechanical input

$W_{22}$  = change in potential energy due to voltage dependent active power loads

$W_{23}$  = change in potential energy due to voltage dependent reactive power loads

$W_{24}+W_{25}$  = change in magnetic energy stored in machine reactances and transmission lines.

2] The kinetic energy term,  $W_{11}$  in Eq. (3.37) can be derived from that of the energy function developed by Padiyar et al. [54] as shown below :

$$W_1 = \frac{1}{2} \sum_{i=1}^m M_i \omega_i^2 = \frac{1}{2} \sum_{\alpha=1}^r \sum_{i=1}^{m_\alpha} M_i \omega_i^2 \quad (3.51)$$

Substituting for  $\omega_i$  in Eq. (3.51) from Eq. (3.10), we have,

$$\begin{aligned} W_1 &= \frac{1}{2} \sum_{\alpha=1}^r \sum_{i=1}^{m_\alpha} M_i (\bar{\omega}_i^\alpha + \omega_o^\alpha)^2 \\ &= \frac{1}{2} \sum_{\alpha=1}^r \sum_{i=1}^{m_\alpha} M_i (\bar{\omega}_i^\alpha)^2 + \frac{1}{2} \sum_{\alpha=1}^r \sum_{i=1}^{m_\alpha} M_i (\omega_o^\alpha)^2 \\ &\quad + \sum_{\alpha=1}^r \sum_{i=1}^{m_\alpha} M_i \bar{\omega}_i^\alpha \omega_o^\alpha \end{aligned}$$

$$\begin{aligned}
&= \frac{1}{2} \sum_{\alpha=1}^r \sum_{i=1}^{m_{\alpha}} M_i (\bar{\omega}_i^{\alpha})^2 + \frac{1}{2} \sum_{\alpha=1}^r M_T^{\alpha} (\omega_0^{\alpha})^2 + \sum_{\alpha=1}^r \omega_0^{\alpha} \left( \sum_{i=1}^{m_{\alpha}} M_i \bar{\omega}_i^{\alpha} \right) \\
&= \frac{1}{2} \sum_{\alpha=1}^r \sum_{i=1}^{m_{\alpha}} M_i (\bar{\omega}_i^{\alpha})^2 + \frac{1}{2} \sum_{\alpha=1}^r M_T^{\alpha} (\omega_0^{\alpha})^2, \text{ in view of Eq. (3.11)}
\end{aligned} \tag{3.52}$$

The first term on the R.H.S. of Eq. (3.52) corresponds to the total energy due to inter-generator swings in each of the  $r$  areas and does not contribute to the system separation. This portion of the kinetic energy need not be absorbed by the network for stability to be maintained and thus can be ignored. This results in an accurate estimation of the transient energy component responsible for system instability. Hence,

$$W_1 = W_{11} = \frac{1}{2} \sum_{\alpha=1}^r M_T^{\alpha} (\omega_0^{\alpha})^2 \tag{3.53}$$

3) The kinetic energy term for the case of two groups can be written from Eq. (3.37) as

$$W_{11} = \frac{1}{2} M_T^1 (\omega_0^1)^2 + \frac{1}{2} M_T^2 (\omega_0^2)^2 \tag{3.54}$$

Using the relation in Eq. (3.7),  $W_{11}$  in Eq. (3.54) can be rewritten after some algebraic manipulation as

$$\begin{aligned}
W_{11} &= \frac{1}{2} M_T^1 (\omega_0^1)^2 + \frac{1}{2} M_T^2 \left( \frac{M_T^1 \omega_0^1}{M_T^2} \right)^2 \\
&= \frac{1}{2} M_T^1 (\omega_0^1)^2 \left( 1 + \frac{M_T^1}{M_T^2} \right) \\
&= \frac{1}{2} \frac{M_T^1 M_T^2}{M_T} \left( \frac{M_T \omega_0^1}{M_T^2} \right)^2
\end{aligned} \tag{3.55}$$

Similarly, it can also be shown that

$$W_{11} = \frac{1}{2} \frac{M_T^1 M_T^2}{M_T} \left( \frac{M_T \omega_o^2}{M_T^1} \right)^2 \quad (3.56)$$

The relative velocity of groups 1 and 2 is given by

$$\begin{aligned} \omega_o^1 - \omega_o^2 &= \omega_o^1 \left( 1 + \frac{M_T^1}{M_T^2} \right), \text{ in view of Eq. (3.7)} \\ &= \frac{M_T^1}{M_T^2} \omega_o^1 \end{aligned} \quad (3.57)$$

$$\text{Also, } \omega_o^1 - \omega_o^2 = - \frac{M_T^1}{M_T^1} \omega_o^2 \quad (3.58)$$

Utilising the relations in Eqs. (3.57) and (3.58),  $W_{11}$  is obtained from Eq. (3.55) or (3.56) as

$$W_{11} = \frac{1}{2} \frac{M_T^1 M_T^2}{M_T} (\omega_o^1 - \omega_o^2)^2 \quad (3.59)$$

Similarly, when a single generator  $k$  separates from the rest of the generators belonging to group  $T-k$  the kinetic energy term can be given as

$$W_{11} = \frac{M_k M_{T-k}}{M_T} (\omega_k - \omega_{T-k})^2 \quad (3.60)$$

4) For constant real power load, the component  $W_{22}$  in Eq. (3.39) of the potential energy function,  $W_2$  can be directly computed from

$$W_{22} = \sum_{i=1}^n P_{L_i} (\varphi_i - \varphi_{i0}) \quad (3.61)$$

In this case, the energy function is a Lyapunov function with the property that its Hessian is positive definite in the region of stability surrounding the stable equilibrium point.

As discussed in Chapter 2, the expression given in Eq. (3.61) can be used as an approximation even for general case of nonlinear loads. However, the time derivative of the modified energy function is not equal to zero and is given by

$$\dot{W}^{\text{mod}} = \sum_{i=1}^n f'_{pi}(V_i) \varphi_i \frac{dV_i}{dt} \quad (3.62)$$

It is observed that the modified energy function neglecting path dependent term gives quite accurate results [71].

5) It has been shown by Padiyar et al. [70] that the components  $W_{24}$  and  $W_{25}$  can be expressed as half the sum of reactive power loss in each element of the network, i.e.,

$$W_{24} + W_{25} = \frac{1}{2} \sum_{r=1}^L Q_r = \frac{1}{2} \left[ \sum_{i=1}^m Q_{Gi} - \sum_{j=1}^n Q_{Lj} \right] \quad (3.63)$$

where

$Q_{Gi}$  = reactive power generation of machine  $i$

$Q_{Lj}$  = reactive power load at bus  $j$

$L$  = number of elements in the network

The R.H.S. of Eq. (3.63) is easily calculated at the end of power flow solution at each step during the transient, thereby simplifying the computation of the overall energy function.

### 3.4 COMPUTATION OF STABILITY REGION

#### 3.4.1 General

An index of the region of stability surrounding the stable equilibrium point (sep) is the critical clearing time for a particular disturbance, typically a three phase fault at the terminals of a generator. The critical clearing time is predicted by computing the critical energy. If at the time of clearing, the total energy is less than the critical energy, the system is stable and unstable otherwise.

The critical energy for a given disturbance has been defined to be the energy evaluated at the controlling uep that lies on the stability boundary nearest to the sustained fault trajectory [30]. The evaluation of the controlling uep can be avoided by the use of PEBS method (see APPENDIX D). This approach is analogous to the equal area criterion used in two machine systems. In a two machine system, the potential energy reaches a maximum along the critically cleared trajectory at which time the kinetic energy (based on the relative velocity) becomes zero for conservative systems. Thus, it can be argued that the kinetic energy gained during the fault-on

period is completely converted into potential energy as the total energy remains constant for the post-fault system.

The application of PEBS method to systems with more than two generators has following problems :

- i) It is not necessary that all the kinetic energy (with reference to COI as used in earlier formulations) gained during the fault-on period be converted into potential energy. Fouad and Stanton [59] has suggested subtracting the (first) minimum value of the kinetic energy along the critically cleared trajectory from the value of the energy at the time of clearing. However, this is a cumbersome procedure and is not justified analytically.
- ii) While the potential energy maximum is same for the faulted trajectory and critically cleared trajectory, this does not extend to a multi-machine system. Since it is easier to evaluate the maximum potential energy along the faulted trajectory, an approximation is introduced by computing the critical energy from this maximum. The relative flatness of PEBS near the critically cleared trajectory is the justification for this approximation [29].  
An iterative method of predicting the critical energy has to be used if this approximation is not valid [73].

The mode of instability plays a major role in determining the amount of kinetic energy that is responsible for system separation. This is clearly brought out by the energy function derived in the previous section. While the potential energy is invariant and identical to that given in Chapter 2, the kinetic energy depends on the nature of coherent groups. Generally, there will be many coherent groups in a large system which may separate from each other. However, it may be conceived that, initially, one group of generators separate from the rest. As the time passes, these two groups may split into many subgroups. It is well known that energy methods as well as the equal area criterion are useful primarily in predicting stability in the first swing. While it is difficult to define 'first swing' stability in a multi-machine system, it is reasonable to expect that the energy methods can predict the onset of instability where one or more generators start separating from the rest.

It is to be noted that the dynamic trajectories of a multi-machine system are extremely complex and characterised by chaotic behaviour [19]. Thus, instability much after the fault clearing, cannot be ruled out. However, the presence of suitably designed controllers in the system to damp out the oscillations can overcome this problem.

### 3.4.2 Computational Procedure

The evaluation of critical clearing time requires the simulation of the faulted system. Although the energy function is derived based on identifying the coherent groups and neglecting the relative motions within a group, simulation is performed without this assumption. Thus, the computer program, described in Chapter 2, is used with a minor modification in the computation of the kinetic energy component of SPEF.

The most severe faults are the three phase faults at the terminals of generators. It is assumed that in the first instance, the generator at whose terminals the fault occurs, tends to separate from the rest. This is a reasonable assumption and its validity is demonstrated by numerical examples.

With the mode of instability thus assumed apriori, the corresponding kinetic energy component is used in the evaluation of critical energy. PEBS method is used with the usual approximation of computing the critical energy from the faulted trajectory.

### 3.5 NUMERICAL EXAMPLES

#### 3.5.1 Description

Three realistic power system examples considered in Chapter 2 are taken up again to illustrate the application of the proposed energy function to direct stability evaluation. Single-line diagrams of the systems are given in Figs.E.1,F.1 and G.1 respectively. The machine constants, line data and the operating data for the three systems are given in Tables E.1-E.3, F.1-F.5 and G.1-G.4 respectively.

It is assumed that a three phase fault occurs at the terminals of a generator. The fault is cleared followed by instantaneous reclosure of the line. The prefault and the post-fault network configurations are, therefore, assumed to be the same. Two types of voltage dependent load characteristics are considered for investigation. For simplicity, load representation at all the buses are assumed to be identical. The following cases are studied :

Example 1 : 7-machine 10-bus (CIGRE) test system

a) Fault at bus 1 ; b) Fault at bus 2 ; c) Fault at bus 3 ;  
d) Fault at bus 5 ; e) Fault at bus 6 ; f) Fault at bus 7.

Types of load characteristics :

$$(i) \quad k_1 V^2 + jk_2 V^2 ; \qquad (ii) \quad k_1 + jk_2 V^2$$

Example 2 : 10-machine 39-bus (NEW ENGLAND) test system

- a) Fault at bus 1 ; b) Fault at bus 3 ; c) Fault at bus 4 ;  
 d) Fault at bus 5 ; e) Fault at bus 6 ; f) Fault at bus 7 ;  
 g) Fault at bus 8 ; h) Fault at bus 9 ; i) Fault at bus 10.

Types of load characteristics :

$$(i) \quad k_1 V^2 + j k_2 V^2 \quad ; \quad (ii) \quad k_1 + j k_2 V^2$$

Example 3 : 13-machine 71-bus (UPSEB) system

- a) Fault at bus 1 (Gen. No.1) ; b) Fault at bus 3 (Gen.No.2) ;  
 c) Fault at bus 6 (Gen. No.3) ; d) Fault at bus 8 (Gen.No.4) ;  
 e) Fault at bus 15(Gen. No.5) ; f) Fault at bus 27(Gen.No.6) ;  
 g) Fault at bus 29(Gen. No.7) ; h) Fault at bus 39(Gen.No.8) ;  
 i) Fault at bus 44(Gen. No.9) ; j) Fault at bus 48(Gen.No.10);  
 k) Fault at bus 64(Gen. No.11); l) Fault at bus 66(Gen.No.12);  
 m) Fault at bus 68(Gen. No.13) .

Types of load characteristics :

$$(i) \quad k_1 V^2 + j k_2 V^2 \quad ; \quad (ii) \quad k_1 + j k_2 V^2$$

### 3.5.2 Results

Critical clearing times are predicted using the proposed SPEF and the SPEF given in Chapter 2 [54]. For all the cases, critical clearing times are also obtained by digital simulation and the results are compared. These are shown in Tables 3.1-3.4

Table 3.1 : Effect of known Modes of instability on the Predicted Critical Clearing time  $t_{cr}$  for 7-machine System.

Fault Location	Gen. No. k	Load Model : i) $k_1 V^2 + jk_2 V^2$			Load Model : ii) $k_1 + jk_2 V^2$		
		Critical Energy, $W_{cr}$ (pu)	$t_{cr}$ (sec) obtained by Energy Function Method (Proposed SPEF) Neglect- ing Mode of Insta- bility	Digital Simulation	Critical Energy, $W_{cr}$ (pu)	$t_{cr}$ (sec) obtained by Energy Function Method (Proposed SPEF) Neglect- ing Mode of Insta- bility	Digital Simulation
Bus 1	1	15.8257	0.339	0.391	0.395-0.400	11.948	0.409 0.412 0.415-0.420
Bus 2	2	15.3988	0.446	0.448	0.450-0.455	12.192	0.394 0.396 0.400-0.405
Bus 3	3	18.463	0.485	0.487	0.485-0.490	-*	-* -*
Bus 5	5	10.085	0.437	0.438	0.435-0.440	-*	-* -*
Bus 6	6	14.925	0.649	0.650	0.650-0.655	13.383	0.593 0.594 0.595-0.600
Bus 7	7	5.896	0.349	0.351	0.350-0.355	-*	-* -*

\* = Network solution does not converge.

Table 3.2 Effect of known Modes of Instability on the Predicted Critical Clearing Time,  $t_{cr}$  for 10-machine System.

Fault Location No.	Gen. k	Load Model : i) $k_1 V^2 + j k_2 V^2$				Load Model : ii) $k_1 + j k_2 V^2$			
		Critical Energy $W_{cr}$ (pu)	$t_{cr}$ (sec)	Energy Function Method (proposed SPEF) Neglect- ing Mode of Insta- bility	Digital Simulation	Critical Energy $W_{cr}$ (pu)	$t_{cr}$ (sec)	Energy Function Method (Proposed SPEF) Neglect- ing Mode of Insta- bility	Digital Simulation
Bus 1	1	7.5771	0.248	0.249	0.260-0.265	6.4175	0.231	0.232	0.230-0.23
Bus 2	3	7.3153	0.218	0.219	0.230-0.235	6.0197	0.200	0.201	0.200-0.20
Bus 4	4	9.8640	0.217	0.219	0.210-0.215	-*	-*	-*	-*
Bus 5	5	2.8465	0.161	0.162	0.175-0.180	2.4043	0.149	0.150	0.160-0.16
Bus 6	6	9.9969	0.236	0.239	0.240-0.245	-*	-*	-*	-*
Bus 7	7	8.8263	0.222	0.224	0.235-0.240	7.5624	0.207	0.209	0.210-0.21
Bus 8	8	8.9164	0.220	0.221	0.230-0.235	8.0419	0.214	0.215	0.215-0.22
Bus 9	9	2.3473	0.109	0.110	0.120-0.125	-*	-*	-*	-*
Bus 10	10	24.7726	0.647	0.680	0.570-0.575	-*	-*	-*	-*

\* = Network solution does not converge.

Table 3.3 : Effect of known Modes of Instability on the  
Predicted Critical Clearing Time,  $t_{cr}$  for  
10-machine System.

Load Model : i)  $k_1 V^2 + j k_2 V^2$

Fault Location	Gen. No. k	Critical Energy $W_{cr}$ (pu)	$t_{cr}$ (sec) obtained by		Digital Simulation
			Energy Function Method (Modified SPEF)		
			Neglecting Mode of Instability	Considering Mode of Instability	
Bus 1	1	9.2701	0.262	0.263	0.260-0.265
Bus 3	3	9.2122	0.232	0.233	0.230-0.235
Bus 4	4	9.8766	0.214	0.215	0.210-0.215
Bus 5	5	3.3192	0.169	0.170	0.175-0.180
Bus 6	6	10.5532	0.238	0.241	0.240-0.245
Bus 7	7	9.5254	0.225	0.228	0.235-0.240
Bus 8	8	10.1766	0.228	0.230	0.230-0.235
Bus 9	9	2.3791	0.108	0.110	0.120-0.125
Bus 10	10	23.5784	0.628	0.658	0.570-0.575



1	2	3	4	5	6	7	8	9	10
Bus 44	9	2.2569	0.331	0.333	0.330-0.335	—*	—*	—*	—*
Bus 48	10	9.0933	0.382	0.384	0.380-0.385	7.8972	0.306	0.308	0.305- 0.310
Bus 64	11	3.5106	0.304	0.307	0.310-0.315	2.9683	0.268	0.272	0.270- 0.275
Bus 66	12	1.5585	0.291	0.293	0.290-0.295	1.2836	0.265	0.267	0.265- 0.270
Bus 68	13	1.0263	0.226	0.227	0.225-0.230	0.8825	0.201	0.202	0.200- 0.205

\* = The network solution does not converge.

for 7-machine, 10-machine and 13-machine systems respectively for load characteristics of types (i) and (ii). Tables 3.2 and 3.3 present the results for 10-machine system for the following cases respectively :

- i) When the path dependent term in the energy function is numerically integrated by trapezoidal rule
- ii) When the energy function is modified to approximate the path dependent term by a path independent term as discussed earlier.

As the results with the modified energy function are more accurate, only this case is considered for 13-machine system the results of which are reported in Table 3.4.

Variables  $\theta$ ,  $V$  and  $\phi$  are monitored corresponding to the critical energy for the contingencies investigated and load characteristic of type (i). These are presented in Tables 3.5 and 3.6 for 7-machine and 10-machine systems respectively.

Figs. 3.2-3.7 show the swing curves, the variation of total energy and its kinetic and potential energy components and also the components of the potential energy function,  $W_2$  for example 1-a) (i) for stable and unstable conditions.

Swing curves for examples 2-a) (i), 2-b)(i), 2-d)(i), 2-e)(i), 2-f)(i), 2-i)(i) and 2-a)(ii) for stable and unstable cases are presented in Figs. 3.8-3.21. The variation of total energy

Table 3.5 Variables Corresponding to the Critical Energy,  
 $W_{cr}$  for 7-machine System (by Trajectory Simulation)  
 Load Model : i)  $k_1 V^2 + j k_2 V^2$   
 $\theta$  and  $\phi$  in radian and  $V$  in pu.

Variables	Fault at bus					
	1	2	3	5	6	7
$\theta_1$	2.6147	-0.2653	-0.3709	-0.1969	-0.3966	-0.3403
$V_1$	0.2716	0.8231	0.8081	0.9254	0.8568	0.9745
$\phi_1$	-0.5229	-0.4056	-0.4866	-0.3181	-0.4896	-0.4514
$\theta_2$	-0.2774	2.5939	-0.1270	-0.1616	-0.4324	-0.3549
$V_2$	0.8319	0.2705	0.6234	0.9211	0.9098	0.9905
$\phi_2$	-0.4096	-0.2633	-0.3267	-0.2716	-0.4952	-0.4416
$\theta_3$	-0.3436	-0.1267	2.4998	-0.1201	-0.4508	-0.3598
$V_3$	0.8453	0.6804	0.2301	0.8471	0.8994	0.9655
$\phi_3$	-0.4590	-0.3455	-0.3003	-0.2749	-0.5197	-0.4628
$\theta_4$	-0.1999	-0.3226	-0.4283	-0.2486	-0.4570	-0.3879
$V_4$	0.6413	0.7469	0.7266	0.8751	0.7872	0.9366
$\phi_4$	-0.4821	-0.4615	-0.5340	-0.3593	-0.5248	-0.4867
$\theta_5$	-0.4972	-0.4183	-0.3637	2.6787	-0.6088	-0.5172
$V_5$	0.8517	0.8303	0.6782	0.1611	0.9130	0.9800
$\phi_5$	-0.5762	-0.5027	-0.5051	-0.0926	-0.6500	-0.5832

Contd.

	1	2	3	5	6	7
$\theta_6$	-0.4910	-0.5622	-0.7059	-0.3964	2.4018	-0.1860
$V_6$	0.8107	0.8558	0.8195	0.9331	0.2351	0.7844
$\phi_6$	-0.5700	-0.5789	-0.6975	-0.4305	0.0755	-0.3579
$\theta_7$	-0.7373	-0.7841	-0.9888	-0.5079	-0.0542	2.4651
$V_7$	0.9323	0.9363	0.8927	0.9771	0.7497	0.3143
$\phi_7$	-0.7556	-0.7703	-0.9545	-0.5404	-0.1490	2.1653
$V_8$	0.8432	0.8519	0.7711	0.9278	0.4966	0.3960
$\phi_8$	-0.6779	-0.6793	-0.8324	-0.5009	-0.2253	-0.2686
$V_9$	0.7711	0.6876	0.3927	0.8277	0.7682	0.8190
$\phi_9$	-0.5841	-0.5190	-0.6329	-0.4147	-0.5678	-0.5313
$V_{10}$	0.7434	0.7852	0.6987	0.5094	0.8451	0.9580
$\phi_{10}$	-0.5643	-0.5114	-0.5480	-0.3454	-0.6208	-0.5646

Table 3.6 Variables Corresponding to the Critical Energy,  $W_{cr}$  for 10-machine

System (by Trajectory Simulation)

Load Model : i)  $k_1 V^2 + j k_2 V^2$

$\underline{\theta}$  and  $\underline{\phi}$  in radian and  $\underline{V}$  in pu

Variables	Fault at bus									
	1	3	4	5	6	7	8	9	10	
$\theta_1$	2.4690	0.3313	0.1909	0.1863	0.1812	0.1890	0.1941	0.1853	0.4099	
$V_1$	0.2388	0.7654	0.9173	0.9574	0.9077	0.9210	0.9253	0.9591	0.8264	
$\phi_1$	0.6901	0.0684	-0.0434	-0.0762	-0.0497	-0.0543	-0.0609	-0.0714	0.1819	
$\theta_2$	-0.2863	-0.2956	-0.2894	-0.2459	-0.3286	-0.2930	-0.2691	-0.2355	-0.5471	
$V_2$	0.9965	0.9975	1.0136	1.0238	1.0110	1.0148	1.0006	1.0196	0.9406	
$\phi_2$	-0.3228	-0.3307	-0.3351	-0.2924	-0.3600	-0.3300	-0.3094	-0.2800	-0.5378	
$\theta_3$	0.4197	0.4445	-0.2703	-0.2590	0.2647	0.2687	0.2657	0.2552	0.5117	
$V_3$	0.7929	0.2699	0.9124	0.9561	0.9021	0.9163	0.9276	0.9602	0.8361	
$\phi_3$	0.1291	0.9343	0.0220	-0.0193	0.0192	0.0102	-0.0045	-0.0174	0.2707	

Contd.....

Variables	Fault at bus								
	1	3	4	5	6	7	8	9	10
$\theta_4$	0.2606	0.2652	2.6103	0.4164	0.3995	0.3658	0.2640	0.2489	0.5633
$V_4$	0.9537	0.9403	0.3406	0.8257	0.8570	0.8792	0.9514	0.9708	0.9030
$\phi_4$	0.0390	0.0482	1.2302	0.1879	0.2013	0.1543	0.0420	0.0312	0.3737
$\theta_5$	0.4217	0.4222	0.7117	2.2958	0.4973	0.4906	0.4330	0.4442	0.6070
$V_5$	0.9744	0.9610	0.6259	0.4763	0.8795	0.9001	0.9712	0.9891	0.9323
$\phi_5$	0.0111	0.0212	0.4858	0.4595	0.1627	0.1220	0.0173	0.0122	0.3174
$\theta_6$	0.2713	0.2739	0.3664	0.2975	2.5313	0.5764	0.2756	0.2671	0.5772
$V_6$	1.0041	0.9902	0.9203	0.9976	0.3250	0.7307	1.0018	1.0220	0.9493
$\phi_6$	0.0547	0.0642	0.1873	0.0786	1.2764	0.3630	0.0586	0.0489	0.4025
$\theta_7$	0.2895	0.2929	0.3898	0.3147	0.7134	2.6246	0.2933	0.2823	0.6050
$V_7$	1.0274	1.0161	0.9589	1.0220	0.7587	0.3014	1.0255	1.0425	0.9829
$\phi_7$	0.0979	0.1070	0.2292	0.1221	0.5649	1.7318	0.1017	0.0903	0.4443
$\theta_8$	0.2423	0.2364	0.2458	0.2294	0.2421	0.2439	2.5664	0.2690	1.1417
$V_8$	0.9759	0.9683	0.9669	1.0047	0.9578	0.9702	0.2383	0.9513	0.6458
$\phi_8$	-0.0098	-0.0101	0.0121	-0.0249	0.0088	0.0019	0.6961	0.0383	0.8359

Variables	Fault at bus									
	1	3	4	5	6	7	8	9	10	
$\phi_9$	0.4310	0.4279	0.4575	0.4521	0.4511	0.4576	0.5392	1.9414	1.0336	
$V_9$	0.9995	0.9925	0.9755	1.0084	0.9677	0.9772	0.9067	0.5639	0.8410	
$\phi_9$	0.0726	0.0758	0.1234	0.0778	0.1235	0.1131	0.1917	0.9797	0.7201	
$\phi_{10}$	-0.0697	-0.0773	-0.0714	-0.0810	-0.0808	-0.0749	0.0486	-0.0595	2.6543	
$V_{10}$	0.9939	0.9863	0.9893	1.0248	0.9811	0.9931	0.8735	0.9928	0.3364	
$\phi_{10}$	-0.1175	-0.1202	-0.1041	-0.1299	-0.1118	-0.1134	-0.0300	-0.0937	1.9390	
$V_{11}$	0.7061	0.6071	0.8997	0.9674	0.8844	0.9070	0.9224	0.9712	0.7796	
$\phi_{11}$	-0.0718	-0.0501	-0.1253	-0.1688	-0.1298	-0.1407	-0.1563	0.1627	0.1010	
$V_{12}$	0.7156	0.5973	0.8820	0.9526	0.8663	0.8898	0.9088	0.9574	0.7682	
$\phi_{12}$	-0.0750	-0.0494	-0.1200	-0.1663	-0.1237	-0.1362	-0.1541	-0.1607	0.1125	
$V_{13}$	0.7441	0.6045	0.8880	0.9632	0.8714	0.8963	0.9194	0.9692	0.7774	
$\phi_{13}$	-0.0750	-0.0455	-0.1115	-0.1605	-0.1143	-0.1284	-0.1487	-0.1555	0.1273	
$V_{14}$	0.7748	0.6941	0.8607	0.9511	0.8413	0.8713	0.9060	0.9601	0.7556	
$\phi_{14}$	-0.1228	-0.1102	-0.1244	-0.1805	-0.1253	-0.1441	-0.1709	-0.1762	0.1256	

Variables	Fault at bus									
	1	3	4	5	6	7	8	9	10	
$V_{15}$	0.8701	0.8258	0.7750	0.9146	0.7471	0.7921	0.9063	0.9489	0.7806	
$\phi_{15}$	-0.1493	-0.1388	-0.0627	-0.1541	-0.0529	-0.0943	-0.1618	-0.1641	0.1825	
$V_{16}$	0.9216	0.8926	0.7489	0.9102	0.7174	0.7685	0.9174	0.9555	0.8019	
$\phi_{16}$	-0.1313	-0.1214	-0.0016	0.1127	0.0144	-0.0395	-0.1289	-0.1297	0.2343	
$V_{17}$	0.9232	0.8985	0.8100	0.9405	0.7837	0.8259	0.8798	0.9250	0.7291	
$\phi_{17}$	-0.1546	-0.1472	-0.0670	-0.1504	-0.0595	-0.0956	-0.1396	-0.1301	0.2562	
$V_{18}$	0.9108	0.8879	0.8396	0.9534	0.8161	0.8534	0.8629	0.9334	0.6766	
$\phi_{18}$	-0.1707	-0.1647	-0.1066	-0.1765	-0.1034	-0.1309	-0.1569	-0.1533	0.2450	
$V_{19}$	0.9822	0.7626	0.4893	0.8022	0.8428	0.8757	0.9789	1.0058	0.9071	
$\phi_{19}$	-0.0484	-0.0377	0.4189	0.0794	0.1115	0.0622	-0.0444	-0.0513	0.2931	
$V_{20}$	0.9416	0.9254	0.5293	0.6197	0.8266	0.8529	0.9384	0.9604	0.8838	
$\phi_{20}$	-0.0717	-0.0612	0.4031	0.1509	0.0852	0.0396	-0.0667	-0.0730	0.2544	
$V_{21}$	0.9439	0.9200	0.8015	0.9340	0.5732	0.6839	0.9403	0.9726	0.8469	
$\phi_{21}$	-0.0931	-0.0825	0.0430	-0.0723	0.1718	0.0685	-0.0901	-0.0949	0.2698	

Variables	Fault at bus									
	1	3	4	5	6	7	8	9	10	
$V_{22}$	0.9799	0.9609	0.8660	0.9715	0.4636	0.6208	0.9769	1.0035	0.9038	
$\phi_{22}$	-0.0233	-0.0127	0.1142	-0.0008	0.4618	0.2415	-0.0198	-0.0278	0.3342	
$V_{23}$	0.9755	0.9559	0.8638	0.9672	0.5533	0.5042	0.9726	0.9988	0.9009	
$\phi_{23}$	-0.0278	-0.0172	0.1101	-0.0053	0.3924	0.2926	-0.0243	-0.0326	0.3301	
$V_{24}$	0.9255	0.8981	0.7622	0.9146	0.6864	0.7243	0.9215	0.9578	0.8129	
$\phi_{24}$	-0.1305	-0.1203	0.0017	-0.1112	0.0424	-0.0217	-0.1279	-0.1300	0.2347	
$V_{25}$	0.9718	0.9599	0.9559	1.0133	0.9428	0.9619	0.6477	0.9330	0.5145	
$\phi_{25}$	-0.1274	-0.1265	-0.0988	-0.1385	-0.1035	-0.1121	-0.0434	-0.0739	0.5653	
$V_{26}$	0.9761	0.9606	0.9606	0.9214	1.0005	0.9045	0.9298	0.8099	0.6788	
$\phi_{26}$	-0.1382	-0.1338	-0.0813	-0.1401	-0.0802	-0.0992	0.0711	0.0175	0.4335	
$V_{27}$	0.9484	0.9288	0.8671	0.9695	0.8460	0.8790	0.8386	0.8451	0.6967	
$\phi_{27}$	-0.1661	-0.1604	-0.0958	-0.1653	-0.0920	-0.1182	-0.1246	-0.0769	0.3283	

$V_{28}$	1.0020	0.9907	0.9625	1.0185	0.9501	0.9673	0.8685	0.6135	0.7681
$\phi_{28}$	-0.0849	-0.0806	-0.0295	-0.0839	-0.0284	-0.0438	0.0144	0.3640	0.5386
$V_{29}$	1.0077	0.9978	0.9731	1.0217	0.9621	0.9768	0.8858	0.5798	0.7959
$\phi_{29}$	0.0405	-0.0364	0.0139	-0.0384	0.0148	0.0008	0.0668	0.5415	0.5941
$V_{30}$	0.9920	0.9875	0.9985	1.0298	0.9905	1.0021	0.9197	1.0060	0.6903
$\phi_{30}$	-0.2588	-0.2643	-0.2527	-0.2431	-0.2781	-0.2604	-0.2415	-0.2205	-0.3315
$V_{31}$	0.9641	0.9516	0.9560	1.0144	0.9427	0.9624	0.7711	0.9618	0.4302
$\phi_{31}$	-0.1498	-0.1496	-0.1264	-0.1613	-0.1332	-0.1395	-0.0964	-0.1169	0.4962
$V_{32}$	0.8923	0.8723	0.8905	0.9764	0.8720	0.9006	0.8368	0.9488	0.5926
$\phi_{32}$	-0.1775	-0.1738	-0.1465	-0.1979	-0.1488	-0.1649	-0.1662	-0.1705	0.2452
$V_{33}$	0.7559	0.7300	0.8751	0.9544	0.8578	0.8843	0.8856	0.9517	0.7110
$\phi_{33}$	-0.1648	-0.1592	-0.1736	-0.2214	-0.1772	-0.1910	-0.2059	-0.2102	0.0862
$V_{34}$	0.6714	0.6958	0.8989	0.9646	0.8840	0.9062	0.9133	0.9652	0.7583
$\phi_{34}$	-0.1317	-0.1307	-0.1750	-0.2134	-0.1817	-0.1898	-0.2011	-0.2050	0.0321

$V_{35}$	0.6512	0.6855	0.9031	0.9672	0.8885	0.9101	0.9186	0.9686	0.7684
$\phi_{35}$	-0.1105	-0.1111	-0.1641	-0.2023	-0.1706	-0.1786	-0.1900	-0.1945	-0.0435
$V_{36}$	0.6718	0.7004	0.8996	0.9608	0.8854	0.9063	0.9132	0.9617	0.7597
$\phi_{36}$	-0.1692	-0.1690	-0.2109	-0.2440	-0.2196	-0.2248	-0.2339	-0.2357	-0.0339
$V_{37}$	0.6851	0.7110	0.9015	0.9614	0.8875	0.9081	0.9141	0.9620	0.7594
$\phi_{37}$	-0.1865	-0.1862	-0.2237	-0.2543	-0.2334	-0.2373	-0.2451	-0.2457	-0.0623
$V_{38}$	0.8780	0.8890	0.9782	1.0100	0.9702	0.9818	0.9763	1.0077	0.8543
$\phi_{38}$	-0.2790	-0.2832	-0.2866	-0.2774	-0.3123	-0.2946	-0.2846	-0.2665	-0.3691
$V_{39}$	0.7345	0.5680	0.9003	0.9695	0.8847	0.9078	0.9263	0.9744	0.7877
$\phi_{39}$	-0.0535	-0.0115	-0.1054	-0.1515	-0.1089	-0.1212	-0.1389	-0.1463	0.1293

its kinetic and potential energy components and also of the components of the potential energy function,  $W_2$  for all these examples except examples 2-d)(i) and 2-i)(i) are shown in Figs. 3.22-3.41 for stable and unstable conditions.

The variation of total energy and its kinetic energy component obtained using the proposed SPEF and the SPEF given in Chapter 2 are compared for stable and unstable cases and is presented as follows :

Figs. 3.4 and 3.5      for example 1-a)(i)  
 Figs. 3.22 and 3.23    for example 2-a)(i)  
 Figs. 3.26 and 3.27    for example 2-b)(i)  
 Figs. 3.30 and 3.31    for example 2-e)(i)  
 Figs. 3.34 and 3.35    for example 2-f)(i)  
 Figs. 3.38 and 3.39    for example 2-a)(ii)

### 3.5.3 Discussion

It is observed from Tables 3.1 - 3.4 that the consideration of the mode of instability in defining the kinetic energy responsible for system separation, results in improvement (although slight) in the predicted values of critical clearing time in, practically, all the cases. The notable exception is the 10-machine system for fault at bus 10 (example 2-i)(i)). However, it is interesting to note that machine 10 does not accelerate.

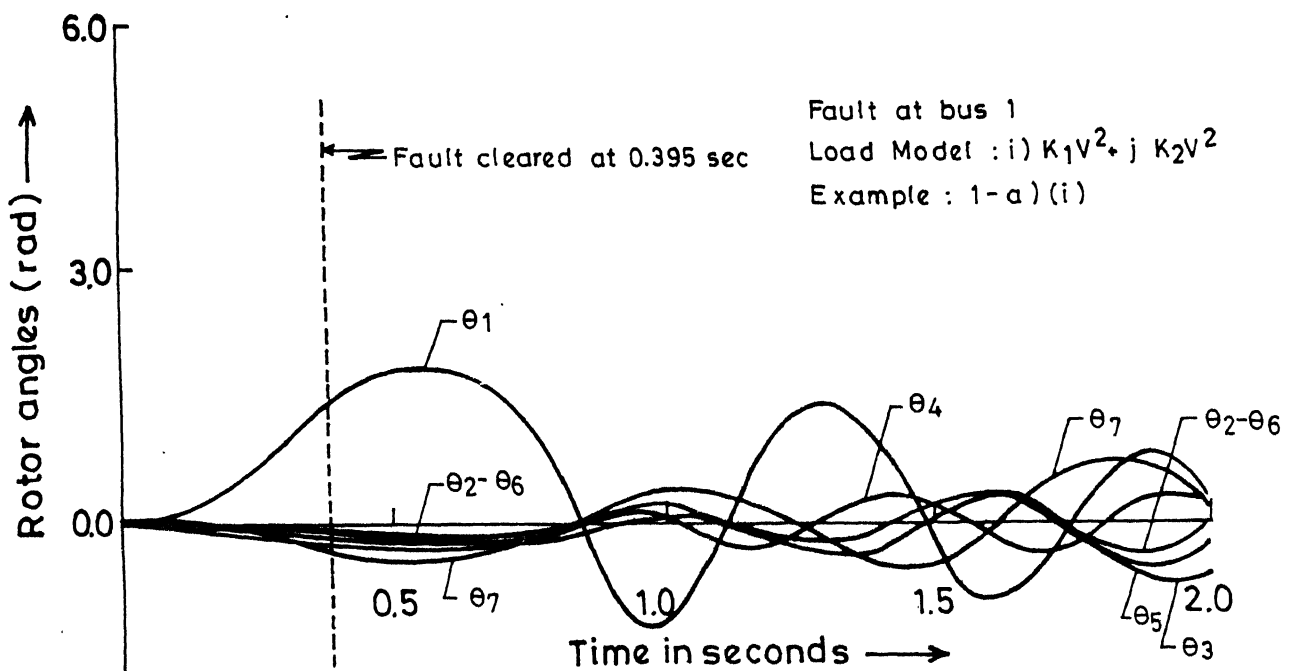


FIG.3.2 SWING CURVES FOR 7-MACHINE SYSTEM, STABLE CASE

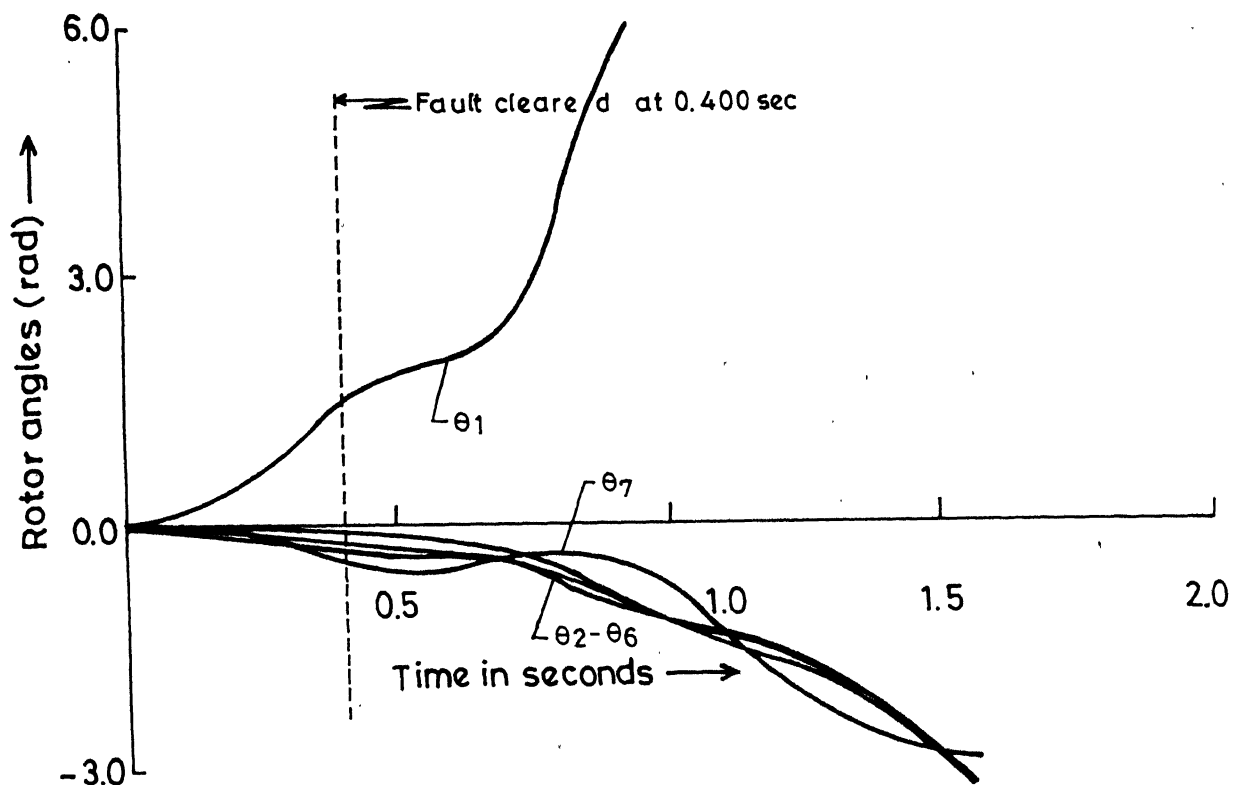


FIG.3.3 SWING CURVES FOR 7-MACHINE SYSTEM, UNSTABLE CASE

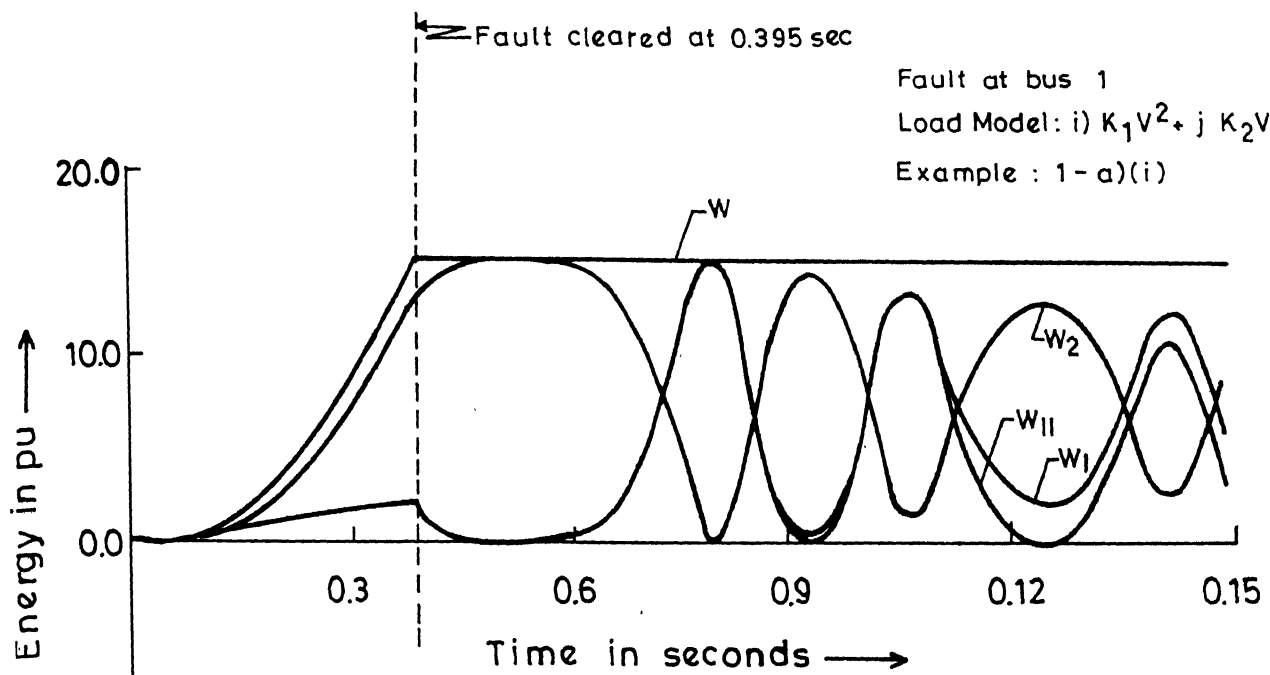


FIG.3.4 VARIATION OF TOTAL ENERGY AND ITS COMPONENTS FOR 7-MACHINE SYSTEM, STABLE CASE

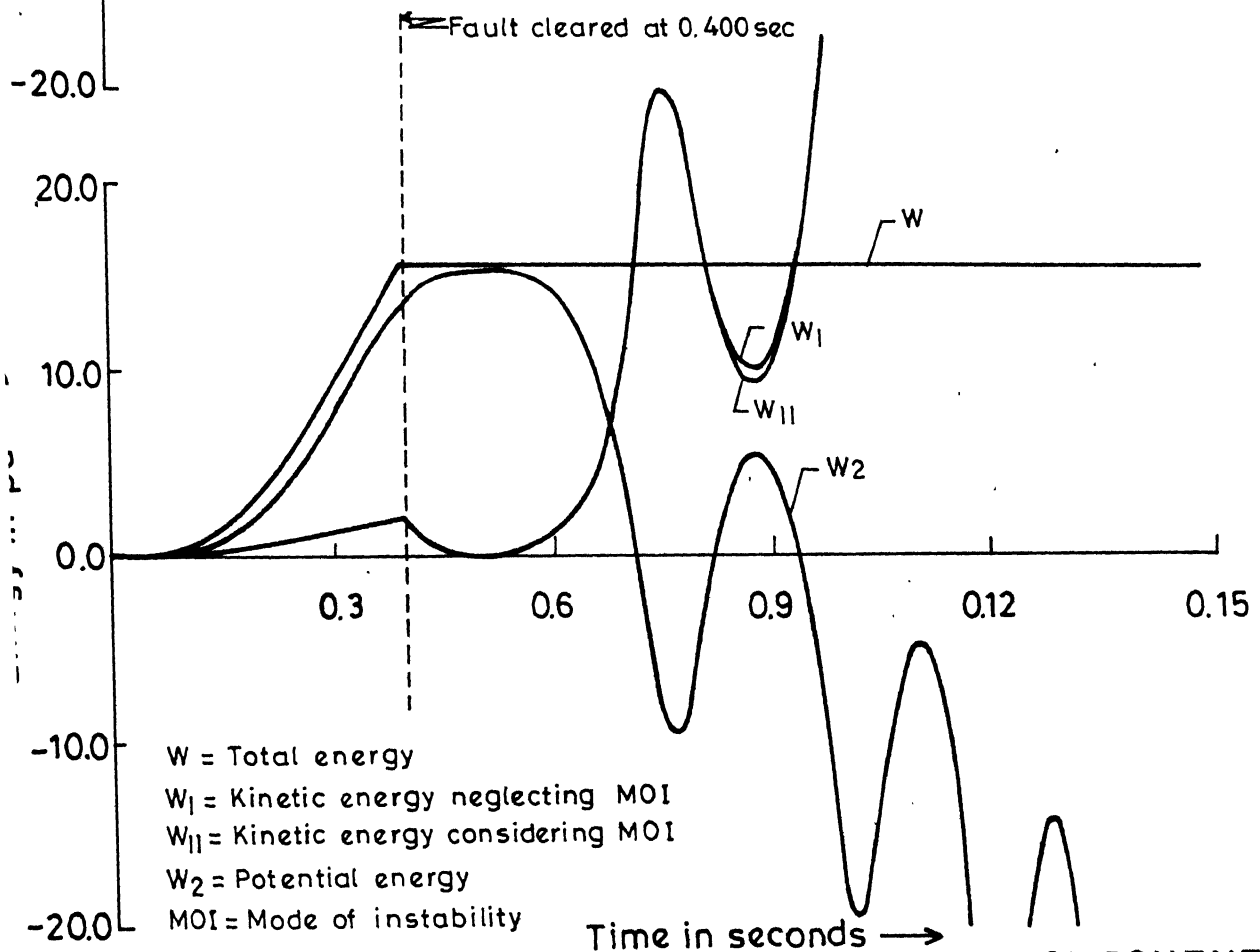


FIG.3.5 VARIATION OF TOTAL ENERGY AND ITS COMPONENTS FOR 7-MACHINE SYSTEM, UNSTABLE CASE

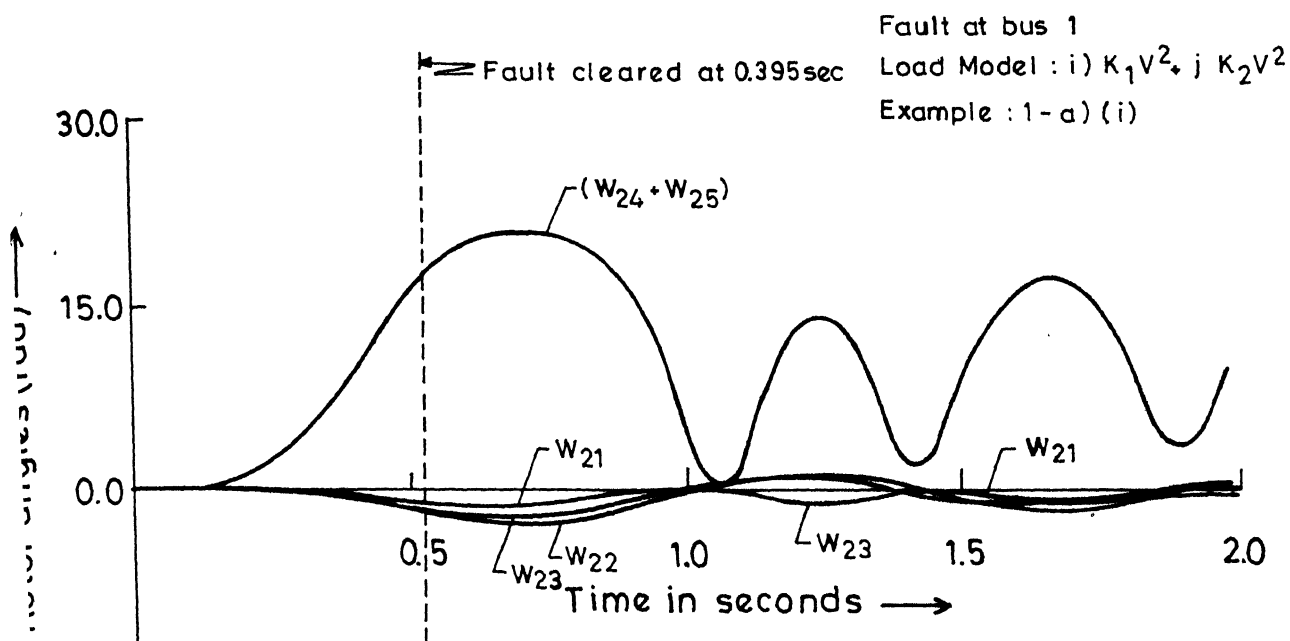


FIG.3.6 VARIATION OF THE COMPONENTS OF POTENTIAL ENERGY FOR 7-MACHINE SYSTEM, STABLE CASE

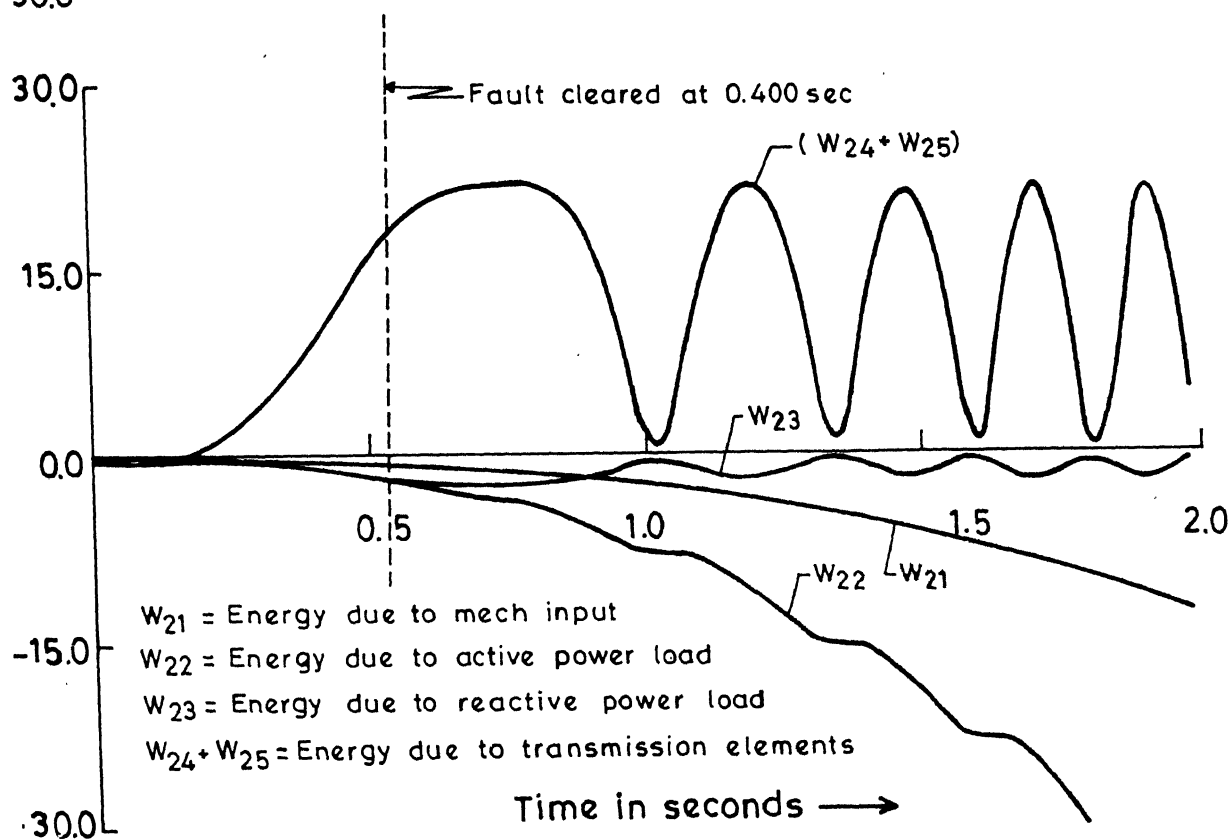


FIG.3.7 VARIATION OF THE COMPONENTS OF POTENTIAL ENERGY FOR 7-MACHINE SYSTEM, UNSTABLE CASE

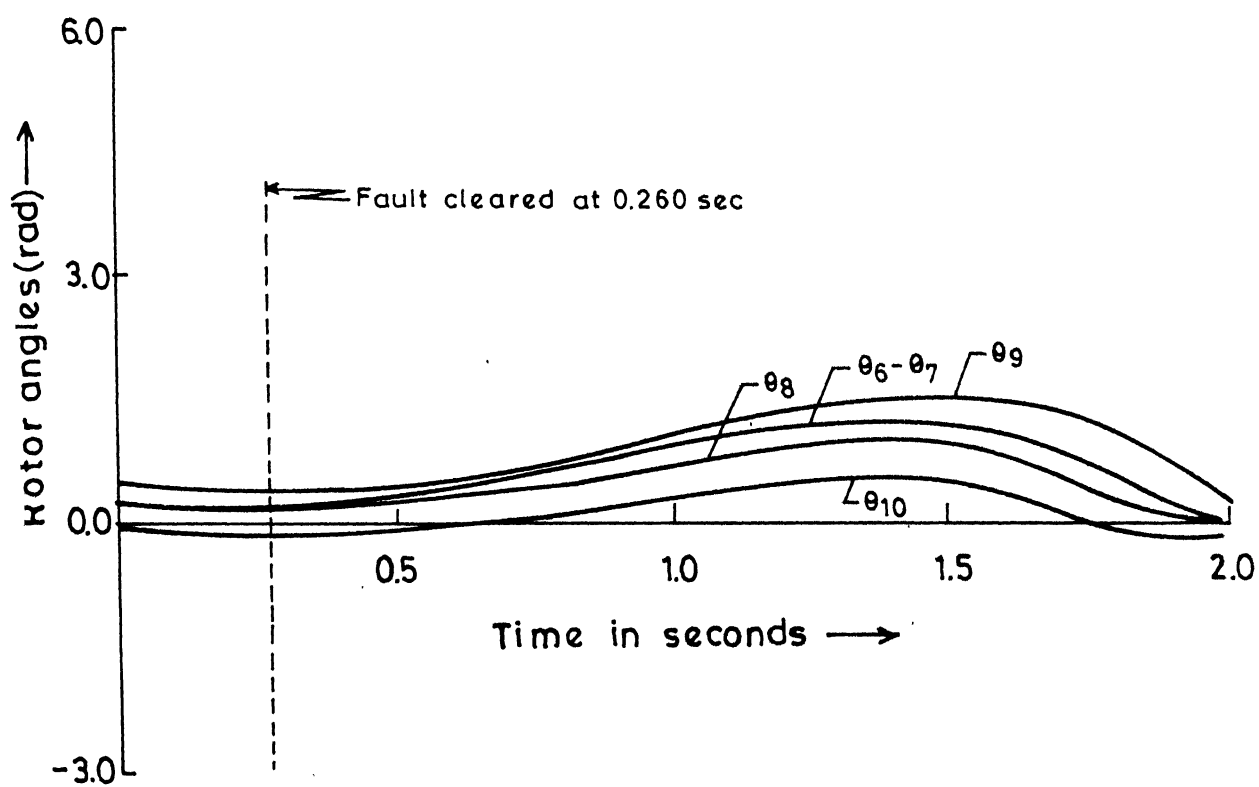
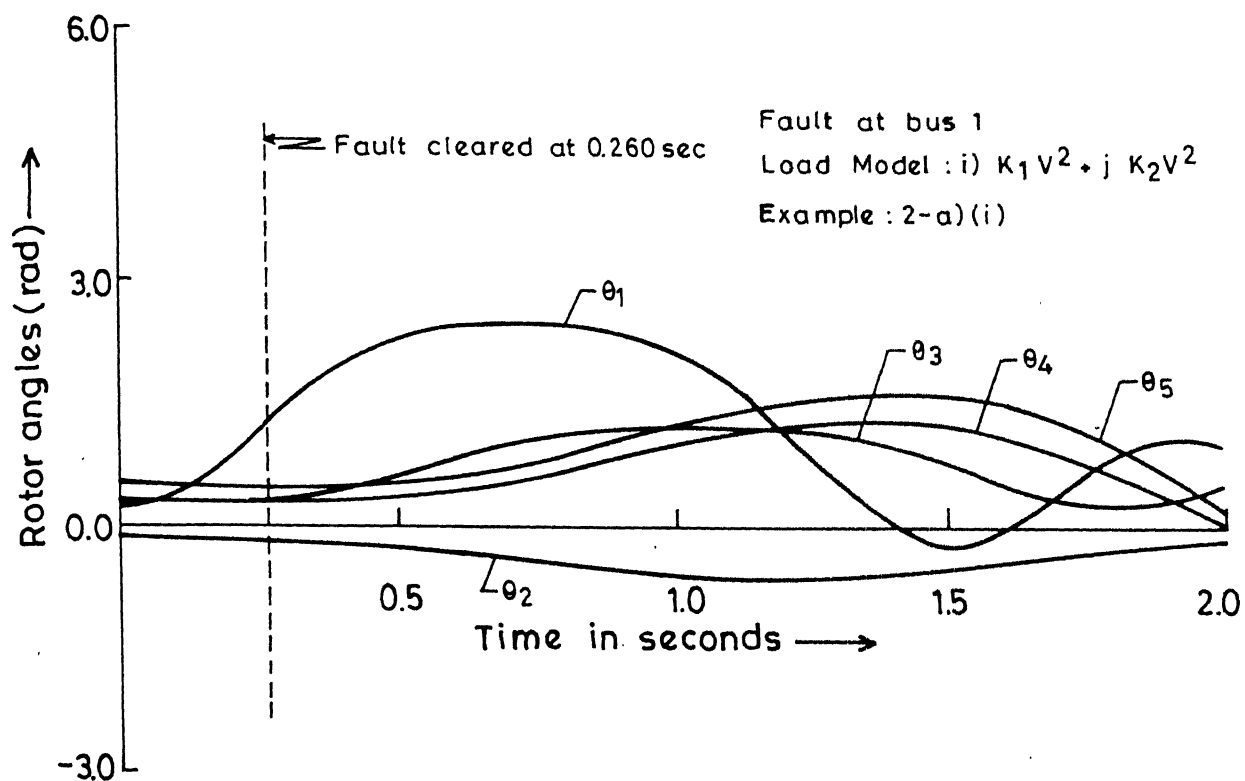


FIG.3.8 SWING CURVES FOR 10-MACHINE SYSTEM, STABLE CASE

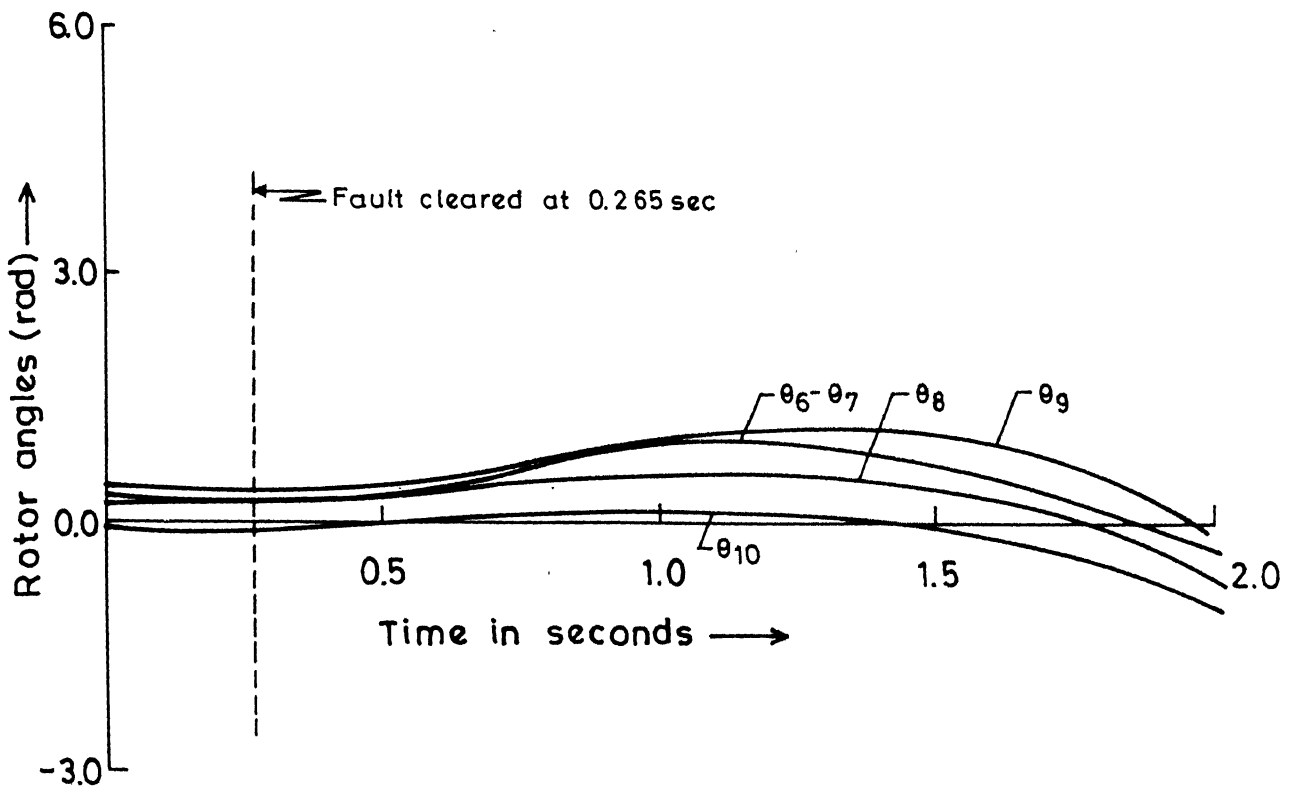
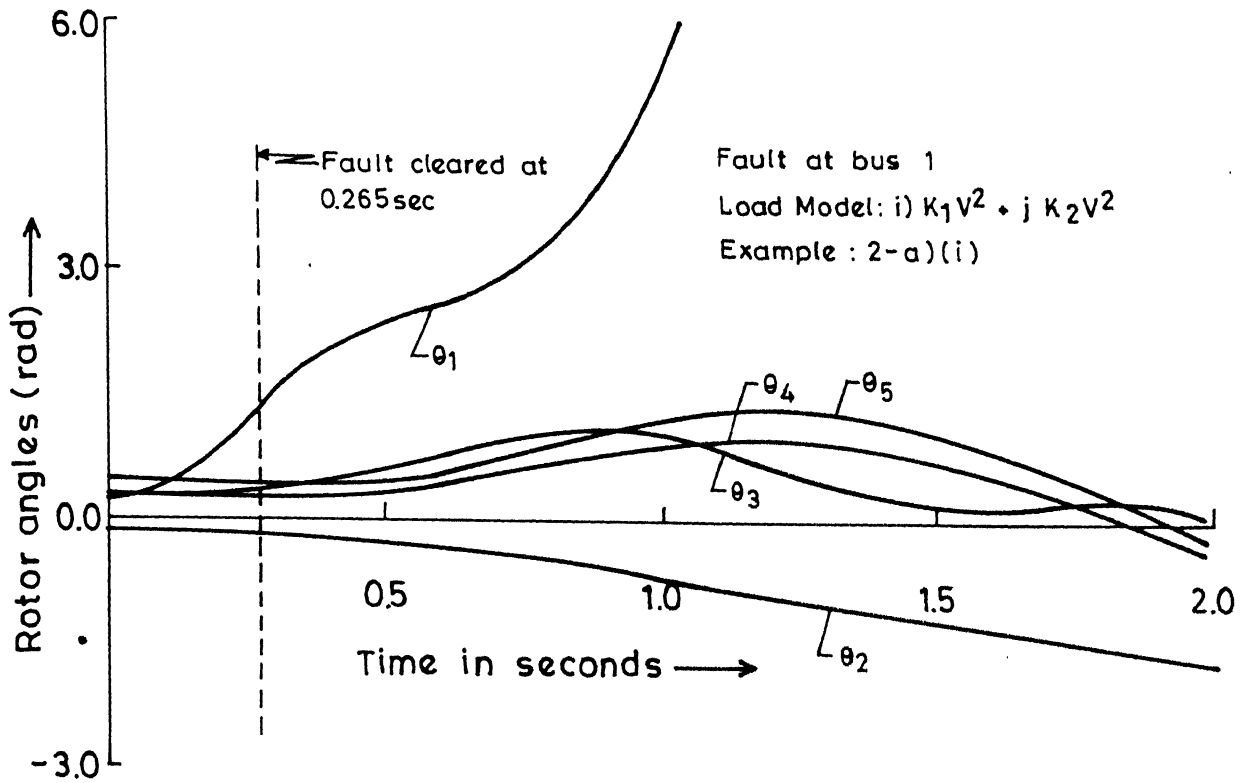


FIG.3.9 SWING CURVES FOR 10-MACHINE SYSTEM, UNSTABLE CASE

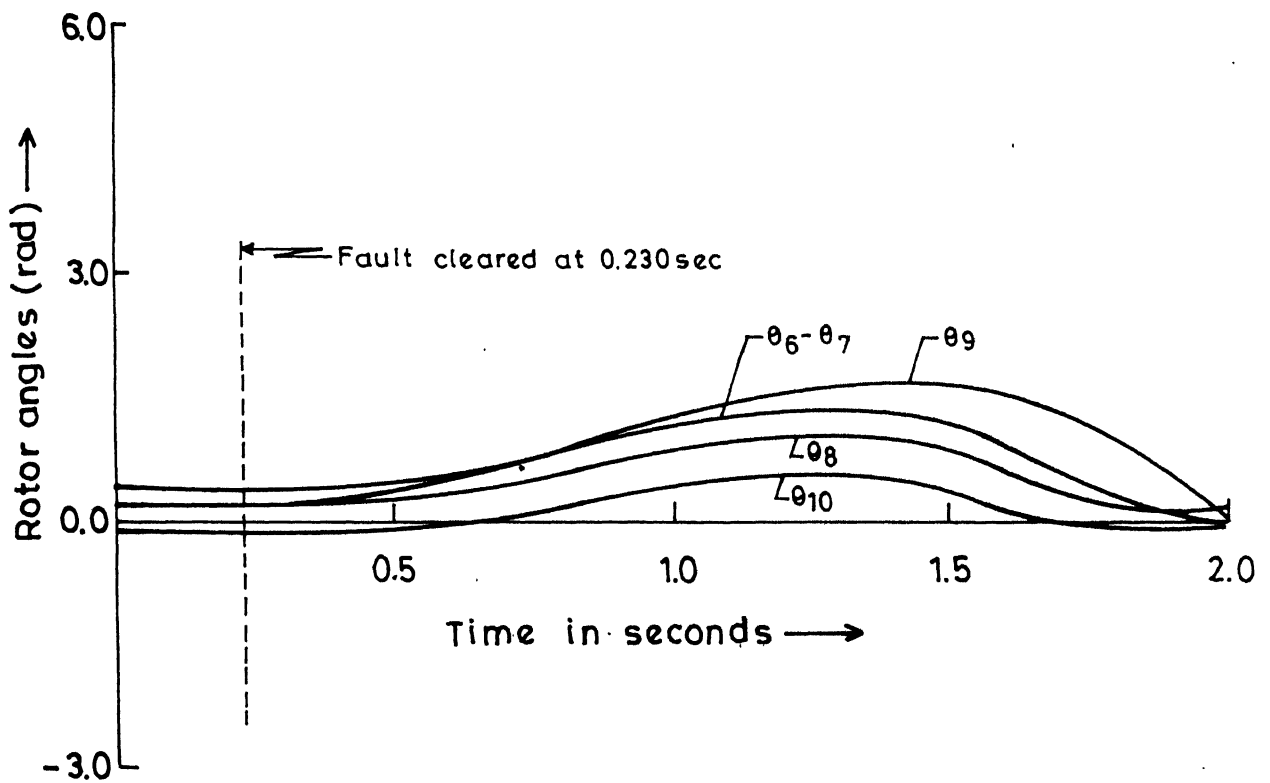
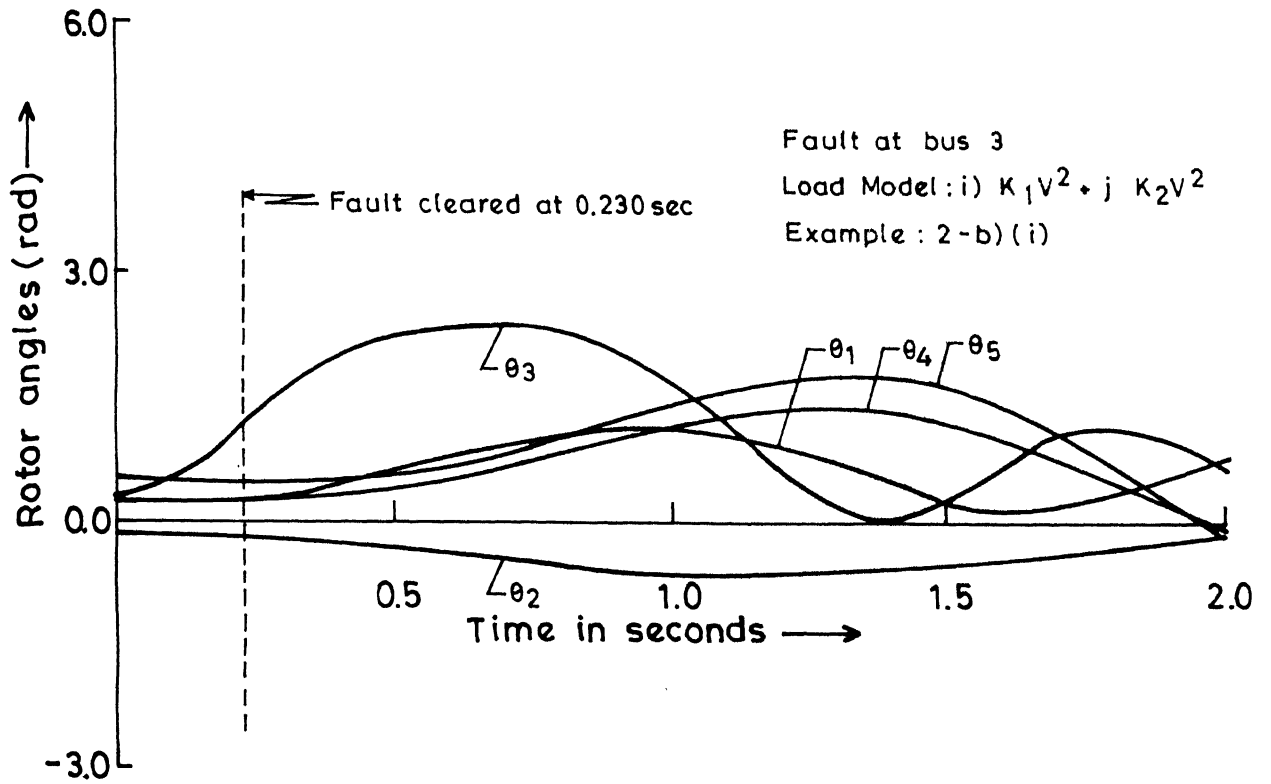


FIG.3.10 SWING CURVES FOR 10-MACHINE SYSTEM, STABLE CASE

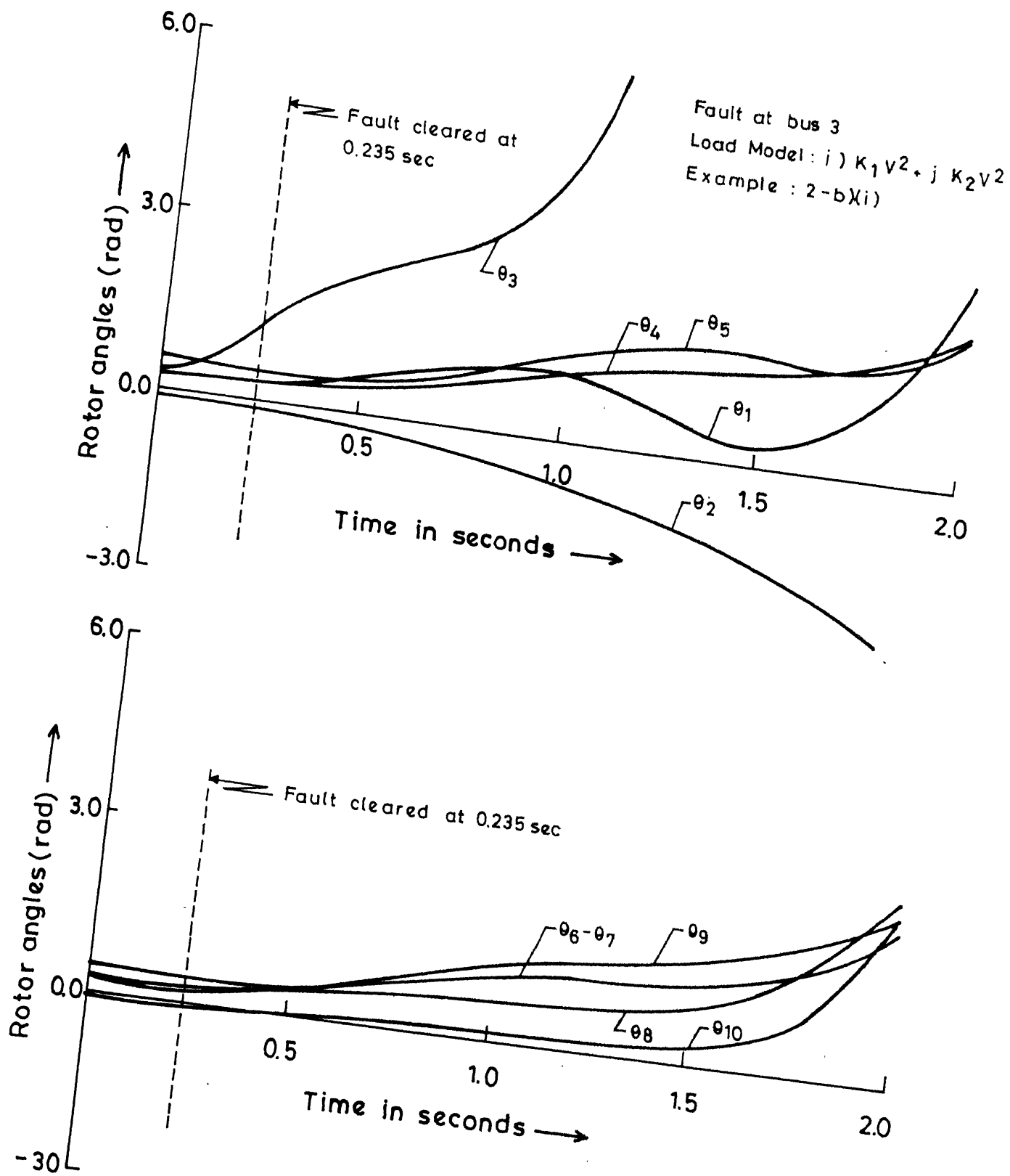


FIG.3.11 SWING CURVES FOR 10-MACHINE SYSTEM, UNSTABLE CASE

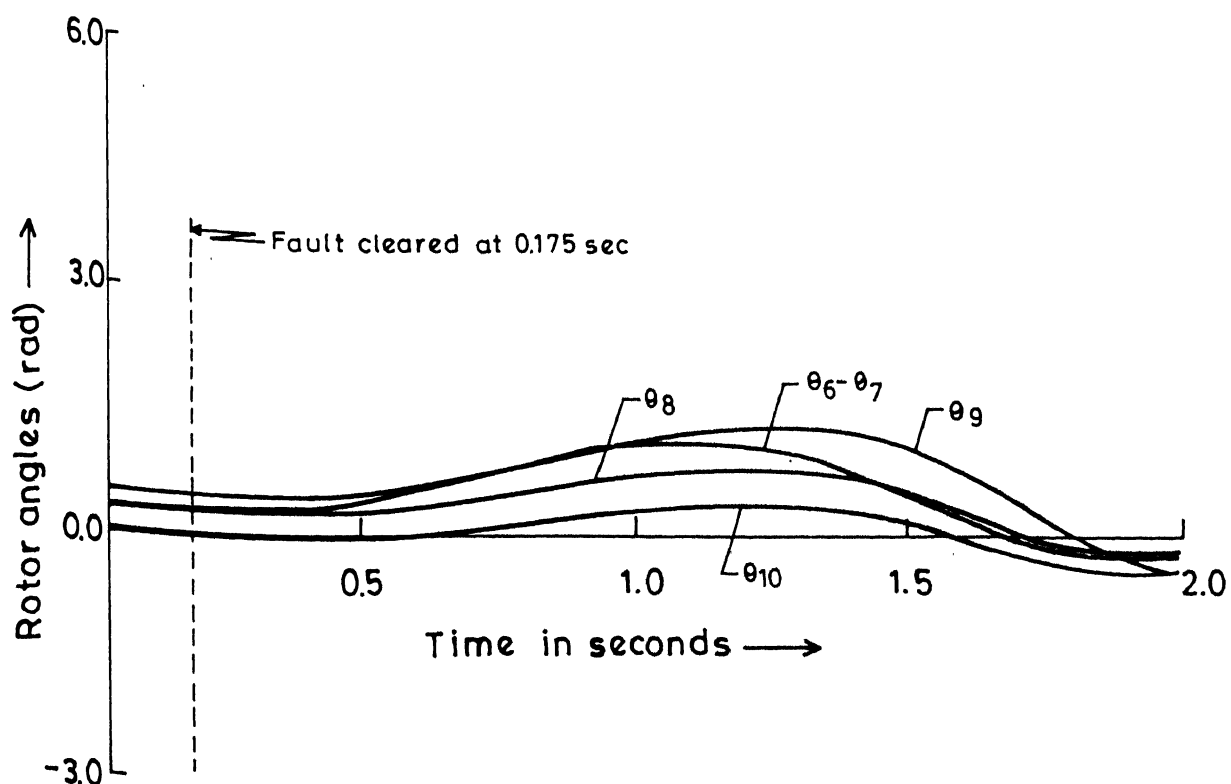
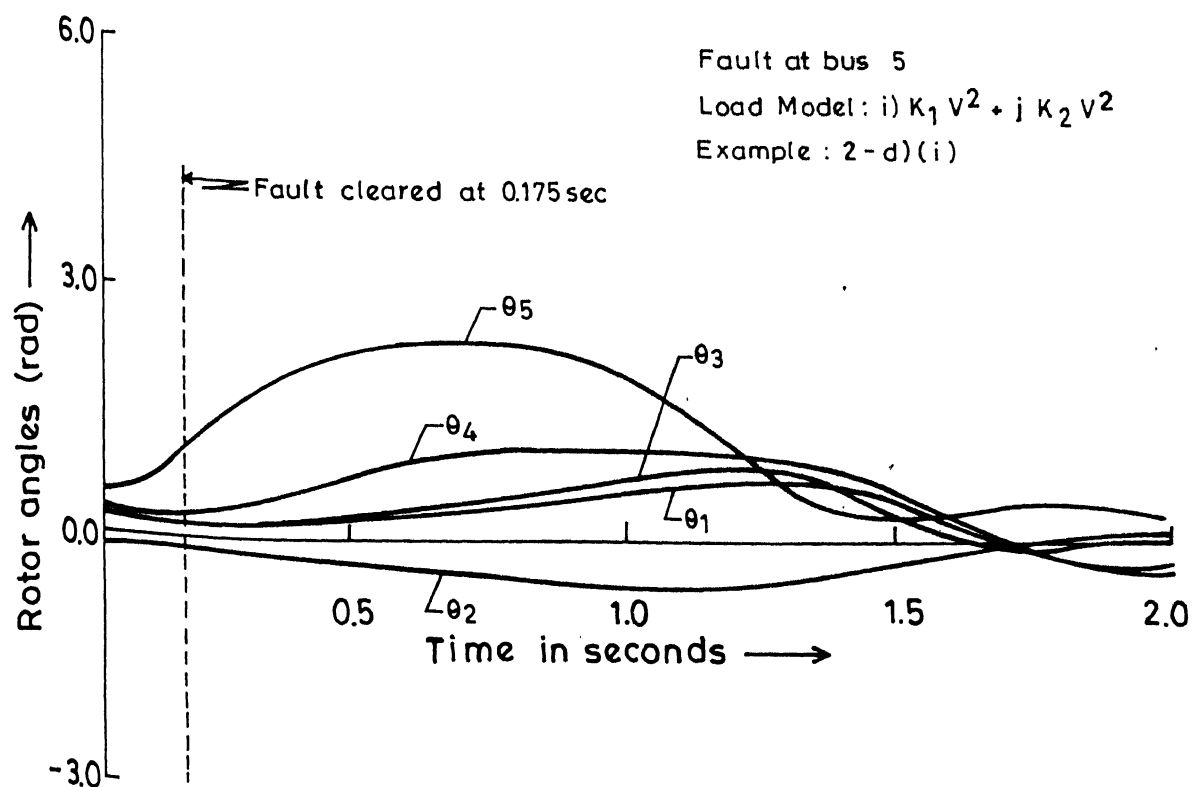


FIG.3.12 SWING CURVES FOR 10 - MACHINE SYSTEM, STABLE CASE

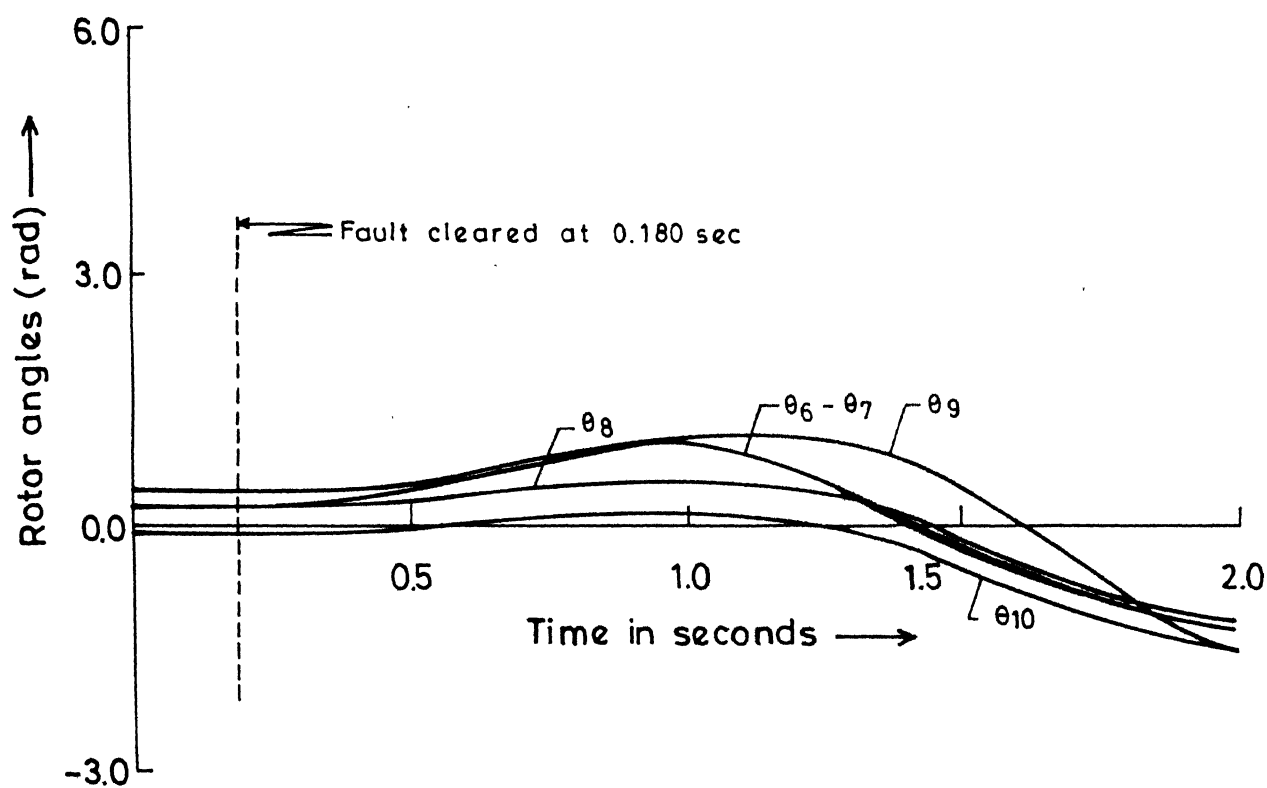
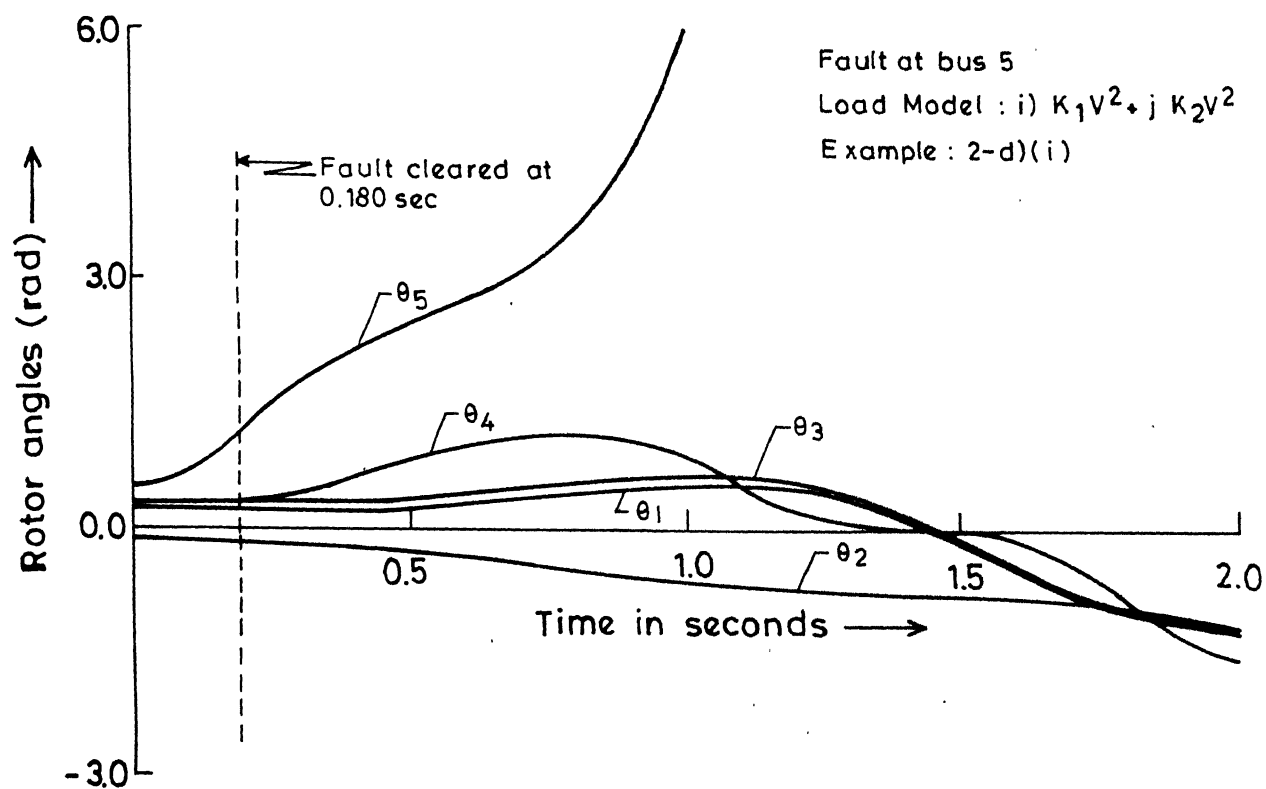


FIG.3.13 SWING CURVES FOR 10-MACHINE SYSTEM, UNSTABLE CASE

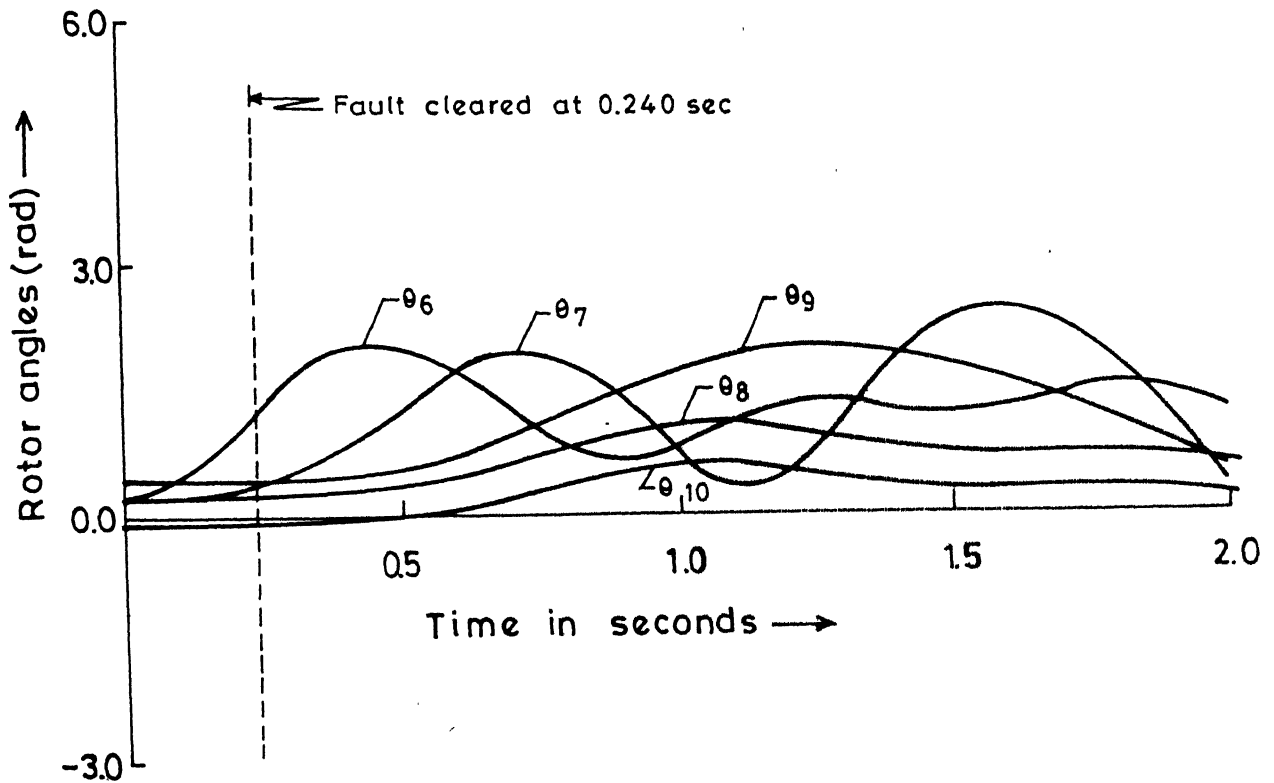
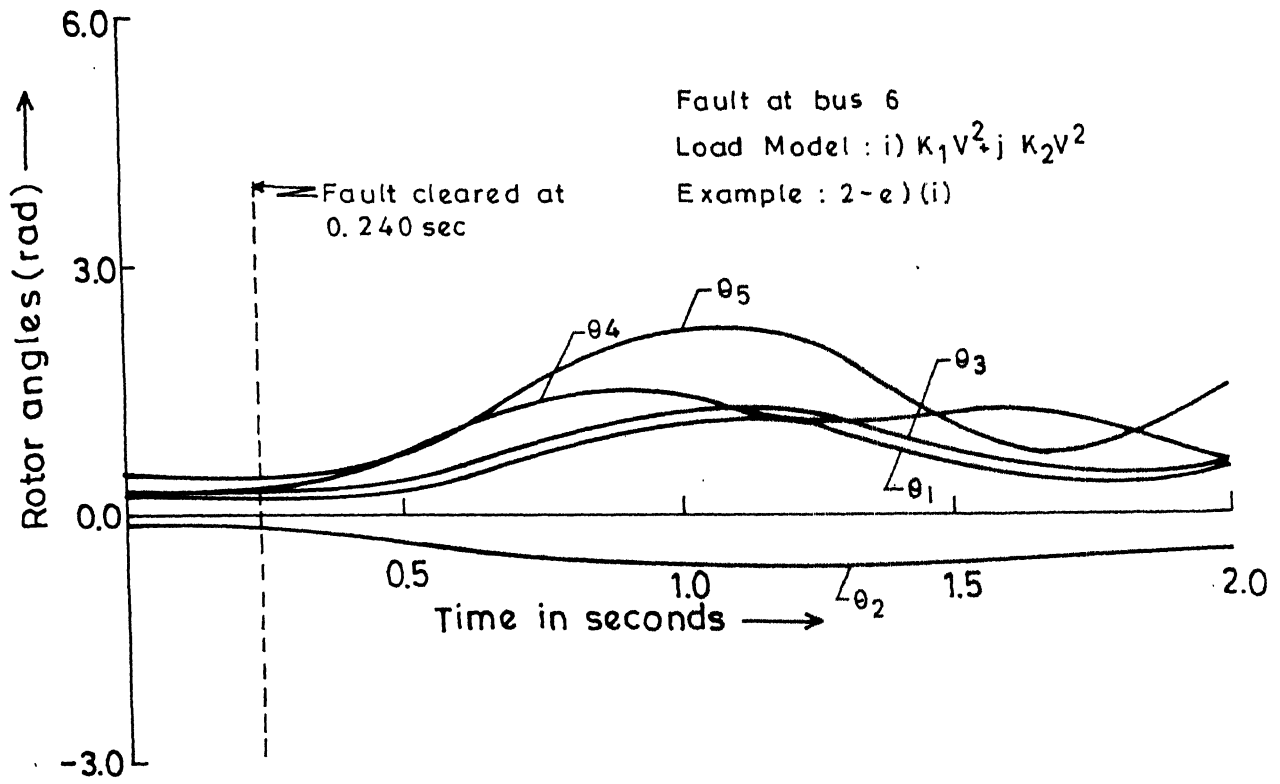


FIG. 3.14 SWING CURVES FOR 10-MACHINE SYSTEM, STABLE CASE

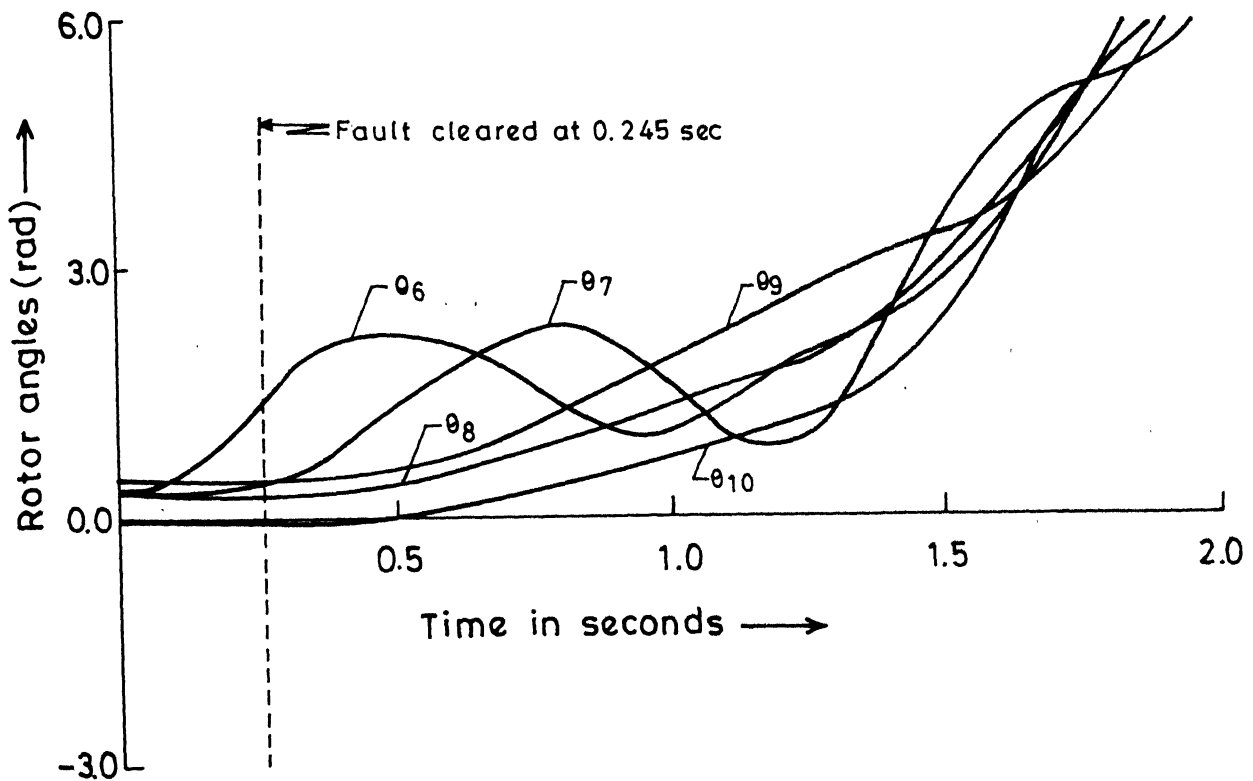
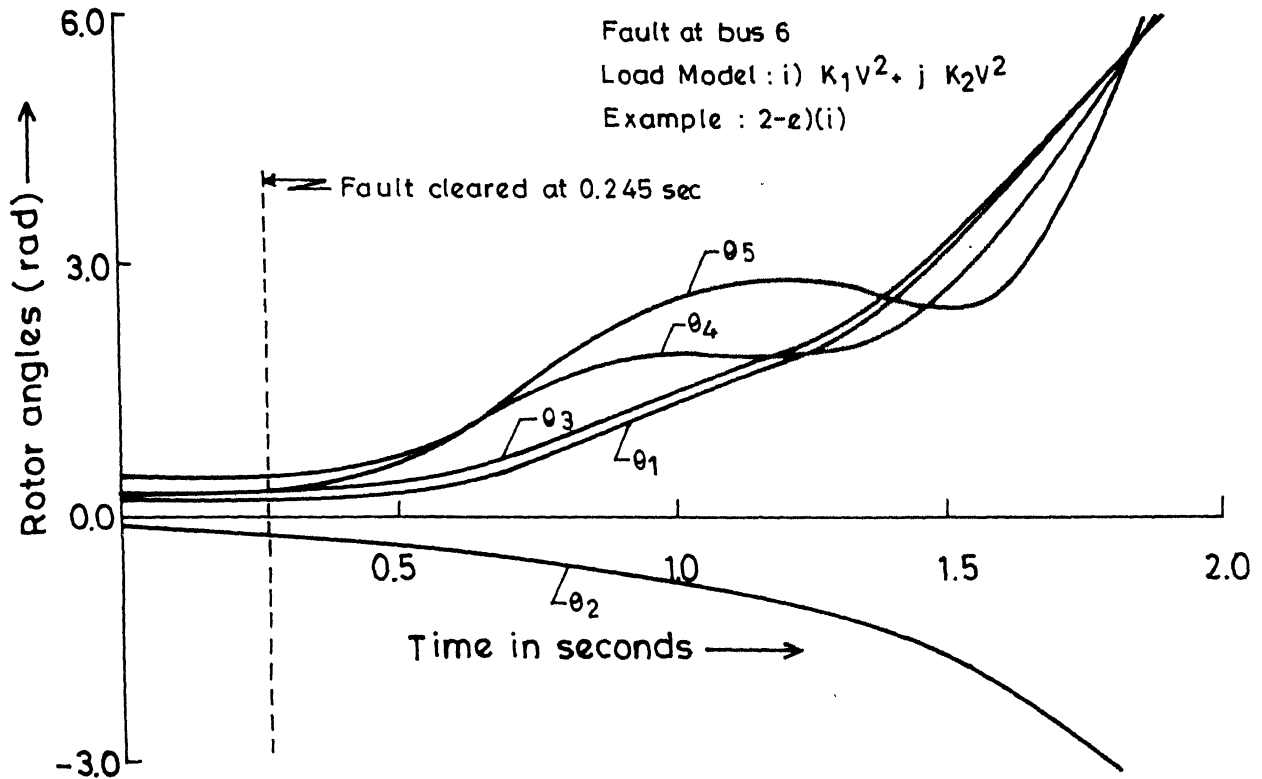


FIG.3.15 SWING CURVES FOR 10-MACHINE SYSTEM, UNSTABLE CASE

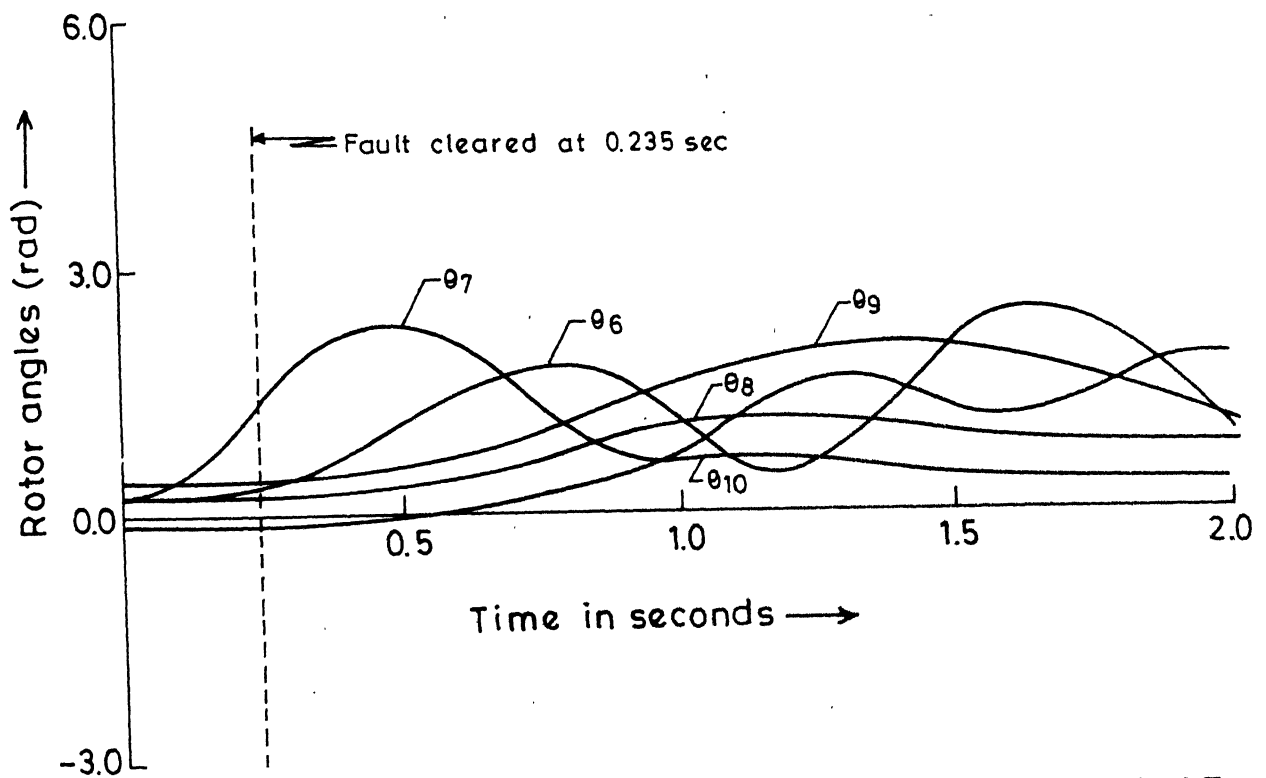
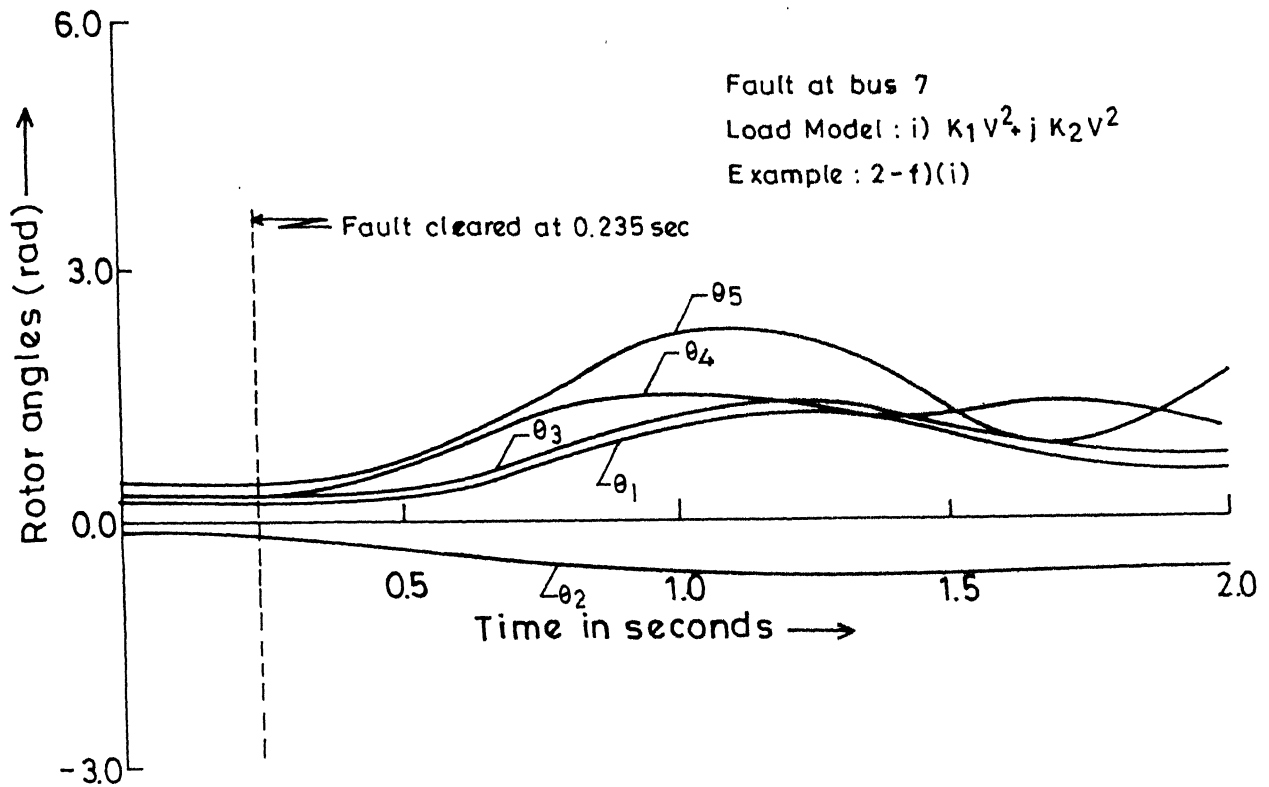


FIG.3.16 SWING CURVES FOR 10-MACHINE SYSTEM, STABLE CASE

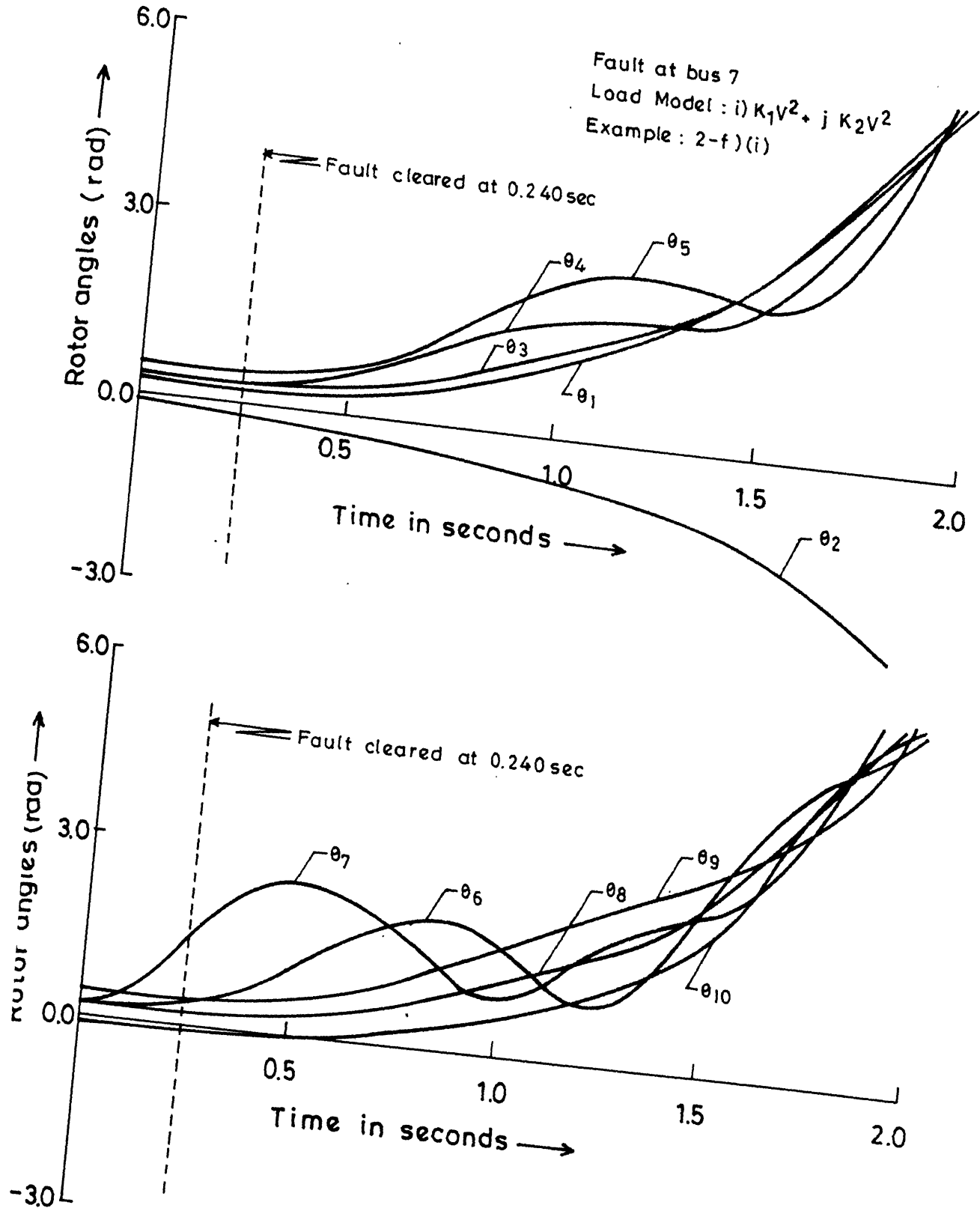


FIG.3.17 SWING CURVES FOR 10-MACHINE SYSTEM, UNSTABLE CASE

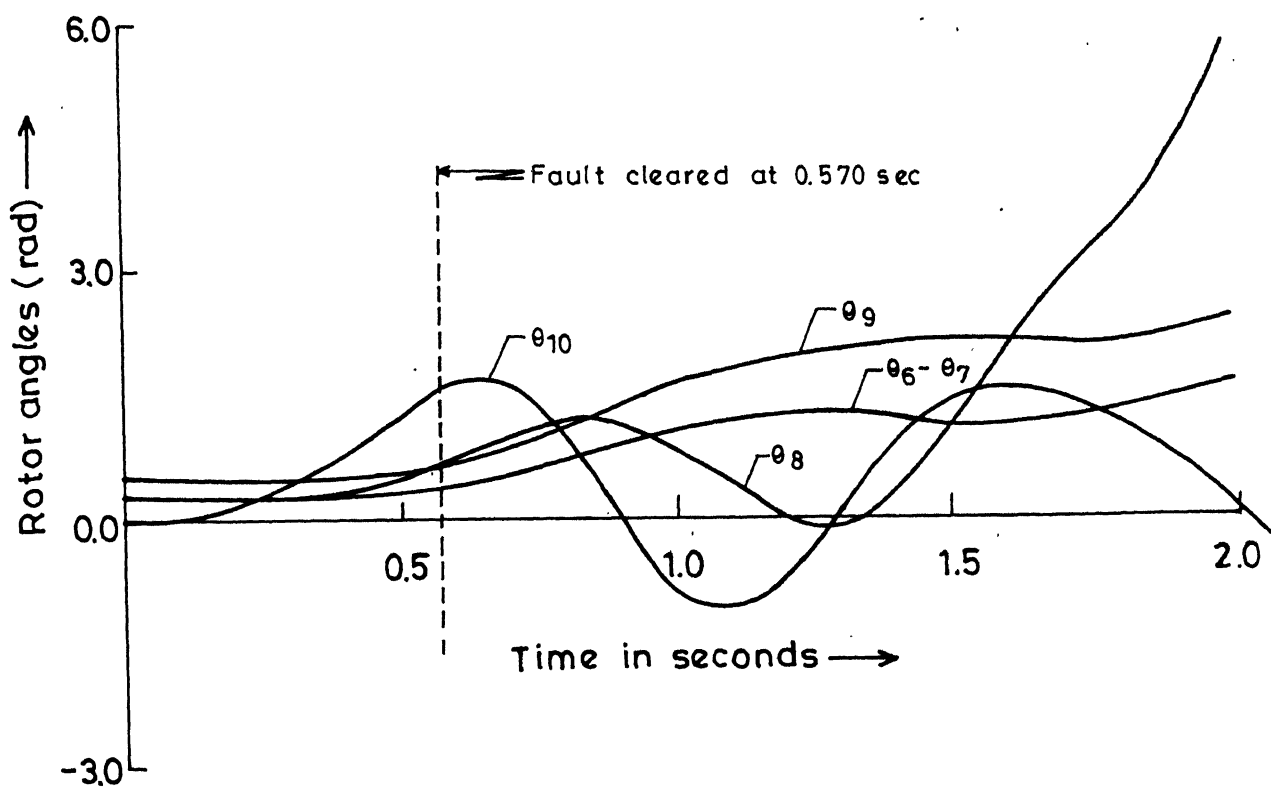
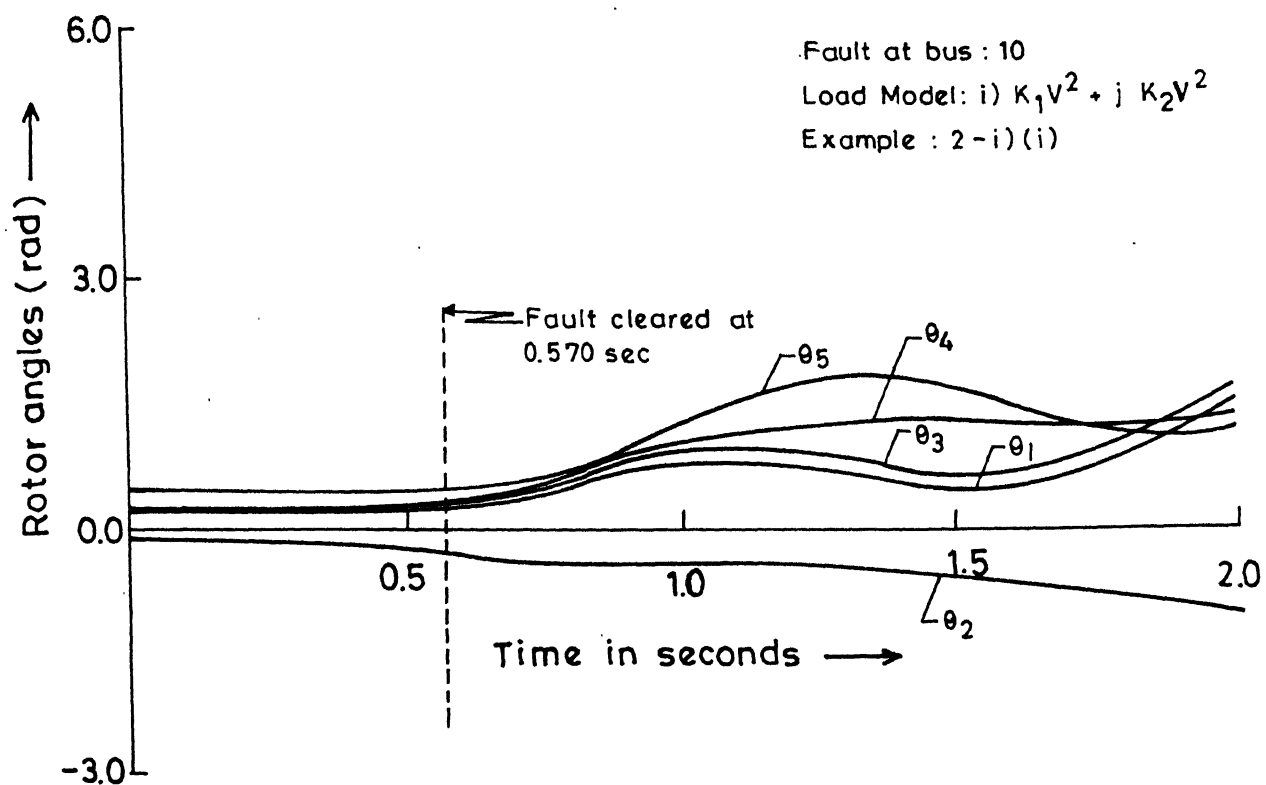


FIG. 3.18 SWING CURVES FOR 10-MACHINE SYSTEM, STABLE CAS

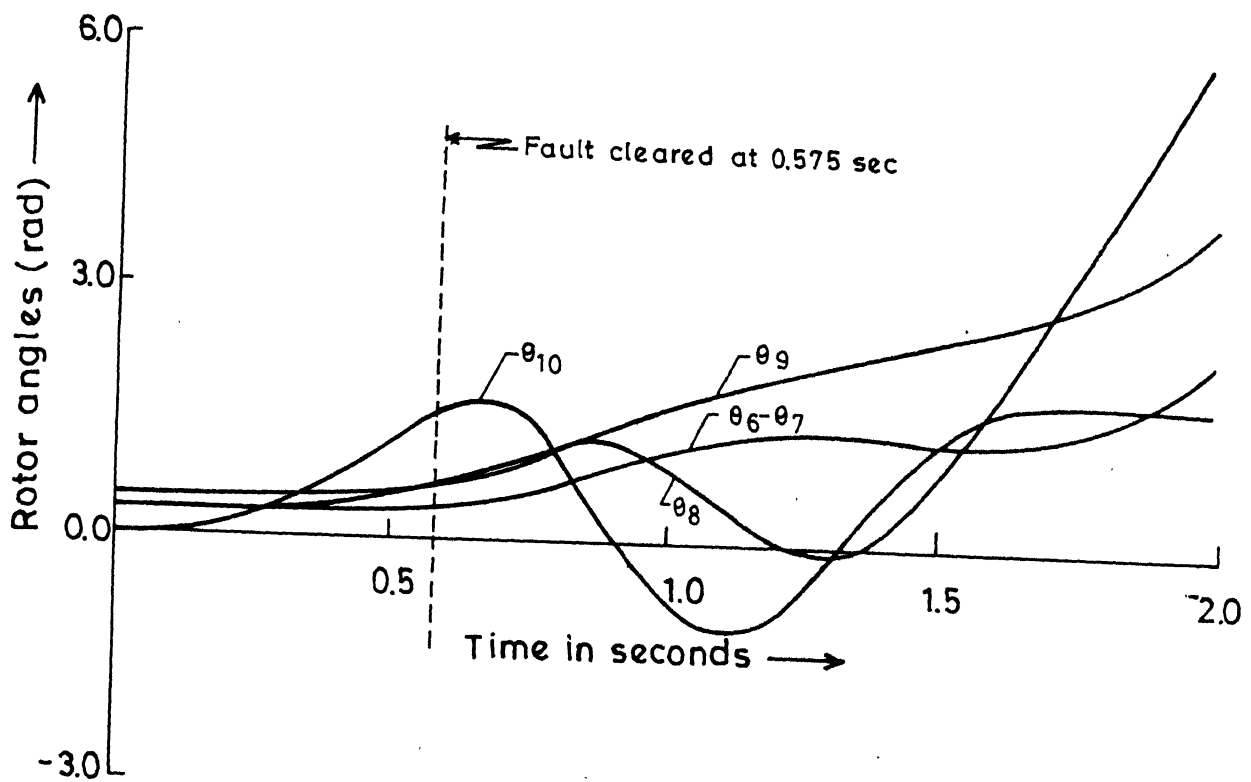
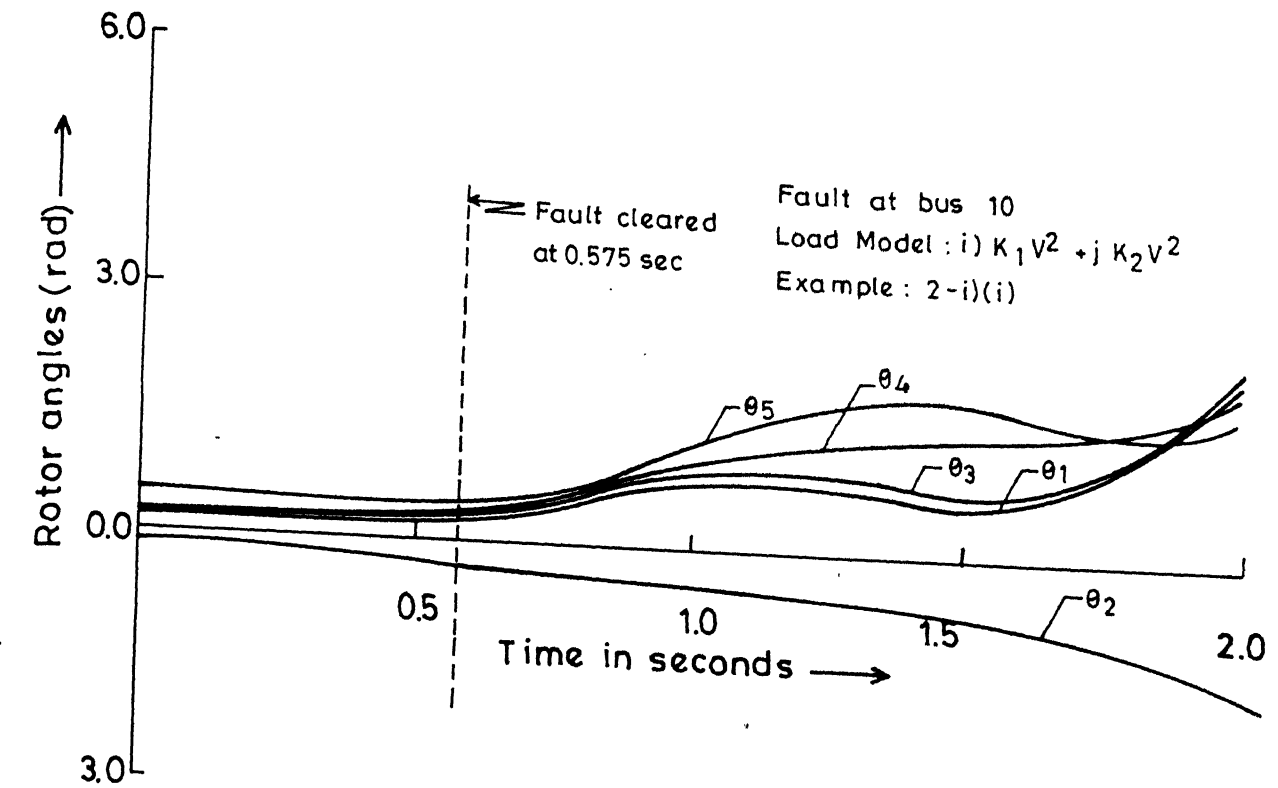


FIG. 3.19 SWING CURVES FOR 10-MACHINE SYSTEM, UNSTABLE CASE

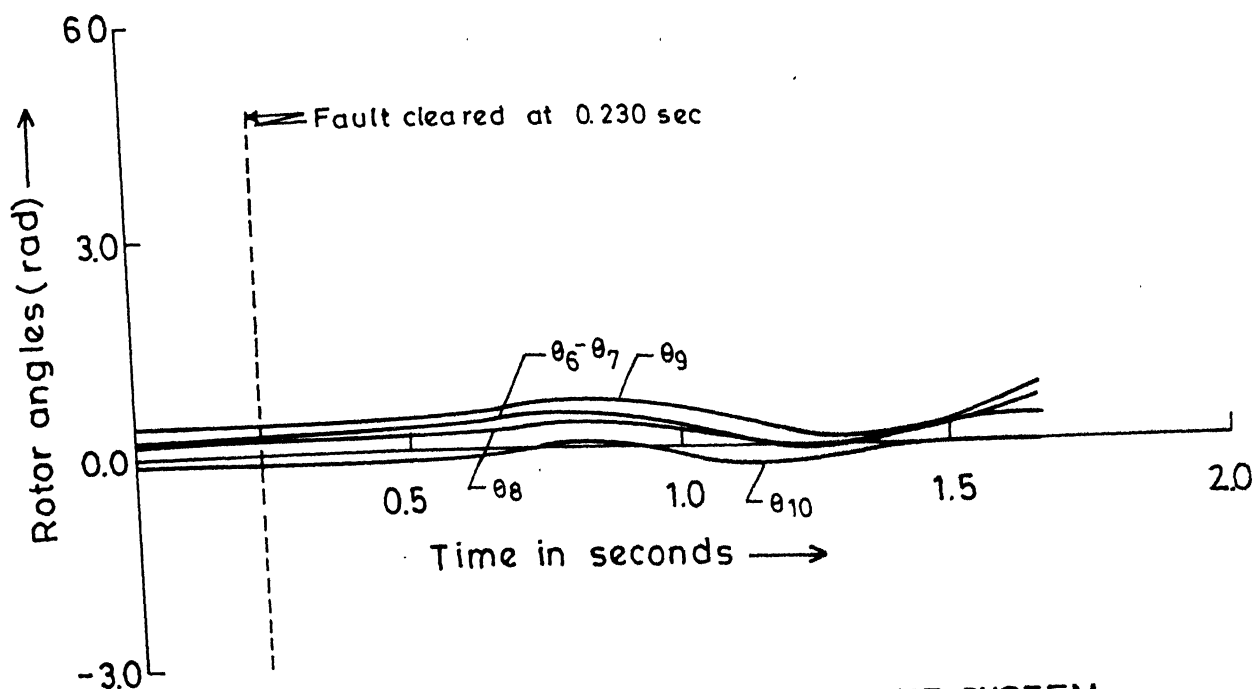
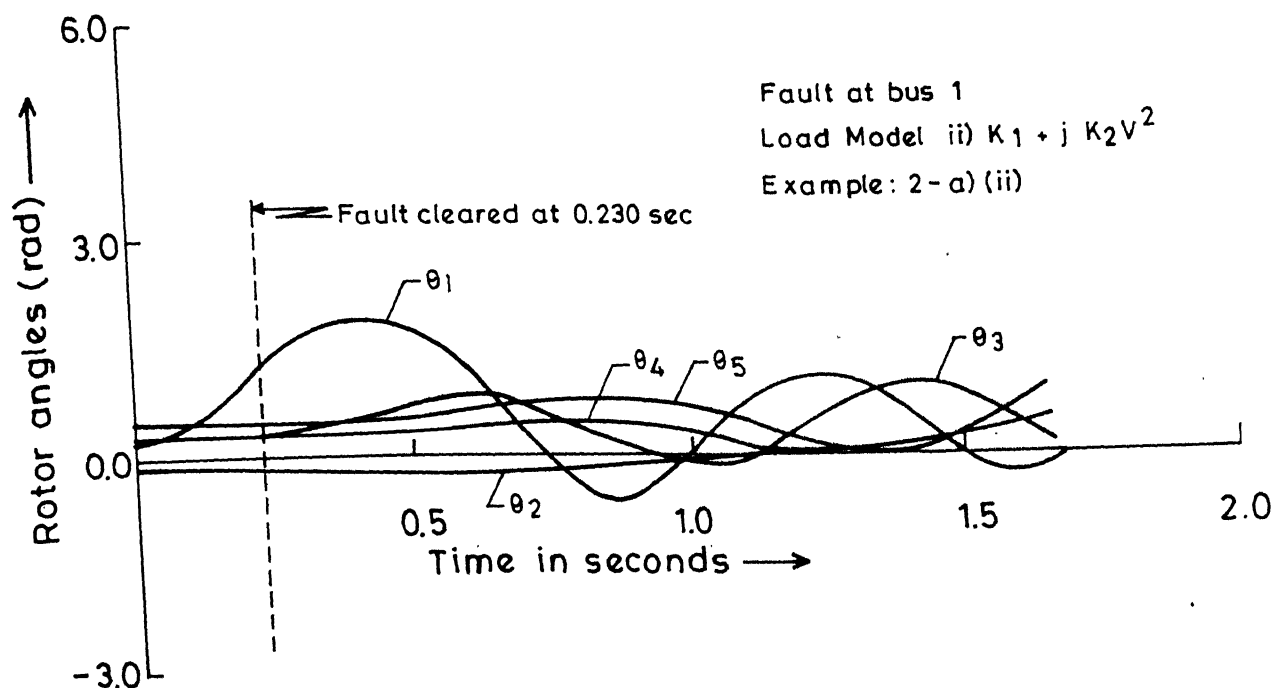


FIG.3.20 SWING CURVES FOR 10-MACHINE SYSTEM, STABLE CASE

Fault at bus 1

Load Model : ii)  $K_1 + j K_2 V^2$

Example : 2- a) (ii)

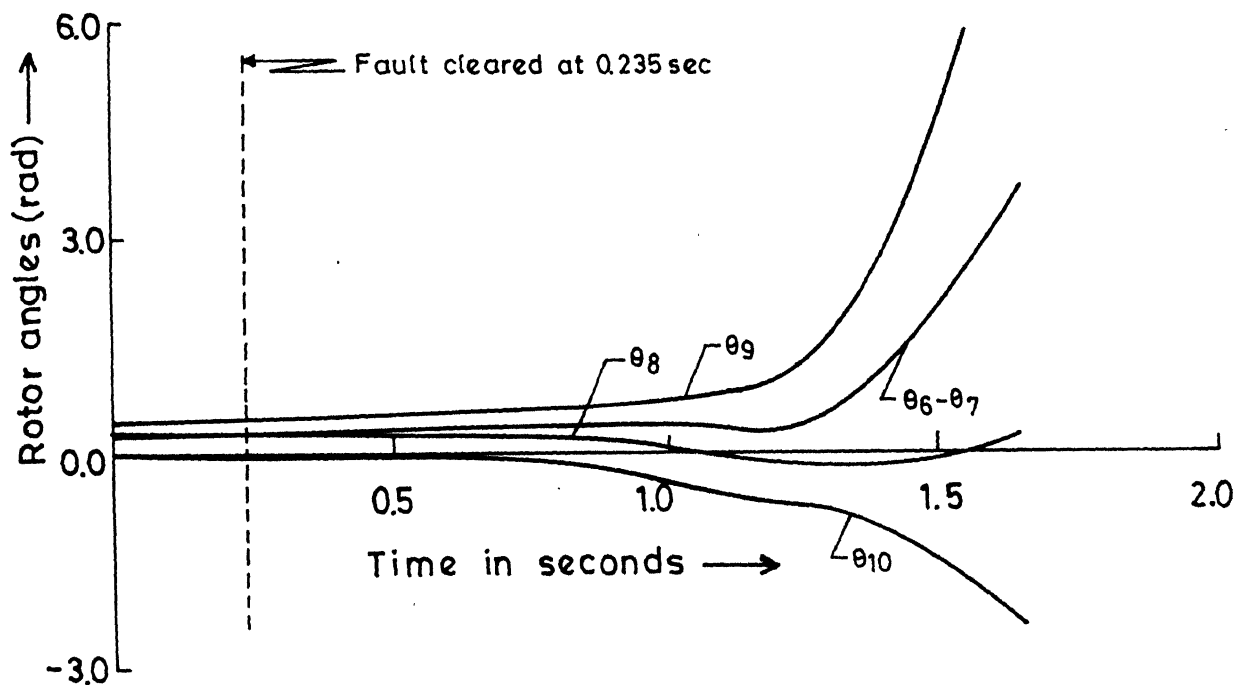
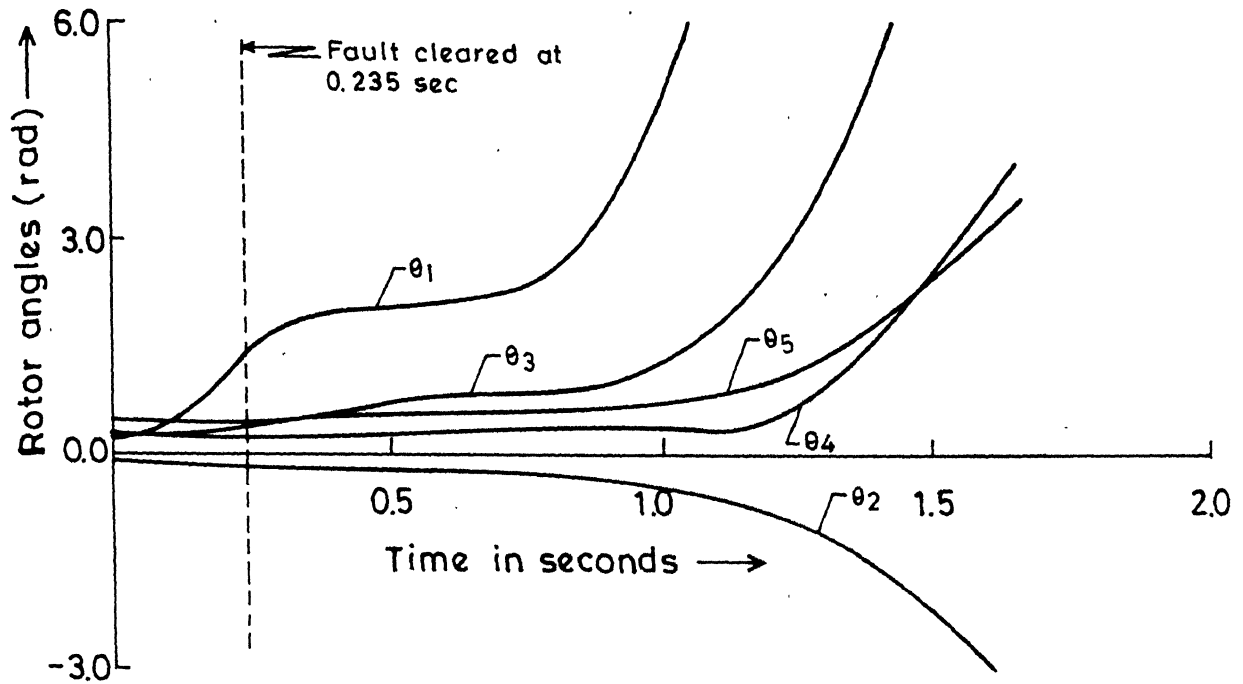


FIG. 3.21 SWING CURVES FOR 10-MACHINE SYSTEM,  
UNSTABLE CASE

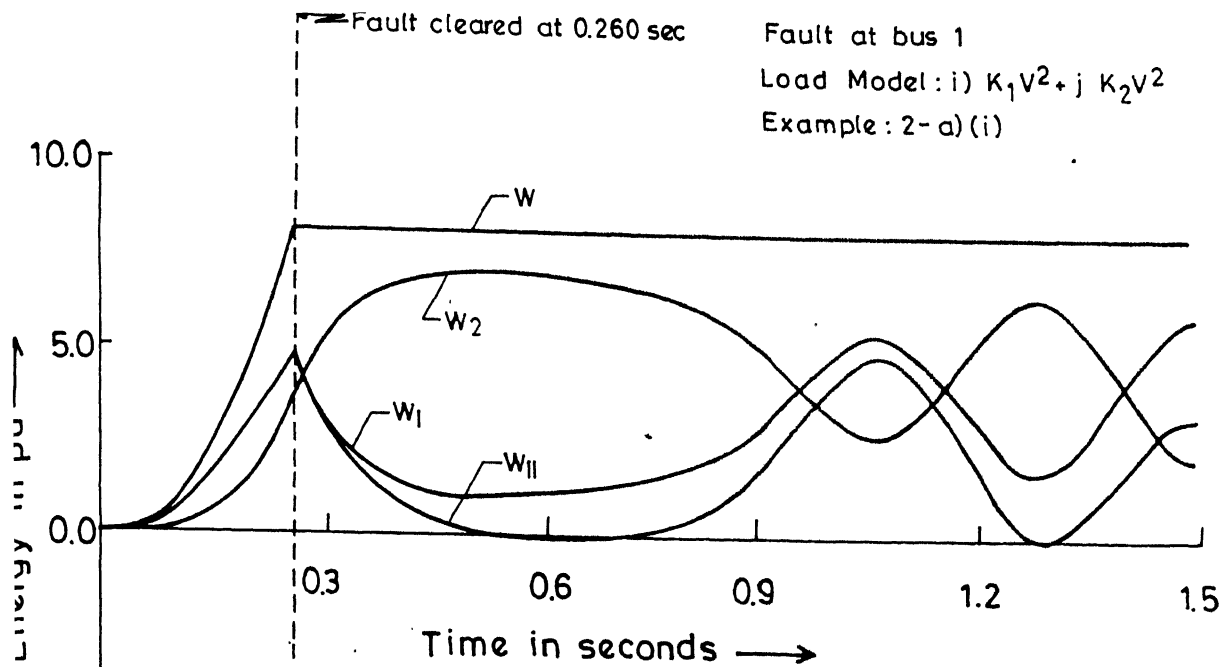


FIG.3.22 VARIATION OF TOTAL ENERGY AND ITS COMPONENTS FOR 10-MACHINE SYSTEM, STABLE CASE

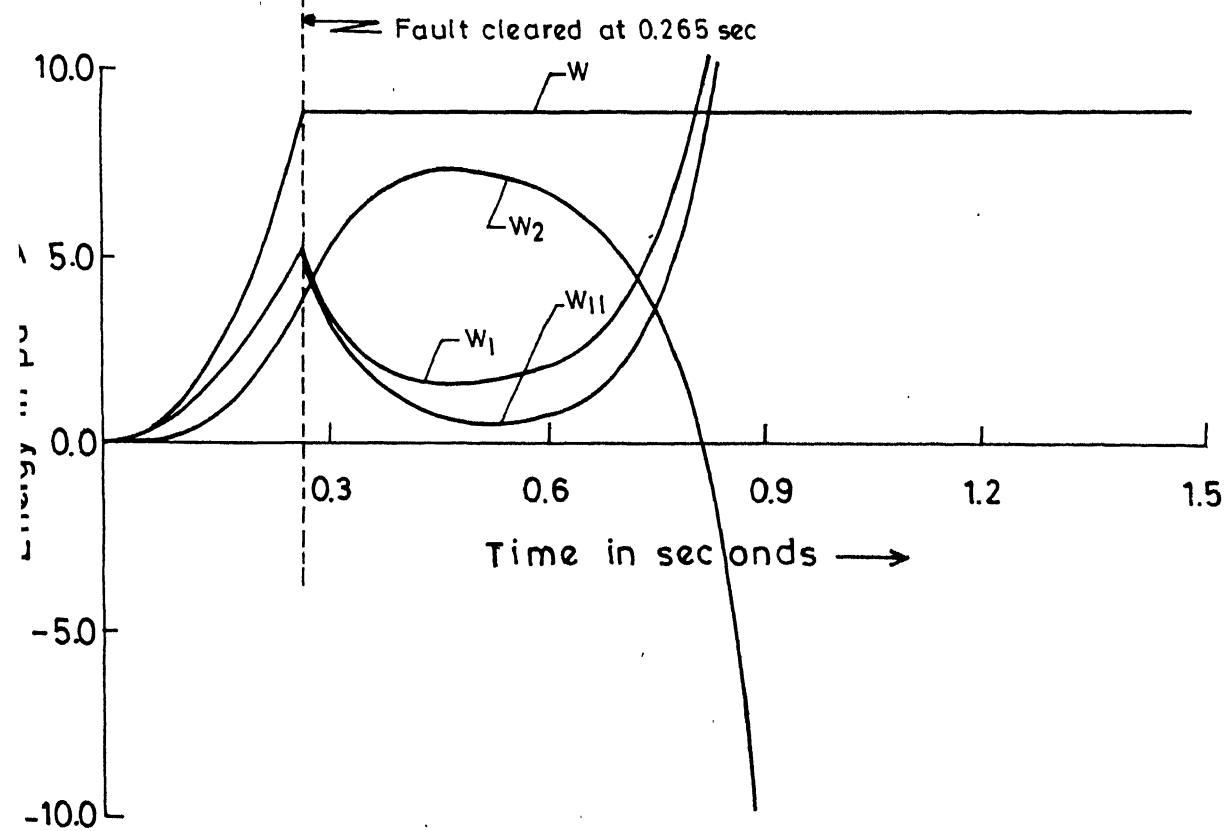


FIG.3.23 VARIATION OF TOTAL ENERGY AND ITS COMPONENTS FOR 10-MACHINE SYSTEM, UNSTABLE CASE

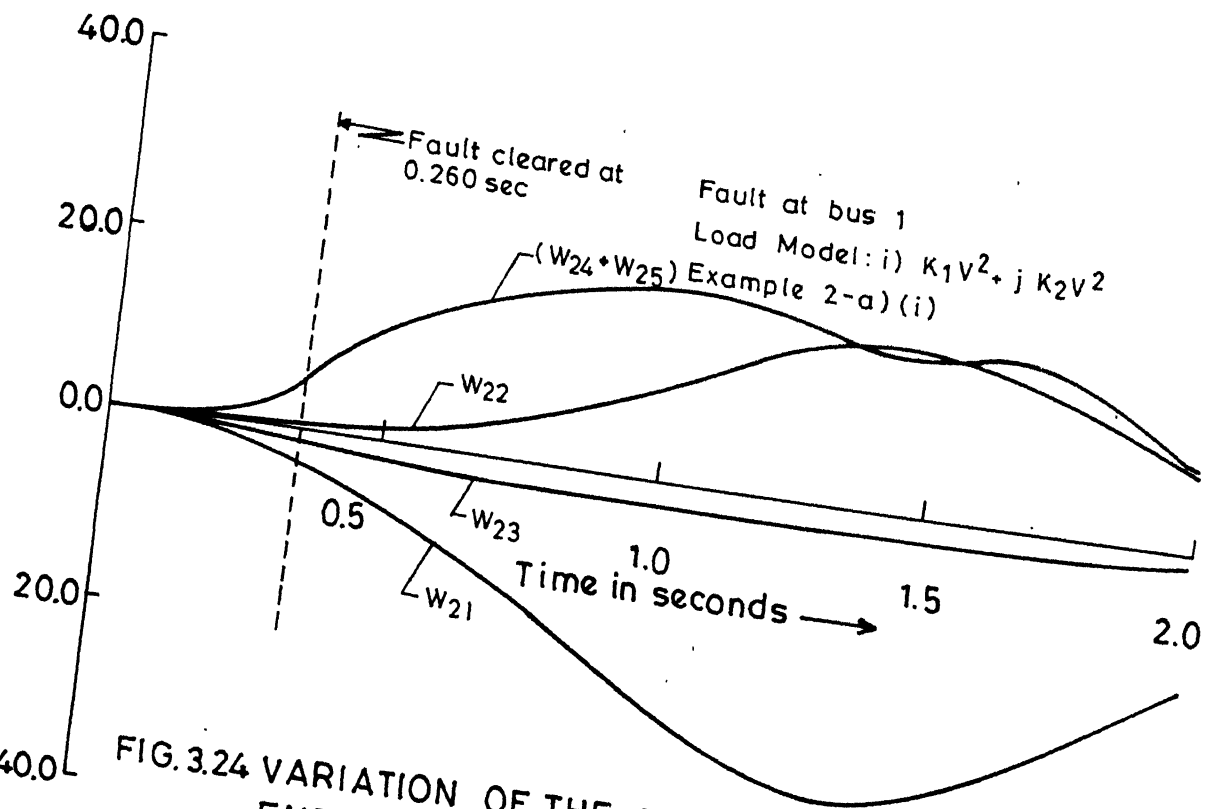


FIG. 3.24 VARIATION OF THE COMPONENTS OF POTENTIAL ENERGY FOR 10-MACHINE SYSTEM, STABLE CASE

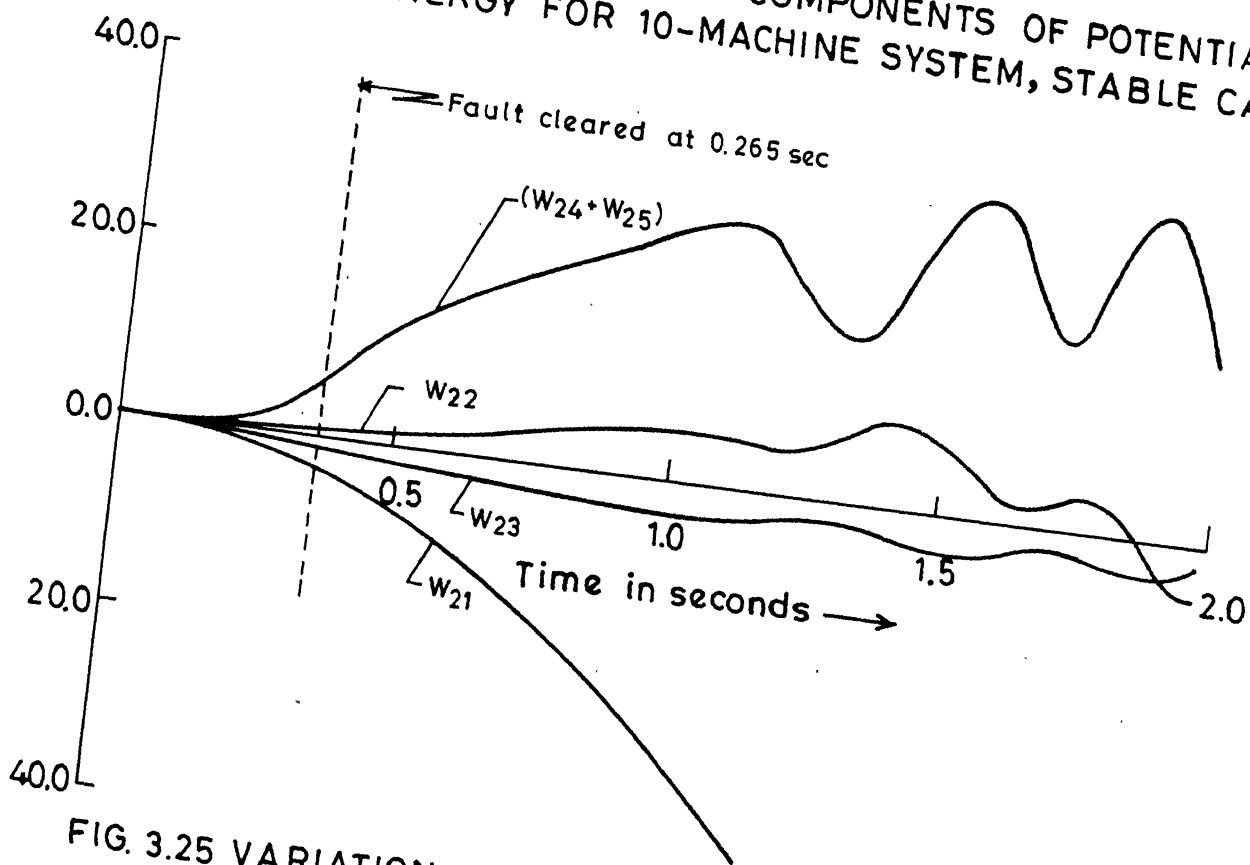


FIG. 3.25 VARIATION OF THE COMPONENTS OF POTENTIAL ENERGY FOR 10-MACHINE SYSTEM, UNSTABLE CASE

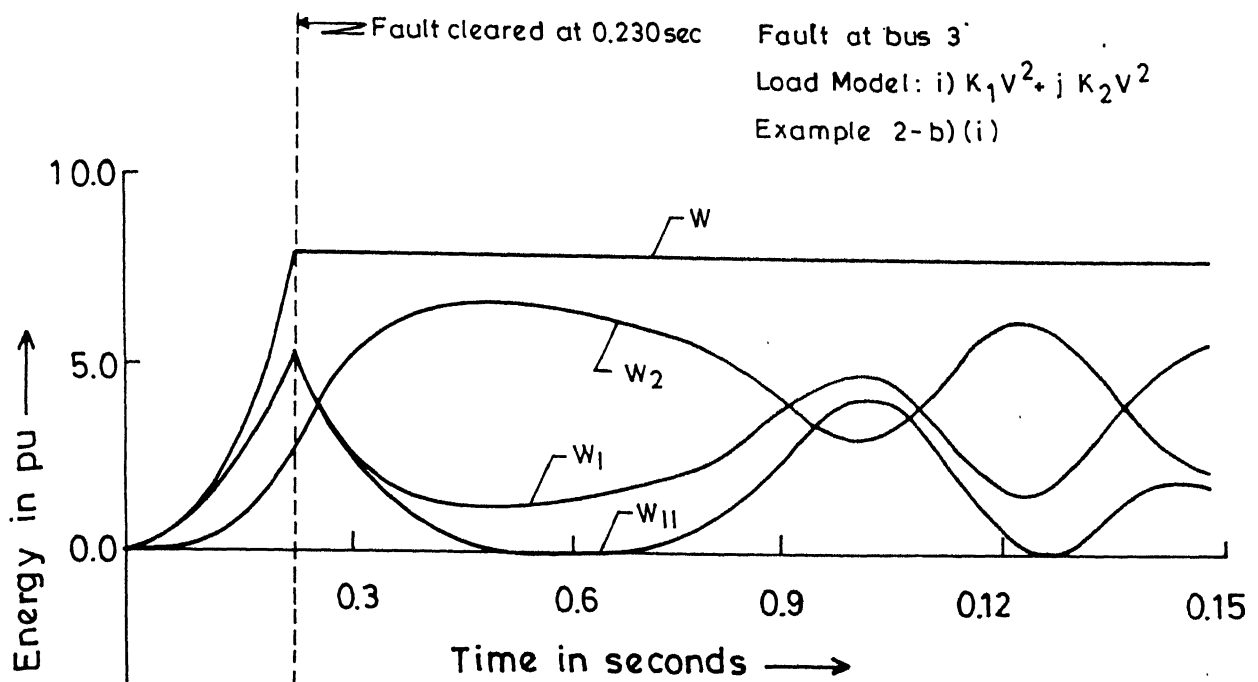


FIG. 3.26 VARIATION OF TOTAL ENERGY AND ITS COMPONENTS FOR 10-MACHINE SYSTEM, STABLE CASE

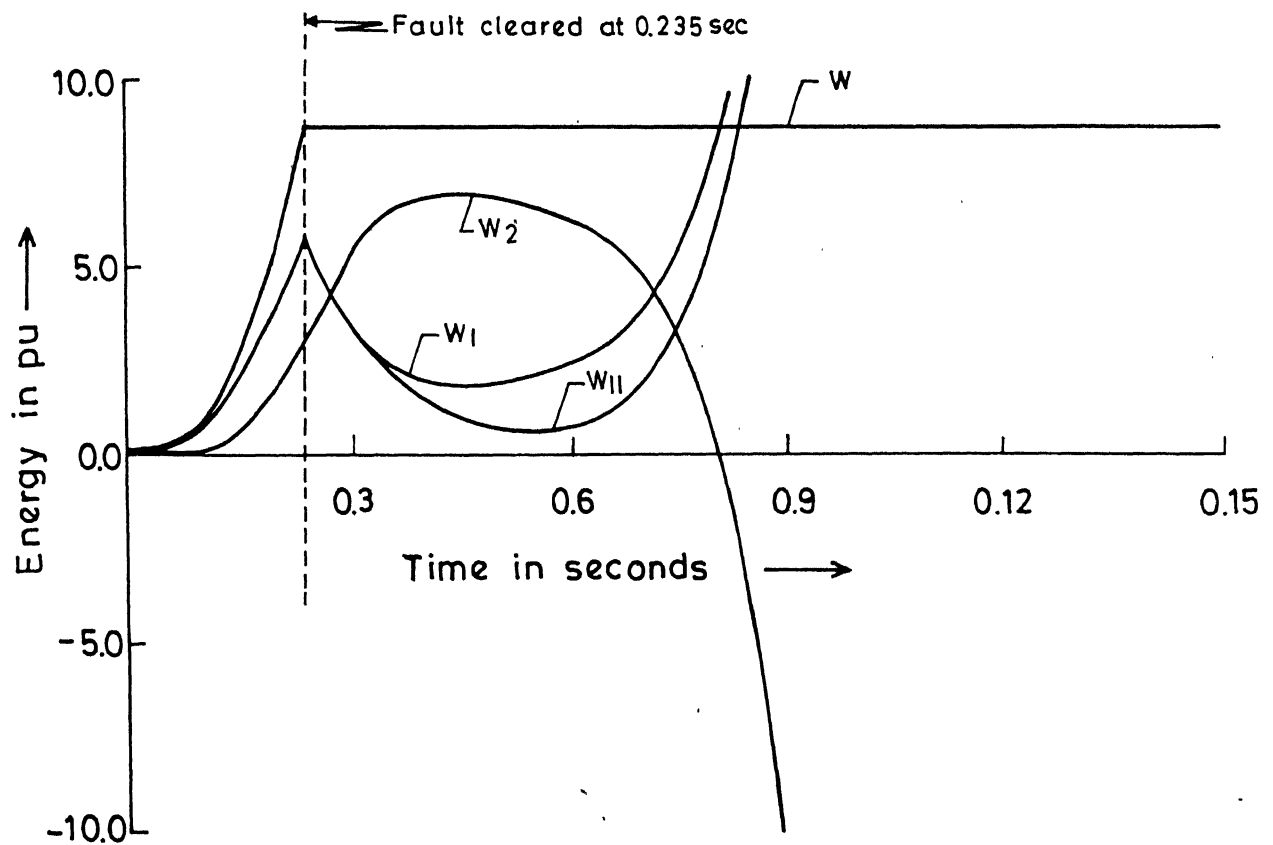


FIG. 3.27 VARIATION OF TOTAL ENERGY AND ITS COMPONENTS FOR 10-MACHINE SYSTEM, UNSTABLE CASE

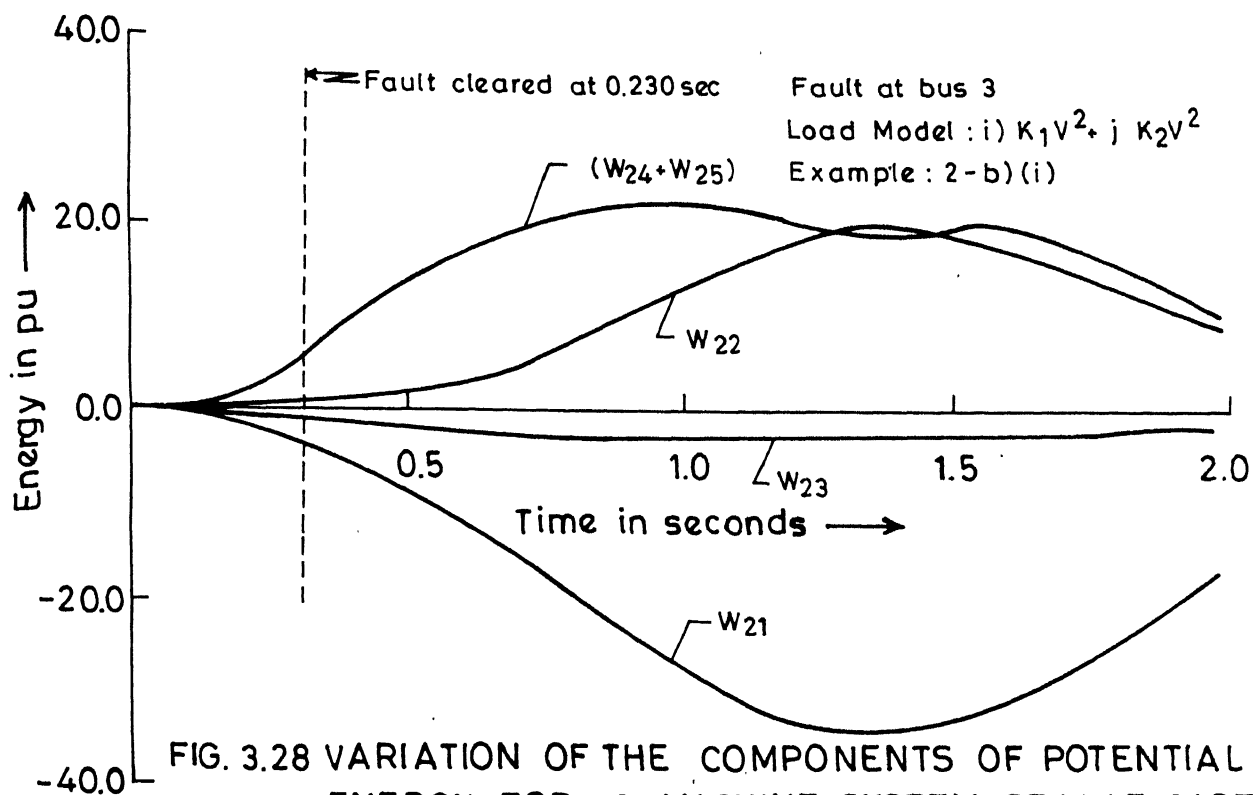


FIG. 3.28 VARIATION OF THE COMPONENTS OF POTENTIAL ENERGY FOR 10-MACHINE SYSTEM, STABLE CASE

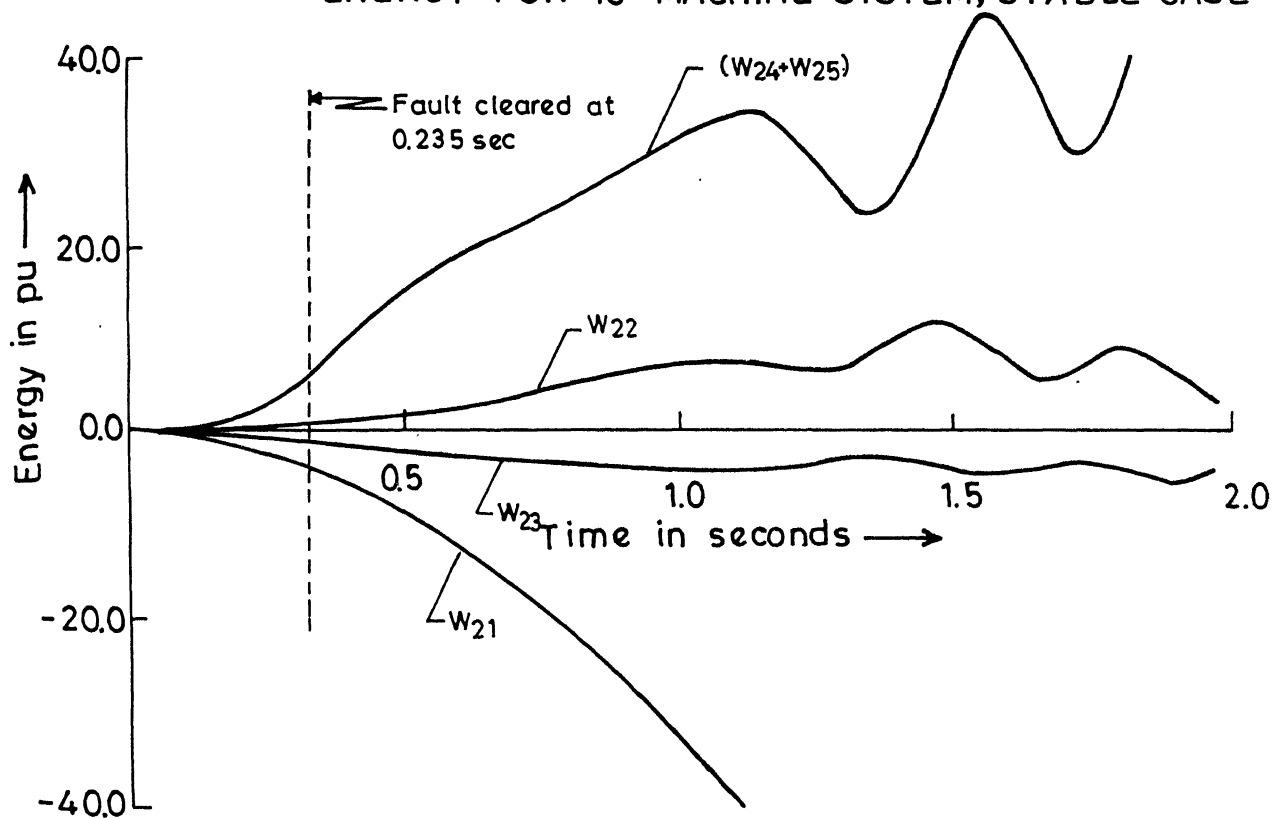


FIG 3.29 VARIATION OF THE COMPONENTS OF POTENTIAL ENERGY FOR 10-MACHINE SYSTEM, UNSTABLE CASE

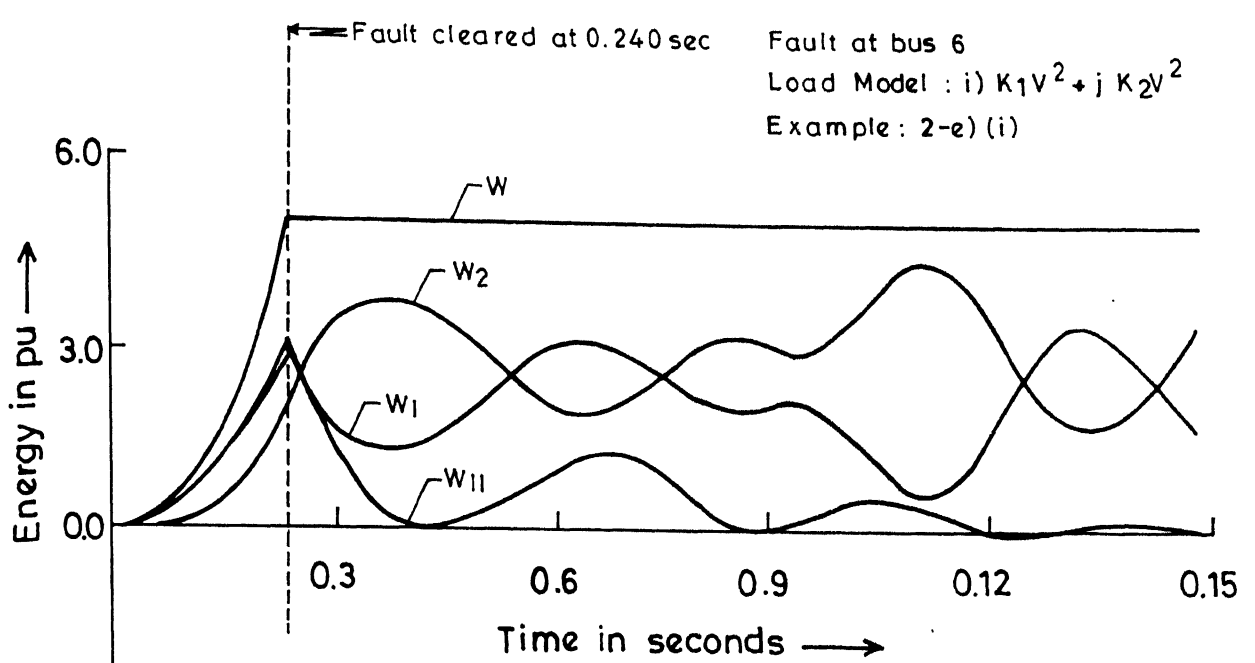


FIG.3.30 VARIATION OF TOTAL ENERGY AND ITS COMPONENTS FOR 10-MACHINE SYSTEM, STABLE CASE

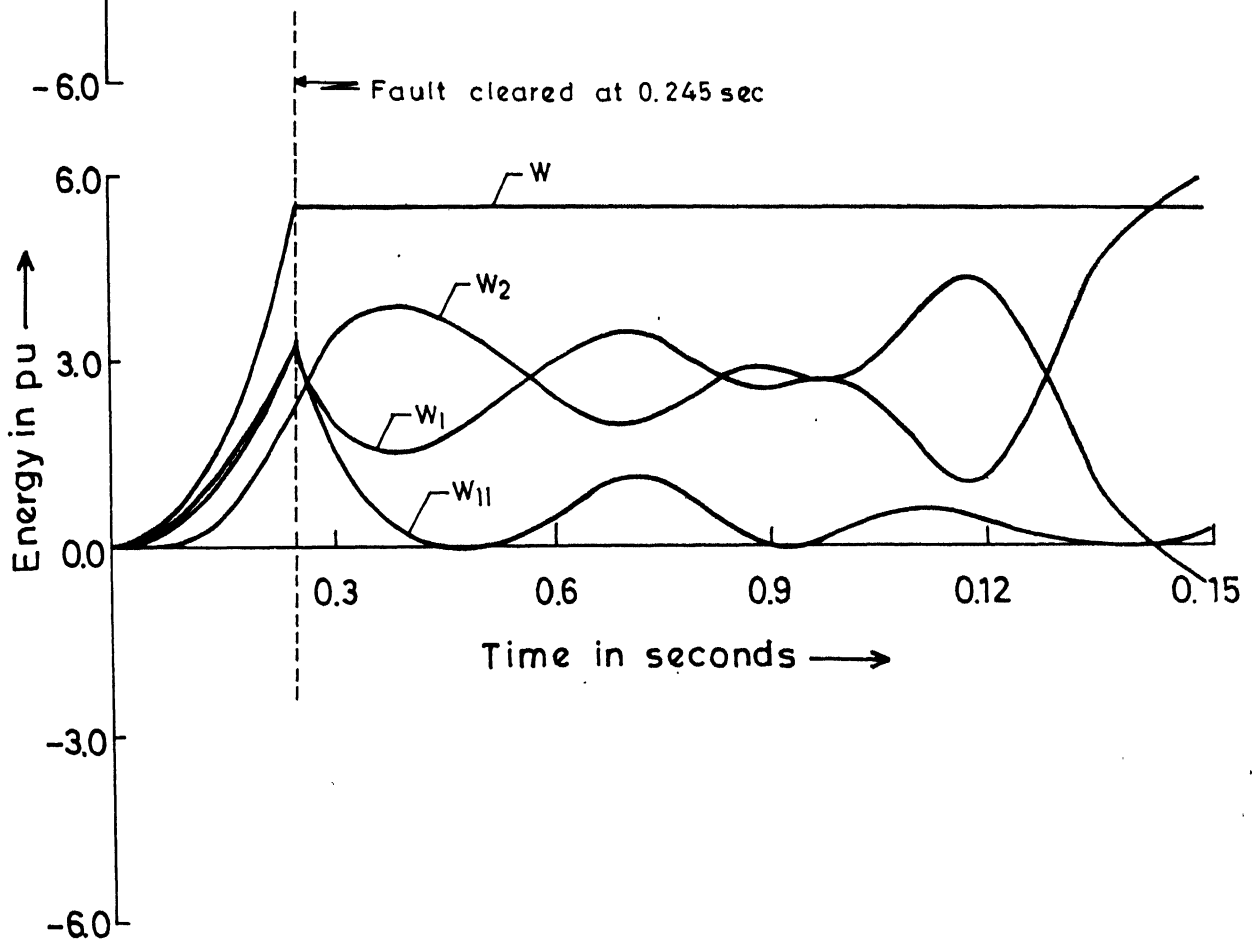


FIG.3.31 VARIATION OF TOTAL ENERGY AND ITS COMPONENTS FOR 10-MACHINE SYSTEM, UNSTABLE CASE

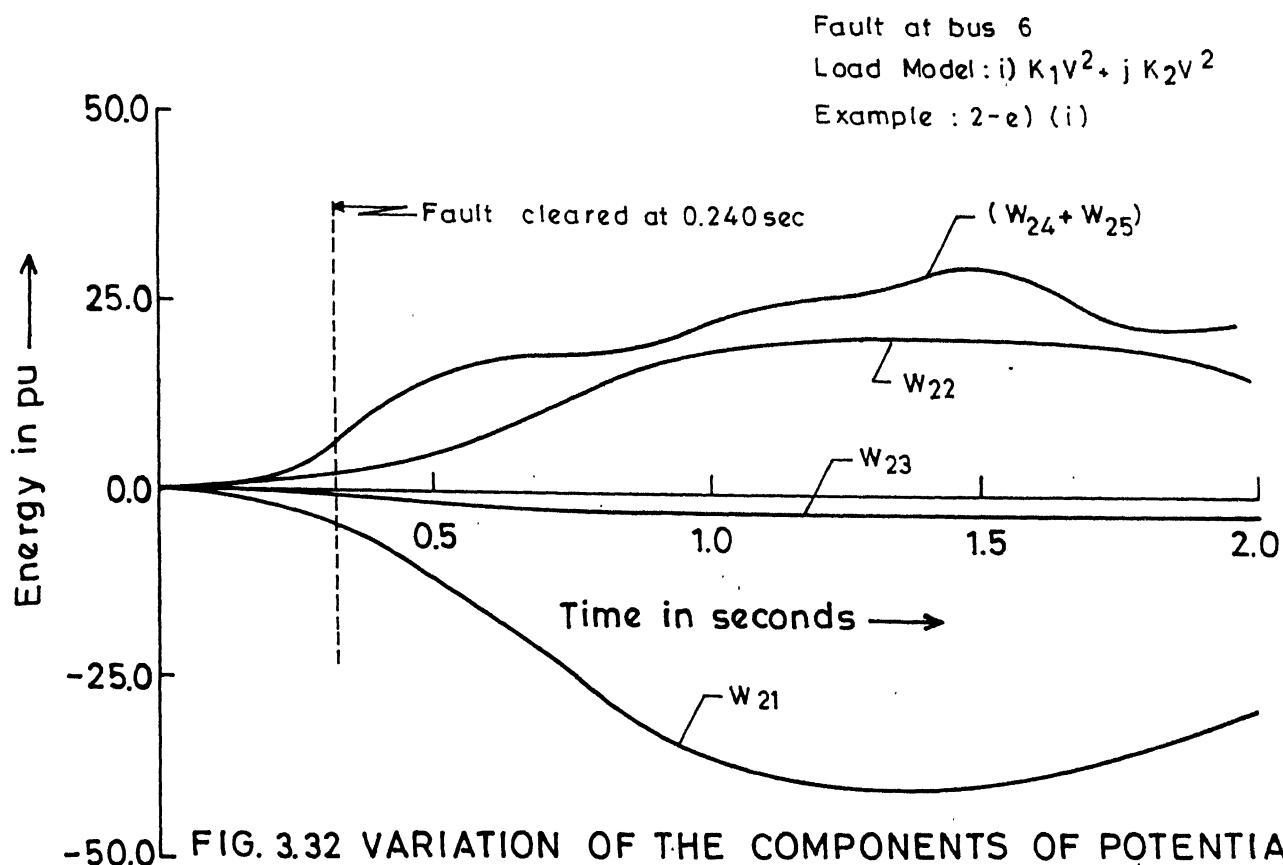


FIG. 3.32 VARIATION OF THE COMPONENTS OF POTENTIAL ENERGY FOR 10-MACHINE SYSTEM, STABLE CASE

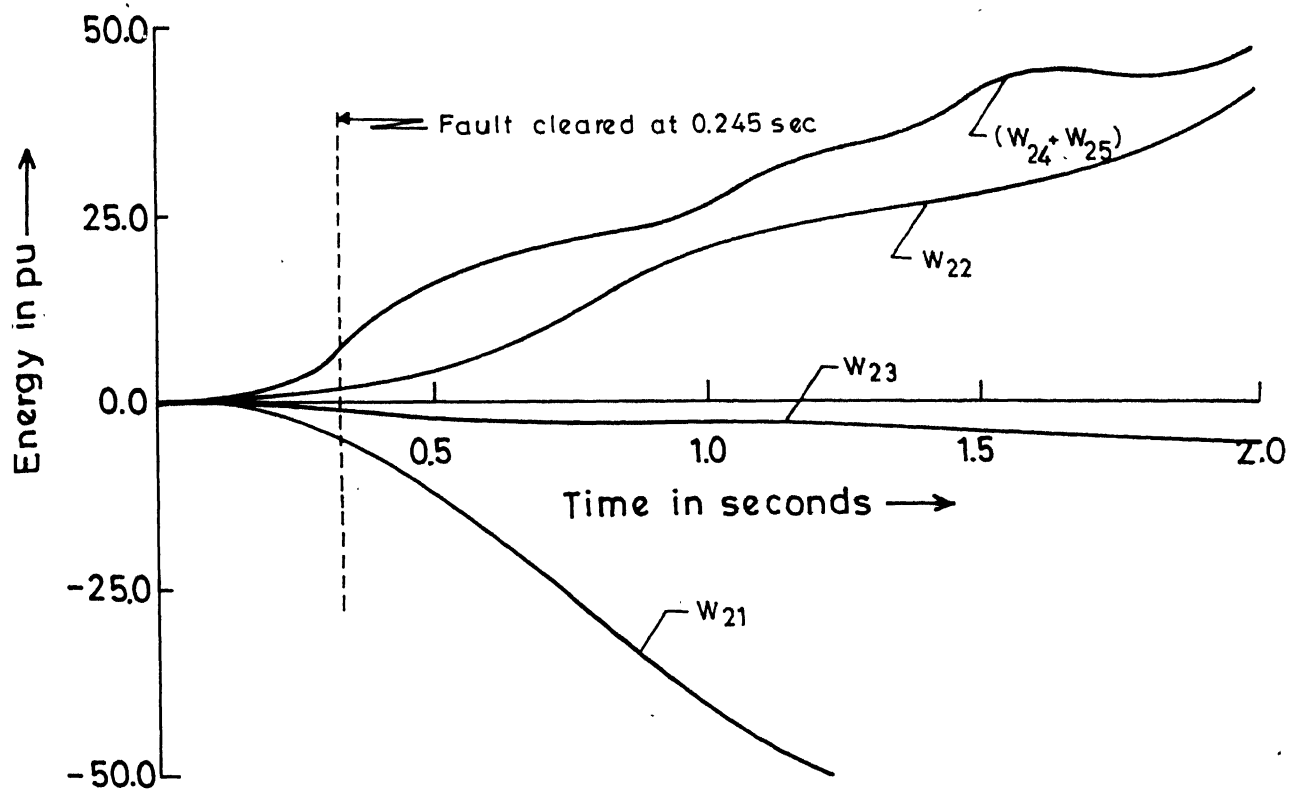


FIG. 3.33 VARIATION OF THE COMPONENTS OF POTENTIAL ENERGY FOR 10-MACHINE SYSTEM, UNSTABLE CASE

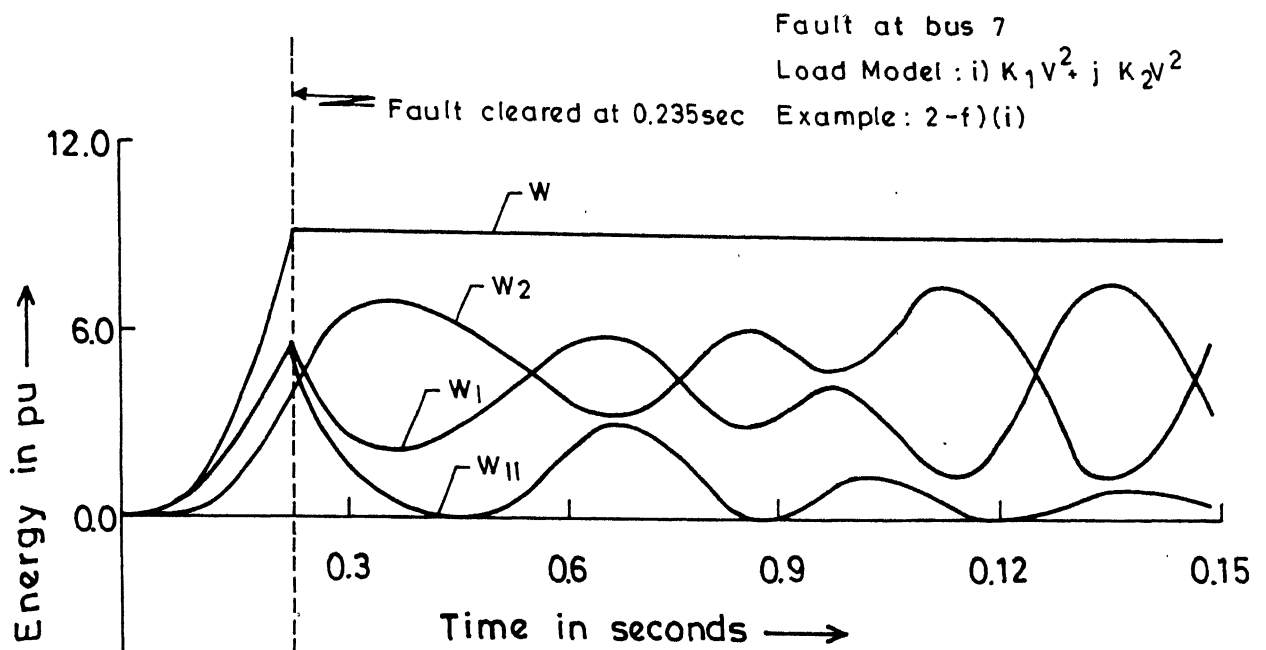


FIG. 3.34 VARIATION OF TOTAL ENERGY AND ITS COMPONENTS FOR 10-MACHINE SYSTEM, STABLE CASE

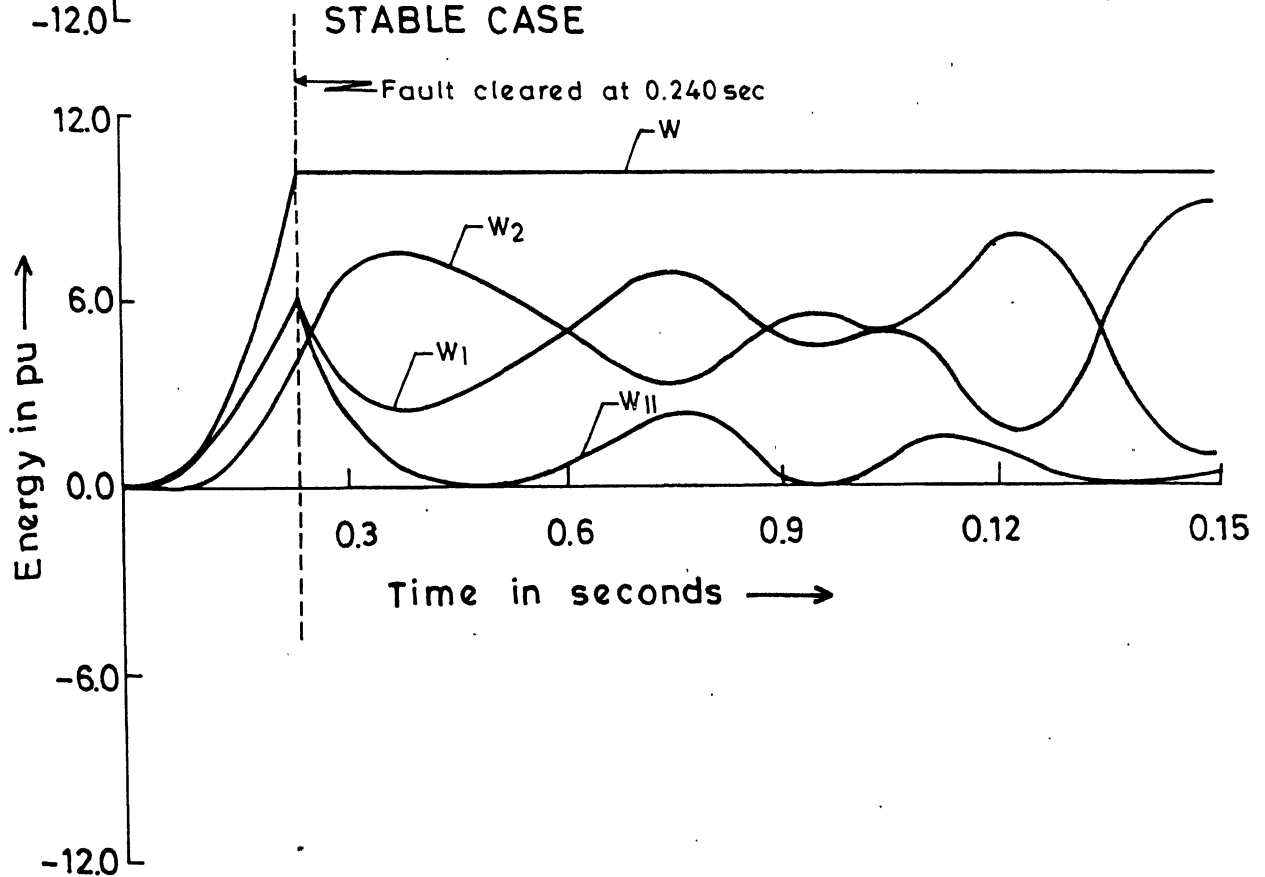


FIG. 3.35 VARIATION OF TOTAL ENERGY AND ITS COMPONENTS FOR 10-MACHINE SYSTEM, UNSTABLE CASE

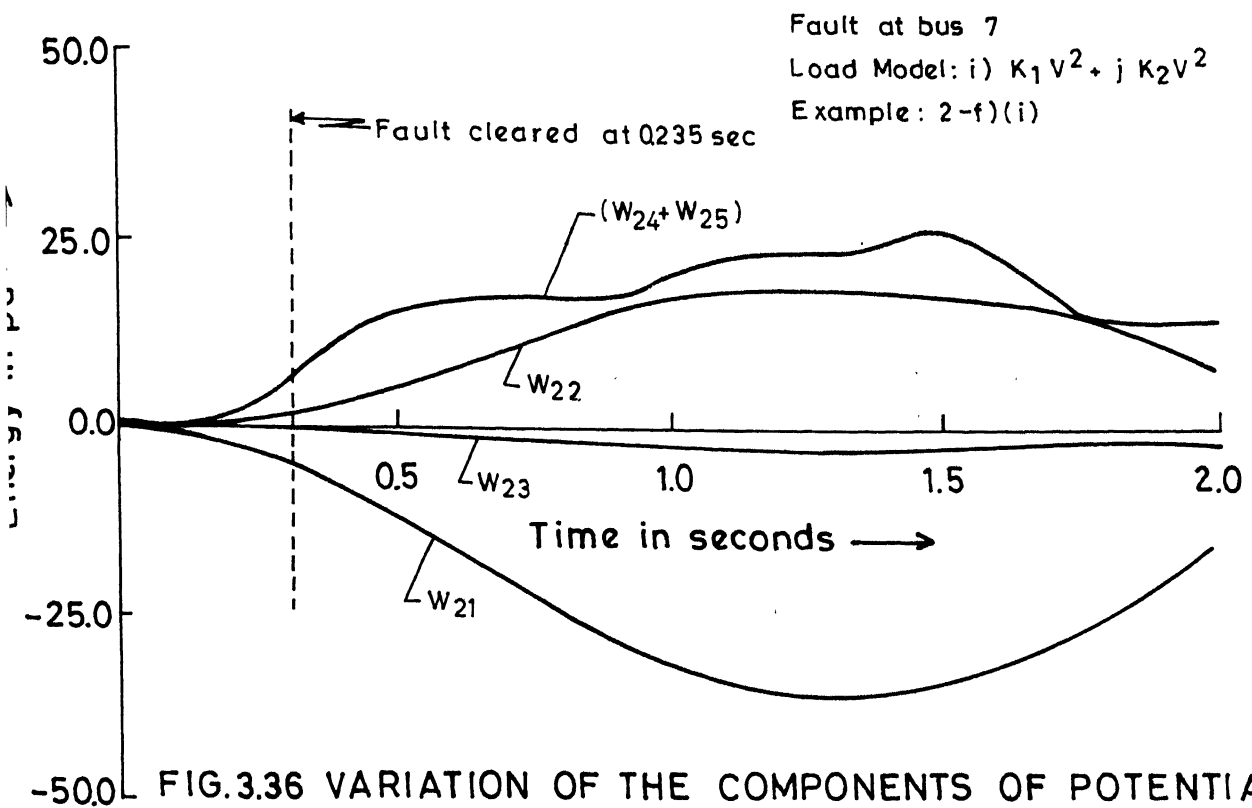


FIG.3.36 VARIATION OF THE COMPONENTS OF POTENTIAL ENERGY FOR 10-MACHINE SYSTEM, STABLE CASE

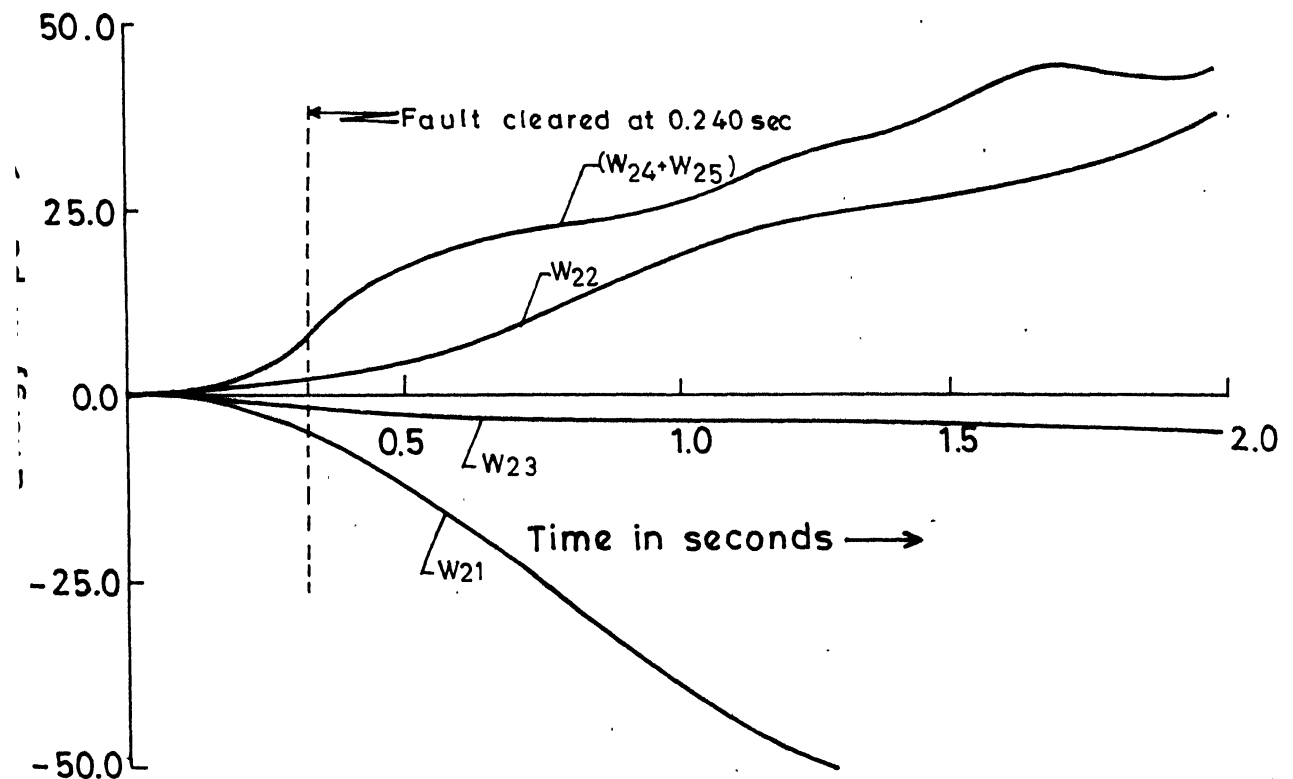


FIG.3.37 VARIATION OF THE COMPONENTS OF POTENTIAL ENERGY FOR 10-MACHINE SYSTEM, UNSTABLE CASE

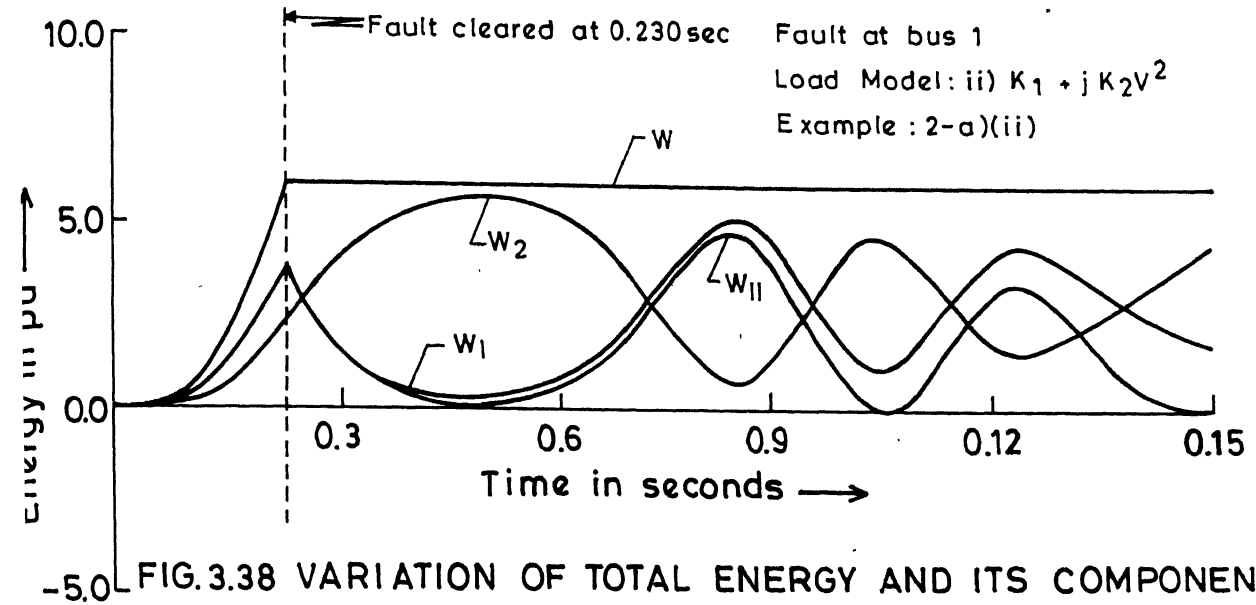


FIG. 3.38 VARIATION OF TOTAL ENERGY AND ITS COMPONENTS FOR 10-MACHINE SYSTEM, STABLE CASE

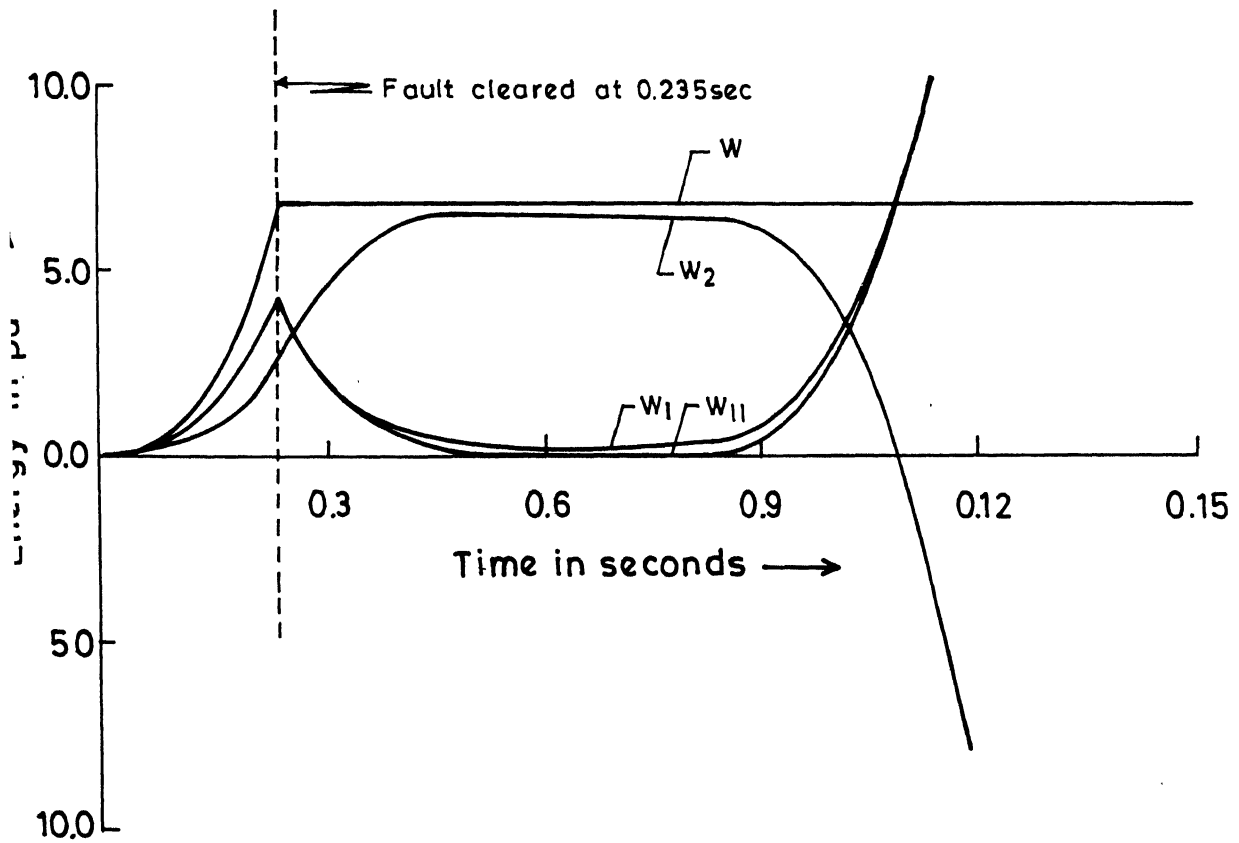


FIG. 3.39 VARIATION OF TOTAL ENERGY AND ITS COMPONENTS FOR 10-MACHINE SYSTEM, UNSTABLE CASE

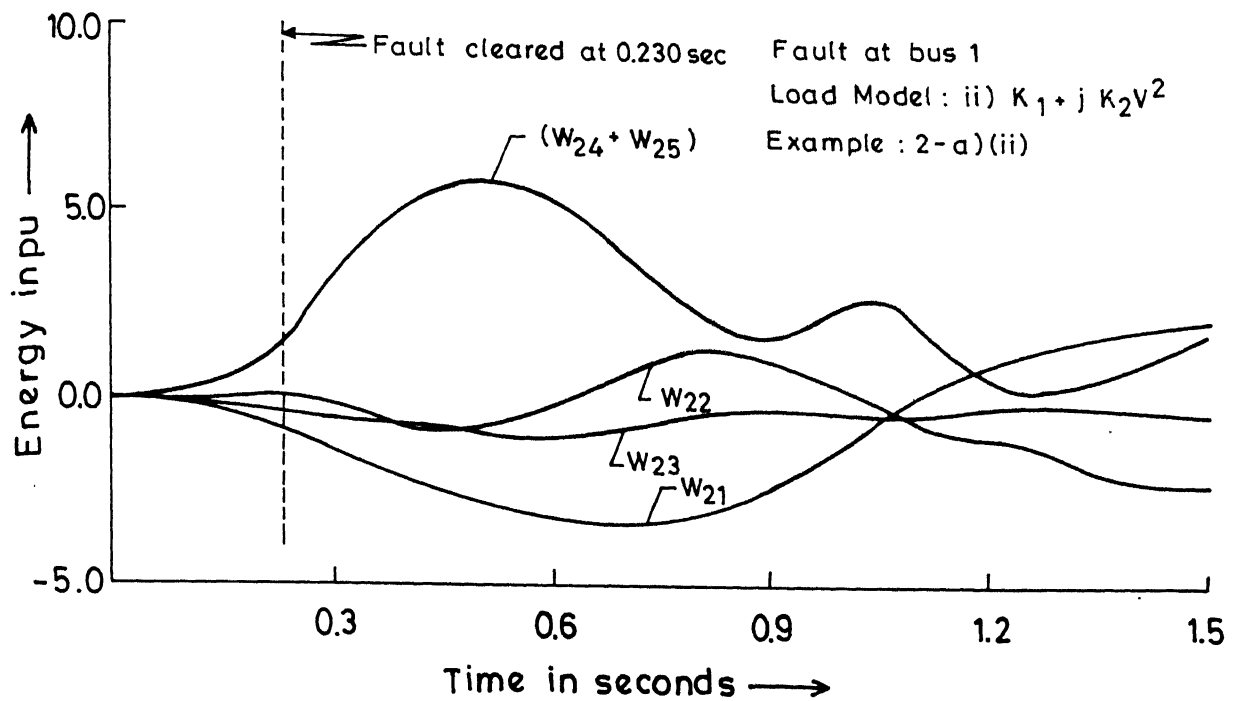


FIG.3.40 VARIATION OF THE COMPONENTS OF POTENTIAL ENERGY FOR 10-MACHINE SYSTEM, STABLE CASE

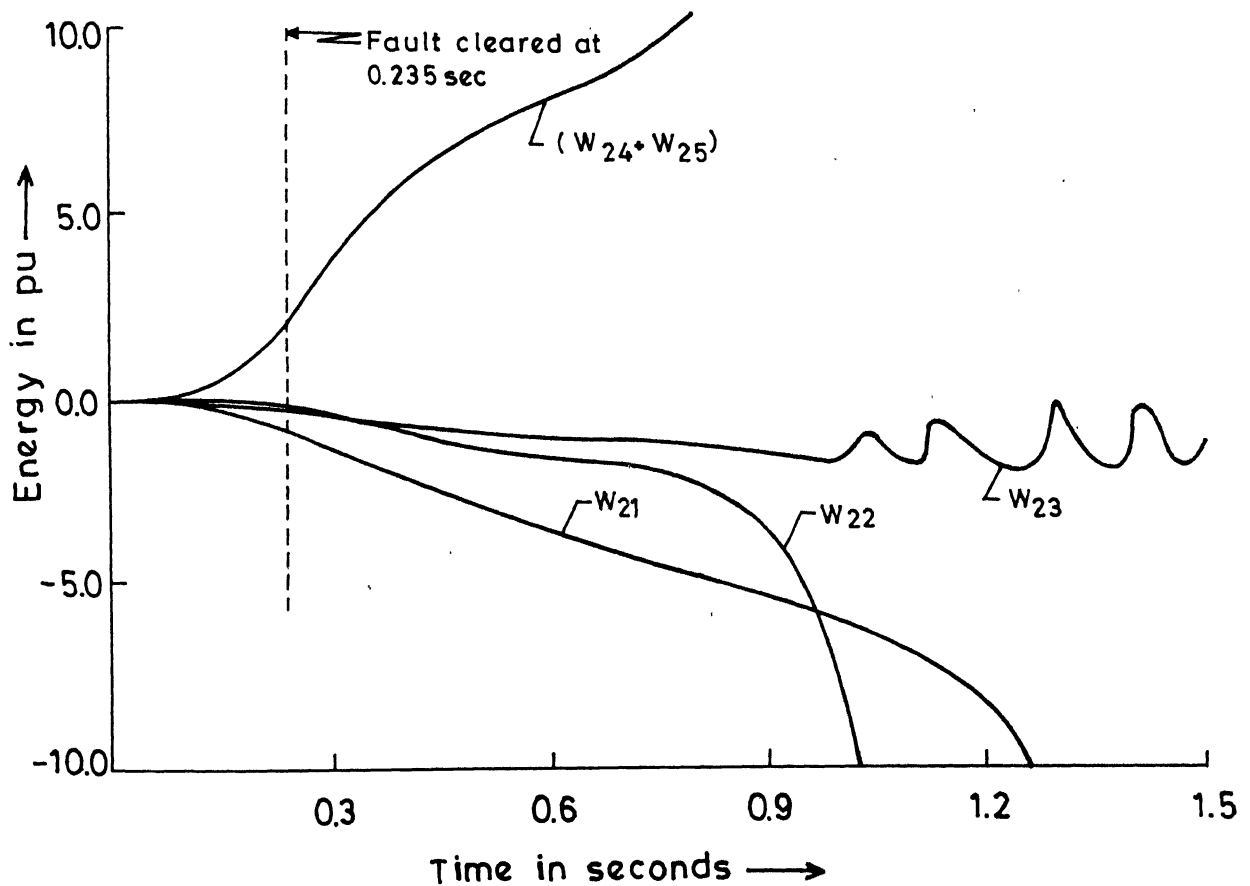


FIG.3.41 VARIATION OF THE COMPONENTS OF POTENTIAL ENERGY FOR 10-MACHINE SYSTEM, UNSTABLE CASE

In general, the mode of instability can be quite complex as seen from the swing curves. Yet it would appear that this complexity does not affect much the predicted results. The major reason for this is that the correction in the kinetic energy term to account for the mode of instability is of secondary importance in comparison with the correction in the potential energy term. Accurate prediction of the mode of instability is essential when the critical energy is determined from the energy evaluated at the controlling ucp as the controlling ucp is related to the mode of instability. However, the accuracy of the PEBS method in determining the critical energy is not dependent on exact knowledge of the mode of instability.

The total kinetic energy consists of two components; i)  $W_{11}$ , defined in Eq. (3.37), which is responsible for system separation and ii)  $W_{12}$ , the component which corresponds to the relative motion of the rotors of the generators within any coherent group. While the energy function derived in Section 3.3 assumed  $W_{12}$  equal to zero, this is not required as long as  $W_{12}$  remains constant along the post-fault trajectory. As perhaps to be expected,  $W_{12}$  does not remain constant (see Figs. 3.22, 3.26, 3.30, 3.34 and 3.38) and oscillates. This is a fact of crucial importance in explaining why the kinetic energy correction neglecting  $W_{12}$  is not adequate.

In stably cleared fault, it is expected that  $W_{11}$  goes through zero following the clearing of the fault. Thus, the minimum of the kinetic energy,  $W_1$ , following the clearing of the fault, is equal to  $W_{12}$ . Fouad and Stanton [59] assume that the minimum kinetic energy is equal to  $W_{12}$  at the time of clearing. However, this is not correct as seen from Figs. 3.22, 3.26, 3.30, 3.34 and 3.38. It is observed that minimum kinetic energy is much larger than  $W_{12}$  at the time of clearing, even though  $W_{11}$  passes through zero following the clearing of the fault in the stable case. This shows that part of the kinetic energy component  $W_{11}$  is transformed into the component  $W_{12}$  which corresponds to the relative motion of the generators within a coherent group. Thus, the correction of the kinetic energy neglecting  $W_{12}$  is not adequate. The kinetic energy correction by considering the minimum kinetic energy (following stably cleared fault) is more accurate. This is shown in Fig. 3.42 for the stable case for example 2-a)(i), where the kinetic energy correction by the later method gives a critical clearing time of 0.263 sec, whereas the predicted time neglecting  $W_{12}$  is 0.249 sec (Table 3.2).

It is interesting to note that for large systems (both 10-machine and 13-machine) neglecting the path dependent term in the energy function (due to the non-constancy of active power loads) gives a very good result which makes the kinetic energy correction superfluous. While it is difficult to explain the

$$W_2^{\max} = W_{cr} = 7.5771 \text{ pu (Table 3.2)}$$

$$W_1^{\min} = 1.0894 \text{ pu}$$

$$W_{cl} = W \text{ at clearing} = 8.4557 \text{ pu}$$

$$W_{cor} = \text{Corrected } W = 8.6665 \text{ pu}$$

$$T_{cr} = 0.263 \text{ sec}$$

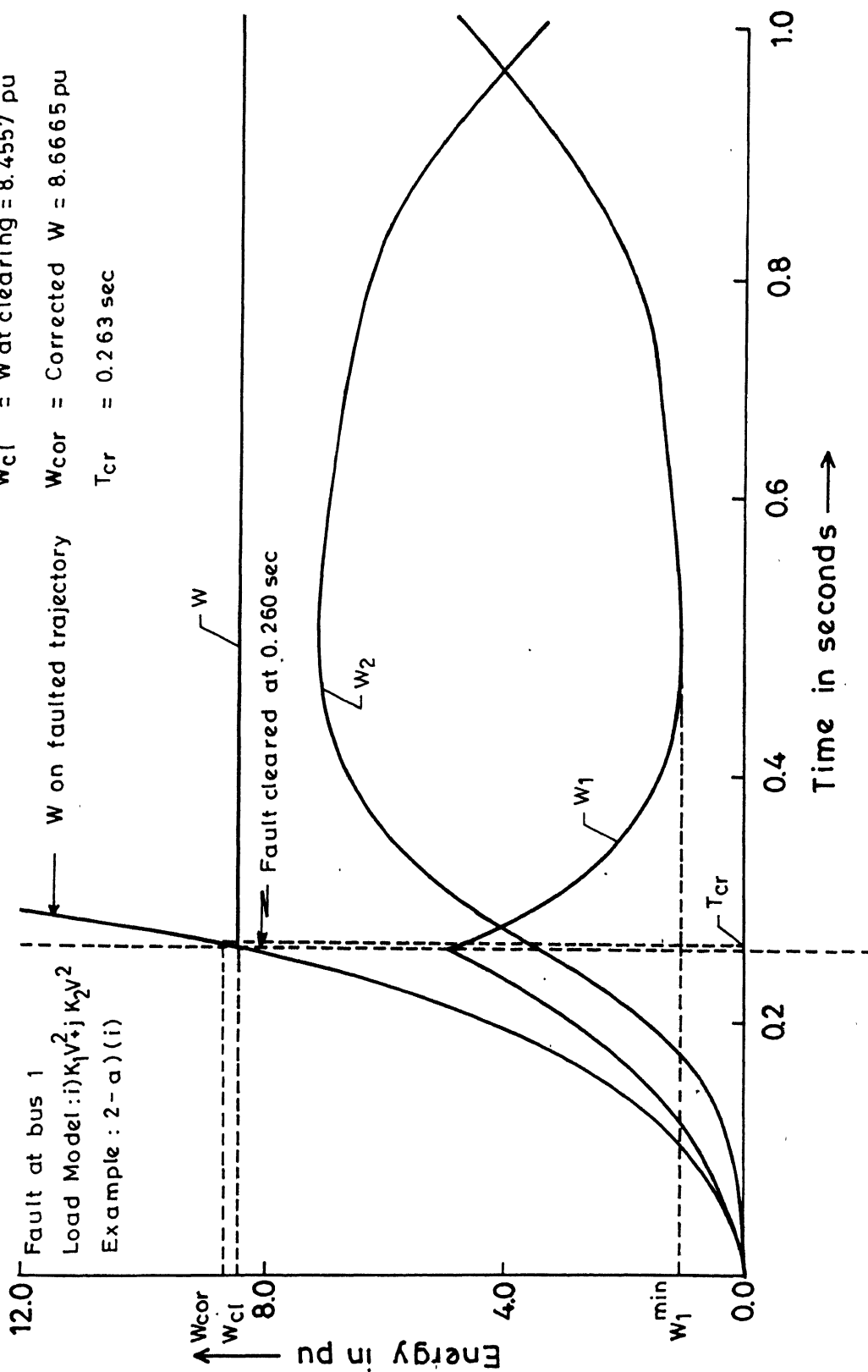


FIG. 3.42 KINETIC ENERGY CORRECTION FOR 10-MACHINE SYSTEM, STABLE CASE

phenomena, it simplifies the computation of the energy function.

The examination of the energy function and its various components brings out the following points and supports the conclusions in Chapter 2:

- i) the instability can be judged from the variation of  $W_1$  or  $W_2$ . While  $W_1$  continues to increase,  $W_2$  continues to decrease (as the total energy is constant along the post-fault trajectory). Instability may occur after the first swing.
- ii)  $W_{23}$ , the component of the potential energy corresponding to the reactive power loads, is insignificant compared to  $W_{22}$  due to the active power loads. This shows that inaccuracies in modelling the reactive power component of loads have negligible effect in predicting the stability region. However, this cannot be said about the modelling of the active power loads.
- iii) The potential energy terms  $W_{24}$  and  $W_{25}$  are always non-negative and bounded even for unstable cases, although higher peaks are reached if the system is unstable.
- iv) The potential energy term  $W_{21}$  due to mechanical input, continues to decrease (or increase) monotonically when the system is unstable.

It is interesting to note that the oscillations in  $W_{11}$  continue to decrease for the two cases (examples 2-e)(i) and 2-f)(i)) even when the system is unstable. This is due to the fact that, in both the cases, all the generators tend to accelerate together and separate from generator 2 which decelerates. This implies that the mode of instability assumed (that the faulted generator separates from the rest) is not correct. However, the effect of this error in predicting  $t_{cr}$  is insignificant.

### 3.6 CONCLUSIONS

In this chapter, a system model is developed based on the aggregation of generators into  $r$  coherent groups on the occurrence of a fault, each group having one or more generators in it. A new structure preserving energy function is then derived assuming that the mode of instability is known apriori. Application of this energy function for predicting the stability regions for three sample systems shows that

- i) the kinetic energy correction neglecting  $W_{12}$  (the component corresponding to the relative motion of the generator rotors within the coherent groups) gives slight improvement in the predicted value of critical clearing time.

- ii) although  $W_{11}$ , the component of kinetic energy that leads to system separation, goes through zero for a stably clear fault, it does not get converted completely into potential energy; part of  $W_{11}$  gets converted into  $W_{12}$ . The exchange in these two components of energy,  $W_{11}$  and  $W_{12}$ , complicates the exact determination of stability region for large multi-machine systems.
- iii) neglecting the path dependent component of the energy function, due to the non-constancy of active power loads, appears to improve the accuracy of prediction even without kinetic energy correction.
- iv) PEBS method using SPEF appears to be quite robust in predicting the critical energy. The kinetic energy correction has, basically, a minor effect on the accuracy.

## CHAPTER 4

### DYNAMIC SECURITY ASSESSMENT USING STRUCTURE PRESERVING ENERGY FUNCTIONS

#### 4.1 INTRODUCTION

While some attempts have been made to apply direct methods, based on energy functions on reduced network models, to on-line dynamic security assessment [64, 65], no attempt has been tried with structure preserving energy functions. The objective of this chapter is to present algorithms and results in applying SPEF for on-line dynamic security assessment.

The security assessment is an important function in modern energy control centres to check whether the present operational state is normal. While the methods of static security assessment are well advanced and implemented in many control centres, the problem of dynamic security assessment is still not well defined. One of the objectives can be the checking of transient stability following a contingency such as a three phase fault at the terminals of a generator.

The use of transient energy margin as an index helps not only in checking the stability, but also to rank the contingencies according to their severities. The computation of transient energy margin requires the computation of critical energy

and the energy at clearing. The later usually requires the simulation of the faulted trajectory. Approximations of the faulted trajectory has been used to simplify the computations [64]. The critical energy can be determined using controlling up or PEBS method. Both require again the simulation of the faulted trajectory. The use of SPEF, although attractive from the view point of preserving the structure of the system, requires more computational efforts in the simulation of the faulted trajectory. Both faulted and post-fault system networks are solved at every step to compute the faulted trajectory and the energy function respectively. Efficient methods for speeding up the computation of transient energy margin would be required before SPEF can be seriously considered for on-line dynamic security assessment.

The method proposed in this chapter assumes that a faulted generator accelerates with respect to the remaining generators and its rotor angle increases monotonically during the fault-on period. If it is assumed that the rest of the generators swing together, then their rotor angles along with the bus voltage magnitudes and angles become implicit functions of the rotor angle of the faulted generator. The potential energy component of the structure preserving energy function also reduces to a function of a single independent variable. With this assumption the estimation of the faulted trajectory is avoided.

The method is illustrated by considering the three system examples of Chapters 2 and 3.

## 4.2 TRANSIENT STABILITY MEASURES

### 4.2.1 General

The energy margin can be used as an index for assessing the robustness of a power system in a given configuration and/or predicting its transient behaviour under abnormal conditions. To the system operator, it offers a means of performing on-line dynamic security assessment.

### 4.2.2 Transient Energy Margin (TEM) [61, 63-65]

The transient energy margin is defined as the difference between the critical energy and the energy at the clearing time. The index serves to indicate the severity of the disturbance.

Thus, if  $W_{cl}$  is the value of the energy function,  $W$  at the clearing time and  $W_{cr}$  the critical energy, the transient energy margin,  $\Delta W$  can be defined [61, 63-65] as

$$\Delta W = W_{cr} - W_{cl} \quad (4.1)$$

The transient energy margin,  $\Delta W$  indicates how close to instability a system might be, for a given system condition and for a particular disturbance. If  $\Delta W$  is positive, then the system is stable. If  $\Delta W$  is negative, the system is unstable.

### Normalised Energy Margin [32]

An alternate measure of transient stability is the ratio of potential energy margin of the system to the kinetic energy at fault clearing. Denoting the kinetic and the potential energy components at clearing by  $W_{1cl}$  and  $W_{2cl}$  respectively, the normalised energy margin,  $\Delta W_n$  may be defined [32] as

$$\Delta W_n = \frac{W_{cr} - W_{2cl}}{W_{1cl}} \quad (4.2)$$

This is used to evaluate the system stability in the following manner :

- i) a value of  $\Delta W_n$  greater than 1 indicates stability; if  $\Delta W_n$  is less than 1, the system is unstable.
- ii) a disturbance which gives the lowest value of  $\Delta W_n$ , constitutes the most severe disturbance.

## 4.3 DYNAMIC SECURITY ASSESSMENT

### 4.3.1 General

Dynamic security evaluation of power systems through the application of transient energy margin or the normalised energy margin, involves the computation of i) critical energy and ii) transient energy and its kinetic and potential energy components at the instant of clearing the fault. Critical energy can be evaluated using the PEBS method which requires the simulation

of the faulted trajectory. Although the application of this method avoids the computation of uep's for evaluating the critical energy, the computation of the faulted trajectory may constitute a limitation in its application to on-line dynamic security assessment. A method is proposed in this section which eliminates the need to determine the faulted trajectory and can speed up the computation of TEM and the normalised TEM.

As discussed in Chapter 3, for a fault at its terminals, a generator (say,  $k$ ) gets severely disturbed and initially tends to separate from the rest of the generators which may be assumed to swing together. This implies that the generator  $k$  accelerates monotonically during the transient. Under the assumption that the remaining generators swing together, their motions can be described by algebraic equations. This permits the rotor angles of these generators and also the bus voltages and their angles to be expressed implicitly as functions of the rotor angle of generator  $k$ . This also reduces the potential energy to a function of single independent variable corresponding to the rotor angle of the generator going out-of-step with respect to the rest of the generators.

#### 4.3.2 Mathematical Formulation

Mathematically, the problem for computation of TEM can be formulated as follows :

Consider the modified energy function (neglecting the path dependent term) defined in Section 3.3, Chapter 3 [Eq. (3.36)] as

$$W = W_{11}(\omega_k) + W_2(\underline{\theta}, \underline{V}, \underline{\varphi}, \theta_k) \quad (4.3)$$

where  $\underline{\theta}$  is  $(m-1)$  vector of rotor angles (excluding the faulted generator),  $\underline{V}$  and  $\underline{\varphi}$  are  $n$  vectors of bus voltage magnitudes and angles respectively.

Under the assumption that all the generators except the faulted generator swing together, it can be shown that the vectors  $\underline{\theta}$  and  $\underline{\varphi}$  are functions of  $\theta_k$ . Using PEBS method, the critical energy can be determined, if  $\dot{\theta}_k^*$  can be determined such that  $W_2(\theta_k^*)$  is maximum along the faulted trajectory.

The energy at the time of clearing can be determined if the values of  $\theta_k$  and  $\omega_k$  at clearing are determined. Thus,

$$W(t=t_{cl}) = W_{11}(\omega_k = \omega_{kcl}) + W_2(\theta_k = \theta_{kcl}) \quad (4.4)$$

#### 4.3.2.1 Computation of $\theta_k^*$ and Critical Energy

The dependence of vectors  $\underline{\theta}$ ,  $\underline{V}$  and  $\underline{\varphi}$  on  $\theta_k$  is shown by the following equations which are taken from Chapter 3 :

There is no loss of generality in assuming that  $k = m$  (this can be done by renumbering the buses, if necessary).

From Eqs. (3.24) which describe the motions of the generators within the coherent group, we have,

$$g_i = 0 = P_{mi} - P_{ei}(\theta_i, V_i, \varphi_i) - \frac{M_i}{M_T} \sum_{i=1}^m [P_{mi} - P_{ei}(\theta_i, V_i, \varphi_i)] \quad (4.5)$$

$$i = 1, 2, \dots, m-2$$

From Eqs. (3.34) and (3.35) which describe the power flow equations at  $n$  buses, we have,

$$g_{m-2+i} = 0 = P_i(\theta_i, V_i, \varphi_i) + f_{pi}(V_i), \quad i = 1, 2, \dots, m \quad (4.6a)$$

$$g_{2m-2+i} = 0 = P_i(V_i, \varphi_i) + f_{pi}(V_i), \quad i = 1, 2, \dots, (n-m) \quad (4.6b)$$

$$g_{m-2+n+i} = 0 = Q_i(\theta_i, V_i, \varphi_i) + f_{qi}(V_i), \quad i = 1, 2, \dots, m \quad (4.7a)$$

$$g_{2m-2+n+i} = 0 = Q_i(V_i, \varphi_i) + f_{qi}(V_i), \quad i = 1, 2, \dots, (n-m) \quad (4.7b)$$

From Eq. (3.7), we have,

$$g_{2n+m-1} = 0 = \sum_{i=1}^m M_i \theta_i \quad (4.8)$$

Eqs. (4.5) - (4.8) can be written in the compact form :

$$\underline{g}(\underline{\theta}, \underline{V}, \underline{\varphi}, \theta_k) = \underline{0} \quad (4.9)$$

In the above expression,  $\underline{g}$  is a vector valued function of dimension of  $(2n+m-1)$ . The total number of unknowns  $\underline{\theta}$ ,  $\underline{V}$  and  $\underline{\varphi}$  are also  $2n+m-1$ . Hence, given  $\theta_k$ , we can solve for the unknown variables from Eqn. (4.9).

Denoting  $[\underline{\theta}, \underline{v}, \underline{\phi}]^T = \underline{x}^T$  and  $\theta_k = u$ , the problem of determining the critical energy,  $W_{cr}$  can be formulated as follows :

$$\text{Max}_u W_2(\underline{x}, u) \quad (4.10)$$

$$\text{subject to } \underline{g}(\underline{x}, u) = \underline{0} \quad (4.11)$$

Let the solution of the problem be  $u = u^*$ . Then,

$$W_{cr} = W_2(\underline{x}^*, u^*) \quad (4.12)$$

where  $\underline{x}^*$  is the solution of

$$\underline{g}(\underline{x}^*, u^*) = \underline{0} \quad (4.13)$$

Note : In the presence of path dependent term in the energy function, numerical integration using trapezoidal rule is used to evaluate these terms and the energy function can be written as

$$W(t=t_r) = W_{11}(\omega_k^r) + W_2(\underline{\theta}^r, \underline{v}^r, \underline{\phi}^r, \underline{v}^{r-1}, \underline{\phi}^{r-1}, \theta_k^r) \quad (4.14)$$

where superscript  $r$  indicates the value of the variable evaluated at  $t = t_r$  and similarly superscript  $r-1$  indicates the value of the variable evaluated at  $t = t_{r-1}$ .

The method of computation of  $W_{cr}$  is now modified as follows :

$$W_{cr} = \text{Max}_{u_r} W_2(\underline{x}_r, \underline{x}_{r-1}, u_r) \quad (4.15)$$

$$\text{subject to } \underline{g}(\underline{x}_{r-1}, u_{r-1}) = \underline{0} \quad (4.16)$$

$$\underline{g}(\underline{x}_r, u_r) = \underline{0} \quad (4.17)$$

$$\text{and } u_r = u_{r-1} + \Delta u_r \quad (4.18)$$

where  $\underline{x}_r = \underline{x}(t = t_r)$ ,  $\underline{x}_{r-1} = \underline{x}(t = t_{r-1})$  and  $u_r = u(t=t_r)$

$\Delta u_r$  can be arbitrarily chosen.

#### 4.3.2.2 Computation of Energy at Clearing

As mentioned earlier, this requires the knowledge of  $\theta_k$  and  $\omega_k$  at clearing which can be obtained from

$$\begin{aligned} M_k \dot{\omega}_k &= P_{mk} - P_{ek} - \frac{M_k}{M_T} \sum_{i=1}^m (P_{mi} - P_{ei}) \\ &= \left(1 - \frac{M_k}{M_T}\right) (P_{mk} - P_{ek}) - \frac{M_k}{M_T} \sum_{i=1, i \neq k}^m (P_{mi} - P_{ei}) \\ &= P_{ak} \end{aligned} \quad (4.19)$$

Under the assumption that the remaining generators swing together throughout the fault-on duration starting from  $t = 0^+$ ,  $P_{ak}$  can be shown to be constant.  $P_{mi}$  ( $i = 1, 2, \dots, m$ ) is constant as classical model is assumed. Power output of generator  $k$ ,  $P_{ek} = 0$  during the fault.  $P_{ei}$  can be calculated from

$$P_{ei} = P_{ei}(\bar{\theta}_i, \bar{V}_i, \bar{\varphi}_i), \quad i = 1, 2, \dots, m-1 \quad (4.20)$$

where

$$\bar{\theta}_i = \theta_i - \theta_{T-k} \quad \text{and} \quad \bar{\varphi}_i = \varphi_i - \theta_{T-k}$$

Define vectors

$$\bar{\underline{\theta}}^T = [\bar{\theta}_1 \ \bar{\theta}_2 \ \dots \ \bar{\theta}_{m-1}] \quad (4.21)$$

$$\bar{\underline{V}}^T = [V_1 \ V_2 \ \dots \ V_{m-1} \ V_{m+1} \ \dots \ V_n] \quad (4.22)$$

$$\bar{\underline{\varphi}}^T = [\bar{\varphi}_1 \ \bar{\varphi}_2 \ \dots \ \bar{\varphi}_{m-1} \ \bar{\varphi}_{m+1} \ \dots \ \bar{\varphi}_n] \quad (4.23)$$

It is to be noted that during the fault,  $V_m = 0$  and  $\bar{\varphi}_m = 0$ .

The vectors,  $\bar{\underline{\theta}}$ ,  $\bar{\underline{V}}$  and  $\bar{\underline{\varphi}}$  can be obtained from the equations :

$$h_i = 0 = P_{mi} - P_{ei}(\bar{\theta}_i, V_i, \bar{\varphi}_i) - \frac{M_i}{M_{T-k}} \sum_{\substack{i=1 \\ \neq k}}^m (P_{mi} - P_{ei}(\bar{\theta}_i, V_i, \bar{\varphi}_i)) \\ i = 1, 2, \dots, m-2 \quad (4.24)$$

$$h_{m-2+i} = 0 = P_i(\bar{\theta}_i, V_i, \bar{\varphi}_i) + f_{pi}(V_i), \quad i = 1, 2, \dots, m-1 \quad (4.25a)$$

$$h_{2m-3+i} = 0 = P_i(V_i, \bar{\varphi}_i) + f_{pi}(V_i), \quad i = 1, 2, \dots, (n-m) \quad (4.25b)$$

$$h_{m-3+n+i} = 0 = Q_i(\bar{\theta}_i, V_i, \bar{\varphi}_i) + f_{qi}(V_i), \quad i = 1, 2, \dots, m-1 \quad (4.26a)$$

$$h_{2m-4+n+i} = 0 = Q_i(V_i, \bar{\varphi}_i) + f_{qi}(V_i), \quad i = 1, 2, \dots, (n-m) \quad (4.26b)$$

and finally,

$$h_{2n+m-3} = 0 = \sum_{\substack{i=1 \\ i \neq k}}^m M_i \bar{\theta}_i \quad (4.27)$$

Eqs. (4.24) - (4.27) can be written in the compact form :

$$\underline{h}(\underline{\bar{\theta}}, \underline{\bar{V}}, \underline{\bar{\phi}}) = \underline{0} \quad (4.28)$$

where  $\underline{h}$  has the dimension of  $(2n+m-3)$ . Eqn. (4.28) can be solved to obtain  $\underline{\bar{\theta}}$ ,  $\underline{\bar{V}}$  and  $\underline{\bar{\phi}}$  which are assumed to remain constant during the faulted period. Once these vectors are determined,  $P_{ei}$  ( $i = 1, 2, \dots, m-1$ ) can be computed and this determines  $P_{ak}$ .

$\omega_{kcl}$  and  $\theta_{kcl}$  are determined from

$$\omega_{kcl} = \frac{P_{ak} t_{cl}}{M_k} \quad (4.29)$$

$$\theta_{kcl} = \theta_{ko} + \frac{P_{ak} (t_{cl})^2}{2M_k} \quad (4.30)$$

where  $t_{cl}$  is the clearing time and  $\theta_{ko} = \theta_k (t = 0)$ .

Substituting Eqs. (4.29) and (4.30) in Eq. (4.4), we can get the kinetic energy and the potential energy at the time of clearing.

#### 4.3.3 Computational Procedure

The major computational effort is the determination of  $\theta_k^*$  to evaluate  $W_{cr}$ .  $\theta_k$ , the rotor angle of the faulted generator,

increases monotonically during the fault. The approach used here is to simulate the trajectory of  $\theta_k$  during the fault and monitor the potential energy,  $W_2$  until it crosses the peak. The trajectory of  $\theta_k$  is simulated by starting from  $\theta_{k0} = \theta_k(t = 0)$  and increasing its value in small steps.

The solution of the set of nonlinear equations (4.9) can be simplified by linearisation.

$$\text{Given } \underline{g}(\underline{x}_{r-1}, u_{r-1}) = \underline{0} \quad (4.31)$$

We can write,

$$\underline{0} = \underline{g}(\underline{x}_r, u_r) \approx \underline{g}(\underline{x}_{r-1}, u_{r-1}) + \left. \frac{\partial \underline{g}}{\partial \underline{x}} \right|_{\substack{\underline{x}=\underline{x}_{r-1} \\ u=u_{r-1}}} + \left. \frac{\partial \underline{g}}{\partial u} \right|_{\substack{\underline{x}=\underline{x}_{r-1} \\ u=u_{r-1}}} \quad (4.32)$$

from which

$$\Delta \underline{x}_r = [S] \Delta u_r \quad (4.33)$$

$$\text{where } [S] = \left[ \frac{\partial \underline{g}}{\partial \underline{x}} \right]^{-1} \left[ \frac{\partial \underline{g}}{\partial u} \right] \quad (4.34)$$

The elements of  $\left( \frac{\partial \underline{g}}{\partial \underline{x}} \right)$  and  $\left( \frac{\partial \underline{g}}{\partial u} \right)$  are given in APPENDIX H.

Thus, given the solution of  $\underline{x}$  at the previous step, the solution at the present step can be obtained as

$$\underline{x}_r = \underline{x}_{r-1} + \Delta \underline{x}_r \quad (4.35)$$

where  $\Delta \underline{x}_r$  is the solution of the linear Eq. (4.33).

The accuracy of the solution of  $\underline{x}$  is controlled by selecting the step size  $\Delta u_r$ .

The algorithm for the determination of critical energy is as follows :

Step 1 : Solve for  $\underline{x}$  at  $t = 0$  from

$$\underline{g}(\underline{x}_0, u_0) = \underline{0} \quad (4.36)$$

using Newton's method.

Step 2 : Compute  $W_2(t = 0) = W_2(\underline{x}_0, u_0)$

Step 3 : Set iteration count  $r = 1$  and  $\Delta u_r = H$

Step 4 : Augment  $u_{r-1}$  by  $\Delta u_r$ , i.e.,

$$u_r = u_{r-1} + \Delta u_r$$

Step 5 : Solve for  $\Delta \underline{x}_r$  using Eq. (4.33), i.e.,

$$\Delta \underline{x}_r = [S] \Delta u_r$$

Step 6 : Update the value of  $\underline{x}_{r-1}$ , i.e.,

$$\underline{x}_r = \underline{x}_{r-1} + \Delta \underline{x}_r$$

Step 7 : Calculate

$$\Delta W_2 = W_2(t_r) - W_2(t_{r-1})$$

If  $\Delta W_2$  is positive, set  $r = r+1$  and go to Step 4.

Otherwise, set  $W_{cr} = W_2(t_{r-1})$  and stop.

## 4.4 NUMERICAL EXAMPLES

### 4.4.1 Description

The three system examples considered in Chapter 2 and Chapter 3 are again taken up to illustrate the application of the proposed method for dynamic security assessment of power systems. It is assumed that a three phase fault occurs at the terminals of generators which is cleared followed by instantaneous reclosure of the line. This implies that the prefault and the post-fault networks are assumed to have identical configuration. For simplicity, all the load buses are considered to have similar characteristics. The following examples are investigated :

Example 1 : 7-machine 10-bus (CIGRE) test system

Fault locations :

- a) bus 1 ; b) bus 2 ; c) bus 3 ; d) bus 5 ;  
e) bus 6 ; f) bus 7

Load models :

- i)  $k_1 V^2 + jk_2 V^2$  ; ii)  $k_1 + jk_2 V^2$

Example 2 : 10-machine 39-bus (NEW ENGLAND) test system.

Fault locations :

- a) bus 1 ; b) bus 3 ; c) bus 4 ; d) bus 5 ;  
e) bus 6 ; f) bus 7 ; g) bus 8 ; h) bus 9

Load models :

$$i) \quad k_1 V^2 + j k_2 V^2 \quad ; \quad ii) \quad k_1 + j k_2 V^2$$

Example 3 : 13-machine 71-bus (UPSEB) system

Fault locations :

- a) bus 6 (Gen. no.3) ; b) bus 15 (Gen. no.5);
- c) bus 27 (Gen. no.6) ; d) bus 39 (Gen. no.8);
- e) bus 44 (Gen. no.9) ; f) bus 64 (Gen. no.11)
- g) bus 68 (Gen. no.13)

Load models :

$$i) \quad k_1 V^2 + j k_2 V^2 \quad ; \quad ii) \quad k_1 + j k_2 V^2$$

#### 4.4.2 Results

The critical value of the energy function is evaluated using PEBS method for all the three examples both by performing the simulation of the faulted trajectory and by the proposed method. The results are then compared and are presented in Tables 4.1-4.3 for examples 1,2 and 3 respectively. An arbitrary step size of  $H = 0.1$  radian is used in the computation of  $\theta_k$ .

The rotor angle and velocity of the faulted generator  $k$  are obtained for example 2 using i) the proposed method and ii) trajectory estimation of the faulted network, for various fault locations and load model (i). The results are compared and are given in Table 4.4. These results are obtained for an arbitrarily selected clearing time,  $t_{c1} = 0.20$  sec.

Table 4.1 Comparison of critical energy,  $W_{cr}$  for 7-machine system  
 $\theta_k^*$  in radians and  $W_{cr}$  in p.u.

Fault Location	Gen. No. k	Load Model : i) $k_1 V + j k_2 V^2$		Load Model : ii) $k_1 + j k_2 V^2$		
		$\theta_k^*$ obtained by Trajectory Simulation Method	$W_{cr}$ obtained by Trajectory Simulation Method	$W_{cr}$ obtained by Trajectory Simulation Method	Proposed Method	
Bus 1	1	2.6147	2.5602	15.8257	12.1921	11.8984
Bus 2	2	2.5939	2.5366	15.3988	11.9425*	11.7832
Bus 3	3	2.4948	2.4229	18.4630	-*	12.3301*
Bus 5	5	2.6787	2.6074	10.0852	-*	-
Bus 6	6	2.4018	2.4693	14.9212	13.3835*	12.9086*
Bus 7	7	2.4651	2.4432	5.8959	-	-

\* = Network solution does not converge.

Table 4.2 Comparison of Critical Energy,  $W_{cr}$  for 10-machine System  
 $\theta_k^*$  in radian and  $W_{cr}$  in p.u.

Fault Location	Gen. No. k	Load Model : i) $k_1 V^2 + jk_2 V^2$		Load Model: ii) $k_1 + jk_2 V^2$			
		$\theta_k^*$ obtained by	$W_{cr}$ obtained by	$W_{cr}$ obtained by			
		Trajectory Simulation	Proposed Method	Trajectory Simulation	Proposed Method		
Bus 1	1	2.4690	2.5135	7.5771	7.7308	6.4175	6.5477
Bus 3	3	2.4645	2.5071	7.3153	7.5602	6.0197*	5.9304*
Bus 4	4	2.6103	2.4850	9.8640	8.9189	-	-
Bus 5	5	2.2958	2.4004	2.8465	2.9621	2.4043*	2.4002*
Bus 6	6	2.8313	2.8091	9.9969	9.9148	-	-
Bus 7	7	2.6246	2.9223	8.8263	8.9502	7.5624	7.2541
Bus 8	8	2.5664	2.5742	8.9164	8.9977	8.0419*	7.9289*
Bus 9	9	1.9414	2.0039	2.3473	2.3611	-	-
Bus 10	10	2.6543	2.5684	24.7726	24.2201		

\* = Network solution does not converge

Table 4.3 Comparison of Critical Energy,  $W_{cr}$  for 13-machine system

Fault Location	Gen. No. k	Load Models			
		$i) k_1 V^2 + j k_2 V^2$		$ii) k_1 + j k_2 V^2$	
		$W_{cr}$ obtained by		$W_{cr}$ obtained by	
		Trajectory Simulation	Proposed Method	Trajectory Simulation	Proposed Method
Bus 6	3	1.8425	1.8857	1.5588	1.5955
Bus 15	5	1.9470	1.9191	1.6458*	1.6222*
Bus 27	6	2.5799	2.6508	-	-
Bus 39	8	0.8694	0.8965	0.7374*	0.7604*
Bus 44	9	2.2569	2.1969	-	-
Bus 64	11	3.5106	3.5432	2.9683	3.1028
Bus 68	13	1.0263	1.0075	0.8825	0.8663

\* = Network solution does not converge

Table 4.4  $\omega_{kcl}$  and  $\theta_{kcl}$  at clearing ( $t_{cl} = 0.20$  sec) for 10-machine system - Load Model : i)  $k_1 V^2 + j k_2 V^2$

Fault Location	Gen. No. k	Trajectory Simulation			Proposed Method	
		$\omega_{kcl}$ (rad/sec)	$\theta_{kcl}$ (rad)	$\omega_{kcl}$ (rad/sec)	$\theta_{kcl}$ (rad)	
Bus 3	3	6.4136	0.9528	6.5318	0.9602	
Bus 4	4	7.8629	1.0777	8.0263	1.0876	
Bus 5	5	7.0378	1.2066	7.1212	1.2125	
Bus 6	6	6.5837	0.9732	6.7284	0.9820	
Bus 7	7	7.5836	1.0861	7.7271	1.0950	
Bus 8	8	7.9797	1.0771	8.1175	1.0860	
Bus 9	9	8.5443	1.3625	8.6699	1.3709	
Bus 10	10	2.0738	0.1778	2.1236	0.1808	

The kinetic energy and the potential energy components of transient energy at clearing are estimated corresponding to the clearing time,  $t_{c1} = 0.20$  sec using i) the proposed method and ii) the faulted trajectory simulation, considering load representation of type (i) for example 2. The transient energy margin,  $\Delta W$  and the normalised transient energy margin,  $\Delta W_n$  are then calculated and the contingencies are ranked based on their severity. Results obtained using the proposed method are presented in Table 4.5 while Table 4.6 shows the results obtained by trajectory simulation.

#### 4.4.3 Discussion

It can be observed from Tables 4.1-4.3 that the value of the critical energy obtained by the proposed method is generally in good agreement with that obtained by performing the trajectory simulation of the faulted system. For 7-machine system, the maximum and minimum differences in the value of critical energy are 3% (fault at bus 3) and 0.39% (fault at bus 6) respectively (Table 4.1) with the loads modelled as (i). For the same load model, the corresponding values for 10-machine system are 9.58% (fault at bus 4) and 0.59% (fault at bus 9) respectively (Table 4.2). For 13-machine system, the maximum and minimum values can be seen (Table 4.3) to be 3.11% (fault at bus 39) and 0.92% (fault at bus 64) respectively. The maximum and minimum differences in the value of the critical energy for load

Table 4.5  $\Delta W$  and  $\Delta W_n$  by the Proposed Method and Ranking of Three phase Faults  
for 10-machine System  
Clearing time,  $t_{cl} = 0.200$  seconds

Fault Location	Gen. No.	Critical Energy, $W_{cr}$ (pu)	Energy at clearing		$\Delta W = W_{cr} - W_{cl}$	$\Delta W_n = \frac{W_{cr} - W_{2cl}}{W_{1cl}}$	Rank	Remarks
			$W_{1cl}$ (pu)	$W_{2cl}$ (pu)				
Bus 3	3	7.5602	4.2456	2.0025	6.2481	1.3121	1.3090	4
Bus 4	4	8.9189	5.0726	3.5857	8.6583	0.2606	1.0514	3
Bus 5	5	2.9621	3.6176	1.1904	4.8080	-1.8459	0.4897	2
Bus 6	6	9.9142	4.3735	2.6829	7.0564	2.8578	1.6536	7
Bus 7	8.9508	9.9502	4.3272	3.0586	7.3858	1.5644	1.3615	6
Bus 8	8	8.9977	4.4835	3.0027	7.4862	1.5115	1.3450	5
Bus 9	9	2.3611	7.1960	2.3047	9.5007	-7.1395	0.0079	1
Bus 10	10	24.2201	0.5309	0.4071	0.9380	23.2821	44.8709	8

Table 4.6  $\Delta W$  and  $\Delta W_n$  by Trajectory Simulation and Ranking of Three Phase Faults for 10-machine System

clearing time,  $t_{c1} = 0.200$  seconds

Fault Location	Gen. No.	Critical Energy, $W_{cr}$ (pu)	Energy at clearing		$\Delta W$ $= W_{cr} - W_{cl}$	$\Delta W_n$ $W_{cr} - W_{2cl}$ $W_{1cl}$	Rank	Remark	
			$W_{1cl}$ (pu)	$W_{2cl}$ (pu)					
Bus 3	3	7.3153	4.0934	1.8219	5.9153	1.4000	1.3420	4	Stable
Bus 4	4	9.8640	4.8681	4.0331	8.9012	0.9628	1.1978	3	Stable
Bus 5	5	2.8465	3.5334	1.0752	4.6086	-1.7621	0.5013	2	Unstable
Bus 6	6	9.9969	4.1873	2.3075	6.4948	3.5021	1.8364	7	Stable
Bus 7	7	8.8263	4.1680	2.5304	6.6984	2.1279	1.5105	6	Stable
Bus 8	8	8.9164	4.2358	2.7391	6.9749	1.9415	1.4584	5	Stable
Bus 9	9	2.3473	6.9890	1.5320	8.5210	-6.1737	0.1167	1	Unstable
Bus 10	10	24.7726	0.5063	0.3834	0.8897	23.8829	48.1714	8	Stable

characteristics of type (ii) are less than those obtained for the load representation of type (i) for the fault locations considered on all the three system examples investigated. The problem of convergence of the network solution is also encountered with constant active power loads as in Chapter 3 and this is indicated in the tables.

It can be seen from Tables 4.5 and 4.6 that the proposed method for computing TEM predicts accurately the stability of the system for all the disturbances considered. Although the values of TEM calculated by the proposed method do not exactly match with the values obtained from simulating the faulted trajectory, it is interesting to observe that the ranking of the contingencies given by both methods are identical. This shows the practical validity of the proposed method.

Actually, the proposed method can be viewed as an extension of the equal area criterion for multi-machine systems, based on the assumption that the faulted generator separates from the rest. Although a two-machine equivalent can be derived under this assumption for constant impedance type loads [32], the procedure given in this chapter does not require such a derivation for simplifying the computation. Also, for structure preserving models, it is not feasible to obtain two-machine equivalents, particularly for nonlinear type loads.

It is interesting to note that the accuracy of the proposed method is not critically dependent on the validity of the assumption about the mode of instability. For example, in the case of 10-machine system it is observed (see Chapter 3 that the faulted generator accelerates along with other generators in the case of faults at buses 6 and 7.

The major computational effort in the evaluation of TEM in the proposed method, lies in determination of  $W_{cr}$ . Even here there is a significant saving in the computations than the usual method of integrating the faulted system equations. The use of SPEF requires the solution of the network equations twice at a step during the simulation of the faulted equations. The proposed method requires the solution of the post-fault system equations and even this is simplified using linearisation. In the numerical examples considered, it required about 20-25 steps to compute  $W_{cr}$  in the proposed method, while it took 40-50 time steps to compute  $W_{cr}$  using the simulation of the faulted equations. Both faulted and post-fault networks were solved for each step during the simulation.

Further computational savings are possible in the proposed method if approximations can be introduced in the sensitivity matrices in each step.

It is interesting to observe that the calculation of  $\theta_{kc}$  and  $\omega_{kcl}$  in the proposed method do not require the knowledge of

faulted trajectory. Also, the computation of energy at clearing requires the solution of one set of nonlinear algebraic equations (to determine the accelerating power of the faulted generator).

#### 4.5 CONCLUSIONS

In this chapter, a novel method using SPEF developed based on an apriori knowledge of the mode of system separation, is presented to evaluate the transient energy margin. This method does not require the simulation of the faulted equations to compute critical energy and energy at clearing and is computationally quite efficient. The application of the proposed method to three large scale sample systems yields encouraging results and lead to the following conclusions :

- i) the proposed method is the first step in the application of SPEF for on-line dynamic security assessment. The results obtained from this method is promising enough to continue the investigation for speeding up the computation required in the on-line dynamic security assessment.
- ii) the normalised transient energy margin is a convenient index for ranking the contingencies (3-phase faults at generator terminals). The proposed method can also serve as an accurate algorithm for contingency ranking.

## CHAPTER 5

### A STRUCTURE PRESERVING ENERGY FUNCTION INCORPORATING TRANSMISSION LINE RESISTANCES

#### 5.1 INTRODUCTION

The structure preserving energy functions so far have neglected the transmission line resistances. While this assumption can be justified due to high values of  $X/R$  ratio of extra high voltage transmission lines, it is used mainly to circumvent analytical difficulties of defining Lyapunov functions for lossy networks.

With the reduced networks by assuming constant impedance load models, transfer conductances cannot be ignored and lot of effort went into the inclusion of transfer conductances into the energy function [30, 50]. There is no adequate solution for this problem and the use of path dependent terms in the energy function is unavoidable. This can result in unreliable prediction of stability regions.

The use of structure preserving model circumvents the problem of transfer conductances and makes it possible to account for voltage dependent load models. Although arbitrary voltage dependent active power load can result in path dependent terms, it has been shown in Chapters 2 and 3 that the use of approximations by neglecting path dependent terms in the energy function

gives very accurate results. In general, it can be argued that path dependent terms which are relatively small in magnitude, can be easily handled by numerical integration. This makes it worthwhile to investigate more detailed models of the system.

A novel approach to develop a structure preserving energy function including transmission line resistances is presented in this chapter. This development of the energy function is based on the result that a network having the same conductance to susceptance ratio ( $G/B$ ) for all its elements, can be transformed to a lossless network with a new set of power injections [67]. Even though  $G/B$  ratio in practical power system networks is not constant, it is possible to introduce approximations by taking the average value of  $G/B$ .

The structure preserving energy function based on the approximation is presented alongwith applications to the direct stability evaluation of two sample systems.

## 5.2 NETWORK TRANSFORMATION

It is shown in [67] that a lossy network with constant  $G/B$  ratio ( $G/B = \alpha$ ) for all its elements, is equivalent to a lossless network with a new set of power injections. The relationship between the two sets of injections is given by

$$P_i = P'_i + \alpha Q'_i \quad (5.1)$$

$$Q_i = -\alpha P'_i + Q'_i \quad (5.2)$$

where  $P_i$  and  $Q_i$  refer to injections for the original network,  $P'_i$  and  $Q'_i$  refer to the injections for the transformed (lossless) network. The susceptance matrices for both networks are identical. Fig. 5.1 shows the original and the transformed networks with 'm' generators (internal) and 'n' load buses (including generator terminal buses).

From Eqs. (5.1) and (5.2), we can write

$$P'_i = \frac{1}{1+\alpha^2} P_i - \frac{\alpha}{1+\alpha^2} Q_i \quad (5.3)$$

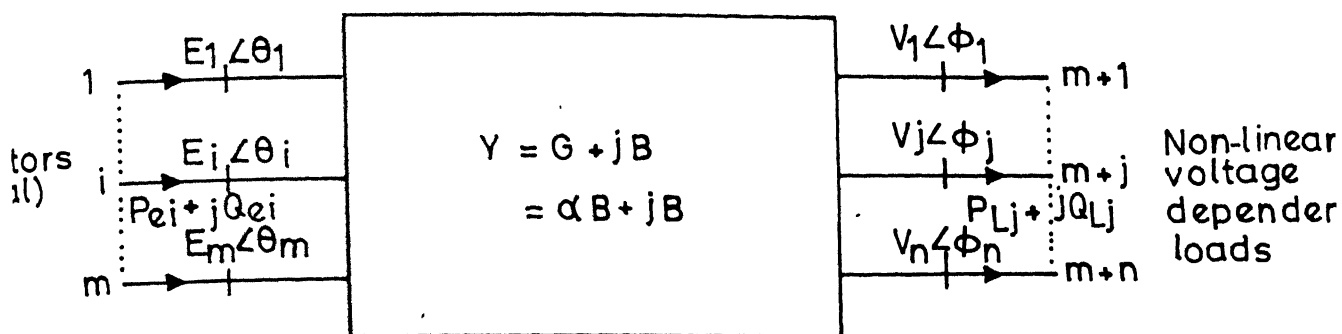
$$Q'_i = \frac{\alpha}{1+\alpha^2} P_i + \frac{1}{1+\alpha^2} Q_i \quad (5.4)$$

The relationships given in Eqs. (5.1) - (5.4) are derived in APPENDIX I.

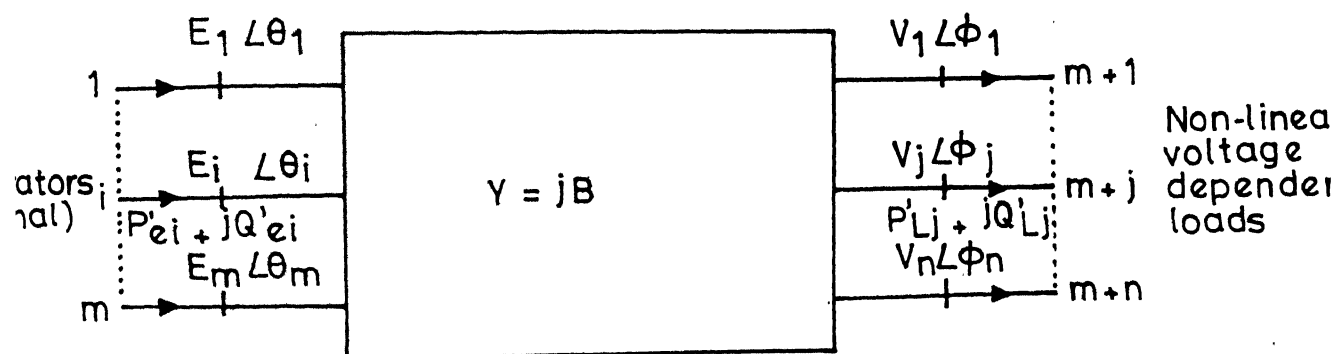
### 5.3 .SYSTEM MODEL

#### 5.3.1 Generator Equations

Consider the system shown in Fig. 5.1(b). Assuming classical model for generators, the motion of the  $i$ th machine can be written as (with respect to an arbitrary synchronous reference frame)



(a) ORIGINAL NETWORK



(b) TRANSFORMED NETWORK

FIG.5.1 A SYSTEM OF  $m$  GENERATORS SUPPLYING POWER TO  $n$  NON-LINEAR VOLTAGE DEPENDENT LOADS

$$\dot{\delta}_i = \omega_i^{\text{syn}} \quad (5.5a)$$

$$M_i \dot{\omega}_i^{\text{syn}} = P_{mi} - P_{ei}, \quad i = 1, 2, \dots, m \quad (5.5b)$$

In view of Eq. (5.1), Eqs. (5.5) can be written as

$$\dot{\delta}_i = \omega_i^{\text{syn}} \quad (5.6a)$$

$$\begin{aligned} M_i \dot{\omega}_i^{\text{syn}} &= P_{mi} - (P'_{ei} + \alpha Q'_{ei}) \\ &= P'_{mi} - P'_{ei}, \quad i = 1, 2, \dots, m \end{aligned} \quad (5.6b)$$

$$\text{where} \quad P'_{mi} = P_{mi} - \alpha Q'_{ei}, \quad i = 1, 2, \dots, m \quad (5.7)$$

Eqs. (5.6) can also be written as (with respect to COI reference)

$$\dot{\theta}_i = \omega_i \quad (5.8a)$$

$$M_i \dot{\omega}_i = P'_{mi} - P'_{ei} - \frac{M_i}{M_T} P'_{\text{COI}}, \quad i = 1, 2, \dots, m \quad (5.8b)$$

$$\text{where} \quad P'_{ei} = b_i E_i V_i \sin(\theta_i - \varphi_i), \quad i = 1, 2, \dots, m \quad (5.9)$$

$$Q'_{ei} = b_i [E_i^2 - E_i V_i \cos(\theta_i - \varphi_i)], \quad i = 1, 2, \dots, m \quad (5.10)$$

$$P'_{\text{COI}} = \sum_{i=1}^m (P'_{mi} - P'_{ei}) \quad (5.11)$$

In the above expressions,  $b_i$  is the susceptance of machine  $i$ .

The dynamics of the COI is described by

$$M_T \dot{\omega}_0 = P'_{\text{COI}} \quad (5.12)$$

$$\text{where } \omega_o = \frac{1}{M_T} \sum_{i=1}^m M_i \omega_i, \quad M_T = \sum_{i=1}^m M_i \quad (5.13)$$

### 5.3.2 Load Model

The real and the reactive power loads at bus  $i$  of the transformed network are modelled as arbitrary functions of the bus voltage, i.e.,

$$P'_{Li} = f'_{pi}(V_i), \quad i = 1, 2, \dots, n \quad (5.14)$$

$$Q'_{Li} = f'_{qi}(V_i), \quad i = 1, 2, \dots, n \quad (5.15)$$

### 5.3.3 Power Flow Equations

The real and reactive power injections at bus  $i$  of the transformed network can be written as

$$\begin{aligned} P'_i &= b_i E_i V_i \sin(\varphi_i - \theta_i) + \sum_{j=1}^n B_{ij} V_i V_j \sin \varphi_{ij}, \quad i = 1, 2, \dots, m \\ &= \sum_{j=1}^n B_{ij} V_i V_j \sin \varphi_{ij}, \quad i = m+1, m+2, \dots, n \end{aligned} \quad (5.16)$$

$$\begin{aligned} Q'_i &= b_i [V_i^2 - E_i V_i \cos(\varphi_i - \theta_i)] - \sum_{j=1}^n B_{ij} V_i V_j \cos \varphi_{ij}, \\ &\quad i = 1, 2, \dots, m \\ &= - \sum_{j=1}^n B_{ij} V_i V_j \cos \varphi_{ij}, \quad i = m+1, m+2, \dots, n \end{aligned} \quad (5.17)$$

where  $[B]$  is the susceptance matrix of the network.

Since the net powers at bus  $i$  is zero, we have the following power flow equations :

$$P_i' + f_{pi}' (V_i) = 0, \quad i = 1, 2, \dots, n \quad (5.18)$$

$$Q_i' + f_{qi}' (V_i) = 0, \quad i = 1, 2, \dots, n \quad (5.19)$$

#### 5.4 STRUCTURE PRESERVING ENERGY FUNCTION (SPEF)

The system model described by Eqs. (5.8) - (5.19) is similar to the model considered in [54]. The only difference is that the transformed mechanical power  $P_{mi}'$  is not constant and varies with time. However, a general structure preserving energy function for lossless networks with time varying mechanical powers input is derived in APPENDIX C. Applying this energy function for the system shown in Fig. 5.1(b), we get

$$W = W_1 + W_2' = W_1 + \sum_{i=1}^5 W_{2i}' \quad (5.20)$$

$$\text{where } W_1 = \frac{1}{2} \sum_{i=1}^m M_i \omega_i^2 \quad (5.21)$$

$$W_{21}' = - \sum_{i=1}^m \int_{t_0}^t P_{mi}' \frac{d\theta_i}{dt} dt \quad (5.22)$$

$$W_{22}' = \sum_{i=1}^n \int_{t_0}^t P_{Li}' \frac{d\phi_i}{dt} dt \quad (5.23)$$

$$W_{23}' = \sum_{i=1}^n \int_{V_{i0}}^{V_i} \frac{f_{qi}'(V_i)}{V_i} dV_i \quad (5.24)$$

$$W'_{24} = \sum_{i=1}^m [E_i^2 + V_i^2 - 2E_i V_i \cos(\theta_i - \varphi_i) - (E_{i0}^2 + V_{i0}^2 - 2E_i V_{i0} \cos(\theta_{i0} - \varphi_{i0}))] \frac{1}{2x'_{di}} \quad (5.25)$$

$$W'_{25} = -\frac{1}{2} \sum_{i=1}^n \sum_{j=1}^n B_{ij} (V_i V_j \cos \varphi_{ij} - V_{i0} V_{j0} \cos \varphi_{ij0}) \quad (5.26)$$

In the above expressions, subscript 'o' indicates the quantities evaluated at the initial stable equilibrium point.

Utilising the relations in Eqs. (5.3), (5.4), (5.7), (5.10) and (5.15), the energy terms  $W'_{21}$ ,  $W'_{22}$  and  $W'_{23}$  can be written as

$$\begin{aligned} W'_{21} &= - \sum_{i=1}^m \int_{t_0}^t [P_{mi} - \alpha b_i (E_i^2 - E_i V_i \cos(\theta_i - \varphi_i))] \frac{d\theta_i}{dt} dt \\ &= - \sum_{i=1}^m \int_{t_0}^t P_{mi} \frac{d\theta_i}{dt} dt + \sum_{i=1}^m \alpha \int_{t_0}^t b_i (E_i^2 - E_i V_i \cos(\theta_i - \varphi_i)) \frac{d\theta_i}{dt} dt \\ &= - \sum_{i=1}^m P_{mi} (\theta_i - \theta_{i0}) + \sum_{i=1}^m \alpha \int_{t_0}^t b_i (E_i^2 - E_i V_i \cos(\theta_i - \varphi_i)) \frac{d\theta_i}{dt} dt \\ &= W_{21} + W_{26} \end{aligned} \quad (5.27)$$

$$\text{where, } W_{21} = - \sum_{i=1}^m P_{mi} (\theta_i - \theta_{i0}). \quad (5.28)$$

$$W_{26} = \sum_{i=1}^m \alpha \int_{t_0}^t b_i (E_i^2 - E_i V_i \cos(\theta_i - \varphi_i)) \frac{d\theta_i}{dt} dt \quad (5.29)$$

$$W'_{22} = \sum_{i=1}^n \int_{t_0}^t \left[ -\frac{1}{1+\alpha^2} (P_{Li} - \alpha Q_{Li}) \right] \frac{d\phi_i}{dt} dt \quad (5.30)$$

$$W'_{23} = \sum_{i=1}^n \int_{V_{i0}}^{V_i} \left[ \frac{1}{1+\alpha^2} \left( \frac{\alpha P_{Li} + Q_{Li}}{V_i} \right) \right] dV_i \quad (5.31)$$

The energy function  $W$  can now be expressed as

$$W = W_1 + W_2 = W_1 + \sum_{i=1}^6 W_{2i} \quad (5.32)$$

where

$$W_{22} = W'_{22} ; \quad W_{23} = W'_{23} ; \quad W_{24} = W'_{24} \quad \text{and} \quad W_{25} = W'_{25} .$$

### Comments

1) As described in Chapter 3, if the mode of instability is known apriori, the kinetic energy term  $W_1$  can be replaced by  $W_{11}$  which corresponds to the kinetic energy component responsible for system separation. If it is assumed that the faulted generator  $k$  separates from the rest of the generators (which swing together), then

$$W_{11} = \frac{1}{2} \frac{M_k M_{T-k}}{M_T} (\omega_k - \omega_{T-k})^2 \quad (5.33)$$

2) The energy term  $W_{26}$  in Eq. (5.29) can be written as

$$\begin{aligned}
 W_{26} &= \sum_{i=1}^m [\alpha b_i E_i^2 \int \frac{d\theta_i}{dt} dt] - \sum_{i=1}^m [\alpha b_i E_i \int_{t_0}^t V_i \cos(\theta_i - \varphi_i) \frac{d\theta_i}{dt} dt] \\
 &= \sum_{i=1}^m \alpha b_i E_i^2 (\theta_i - \theta_{i0}) - \sum_{i=1}^m [\alpha b_i E_i \int_{t_0}^t V_i \cos(\theta_i - \varphi_i) \frac{d\theta_i}{dt} dt] \\
 &= W_{261} + W_{262}
 \end{aligned} \tag{5.34}$$

$$\text{where } W_{261} = \sum_{i=1}^m \alpha b_i E_i^2 (\theta_i - \theta_{i0}) \tag{5.35}$$

$$W_{262} = \sum_{i=1}^m \alpha b_i E_i \int_{t_0}^t V_i \cos(\theta_i - \varphi_i) \frac{d\theta_i}{dt} dt \tag{5.36}$$

In the above expressions, while the term  $W_{261}$  is path independent, the term  $W_{262}$  is path dependent and can be evaluated by numerical integration using trapezoidal rule [75].

3) For constant real and reactive power loads, the term  $W_{22}$  and  $W_{23}$  can be directly computed from

$$W_{22} = \sum_{i=1}^n \left[ \frac{1}{1+\alpha^2} [P_{Li} - \alpha Q_{Li}] (\varphi_i - \varphi_{i0}) \right] \tag{5.37}$$

$$W_{23} = \sum_{i=1}^n \left[ \frac{1}{1+\alpha^2} [\alpha P_{Li} + Q_{Li}] (\log_e V_i - \log_e V_{i0}) \right] \tag{5.38}$$

It is interesting to observe that an additional condition of reactive power components of the loads being independent of the

2) The energy term  $W_{26}$  in Eq. (5.29) can be written as

$$\begin{aligned}
 W_{26} &= \sum_{i=1}^m [\alpha b_i E_i^2 \int \frac{d\theta_i}{dt} dt] - \sum_{i=1}^m [\alpha b_i E_i \int_{t_0}^t V_i \cos(\theta_i - \varphi_i) \frac{d\theta_i}{dt} dt] \\
 &= \sum_{i=1}^m \alpha b_i E_i^2 (\theta_i - \theta_{i0}) - \sum_{i=1}^m [\alpha b_i E_i \int_{t_0}^t V_i \cos(\theta_i - \varphi_i) \frac{d\theta_i}{dt} dt] \\
 &= W_{261} + W_{262}
 \end{aligned} \tag{5.34}$$

$$\text{where } W_{261} = \sum_{i=1}^m \alpha b_i E_i^2 (\theta_i - \theta_{i0}) \tag{5.35}$$

$$W_{262} = \sum_{i=1}^m \alpha b_i E_i \int_{t_0}^t V_i \cos(\theta_i - \varphi_i) \frac{d\theta_i}{dt} dt \tag{5.36}$$

In the above expressions, while the term  $W_{261}$  is path independent, the term  $W_{262}$  is path dependent and can be evaluated by numerical integration using trapezoidal rule [75].

3) For constant real and reactive power loads, the term  $W_{22}$  and  $W_{23}$  can be directly computed from

$$W_{22} = \sum_{i=1}^n \left[ \frac{1}{1+\alpha^2} [P_{Li} - \alpha Q_{Li}] (\varphi_i - \varphi_{i0}) \right] \tag{5.37}$$

$$W_{23} = \sum_{i=1}^n \left[ \frac{1}{1+\alpha^2} [\alpha P_{Li} + Q_{Li}] (\log_e V_i - \log_e V_{i0}) \right] \tag{5.38}$$

It is interesting to observe that an additional condition of reactive power components of the loads being independent of the

voltage, is required in this case compared to the case in lossless network to make the terms  $W_{22}$  and  $W_{23}$  path independent.

4) The component  $W_{26}$  is always path dependent as

$$W_{262} = \sum_{i=1}^m \alpha b_i E_i \int_{t_0}^t V_i \cos(\theta_i - \phi_i) \frac{d\theta_i}{dt} dt \quad (5.39)$$

cannot be integrated exactly. This implies that there is always a path dependent term in the energy function when the transmission line losses are considered. However, if this term is small in magnitude, it should not affect the accuracy in prediction significantly.

5) For practical power systems, G/B ratio for all the elements is not the same. However, the proposed energy function can still be employed to predict the critical clearing time using an average value for G/B.

PEBS method is employed again, as in Chapter 3 for a lossless system, to evaluate the critical energy for a fault at the terminals of a generator in a lossy network. The computer program described in Chapter 2 can be used with a minor modification to incorporate the calculation of the energy term  $W_{26}$  in Eq. (5.29) in the computation of SPEF. This term is path dependent and can be evaluated by numerical integration. To accommodate the known mode of instability, the kinetic energy term  $W_1$  is also modified.

## 5.5 NUMERICAL EXAMPLES

### 5.5.1 Description

Two system examples (7-machine and 10-machine) are studied to investigate the transient stability of lossy power system networks. The single-line diagrams alongwith system and operating data are given in APPENDICES E and F.

Three phase faults at different buses are considered for analysis. Fault clearing is followed by instantaneous reclosure of the line. This implies that the prefault and the post-fault network configurations are the same. Two different load characteristics are selected to illustrate the applicability of the proposed method to voltage dependent load models. Different load buses are assumed to have identical characteristics for the sake of simplicity in analysis. The following cases are investigated.

Example 1 : 7-machine 10-bus (CIGRE) test system

- a) Fault at bus 1 ; b) Fault at bus 2 ; c) Fault at bus 3 ;
- d) Fault at bus 5 ; e) Fault at bus 6 ; f) Fault at bus 7.

Types of load characteristics :

$$\text{i) } k_1 V^2 + j k_2 V^2 \quad ; \quad \text{ii) } k_1 + j k_2 V^2$$

Average  $\alpha = 0.2$ .

Example 2 : 10-machine 39-bus (NEW ENGLAND) test system

- a) Fault at bus 1 ; b) Fault at bus 3 ; c) Fault at bus 4 ;  
 d) Fault at bus 5 ; e) Fault at bus 6 ; f) Fault at bus 7 ;  
 g) Fault at bus 8 ; h) Fault at bus 9 .

Types of load characteristics :

$$i) k_1 V^2 + jk_2 V^2 \quad ; \quad ii) k_1 + jk_2 V^2$$

Average  $\alpha = 0.07$ .

In both the cases, results are also obtained for two arbitrary values of  $\alpha$  ; (i) 0.1 and (ii) 0.2.

#### 5.5.2 Results

In all the cases, critical clearing time is predicted using the proposed energy function for the assumed and average values for G/B and load characteristics of types (i) and (ii). The result is compared with that obtained by digital simulation and presented in Tables 5.1 - 5.2 and 5.4 - 5.6 for 7-machine and 10-machine systems respectively alongwith the critical energy. The predicted results are quite close to the results obtained by digital simulation.

Critical clearing time is also obtained by digital simulation for the average value for G/B of the systems under investigation and their actual line resistances for load representation of types (i) and (ii) and compared in Tables 5.3 and 5.7 for 7-machine and 10-machine systems respectively.

Table 5.1 Effect of transmission line resistance on critical energy,  $W_{cr}$  and predicted critical clearing time,  $t_{cr}$  for 7-machine System  
 $\alpha = 0.1$  ;  $t_{cr}$  in sec and  $W_{cr}$  in pu

Fault Location	Gen. No. k	Load Model : i) $k_1 V^2 + jk_2 V^2$			Load Model : ii) $k_1 + jk_2 V^2$				
		Critical Energy, $W_{cr}$	$t_{cr1}$	$t_{cr2}$	$t_{cr3}$	Critical Energy, $W_{cr}$	$t_{cr1}$	$t_{cr2}$	$t_{cr3}$
Bus 1	1	15.3525	0.383	0.385	0.390- 0.395	13.7567	0.417	0.423	0.425- 0.430
Bus 2	2	16.1474	0.443	0.446	0.450- 0.455	13.9060	0.380	0.386	0.390- 0.395
Bus 3	3	17.1216	0.457	0.461	0.460- 0.465	*	*	*	* -
Bus 5	5	9.5458	0.413	0.414	0.415- 0.420	*	*	*	* -
Bus 6	6	13.9285	0.607	0.608	0.610- 0.615	14.3976	0.595	0.604	0.600- 0.605
Bus 7	7	6.5627	0.360	0.361	0.360- 0.365	*	*	*	* -

$t_{cr1}$  = Critical clearing time obtained neglecting the mode of instability (by prediction)  
 $t_{cr2}$  = Critical clearing time obtained considering the mode of instability (by prediction)  
 $t_{cr3}$  = Critical clearing time obtained by digital simulation  
 \* = Network solution does not converge

Table 5.2 Effect of transmission line resistance on critical energy,  $W_{cr}$  and predicted critical clearing time,  $t_{cr}$  for 7-machine system  
 $\alpha = 0.2$  ;  $t_{cr}$  in sec and  $W_{cr}$  in pu

Fault Location	Gen. No.	Load Model : i) $k_1 V^2 + jk_2 V^2$			Load Model: ii) $k_1 + jk_2 V^2$				
		Critical Energy $W_{cr}$	$t_{cr1}$	$t_{cr2}$	$t_{cr3}$	Critical Energy $W_{cr}$	$t_{cr1}$	$t_{cr2}$	$t_{cr3}$
Bus 1	1	17.8174	0.401	0.403	0.405-0.410	16.5406	0.435	0.439	0.440-0.445
Bus 2	2	18.6679	0.465	0.467	0.470-0.475	16.8239	0.397	0.401	0.405-0.410
Bus 3	3	19.4162	0.480	0.482	0.480-0.485	*	*	*	*
Bus 5	5	10.6388	0.424	0.425	0.425-0.430	*	*	*	*
Bus 6	6	15.4196	0.631	0.633	0.635-0.640	16.5584	0.618	0.623	0.620-0.625
Bus 7	7	7.5794	0.378	0.379	0.380-0.385	*	*	*	*

\* = Network solution does not converge

Table 5.3 Comparison of critical clearing time,  $t_{cr}$  by digital simulation for 7-machine system  
 $t_{cr}$  in sec

Fault Location	Gen. No. k	Load Model : i) $k_1 V^2 + jk_2 V^2$		Load Model : ii) $k_1 + jk_2 V^2$	
		$t_{cr}$ with actual line resistance	$t_{cr}$ with average value for $\alpha=0.2$	$t_{cr}$ with actual line resistance	$t_{cr}$ with average value for $\alpha = 0.2$
Bus 1	1	0.400-0.405	0.405-0.410	0.435-0.440	0.440-0.445
Bus 2	2	0.470-0.475	0.470-0.475	0.405-0.410	0.405-0.410
Bus 3	3	0.485-0.490	0.480-0.485	- *	- *
Bus 5	5	0.430-0.435	0.425-0.430	- *	- *
Bus 6	6	0.630-0.635	0.635-0.640	0.620-0.625	0.620-0.625
Bus 7	7	0.380-0.385	0.380-0.385	- *	- *

\* = Network solution does not converge

Table 5.4 Effect of transmission line resistance on critical energy,  $W_{cr}$  and predicted critical clearing time,  $t_{cr}$  for 10-machine system  
 $\alpha = 0.1$  ;  $t_{cr}$  in sec and  $W_{cr}$  in pu

Fault Location	Gen. No. k	Load Model : i) $k_1V^2 + jk_2V^2$			Load Model : ii) $k_1 + jk_2V^2$				
		Critical Energy, $W_{cr}$	$t_{cr1}$	$t_{cr2}$	$t_{cr3}$	Critical Energy, $W_{cr}$	$t_{cr1}$	$t_{cr2}$	$t_{cr3}$
Bus 1	1	8.6607	0.257	0.258	0.270-0.275	7.0444	0.237	0.238	0.235-0.240
Bus 3	3	8.4144	0.227	0.228	0.240-0.245	6.5292	0.205	0.205	0.205-0.210
Bus 4	4	11.9475	0.230	0.232	0.235-0.240	*	*	*	*
Bus 5	5	4.2518	0.185	0.186	0.195-0.200	3.1525	0.163	0.163	0.170-0.175
Bus 6	6	12.1926	0.250	0.254	0.255-0.260	*	*	*	*
Bus 7	7	10.4329	0.233	0.236	0.245-0.250	*	*	*	*
Bus 8	8	10.4947	0.231	0.232	0.240-0.245	9.2487	0.220	0.221	0.220-0.225
Bus 9	9	3.7250	0.134	0.134	0.145-0.150	*	*	*	*

\* = Network solution does not converge

Table 5.5 Effect of transmission line resistance on critical energy,  $W_{cr}$  and critical clearing time,  $t_{cr}$  for 10-machine system  
 $\alpha = 0.2$

Fault Location	Gen. No. k	Load Model : i) $k_1 V^2 + jk_2 V^2$					Load Model : ii) $k_1 + jk_2 V^2$				
		Critical Energy, $W_{cr}$ (pu)	Critical clearing time			Critical Energy, $W_{cr}$ (pu)	Critical clearing time, $t_{cr}$ (sec)				
			$t_{cr1}$	$t_{cr2}$	$t_{cr3}$		$t_{cr1}$	$t_{cr2}$	$t_{cr3}$		
Bus 1	1	10.8214	0.277	0.278	0.290-0.295	8.8267	0.255	0.256	0.255-0.260		
Bus 3	3	10.7015	0.246	0.247	0.260-0.265	8.2722	0.221	0.222	0.220-0.225		
Bus 4	4	14.1525	0.243	0.246	0.250-0.255	*	*	*	*		
Bus 5	5	5.9082	0.208	0.209	0.215-0.220	*	*	*	*		
Bus 6	6	15.1326	0.268	0.273	0.275-0.280	*	*	*	*		
Bus 7	7	12.7624	0.250	0.253	0.260-0.265	*	*	*	*		
Bus 8	8	12.8183	0.247	0.249	0.255-0.260	11.3751	0.236	0.237	0.235-0.240		
Bus 9	9	4.5109	0.144	0.145	0.155-0.160	*	*	*	*		

\* = Network solution does not converge

Table 5.6 Effect of transmission line resistance on critical energy,  $W_{cr}$  and predicted critical clearing time,  $t_{cr}$  for average value of  $\alpha$  for 10-machine system  
Average value of  $\alpha = 0.07$  ;  $t_{cr}$  in sec and  $W_{cr}$  in pu

Fault Location	Gen. No. k	Load Model : i) $k_1 V^2 + jk_2 V^2$			Load Model : ii) $k_1 + jk_2 V^2$				
		Critical Energy, $W_{cr}$	$t_{cr1}$	$t_{cr2}$	$t_{cr3}$	Critical Energy, $W_{cr}$	$t_{cr1}$	$t_{cr2}$	$t_{cr3}$
Bus 1	1	8.1127	0.252	0.253	0.265-0.270	6.6252	0.233	0.233	0.230-0.235
Bus 3	3	7.8481	0.221	0.222	0.235-0.240	6.1165	0.200	0.200	0.200-0.205
Bus 4	4	11.3502	0.226	0.228	0.230-0.235	*	*	*	*
Bus 5	5	3.8320	0.179	0.180	0.190-0.195	2.8288	0.157	0.157	0.165-0.170
Bus 6	6	11.4569	0.245	0.248	0.250-0.255	*	*	*	*
Bus 7	7	9.8369	0.229	0.231	0.240-0.245	7.5868	0.207	0.208	0.205-0.210
Bus 8	8	9.8693	0.227	0.228	0.235-0.240	8.7484	0.216	0.217	0.225-0.230
Bus 9	9	3.5067	0.130	0.130	0.140-0.145	*	*	*	*

\* = Network solution does not converge

Table 5.7 Comparison of critical clearing time,  $t_{cr}$  by Digital Simulation for 10-machine system  
 $t_{cr}$  in sec

Fault Location	Gen. No. k	Load Model : i) $k_1 V^2 + jk_2 V^2$	Load Model : ii) $k_1 + jk_2 V^2$
		$t_{cr}$ with actual line resistance value of $\alpha=0.07$	$t_{cr}$ with actual line resistance value of $\alpha = 0.07$
Bus 1	1	0.265-0.270	0.230-0.235
Bus 3	3	0.235-0.240	0.200-0.205
Bus 4	4	0.230-0.235	* -
Bus 5	5	0.185-0.190	0.165-0.170
Bus 6	6	0.245-0.250	* -
Bus 7	7	0.240-0.245	0.205-0.210
Bus 8	8	0.235-0.240	0.220-0.225
Bus 9	9	0.135-0.140	* -

\* = Network solution does not converge

Swing curves for examples 2-a)(i), 2-b)(i), 2-c)(i), 2-f)(i) and 2-g)(i) are shown in Figs. 5.2-5.11 for stable and unstable cases for  $G/B = 0.1$  and load characteristic of type (i).

The variation of total energy, kinetic and potential energy components for examples 2-a)(i), 2-b)(i), 2-c)(i), 2-f)(i) and 2-g)(i) are shown in Figs. 5.12-5.13, 5.16-5.17, 5.20-5.21, 5.24-5.25 and 5.28-5.29 for stable and unstable conditions for the assumed value for  $G/B = 0.1$  with the loads modelled as type (i). The corresponding variation of the components of potential energy function,  $W_2$  are shown in Figs. 5.14-5.15, 5.18-5.19, 5.22-5.23, 5.26-5.27 and 5.30-5.31 respectively. The variation of the components of the energy term  $W_{26}$  is shown in Fig. 5.32 for the stable case with  $G/B = 0.1$  and loads modelled as type (i).

### 5.5.3 Discussion

It can be observed from the tables that the proposed energy function including the transmission line resistances yields a higher estimate of the critical clearing time for higher values of resistances. Also, the predicted values are in close agreement with the results obtained by digital simulation.

From Tables 5.3 and 5.7 it can be seen that the use of an average value for  $G/B$  gives accurate results in comparison

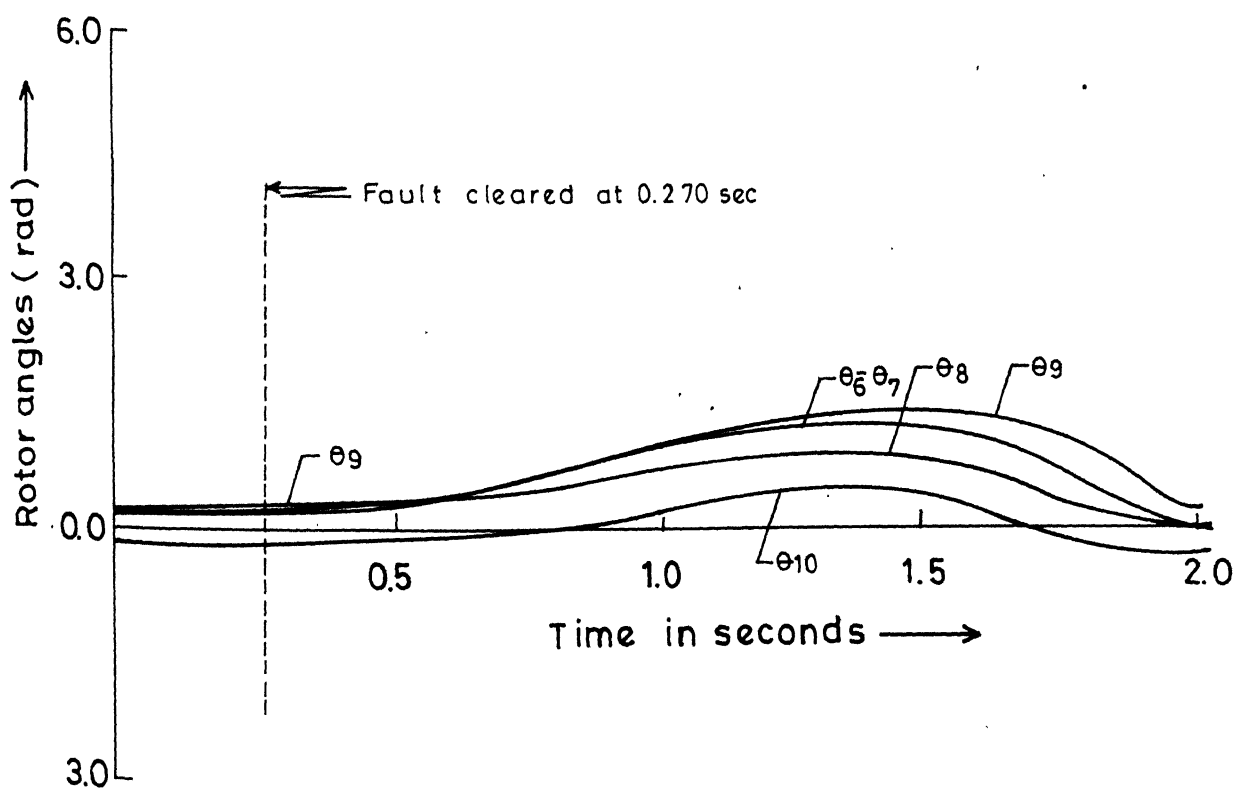
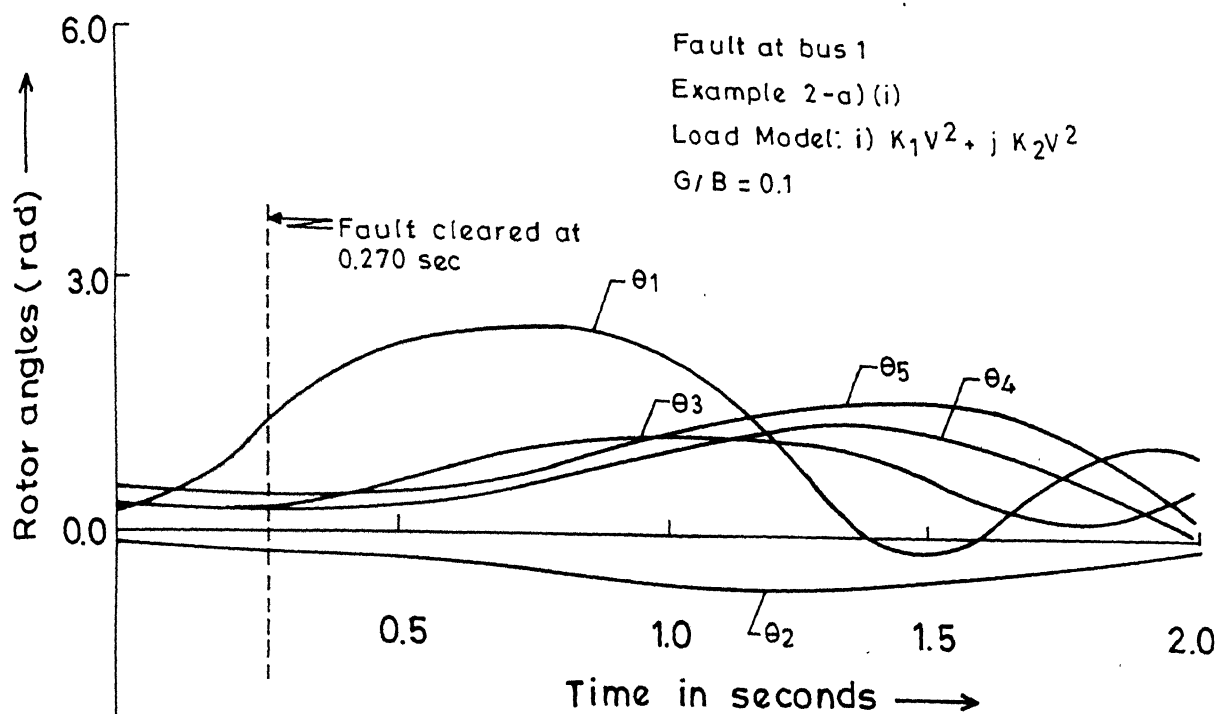


FIG. 5.2 SWING CURVES FOR 10-MACHINE SYSTEM, STABLE CASE

Fault at bus 1

Example 2-a)(i)

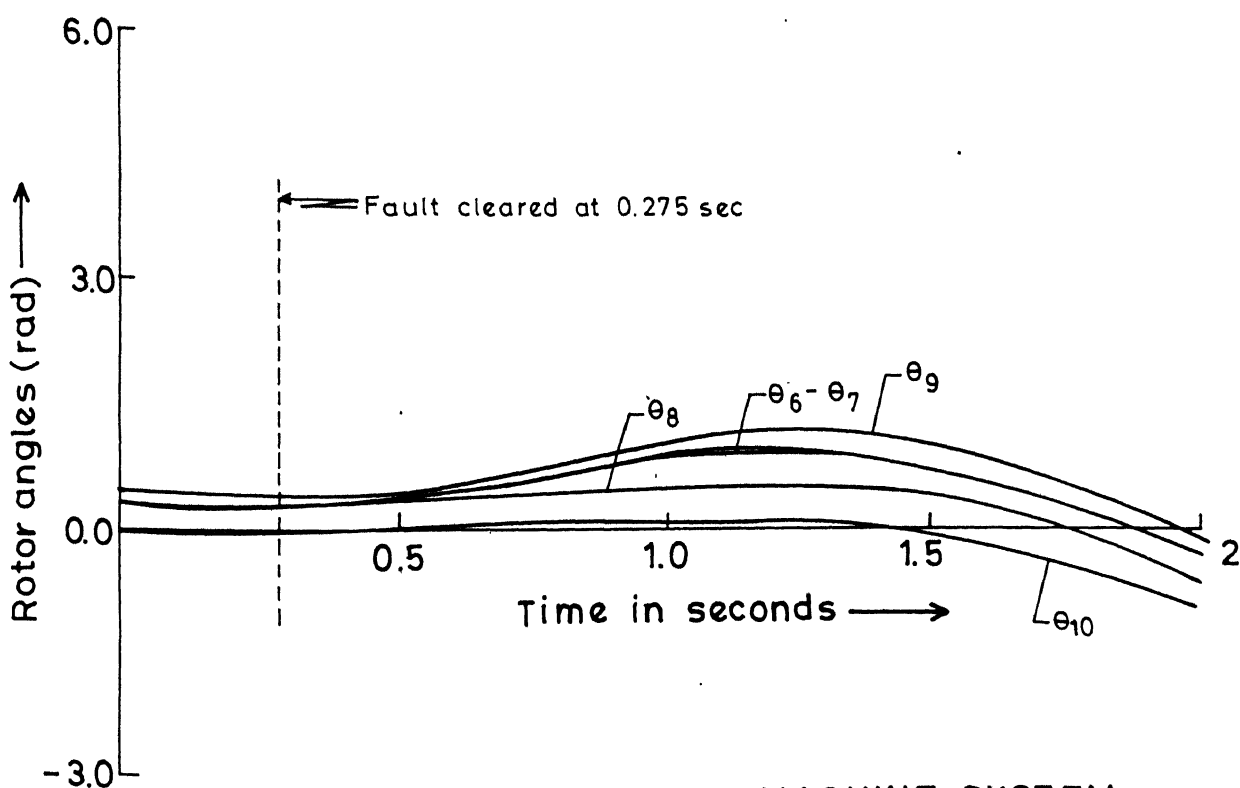
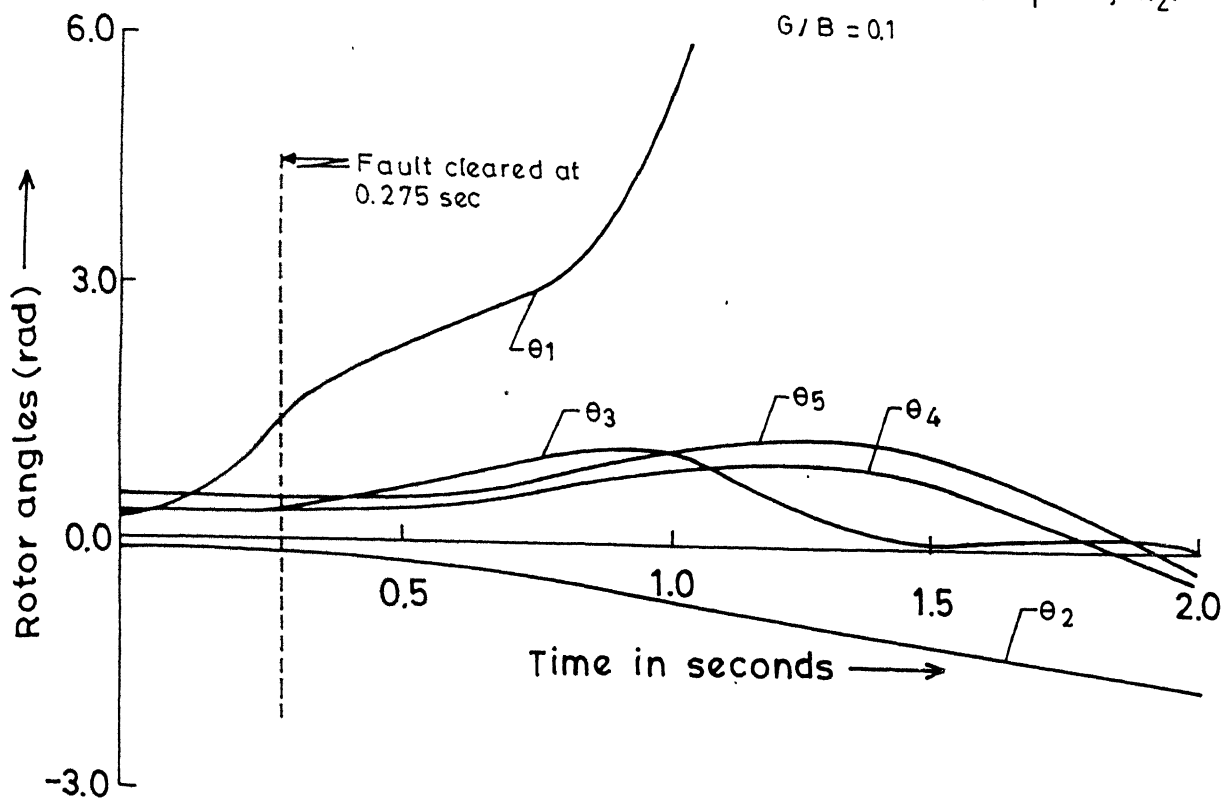
Load Model: i)  $K_1 V^2 + j K_2 V^2$  $G/B = 0.1$ 

FIG.5.3 SWING CURVES FOR 10-MACHINE SYSTEM,  
UNSTABLE CASE

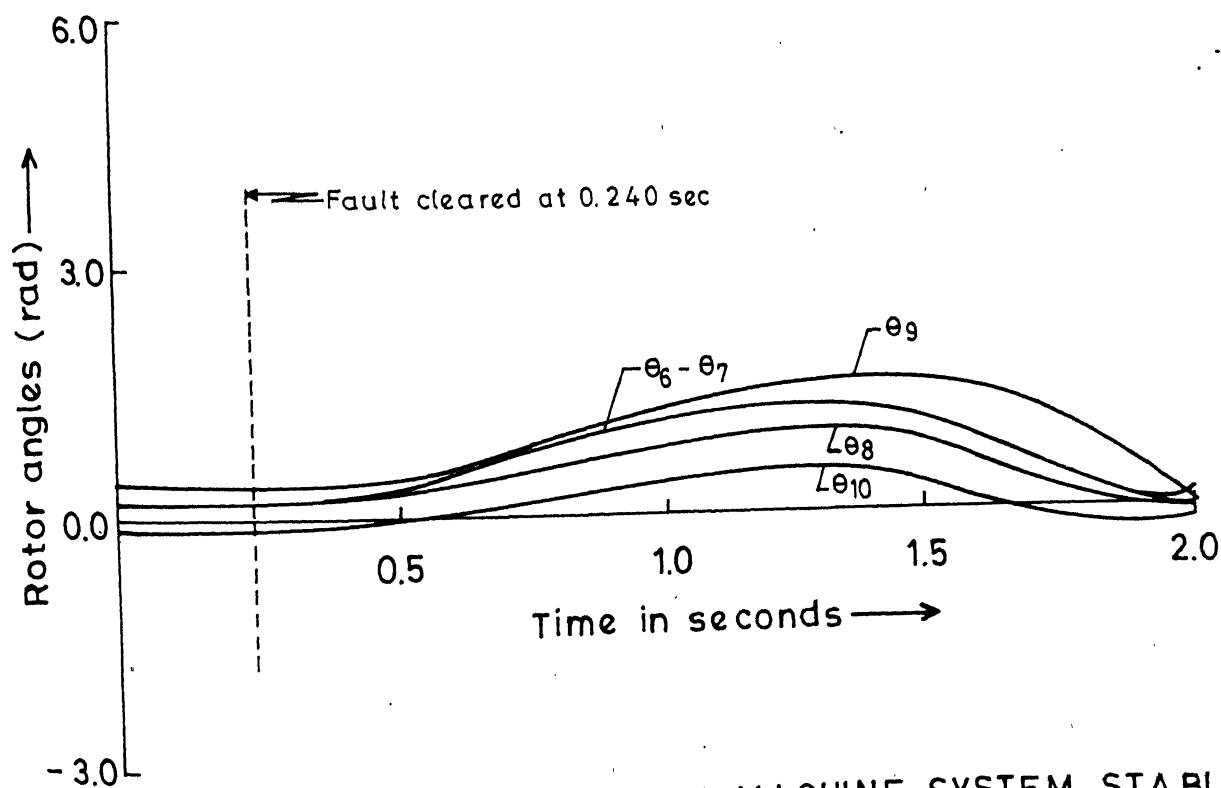
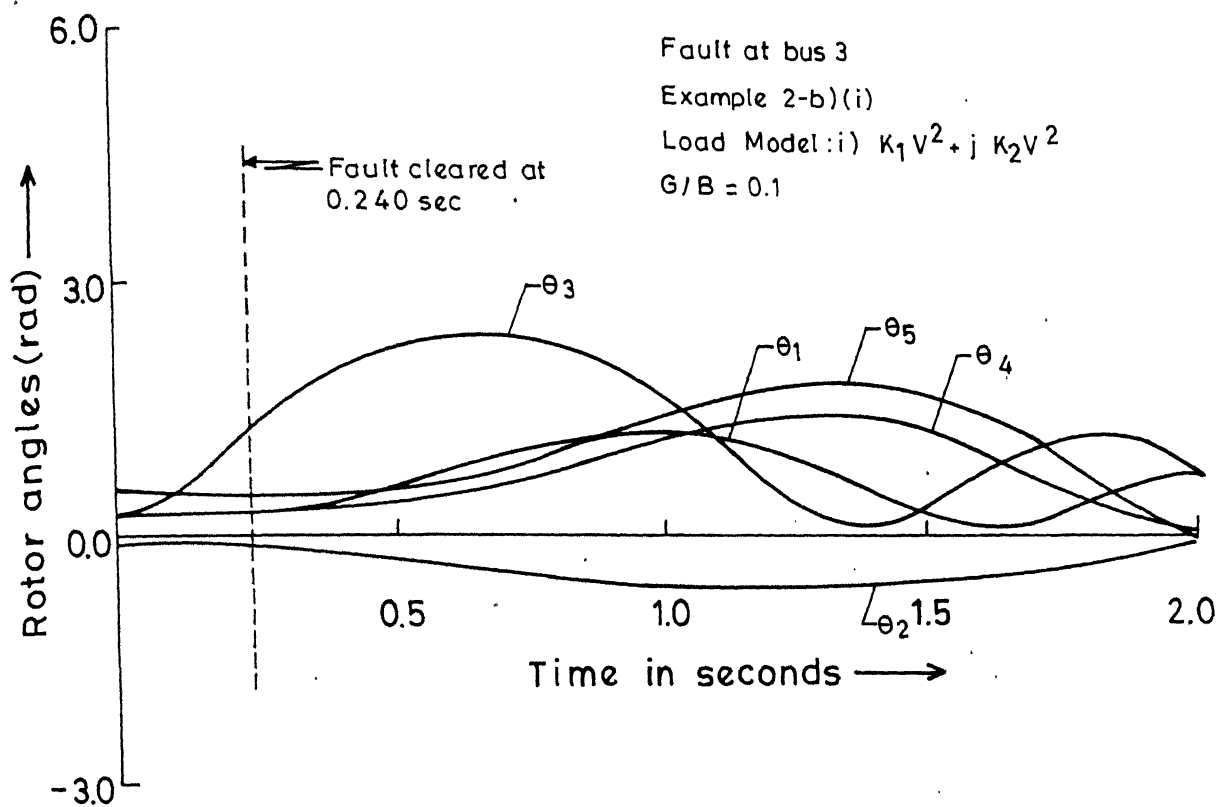


FIG.5.4 SWING CURVES FOR 10-MACHINE SYSTEM, STABLE CASE

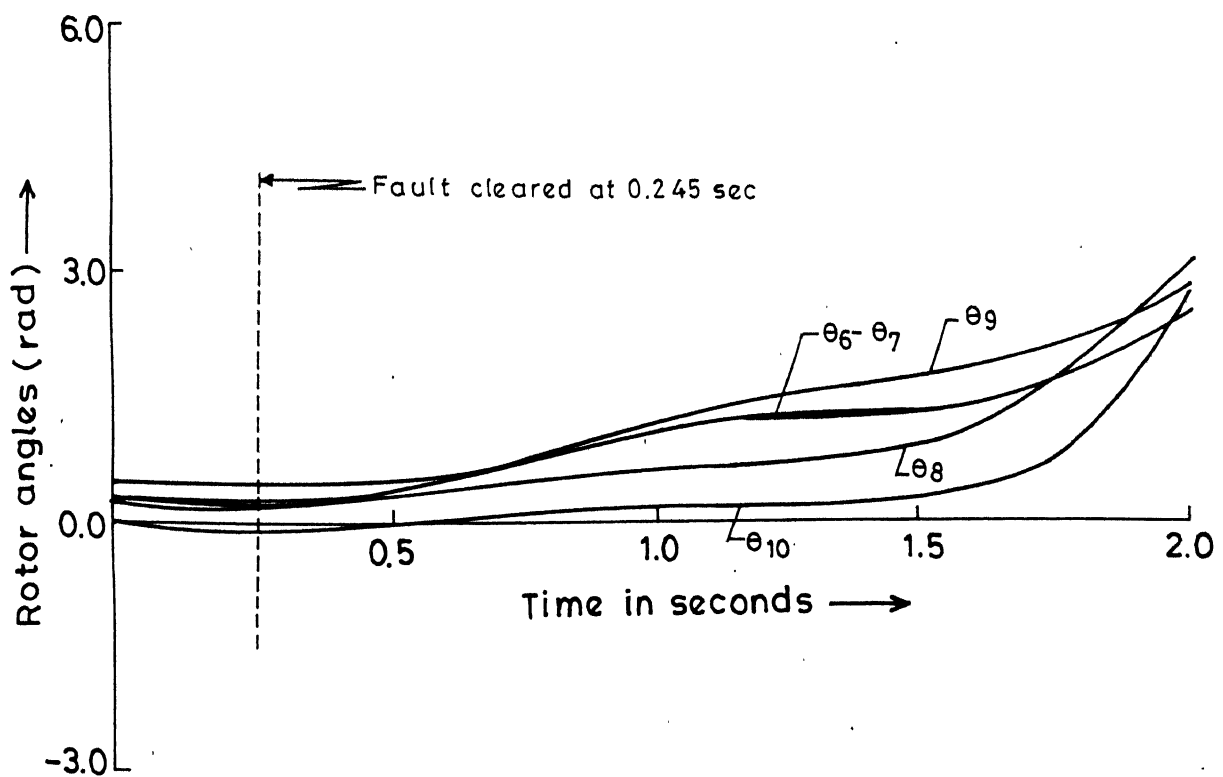
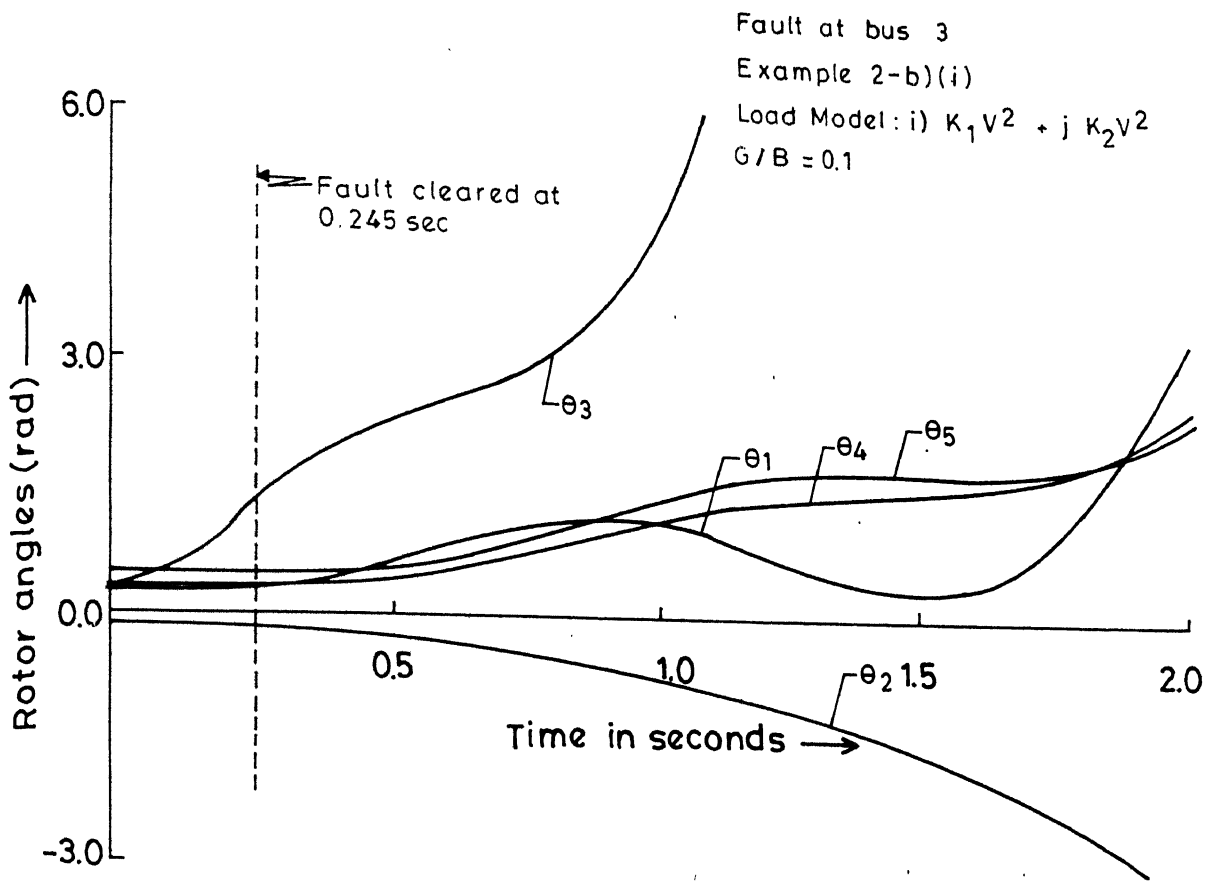


FIG.5.5 SWING CURVES FOR 10-MACHINE SYSTEM,  
UNSTABLE CASE

Fault at bus 4

Example 2-c) (i)

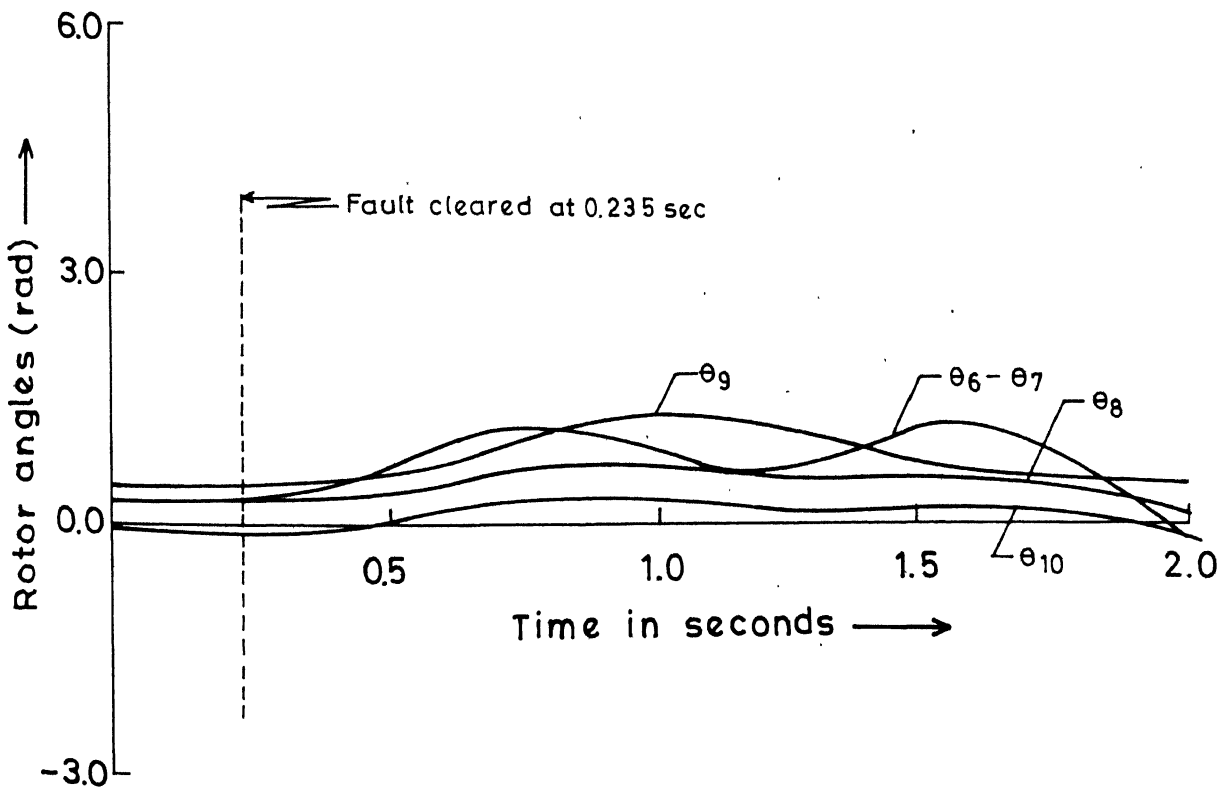
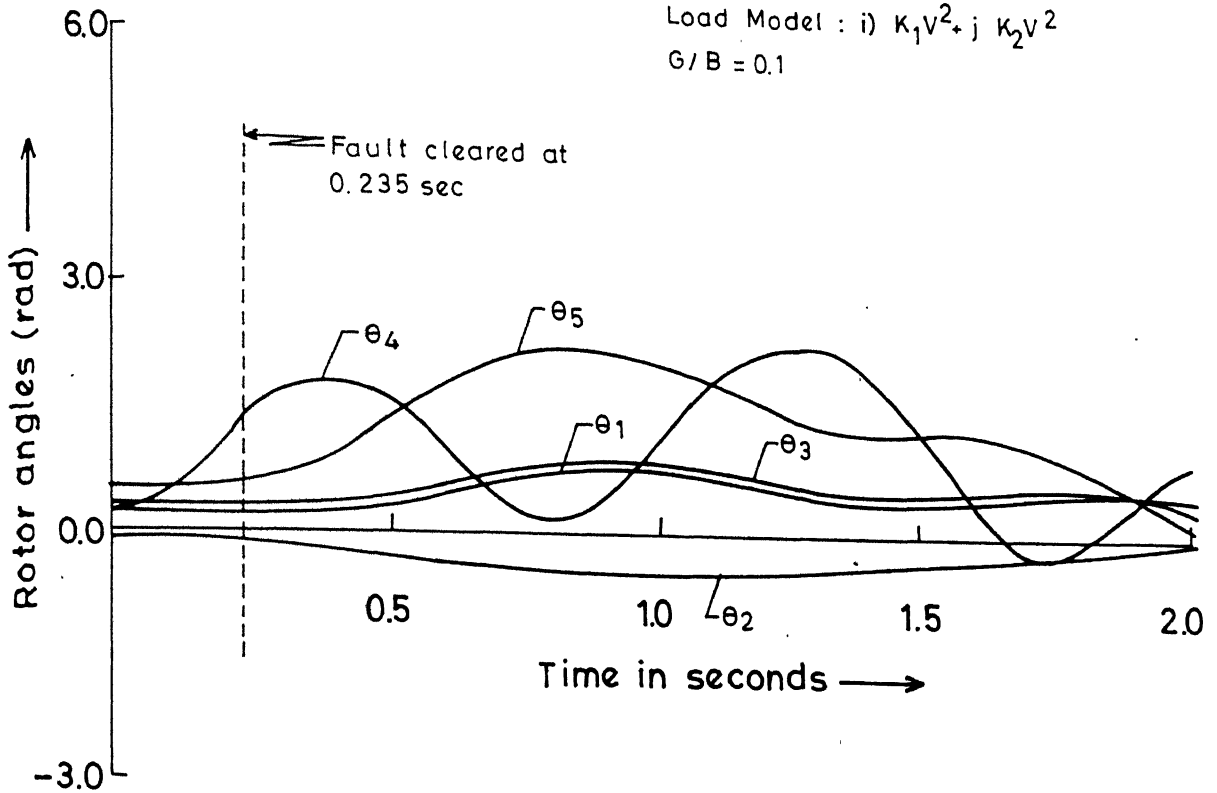
Load Model : i)  $K_1 V^2 + j K_2 V^2$  $G/B = 0.1$ 

FIG. 5.6 SWING CURVES FOR 10-MACHINE SYSTEM, STABLE CASE

Load Model : i)  $K_1 V^2 + j K_2 V^2$   
 $G/B = 0.1$

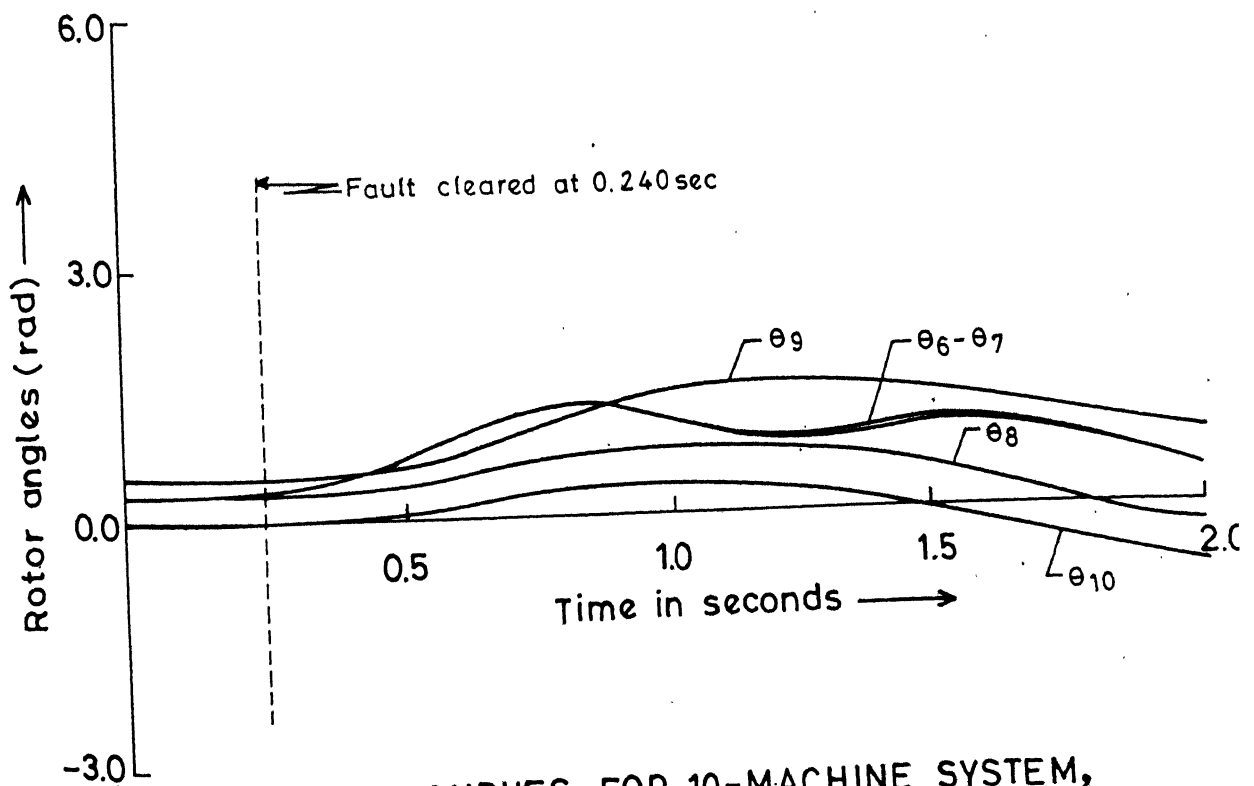
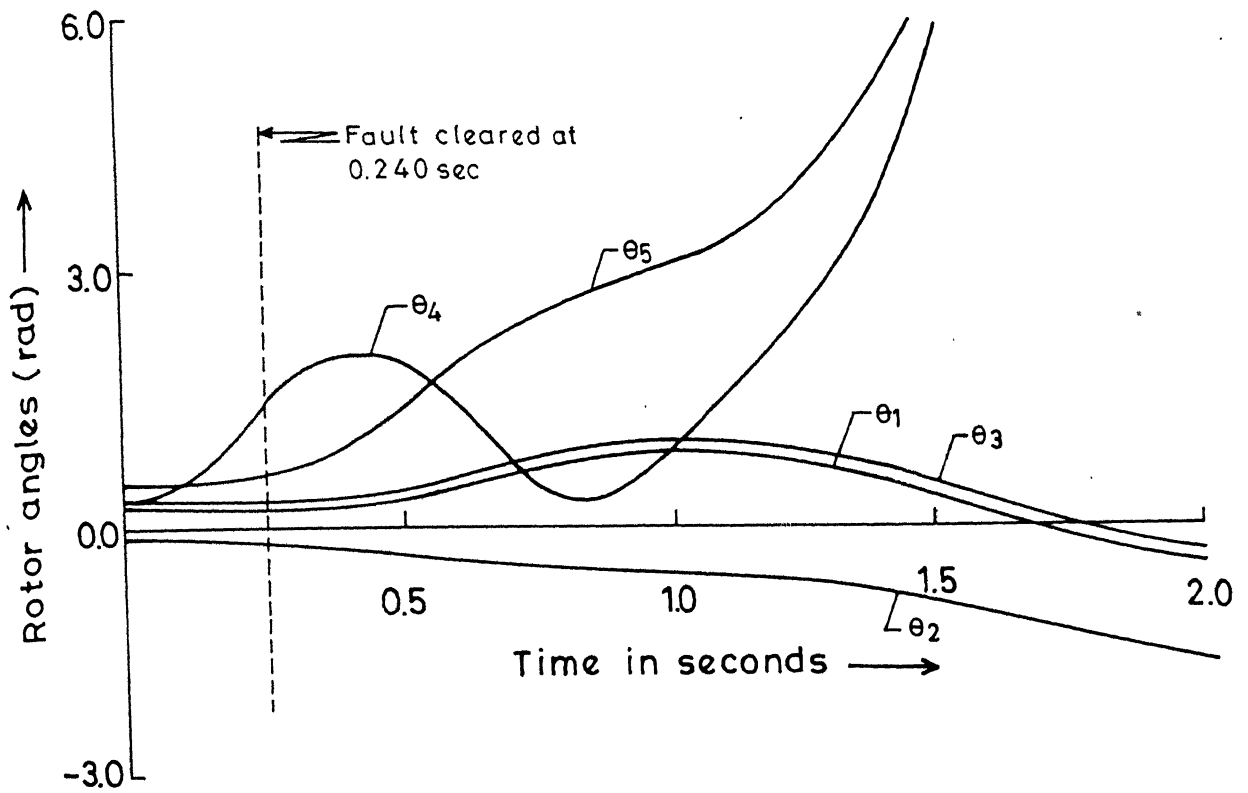


FIG.5.7 SWING CURVES FOR 10-MACHINE SYSTEM,  
 UNSTABLE CASE

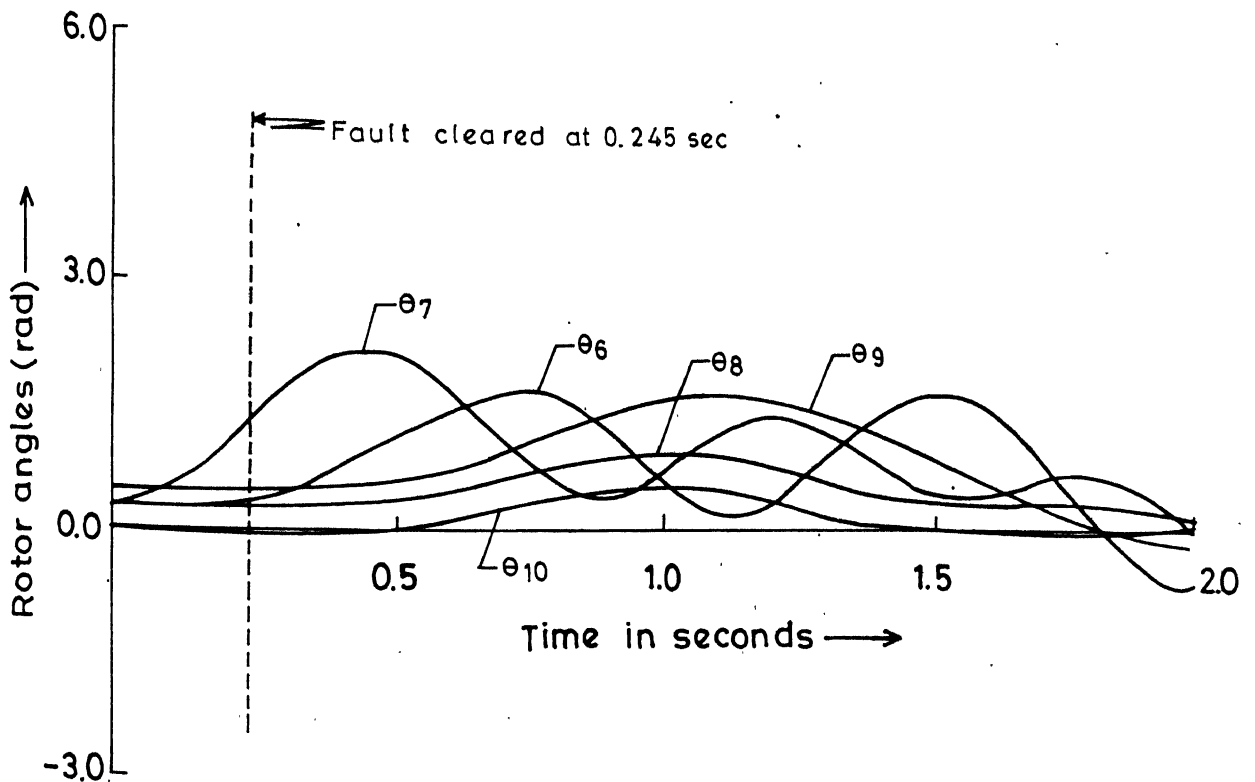
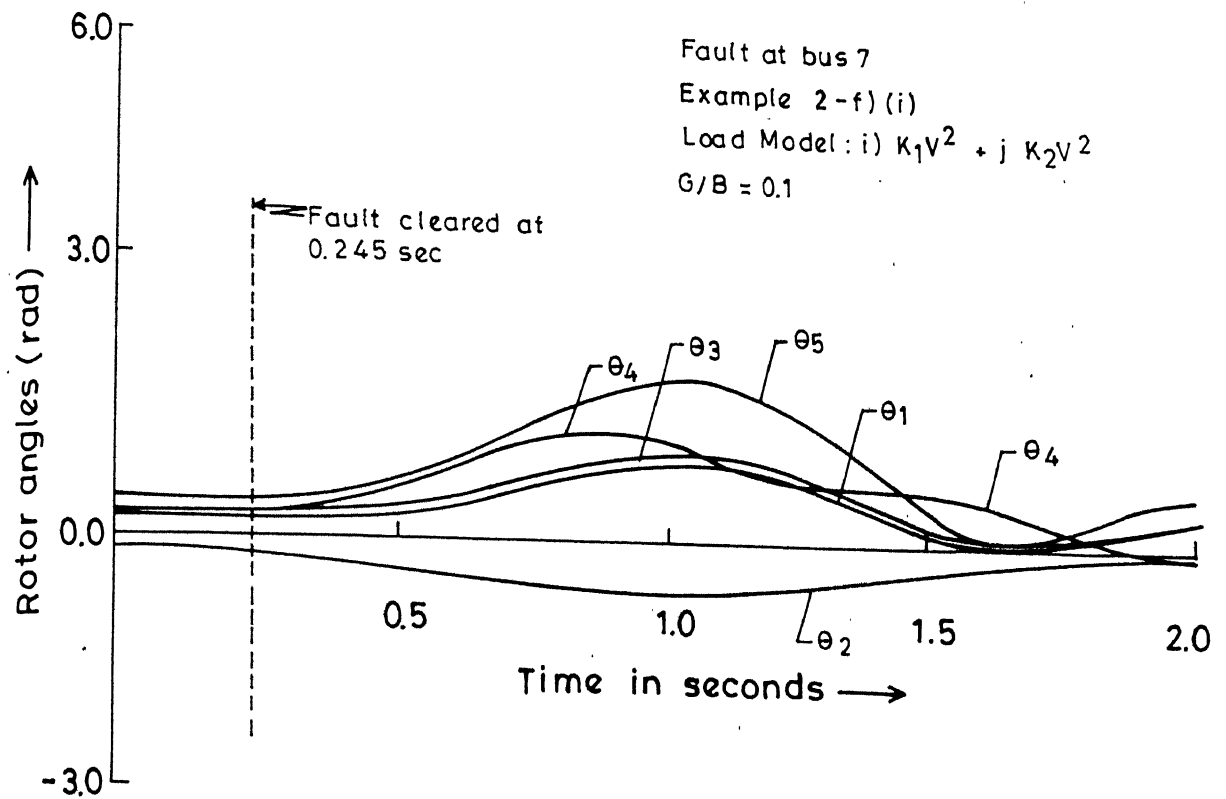


FIG.5.8 SWING CURVES FOR 10-MACHINE SYSTEM, STABLE CASE

Fault at bus 7

Example : 2-f)(i)

Load Model : i)  $K_1 V^2 + j K_2 V^2$

$G/B = 0.1$

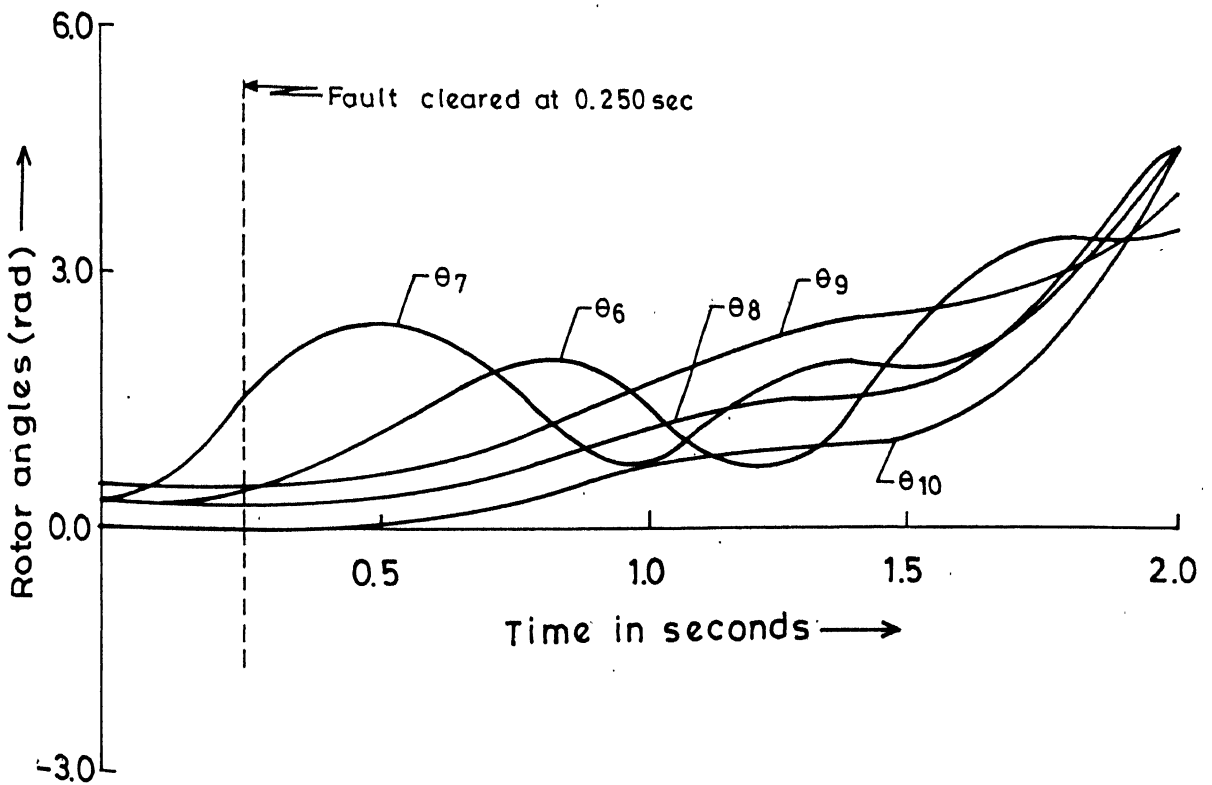
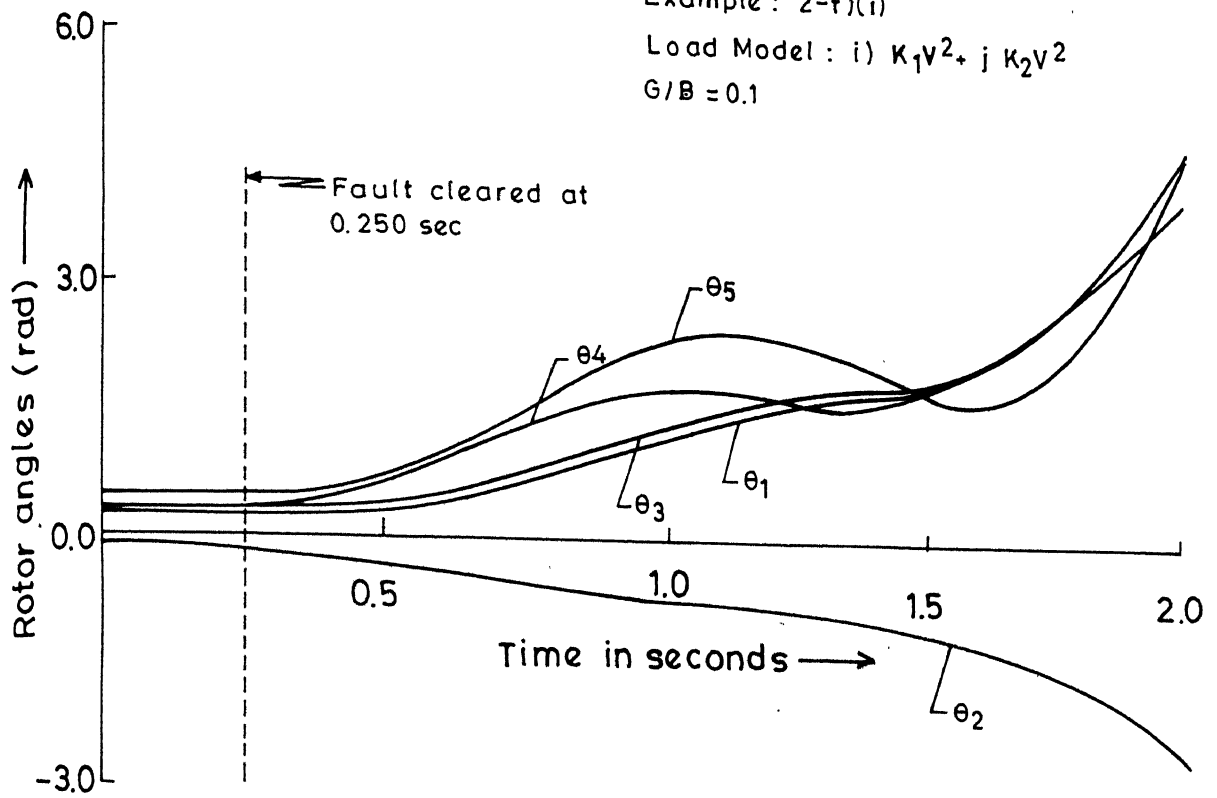


FIG.5.9 SWING CURVES FOR 10-MACHINE SYSTEM, UNSTABLE CASE

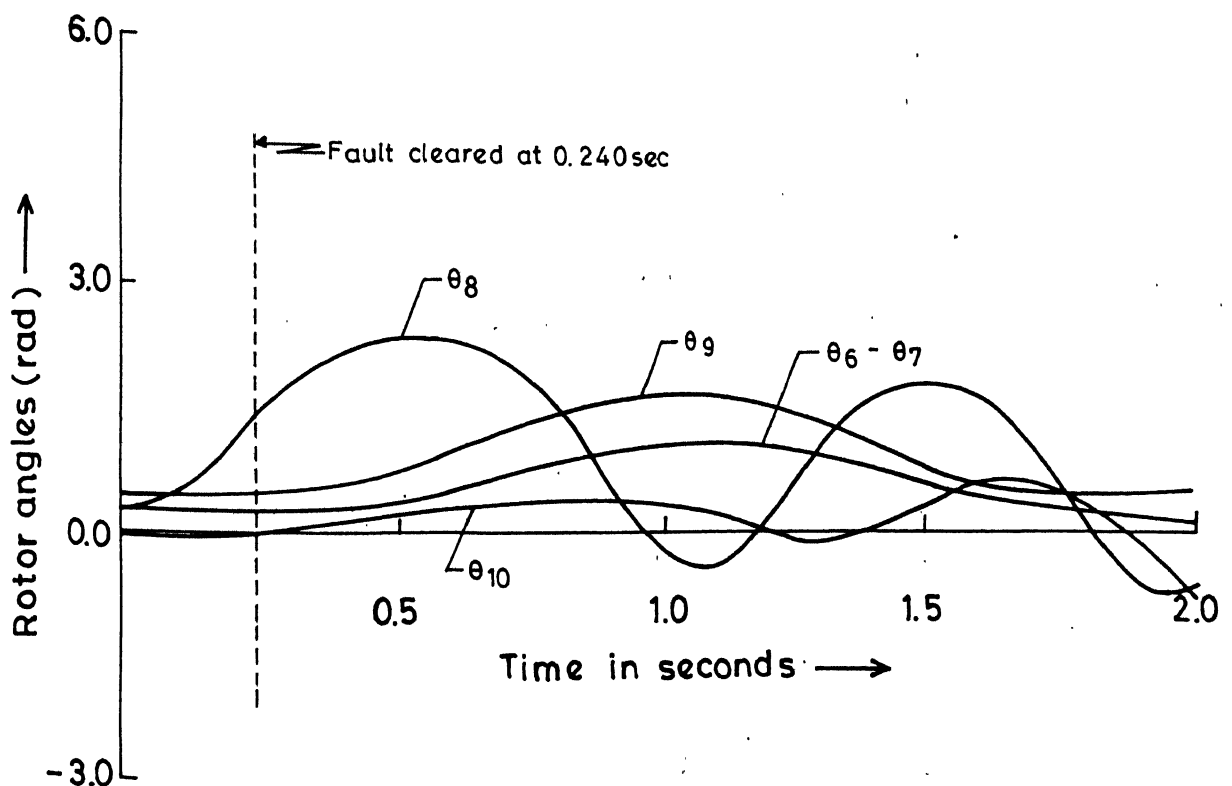
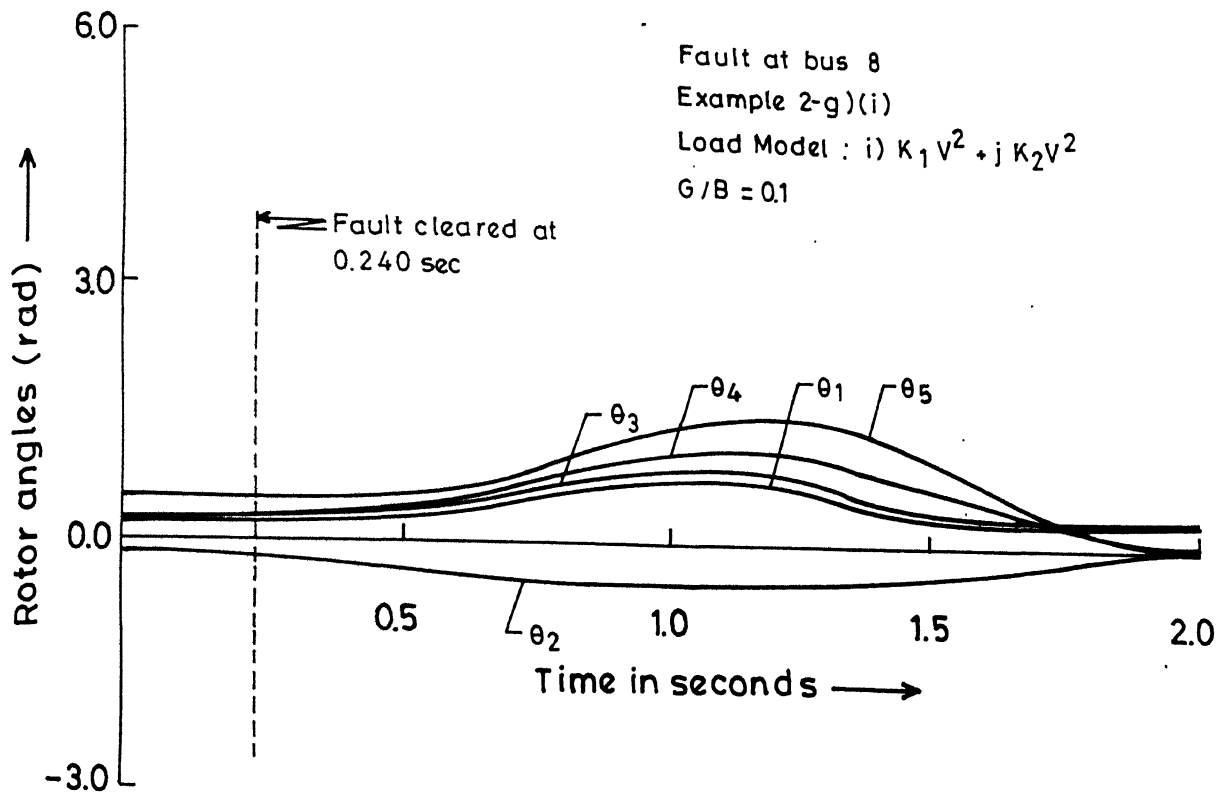


FIG. 5.10 SWING CURVES FOR 10-MACHINE SYSTEM, STABLE CASE

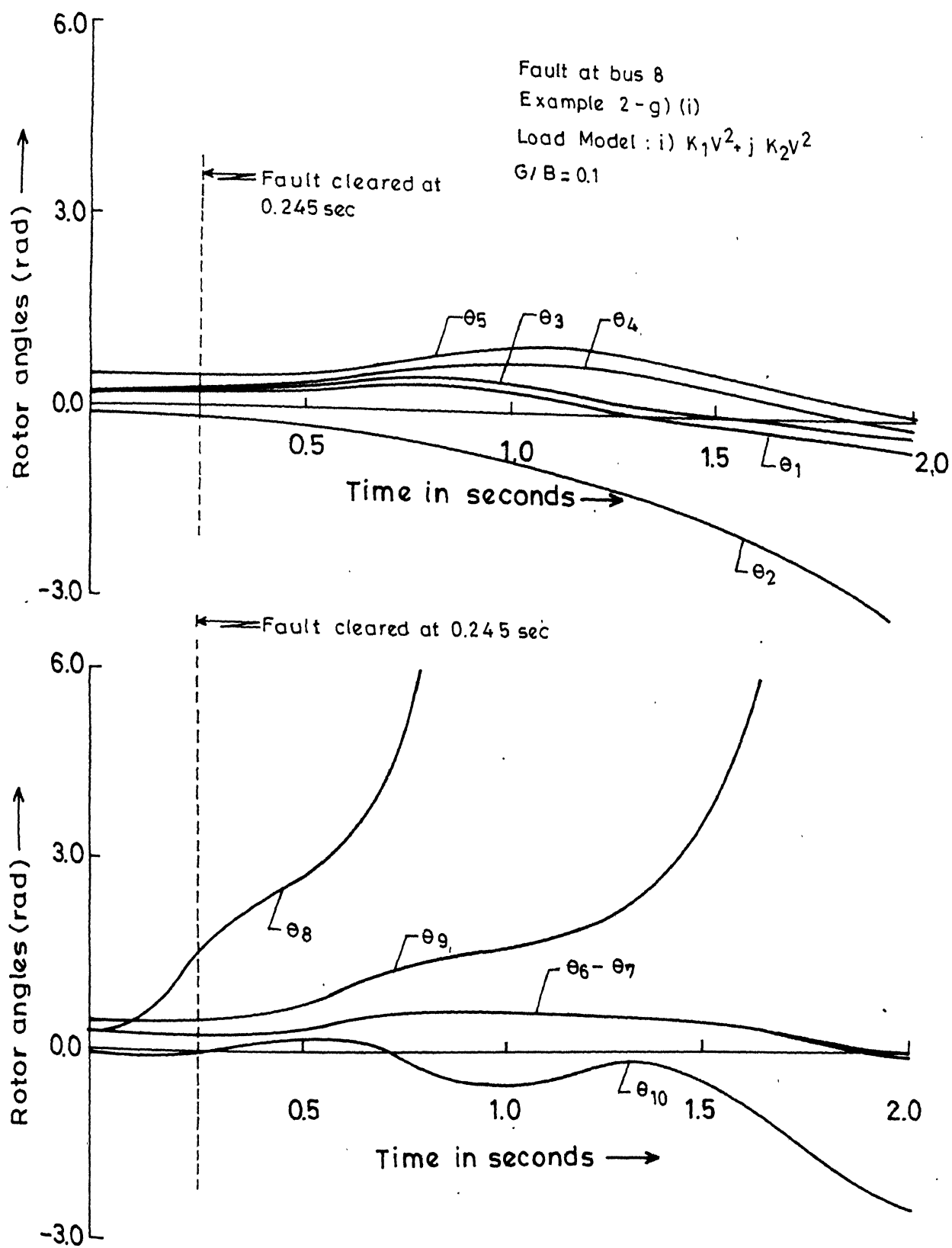


FIG. 5.11 SWING CURVES FOR 10-MACHINE SYSTEM, UNSTABLE CASE

Load Model : i)  $K_1 V^2 + j K_2 V^2$   
 $G/B = 0.1$

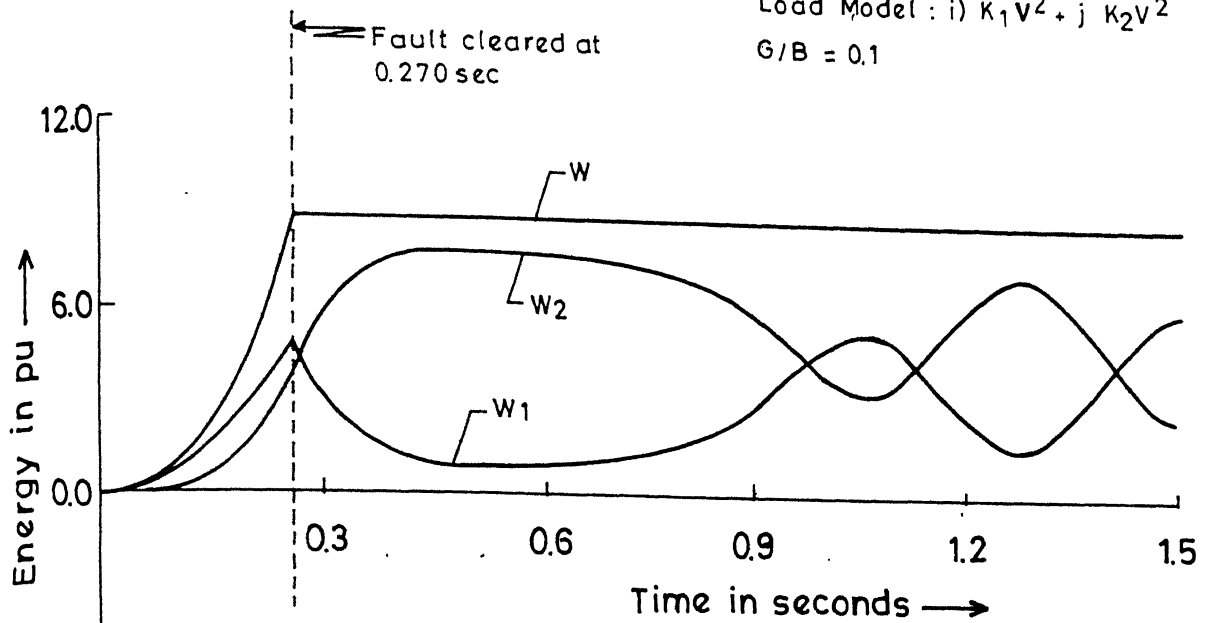


FIG.5.12 VARIATION OF TOTAL ENERGY AND ITS COMPONENTS FOR 10-MACHINE SYSTEM, STABLE CASE

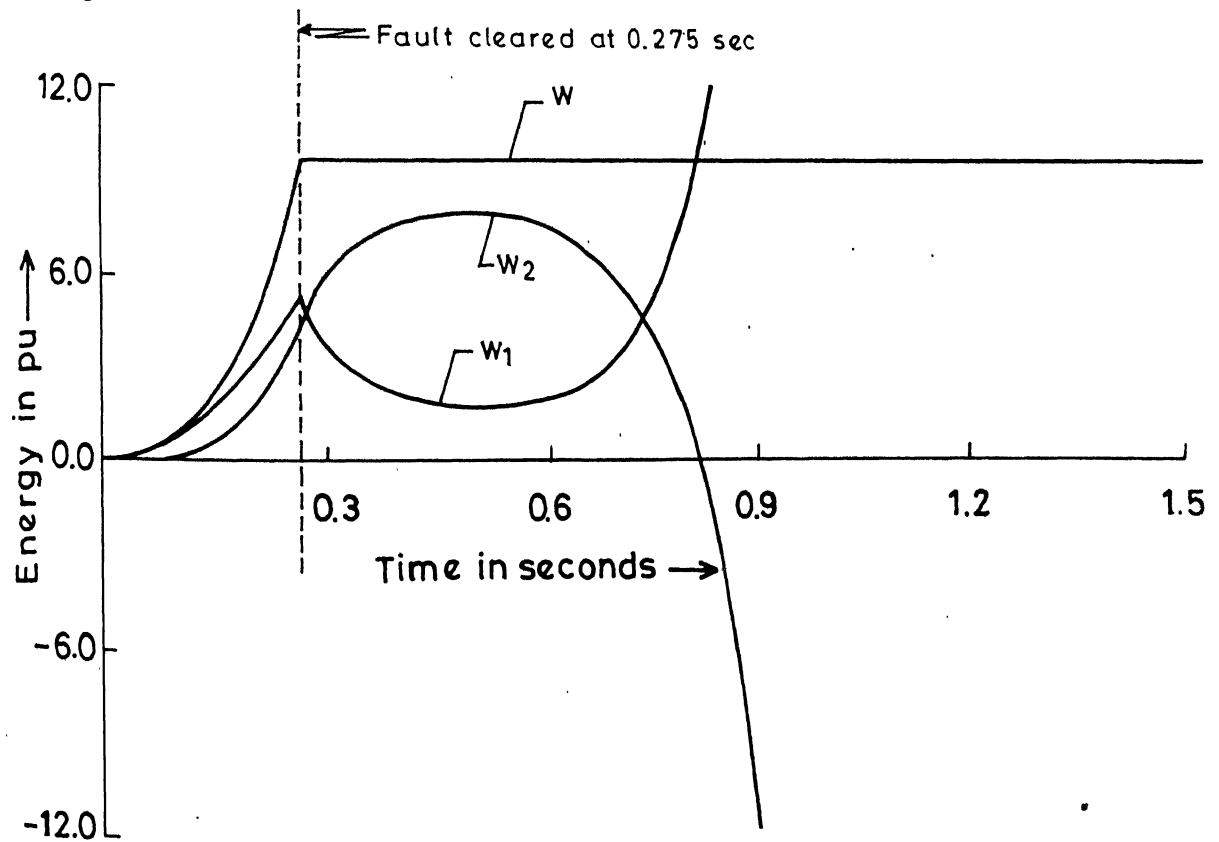
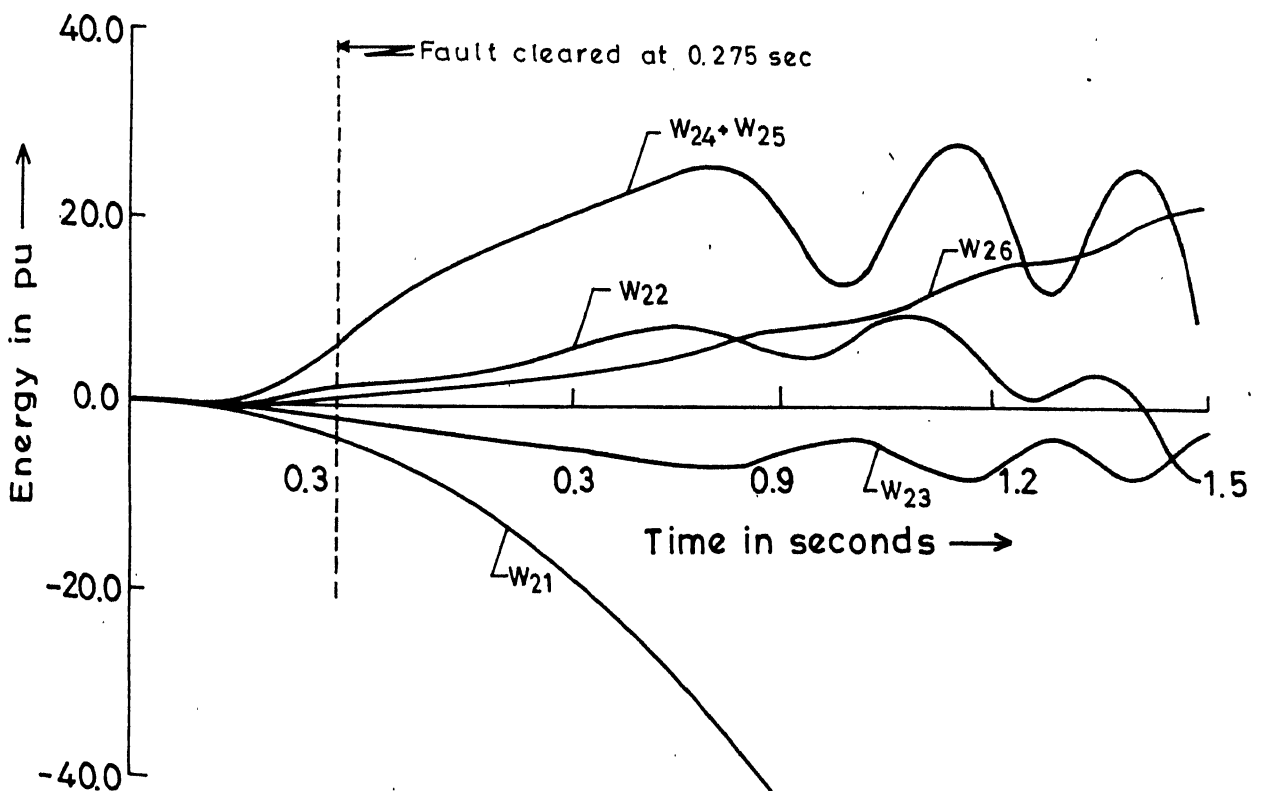
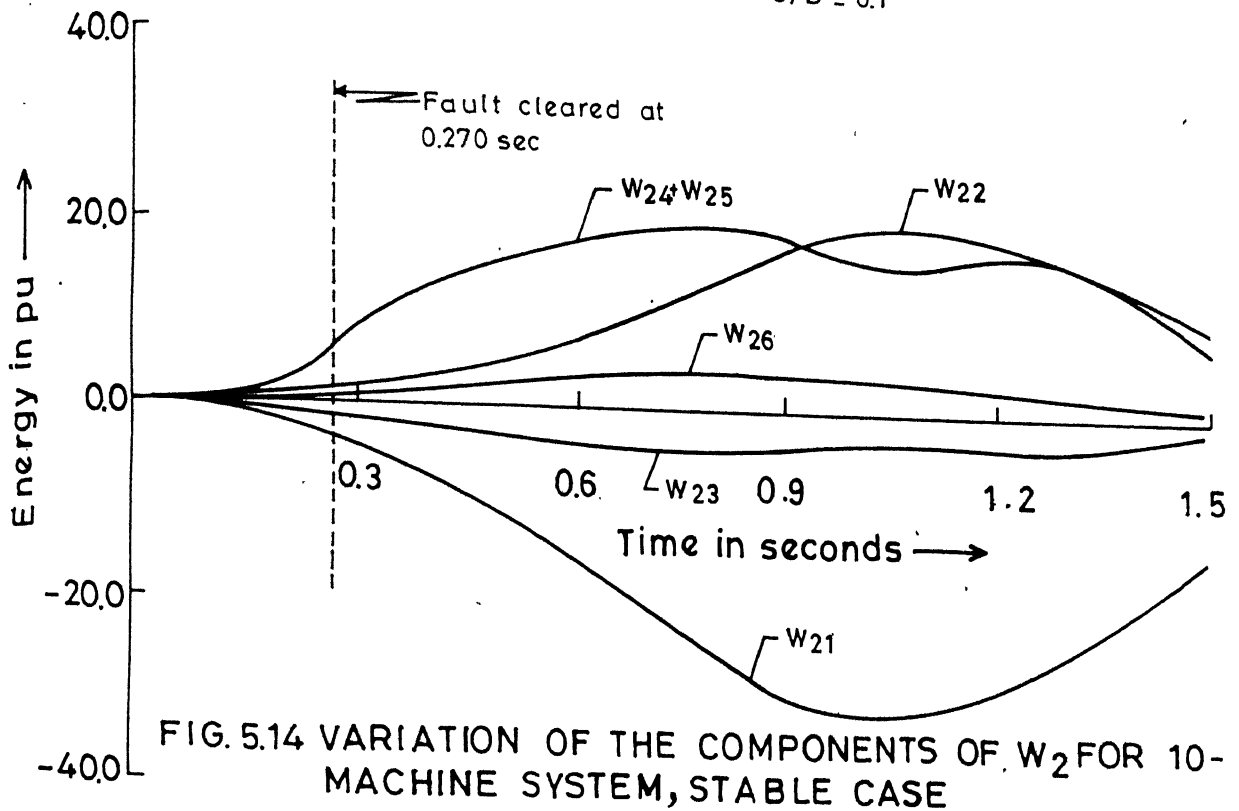


FIG.5.13 VARIATION OF TOTAL ENERGY AND ITS COMPONENTS FOR 10-MACHINE SYSTEM, UNSTABLE CASE

Example: 2-a) (i)

Load Model:  $K_1 V^2 + j K_2 V^2$  $G/B = 0.1$ 

Fault at bus 3

Example : 2-b) (i)

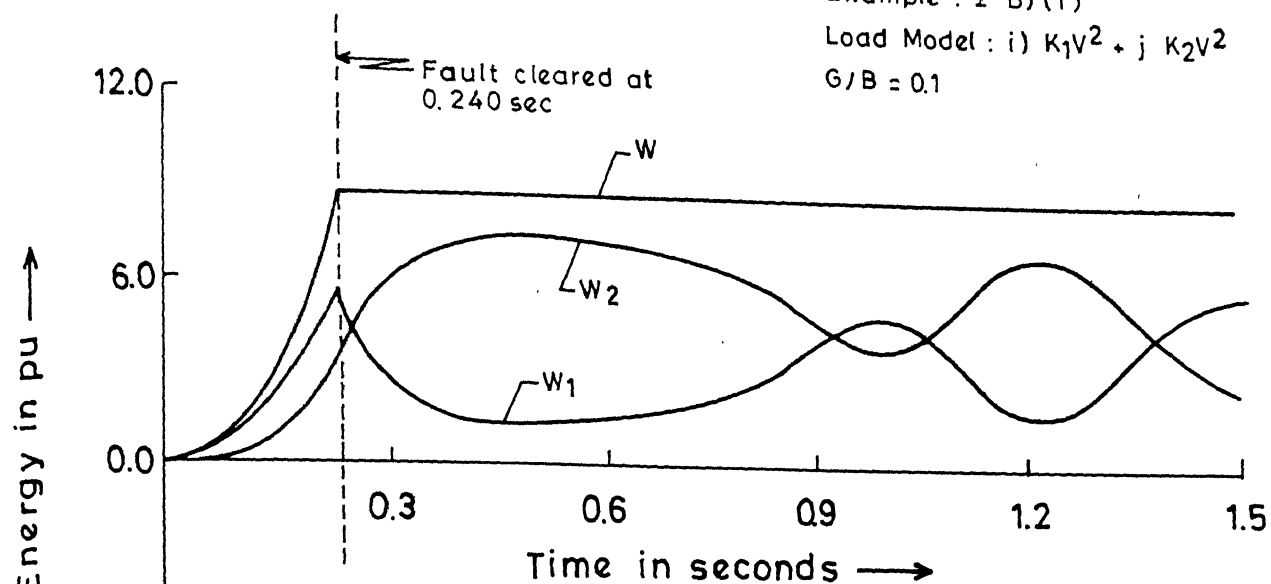
Load Model : i)  $K_1 V^2 + j K_2 V^2$  $G/B = 0.1$ 

FIG.5.16 VARIATION OF TOTAL ENERGY AND ITS COMPONENTS FOR 10-MACHINE SYSTEM, STABLE CASE

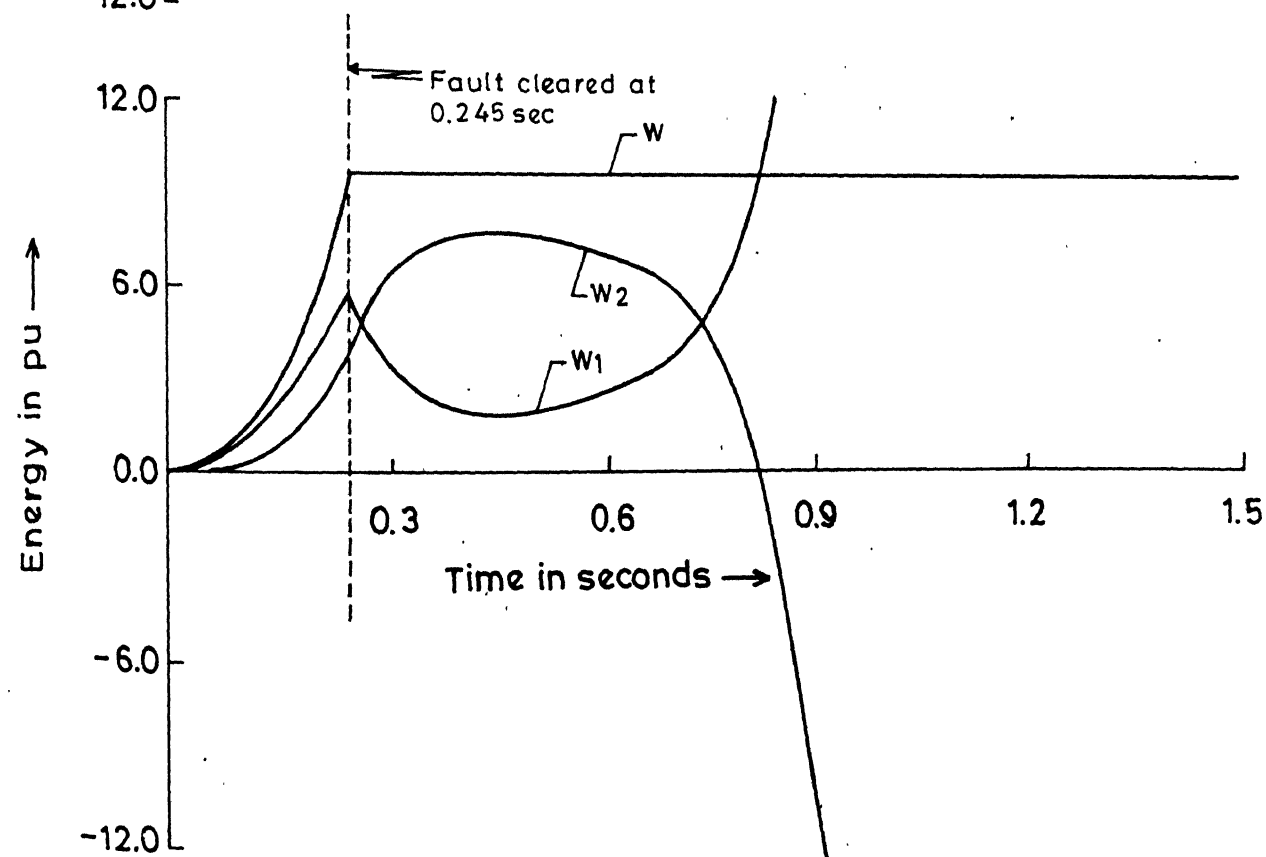


FIG.5.17 VARIATION OF TOTAL ENERGY AND ITS COMPONENTS FOR 10-MACHINE SYSTEM, UNSTABLE CASE

Fault at bus 3

Example : 2-b)(i)

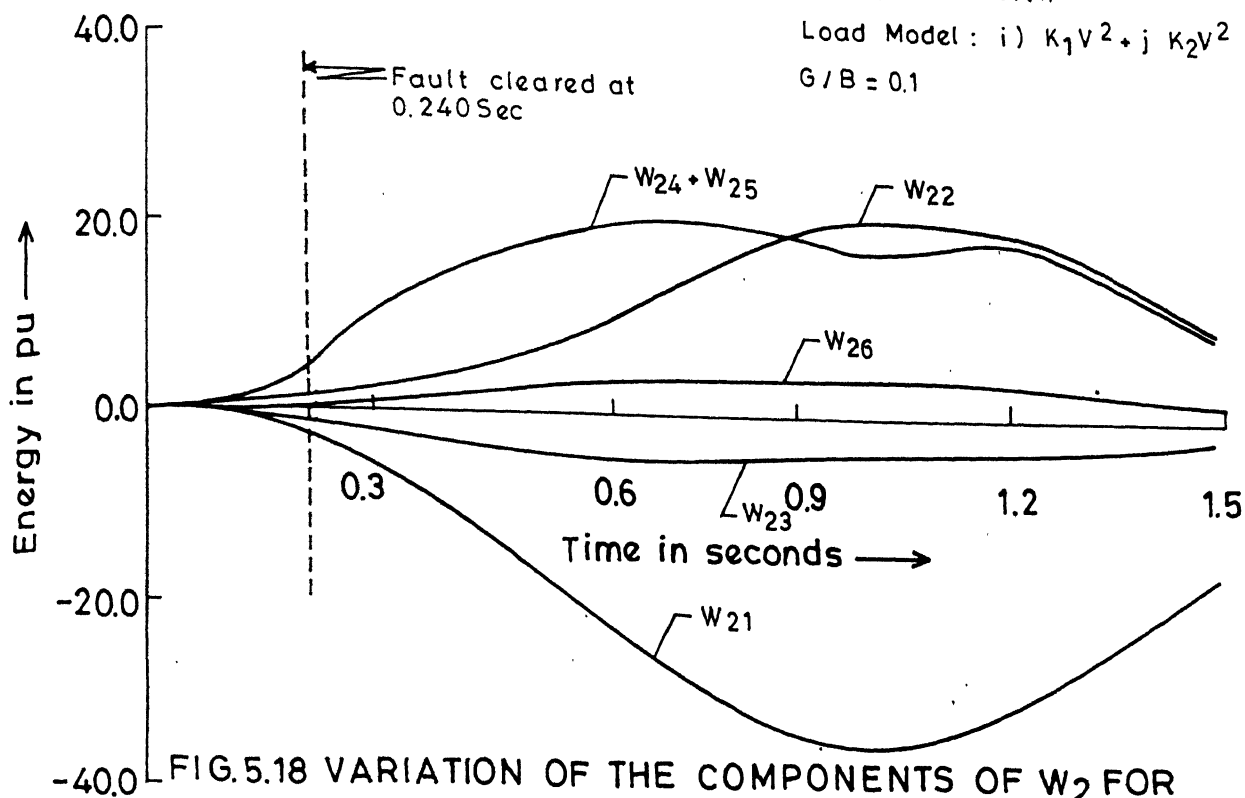
Load Model : i)  $K_1 V^2 + j K_2 V^2$  $G/B = 0.1$ 

FIG.5.18 VARIATION OF THE COMPONENTS OF  $W_2$  FOR 10-MACHINE SYSTEM, STABLE CASE

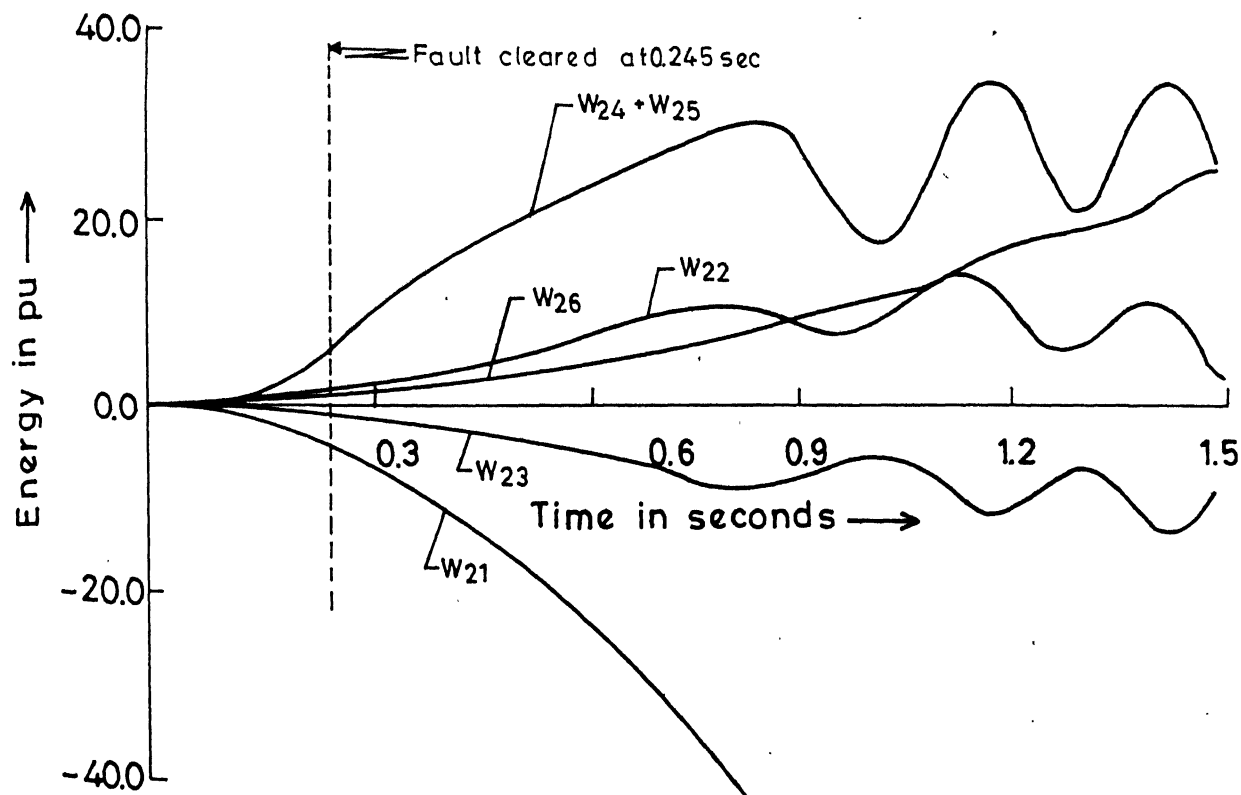
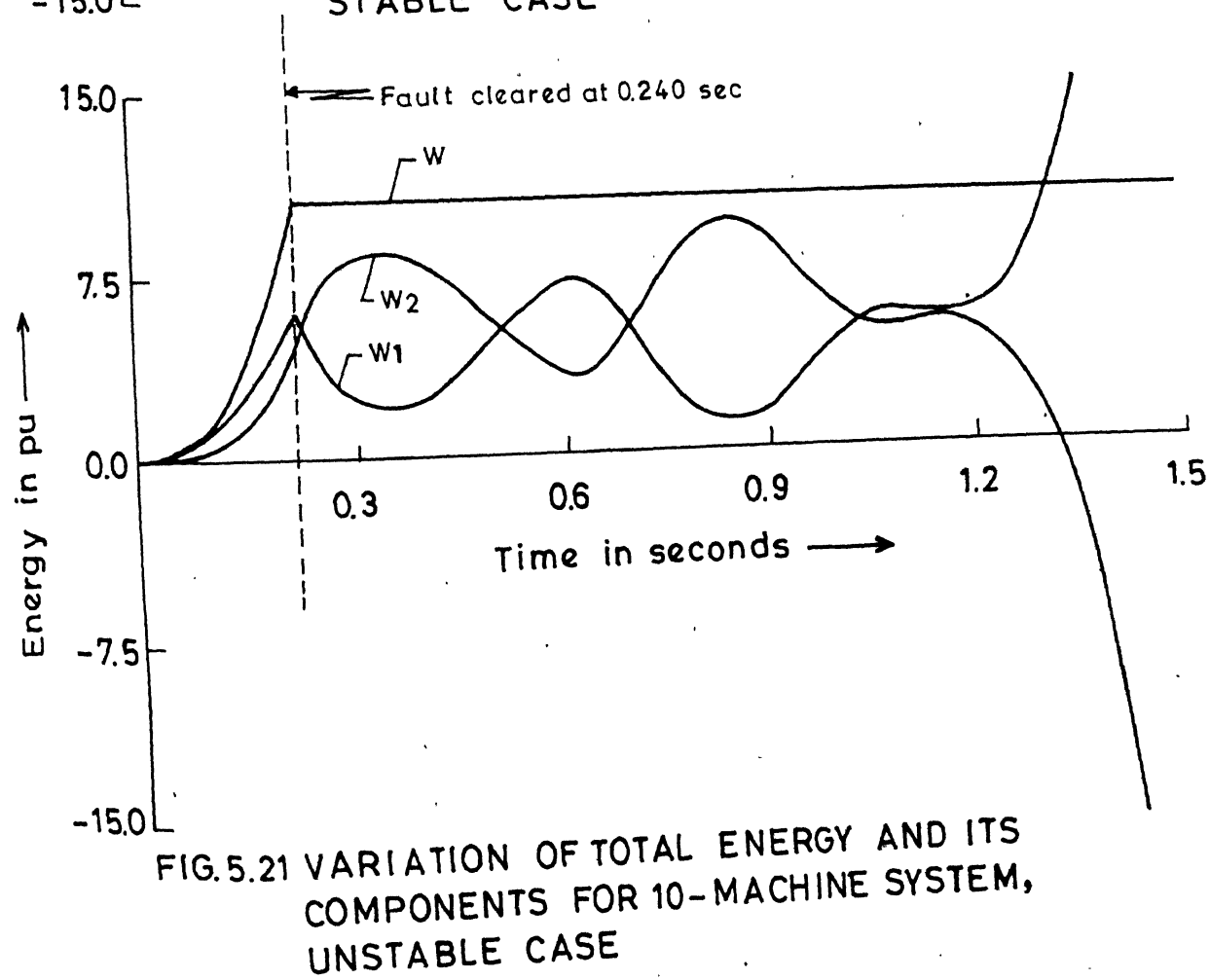
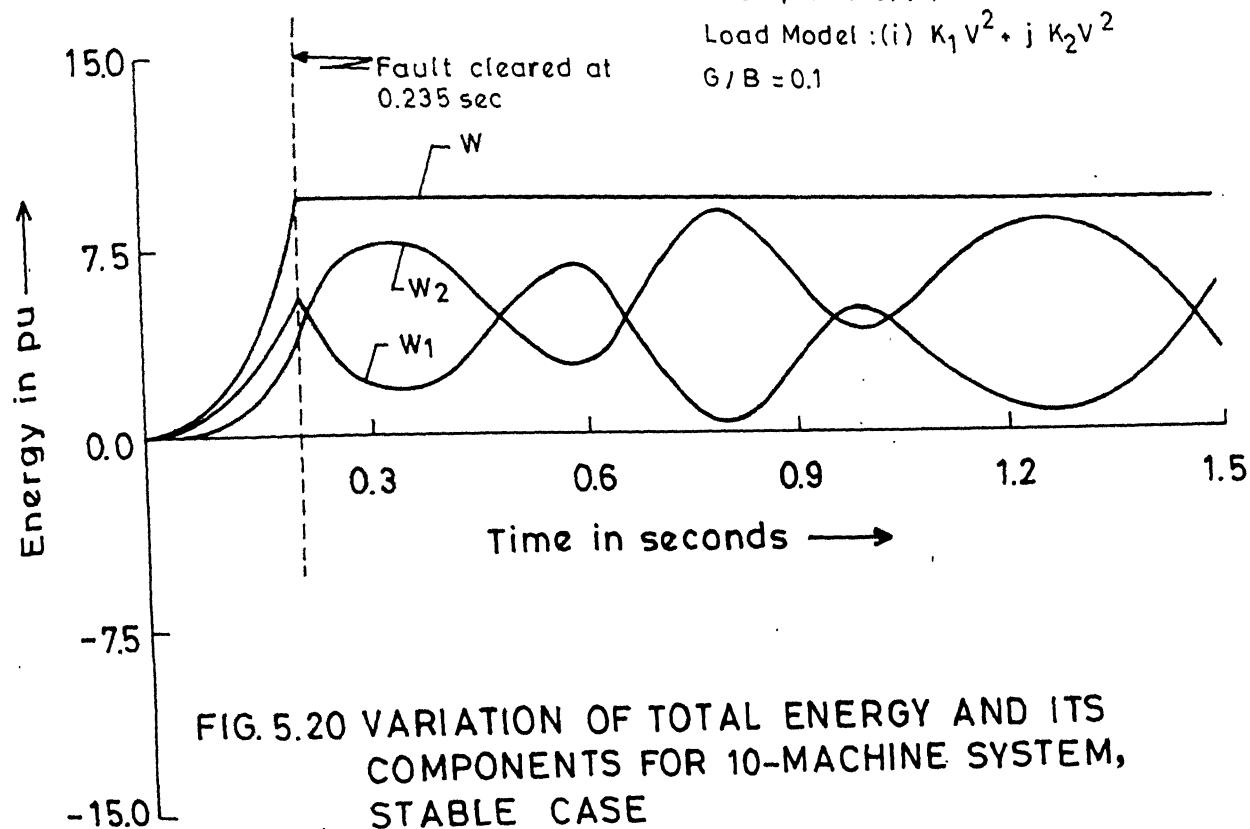
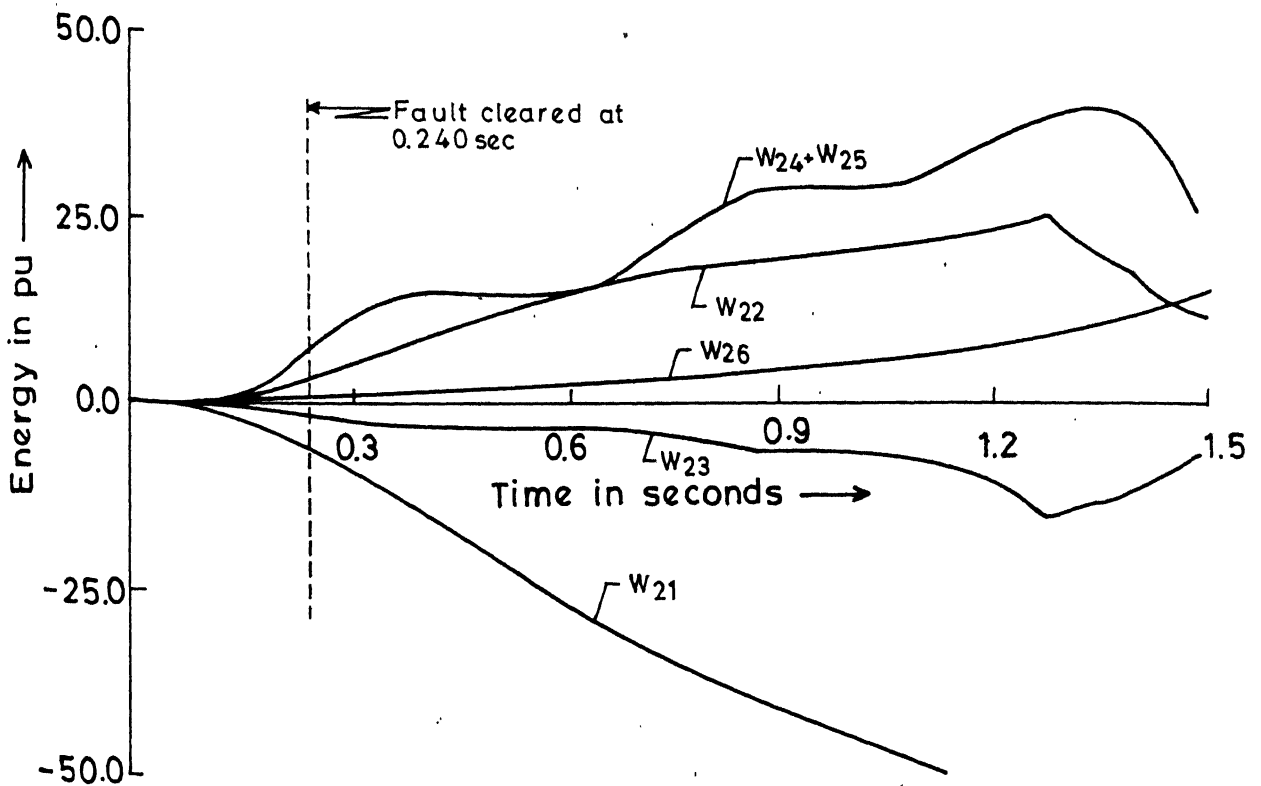
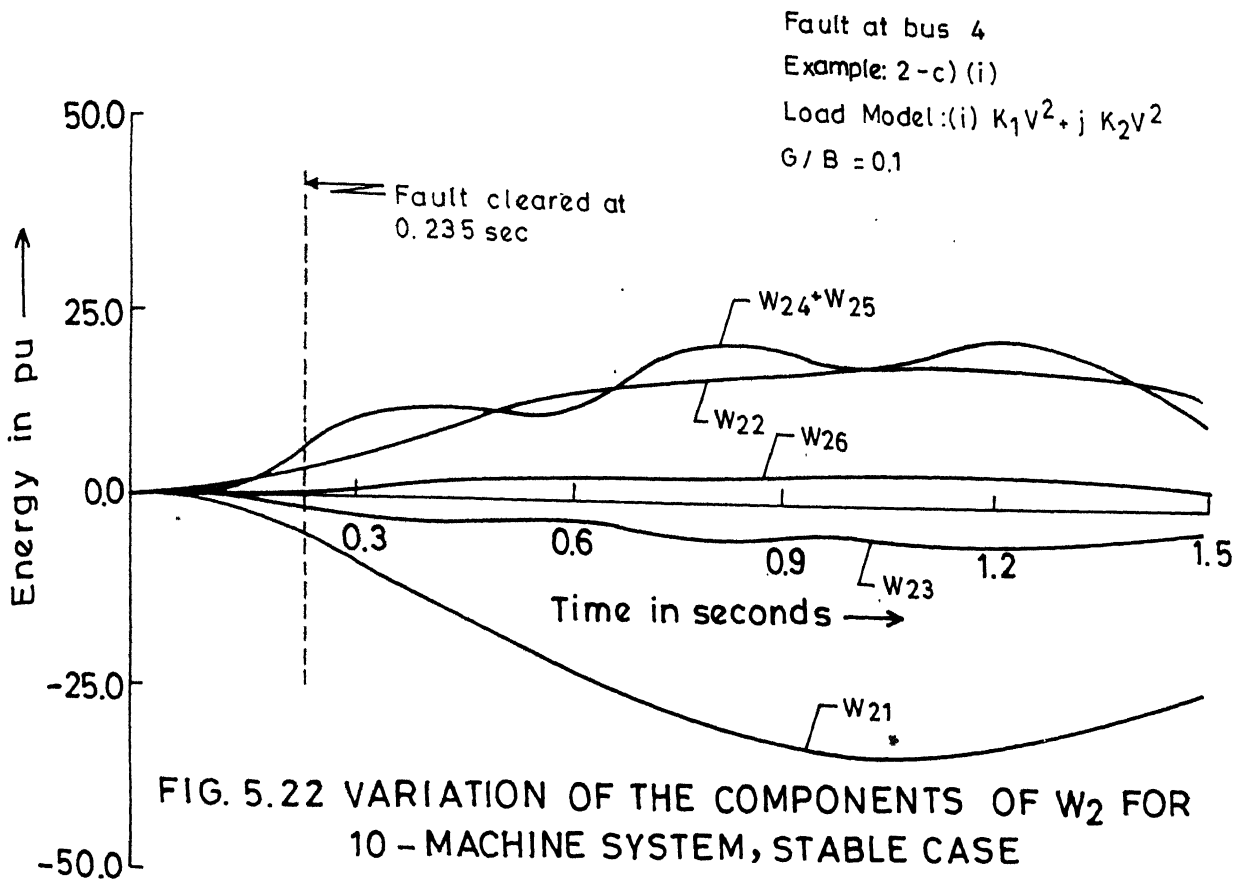


FIG.5.19 VARIATION OF THE COMPONENTS OF  $W_2$  FOR 10-MACHINE SYSTEM, UNSTABLE CASE

Fault at bus 4

Example : 2-c)(i)

Load Model : (i)  $K_1 V^2 + j K_2 V^2$  $G/B = 0.1$ 



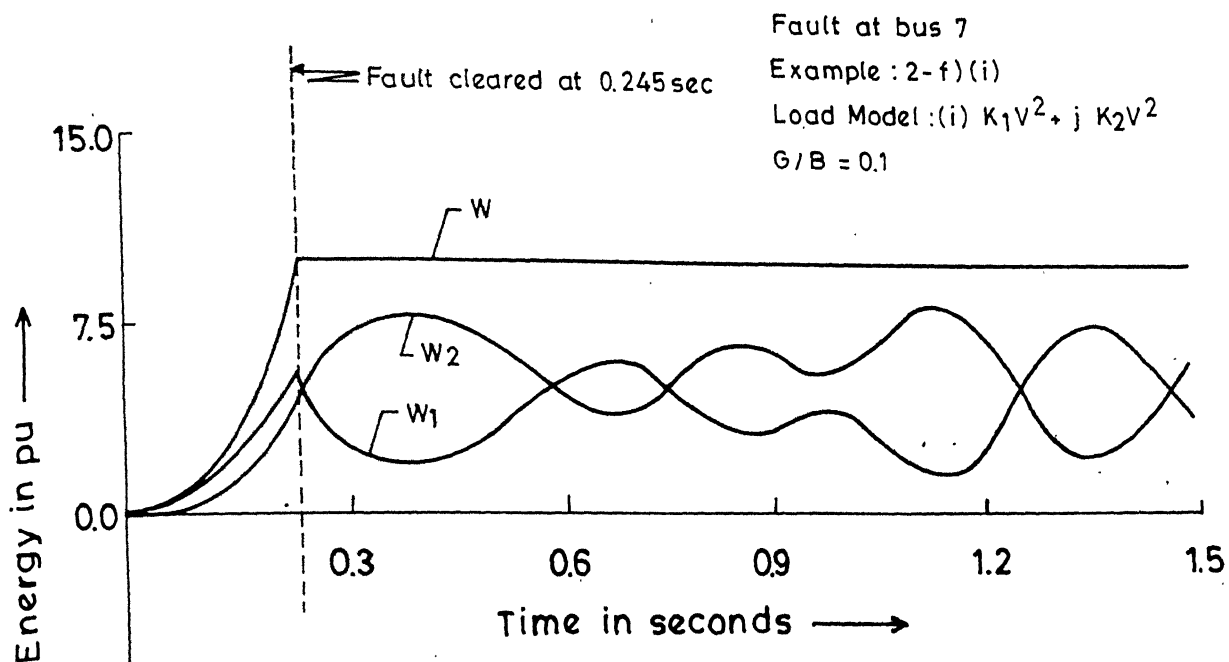


FIG. 5.24 VARIATION OF TOTAL ENERGY AND ITS COMPONENTS FOR 10-MACHINE SYSTEM, STABLE CASE

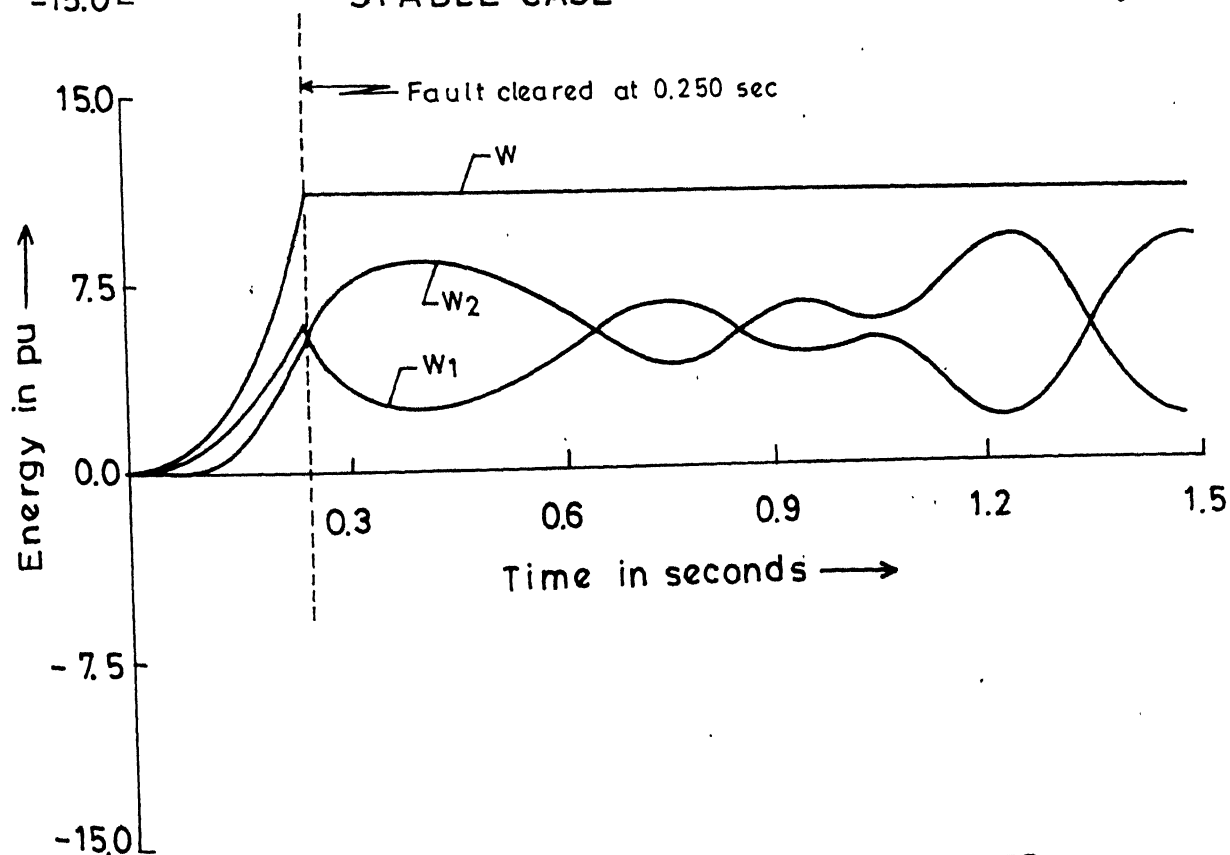


FIG. 5.25 VARIATION OF TOTAL ENERGY AND ITS COMPONENTS FOR 10-MACHINE SYSTEM, UNSTABLE CASE

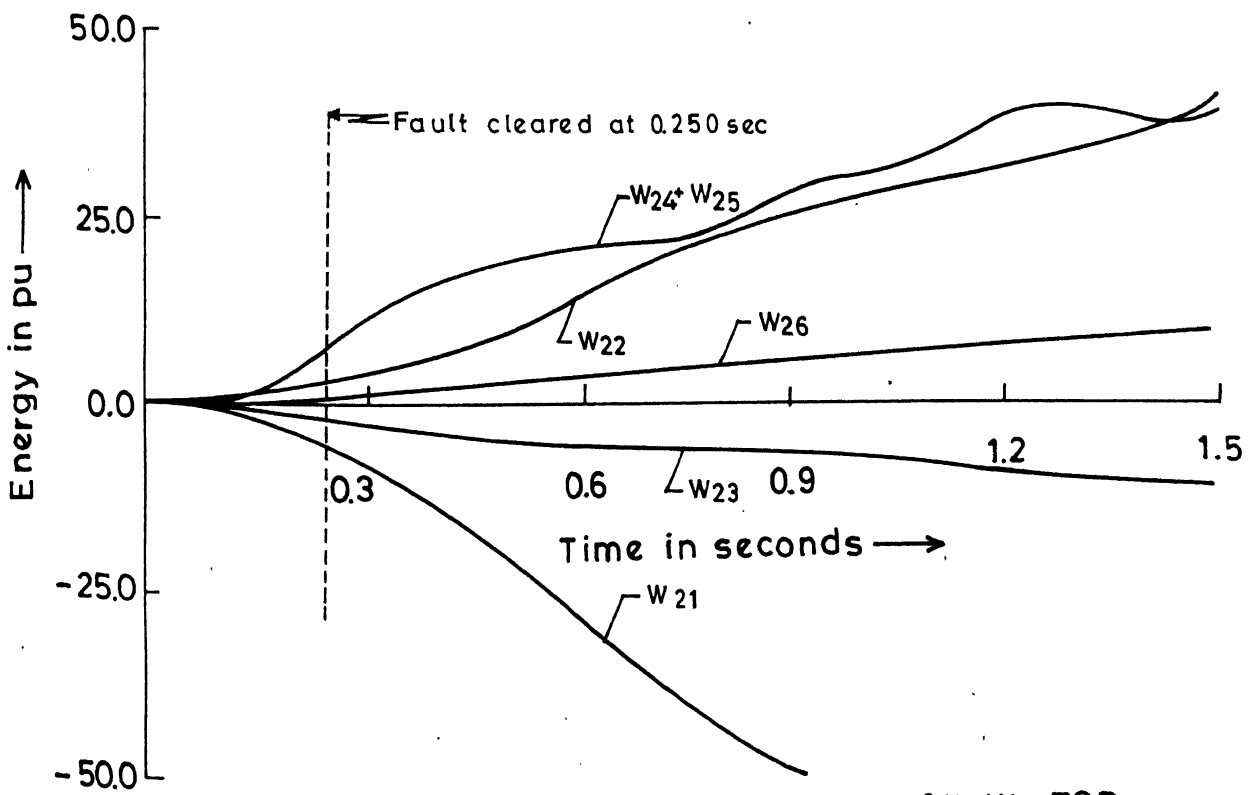
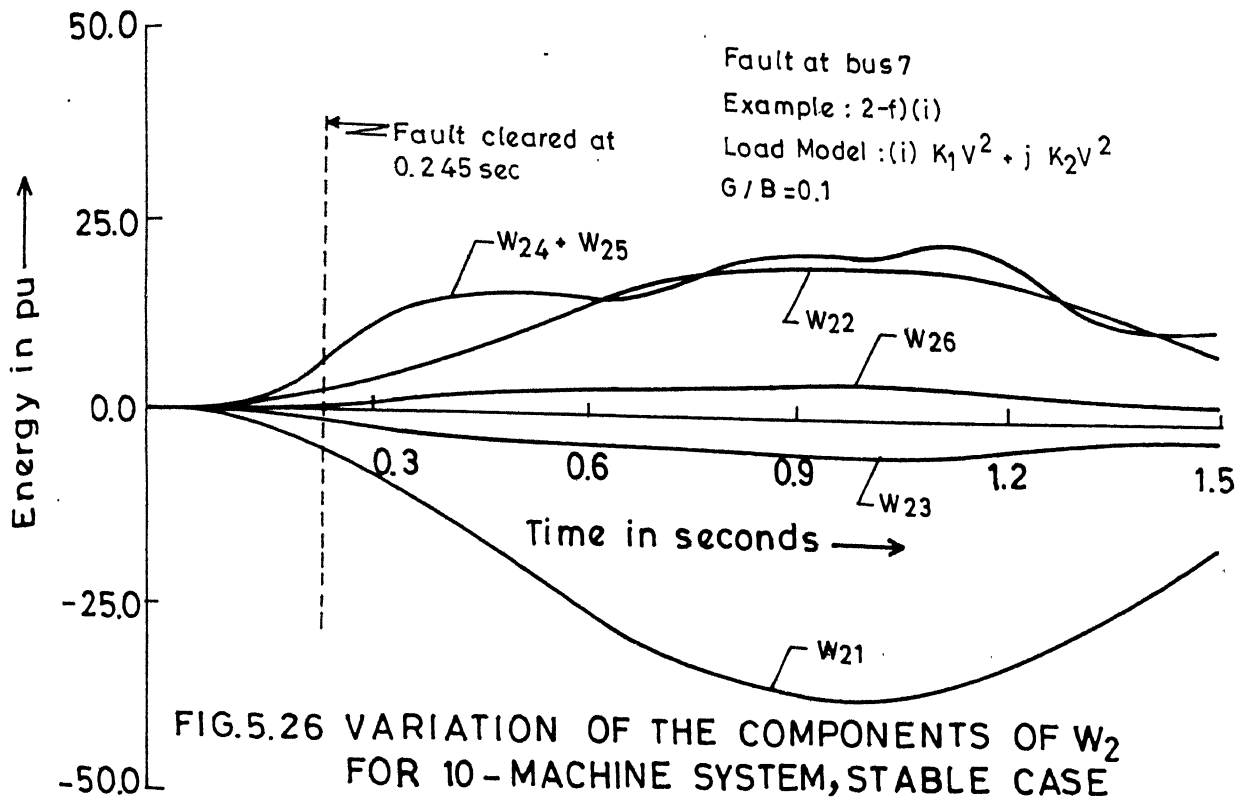


FIG.5.27 VARIATION OF THE COMPONENTS OF  $W_2$  FOR 10 - MACHINE SYSTEM, UNSTABLE CASE

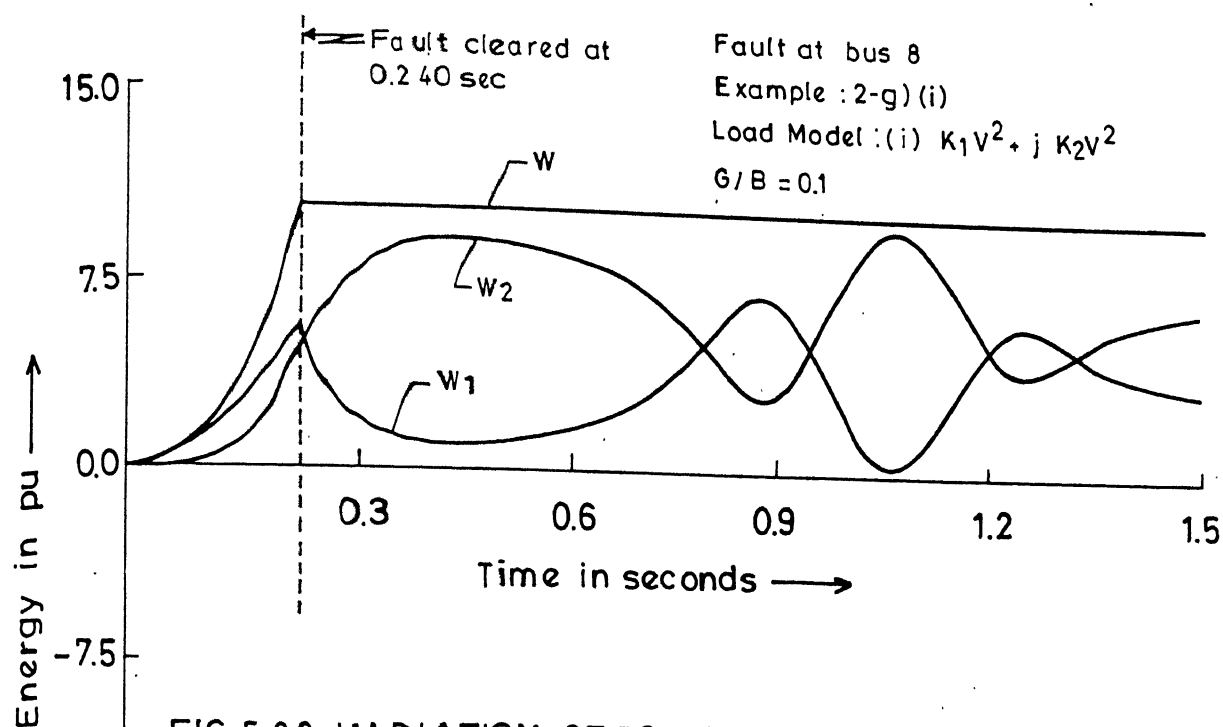


FIG.5.28 VARIATION OF TOTAL ENERGY AND ITS COMPONENTS FOR 10-MACHINE SYSTEM, STABLE CASE

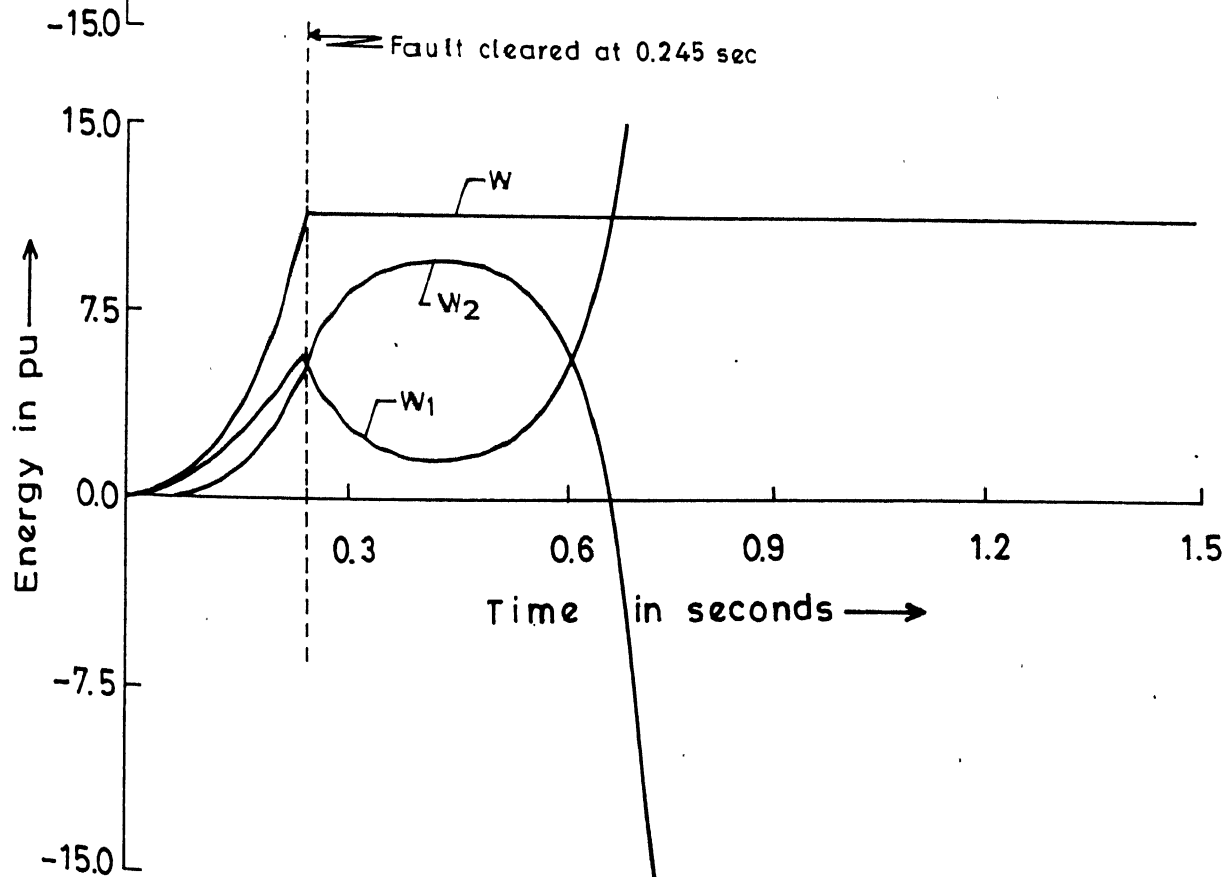


FIG.5.29 VARIATION OF TOTAL ENERGY AND ITS COMPONENTS FOR 10-MACHINE SYSTEM, UNSTABLE CASE

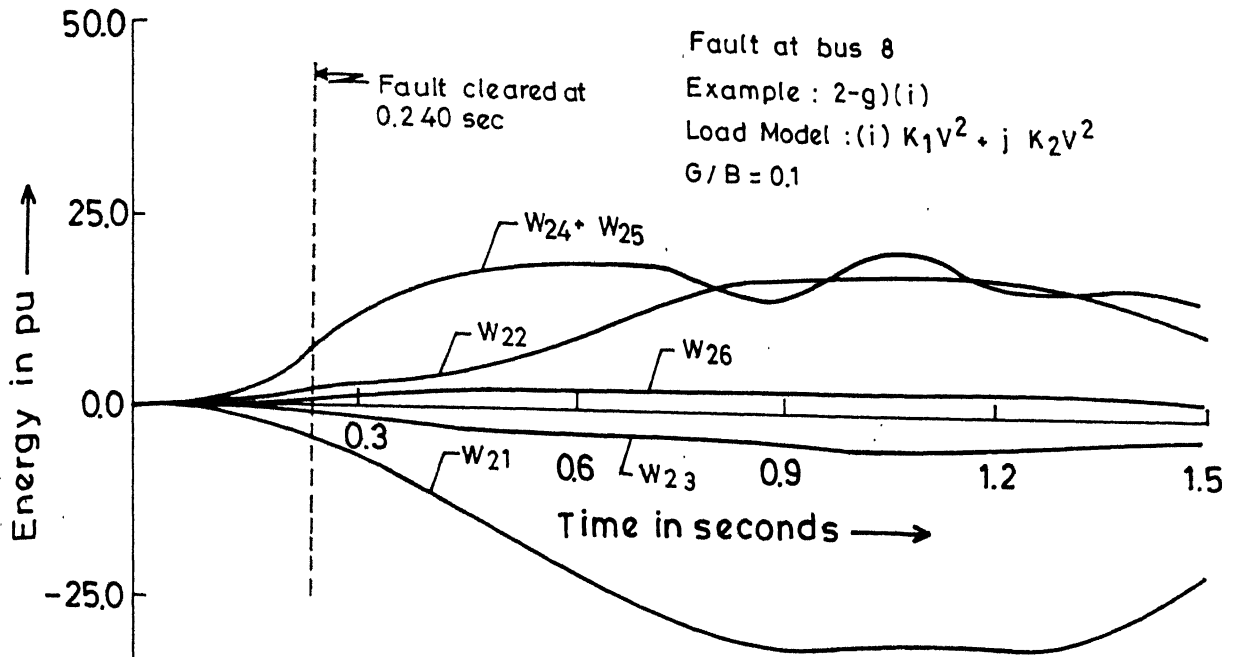


FIG. 5.30 VARIATION OF THE COMPONENTS OF  $W_2$  FOR 10-MACHINE SYSTEM, STABLE CASE

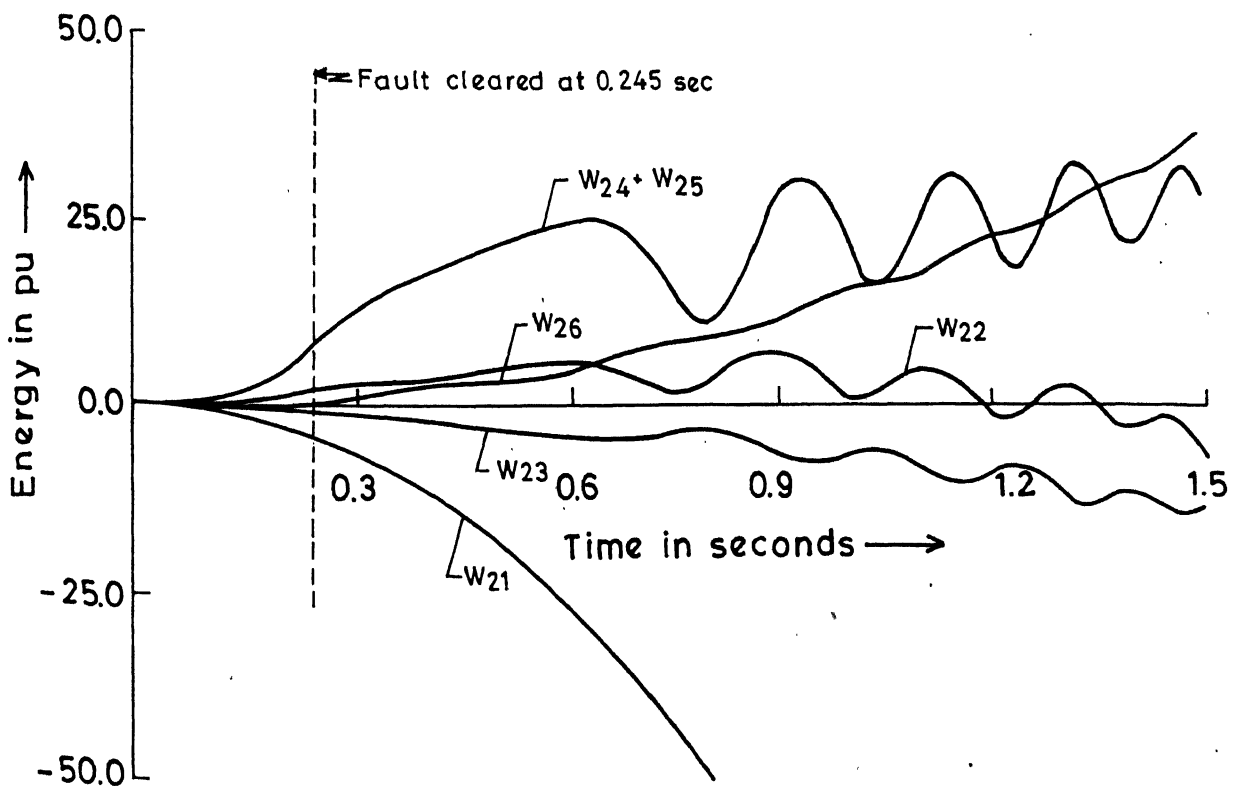


FIG. 5.31 VARIATION OF THE COMPONENTS OF  $W_2$  FOR 10-MACHINE SYSTEM, UNSTABLE CASE

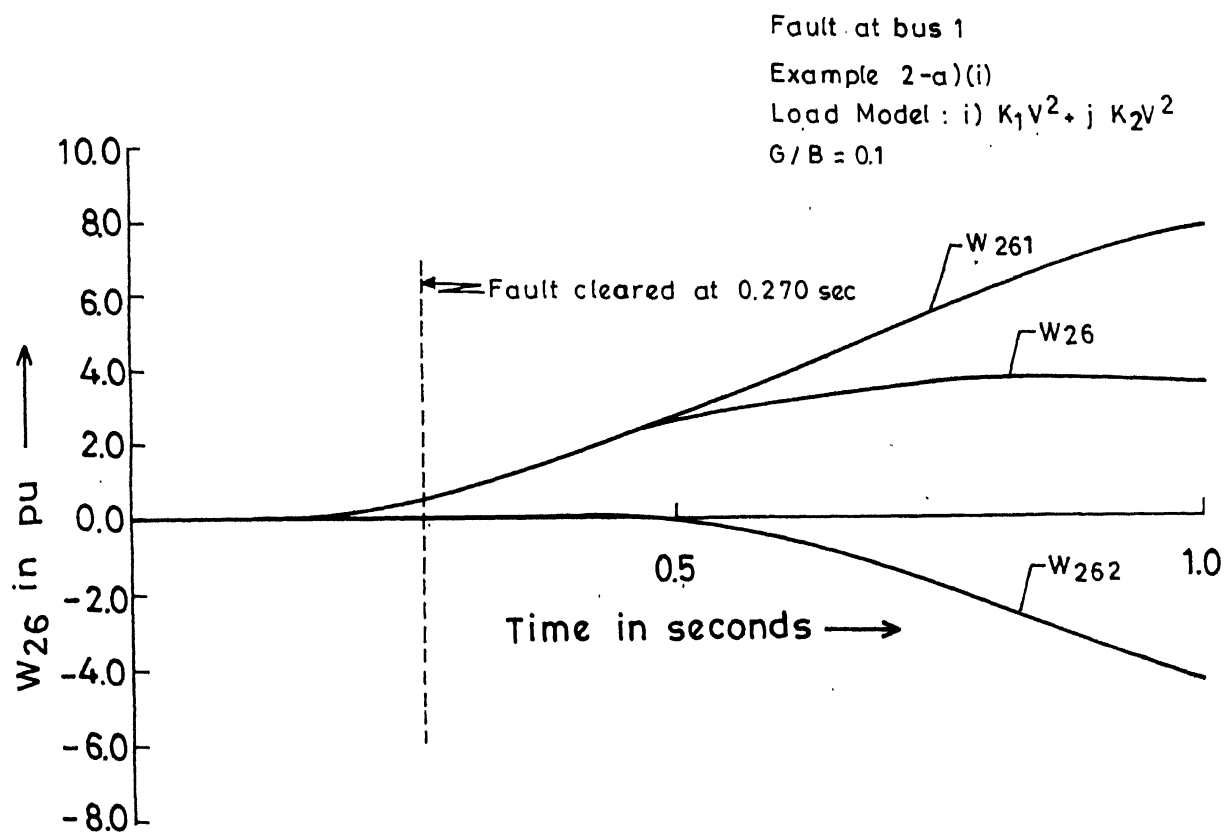


FIG. 5.32 VARIATION OF THE COMPONENTS OF  $W_{26}$  FOR 10-MACHINE SYSTEM, STABLE CASE

to those obtained considering the actual line resistances. Thus, the proposed method to account for the resistances is quite satisfactory.

The replacement of the kinetic energy term  $W_1$  by  $W_{11}$  results in a slight improvement in the predicted result of critical clearing time. As in Chapter 3,  $W_{11}$  was calculated by considering the faulted generator going out-of-step with respect to the rest of the generators. As observed in Chapter 3, this procedure of the kinetic energy correction does not significantly affect the results.

Out of the 6 components of the potential energy,  $W_{21}$ ,  $W_{24}$  and  $W_{25}$  are identical to the similar components defined in Chapters 2 and 3 and their variations are similar to those observed in Chapters 2 and 3. It is also observed here that  $W_{22}$  is significantly larger than  $W_{23}$ . However, in comparison to the lossless case, the magnitude of  $W_{23}$  is slightly larger. It is interesting to observe that in all stable cases  $W_{26}$  (which is positive) is of similar magnitude as of  $W_{23}$  (which is negative) and tends to cancel each other. In unstable cases,  $W_{26}$  tends to increase without limit although the rate of increase is smaller than the rate of decrease of  $W_{21}$ .

The variations of the component  $W_{26}$  alongwith its sub-components  $W_{261}$  and  $W_{262}$  are shown in Fig. 5.32 for example 2-a)(i). It is interesting to observe that the path dependent

term  $W_{262}$  is negligible initially and also  $W_{261}$  which is path independent, dominates over  $W_{262}$ . This shows that the accuracy in the prediction of critical clearing time is not significantly affected by the presence of the path dependent term whose contribution is negligible.

## 5.6 CONCLUSIONS

In this chapter, a structure preserving energy function has been developed including the effects of transmission line resistances. The function has been applied to two sample power systems and based on this study, the following conclusions are drawn :

- i) The predicted value of  $t_{cr}$  agrees closely with that obtained by digital simulation.
- ii) Inclusion of transmission line resistances in the energy function gives an estimate of  $t_{cr}$  which is, in general, higher than that obtained for the lossless system.
- iii)  $t_{cr}$  obtained by digital simulation using the average value for  $G/B$  agrees well with that obtained using the actual resistances of the elements of the system. Thus, the approximation introduced by the assumption of same  $G/B$  ratio for all the elements of a network, appears to be fairly accurate.

## CHAPTER 6

# A STRUCTURE PRESERVING ENERGY FUNCTION WITH DETAILED GENERATOR MODELS

### 6.1 INTRODUCTION

A structure preserving energy function was developed in Chapter 3 representing the generator by the simple model, i.e., a constant voltage source behind the transient reactance. Recently, Padiyar et al [58] have considered detailed models for generators including flux decay, transient saliency, AVR and exciter to evaluate the transient stability of power systems. The SPEF considered in [58] has a time derivative that, along the post-fault trajectory, is non-positive which results in pessimistic estimates of the region of stability.

The principal aim of this chapter is to reexamine the work reported in ref. [58] and try to remove the limitations mentioned above. A new structure preserving energy function is developed which is constant on the post-fault trajectory. This should lead to better accuracy in the prediction of stability using PEBS method. Moreover, the generator model is improved upon by the addition of a damper winding on the quadrature axis. Simpler and more general expressions for the energy functions are then derived where the use of the classical model becomes a special case. The simplification in the

expressions can lead to increasing the speed of computation of SPEF. Investigations are carried out on a 4-machine and a 10-machine system examples to illustrate the proposed method.

## 6.2 SYSTEM MODEL

### 6.2.1 Generator Model

Consider the 'm' machine system supplying 'n' nonlinear voltage dependent loads, as shown in Fig. 3.1 (Chapter 3). Usually, in transient stability studies, the generators close to the fault are modelled in greater detail [24, 57]. The complexity in modelling the generators more realistically depends on the number of rotor circuits represented. The model considered here includes two circuits on the rotor; i) the field winding on the direct axis and ii) a damper winding on the quadrature axis. It is assumed that the mechanical input to the generator is constant. The dynamics of the machines are then described by the following differential-algebraic equations (with respect to COI reference frame) :

For  $i = 1, 2, \dots, m$

$$\dot{\theta}_i = \omega_i \quad (6.1)$$

$$M_i \dot{\omega}_i = P_{mi} - P_{ei} - \frac{M_i}{M_T} P_{COI} \quad (6.2)$$

$$\text{where } P_{ei} = [E'_{qi} + (x'_{di} - x'_{qi}) i_{di}] i_{qi} + E'_{di} i_{di} \quad (6.3)$$

$$P_{COI} = \sum_{i=1}^m (P_{mi} - P_{ei}) \quad (6.4)$$

$$T'_{doi} E'_{qi} = E_{fdi} - E'_{qi} + (x_{di} - x'_{di}) i_{di} \quad (6.5)$$

$$T'_{qoi} E'_{di} = -[E'_{di} + (x_{qi} - x'_{qi}) i_{qi}] \quad (6.6)$$

$$V_{qi} = E'_{qi} + x'_{di} i_{di} \quad (6.7)$$

$$V_{di} = E'_{di} - x'_{qi} i_{qi} \quad (6.8)$$

$$V_i e^{j\varphi_i} = (V_{qi} + jV_{di}) e^{j\theta_i} \quad (6.9)$$

From Eq. (6.9) we get,

$$V_{qi} = V_i \cos(\theta_i - \varphi_i) \quad (6.10)$$

$$V_{di} = -V_i \sin(\theta_i - \varphi_i) \quad (6.11)$$

From Eqs. (6.7) - (6.11),  $i_{di}$  and  $i_{qi}$  are obtained as

$$i_{di} = [V_i \cos(\theta_i - \varphi_i) - E'_{qi}] / x'_{di} \quad (6.12)$$

$$i_{qi} = \frac{E'_{di} + V_i \sin(\theta_i - \varphi_i)}{x'_{qi}} \quad (6.13)$$

Substituting for  $i_{di}$  and  $i_{qi}$  from Eqs. (6.12) and (6.13) in Eq. (6.3) and simplifying, we get,

$$P_{ei} = \frac{E'_{qi} V_i \sin(\theta_i - \varphi_i)}{x'_{di}} + \frac{E'_{di} V_i \cos(\theta_i - \varphi_i)}{x'_{qi}} + V_i^2 \frac{x'_{di} - x'_{qi}}{2x'_{di}x'_{qi}} \sin 2(\theta_i - \varphi_i) \quad (6.14)$$

Eliminating  $i_{di}$  and  $i_{qi}$  in Eqs. (6.5) and (6.6) using Eqs. (6.12) and (6.13), we get,

$$T'_{doi} \dot{E}'_{qi} = E_{fdi} - \frac{x_{di}}{x'_{di}} E'_{qi} + \frac{V_i \cos(\theta_i - \phi_i)}{x'_{di}} (x_{di} - x'_{di}) \quad (6.15)$$

$$T'_{qoi} \dot{E}'_{di} = -\left[\frac{x_{qi}}{x'_{qi}} E'_{di} + \frac{V_i \sin(\theta_i - \phi_i)}{x'_{qi}} (x_{qi} - x'_{qi})\right] \quad (6.16)$$

### 6.2.2 Excitation System and Voltage Regulator Model

The excitation system and voltage regulator model used here is IEEE type 1 taken from ref. [76]. The block diagram of the system is shown in Fig. 6.1. The system is described by the following dynamic and algebraic equations :

$$V_{ei} = V_{Refi} - V_i - V_{si} \quad (6.17)$$

$$\dot{V}_{Ri} = (K_A V_{ei} - V_{Ri})/T_A \quad (6.18)$$

$$V_{RLi} = V_{Ri} \quad \text{if} \quad V_{Rmin} \leq V_{Ri} \leq V_{Rmax} \quad (6.19)$$

$$= V_{Rmin} \quad \text{if} \quad V_{Ri} < V_{Rmin} \quad (6.20)$$

$$= V_{Rmax} \quad \text{if} \quad V_{Ri} > V_{Rmax} \quad (6.21)$$

$$\dot{E}_{fdi} = [V_{RLi} - A_{ex} e^{B_{ex}} E_{fdi} - K_E E_{fdi}]/T_E \quad (6.22)$$

$$V_{si} = \frac{K_s}{T_s} E_{fdi} - V_{sLi} \quad (6.23)$$

where,

$$\dot{V}_{sLi} = \frac{1}{T_s} \left( \frac{K_s}{T_s} E_{fdi} - V_{sLi} \right) \quad (6.24)$$

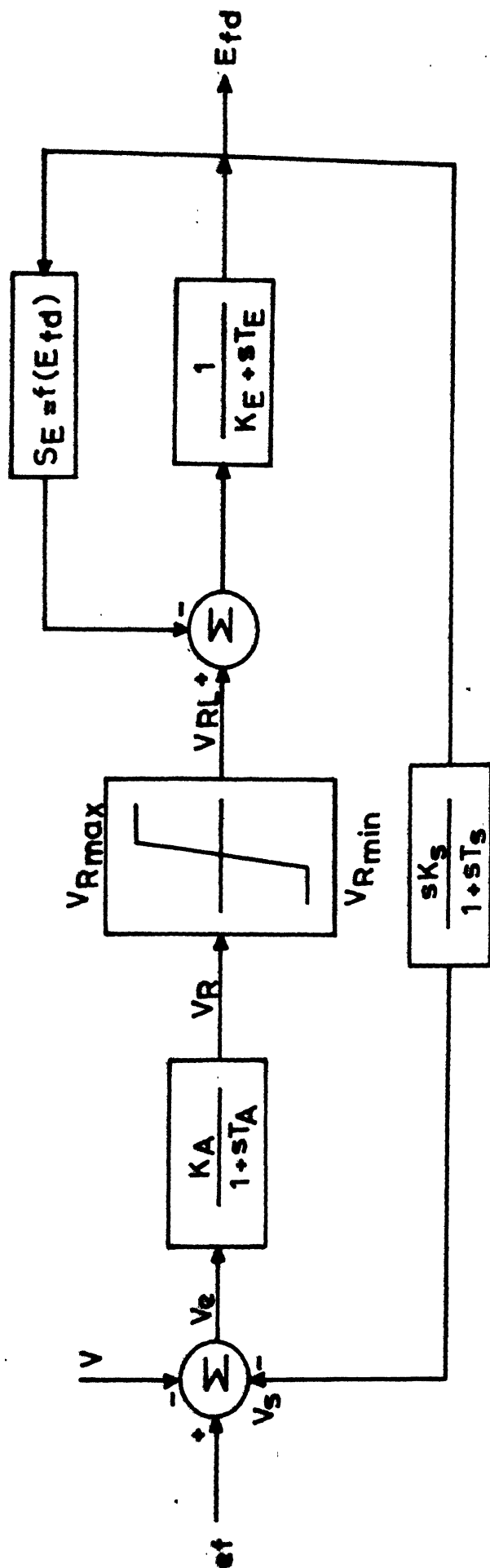


FIG.6.1 BLOCK DIAGRAM OF IEEE TYPE I EXCITATION SYSTEM

### 6.2.3 Load Model

The load model given in Chapter 3 is used.

### 6.2.4 Power Flow Equations

For the lossless system shown in Fig. 3.1 (Chapter 3), the following equations can be written at bus  $i$  :

$$\begin{aligned}
 P_i &= \frac{E'_{qi} V_i \sin(\varphi_i - \theta_i)}{x'_{di}} - \frac{E'_{di} V_i \cos(\theta_i - \varphi_i)}{x'_{qi}} \\
 &\quad + \frac{V_i^2 (x'_{di} - x'_{qi})}{2x'_{di} x'_{qi}} \sin 2(\varphi_i - \theta_i) \\
 &\quad + \sum_{j=1}^n B_{ij} V_i V_j \sin \varphi_{ij}, \quad i = 1, 2, \dots, m \\
 &= \sum_{j=1}^n B_{ij} V_i V_j \sin \varphi_{ij}, \quad i = m+1, m+2, \dots, n \quad (6.25)
 \end{aligned}$$

$$\begin{aligned}
 Q_i &= \frac{V_i^2}{x'_{di}} - \frac{E'_{qi} V_i \cos(\theta_i - \varphi_i)}{x'_{di}} - \frac{E'_{di} V_i \sin(\varphi_i - \theta_i)}{x'_{qi}} \\
 &\quad - \frac{V_i^2 (x'_{di} - x'_{qi})}{2x'_{di} x'_{qi}} [\cos 2(\theta_i - \varphi_i) - 1] - \sum_{j=1}^n B_{ij} V_i V_j \cos \varphi_{ij}, \\
 &\quad i = 1, 2, \dots, m \\
 &= - \sum_{j=1}^n B_{ij} V_i V_j \cos \varphi_{ij}, \quad i = m+1, m+2, \dots, n \quad (6.26)
 \end{aligned}$$

In the above expressions  $B_{ij} = \text{Im} [Y_{ij}]$  where  $[Y]$  is the admittance matrix of the network (excluding machine reactances).

The power flow equations, as given in Chapter 3, are

$$P_i + f_{pi}(V_i) \quad , \quad i = 1, 2, \dots, n \quad (6.27)$$

$$Q_i + f_{qi}(V_i) \quad , \quad i = 1, 2, \dots, n \quad (6.28)$$

### 6.3 STRUCTURE PRESERVING ENERGY FUNCTION (SPEF)

In what follows, a structure preserving energy function, which incorporates the effect of AVR, transient saliency, damper winding and voltage dependent active and reactive power loads, is developed.

Consider the function defined for the post-fault system,

$$W(\theta, \omega, E'_q, E'_d, V, \varphi, E_{fd}, t) = W_1 + W_2 = W_1 + \sum_{i=1}^{13} W_{2i} \quad (6.29)$$

where

$$W_1(\omega) = \frac{1}{2} \sum_{i=1}^m M_i \omega_i^2 \quad (6.30)$$

$$W_{21}(\theta) = - \sum_{i=1}^m P_{mi}(\theta_i - \theta_{i0}) \quad (6.31)$$

$$W_{22}(t) = \sum_{i=1}^n \int_{t_0}^t f_{pi}(V_i) \frac{d\varphi_i}{dt} dt \quad (6.32)$$

$$W_{23}(V) = \sum_{i=1}^n \int_{V_{i0}}^{V_i} \frac{f_{qi}(V_i)}{V_i} dV_i \quad (6.33)$$

$$W_{24}(\theta, E'_q, V, \varphi) = \sum_{i=1}^m [E_{qi}^2 + V_i^2 - 2E'_{qi} V_i \cos(\theta_i - \varphi_i) - (E_{qio}^2 + V_{io}^2 - 2E'_{qio} V_{io} \cos(\theta_{io} - \varphi_{io}))] \frac{1}{2x_{di}} \quad (6.34)$$

$$W_{25}(V, \varphi) = -\frac{1}{2} \sum_{i=1}^n \sum_{j=1}^n B_{ij} (V_i V_j \cos \varphi_{ij} - V_{io} V_{jo} \cos \varphi_{ijo}) \quad (6.35)$$

$$W_{26}(\theta, V, \varphi) = - \sum_{i=1}^m [V_i^2 \{ \cos 2(\theta_i - \varphi_i) - 1 \} - V_{io}^2 \{ \cos 2(\theta_{io} - \varphi_{io}) - 1 \}]$$

$$\frac{x'_{di} - x'_{qi}}{4x'_{di} x'_{qi}} \quad (6.36)$$

$$W_{27}(t) = - \sum_{i=1}^m \int_{t_0}^t \frac{E_{fdi}}{(x_{di} - x'_{di})} \frac{dE'_{qi}}{dt} dt \quad (6.37)$$

$$W_{28}(E'_q) = \sum_{i=1}^m \frac{E'^2_{qi} - E'^2_{qio}}{2(x_{di} - x'_{di})} \quad (6.38)$$

$$W_{29}(t) = \sum_{i=1}^m \int_{t_0}^t \frac{T'_{doi}}{(x_{di} - x'_{di})} \left( \frac{dE'_{qi}}{dt} \right)^2 dt \quad (6.39)$$

$$W_{210}(\theta, E'_d, V, \varphi) = \sum_{i=1}^m [E'^2_{di} + V_i^2 + 2E'_d V_i \sin(\theta_i - \varphi_i) - (E'^2_{dio} + V_{io}^2 + 2E'_d V_{io} \sin(\theta_{io} - \varphi_{io}))] \frac{1}{2x'_{qi}} \quad (6.40)$$

$$W_{211}(V) = - \sum_{i=1}^m \frac{V_i^2 - V_{io}^2}{2x'_{qi}} \quad (6.41)$$

$$W_{212}(t) = \sum_{i=1}^m \int_{t_0}^t \frac{T'_{qoi}}{(x_{qi} - x'_{qi})} \left( \frac{dE'_{di}}{dt} \right)^2 dt \quad (6.42)$$

$$W_{213}(E'_d) = \sum_{i=1}^m \frac{E'^2_{di} - E'^2_{dio}}{2(x_{qi} - x'_{qi})} \quad (6.43)$$

Subscript 'o' in the above expressions indicates the quantities at the initial sep.

Now it will be shown that the time derivative of the function defined in Eq. (6.29) is zero.

Partially differentiating  $W_2$  with respect to  $E'_{qi}$ ,  $E'_{di}$ ,  $V_i$ ,  $\varphi_i$ ,  $\theta_i$  and  $t$ , we get,

$$\begin{aligned}
 \frac{\partial W_2}{\partial E'_{qi}} &= \frac{E'_{qi}}{x'_{di}} - \frac{V_i \cos(\theta_i - \varphi_i)}{x'_{di}} + \frac{E'_{qi}}{(x_{di} - x'_{di})} \\
 &= - \frac{V_i \cos(\theta_i - \varphi_i)}{x'_{di}} + \frac{x_{di}}{x'_{di}} \frac{E'_{qi}}{(x_{di} - x'_{di})} \\
 &= - \frac{T'_{doi} \dot{E}'_{qi}}{(x_{di} - x'_{di})} + \frac{E_{fdi}}{(x_{di} - x'_{di})}, \text{ from Eq. (6.15)} \quad (6.44)
 \end{aligned}$$

$$\begin{aligned}
 \frac{\partial W_2}{\partial E'_{di}} &= \frac{E'_{di}}{x'_{qi}} + \frac{V_i \sin(\theta_i - \varphi_i)}{x'_{qi}} + \frac{E'_{di}}{(x_{qi} - x'_{qi})} \\
 &= \frac{x_{qi}}{x'_{qi}} \frac{E'_{di}}{(x_{qi} - x'_{qi})} + \frac{V_i \sin(\theta_i - \varphi_i)}{x'_{qi}} \\
 &= - \frac{T'_{qoi} \dot{E}'_{di}}{(x_{qi} - x'_{qi})}, \text{ from Eq. (6.16)} \quad (6.45)
 \end{aligned}$$

$$\begin{aligned}
 \frac{\partial W_2}{\partial V_i} &= \frac{1}{V_i} [f_{qi}(V_i) + \frac{V_i^2}{x'_{di}} - \frac{E'_{qi} V_i \cos(\theta_i - \varphi_i)}{x'_{di}} - \sum_{j=1}^n B_{ij} V_i V_j \cos \varphi_{ij} \\
 &\quad - \frac{V_i^2}{2x'_{di} x'_{qi}} \{ \cos 2(\theta_i - \varphi_i) - 1 \} + \frac{E'_{di} V_i \sin(\theta_i - \varphi_i)}{x'_{qi}}], i=1, 2, \dots, m \\
 &= \frac{1}{V_i} [f_{qi}(V_i) - \sum_{j=1}^n B_{ij} V_i V_j \cos \varphi_{ij}], i = m+1, m+2, \dots, n,
 \end{aligned}$$

$$= \frac{1}{V_i} [Q_i + f_{qi}(V_i)] , \quad i = 1, 2, \dots, n$$

in view of Eq. (6.26)

$$= 0 , \text{ from Eq. (6.28)} \quad (6.46)$$

$$\begin{aligned} \frac{\partial W_2}{\partial \varphi_i} &= - \frac{E'_{qi} V_i \sin(\theta_i - \varphi_i)}{x'_{di}} + \sum_{j=1}^n B_{ij} V_i V_j \sin \varphi_{ij} \\ &\quad - \frac{V_i^2 (x'_{di} - x'_{qi})}{2x'_{di} x'_{qi}} \sin 2(\theta_i - \varphi_i) - \frac{E'_{di} V_i \cos(\theta_i - \varphi_i)}{x'_{qi}}, i=1, 2, \dots, m \\ &= \sum_{j=1}^n B_{ij} V_i V_j \sin \varphi_{ij} \quad i = m+1, m+2, \dots, n \end{aligned}$$

$$= P_i , \text{ from Eq. (6.25)} \quad (6.47)$$

$$\begin{aligned} \frac{\partial W_2}{\partial \theta_i} &= -P_{mi} + \frac{E'_{qi} V_i \sin(\theta_i - \varphi_i)}{x'_{di}} + \frac{V_i^2 (x'_{di} - x'_{qi})}{2x'_{di} x'_{qi}} \sin 2(\theta_i - \varphi_i) \\ &\quad + \frac{E'_{di} V_i \cos(\theta_i - \varphi_i)}{x'_{qi}} \end{aligned}$$

$$= -P_{mi} + P_{ei}, \text{ in view of Eq. (6.14)} \quad (6.48)$$

$$\begin{aligned} \frac{\partial W_2}{\partial t} &= \sum_{i=1}^n f_{pi}(V_i) \frac{d\varphi_i}{dt} - \sum_{i=1}^m \frac{E_{fdi}}{(x_{di} - x'_{di})} \frac{dE'_{qi}}{dt} \\ &\quad + \sum_{i=1}^m \frac{T'_{doi}}{(x_{di} - x'_{di})} \left( \frac{dE'_{qi}}{dt} \right) + \sum_{i=1}^m \frac{T'_{qoi}}{(x_{qi} - x'_{qi})} \left( \frac{dE'_{di}}{dt} \right)^2 \quad (6.49) \end{aligned}$$

Partially differentiating  $W_1$  with respect to  $\omega_i$ , we have,

$$\frac{\partial W_1}{\partial \omega_i} = M_i \omega_i \quad (6.50)$$

Substituting from Eqs. (6.48) and (6.50) we get,

$$\begin{aligned}
 \frac{\partial W_1}{\partial \omega_i} \frac{d\omega_i}{dt} + \frac{\partial W_2}{\partial \theta_i} \frac{d\theta_i}{dt} &= M_i \omega_i \dot{\omega}_i - P_{mi} \omega_i + P_{ei} \omega_i \\
 &= (M_i \dot{\omega}_i - P_{mi} + P_{ei}) \omega_i \\
 &= - \frac{M_i \omega_i}{M_T} P_{COI}, \text{ from Eq. (6.2)}
 \end{aligned} \tag{6.51}$$

Thus,

$$\begin{aligned}
 \sum_{i=1}^m \left( \frac{\partial W_1}{\partial \omega_i} \frac{d\omega_i}{dt} + \frac{\partial W_2}{\partial \theta_i} \frac{d\theta_i}{dt} \right) &= - \sum_{i=1}^m \frac{M_i \omega_i}{M_T} P_{COI} \\
 &= - \frac{P_{COI}}{M_T} \sum_{i=1}^m M_i \omega_i = 0, \text{ from the definition of COI} \\
 &\quad \text{variables}
 \end{aligned} \tag{6.52}$$

$$\sum_{i=1}^n \frac{\partial W_2}{\partial V_i} \frac{dV_i}{dt} = 0, \text{ from Eq. (6.46)} \tag{6.53}$$

Substituting from Eqs. (6.47) and (6.49), we have,

$$\begin{aligned}
 \sum_{i=1}^n \left( \frac{\partial W_2}{\partial \phi_i} \frac{d\phi_i}{dt} \right) + \frac{\partial W_2}{\partial t} &= \sum_{i=1}^n [P_i + f_{pi}(V_i)] - \sum_{i=1}^m \frac{E_{fdi}}{(x_{di} - x'_{di})} \frac{dE'_{qi}}{dt} \\
 &\quad + \sum_{i=1}^m \frac{T'_{doi}}{(x_{di} - x'_{di})} \left( \frac{dE'_{qi}}{dt} \right)^2 + \sum_{i=1}^m \frac{T'_{qoi}}{(x_{qi} - x'_{qi})} \left( \frac{dE'_{di}}{dt} \right)^2 \\
 &= - \sum_{i=1}^m \frac{E_{fdi}}{(x_{di} - x'_{di})} \frac{dE'_{qi}}{dt} + \sum_{i=1}^m \frac{T'_{doi}}{(x_{di} - x'_{di})} \left( \frac{dE'_{qi}}{dt} \right)^2 \\
 &\quad + \sum_{i=1}^m \frac{T'_{qoi}}{(x_{qi} - x'_{qi})} \left( \frac{dE'_{di}}{dt} \right)^2, \text{ using Eq. (6.27)}
 \end{aligned} \tag{6.54}$$

Substituting from Eqs. (6.44), (6.45) and (6.54), we get,

$$\begin{aligned}
 & \sum_{i=1}^m \left( \frac{\partial W_2}{\partial E'_{qi}} \frac{dE'_{qi}}{dt} \right) + \sum_{i=1}^m \left( \frac{\partial W_2}{\partial E'_{di}} \frac{dE'_{di}}{dt} \right) + \sum_{i=1}^n \left( \frac{\partial W_2}{\partial \varphi_i} \frac{d\varphi_i}{dt} \right) + \frac{\partial W_2}{\partial t} \\
 &= \sum_{i=1}^m \left[ - \frac{T'_{doi} (\dot{E}'_{qi})^2}{(x_{di} - x'_{di})} + \frac{E_{fdi} E_{qi}}{(x_{di} - x'_{di})} \right] - \sum_{i=1}^m \frac{T'_{qoi} (\dot{E}'_{di})^2}{(x_{qi} - x'_{qi})} \\
 & - \sum_{i=1}^m \frac{E_{fdi} \dot{E}'_{qi}}{(x_{di} - x'_{di})} + \sum_{i=1}^m \frac{T'_{doi} (\dot{E}'_{qi})^2}{(x_{di} - x'_{di})} + \sum_{i=1}^m \frac{T'_{qoi} (\dot{E}'_{di})^2}{(x_{qi} - x'_{qi})} \\
 &= 0
 \end{aligned} \tag{6.55}$$

Hence,

$$\begin{aligned}
 \frac{dW}{dt} &= \frac{d}{dt} (W_1 + W_2) = \sum_{i=1}^m \left( \frac{\partial W_1}{\partial \omega_i} \frac{d\omega_i}{dt} + \frac{\partial W_2}{\partial \theta_i} \frac{d\theta_i}{dt} \right) + \sum_{i=1}^n \left( \frac{\partial W_2}{\partial V_i} \frac{dV_i}{dt} \right) \\
 &+ \left[ \sum_{i=1}^m \left( \frac{\partial W_2}{\partial E'_{qi}} \frac{dE'_{qi}}{dt} \right) + \sum_{i=1}^m \left( \frac{\partial W_2}{\partial E'_{di}} \frac{dE'_{di}}{dt} \right) + \sum_{i=1}^n \left( \frac{\partial W_2}{\partial \varphi_i} \frac{d\varphi_i}{dt} \right) + \frac{\partial W_2}{\partial t} \right] \\
 &= 0, \text{ in view of Eqs. (6.52), (6.53) and (6.55)}
 \end{aligned} \tag{6.56}$$

### Comments

1) The last 4 terms  $W_{210}$ ,  $W_{211}$ ,  $W_{212}$  and  $W_{213}$  correspond to the change in energy due to the presence of damper winding on the quadrature axis. In the absence of this winding,  $E'_d = 0$  and these terms vanish. Thus, there are only 9 terms in the energy function when one-axis model of the generator is used. Out of these, the first 8 terms are the same as those given in [58, 71].

The 9th term is introduced as the energy function defined here is constant along the post-fault trajectory. It is to be noted that the energy function defined in [58, 71] has a time derivative given by

$$- \sum_{i=1}^m \frac{T'_{doi}}{(x_{di} - x'_{di})} \left( \frac{dE'_{qi}}{dt} \right)^2 \quad (6.57)$$

which is non-positive.

2) The term  $W_{26}$  in Eq. (6.36) is the change in energy stored due to saliency in absence of which it is zero.

3) In the absence of AVR,  $E_{fd}$  is constant and  $W_{27}$  in Eq. (6.37) can be expressed as

$$- \sum_{i=1}^m E_{fdi} \frac{E'_{qi} - E'_{qio}}{x_{di} - x'_{di}} \quad (6.58)$$

With this simplification the sum of the first 8 terms of the energy function are equivalent to that given in ref. [57] for the one-axis model including flux decay but neglecting AVR. It is to be noted that ref. [57] considers only constant P-Q type loads.

4) If a fault at its terminals separates generator  $k$  from the rest of the generators, then the kinetic energy term can be modified to  $W_{11}$  defined below (see Chapter 3)

$$W_{11} = \frac{1}{2} \frac{M_k M_{T-k}}{M_T} (\omega_k - \omega_{T-k})^2 \quad (6.59)$$

5) As discussed in Chapter 2,  $W_{22}$ , the potential energy component due to active power loads, can be approximated as

$$W_{22} = \sum_{i=1}^m [f_{pi}(V_i) \phi_i - f_{pi}(V_{io}) \phi_{io}] \quad (6.60)$$

### A Simpler Expression for SPEF

The terms  $W_{24}$ ,  $W_{25}$ ,  $W_{26}$ ,  $W_{210}$  and  $W_{211}$  correspond to the change in energy stored in the machine reactances and transmission lines. It is shown in Appendix J that this change is half the sum of the change in reactive power loss in the network, i.e.,

$$\begin{aligned} W_{24} + W_{25} + W_{26} + W_{210} + W_{211} &= \frac{1}{2} Q_{\text{LOSS}} \\ &= \frac{1}{2} \left[ \sum_{i=1}^m (Q_{Gi} - Q_{Gio}) - \sum_{j=1}^n (Q_{Li} - Q_{Lio}) \right] \end{aligned} \quad (6.61)$$

From Eq. (6.5) we get,

$$i_{di} = - \frac{E_{fdi}}{(x_{di} - x'_{di})} + \frac{E'_{qi}}{(x_{di} - x'_{di})} + \frac{T'_{doi} E'_{qi}}{(x_{di} - x'_{di})} \quad (6.62)$$

Multiplying both sides of Eq. (6.62) by  $dE'_{qi}/dt$  and integrating, we get the following equation after summing over all values of  $i$

$$\begin{aligned} \sum_{i=1}^m \int_{t_0}^t i_{di} \frac{dE'_{qi}}{dt} dt &= - \sum_{i=1}^m \int_{t_0}^t \frac{E_{fdi}}{(x_{di} - x'_{di})} \frac{dE'_{qi}}{dt} dt \\ &\quad + \sum_{i=1}^m \int_{t_0}^t \frac{E'_{qi}}{(x_{di} - x'_{di})} \frac{dE'_{qi}}{dt} dt \\ &\quad + \sum_{i=1}^m \int_{t_0}^t \frac{T'_{doi}}{(x_{di} - x'_{di})} \left( \frac{dE'_{qi}}{dt} \right)^2 dt \\ &= W_{27} + W_{28} + W_{29}, \text{ in view of Eqs. (6.37)-(6.39)} \end{aligned} \quad (6.63)$$

Again, from Eqs. (6.6) we have,

$$-i_{qi} = \frac{E'_{di}}{(x_{qi} - x'_{qi})} + \frac{T'_{qoi} \dot{E}'_{di}}{(x_{qi} - x'_{qi})} \quad (6.64)$$

Multiplying both sides of Eq. (6.64) by  $dE'_{di}/dt$  and integrating, we get the following equation after summing over all values of  $i$

$$\begin{aligned} - \sum_{i=1}^m \int_{t_0}^t i_{qi} \frac{dE'_{di}}{dt} dt &= \sum_{i=1}^m \int_{t_0}^t \frac{E'_{di}}{(x_{qi} - x'_{qi})} \frac{dE'_{di}}{dt} dt \\ &+ \sum_{i=1}^m \int_{t_0}^t \frac{T'_{qoi}}{(x_{qi} - x'_{qi})} \left( \frac{dE'_{di}}{dt} \right)^2 dt \\ &= W_{212} + W_{213}, \text{ in view of Eqs. (6.42)-(6.43)} \end{aligned} \quad (6.65)$$

Thus, substituting from Eqs. (6.61), (6.63) and (6.65), the energy function in Eq. (6.29) can be written as

$$W = W_1 + W_{21} + W_{22} + W_{23} + W'_{24} + W'_{25} + W'_{26} \quad (6.66)$$

where,

$$W'_{24} = \frac{1}{2} \left[ \sum_{i=1}^m (Q_{Gi} - Q_{Gio}) - \sum_{j=1}^n (Q_{Li} - Q_{Lio}) \right] \quad (6.67)$$

$$W'_{25} = \sum_{i=1}^m \int_{t_0}^t i_{di} \frac{dE'_{di}}{dt} dt \quad (6.68)$$

$$W'_{26} = - \sum_{i=1}^m \int_{t_0}^t i_{qi} \frac{dE'_{di}}{dt} dt \quad (6.69)$$

The expression for the energy function in Eq. (6.66) is much simpler and requires less computations than that given in Eq.(6.29).  $W'_{25}$  accounts for the effect of flux decay and AVR and  $W'_{26}$  accounts for the effect of damper winding on the quadrature axis. It is obvious that both these terms would vanish when the generator is represented by the classical model and the expression for the energy function will be the same as that used in Chapter 2.

The SPEF defined in Eq. (6.66) can be evaluated using the computer program described in Chapter 2 with modifications to include the computation of the terms  $W'_{24}$ ,  $W'_{25}$  and  $W'_{26}$  in the subroutine TEF for the computation of SPEF.

## 6.4 NUMERICAL EXAMPLES

### 6.4.1 Description

A 4-machine and a 10-machine system examples are considered here. The 10-machine system has already been described in previous chapters while the 4-machine system example is taken from [14]. The single-line diagram of 4-machine system is shown in Fig. K.1 and the system parameters and the operating data are given in APPENDIX K. The disturbance considered is a three phase fault which is cleared followed by instantaneous reclosure of the line. The prefault and the post-fault configurations of the systems are, therefore, assumed to be the same. Impedance type load characteristics are assumed for all the buses. Critical energy is evaluated using the PEBS method. The following cases are investigated.:

Example 1 : 4-machine system

Fault location : bus 3

Machines 2 and 3 which are close to the fault are modelled in detail considering voltage regulator, while machines 1 and 4 are represented by classical models.

Example 2 : 10-machine (NEW ENGLAND) test system

Fault locations : 1) bus 3

i) Machine modelled in detail: 3

ii) Machines modelled in detail: 1,3

2) bus 4

Machines modelled in detail : 4,5

3) bus 8

Machines 8 and 9 are represented with realistic models.

The following is the data for AVR [71] :

$$K_A = 50 ; \quad T_A = 0.02 ; \quad K_E = -0.037$$

$$T_E = 0.146; \quad K_s = 0.057; \quad T_s = 0.45$$

$$A_{ex} = 0.015; \quad B_{ex} = 0.6 ; \quad V_{Rmax} = 5.0$$

$$V_{Rmin} = -5.0$$

For both the examples, the following cases are considered :

A. Without Damper Winding

1. without AVR ; a) with saliency; b) without saliency

2. with AVR : a) with saliency; b) without saliency

## B. With Damper Winding

1. without AVR : a) with saliency; b) without saliency
2. with AVR : a) with saliency; b) without saliency

### 6.4.2 Results and Discussion

#### Critical Energies and Clearing Times

Critical energy and critical clearing time obtained by prediction and digital simulation for various cases are presented in Table 6.1 for 4-machine system and Tables 6.2-6.4 for 10-machine systems. The results in Tables 6.3-6.4 are obtained using the modified energy function neglecting the path dependent term in  $W_{22}$ , the energy component due to the active power of loads.

From an examination of Tables, it is observed that the effect of flux decay alone is to reduce  $t_{cr}$  while the effect of transient saliency is to increase  $t_{cr}$ . However, the effect of flux decay predominates the effect of transient saliency. The presence of the damper winding marginally improves the transient stability. The deleterious effect of flux decay is counteracted by the AVR. In the case of 4-machine system, the critical clearing time is higher than that obtained using the classical model. This is not observed always in the case of 10-machine system. From Table 6.2 it is observed that providing AVR on more than one machine is beneficial in

Table 6.1 Comparison of Critical Energy,  $W_{cr}$  and Critical Clearing Time,  $t_{cr}$  for 4-machine system using proposed SPEF  
 Load Model :  $k_1 V^2 + jk_2 V^2$  ; Fault at bus 3  
 Machines modelled in detail : 2 and 3

A. Without damper winding				B. With damper winding					
	$W_{cr}$ (pu)	$t_{cr}$ (sec) obtained by	$W_{cr}$ (pu)	$t_{cr}$ (sec) obtained by	Prediction		Digital Simula- tion		
					Neglecting Mode of Instability			Considering Mode of Instability	
Classical Model	2.1577	0.480	0.482	2.1577	0.480	0.482	0.480- 0.485		
1. Without AVR									
a) With saliency	1.8935	0.484	0.488	1.9019	0.485	0.489	0.485- 0.490		
b) Without saliency	1.8350	0.475	0.480	1.8469	0.478	0.484	0.480- 0.485		
2. With AVR									
a) With saliency	2.7993	0.510	0.517	2.8860	0.511	0.518	0.510- 0.515		
b) Without saliency	2.5019	0.503	0.509	2.5162	0.503	0.509	0.505- 0.510		

Table 6.2 Comparison of Critical Energy,  $W_{cr}$  and Critical Clearing Time,  $t_{cr}$  for 10-machine System using proposed SPEF  
 Load Model :  $k_1 V^2 + jk_2 V^2$  ; Fault at bus 3

Machines Modelled in detail		A. Without damper winding				B. With damper winding			
		$W_{cr}$ (pu)	$t_{cr}$ (sec) obtained by		$W_{cr}$ (pu)	$t_{cr}$ (sec) obtained by		Digit Simul tion	
			Prediction	Digital Simula- tion		Prediction	Consi- dering Mode of Insta- bility		
Classical Model	-	7.3153	0.218	0.219	7.3153	0.218	0.219	0.230 0.235	
1. Without AVR									
a) With saliency	3	6.1809	0.205	0.206	6.2005	0.206	0.207	0.215 0.220	
ii)	1,3	5.9896	0.204	0.205	6.1080	0.205	0.206	0.215 0.220	
b) Without saliency									
i)	3	5.9835	0.204	0.206	6.0974	0.206	0.208	0.215 0.220	
ii)	1,3	5.9387	0.201	0.203	6.0667	0.201	0.202	0.210 0.215	
2. With AVR									
a) With saliency	3	8.3803	0.226	0.227	8.4302	0.227	0.228	0.235 0.240	
ii)	1,3	8.9461	0.232	0.233	9.0517	0.234	0.235	0.240 0.245	

contd ...

b) Without saliency

i)	3	7.4758	0.221	0.224	0.235- 0.240	7.6302	0.225	0.227	0.235- 0.240
ii)	1,3	7.5004	0.222	0.225	0.235- 0.240	7.6425	0.223	0.226	0.235- 0.240

---

Table 6.3 Comparison of Critical Energy,  $W_{cr}$  and Critical Clearing Time,  $t_{cr}$  for IO-machine system using modified  $W_{22}$  in SPEF  
 Load Model:  $k_1 V^2 + jk_2 V^2$ ; Fault at bus 4  
 Machines modelled in detail : 4 and 5

A. Without damper winding				B. With damper winding			
	$W_{cr}$ (pu)	$t_{cr}$ (sec) obtained by		$W_{cr}$ (pu)	$t_{cr}$ (sec) obtained by		Digital Simulati
		Prediction			Prediction		
		Neglecting Mode of Instabili- ty	Consider- ing Mode of Insta- bility		Neglecting Mode of Instabi- lity	Consider- ing Mode of Insta- bility	
Classical Model	9.8766	0.214	0.215	9.8766	0.214	0.215	0.210- 0.215
1. Without AVR							
a) With saliency	8.4058	0.205	0.206	8.4940	0.206	0.208	0.205- 0.210
b) Without saliency	8.2216	0.196	0.198	8.3030	0.197	0.199	0.195- 0.200
2. With AVR							
a) With saliency	11.2079	0.221	0.223	11.3909	0.223	0.225	0.225- 0.230
b) Without saliency	9.9288	0.215	0.217	10.1288	0.217	0.219	0.220- 0.225

Table 6.4 Comparison of Critical Energy,  $W_{cr}$  and Critical clearing Time,  $t_{cr}$  for 10-machine System using Modified  $W_{22}$  in the SPEF  
 Load Model :  $k_1 V^2 + j k_2 V^2$  ; Fault at bus 8  
 Machines modelled in detail : 8 and 9

A. Without damper winding				B. With damper winding			
	$W_{cr}$ (pu)	$t_{cr}$ (sec) obtained by		$W_{cr}$ (pu)	$t_{cr}$ (sec) obtained by		Digital Simulation
		Prediction	Considering Mode of Instability		Neglecting Mode of Instability	Prediction	
Classical Model	10.1766	0.228	0.230	10.1766	0.228	0.230	0.230- 0.235
1. Without AVR							
a) With saliency	8.8456	0.219	0.222	9.7774	0.224	0.227	0.225- 0.230
b) Without saliency	8.7879	0.213	0.215	8.8995	0.217	0.220	0.220- 0.225
2. With AVR							
a) With saliency	11.6470	0.238	0.242	11.6723	0.239	0.244	0.240- 0.245
b) Without saliency	10.3711	0.230	0.233	10.8350	0.233	0.236	0.235 0.240

increasing critical energies and critical clearing times. This is particularly true when transient saliency is considered. In general, it would be reasonably accurate to state that the classical model is a good and slightly conservative approximation for the detailed model of a generator including AVR.

In, practically, all the cases considered, the predicted values of critical clearing times are fairly close to the values obtained by digital simulation. The accuracy is slightly improved by including the kinetic energy correction as given in Chapter 3. The most significant observation is that the effects of flux decay, transient saliency, damper winding and AVR are correctly reflected in the predicted values of critical energies and critical clearing times. This shows that the proposed SPEF can be used successfully in studying the stability characteristics of a power system.

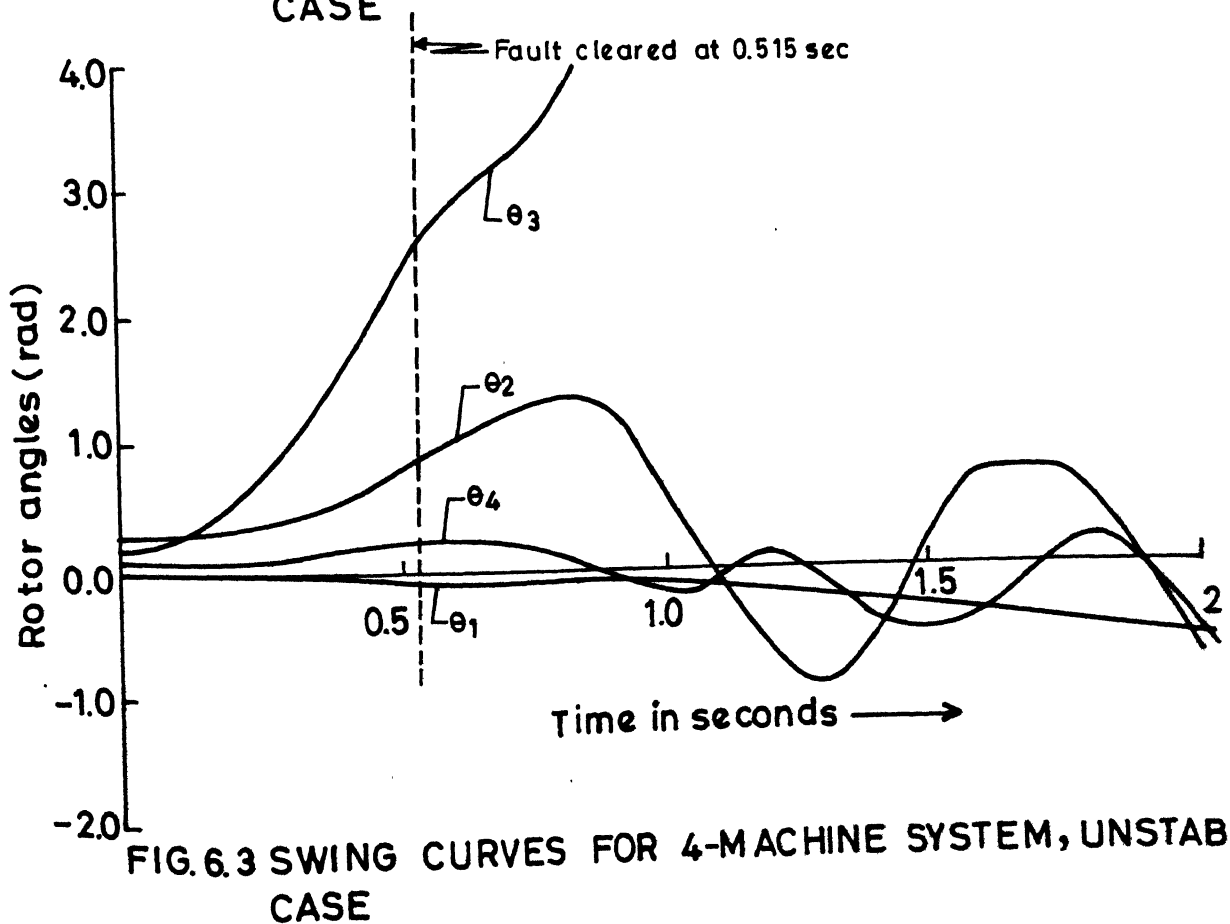
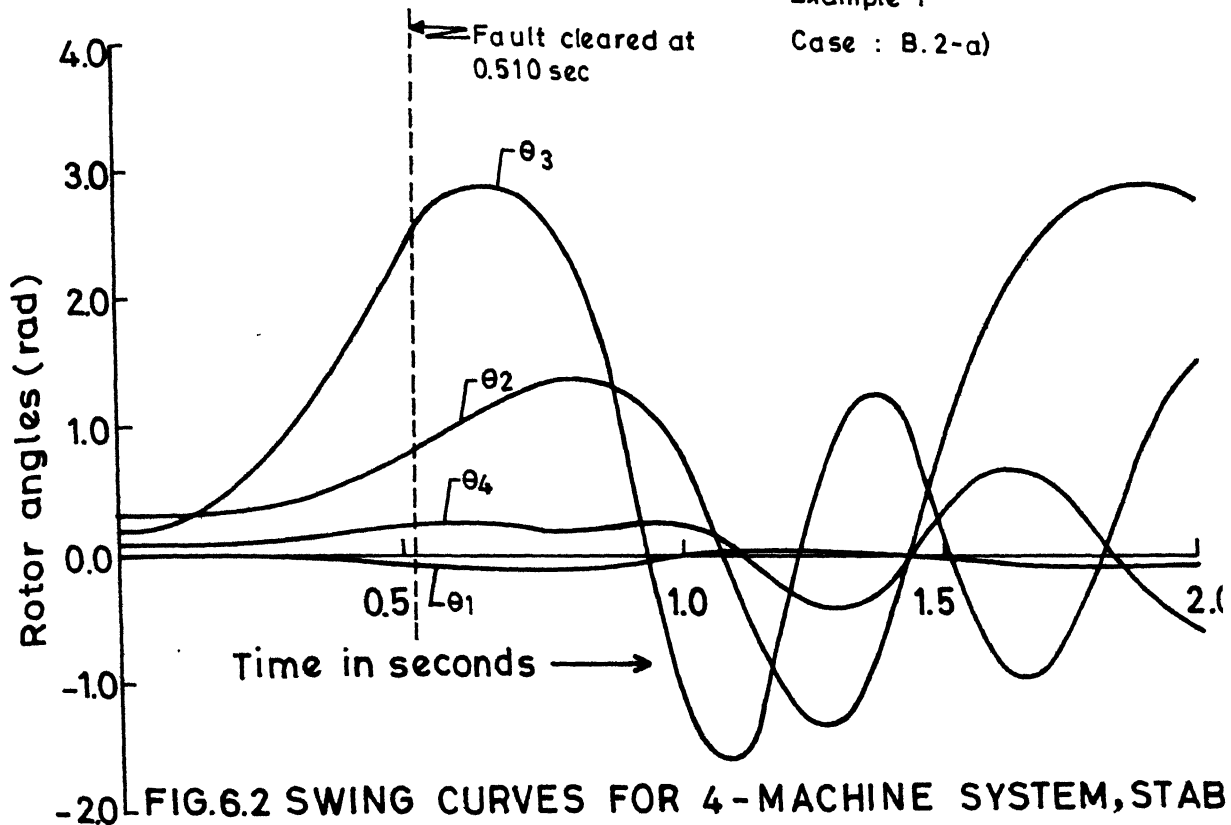
#### Variations of Rotor Angles, Energy Components and other Variables

Figs. 6.2-6.3 show the swing curves for example 1 [B. 2-a)] for the stable and unstable cases for fault at bus 3 of 4-machine system. Variations in the field voltage ( $E_{fd}$ ),  $E'_q$  and  $E'_d$  are given in Figs. 6.4-6.9 both for stable and unstable cases. Figs. 6.10-6.19 show the variations in the total energy, kinetic energy, potential energy and its various components for the stable and unstable cases.

Fault at bus 3

Example 1

Case : B.2-a)



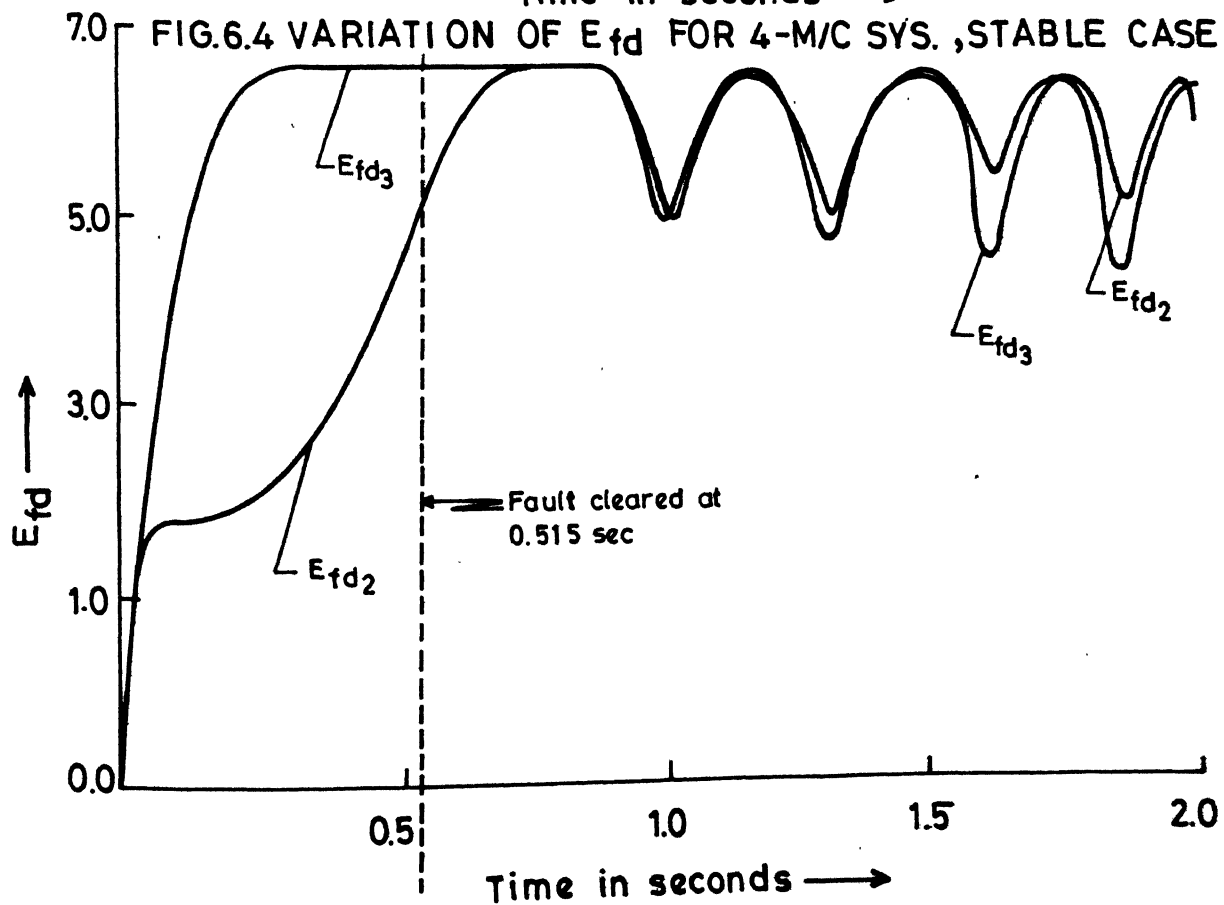
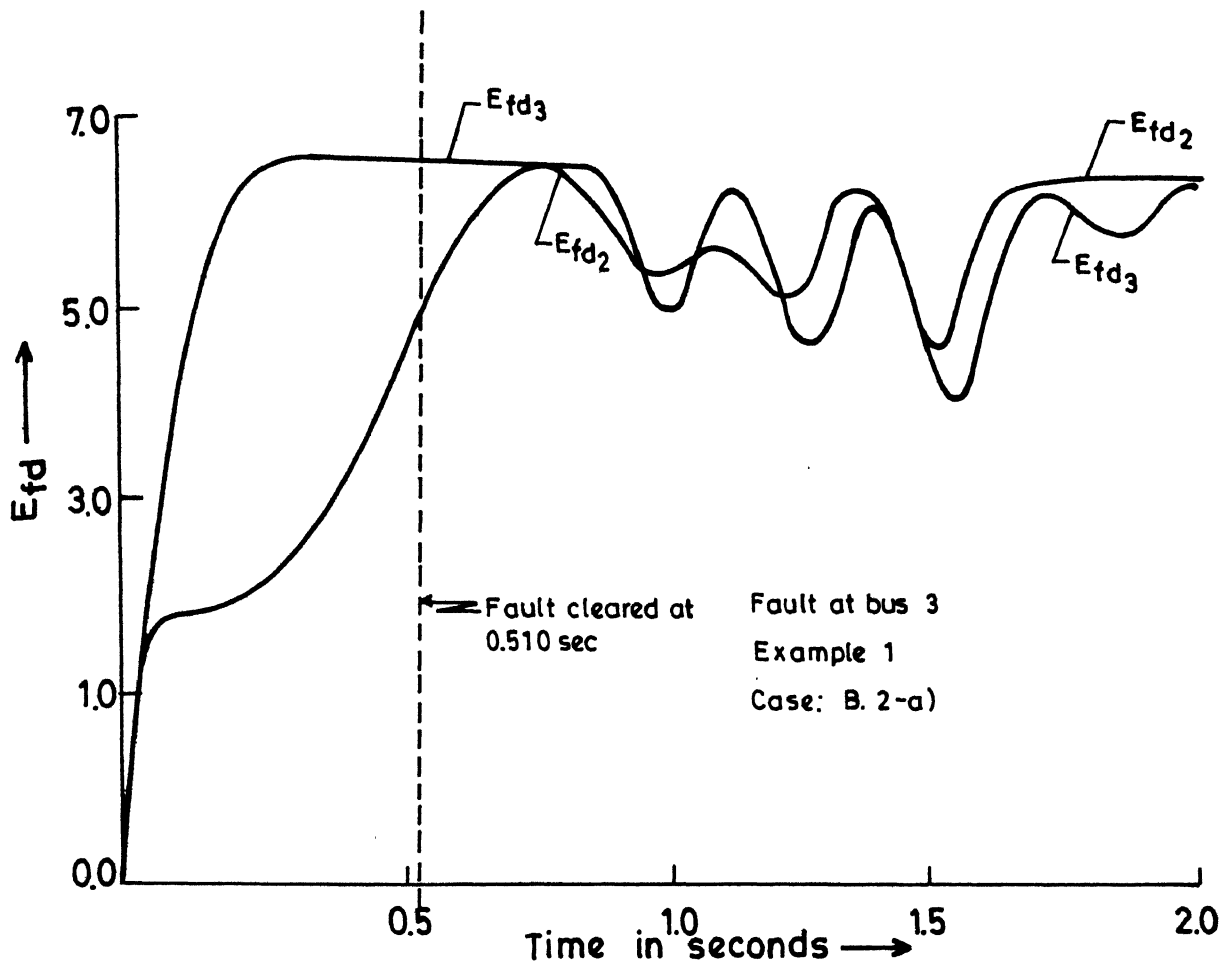


FIG.6.5 VARIATION OF  $E_{fd}$  FOR 4-MACHINE SYSTEM,

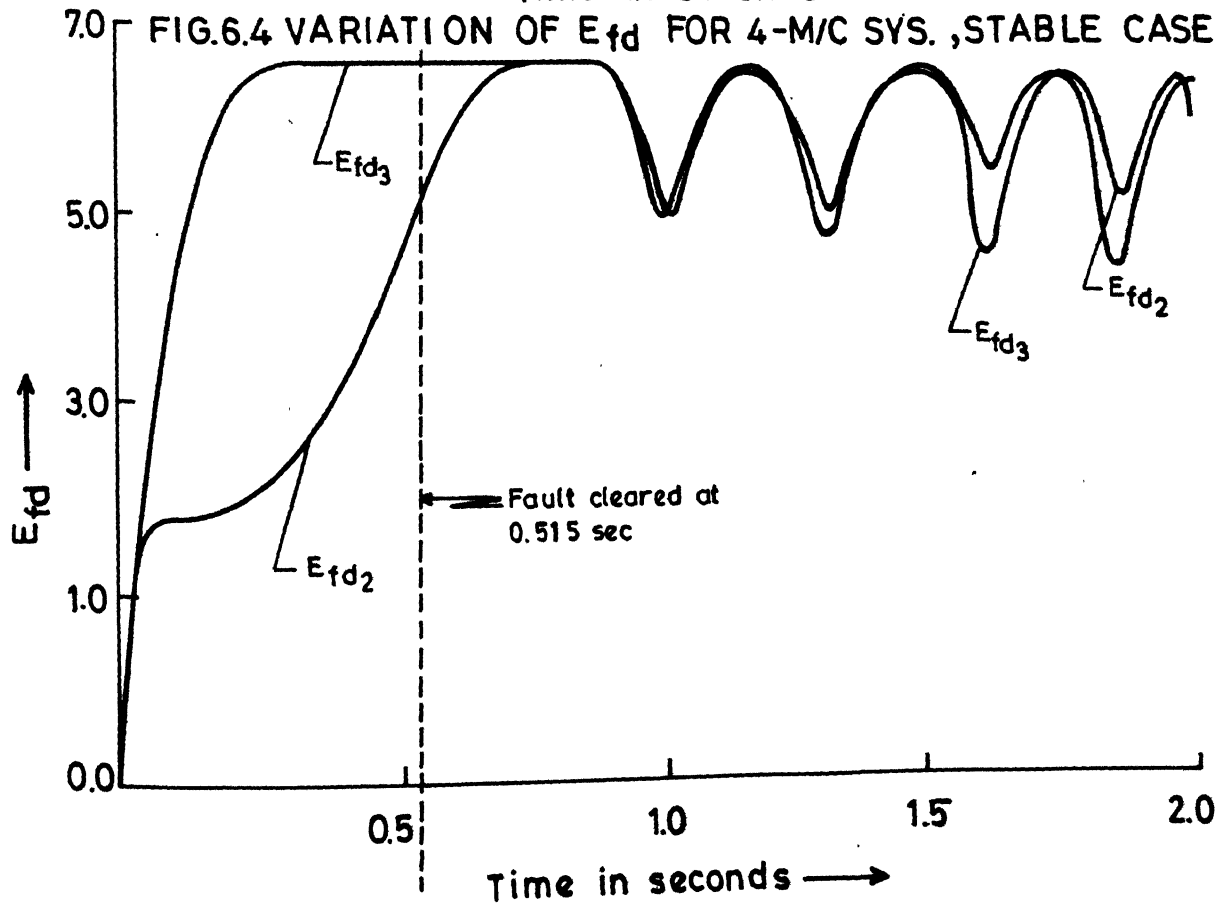
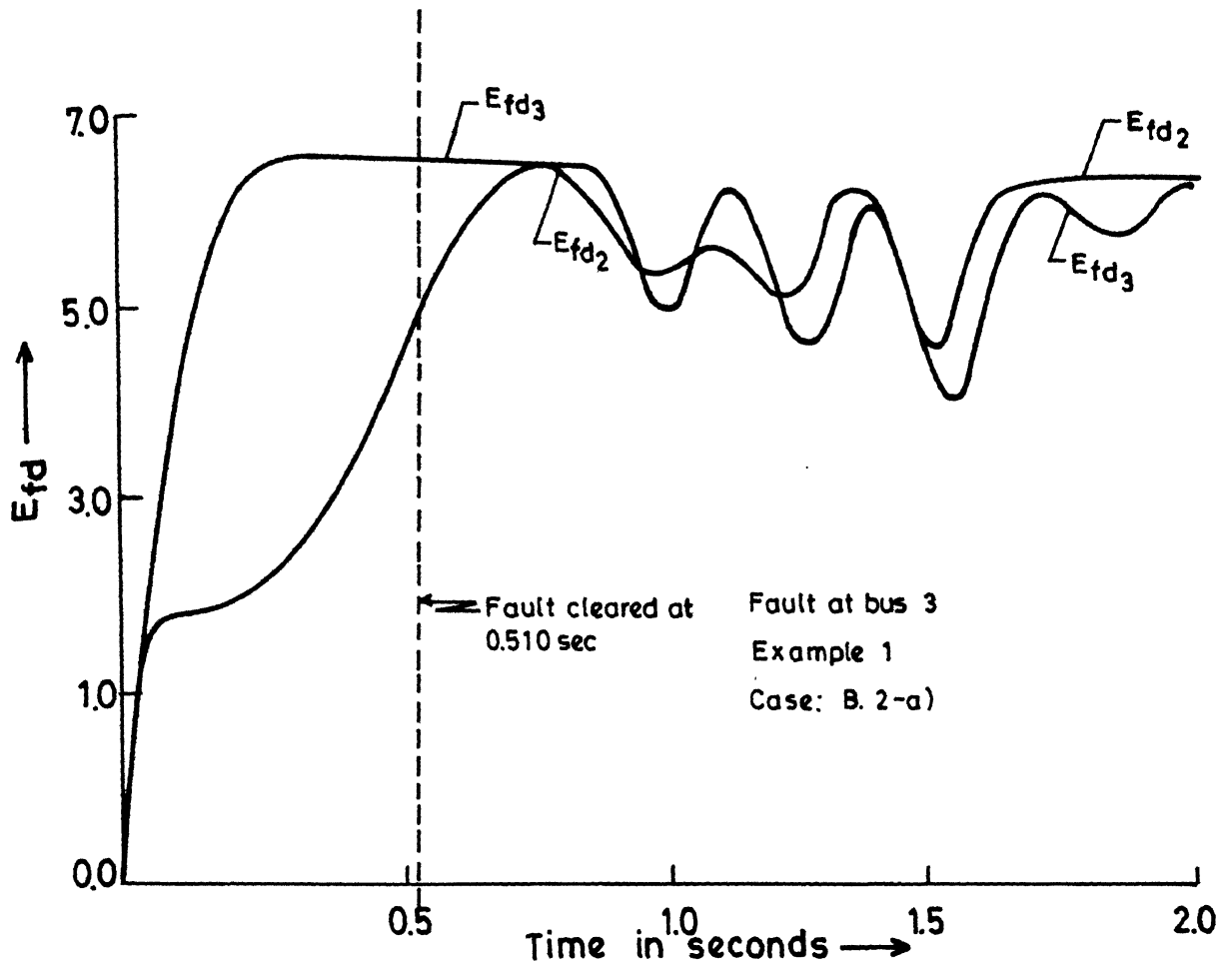


FIG.6.5 VARIATION OF  $E_{fd}$  FOR 4-MACHINE SYSTEM,

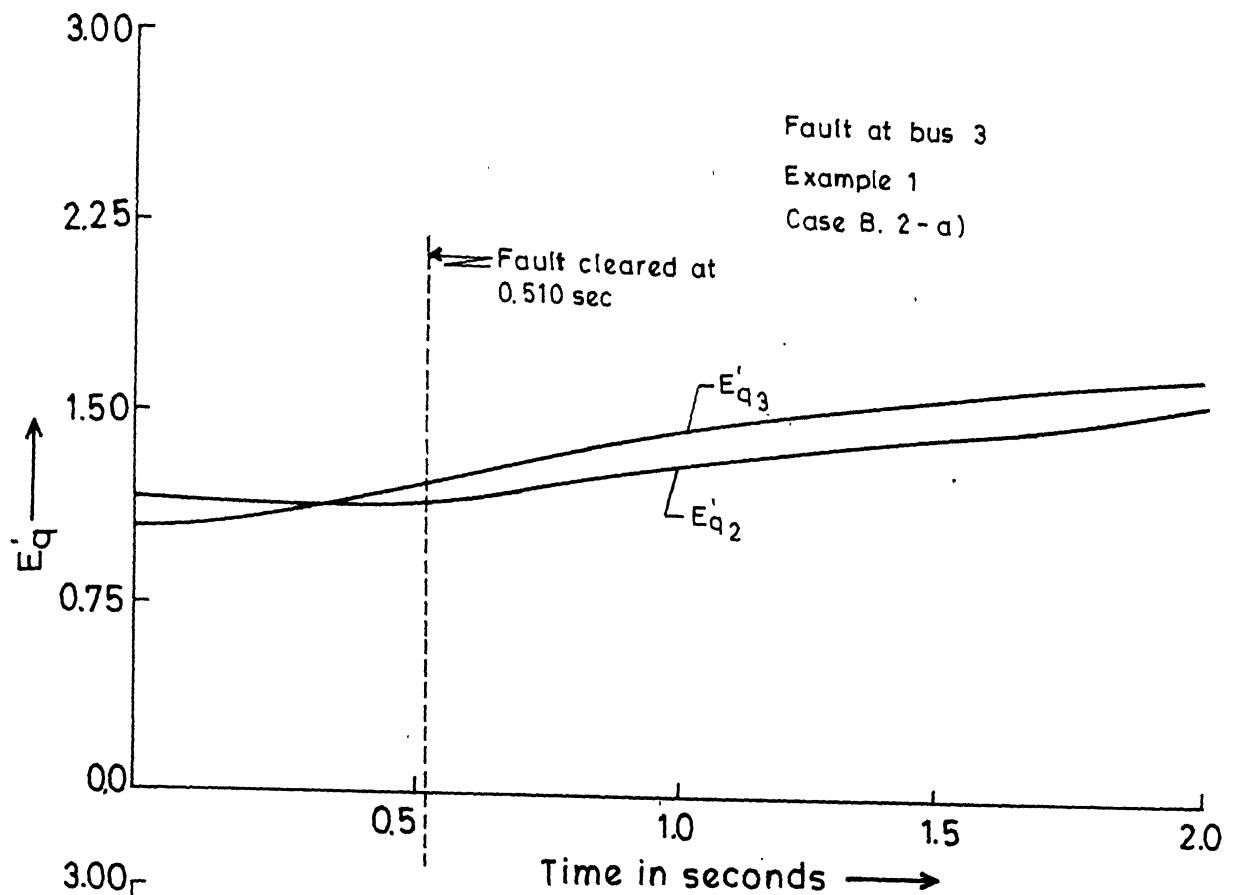


FIG. 6.6 VARIATION OF  $E'_q$  FOR 4-MACHINE SYSTEM, STABLE CASE

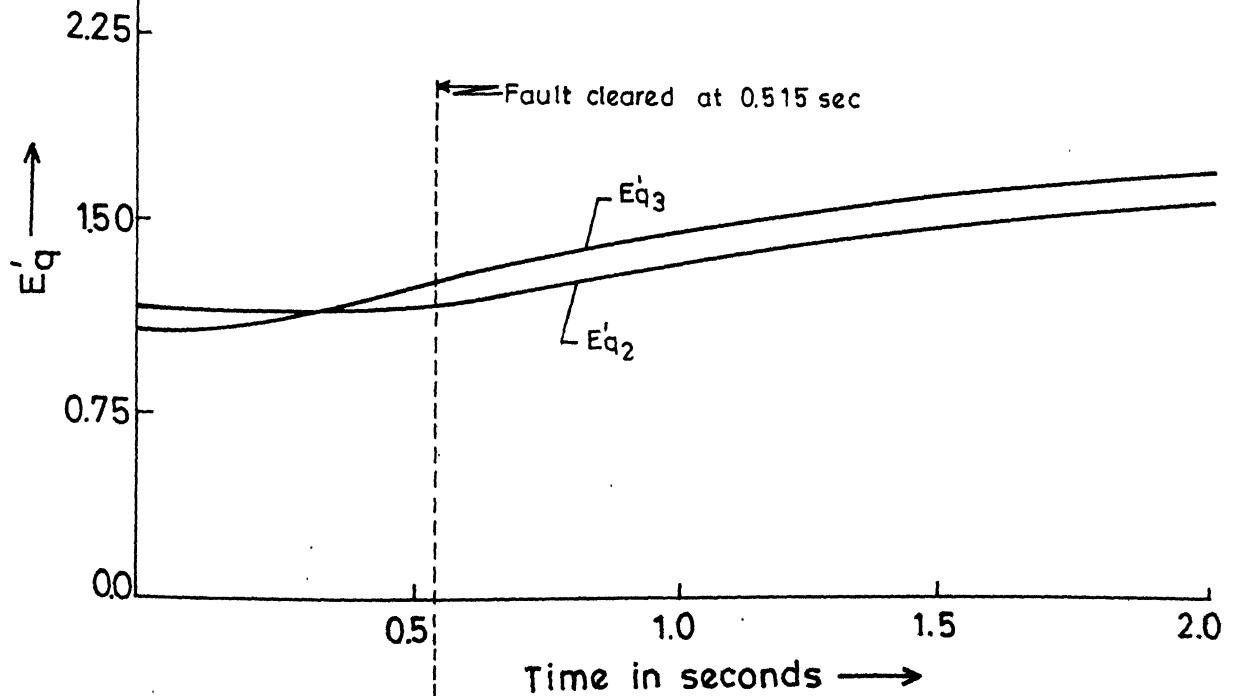


FIG. 6.7 VARIATION OF  $E'_q$  FOR 4-MACHINE SYSTEM, STABLE CASE

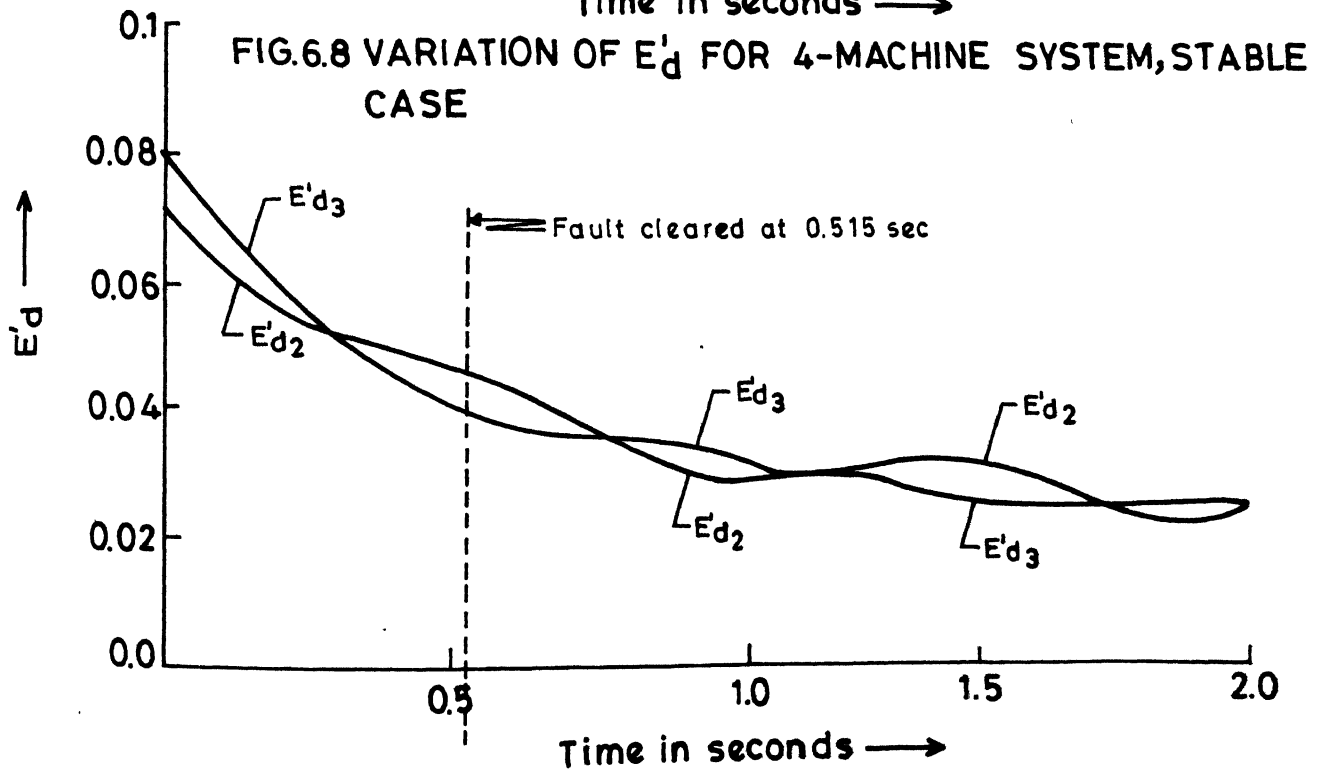
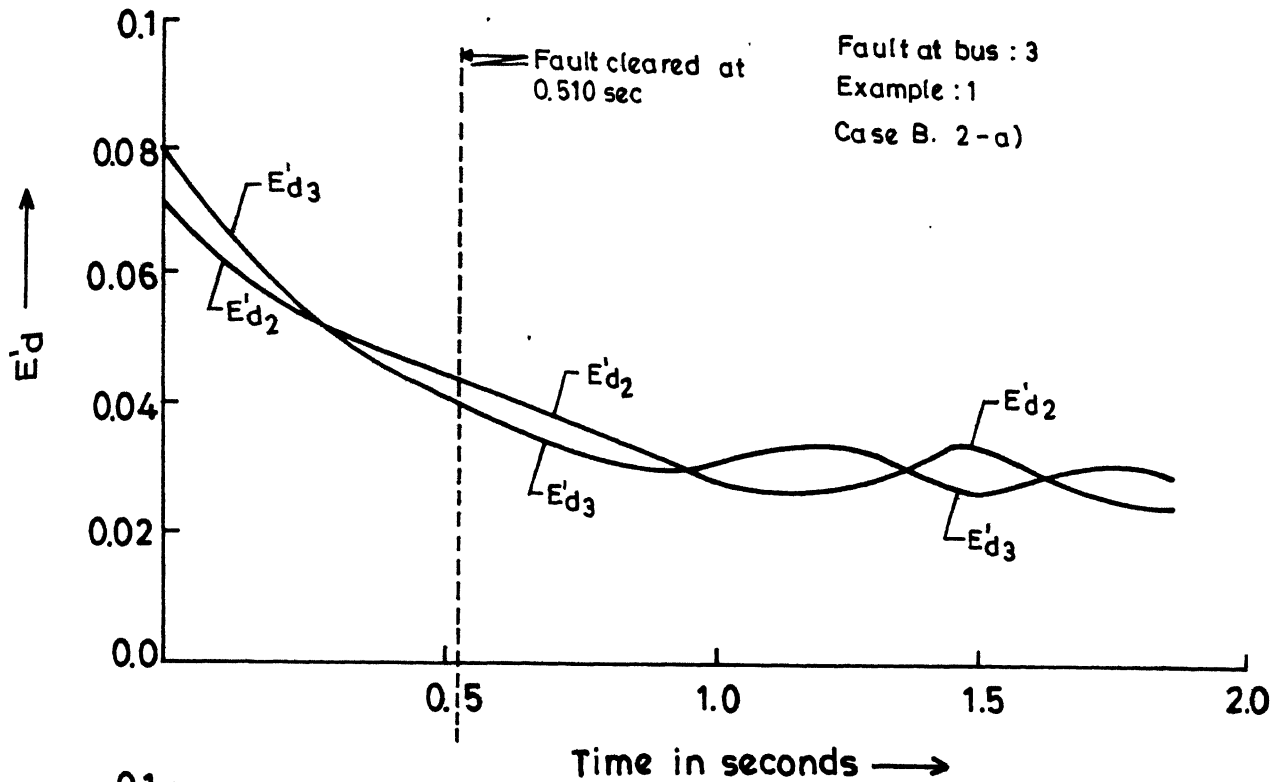


FIG.6.9 VARIATION OF  $E'd$  FOR 4-MACHINE SYSTEM, UNSTABLE CASE

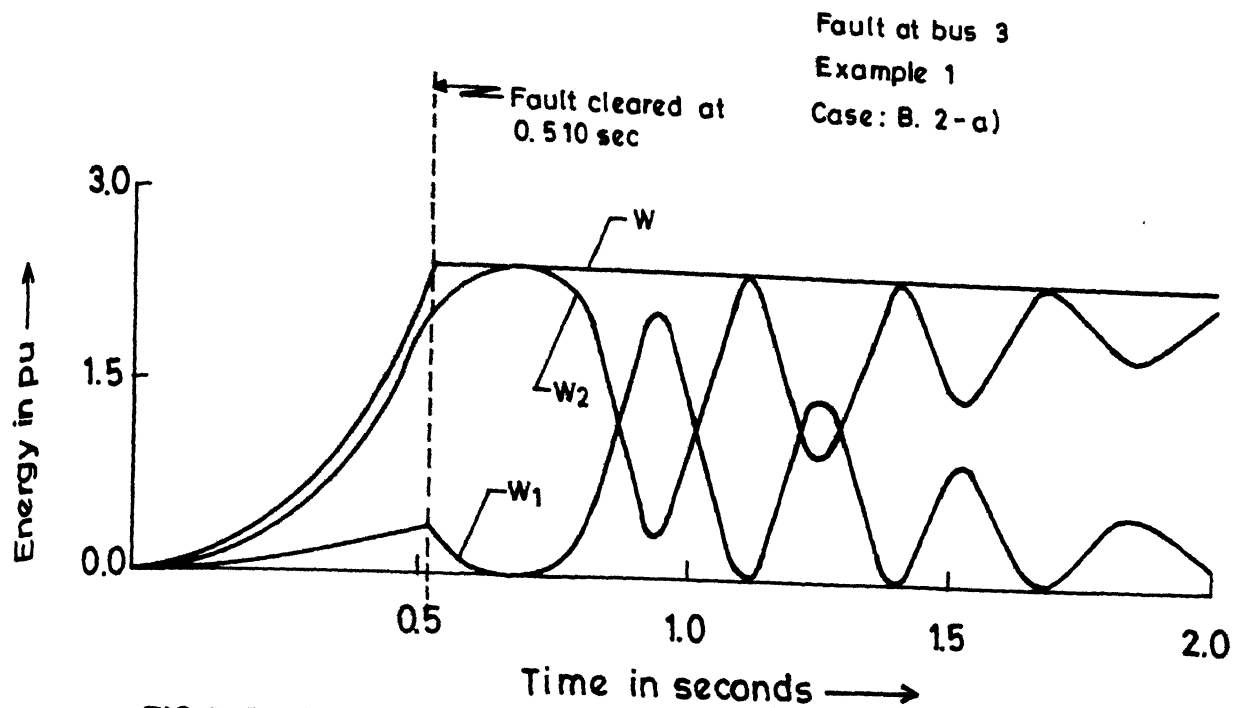


FIG.6.10 VARIATION OF TOTAL ENERGY AND ITS COMPONENTS  
FOR 4-MACHINE SYSTEM, STABLE CASE

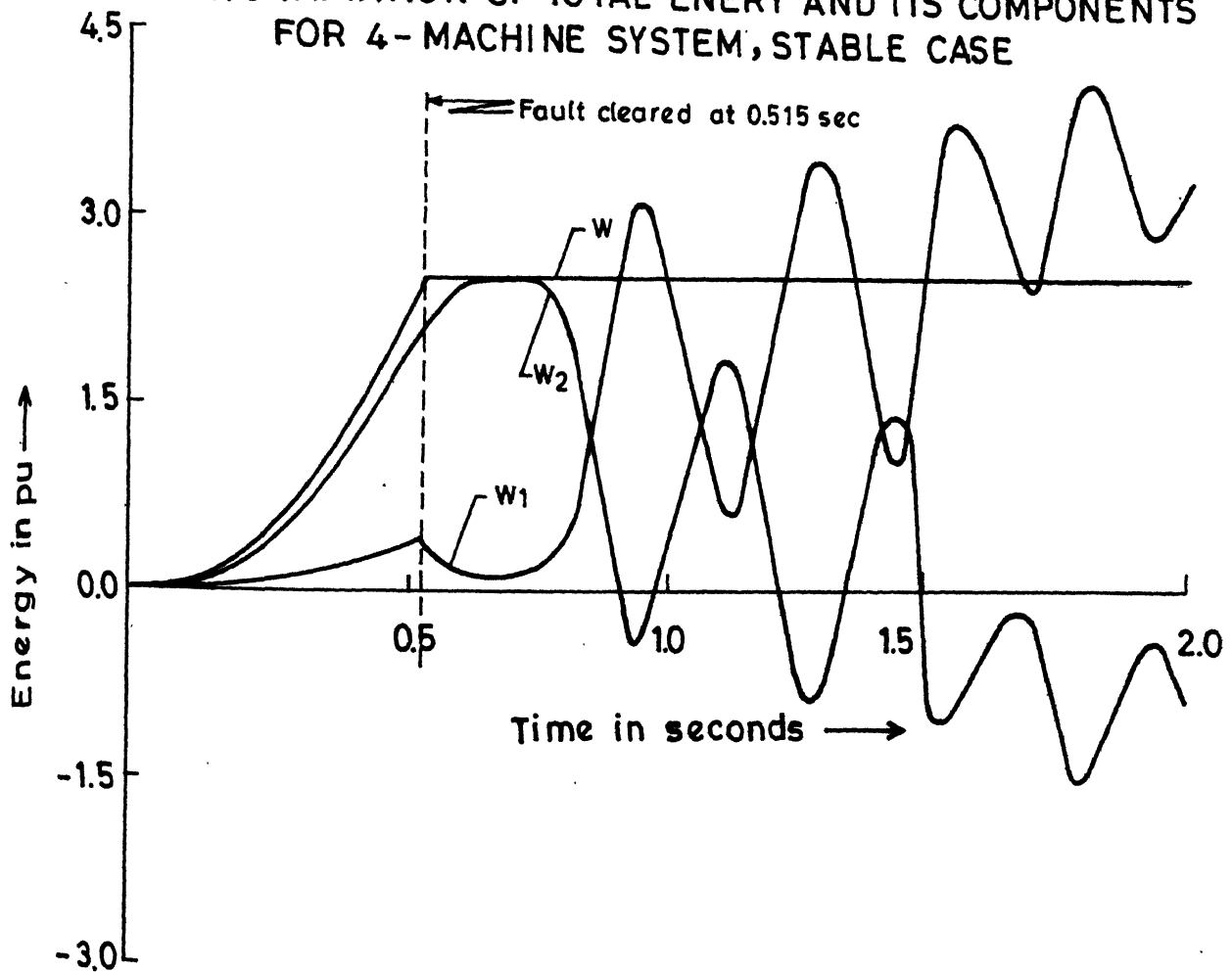


FIG. 6.11 VARIATION OF TOTAL ENERGY AND ITS COMPONENTS  
FOR 4-MACHINE SYSTEM, UNSTABLE CASE

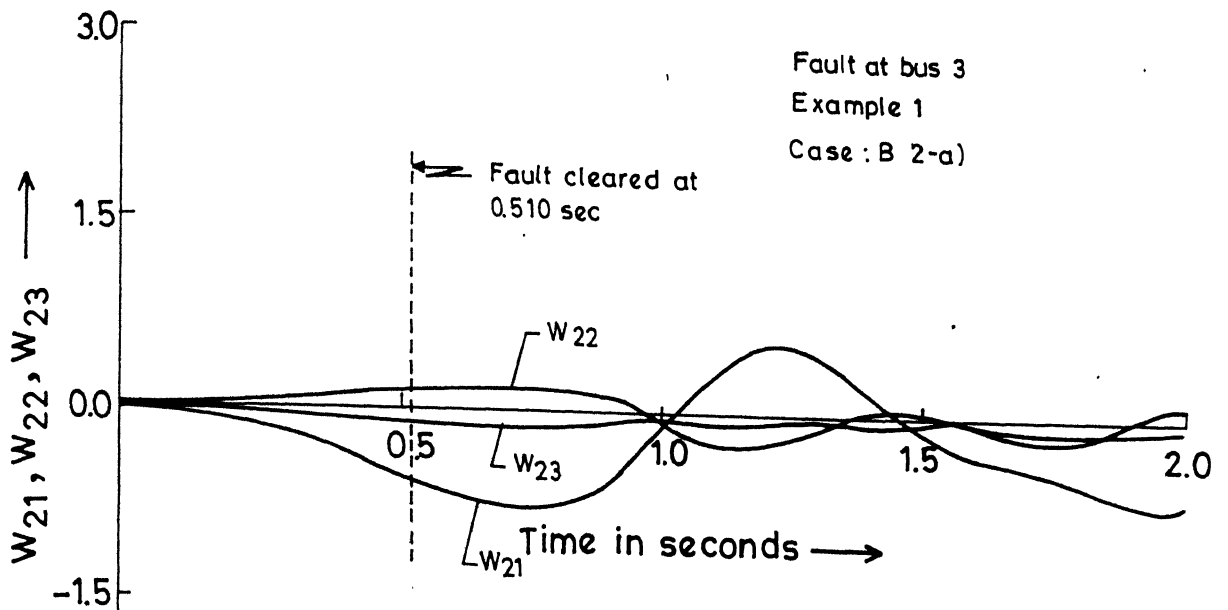


FIG.6.12 VARIATION OF SOME COMPONENTS OF  $W_2$  FOR 4 - MACHINE SYSTEM, STABLE CASE

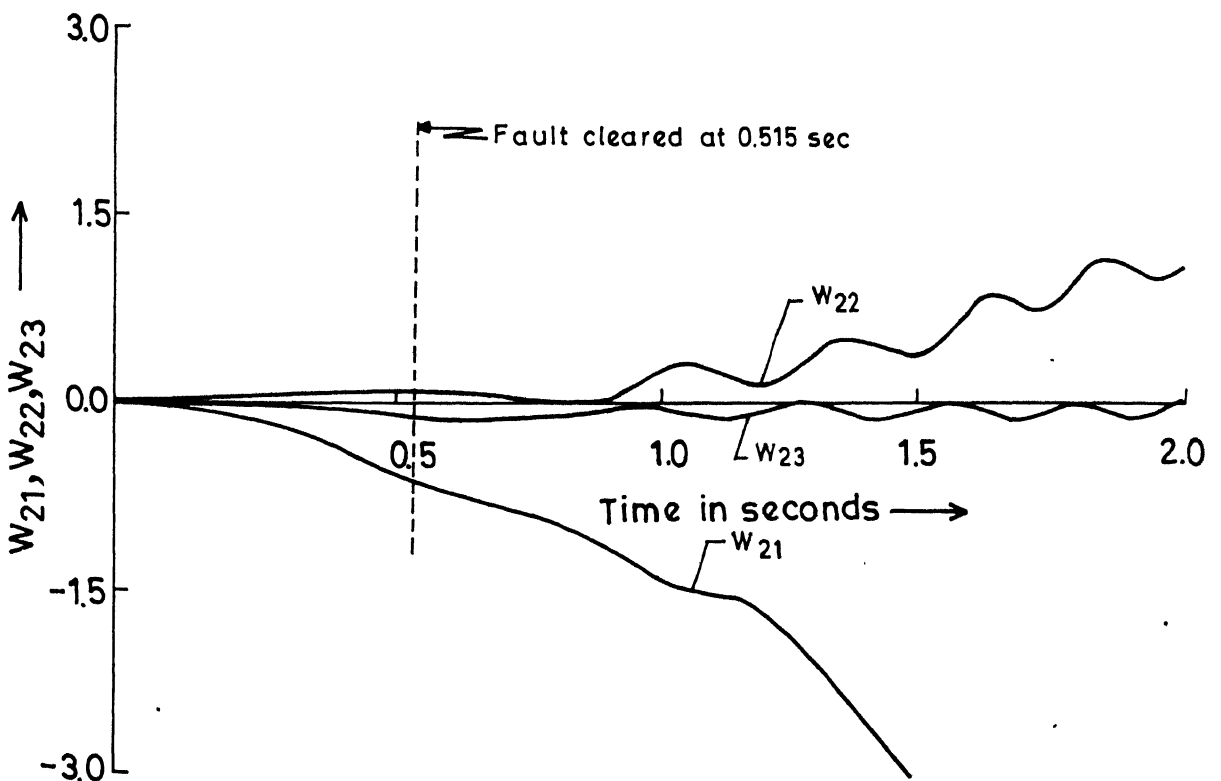


FIG.6.13 VARIATION OF SOME COMPONENTS OF  $W_2$  FOR 4 - MACHINE SYSTEM, UNSTABLE CASE

Example 1  
Case: B. 2-a)

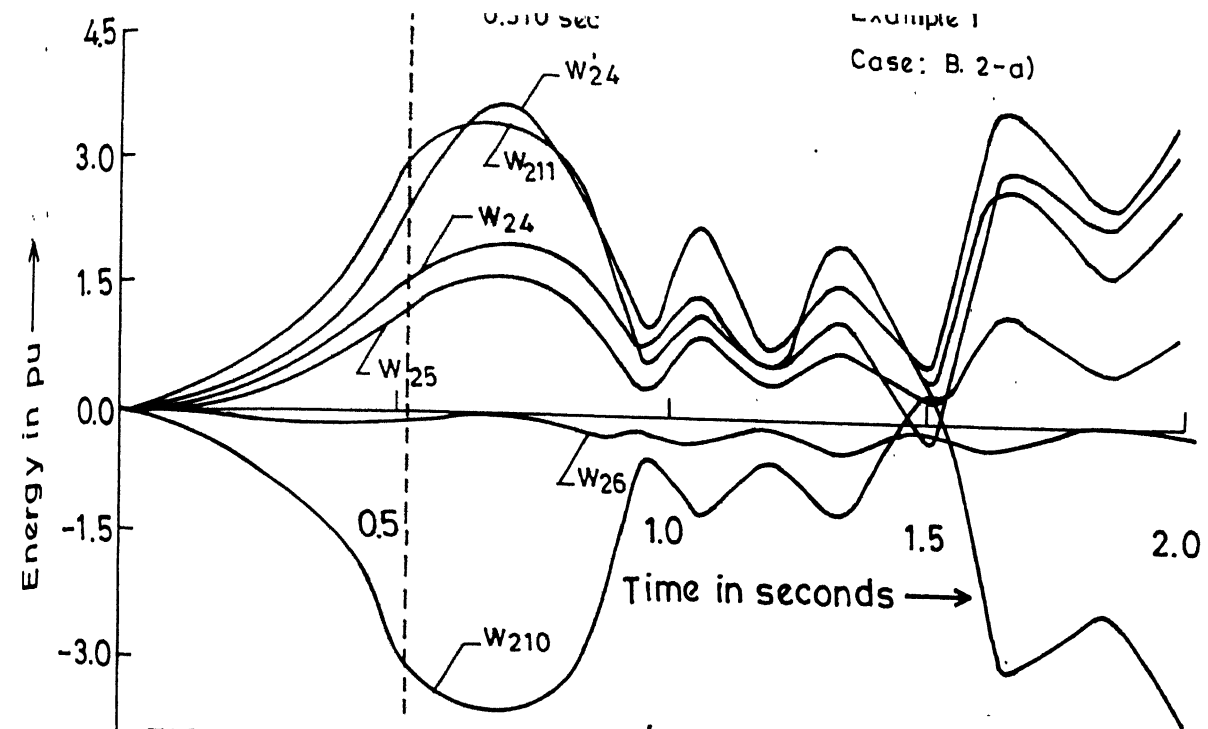


FIG. 6.14 VARIATION OF  $W'_{24}$  AND ITS COMPONENTS FOR 4-MACHINE SYSTEM, STABLE CASE

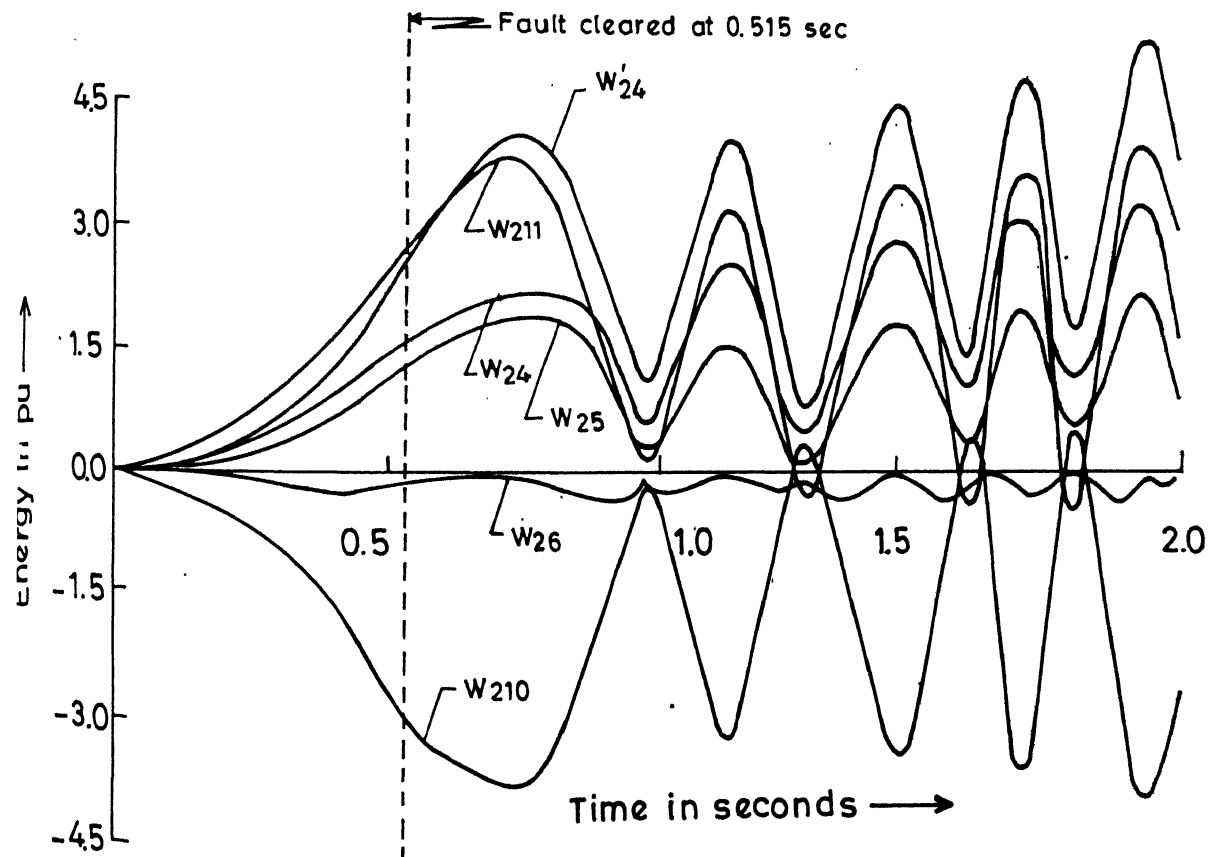


FIG. 6.15 VARIATION OF  $W'_{24}$  AND ITS COMPONENTS FOR 4-MACHINE SYSTEM, UNSTABLE CASE

Fault at bus 3  
Example: i)  
Case : B. 2-a)

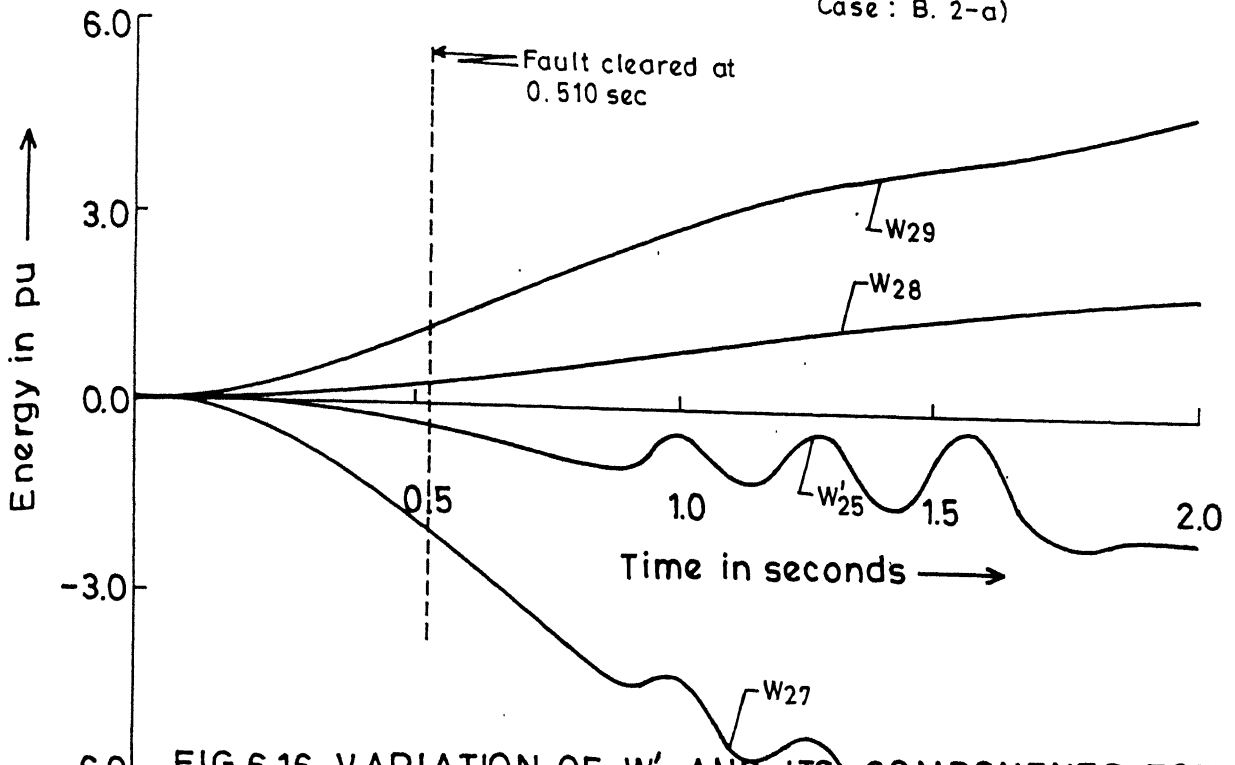


FIG.6.16 VARIATION OF  $W'_{25}$  AND ITS COMPONENTS FOR 4-MACHINE SYSTEM, STABLE CASE

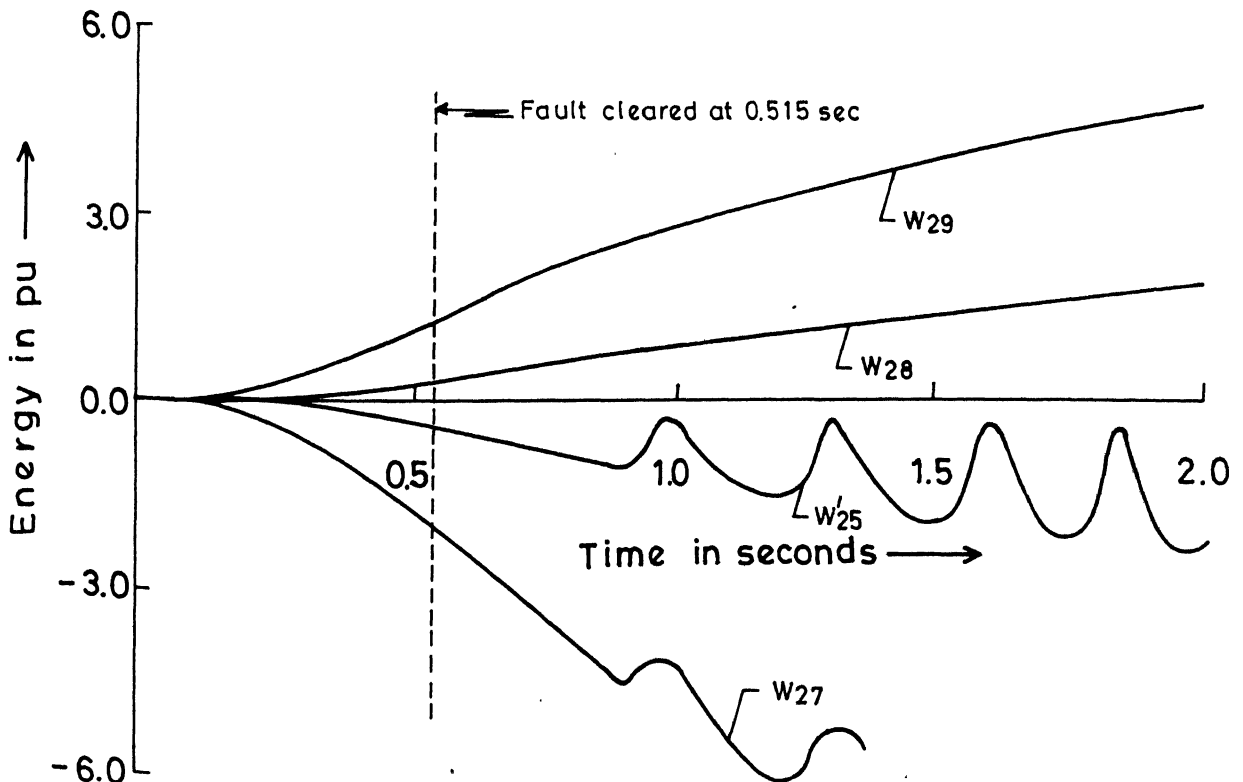


FIG.6.17 VARIATION OF  $W'_{25}$  AND ITS COMPONENTS FOR 4-MACHINE SYSTEM, UNSTABLE CASE

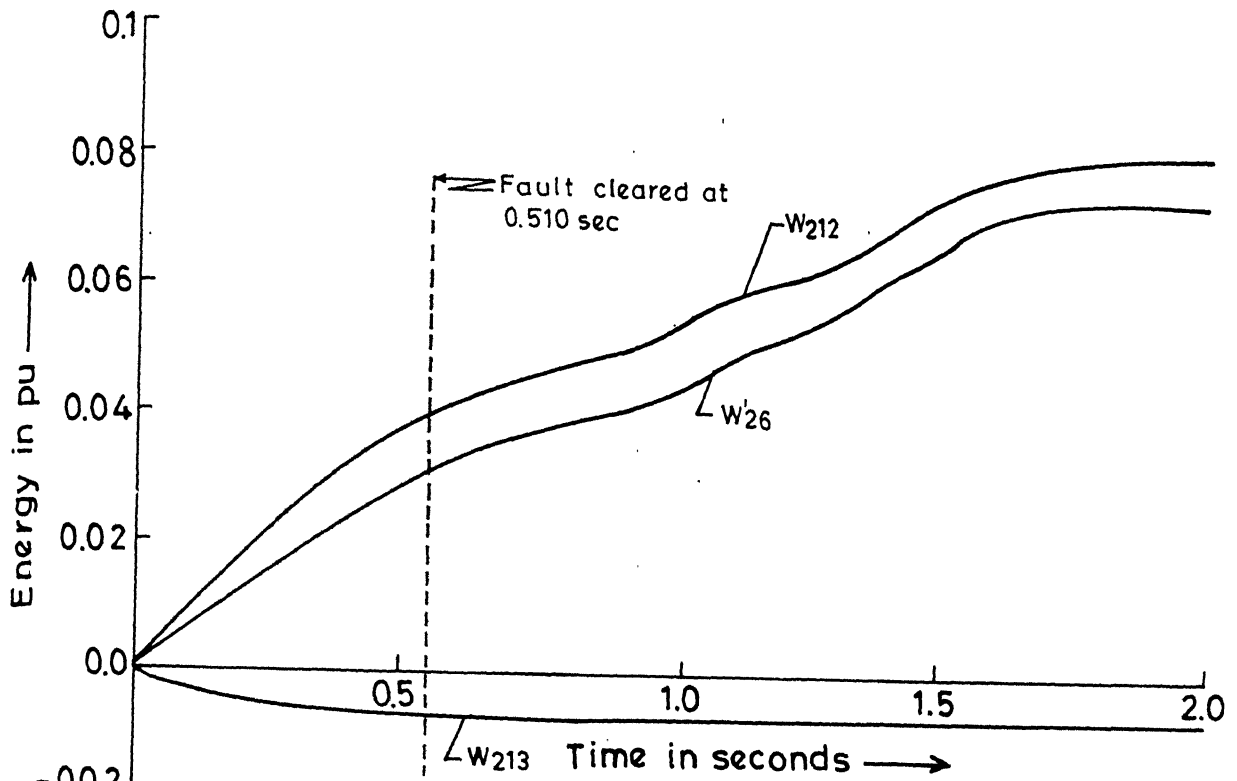


FIG. 6.18 VARIATION OF  $W'_{26}$  AND ITS COMPONENTS FOR 4-MACHINE SYSTEM, STABLE CASE

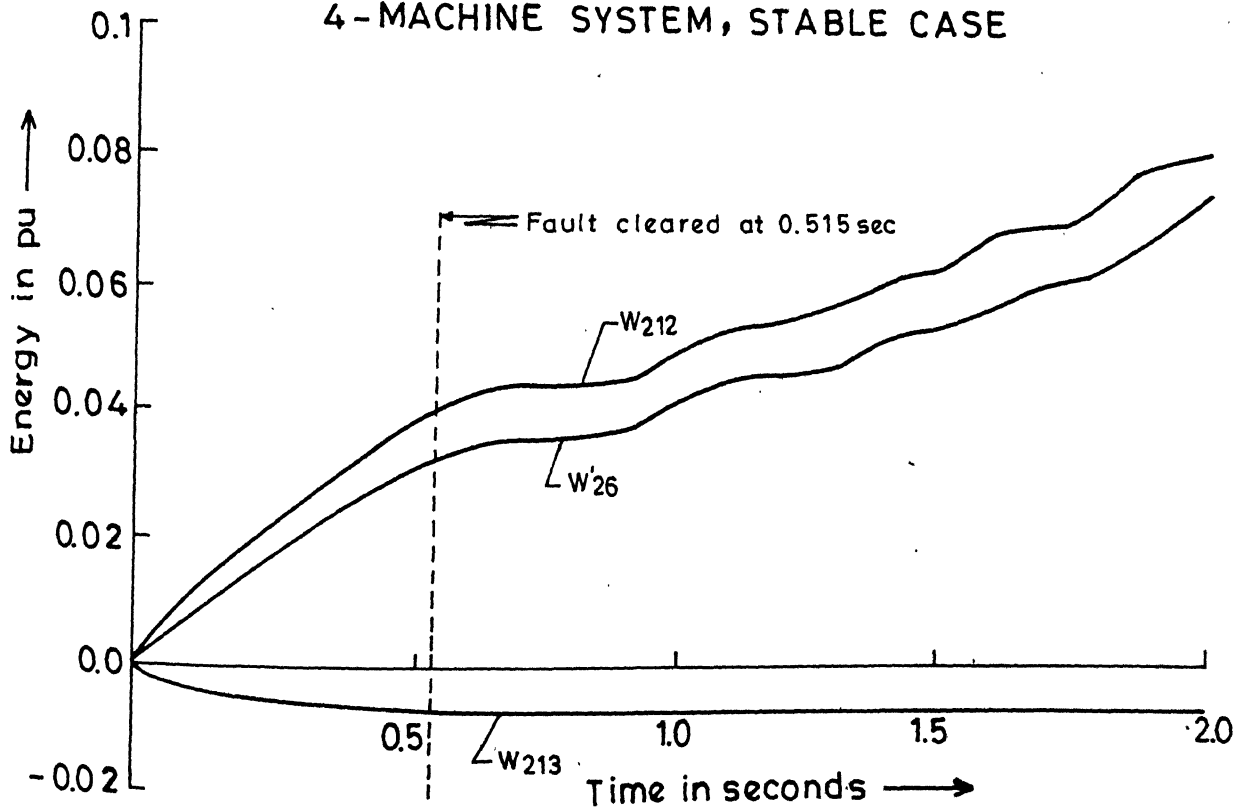


FIG. 6.19 VARIATION OF  $W'_{26}$  AND ITS COMPONENTS FOR 4-MACHINE SYSTEM, UNSTABLE CASE

The variations in the rotor angles,  $E_{fd}$ ,  $E'_q$ ,  $E'_d$ , energy and its various components for one case for fault at bus 3 in the 10-machine system [B.2-a)] are shown in Figs. 6.20-6.37. Both stable and unstable cases are included here.

In the case of the larger 10-machine system, when the system is unstable, there appear to be 3 distinct groups of generators that separate from each other (machine 2, machine 3 and the remaining machines). In comparison with Fig. 3.11 (Chapter 3), it appears that the provision of AVR on machine 1 results in reducing the magnitude of oscillation within the coherent group. Even though it is not evident from the swing curves, the rotor oscillations tend to increase in magnitude for the critically cleared fault, which is reflected in the variation of  $W_1$  or  $W_2$  (see Fig. 6.28). This problem could be due to dynamic instability and is normally cured by providing power system stabilisers which modulate the reference value (set point) of the AVRs. It is interesting to observe that this problem is not encountered in the case of 4-machine system.

The action of AVRs is field forcing during the fault and immediately after the fault is cleared. This results in increase of  $E'_q$ . However, the AVR has little effect on  $E'_d$  which tends to reduce from its initial value. But this has little effect on the stability.

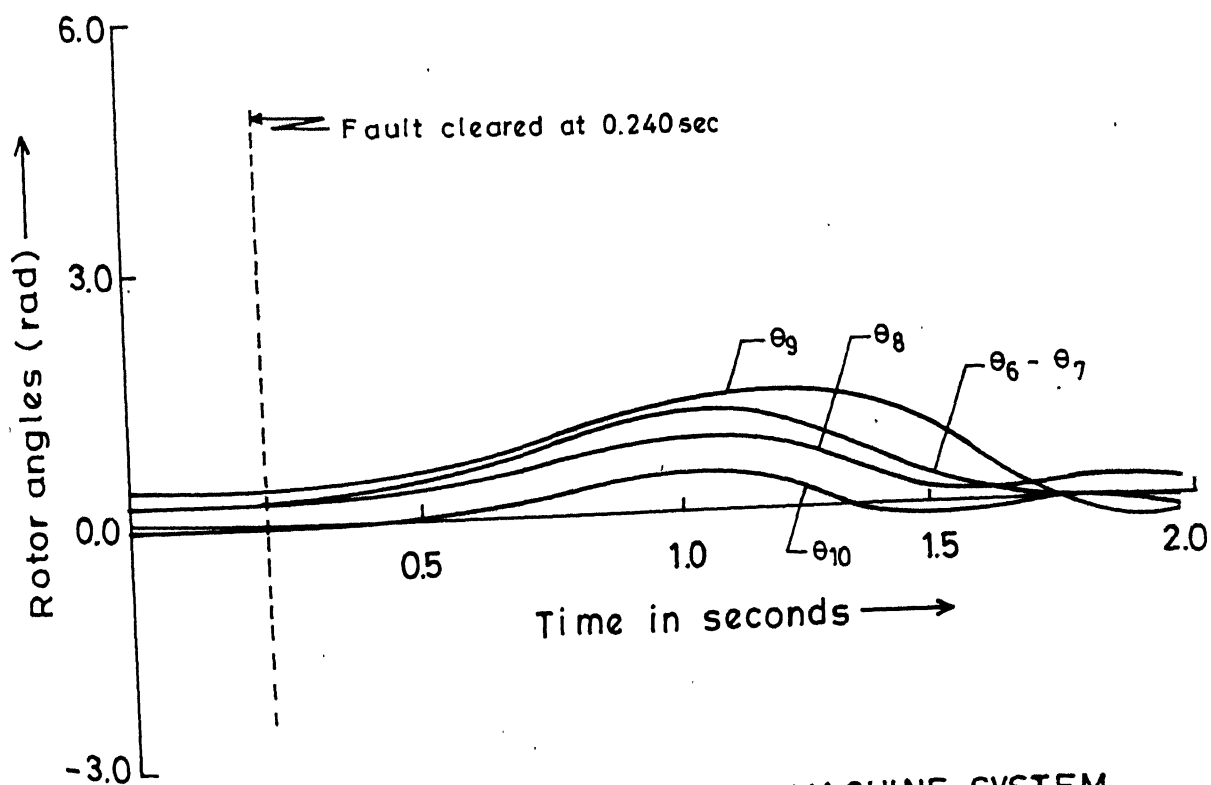
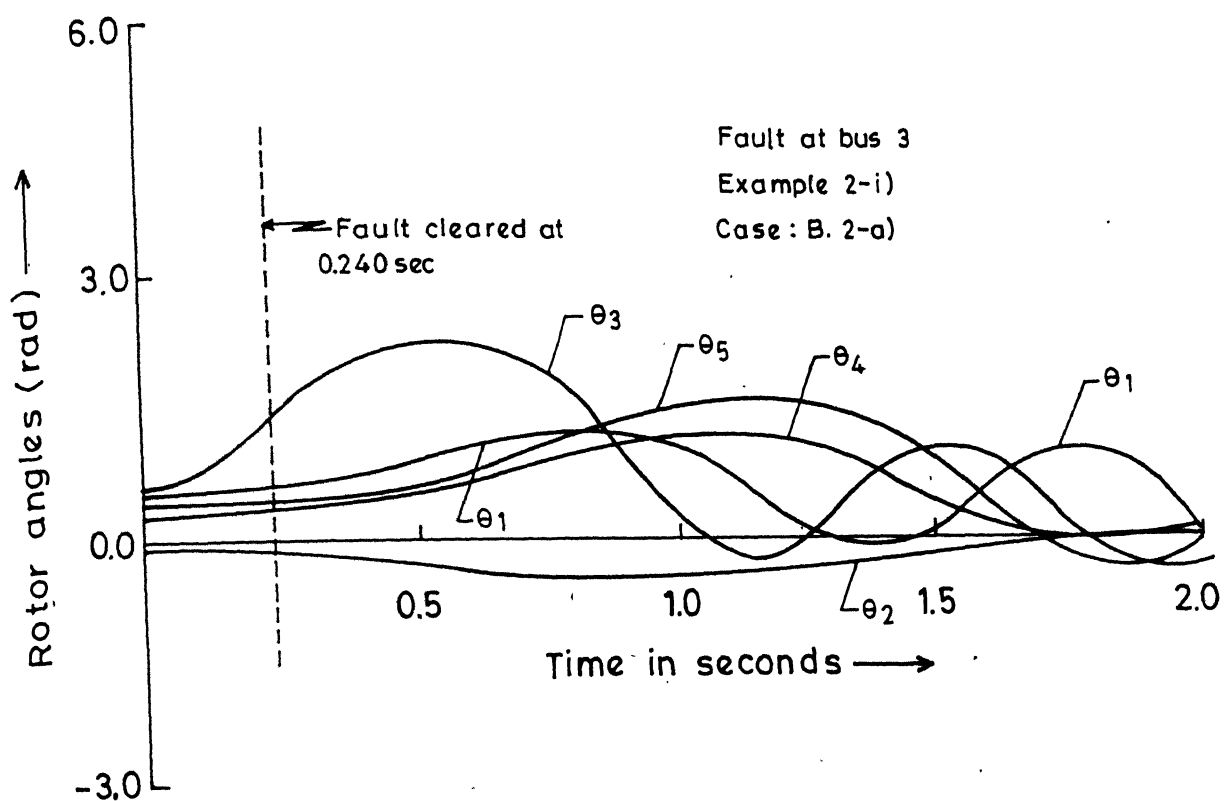


FIG. 6.20 SWING CURVES FOR 10-MACHINE SYSTEM,  
 STABLE CASE

Fault at bus 3

Example 2-i)

Case: B 2-a)

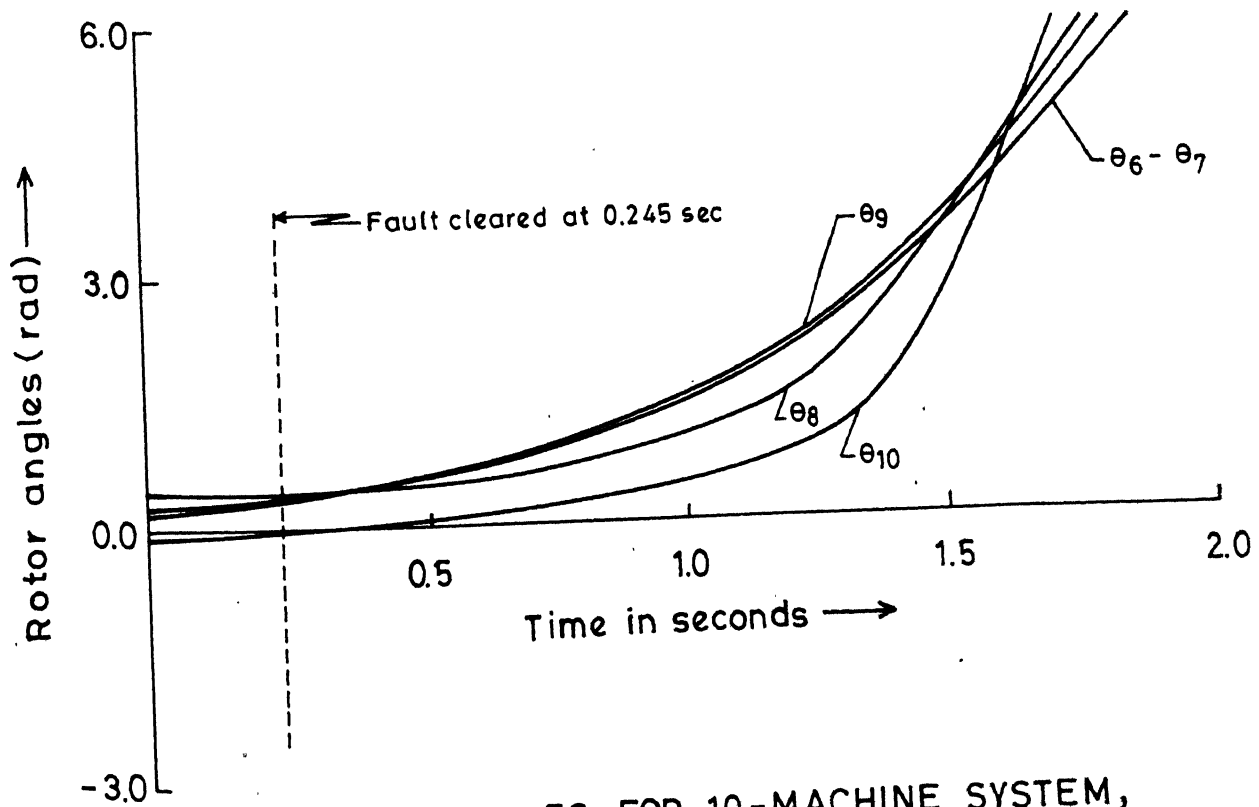
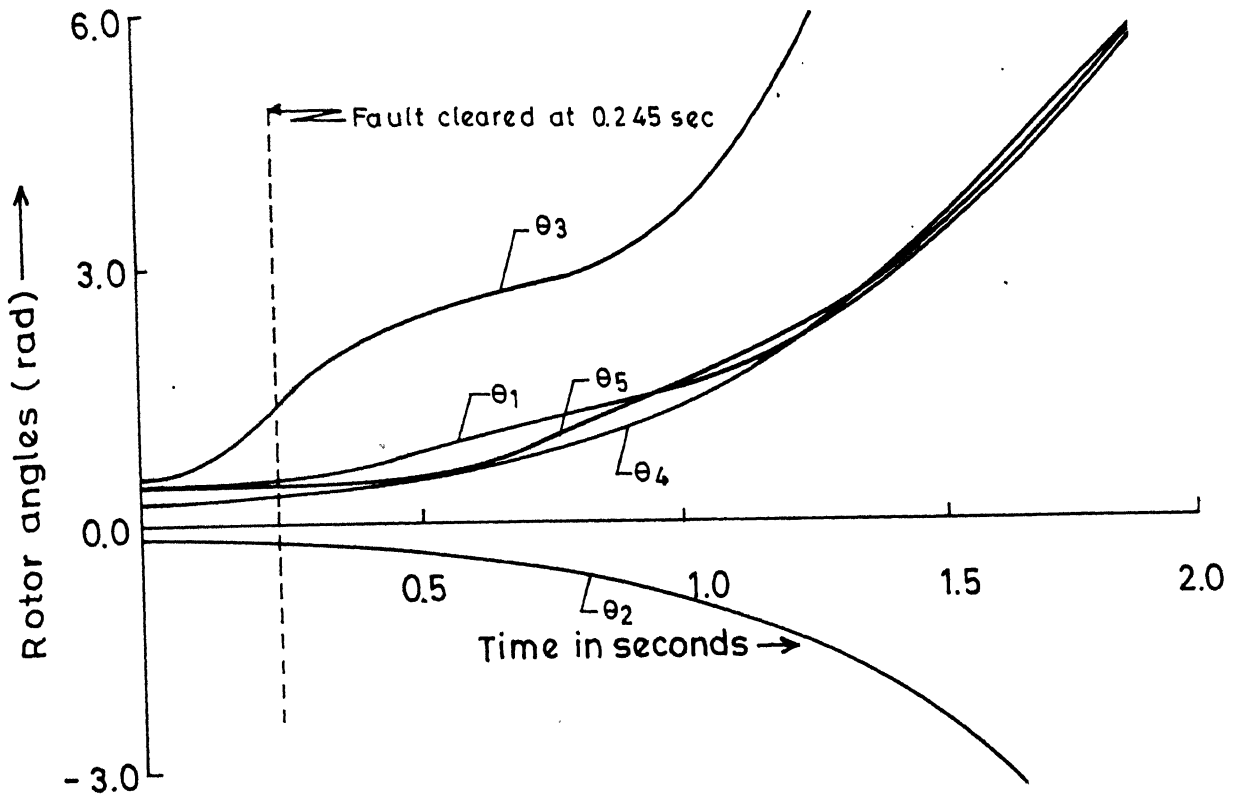


FIG. 6.21 SWING CURVES FOR 10-MACHINE SYSTEM, UNSTABLE CASE

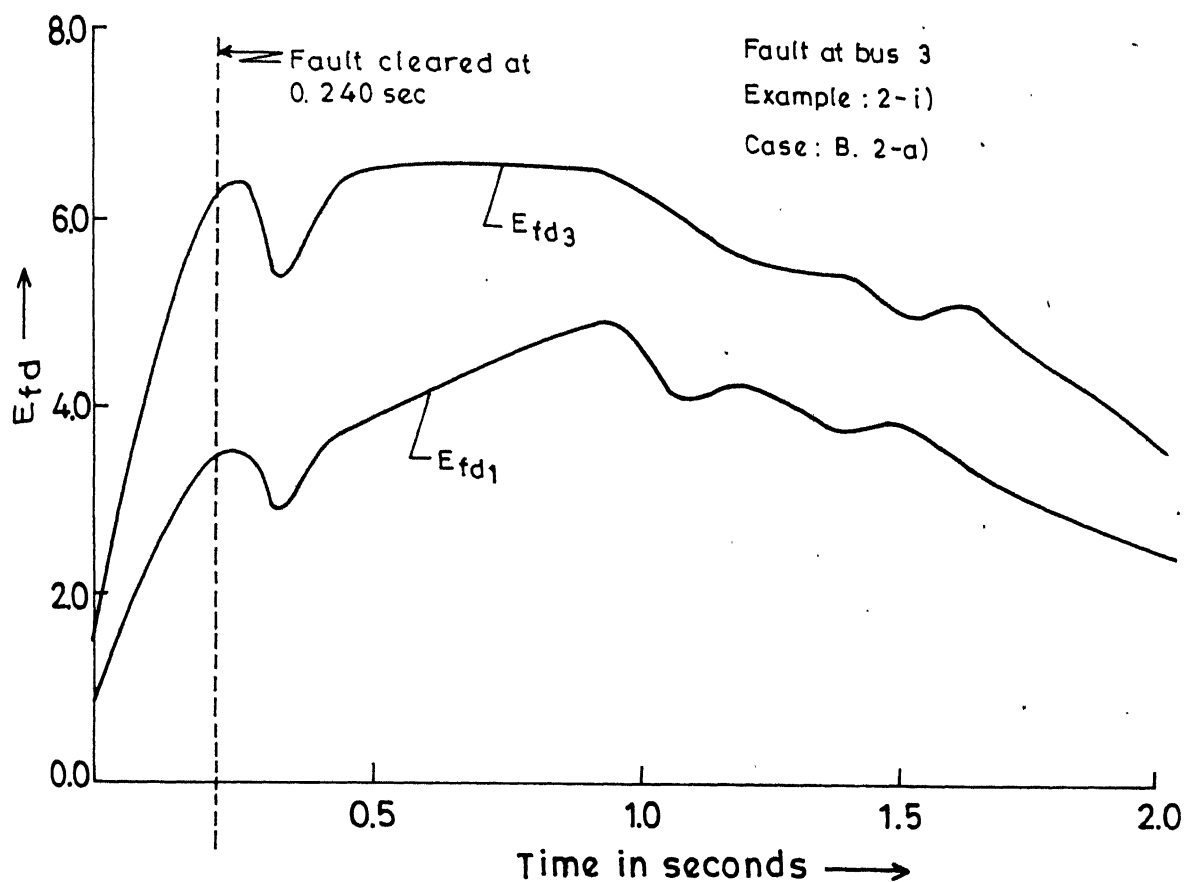


FIG.6.22 VARIATION OF  $E_{fd}$  FOR 10-MACHINE SYSTEM, STABLE CASE

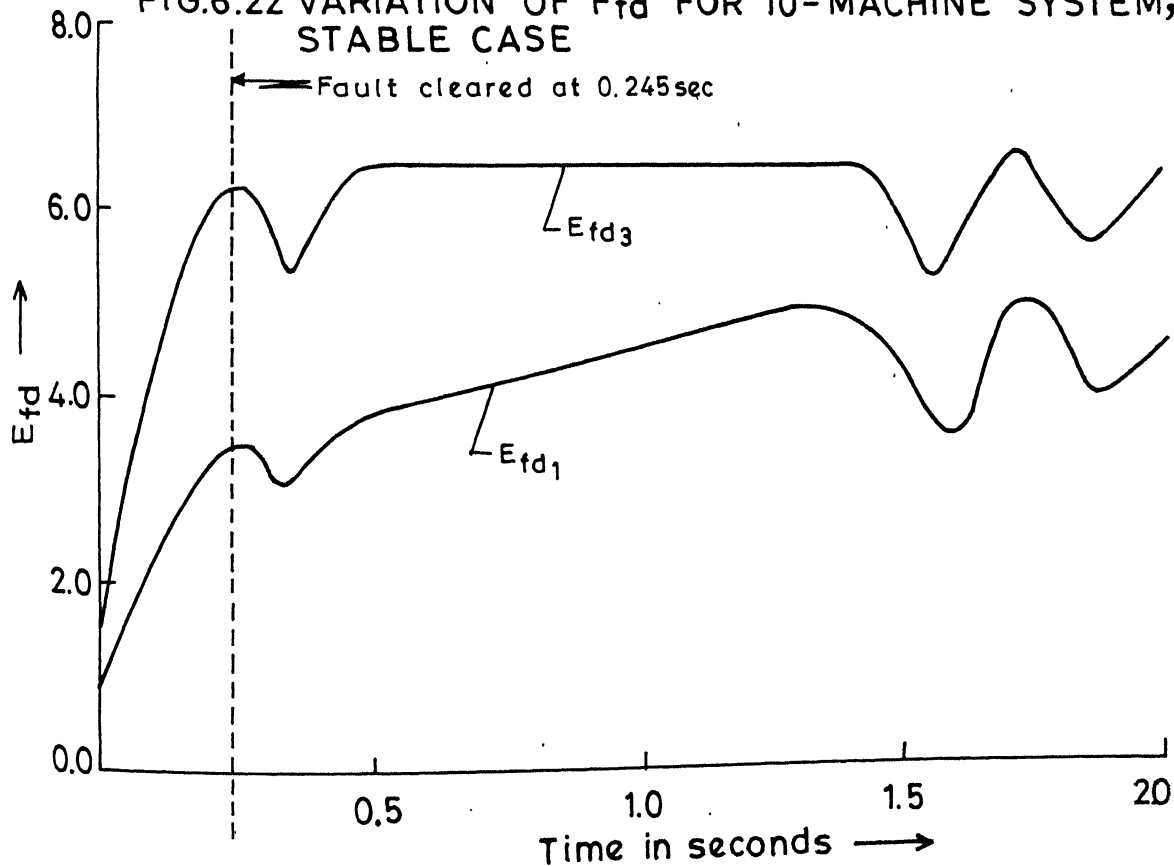


FIG.6.23 VARIATION OF  $E_{fd}$  FOR 10-MACHINE SYSTEM, UNSTABLE

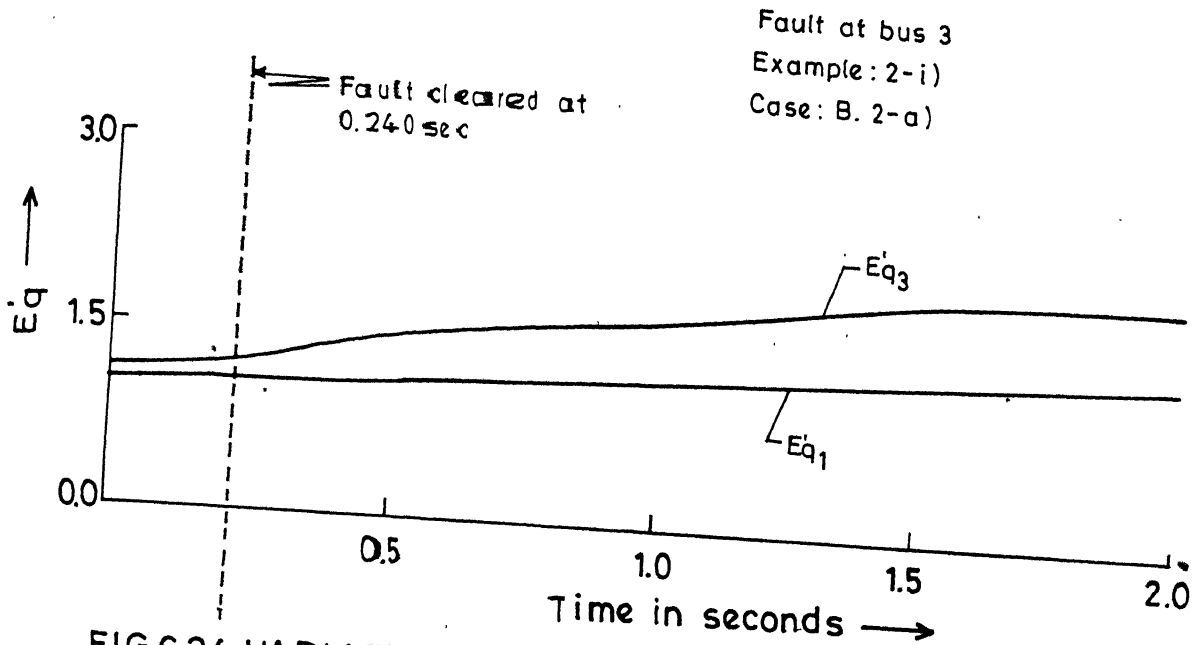


FIG.6.24 VARIATION OF  $E'q$  FOR 10-MACHINE SYSTEM, STABLE CASE

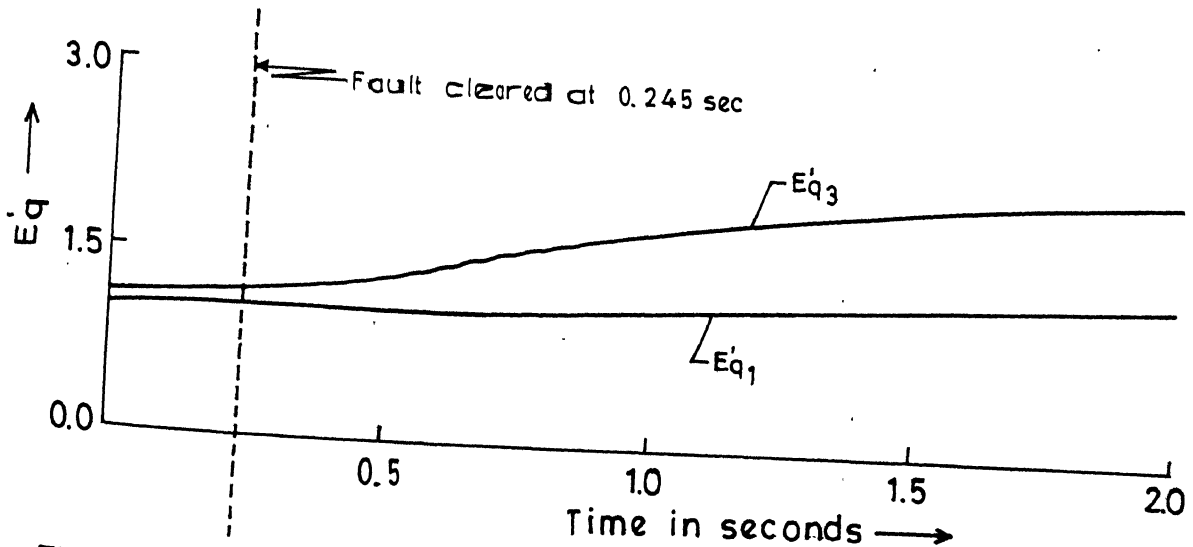


FIG.6.25 VARIATION OF  $E'q$  FOR 10-MACHINE SYSTEM, UNSTABLE CASE

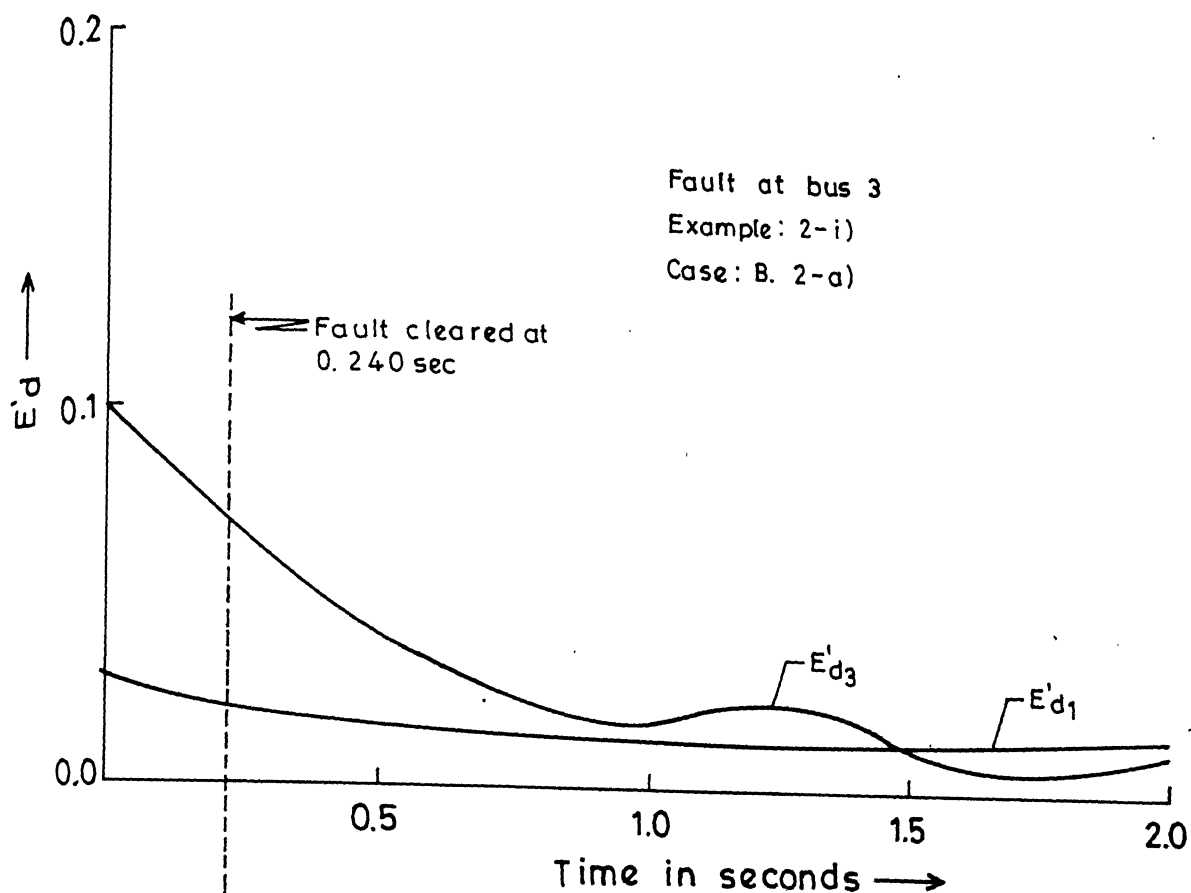


FIG. 6.26 VARIATION OF  $E'd$  FOR 10-MACHINE SYSTEM, STABLE CASE

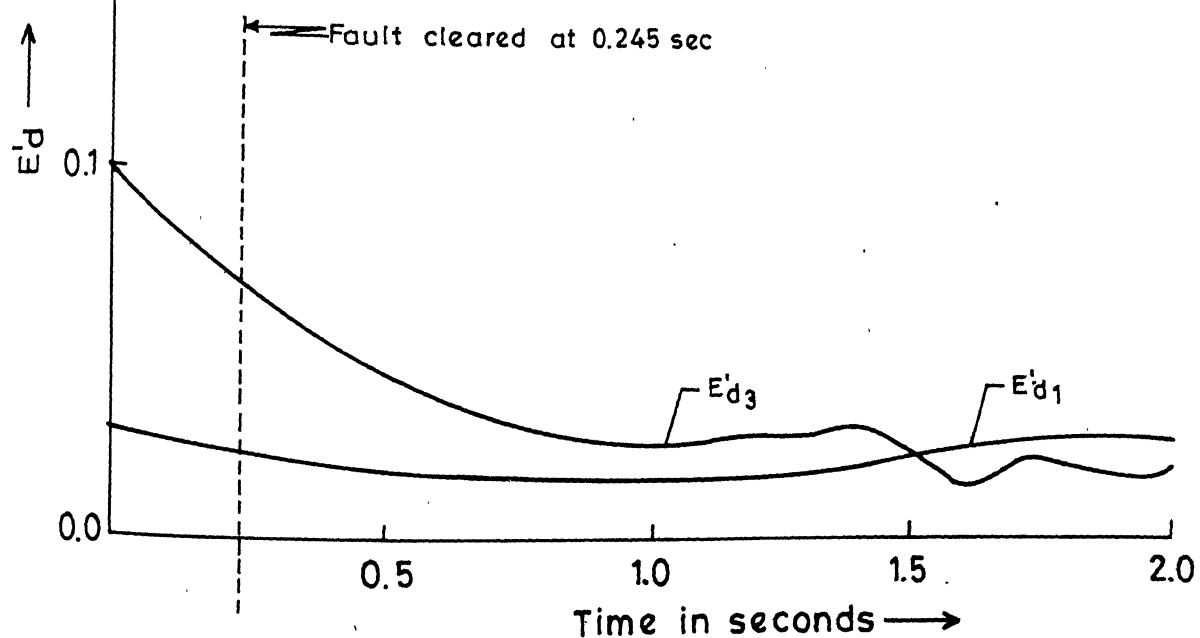


FIG. 6.27 VARIATION OF  $E'd$  FOR 10-MACHINE SYSTEM, UNSTABLE CASE

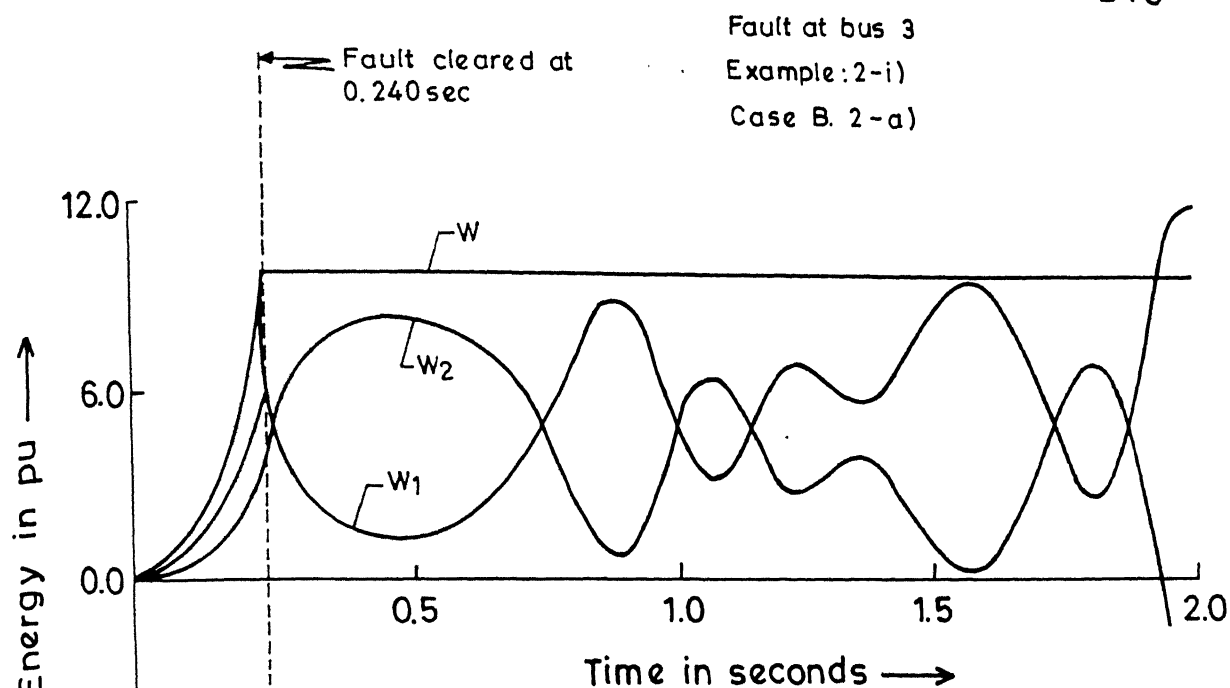


FIG.6.28 VARIATION OF TOTAL ENERGY AND ITS COMPONENTS FOR 10-MACHINE SYSTEM, STABLE CASE

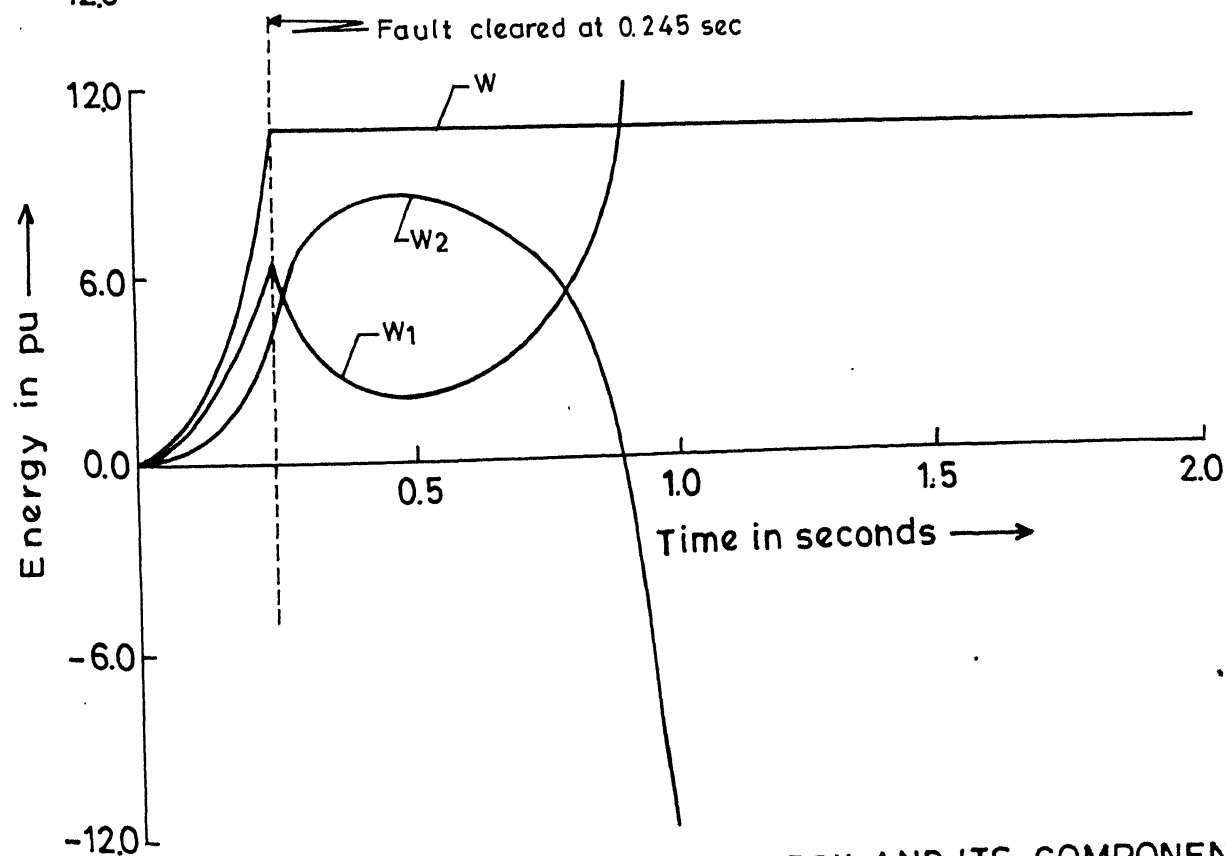


FIG.6.29 VARIATION OF TOTAL ENERGY AND ITS COMPONENTS FOR 10-MACHINE SYSTEM, UNSTABLE CASE

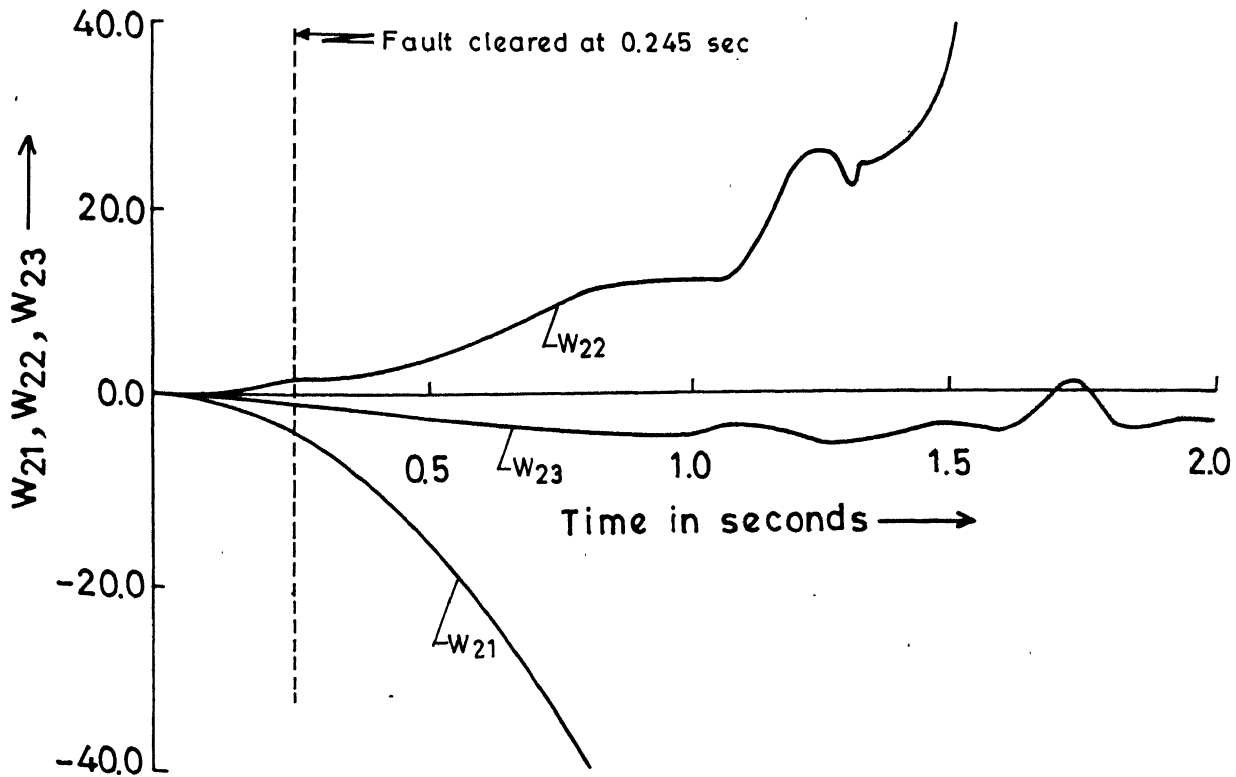
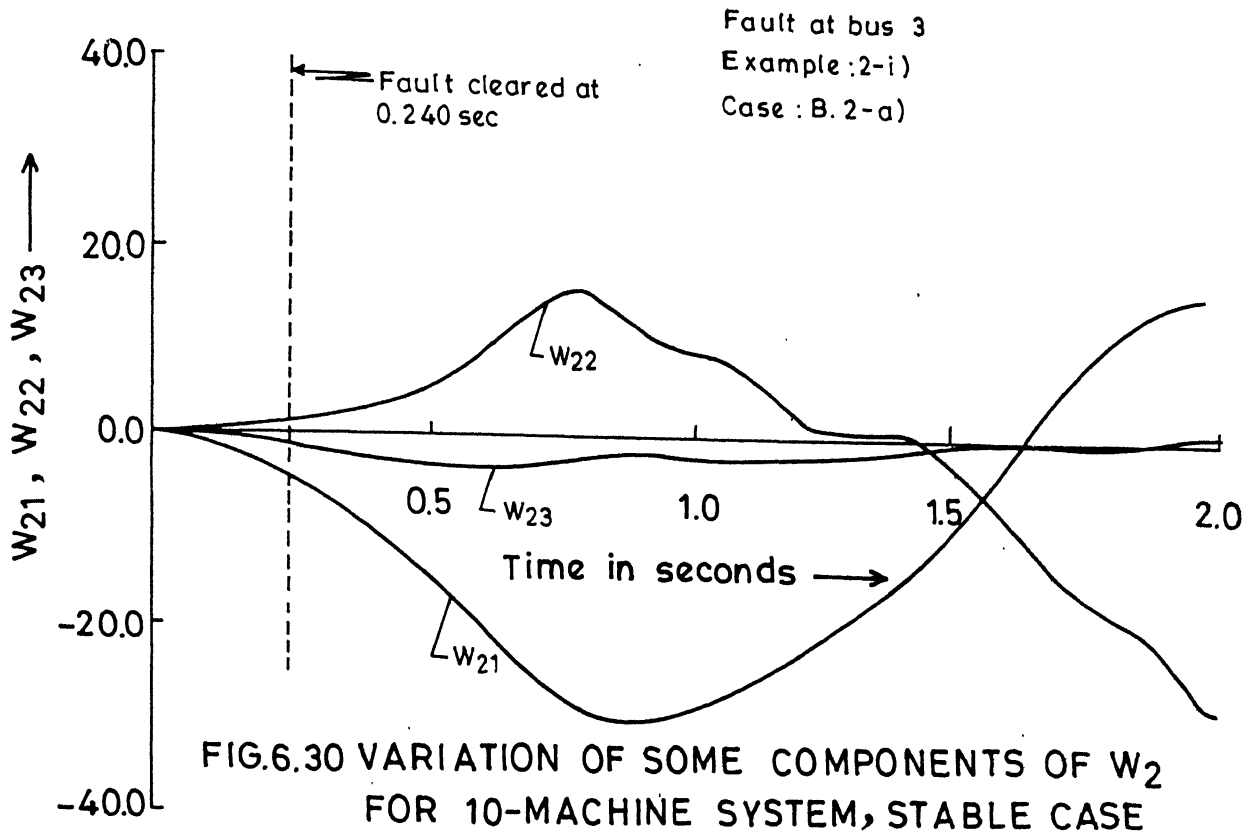


FIG.6.31 VARIATION OF SOME COMPONENTS OF  $W_2$

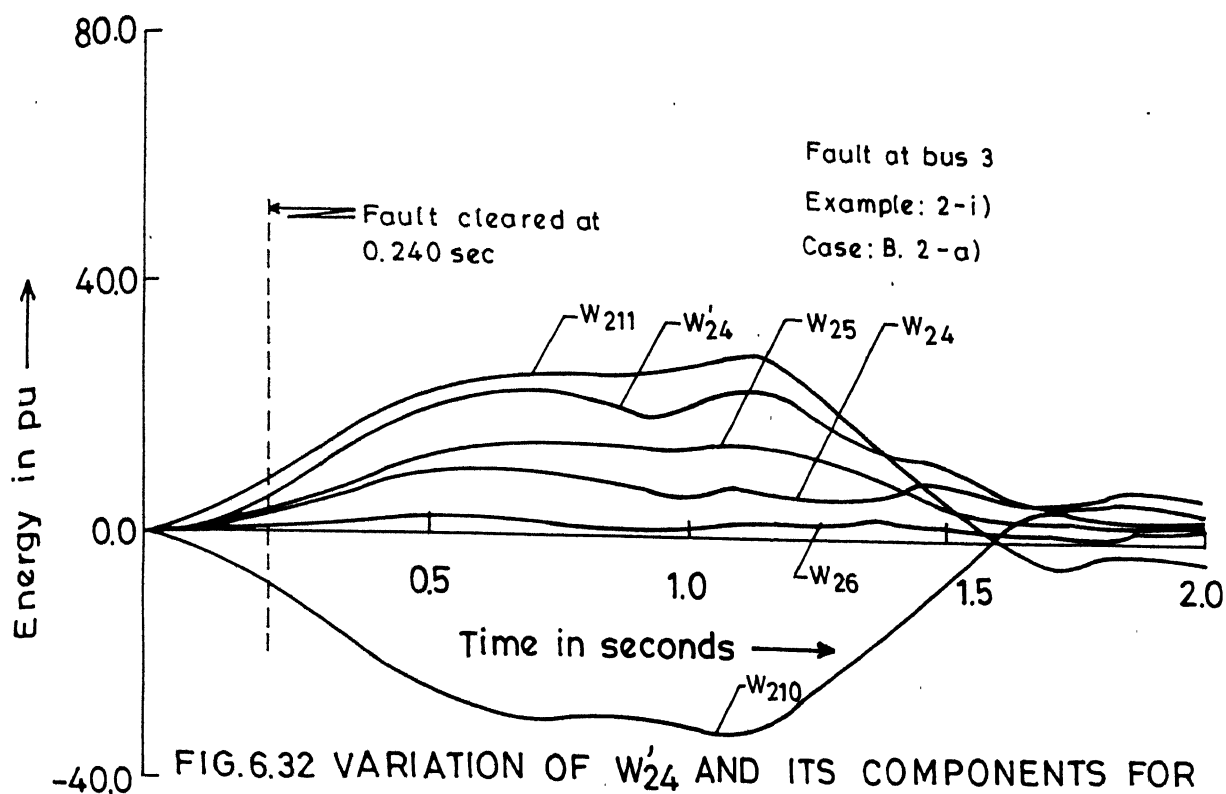


FIG.6.32 VARIATION OF  $W'_{24}$  AND ITS COMPONENTS FOR 10-MACHINE SYSTEM, STABLE CASE

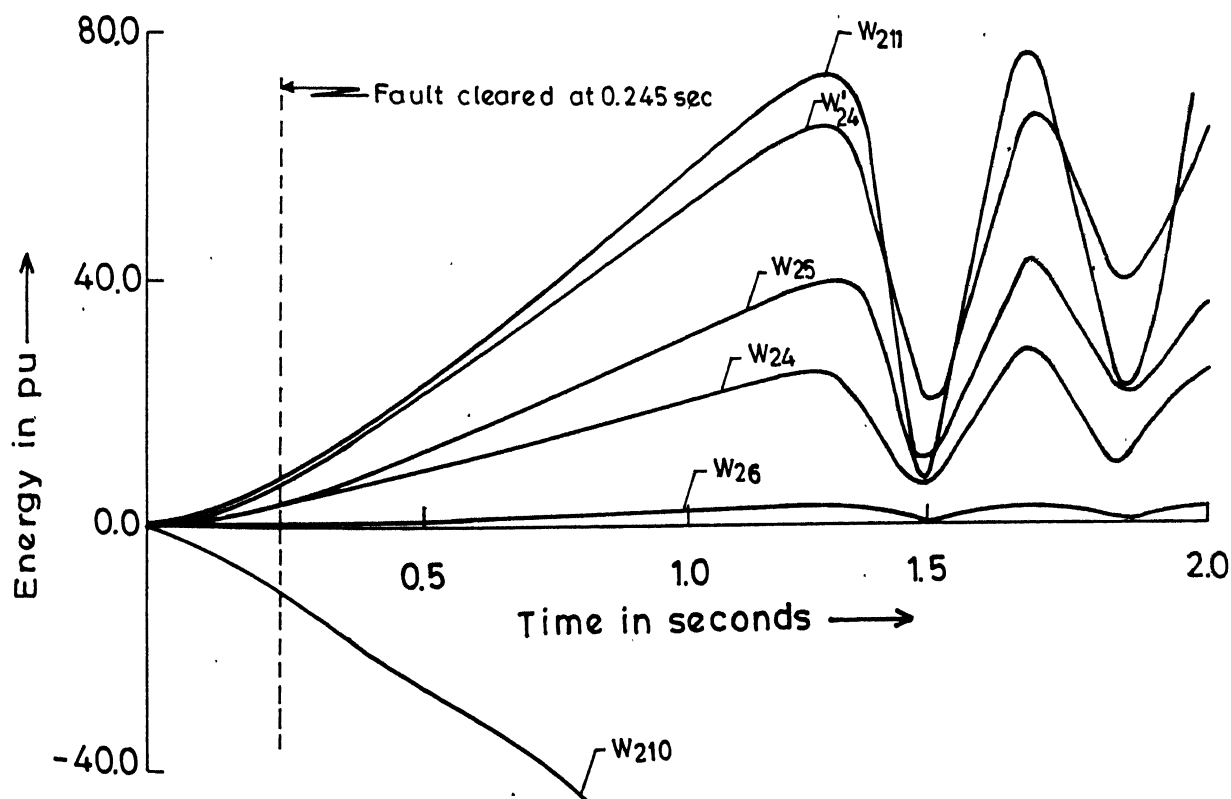


FIG.6.33 VARIATION OF  $W'_{24}$  AND ITS COMPONENTS FOR 10-MACHINE SYSTEM, UNSTABLE CASE

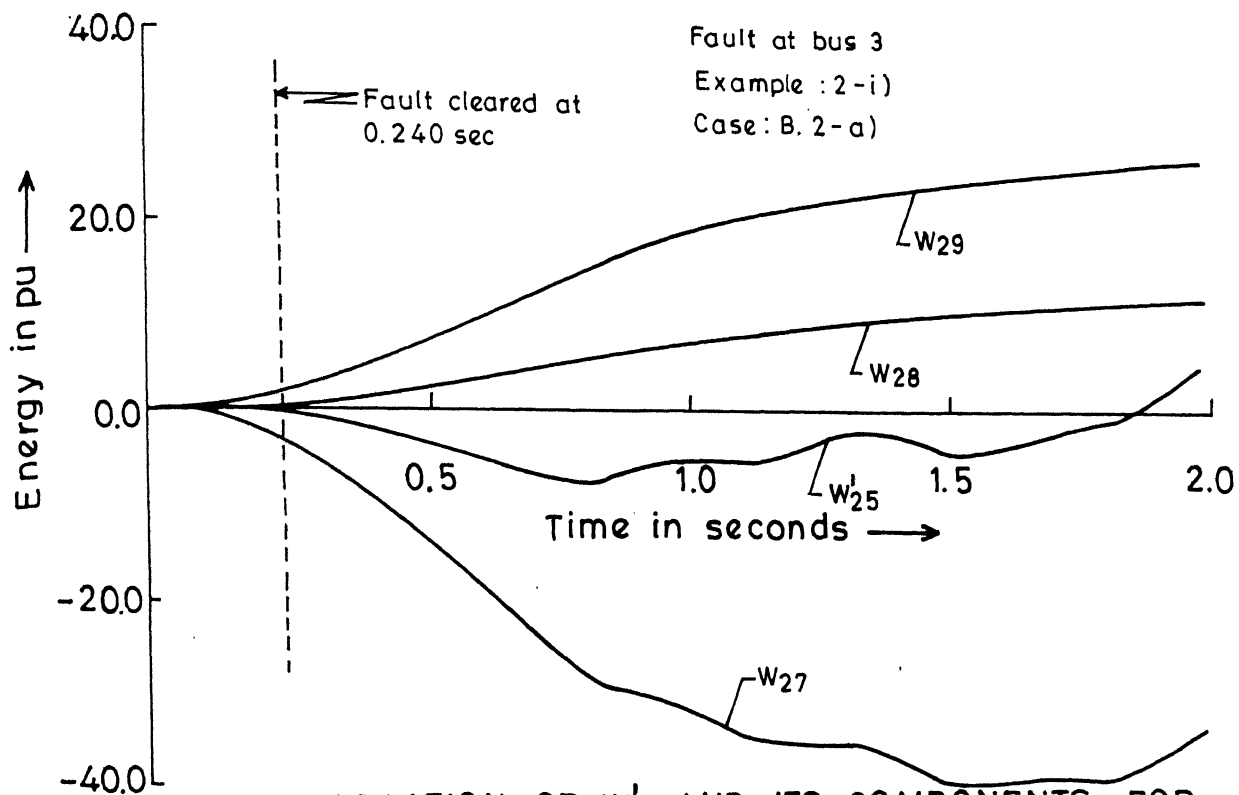


FIG.6.34 VARIATION OF  $W_{25}'$  AND ITS COMPONENTS FOR 10-MACHINE SYSTEM, STABLE CASE

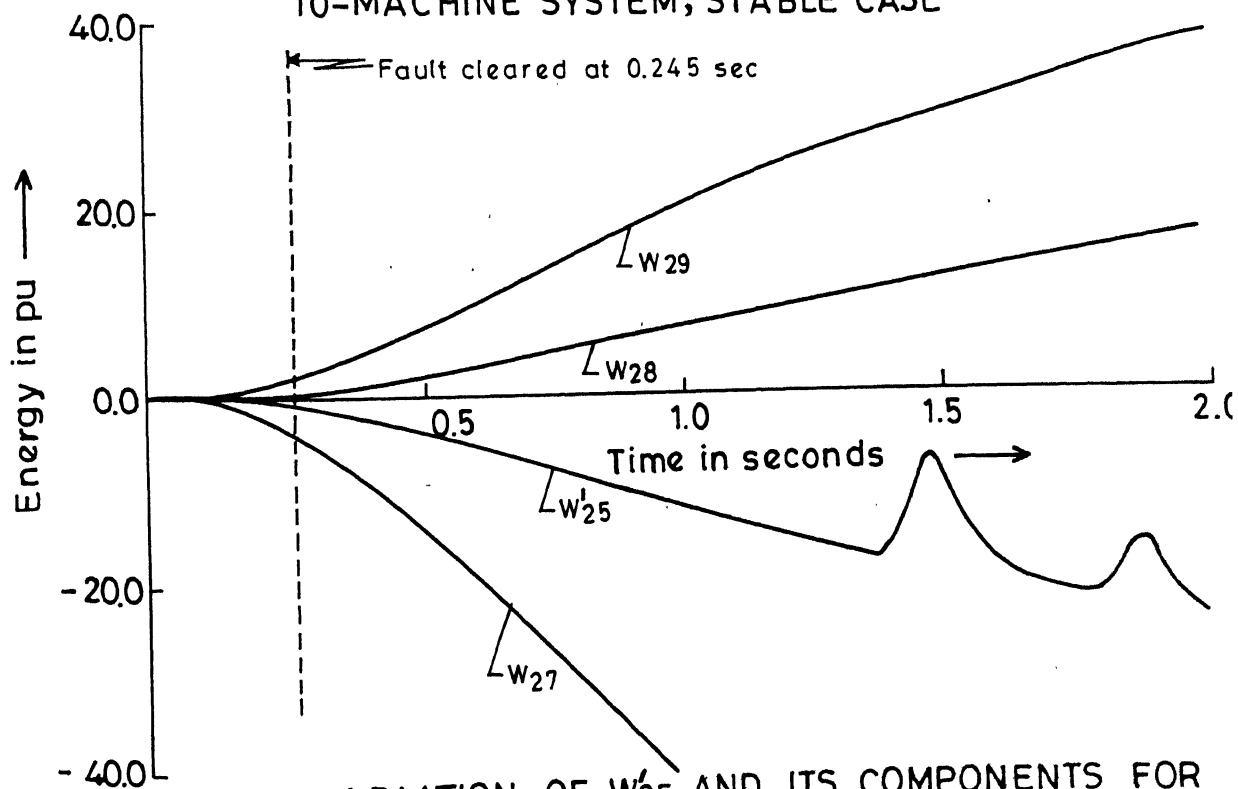


FIG.6.35 VARIATION OF  $W_{25}'$  AND ITS COMPONENTS FOR 10-MACHINE SYSTEM, UNSTABLE CASE

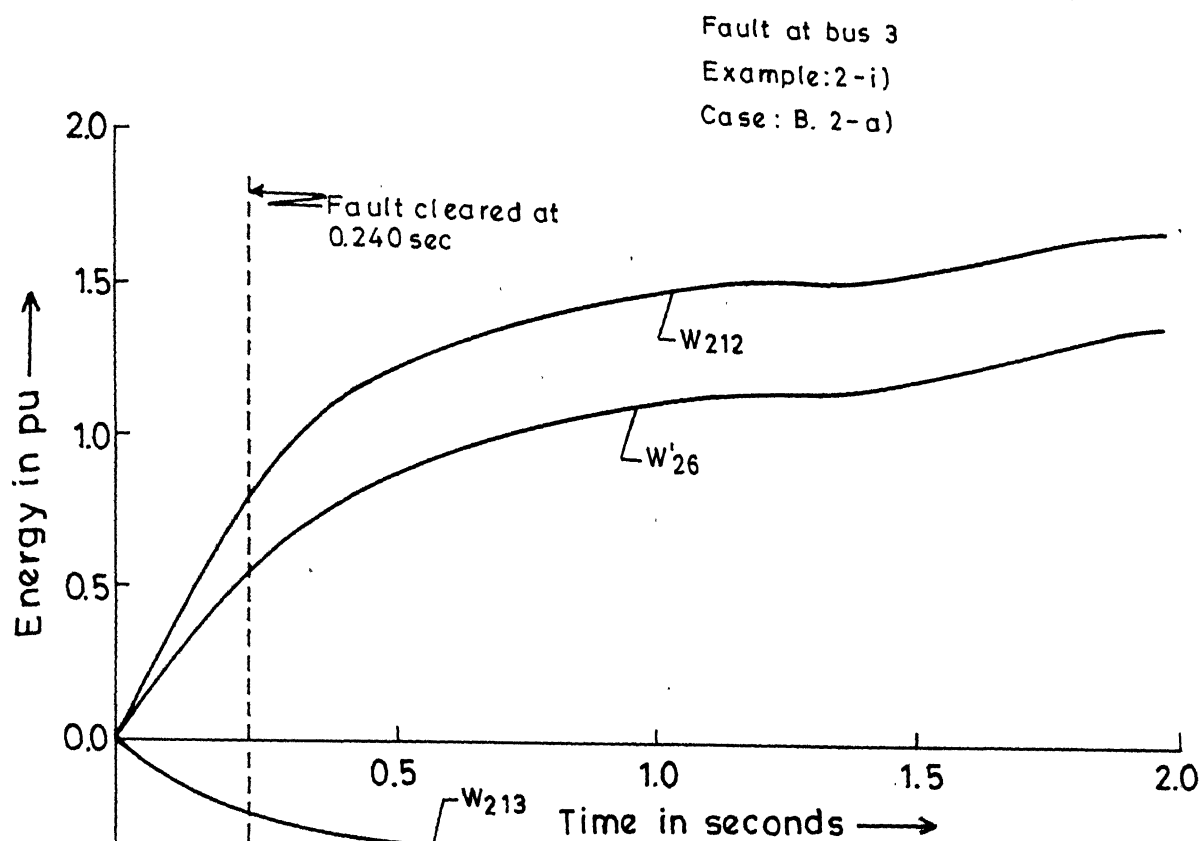


FIG. 6.36 VARIATION OF  $W'_{26}$  AND ITS COMPONENTS FOR 10-MACHINE SYSTEM, STABLE CASE

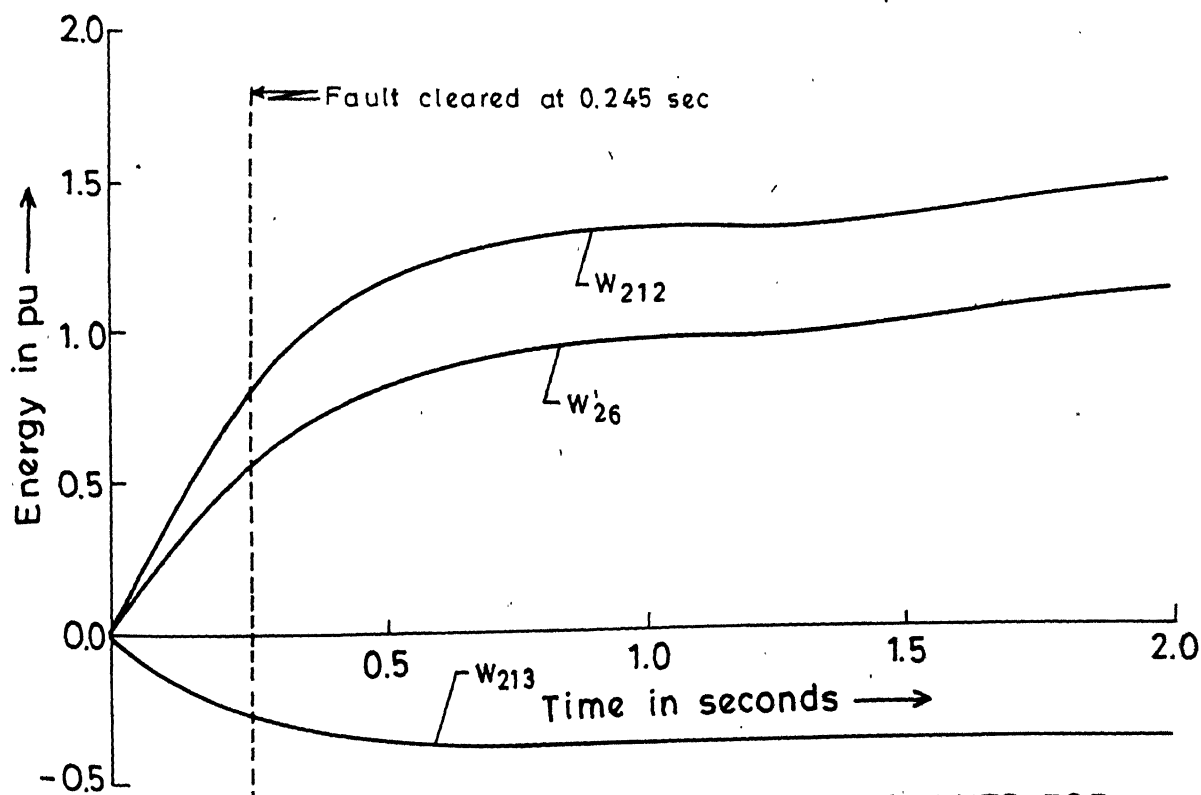


FIG. 6.37 VARIATION OF  $W'_{26}$  AND ITS COMPONENTS FOR 10-MACHINE SYSTEM, UNSTABLE CASE

Variations in  $W'_{24}$ ,  $W'_{25}$  and  $W'_{26}$  are shown alongwith the constituent components.  $W'_{24}$  has 5 components and their variations appear to be correlated.  $W'_{26}$  has 2 components but their magnitudes are negligible compared to other components. This is not surprising as  $W'_{26}$  is due to the damper winding which has a very small effect on the transient stability.

It is interesting to note that although the components of  $W'_{25}$  have large magnitudes (particularly,  $W_{27}$  and  $W_{29}$ ), the magnitude of  $W'_{25}$  is relatively small. This observation confirms the earlier statement that the use of the classical model is good approximation of the detailed model of the generator with AVR. This conclusion follows from the fact that the component  $W'_{25}$  identically vanishes when the classical model is considered.

## 6.5 CONCLUSIONS

In this chapter, a new SPEF is derived which takes into account the detailed models of generators including flux decay, transient saliency, AVR and damper winding. This energy function is constant along the post-fault trajectory. The potential energy has 13 components which are finally shown equivalent to 6 components which can be speedily evaluated. A 4-machine and a 10-machine system examples are used to illustrate the application of the proposed SPEF for direct stability evaluation. The following are the conclusions of the analysis :

- i)  $t_{cr}$  increases with transient saliency, AVR and the inclusion of damper winding.
- ii) The predicted values of  $t_{cr}$  using the proposed energy function are close to the actual ones and the effects of flux decay, transient saliency, AVR and the damper winding can be accurately determined.
- iii) The variations of  $E_{fd}$  and  $E'_q$  have predominant effect on the system energy during the transient.
- iv) Variation of  $E'_d$  and its effect on the transient energy is negligible.
- v) Although the detailed models of the generators including AVR are necessary for accurate evaluation of stability regions, the use of classical models is adequate as a first approximation.

## CHAPTER 7

### CONCLUSIONS

#### 7.1 GENERAL

Direct methods for transient stability analysis are potentially useful both as off-line tools for planning purposes as well as on-line dynamic security assessment. Although much research work has been reported in this area, the application of this method has been limited by conservativeness or accuracy of results, computational burden in determining stability regions and the use of simple (classical) models of generators and loads. Recent advances in the techniques of direct methods such as the use of energy functions in COI variables, the concept of controlling up and PEBS in evaluating the region of stability have been directed at eliminating the limitations due to conservativeness of results thereby enhancing the accuracy and reliability of these methods. However, the use of reduced networks and classical machine models are major handicaps.

Subsequent research work in the area has been aimed at removing the limitations due to system models. Structure preserving model which was first proposed by Bergen and Hill [52] is promising in that it allows detailed load representations. Recently, Padiyar and Sastry [58] have developed a

'topological' energy function which includes detailed generator and load representations. Preservation of network is also advantageous in on-line dynamic security assessment. However, the application of direct methods using structure preserving energy functions to on-line dynamic security assessment requires further developments due to i) more computational burden with nonlinear load models than with reduced models, ii) need to improve system models used and iii) the necessity to provide effective tools to the user for stability evaluation (both at the planning stage and in the operational level) of large systems. This thesis has been aimed at eliminating some of these limitations to make the direct methods acceptable to utilities. In this chapter, the major contributions of the thesis are reviewed and suggestions for further work are given.

## 7.2 COMPUTATION OF SPEF IN DYNAMIC SIMULATION PROGRAM

Although efficient computer programs to perform digital simulation for stability evaluation are available and capable of accommodating detailed generator models, the non-availability of effective programs for the computation of energy functions has prevented extensive application of direct methods to system planning. However, the existing programs, if suitably modified, can be used to study the transient behaviour of power systems through direct methods or simulation. In Chapter 2, an existing digital simulation program [66] has been i) modified to

include voltage dependent loads and then ii) augmented to include the computation of SPEF and its various components by incorporating two new subroutines PFSOL and TEF. While subroutine PFSOL solves the post-fault network equations at the end of each step of integration of the swing equations describing the system dynamics, subroutine TEF evaluates the SPEF and its components utilising the bus voltage magnitudes and the bus angles obtained as outputs of PFSOL. The resultant program can, thus, be conveniently used to analyse the transient stability of power systems both by digital simulation and by direct methods based on the computation of SPEF.

The analysis of the variations of kinetic and potential energy components is helpful in deciding system stability thereby avoiding the need to scrutinise the voluminous results in the form of swing curves.

### 7.3 STRUCTURE PRESERVING ENERGY FUNCTIONS WITH KNOWN MODES OF INSTABILITY

In the application of PEBS method, it is assumed that the kinetic energy gained by the faulted system at the instant of clearing gets fully converted into the potential energy of the post-fault system. Though the assumption is true for a two-machine system, it has been shown [59] that the total kinetic energy need not be converted into potential energy in the case of multi-machine systems. It is the kinetic energy

at clearing corresponding to a particular step-out mode that is responsible for system separation [32]. In this thesis, a novel structure preserving energy function has been developed (in Chapter 3) using COI variables under the assumption that the system splits into  $r$  groups ( $r \geq 2$ ) on the onset of instability and that the generators within a group swing together. The kinetic energy component of the energy function excludes the energy due to inter-generator swings within the group and thus gives better estimate of the energy associated with system separation. Although this energy component can be derived from the SPEF used in Chapter 2 [54], the proposed SPEF is derived directly from a system model based on the mode of instability.

Numerical examples demonstrate that the kinetic energy correction by the application of the proposed SPEF improves the predicted results only marginally. This is because the kinetic energy component  $W_{12}$  due to the relative motion of rotors of generators in a coherent group is not zero and does not remain constant along the post-fault trajectory. There is an exchange of energy between the two components of the kinetic energy term. This fact seems to be ignored in the previous literature on the subject.

The presence of non-constant active power loads results in path dependent terms in the energy function. These terms can be integrated numerically without difficulties. However, it is

angles become implicit functions of the faulted generator rotor angle. While the trajectory of the faulted generator rotor which accelerates monotonically during the fault-on period, can be determined by increasing its angle from its initial value by an arbitrarily selected step size, the remaining system variables required for the computation of SPEF can be obtained by solving a set of algebraic equations. Further, the assumption of constant accelerating power for the faulted generator till the instant of fault clearing, speeds up the computation of energy at clearing thereby reducing the overall computation time for TEM. The algorithm for the calculation of TEM is validated by the correct prediction of stability or instability of the systems investigated and the ranking of the contingencies considered.

The work reported in this thesis is first step in the work required to implement the application of SPEF for on-line dynamic security assessment. The elimination of the computation of the faulted trajectory in detail is significant not only in terms of reducing the computations but allowing the introduction of sensitivity analysis for handling changes in loading conditions and the network configurations.

The algorithm given in Chapter 4 is based on the assumption that the faulted generator tends to separate from the rest. As seen from the results in Chapters 2 and 3, this assumption is

valid for most of the cases. Where it is not applicable (for example, fault at the terminals of generator 10 of the 10-machine system), the contingency would be, usually, not critical and the results of the security assessment would not be affected.

## 7.5 STRUCTURE PRESERVING ENERGY FUNCTIONS WITH DETAILED SYSTEM MODELS

A novel method has been presented in Chapter 5 to account for transmission line resistances in the SPEF. The method exploits the equivalence of a lossy network having same  $G/B$  ratio for all its elements to a lossless network with a new set of power injections. The new SPEF developed using COI variables has a path dependent term which can be numerically integrated without affecting the accuracy in the predicted results. The error due to the approximation in assuming constant  $G/B$  ratio for all the lines is found to be small.

Reduced networks where the elimination of load buses introduces transfer conductances which are predominant, require the inclusion of path dependent term in the energy function. As remarked earlier, the presence of large path dependent terms is not desirable and perhaps explains the reason for the failure of the PEBS method in accurately predicting the critical energy sometimes as reported in the literature. The accuracy of the

SPEF developed in Chapter 5 is very good perhaps due to relatively small path dependent term in the energy function. The effect of line resistances seem to improve the critical clearing time and this is accurately predicted by the SPEF.

A SPEF has been developed in this thesis considering flux decay, transient saliency, exciter, AVR and a damper winding on the quadrature axis. Recently, a 'topological' energy function (TEF) considering realistic generator models (these do not include the damper winding) has been reported in ref.[58]. However, the TEF in ref.[58] has a time derivative which is negative semi-definite along the post-fault trajectory and gives conservative estimates of the region of stability. The SPEF proposed in this work removes the conservativeness of the results. Moreover, a general expression for the SPEF is derived which simplifies the computation of the energy function. From a study of two system examples considered, the following conclusions can be derived :

- i) The effect of transient saliency, AVR and damper winding is to increase the stability region. However, the effect of damper winding on system stability is not very perceptible.
- ii) The use of SPEF gives reliable results and correctly shows the effects with control equipments.
- iii) For stability analysis, the use of a classical model for generators is a good approximation for the detailed models.

## 7.6 SUGGESTIONS FOR FURTHER WORK

Based on the observations made in the previous sections, the following suggestions are made for further work in this area :

- i) An algorithm for accurately predicting the mode of instability for a given contingency without computing the system trajectory is not yet available and requires investigation.
- ii) In this work, a beginning has been made in the application of SPEF for on-line dynamic security assessment. This work can be extended to further simplify the computations and implement the use of SPEF in energy control centres. This would require the following developments :
  - a) The use of sensitivity analysis for changing load conditions and the network configurations.
  - b) At present, the direct method considers only a single element such as fault followed by its clearing. An emergency state can lead to a series of events. It is worthwhile examining whether SPEF can handle the analysis of such events.
  - c) Before actual implementation extensive testing on large systems is required.

## APPENDIX A

## DERIVATION OF SYNCHRONOUS GENERATOR EQUATIONS [2, 66]

## A.1 PARK EQUATIONS

The Park equations of synchronous generator with a d-axis field winding and a q-axis damper winding are given below :

Direct axis :

$$\Psi_d = L_{ad}i_f + L_d i_d \quad (A.1)$$

$$\Psi_f = L_{ff}i_f + L_{ad}i_d \quad (A.2)$$

$$v_d = - \frac{d\Psi_d}{dt} - r_a i_d - \Psi_q \omega \quad (A.3)$$

$$v_f = \frac{d\Psi_f}{dt} + r_f i_f \quad (A.4)$$

Quadrature axis :

$$\Psi_q = -L_{aq}i_{kq} + L_q i_q \quad (A.5)$$

$$\Psi_{kq} = L_{kkq}i_{kq} - L_{aq}i_q \quad (A.6)$$

$$v_q = - \frac{d\Psi_q}{dt} - r_a i_q + \Psi_d \omega \quad (A.7)$$

$$0 = \frac{d\Psi_{kq}}{dt} + r_{kq}i_{kq} \quad (A.8)$$

## A.2 STATOR EQUATIONS

In this section the stator equations which are suited for use in the generator model are derived. For the purpose of transient and dynamic stability studies the stator transformer voltages can be neglected. Eqs. (A.3) and (A.7), therefore, become :

$$v_d = -r_a i_d - \omega \Psi_q \quad (\text{A.9})$$

$$v_q = -r_a i_q + \omega \Psi_d \quad (\text{A.10})$$

The q-axis stator equation is firstly derived by eliminating  $i_f$  from (A.1) and (A.2),

$$\omega \Psi_d = \omega \Psi_f L_{ad} / L_{ff} + \omega (L_d - L_{ad}^2 / L_{ff}) i_d \quad (\text{A.11})$$

Define the d-axis transient inductance,

$$L'_d = L_d - L_{ad}^2 / L_{ff} \quad (\text{A.12})$$

and the q-axis transient voltage,

$$E'_q = \omega \Psi_f L_{ad} / L_{ff} \quad (\text{A.13})$$

and substitute into (A.11),

$$\omega \Psi_d = E'_q + \omega L'_d i_d \quad (\text{A.14})$$

Substitute (A.14) into (A.10),

$$v_q = E'_q + \omega L'_d i_d - r_a i_q \quad (\text{A.15})$$

The d-axis stator equation is now derived by firstly eliminating  $i_{kq}$  from (A.5) and (A.6),

$$\omega \Psi_q = -\omega \Psi_{kq} L_{aq}/L_{kkq} + \omega(L_q - L_{aq}^2/L_{kkq})i_q \quad (A.16)$$

Define the q-axis transient inductance,

$$L'_q = L_q - L_{aq}^2/L_{kkq} \quad (A.17)$$

and the d-axis transient voltage,

$$E'_d = \omega \Psi_{kq} L_{aq}/L_{kkq} \quad (A.18)$$

and substitute into (A.16),

$$\omega \Psi_q = -E'_d + \omega L'_q i_q \quad (A.19)$$

Substitute (A.19) into (A.9),

$$v_d = E'_d - \omega L'_q i_q - r_a i_q \quad (A.20)$$

### A.3 ROTOR WINDING EQUATIONS

The d-axis field winding equation is derived as follows:

Multiply (A.4) by  $\omega L_{ad}/r_f$

$$v_f \frac{\omega L_{ad}}{r_f} = \omega L_{ad} i_f + \frac{\omega L_{ad}}{r_f} \frac{d\Psi_f}{dt} \quad (A.21)$$

Define,

$$E_f = \frac{\omega L_{ad}^o}{r_f} v_f = \frac{\omega L_{ad}}{k_f r_f} v_f \quad (A.22)$$

From (A.2),

$$i_f = \Psi_f / L_{ff} - L_{ad} i_d / L_{ff} \quad (A.23)$$

Substitute (A.22) and (A.23) into (A.21),

$$k_f E_f = \frac{\omega L_{ad}}{L_{ff}} \Psi_f - \frac{\omega L_{ad}^2}{L_{ff}} i_d + \frac{\omega L_{ad}}{r_f} \frac{d\Psi_f}{dt} \quad (A.24)$$

Define the d-axis open circuit transient time constant,

$$T'_{do} = L_{ff} / r_f \quad (A.25)$$

Combine (A.12), (A.13), (A.25) into (A.24),

$$k_f E_f = E'_q - \omega(L_d - L'_d) i_d + T'_{do} \frac{dE'_q}{dt} \quad (A.26)$$

The q-axis damper equation is derived as follows : Multiply (A.8) by  $\omega L_{aq} / r_{kq}$ ,

$$0 = \omega L_{aq} i_{kq} + \frac{\omega L_{aq}}{r_{kq}} \frac{d\Psi_{kq}}{dt} \quad (A.27)$$

From (8.6),

$$i_{kq} = \Psi_{kq} / L_{kkq} + L_{aq} i_q / L_{kkq} \quad (A.28)$$

Substitute (A.28) into (A.27),

$$0 = \frac{\omega L_{aq}}{L_{kkq}} \Psi_{kq} + \frac{\omega L_{aq}^2}{L_{kkq}} i_q + \frac{\omega L_{aq}}{r_{kq}} \frac{d\Psi_{kq}}{dt} \quad (A.29)$$

Define the q-axis open circuit transient time constant,

$$T'_{qo} = L_{kkq} / r_{kq} \quad (A.30)$$

Combine (A.18), (A.19) and (A.30) into (A.29),

$$0 = E'_d + \omega(L_q - L'_q) i_q + T'_{qo} \frac{dE'_d}{dt} \quad (A.31)$$

#### A.4 AIR GAP VOLTAGE EQUATIONS

The d and q-axis air gap voltages are defined by,

$$E_{aq} = \omega \Psi_{ad} = \omega(\Psi_d + L_1 i_d) \quad (A.32)$$

and 
$$E_{ad} = -\omega \Psi_{aq} = -\omega(\Psi_q + L_1 i_q) \quad (A.33)$$

The equations used in the generator model are obtained as follows : Substitute (A.14) into (A.32),

$$E_{aq} = E'_q + \omega(L'_d + L_1) i_d \quad (A.34)$$

Substitute (A.19) into (A.33),

$$E_{ad} = E'_d - \omega(L'_q + L_1) i_q \quad (A.35)$$

In Sections A.1 to A.4 the generator model equations have been developed in terms of inductances. For transient stability studies the deviations in frequency are small and one can substitute  $\omega L = x$ , ( $x$  is the reactance at synchronous frequency) in the equations derived.

#### A.5 STEADY STATE GENERATOR EQUATIONS

The vector diagram for synchronous generator in the steady state is shown in Fig. A.1. The voltage  $\bar{E}_q$  is defined as

$$\bar{E}_q = (V_q + jV_d) + (r_a + jx_q)(I_q + jI_d) \quad (A.36)$$

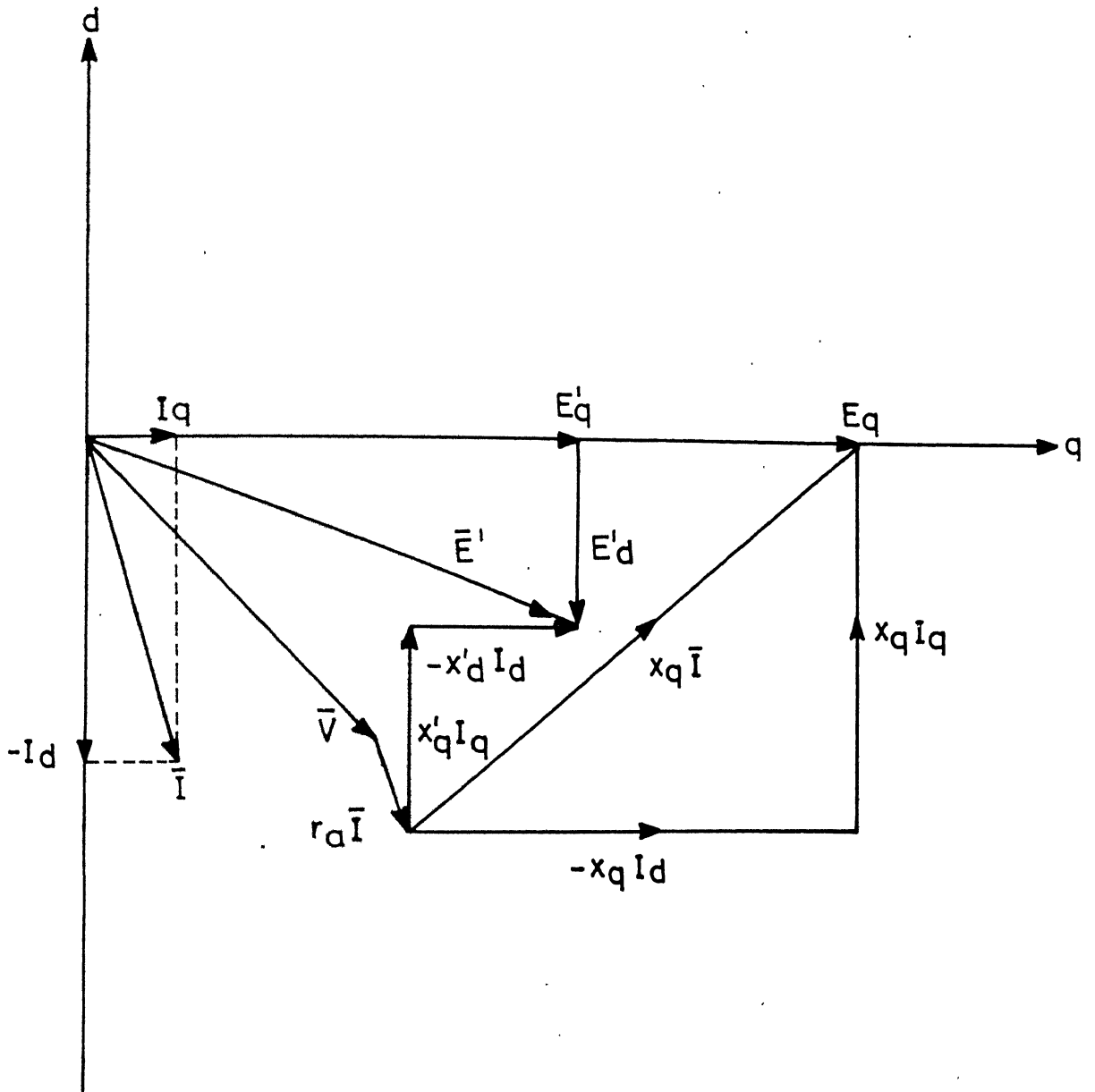


FIG. A.1 STEADY STATE SYNCHRONOUS GENERATOR VECTOR DIAGRAM

During the steady state  $E_q$  lies on the quadrature axis, since,

$$\text{Im}[\bar{E}_q] = V_d + r_a I_d + x_q I_q \quad (\text{A.37})$$

and from (A.5) and (A.9)

$$V_d + r_a I_d + x_q I_q = x_{aq} I_{kq} \quad (\text{A.38})$$

In the steady-state,  $I_{kq} = 0$  and, therefore,  $\text{Im}[\bar{E}_q] = 0$ . This property of  $\bar{E}_q$  is used in calculating the generator initial conditions since the terminal voltage and current are given in terms of the synchronous reference frame. The position of the generator q-axis is given by calculating,

$$\bar{E}_q = (r_a + jx_q) \bar{I} \quad (\text{A.39})$$

$$\text{and } \delta = \text{Arg}(\bar{E}_q) \quad (\text{A.40})$$

From the vector diagram it can also be seen that in the steady state,

$$E'_q = E_q - (x_q - x'_d) I_d \quad (\text{A.41})$$

The other equations which are used in calculating the generator initial conditions are obtained by setting derivatives to zero in (A.26) and (A.31),

$$E_f = [E'_q - (x_d - x'_d) I_d] / k_f \quad (\text{A.42})$$

$$0 = E'_d + (x_q - x'_q) I_q \quad (\text{A.43})$$

## APPENDIX B

## NETWORK SOLUTION WITH NONLINEAR VOLTAGE DEPENDENT LOADS [69]

In the presence of nonlinear voltage dependent loads, the computation of faulted trajectory requires iterative solution of the nonlinear algebraic network equations. An algorithm giving fast convergence is discussed here.

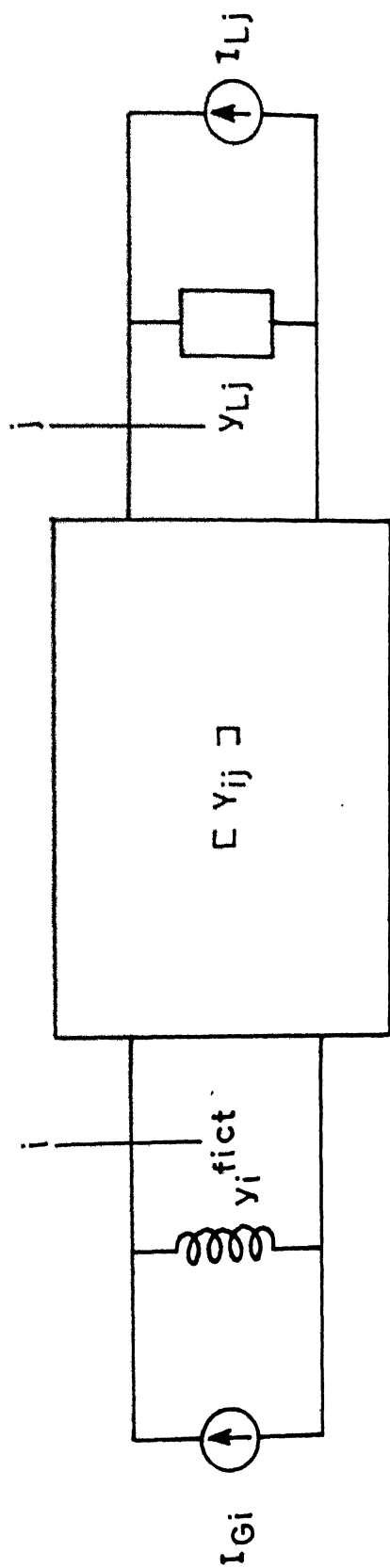
The admittance matrix  $[Y_{ij}]$  for the system network is formulated (excluding machine reactance). A generator is represented by its Norton's equivalent i.e., a current source in parallel with a fictitious admittance to be obtained as

$$y_i^{\text{fict}} = \frac{r_{ai} - j \frac{1}{2} (x'_{di} + x'_{qi})}{r_{ai}^2 + x'_{di} x'_{qi}} \quad (\text{B.1})$$

A load is represented as a current source in parallel with a constant admittance (see Fig. B.1). Admittance,  $y_{Lj}$  at bus  $j$  is evaluated from the initial load flow and hence, initially,  $I_{Lj}$  is zero. The admittance matrix  $[Y_{ij}]$  is augmented to include  $y_i^{\text{fict}}$  at the generator bus  $i$  and  $y_{Lj}$  at the load bus  $j$ . Let the augmented admittance matrix be  $[Y]$ . Then the network equations are :

$$\begin{bmatrix} \underline{I}_G \\ 0 \end{bmatrix} + [\underline{I}_L] = [Y] [\underline{V}] \quad (\text{B.2})$$

$$\text{where } I_{Gi} = E_i^{\text{fict}} y_i^{\text{fict}}, \quad i = 1, 2, \dots, m \quad (\text{B.3})$$

FIG.B.1 NET WORK FOR OBTAINING  $[Y]$

$E_i^{fict}$  is the voltage behind the fictitious admittance  $y_i^{fict}$  of  $i$ th generator and is calculated from

$$\bar{E}_i^{fict} = \bar{E}_i' + \frac{j \frac{1}{2} (x_{qi}' - x_{di}')}{r_{ai} - j \frac{1}{2} (x_{di}' + x_{qi}')} (\bar{E}_i'^* - \bar{V}_i^*) e^{j2\theta}, \quad i=1,2,\dots, m \quad (B.4)$$

$$\text{where } \bar{E}_i' = E_{qi}' + jE_{di}', \quad i = 1,2, \dots, m \quad (B.5)$$

vector  $[\underline{I}_L]$  represents the current injections due to loads.

Current injection  $I_{Lj}$  at a load bus  $j$  can be obtained from

$$I_{Lj} = \frac{(a_j V_j^2 - j d_j V_j^2) - (P_{Lj} - j Q_{Lj})}{V_j^*}, \quad j = 1,2, \dots, n \quad (B.6)$$

The admittance matrix changes whenever the network changes due to fault, line switching, etc., otherwise it remains constant at all iteration steps.

If all the loads are represented as impedances, the Eq. (B.2) would be non-iterative with  $[\underline{I}_L] = \underline{0}$ . If the loads are not modelled as impedances, then  $[\underline{I}_L]$  is adjusted iteratively to account for the difference between the quadratic voltage dependence of the impedance and the specified voltage dependence

## APPENDIX C

## TIME DERIVATIVE OF ENERGY FUNCTION WITH NONCONSTANT MECHANICAL POWER

The structure preserving energy function including the nonconstant mechanical power can be written as

$$W = W_1 + W_2 = W_1 + \sum_{i=1}^5 W_{2i} \quad (C.1)$$

where

$$W_1 = \frac{1}{2} \sum_{i=1}^m M_i \omega_i^2 \quad (C.2)$$

$$W_{21} = - \sum_{i=1}^m \int_{t_0}^t P_{mi} \frac{d\theta_i}{dt} dt \quad (C.3)$$

$$W_{22} = \sum_{i=1}^n \int_{t_0}^t f_{pi}(V_i) \frac{d\varphi_i}{dt} dt \quad (C.4)$$

$$W_{23} = \sum_{i=1}^n \int_{V_{i0}}^{V_i} \frac{f_{qi}(V_i)}{V_i} dV_i \quad (C.5)$$

$$W_{24} = \sum_{i=1}^m [E_i^2 + V_i^2 - 2E_i V_i \cos(\theta_i - \varphi_i) - \{E_i^2 + V_{i0}^2 - 2E_i V_{i0} \cos(\theta_{i0} - \varphi_{i0})\}] \frac{1}{2x'_{di}} \quad (C.6)$$

$$W_{25} = - \sum_{i=1}^n \sum_{j=1}^n B_{ij} (V_i V_j \cos \varphi_{ij} - V_{i0} V_{j0} \cos \varphi_{ij0}) \quad (C.7)$$

The time derivative of the function  $W$  in Eq. (C.1) can be shown to be zero by direct verification as follows :

Differentiating  $W_1$  with respect to  $\omega_i$ , we have,

$$\frac{\partial W_1}{\partial \omega_i} = M_i \omega_i, \quad i = 1, 2, \dots, m \quad (C.8)$$

Taking the partial derivative of  $W_2$  with respect to  $\theta_i, V_i$ , and  $t$  respectively, we get,

$$\frac{\partial W_2}{\partial \theta_i} = \frac{E_i V_i \sin(\theta_i - \varphi_i)}{x'_{di}} = P_{ei}, \quad i = 1, 2, \dots, m \quad (C.9)$$

$$\frac{\partial W_2}{\partial V_i} = \left[ \frac{V_i^2}{x'_{di}} - \frac{E_i V_i \cos(\theta_i - \varphi_i)}{x'_{di}} + f_{qi}(V_i) - \sum_{j=1}^n B_{ij} V_i V_j \cos \varphi_{ij} \right]$$

$$i = 1, 2, \dots, m$$

$$= [f_{qi}(V_i) - \sum_{j=1}^n B_{ij} V_i V_j \cos \varphi_{ij}] \frac{1}{V_i}, \quad i = m+1, m+2, \dots, n$$

$$= \frac{1}{V_i} [Q_{Li} + Q_i], \quad i = 1, 2, \dots, n \quad (C.10)$$

$$= 0 \quad (C.10)$$

$$\frac{\partial W_2}{\partial \varphi_i} = - \frac{E_i V_i \sin(\theta_i - \varphi_i)}{x'_{di}} + \sum_{j=1}^n B_{ij} V_i V_j \sin \varphi_{ij}, \quad i=1, 2, \dots, m$$

$$= \sum_{j=1}^n B_{ij} V_i V_j \sin \varphi_{ij}, \quad i = m+1, m+2, \dots, n$$

$$= P_i, \quad i = 1, 2, \dots, n \quad (C.11)$$

$$\frac{\partial W_2}{\partial t} = - \sum_{i=1}^m P_{mi} \frac{d\theta_i}{dt} + \sum_{i=1}^n P_{Li} \frac{d\phi_i}{dt} \quad (C.12)$$

From Eqs. (C.8), (C.9), (C.11) and (C.12), we get after rearranging the terms,

$$\begin{aligned} & \sum_{i=1}^m \frac{\partial W_1}{\partial \omega_i} \frac{d\omega_i}{dt} + \sum_{i=1}^m \frac{\partial W_2}{\partial \theta_i} \frac{d\theta_i}{dt} + \sum_{i=1}^n \frac{\partial W_2}{\partial \phi_i} \frac{d\phi_i}{dt} + \frac{\partial W_2}{\partial t} \\ &= \sum_{i=1}^m M_i \dot{\omega}_i \omega_i + \sum_{i=1}^m P_{ei} \omega_i + \sum_{i=1}^n P_i \frac{d\phi_i}{dt} - \sum_{i=1}^m P_{mi} \omega_i + \sum_{i=1}^n P_{Li} \frac{d\phi_i}{dt} \\ &= \sum_{i=1}^m (M_i \dot{\omega}_i - P_{mi} + P_{ei}) \omega_i + \sum_{i=1}^n (P_i + P_{Li}) \frac{d\phi_i}{dt} \\ &= - \sum_{i=1}^m \frac{M_i \omega_i}{M_T} P_{COI} + \sum_{i=1}^n (P_i + P_{Li}) \frac{d\phi_i}{dt} \\ &= - \frac{P_{COI}}{M_T} \sum_{i=1}^m M_i \omega_i + \sum_{i=1}^n (P_i + P_{Li}) \frac{d\phi_i}{dt} \\ &= 0 \end{aligned} \quad (C.13)$$

Hence,

$$\begin{aligned} \frac{dW}{dt} &= \frac{d}{dt} (W_1 + W_2) \\ &= \left[ \sum_{i=1}^m \left( \frac{\partial W_1}{\partial \omega_i} \frac{d\omega_i}{dt} + \frac{\partial W_2}{\partial \theta_i} \frac{d\theta_i}{dt} \right) + \sum_{i=1}^n \frac{\partial W_2}{\partial \phi_i} \frac{d\phi_i}{dt} + \frac{\partial W_2}{\partial t} \right] \\ &\quad + \left[ \sum_{i=1}^n \frac{\partial W_2}{\partial V_i} \frac{dV_i}{dt} \right] \\ &= 0, \text{ in view of Eqs. (C.10) and (C.13)} \end{aligned} \quad (C.14)$$

## APPENDIX D

## PEBS METHOD OF DETERMINING STABILITY REGION

As discussed earlier in Chapter 1, the potential energy boundary surface is the surface in the angle space of the points corresponding to the first maxima of the potential energy with respect to the stable equilibrium point where its directional derivative is zero. The method of computing stability region using PEBS is explained below :

The basic idea of PEBS method is to replace the study of the following model of power system consisting of  $m$  generators

$$\dot{\theta}_i = \omega_i, \quad i = 1, 2, \dots, m \quad (D.1a)$$

$$M_i \dot{\omega}_i = P_{mi} - P_{ei} - \frac{M_i}{M_T} P_{COI}, \quad i = 1, 2, \dots, m \quad (D.1b)$$

by the study of simple gradient system [77]

$$\underline{s} = - \frac{\partial W_2}{\partial \theta} \quad (D.2)$$

In the PEBS method we calculate the critical energy from the system (D.2) rather than from system (D.1) using the properties of the gradient system. However, it has been shown in ref.[77] that the boundary of the stability region of the system described by Eqs. (D.1) is related to that of the gradient system of Eq. (D.2).

The structure preserving energy function can be written as

$$W(\underline{\theta}, \underline{\omega}, \underline{V}, \underline{\varphi}, t) = W_1(\underline{\omega}) + W_2(\underline{\theta}, \underline{V}, \underline{\varphi}, t) \quad (D.3)$$

Hence,

$$\frac{dW_1}{dt} = \sum_{i=1}^m \frac{\partial W_1}{\partial \omega_i} \frac{d\omega_i}{dt} \quad (D.4)$$

$$\begin{aligned} \frac{dW_2}{dt} &= \sum_{i=1}^m \frac{\partial W_2}{\partial \theta_i} \frac{d\theta_i}{dt} + \sum_{i=1}^n \left[ \frac{\partial W_2}{\partial \varphi_i} \frac{d\varphi_i}{dt} + \frac{\partial W_2}{\partial V_i} \frac{dV_i}{dt} \right] + \frac{\partial W_2}{\partial t} \\ &= \sum_{i=1}^m \frac{\partial W_2}{\partial \theta_i} \frac{d\theta_i}{dt} + \sum_{i=1}^n \left[ \frac{\partial W_2}{\partial \varphi_i} \frac{d\varphi_i}{dt} + \frac{\partial W_2}{\partial V_i} \frac{dV_i}{dt} \right] = \sum_{i=1}^m \frac{\partial W_2}{\partial \theta_i} \frac{d\theta_i}{dt} \end{aligned} \quad (D.5)$$

$$\frac{dW}{dt} = \sum_{i=1}^m M_i \omega_i \dot{\omega}_i + \sum_{i=1}^m \frac{\partial W_2}{\partial \theta_i} \dot{\theta}_i = \sum_{i=1}^m (M_i \dot{\omega}_i + \frac{\partial W_2}{\partial \theta_i}) \omega_i \quad (D.6)$$

$$\text{Let vector } \underline{S} = [M_1 \dot{\omega}_1 \quad M_2 \dot{\omega}_2 \quad \dots \quad M_m \dot{\omega}_m]^T$$

$$\text{and } \frac{\partial W_2}{\partial \underline{\theta}} = \left[ \frac{\partial W_2}{\partial \theta_1} \quad \frac{\partial W_2}{\partial \theta_2} \quad \dots \quad \frac{\partial W_2}{\partial \theta_m} \right]^T$$

Therefore,

$$\begin{aligned} \frac{dW}{dt} &= (\underline{S} + \frac{\partial W_2}{\partial \underline{\theta}}) \cdot \underline{\omega} \\ &= 0 \end{aligned} \quad (D.7)$$

for a conservative system. From this it follows then,

$$\underline{S} = - \frac{\partial W_2}{\partial \underline{\theta}} \quad (D.8)$$

The direction of the torque vector  $\underline{S}$  is in a direction negative to the gradient of  $W_2$ , i.e.,  $\underline{S} = -\nabla W_2$ .

By definition  $\underline{\nabla W_2}$  is in a direction normal to  $W_2 =$  constant in the angle space. Hence, torque is always orthogonal to the equipotential surfaces and in the direction of decreasing  $W_2$ . Consider a trajectory crossing the PEBS. Inside the region surrounded by PEBS and containing the sep, the projection of  $\underline{S}$  on the velocity vector  $\underline{\omega}$  is in a direction opposing the motion, i.e., towards sep. Outside PEBS, projection of  $\underline{S}$  is in the direction of the velocity vector  $\underline{\omega}$ . Thus, the dot product of  $\underline{\nabla W_2}$  with velocity vector  $\underline{\omega}$  changes sign in the vicinity of the PEBS.

From Eq. (D.7), we get,

$$\underline{S} \cdot \underline{\omega} = -\frac{\partial W_2}{\partial \underline{\theta}} \cdot \underline{\omega} = -\sum_{i=1}^m \frac{\partial W_2}{\partial \theta_i} \frac{d\theta_i}{dt} = -\dot{W}_2 \quad (D.9)$$

in view of Eq. (D.5).

Hence,  $\dot{W}_2 > 0$  inside the PEBS and  $< 0$  outside it and vice versa is true with  $\dot{W}_1$ . This implies that inside the stable region the potential energy increases and the kinetic energy decreases. The opposite is true outside the PEBS. Consequently, when  $\dot{W}_2$  or  $\dot{W}_1$  changes sign can be interpreted to be the instant when the trajectory crosses the PEBS [29].

The computation of critical energy,  $W_{cr}$  and critical clearing time,  $t_{cr}$  by the PEBS method consists of the following procedure :

- 1) Compute the fault-on trajectory.
- 2) Monitor  $W_2^{\max}$ , the maximum value of  $W_2$ , on the fault-on trajectory. Critical energy,  $W_{cr} = W_2^{\max}$ .
- 3) Find  $t_{c1}$  such that

$$W(t_{c1}) = W_1(t_{c1}) + W_2(t_{c1}) = W_{cr}$$

- 4) The  $t_{c1}$  of Step 3 is the PEBS method solution for the critical clearing time.

## APPENDIX E

## DATA FOR THE 7-MACHINE (CIGRE) TEST SYSTEM

Number of machines : 7  
 Number of buses : 10  
 Number of lines : 13  
 Number of loads : 7  
 Base MVA : 100      Base kV : 225

Table E.1 Machine Constants

Generator No.	$M$ in pu - $\text{sec}^2/\text{rad}$	$x'_d$ in pu
1	0.0602	0.074
2	0.0602	0.074
3	0.0759	0.062
4	0.0954	0.049
5	0.0411	0.118
6	0.0677	0.071
7	0.0568	0.087

Table E.2 Line Data

Line No.	From Bus	To Bus	Line reactance in ohms	Half-line charging ( $\mu$ s)
1	2	3	24.5	200
2	2	4	24.5	100
3	3	5	62.6	200
4	5	10	32.3	300
5	3	4	39.5	300
6	3	9	28.0	200
7	4	1	10.0	200
8	4	6	24.8	100
9	4	9	97.0	200
10	4	10	33.0	300
11	6	8	31.8	200
12	7	8	39.5	300
13	8	9	97.0	200

Table E.3 Operating Data

Bus No.	Voltage Magnitude in pu	Bus angle in deg	Generation		Load	
			Active power in pu	Reactive power in pu	Active power in pu	Reactive power in pu
1	1.0343	-1.4640	2.30	1.0	0.0	0.00
2	1.0448	-0.1852	2.00	0.7346	0.0	0.00
3	1.0363	-1.6300	2.56	0.8536	0.0	0.00
4	1.0141	-3.9461	3.00	1.7880	6.5	4.05
5	1.0257	-7.0880	1.20	1.0602	2.0	1.20
6	1.0125	-2.8794	1.60	0.2919	0.8	0.30
7	1.0103	-0.6210	1.74	0.3832	0.9	0.40
8	1.0017	-4.3339	0.00	0.0	1.0	0.50
9	0.9829	-7.12	0.00	0.0	2.3	1.40
10	1.0148	-7.15	0.00	0.0	0.9	0.45

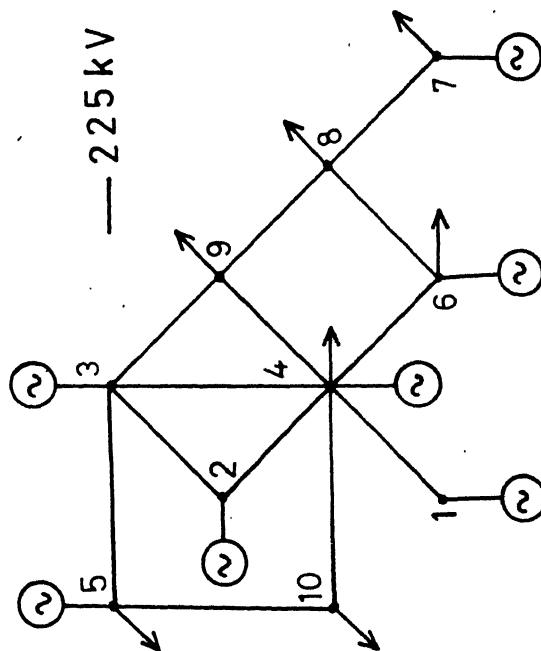


FIG.E.1 ONE-LINE DIAGRAM OF 7-MACHINE SYSTEM

## APPENDIX F

## DATA FOR THE 10-MACHINE (NEW ENGLAND) TEST SYSTEM

Number of machines : 10  
 Number of buses : 39  
 Number of lines : 34  
 Number of transformers: 12  
 Number of loads : 19

Table F.1 Machine Constants

Generator No.	Bus No.	H in sec.	$x_d'$ in pu	$x_q$ in pu	$x_d$ in pu	$T_{do}'$ in sec
1	1	30.3	0.0647	0.1543	0.1812	7.5
2	2	500.0	0.006	-	-	-
3	3	35.8	0.0531	0.1261	0.1493	5.8
4	4	28.6	0.0436	0.1040	0.1224	5.1
5	5	26.0	0.1320	0.3142	0.3696	10.0
6	6	34.8	0.05	-	-	-
7	7	26.4	0.049	-	-	-
8	8	24.3	0.057	0.1359	0.1596	6.0
9	9	34.5	0.057	0.1359	0.1596	6.0
10	10	42.0	0.031	-	-	-

Table F.2 Line Data

Line No.	From Bus	To Bus	Line impedance		Half-line Charging in pu
			Resistance in pu	Reactance in pu	
1	2	3	4	5	6
1	30	31	0.0035	0.0411	0.3494
2	30	2	0.0010	0.0250	0.3750
3	31	32	0.0013	0.0151	0.1286
4	31	25	0.0070	0.0086	0.0730
5	32	35	0.0013	0.0213	0.1107
6	32	18	0.0011	0.0133	0.1069
7	33	34	0.0008	0.0128	0.0671
8	33	14	0.0008	0.0129	0.0691
9	34	35	0.0002	0.0026	0.0217
10	34	37	0.0008	0.0112	0.0738
11	35	36	0.0006	0.0092	0.0565
12	35	11	0.0007	0.0082	0.0695
13	36	37	0.0004	0.0046	0.0390
14	37	38	0.0023	0.0363	0.1902
15	38	2	0.0010	0.0250	0.6000
16	39	11	0.0004	0.0043	0.0365
17	39	13	0.0004	0.0043	0.0365
18	13	14	0.0009	0.0101	0.0862
19	14	15	0.0018	0.0217	0.1830
20	15	16	0.0009	0.0094	0.0855

contd ...

---

1	2	3	4	5	6
21	16	17	0.0007	0.0089	0.0671
22	16	19	0.0016	0.0195	0.1520
23	16	21	0.0008	0.0135	0.1274
24	16	24	0.0003	0.0059	0.0340
25	17	18	0.0007	0.0082	0.0659
26	17	27	0.0013	0.0173	0.1608
27	21	22	0.0008	0.0135	0.1274
28	22	23	0.0006	0.0096	0.0923
29	23	24	0.0022	0.0350	0.1805
30	25	26	0.0032	0.0323	0.2565
31	26	27	0.0014	0.0147	0.1198
32	26	28	0.0043	0.0474	0.3901
33	26	29	0.0057	0.0625	0.5145
34	28	29	0.0014	0.0151	0.1245

---

Table F.3 Transformer Data

Transformer No.	From Bus	To Bus	Impedance		Turns ratio
			Resistance in pu	Reactance in pu	
1	12	11	0.0016	0.0435	1.006
2	12	13	0.0016	0.0435	1.006
3	35	1	0.0	0.0250	1.070
4	39	3	0.0	0.0200	1.070
5	19	4	0.0007	0.0142	1.070
6	20	5	0.0009	0.0180	1.009
7	22	6	0.0	0.0143	1.025
8	23	7	0.0005	0.0272	1.0
9	25	8	0.0006	0.0232	1.025
10	31	10	0.0	0.0181	1.025
11	29	9	0.0008	0.0156	1.025
12	19	20	0.0007	0.0138	1.060

Table F.4 Operating Data (Including line resistance)

Bus No.	Voltage Magnitude in pu	Bus angle in deg	Generation		Loads	
			Active power in pu	Reactive power in pu	Active power in pu	Reactive power in pu
1	2	3	4	5	6	7
1	0.9820	0.0	5.484	2.157	0.092	0.046
2	1.0300	-10.6620	10.000	0.983	11.040	2.500
3	0.9831	2.0860	6.500	2.230	0.0	0.0
4	0.9972	3.4710	6.320	1.444	0.0	0.0
5	1.0123	2.4320	5.080	1.816	0.0	0.0
6	1.0493	4.6790	6.500	2.596	0.0	0.0
7	1.0635	7.3490	5.600	1.323	0.0	0.0
8	1.0278	1.7331	5.400	0.1184	0.0	0.0
9	1.0265	7.1022	8.300	0.3486	0.0	0.0
10	1.0475	-4.0150	2.500	1.6155	0.0	0.0
11	1.0089	-6.7821	0.0	0.0	0.0	0.0
12	0.9958	-6.7621	0.0	0.0	0.075	0.880
13	1.0097	-6.6363	0.0	0.0	0.0	0.0
14	1.0053	-8.2621	0.0	0.0	0.0	0.0
15	1.0033	-8.5024	0.0	0.0	3.200	1.530
16	1.0175	-6.9806	0.0	0.0	3.294	0.323
17	1.0228	-8.0752	0.0	0.0	0.0	0.0
18	1.0220	-8.9790	0.0	0.0	1.580	0.300
19	1.0446	-1.7585	0.0	0.0	0.0	0.0
20	0.9883	-2.7550	0.0	0.0	6.280	1.030

contd ...

1	2	3	4	5	6	7
21	1.0215	-4.5945	0.0	0.0	2.740	1.150
22	1.0432	-0.3143	0.0	0.0	0.0	0.0
23	1.0369	-0.5562	0.0	0.0	2.745	0.846
24	1.0149	-6.8910	0.0	0.0	3.086	0.922
25	1.0549	-5.0647	0.0	0.0	2.240	0.472
26	1.0468	-6.2636	0.0	0.0	1.390	0.170
27	1.0298	-8.2627	0.0	0.0	2.810	0.755
28	1.0474	-2.7362	0.0	0.0	2.060	0.276
29	1.0481	0.0313	0.0	0.0	2.835	0.269
30	1.0464	-9.0820	0.0	0.0	0.0	0.0
31	1.0460	-6.4410	0.0	0.0	0.0	0.0
32	1.0243	-9.2300	0.0	0.0	3.220	0.024
33	0.9985	-10.2040	0.0	0.0	5.00	1.840
34	1.0014	-9.0998	0.0	0.0	0.0	0.0
35	1.0040	-8.4120	0.0	0.0	0.0	0.0
36	0.9934	-10.6170	0.0	0.0	2.338	0.840
37	0.9925	-11.1200	0.0	0.0	5.220	1.760
38	1.0268	-10.8900	0.0	0.0	0.0	0.0
39	1.0133	-5.9400	0.0	0.0	0.0	0.0

Table F.5 Operating Data (neglecting line resistance)

Bus No.	Voltage Magnitude in pu	Bus angle in deg	Generation		Loads	
			Active power in pu	Reactive power in pu	Active power in pu	Reactive power in pu
1	2	3	4	5	6	7
1	0.982	0.0	5.045	1.9164	0.092	0.046
2	1.030	-9.538	10.0	0.684	11.04	2.5
3	0.9831	2.9	6.5	2.159	0.0	0.0
4	0.9972	4.806	6.32	1.57	0.0	0.0
5	1.0123	3.834	5.08	1.852	0.0	0.0
6	1.0493	5.903	6.5	2.547	0.0	0.0
7	1.0635	8.584	5.6	1.376	0.0	0.0
8	1.0278	2.853	5.4	0.46	0.0	0.0
9	1.0265	8.378	8.3	0.597	0.0	0.0
10	1.0475	-2.7	2.5	1.256	0.0	0.0
11	1.0116	-5.99	0.0	0.0	0.0	0.0
12	0.9989	-5.98	0.0	0.0	0.075	0.88
13	1.0129	-5.79	0.0	0.0	0.0	0.0
14	1.0122	-7.34	0.0	0.0	0.0	0.0
15	1.0131	-7.42	0.0	0.0	3.2	1.53
16	1.0256	-5.8	0.0	0.0	3.294	0.323
17	1.0320	-6.87	0.0	0.0	0.0	0.0
18	1.0322	-7.774	0.0	0.0	1.58	0.30
19	1.0475	-0.468	0.0	0.0	0.0	0.0
20	0.9924	-1.436	0.0	0.0	6.28	1.03

contd ...

1	2	3	4	5	6	7
21	1.0270	-3.443	0.0	0.0	2.74	1.15
22	1.0439	0.913	0.0	0.0	0.0	0.0
23	1.0382	0.655	0.0	0.0	2.745	0.846
24	1.0230	-5.71	0.0	0.0	3.086	0.922
25	1.0503	-3.978	0.0	0.0	2.24	0.472
26	1.0526	-5.01	0.0	0.0	1.39	0.17
27	1.0393	-7.037	0.0	0.0	2.81	0.755
28	1.0530	-1.44	0.0	0.0	2.06	0.276
29	1.0508	1.31	0.0	0.0	2.835	0.269
30	1.0496	-7.842	0.0	0.0	0.0	0.0
31	1.0524	-5.112	0.0	0.0	0.0	0.0
32	1.0343	-8.1	0.0	0.0	3.22	0.024
33	1.0073	-9.286	0.0	0.0	5.0	1.84
34	1.0074	-8.34	0.0	0.0	0.0	0.0
35	1.0089	-7.686	0.0	0.0	0.0	0.0
36	1.0006	-9.863	0.0	0.0	2.338	0.84
37	1.0003	-10.345	0.0	0.0	5.22	1.76
38	1.0299	-9.861	0.0	0.0	0.0	0.0
39	1.0148	-5.112	0.0	0.0	0.0	0.0

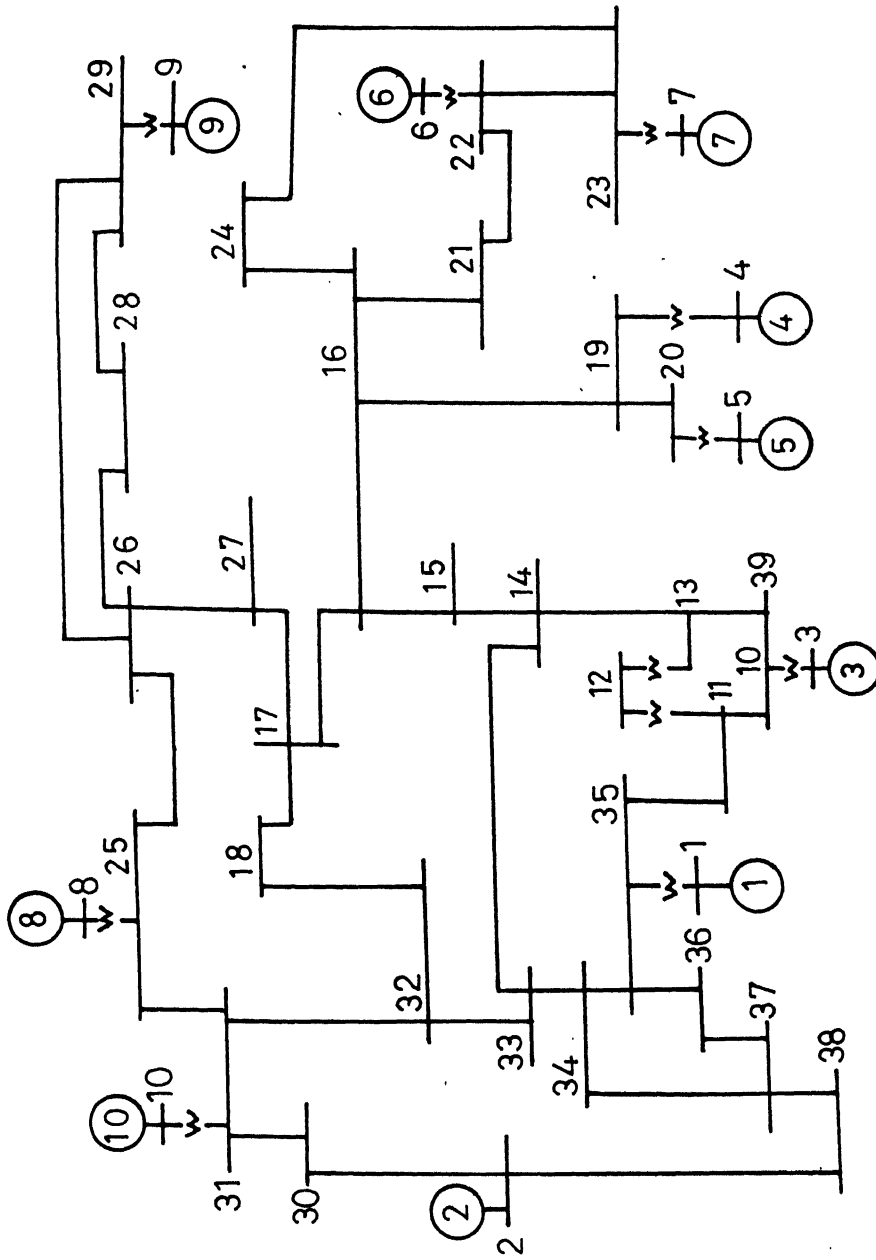


FIG.F.1 ONE-LINE DIAGRAM OF 10-MACHINE SYSTEM.

## APPENDIX G

## DATA FOR THE 13-MACHINE SYSTEM

Number of buses = 71      Number of machines = 13  
 Number of lines = 94      Number of shunt capacitors = 23  
 Base MVA = 200

Table.G.1 : Machine constants.

Gen. No.	Bus No.	Rated MVA	H (in sec)	$T'_{do}$ (in sec)	$x_d$ (in pu)	$x'_d$ (in pu)
1	1	1175.0	12.9	7.0	0.36	0.0488
2	3	665.0	9.0	6.5	0.535	0.069
3	6	110.0	1.923	6.0	1.638	0.5278
4	8	335.0	6.648	6.0	0.567	0.201
5	15	275.0	2.59	6.0	0.6	0.244
6	27	400.0	2.55	6.0	0.9	0.1455
7	29	300.0	2.70	6.0	1.578	0.1355
8	39	51.75	1.035	6.0	2.705	1.082
9	44	220.0	5.43	6.0	0.9118	0.227
10	48	500.0	7.808	6.0	0.74	0.0595
11	64	376.0	7.14	6.0	0.532	0.13
12	66	127.8	2.176	6.0	1.405	0.486
13	68	103.5	1.473	6.0	2.28	0.599

Table G.2 : Line Data

Line No.	From Bus	To Bus	Line R	Impedance X	$\frac{1}{2} Y_{charge}$	Turns Ratio
1	9	8	0.0	0.0570	0.0	1.05
2	9	7	0.0320	0.0780	0.0090	1.00
3	9	5	0.0660	0.1600	0.0047	1.00

Continued ....

Line No.	From Bus	To Bus	Line R	Impedance X	$\frac{1}{2} Y_{\text{change}}$	Turns Ratio
4	9	10	0.0520	0.1270	0.0140	1.00
5	10	11	0.0660	0.1610	0.0180	1.00
6	7	10	0.0270	0.0700	0.0070	1.00
7	12	11	0.0	0.0530	0.0	0.95
8	11	13	0.0600	0.1480	0.0360	1.00
9	14	13	0.0	0.0800	0.0	1.00
10	13	16	0.0970	0.2380	0.270	1.00
11	17	15	0.0	0.0920	0.0	1.05
12	7	6	0.0	0.2220	0.0	1.05
13	7	4	0.0	0.0800	0.0	1.00
14	4	3	0.0	0.0330	0.0	1.05
15	4	5	0.0	0.1600	0.0	1.00
16	4	12	0.0160	0.0790	0.0710	1.00
17	12	14	0.0160	0.0790	0.0710	1.00
18	17	16	0.0	0.0800	0.0	0.95
19	2	4	0.0	0.0620	0.0	1.00
20	4	26	0.0190	0.0950	0.1930	1.00
21	2	1	0.0	0.0340	0.0	1.05
22	31	26	0.0340	0.1670	0.1500	1.00
23	26	25	0.0	0.0800	0.0	0.95
24	25	23	0.2040	0.5200	0.0130	1.00
25	22	23	0.0	0.0800	0.0	0.95
26	24	22	0.0	0.0840	0.0	0.95
27	22	17	0.0480	0.2500	0.0505	1.00
28	2	24	0.0100	0.0200	0.3353	1.00
29	23	21	0.0366	0.1412	0.0140	1.00
30	21	20	0.0720	0.1860	0.0050	1.00
31	20	19	0.1460	0.3740	0.0100	1.00
32	19	18	0.0590	0.1500	0.0040	1.00
33	18	16	0.0300	0.0755	0.0080	1.00
34	28	27	0.0	0.0810	0.0	1.05
35	30	29	0.0	0.0610	0.0	1.05

Continued ...

Line No.	From Bus	To Bus	Line R	Impedance X	$\frac{1}{2}$ Y charge	Turns Ratio
36.	32	31	0.0	0.0930	0.0	0.95
37.	31	30	0.0	0.0800	0.0	0.95
38	28	32	0.005	0.0510	0.6706	1.00
39	31	33	0.0130	0.0640	0.0580	1.00
40	31	47	0.0100	0.0790	0.1770	1.00
41.	2	32	0.0158	0.1570	0.5100	1.00
42.	33	34	0.0	0.0800	0.0	0.95
43	35	33	0.0	0.0840	0.0	0.95
44.	35	24	0.0062	0.0612	0.2012	1.00
45.	34	36	0.0790	0.2010	0.0220	1.00
46	36	37	0.1690	0.4310	0.0110	1.00
47	37	38	0.0840	0.1880	0.0210	1.00
48	40	39	0.0	0.3800	0.0	1.05
49.	40	38	0.0890	0.2170	0.0250	1.00
50.	38	41	0.1090	0.1960	0.0220	1.00
51	41	51	0.2350	0.6000	0.0160	1.00
52	42	41	0.0	0.0530	0.0	0.95
53.	43	42	0.0	0.0840	0.0	0.95
54.	47	49	0.0210	0.1030	0.0920	1.00
55.	49	48	0.0	0.0460	0.0	1.05
56.	49	50	0.0170	0.0840	0.0760	1.00
57	49	42	0.0370	0.1950	0.0390	1.00
58.	50	51	0.0	0.0530	0.0	0.95
59.	52	50	0.0	0.0840	0.0	0.95
60.	50	55	0.0290	0.1520	0.0300	1.00
61	50	53	0.0100	0.0520	0.0390	1.00
62	53	54	0.0	0.0800	0.0	0.95
63	51	54	0.0220	0.0540	0.0060	1.00
64.	55	56	0.0160	0.0850	0.0170	1.00
65	56	57	0.0	0.0800	0.0	1.00
66.	57	59	0.0280	0.0720	0.0070	1.00
67	59	58	0.0480	0.1240	0.0120	1.00

Continued ....

Line No.	From Bus	To Bus	Line R	Impedance X	$\frac{1}{2}$ Y charge	Turns Ratio
68	60	59	0.0	0.0800	0.0	1.00
69.	53	60	0.0360	0.1840	0.0370	1.00
70.	45	44	0.0	0.1200	0.0	1.05
71.	45	46	0.0370	0.0900	0.0100	1.00
72.	46	41	0.0830	0.1540	0.0170	1.00
73	46	59	0.1070	0.1970	0.0210	1.00
74	60	61	0.0160	0.0830	0.0160	1.00
75	61	62	0.0	0.0800	0.0	0.95
76.	53	62	0.0420	0.1080	0.0020	1.00
77.	62	63	0.0350	0.0890	0.0090	1.00
78	69	68	0.0	0.2220	0.0	1.05
79.	69	61	0.0230	0.1160	0.1040	1.00
80.	67	66	0.0	0.1880	0.0	1.05
81.	65	64	0.0	0.0630	0.0	1.05
82.	65	56	0.0280	0.1440	0.0290	1.00
83.	65	61	0.0230	0.1140	0.0240	1.00
84	65	67	0.0240	0.0600	0.0950	1.00
85	67	63	0.0390	0.0990	0.0100	1.00
86.	61	42	0.0230	0.2293	0.0695	1.00
87	57	67	0.0550	0.2910	0.0070	1.00
88.	45	70	0.1840	0.4680	0.0120	1.00
89.	70	38	0.1650	0.4220	0.0110	1.00
90.	33	71	0.0570	0.2960	0.0590	1.00
91.	71	37	0.0	0.0800	0.0	0.95
92	45	41	0.1530	0.3880	0.0100	1.00
93.	35	43	0.0131	0.1306	0.4293	1.00
94.	32	52	0.0164	0.1632	0.5360	1.00

Table G.3 : Shunt Capacitor Data.

S.No.	Bus No.	Shunt Load	Admittance
1	2	0.0	-0.4275
2	13	0.0	0.1500
3	20	0.0	0.0800
4	24	0.0	-0.2700
5	28	0.0	-0.3375
6	31	0.0	0.2000
7	32	0.0	-0.8700
8	34	0.0	0.2250
9	35	0.0	-0.3220
10	36	0.0	0.100
11	37	0.0	0.3500
12	38	0.0	0.2000
13	41	0.0	0.200
14	43	0.0	-0.2170
15	46	0.0	0.1000
16	47	0.0	0.3000
17	50	0.0	0.1000
18	51	0.0	0.1750
19	52	0.0	-0.2700
20	54	0.0	0.1500
21	57	0.0	0.1000
22	59	0.0	0.0750
23	21	0.0	0.0500

Table G.4 : Operating Data

Bus No.	Generation		Load Power		Bus Voltage	
	(MW)	(MVAR)	(MW)	(MVAR)	Mag.(pu)	Ang.(deg)
1	630.667	169.722	0.0	0.0	1.030	0.0
2	0.0	0.0	0.0	0.0	1.057	-5.931
3	506.0	149.492	0.0	0.0	1.025	- 1.406
4	0.0	0.0	0.0	0.0	1.054	- 6.061
5	0.0	0.0	0.0	0.0	1.047	- 5.064
6	98.0	31.986	0.0	0.0	1.025	0.397
7	0.0	0.0	12.8	8.3	1.045	- 5.723
8	297.0	124.227	0.0	0.0	1.025	- 0.204
9	0.0	0.0	185.0	130.0	1.0433	- 4.976
10	0.0	0.0	80.0	50.0	1.026	- 7.413
11	0.0	0.0	155.0	96.0	1.023	-11.762
12	0.0	0.0	0.0	0.0	1.003	-10.057
13	0.0	0.0	100.0	62.0	1.007	-13.839
14	0.0	0.0	0.0	0.0	1.004	-11.984
15	184.08	114.0	0.0	0.0	1.005	- 9.413
16	0.0	0.0	73.0	45.5	1.024	-16.682
17	0.0	0.0	36.0	22.4	1.005	-14.460
18	0.0	0.0	16.0	9.9	1.009	-17.881
19	0.0	0.0	32.0	19.8	0.981	-19.786
20	0.0	0.0	27.0	16.8	1.003	-21.838
21	0.0	0.0	32.0	19.8	1.016	-21.376
22	0.0	0.0	0.0	0.0	1.008	-17.625
23	0.0	0.0	75.0	46.6	1.036	-19.815
24	0.0	0.0	0.0	0.0	0.985	-16.193
25	0.0	0.0	133.0	82.5	1.039	-17.441
26	0.0	0.0	0.0	0.0	1.016	-14.382
27	304.0	76.287	0.0	0.0	1.025	- 5.453

Bus No.	Generation		Load Power		Bus Voltage	
	(MW)	(MVAR)	(MW)	(MVAR)	Mag. (pu)	Ang. (deg)
28	0.0	0.0	30.0	20.0	1.055	-12.342
29	261.0	70.506	0.0	0.0	1.025	-15.519
30	0.0	0.0	120.0	74.5	1.057	-19.947
31	0.0	0.0	160.0	99.4	1.014	-22.817
32	0.0	0.0	0.0	0.0	1.025	-15.936
33	0.0	0.0	0.0	0.0	0.998	-25.515
34	0.0	0.0	112.0	69.5	1.306	-29.639
35	0.0	0.0	0.0	0.0	0.966	-21.803
36	0.0	0.0	50.0	32.0	0.994	-34.030
37	0.0	0.0	147.0	92.0	0.967	-37.982
38	0.0	0.0	93.5	88.0	0.972	-37.638
39	25.0	30.383	0.0	0.0	1.025	-34.166
40	0.0	0.0	0.0	0.0	1.018	-36.913
41	0.0	0.0	255.0	123.0	1.007	-34.778
42	0.0	0.0	0.0	0.0	0.979	-31.484
43	0.0	0.0	0.0	0.0	0.946	-27.835
44	180.0	55.037	0.0	0.0	1.025	-24.448
45	0.0	0.0	0.0	0.0	1.048	-30.514
46	0.0	0.0	78.0	38.6	1.020	-32.678
47	0.0	0.0	234.0	145.0	0.989	-29.053
48	341.0	256.0	0.0	0.0	1.005	-25.781
49	0.0	0.0	295.0	183.0	0.997	-30.500
50	0.0	0.0	40.0	24.6	0.977	-32.056
51	0.0	0.0	227.0	142.0	1.005	-35.309
52	0.0	0.0	0.0	0.0	0.957	-26.552
53	0.0	0.0	0.0	0.0	0.972	-32.845
54	0.0	0.0	108.0	68.0	1.004	-35.318
55	0.0	0.0	25.5	48.0	0.985	-31.313
56	0.0	0.0	0.0	0.0	1.013	-29.253

Bus No.	Generation		Load Power		Bus Voltage	
	(MW)	(MVAR)	(MW)	(MVAR)	Mag(pu)	Ang.(deg)
57	0.0	0.0	55.6	35.6	1.016	-29.967
58	0.0	0.0	42.0	27.0	1.018	-30.261
59	0.0	0.0	57.0	27.4	1.013	-30.715
60	0.0	0.0	0.0	0.0	1.008	-29.974
61	0.0	0.0	0.0	0.0	1.019	-27.874
62	0.0	0.0	40.0	27.0	1.044	-28.940
63	0.0	0.0	33.2	20.6	1.042	-27.695
64	300.0	72.882	0.0	0.0	1.025	-19.401
65	0.0	0.0	0.0	0.0	1.057	-24.662
66	96.0	25.636	0.0	0.0	1.025	-20.610
67	0.0	0.0	14.0	6.5	1.055	-25.641
68	89.0	26.689	0.0	0.0	1.025	-19.829
69	0.0	0.0	0.0	0.0	1.050	-25.363
70	0.0	0.0	11.4	7.0	0.998	-34.790
71	0.0	0.0	0.0	0.0	0.927	-35.329

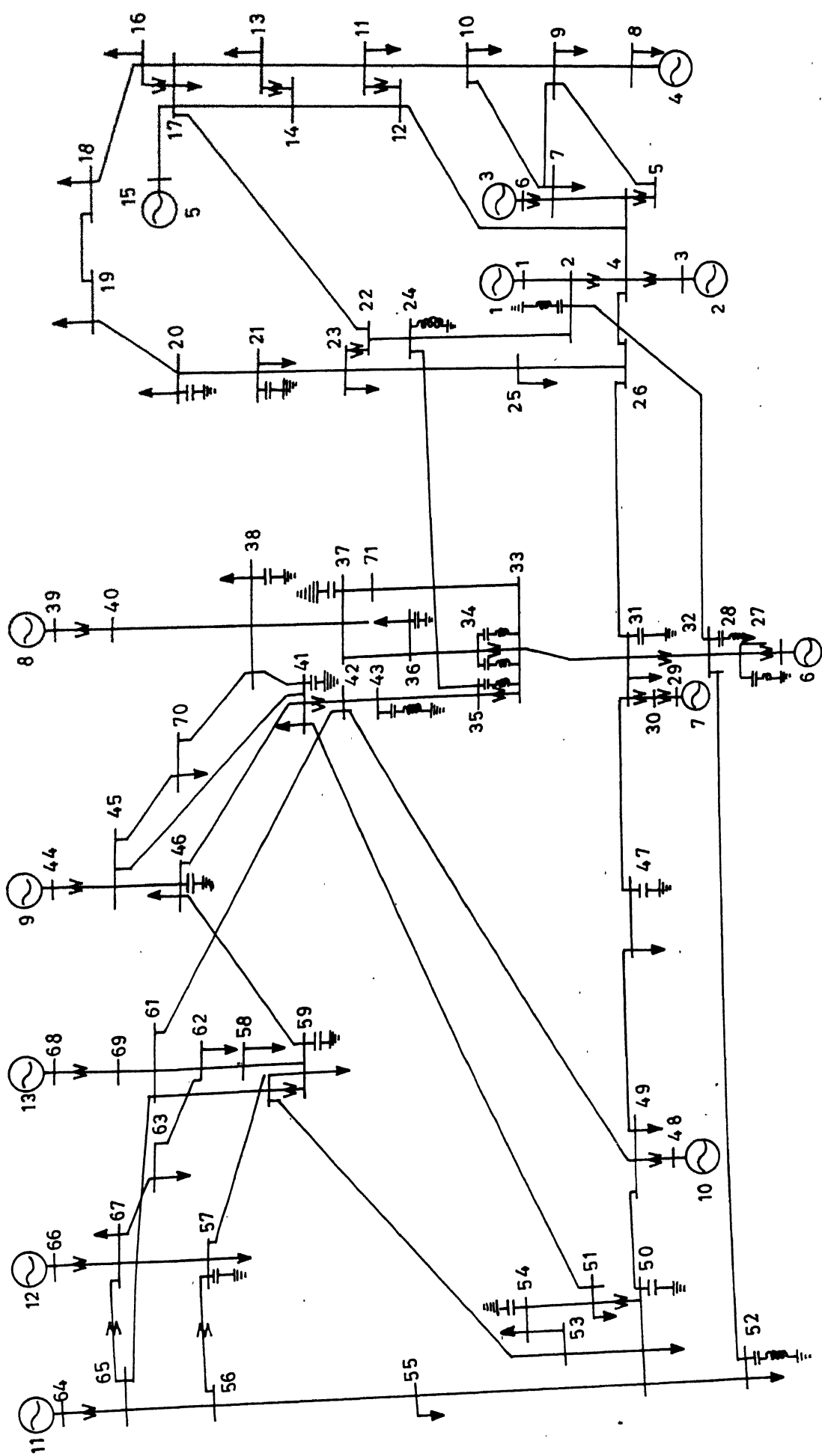


FIG.G.1 SINGLE LINE DIAGRAM OF 13 - MACHINE SYSTEM

## APPENDIX - H

ELEMENTS OF  $[\partial g / \partial \underline{x}]$  AND  $[\partial g / \partial u]$  IN EQ. (4.34)The elements of  $[\partial g / \partial \underline{x}]$  can be expressed as

$$\frac{\partial g_i}{\partial \theta_i} = \left( \frac{M_i}{M_T} - 1 \right) \frac{E_i V_i \cos(\theta_i - \phi_i)}{x'_{di}},$$

$$i = 1, 2, \dots, (m-2) \quad (H-1)$$

$$\frac{\partial g_i}{\partial \theta_j} = \frac{M_i}{M_T} \frac{E_j V_j \cos(\theta_j - \phi_j)}{x'_{dj}},$$

$$i = 1, 2, \dots, (m-2)$$

$$j = 1, 2, \dots, (m-1)$$

$$j \neq i \quad (H-2)$$

$$\frac{\partial g_{m-2+i}}{\partial \theta_i} = - \frac{E_i V_i \cos(\phi_i - \theta_i)}{x'_{di}},$$

$$i = 1, 2, \dots, (m-1) \quad (H-3)$$

$$\frac{\partial g_{m-2+i}}{\partial \theta_j} = 0,$$

$$i = 1, 2, \dots, m$$

$$j = 1, 2, \dots, (m-1)$$

$$j \neq i \quad (H-4)$$

$$\frac{\partial g_{2m-2+i}}{\partial \theta_j} = 0,$$

$$i = 1, 2, \dots, (n-m)$$

$$j = 1, 2, \dots, (m-1) \quad (H-5)$$

$$\frac{\partial g_{m-2+n+i}}{\partial \theta_i} = \frac{E_i V_i \sin(\theta_i - \phi_i)}{x'_{di}}, \quad i = 1, 2, \dots, (m-1) \quad (H.6)$$

$$\frac{\partial g_{m-2+n+i}}{\partial \theta_j} = 0, \quad \begin{array}{l} i = 1, 2, \dots, m \\ j = 1, 2, \dots, m-1 \\ j \neq i \end{array} \quad (H.7)$$

$$\frac{\partial g_{2m-2+n+i}}{\partial \theta_j} = 0, \quad \begin{array}{l} i = 1, 2, \dots, (n-m) \\ j = 1, 2, \dots, (m-1) \end{array} \quad (H.8)$$

$$\frac{\partial g_{2n+m-1}}{\partial \theta_i} = M_i, \quad i = 1, 2, \dots, (m-1) \quad (H.9)$$

$$\frac{\partial g_i}{\partial v_i} = \left( \frac{M_i}{M_T} - 1 \right) \frac{E_i \sin(\theta_i - \phi_i)}{x'_{di}}, \quad i = 1, 2, \dots, (m-2) \quad (H.10)$$

$$\frac{\partial g_i}{\partial v_j} = \frac{M_i}{M_T} \frac{E_j \sin(\theta_j - \phi_j)}{x'_{dj}}, \quad \begin{array}{l} i = 1, 2, \dots, (m-2) \\ j = 1, 2, \dots, n \\ j \neq i \end{array} \quad (H.11)$$

$$\begin{aligned} \frac{\partial g_{m-2+i}}{\partial v_i} &= \frac{E_i \sin(\phi_i - \theta_i)}{x'_{di}} + \sum_{j=1}^n B_{ij} V_j \sin \phi_{ij} \\ &+ \frac{df_{pi}(V_i)}{dv_i}, \quad i = 1, 2, \dots, m \end{aligned} \quad (H.12)$$

$$\frac{\partial g_{m-2+i}}{\partial V_j} = B_{ij} V_i \sin \phi_{ij},$$

$$i = 1, 2, \dots, m$$

$$j = 1, 2, \dots, n$$

$$j \neq i \quad (H.13)$$

$$\frac{\partial g_{2m-2+i}}{\partial V_i} = \sum_{j=1}^n B_{ij} V_j \sin \phi_{ij} + \frac{df_{pi}(V_i)}{dV_i},$$

$$i = 1, 2, \dots, (n-m) \quad (H.14)$$

$$\frac{\partial g_{2m-2+i}}{\partial V_j} = B_{ij} V_i \sin \phi_{ij}, \quad i = 1, 2, \dots, (n-m)$$

$$j = 1, 2, \dots, n$$

$$j \neq i \quad (H.15)$$

$$\frac{\partial g_{m-2+n+i}}{\partial V_i} = \frac{2V_i}{x_{di}'} - \frac{E_i \cos(\theta_i - \phi_i)}{x_{di}'}$$

$$- 2B_{ii}V_i - \sum_{\substack{j=1 \\ j \neq i}}^n B_{ij} V_j \cos \phi_{ij}$$

$$+ \frac{df_{qi}(V_i)}{dV_i}, \quad i = 1, 2, \dots, m \quad (H.16)$$

$$\frac{\partial g_{m-2+n+i}}{\partial V_j} = -B_{ij} V_i \cos \phi_{ij}, \quad i = 1, 2, \dots, m$$

$$j = 1, 2, \dots, n$$

$$j \neq i \quad (H.17)$$

$$\frac{\partial g_{2m-2+n+i}}{\partial V_i} = -2B_{ii}V_i - \sum_{\substack{j=1 \\ j \neq i}}^n B_{ij} V_j \cos \phi_{ij}$$

$$+ \frac{df_{qi}(V_i)}{dV_i}, \quad i = 1, 2, \dots, (n-m) \quad (H.18)$$

$$\begin{aligned} \frac{\partial g_{2m-2+n+i}}{\partial V_j} &= - B_{ij} V_i \cos \phi_{ij}, \quad i = 1, 2, \dots, (n-m) \\ &\quad j = 1, 2, \dots, n \\ &\quad j \neq i \end{aligned} \quad (H.19)$$

$$\frac{\partial g_{2n+m-1}}{\partial V_i} = 0, \quad i = 1, 2, \dots, n \quad (H.20)$$

$$\begin{aligned} \frac{\partial g_i}{\partial \phi_i} &= \left(1 - \frac{M_i}{M_T}\right) \frac{E_i V_i \cos(\theta_i - \phi_i)}{x'_{di}} \\ &\quad i = 1, 2, \dots, (m-2) \end{aligned} \quad (H.21)$$

$$\begin{aligned} \frac{\partial g_i}{\partial \phi_j} &= - \frac{M_i}{M_T} \frac{E_j V_j \cos(\theta_j - \phi_j)}{x'_{dj}}, \\ &\quad i = 1, 2, \dots, (m-2) \\ &\quad j = 1, 2, \dots, n \\ &\quad j \neq i \end{aligned} \quad (H.22)$$

$$\begin{aligned} \frac{\partial g_{m-2+i}}{\partial \phi_i} &= \frac{E_i V_i \cos(\phi_i - \theta_i)}{x'_{di}} \\ &\quad + \sum_{j=1}^n B_{ij} V_i V_j \cos \phi_{ij}, \\ &\quad i = 1, 2, \dots, m \end{aligned} \quad (H.23)$$

$$\begin{aligned} \frac{\partial g_{m-2+i}}{\partial \phi_j} &= - B_{ij} V_i V_j \cos \phi_{ij}, \\ &\quad i = 1, 2, \dots, m \\ &\quad j = 1, 2, \dots, n \\ &\quad j \neq i \end{aligned} \quad (H.24)$$

$$\frac{\partial g_{2m-2+i}}{\partial \phi_i} = \sum_{j=1}^n B_{ij} v_i v_j \cos \phi_{ij},$$

$$i = 1, 2, \dots, (n-m) \quad (H.25)$$

$$\frac{\partial g_{2m-2+i}}{\partial \phi_j} = - B_{ij} v_i v_j \cos \phi_{ij},$$

$$i = 1, 2, \dots, (n-m)$$

$$j = 1, 2, \dots, n$$

$$j \neq i \quad (H.26)$$

$$\frac{\partial g_{m-2+n+i}}{\partial \phi_i} = - \frac{E_i v_i \sin(\theta_i - \phi_i)}{x'_{di}}$$

$$+ \sum_{j=1}^n B_{ij} v_i v_j \sin \phi_{ij}$$

$$i = 1, 2, \dots, m \quad (H.27)$$

$$\frac{\partial g_{m-2+n+i}}{\partial \phi_j} = - B_{ij} v_i v_j \sin \phi_{ij}$$

$$i = 1, 2, \dots, m$$

$$j = 1, 2, \dots, n$$

$$j \neq i \quad (H.28)$$

$$\frac{\partial g_{2m-2+n+i}}{\partial \phi_i} = \sum_{j=1}^n B_{ij} v_i v_j \sin \phi_{ij},$$

$$i = 1, 2, \dots, (n-m) \quad (H.29)$$

$$\frac{\partial g_{2m-2+n+i}}{\partial \phi_j} = - B_{ij} v_i v_j \sin \phi_{ij},$$

$$i = 1, 2, \dots, (n-m)$$

$$j = 1, 2, \dots, n$$

$$j \neq i \quad (H.30)$$

$$\frac{\partial g_{2n+m-1}}{\partial \phi_i} = 0, \quad i = 1, 2, \dots, n \quad (\text{H.31})$$

The elements of  $[\partial g / \partial u]$  are as follows :

$$\frac{\partial g_i}{\partial \theta_k} = 0, \quad i = 1, 2, \dots, (m-2) \quad (\text{H.32})$$

$$\frac{\partial g_{m-2+i}}{\partial \theta_k} = - \frac{E_k v_k \cos(\phi_k - \theta_k)}{x'_{dk}} \quad i = k = m \quad (\text{H.33a})$$

$$= 0, \quad \begin{matrix} i = 1, 2, \dots, m \\ k \neq i \end{matrix} \quad (\text{H.33b})$$

$$\frac{\partial g_{2m-2+i}}{\partial \theta_k} = 0, \quad i = 1, 2, \dots, (n-m) \quad (\text{H.34})$$

$$\frac{\partial g_{m-2+n+i}}{\partial \theta_k} = - \frac{E_k v_k \sin(\phi_k - \theta_k)}{x'_{dk}} \quad i = k = m \quad (\text{H.35a})$$

$$= 0, \quad \begin{matrix} i = 1, 2, \dots, m \\ k \neq i \end{matrix} \quad (\text{H.35b})$$

$$\frac{\partial g_{2m-2+n+i}}{\partial \theta_k} = 0, \quad i = 1, 2, \dots, (n-m) \quad (\text{H.36})$$

$$\frac{\partial g_{2n+m-1}}{\partial \theta_k} = M_k \quad (\text{H.37})$$

## APPENDIX - I

## RELATIONSHIP BETWEEN POWER INJECTIONS IN LOSSY AND LOSSLESS NETWORKS [67]

For an element  $ij$  (connected across nodes  $i$  and  $j$  in the network, the real and reactive power flows at node  $i$ , are given by

$$P_{ij} = (V_i^2 - V_i V_j \cos \phi_{ij}) g_{ij} + b_{ij} V_i V_j \sin \phi_{ij} \quad (I.1)$$

$$Q_{ij} = (V_i^2 - V_i V_j \cos \phi_{ij}) b_{ij} - g_{ij} V_i V_j \sin \phi_{ij} \quad (I.2)$$

From the above one can write

$$P_{ij} - \alpha Q_{ij} = (1 + \alpha^2) b_{ij} V_i V_j \sin \phi_{ij} \quad (I.3)$$

$$\frac{\alpha}{1 + \alpha^2} P_{ij} + \frac{1}{1 + \alpha^2} Q_{ij} = b_{ij} (V_i^2 - V_i V_j \cos \phi_{ij}) \quad (I.4)$$

where  $\alpha = g_{ij}/b_{ij}$  for all  $ij$ .

Defining

$$P'_{ij} = b_{ij} V_i V_j \sin \phi_{ij} \quad (I.5)$$

$$Q'_{ij} = b_{ij} (V_i^2 - V_i V_j \cos \phi_{ij}) \quad (I.6)$$

we have,

$$P'_{ij} = \frac{1}{1 + \alpha^2} P_{ij} - \frac{\alpha}{1 + \alpha^2} Q_{ij} \quad (1.7)$$

$$Q'_{ij} = \frac{\alpha}{1 + \alpha^2} P_{ij} + \frac{1}{1 + \alpha^2} Q_{ij} \quad (1.8)$$

Equations (1.5) and (1.6) describe a lossless network element. It is easy to see that the above equations still apply when  $P_{ij}$  and  $Q_{ij}$  are replaced by  $P_i$  and  $Q_i$  and similarly for  $P'_{ij}$  and  $Q'_{ij}$ . Thus, we have,

$$\begin{vmatrix} P'_i \\ Q'_i \end{vmatrix} = \frac{1}{1 + \alpha^2} \begin{vmatrix} 1 & -\alpha \\ \alpha & 1 \end{vmatrix} \begin{vmatrix} P_i \\ Q_i \end{vmatrix} \quad (1.9)$$

From Eq.(1.9), Eqs. (5.1) and (5.2) are easily derived.

## APPENDIX - J

## ENERGY STORED IN MACHINE REACTANCES AND TRANSMISSION LINES

J.1. Energy Stored in Machine Reactances

It was mentioned in Chapter 6 that the energy stored in the machine reactances is given by

$$\begin{aligned}
 & \sum_{i=1}^m [(E'_{qi})^2 + V_i^2 - 2E'_{qi} V_i \cos(\theta_i - \phi_i)] \frac{1}{2x'_{di}} \\
 & - V_i^2 \frac{x'_{di} - x_{qi}}{4x'_{di} x_{qi}} (\cos(2\theta_i - 2\phi_i) - 1) \\
 & + (E'_{di})^2 + V_i^2 - 2E'_{di} V_i \cos(\theta_i - \phi_i) \left[ \frac{1}{2x'_{qi}} - \frac{V_i^2}{2x'_{qi}} \right]
 \end{aligned}
 \tag{J.1}$$

In general, it has been shown in [70] that the energy stored in a line element is equal to half the reactive power loss. It will be shown here that the energy term given in Eq.(J.1) is actually half the reactive power loss within the generator.

The reactive power generation at the internal bus of the  $i$ -th machine is

$$Q_{ei} = \text{Im} [E'_{qi} + j E'_{di}] [i_{qi} - j i_{di}] = E'_{di} i_{qi} - E'_{qi} i_{di}
 \tag{J.2}$$

The reactive power output at the terminal bus is

$$Q_i = \text{Im} [V_{qi} + j V_{di}][i_{qi} - j i_{di}] = V_{di} i_{qi} - V_{qi} i_{di} \quad (\text{J.3})$$

Hence, the reactive power loss in the machine reactance is

$$Q_{ri} = Q_{ei} - Q_i = i_{qi}(E'_{di} - V_{di}) - i_{di}(E'_{qi} - V_{qi}) \quad (\text{J.4})$$

For the machine model considered,

$$V_{qi} = E'_{qi} + x'_{di} i_{di} \quad (\text{J.5})$$

$$\text{and } V_{di} = E'_{di} - x'_{qi} i_{qi} \quad (\text{J.6})$$

$$\text{Thus, } Q_{ri} = x'_{qi} i_{qi}^2 + x'_{di} i_{di}^2 \quad (\text{J.7})$$

$$\text{Also, } V_{qi} = V_i \cos(\theta_i - \phi_i) \quad (\text{J.8})$$

$$V_{di} = -V_i \sin(\theta_i - \phi_i) \quad (\text{J.9})$$

Thus ,

$$i_{qi} = \frac{E'_{di} + V_i \sin(\theta_i - \phi_i)}{x'_{qi}} \quad \text{and}$$

$$i_{di} = \frac{V_i \cos(\theta_i - \phi_i) - E'_{qi}}{x'_{di}}, \quad (\text{J.10})$$

from Eqs.(6.12) and (6.13) in Chapter 6.

Hence,

$$\begin{aligned} x'_{qi} i_{qi}^2 &= x'_{qi} \left[ \frac{E'_{di} + V_i \sin(\theta_i - \phi_i)}{x'_{qi}} \right]^2 \\ &= \frac{[E'_{di} + V_i \sin(\theta_i - \phi_i)]^2}{x'_{qi}} \end{aligned} \quad (J.11)$$

$$\begin{aligned} x'_{di} i_{di}^2 &= x'_{di} \left[ \frac{V_i \cos(\theta_i - \phi_i) - E'_{qi}}{x'_{di}} \right]^2 \\ &= \frac{[V_i \cos(\theta_i - \phi_i) - E'_{qi}]^2}{x'_{di}} \end{aligned} \quad (J.12)$$

$$Q_{ri} = \frac{[E'_{di} + V_i \sin(\theta_i - \phi_i)]^2}{x'_{qi}} + \frac{[V_i \cos(\theta_i - \phi_i) - E'_{qi}]^2}{x'_{di}} \quad (J.13)$$

Expanding the R.H.S. of Eq.(J.13) and replacing  $\sin^2(\theta_i - \phi_i)$  by  $\frac{1}{2} [1 - \cos 2(\theta_i - \phi_i)]$  and  $\cos^2(\theta_i - \phi_i)$  by  $\frac{1}{2} [\cos 2(\theta_i - \phi_i) + 1]$ , we get after rearranging the terms,

$$\begin{aligned} Q_{ri} &= \frac{E'_{qi}{}^2 - 2E'_{qi} V_i \cos(\theta_i - \phi_i)}{x'_{di}} + \frac{V_i^2}{2x'_{di}} [\cos 2(\theta_i - \phi_i) + 1] \\ &\quad + \frac{E'_{di}{}^2 + 2E'_{di} V_i \sin(\theta_i - \phi_i)}{x'_{qi}} + \frac{V_i^2}{2x'_{qi}} [1 - \cos 2(\theta_i - \phi_i)] \end{aligned} \quad (J.14)$$

Adding and subtracting the term  $\frac{V_i^2}{x'_{qi}}$  from the R.H.S. of Eq. (J.14) and simplifying, we get,

$$\begin{aligned}
Q_{ri} &= [E_{qi}^2 + V_i^2 - 2E_{qi}' V_i \cos(\theta_i - \phi_i)] \frac{1}{x_{di}'} \\
&\quad - V_i^2 [\cos(2\theta_i - 2\phi_i) - 1] \frac{x_{di}' - x_{qi}'}{2x_{di}' x_{qi}'} \\
&\quad + [E_{di}^2 + V_i^2 + 2E_{di}' V_i \sin(\theta_i - \phi_i)] \frac{1}{x_{qi}'} - \frac{V_i^2}{x_{qi}'} \quad (J.15)
\end{aligned}$$

Eq.(J.15) gives the reactive power loss in the reactances of a single machine. The total reactive power loss in the reactances of machines for a system having  $m$  machines, is given by

$$\begin{aligned}
Q_{r\sum} &= \sum_{i=1}^m Q_{ri} = \sum_{i=1}^m [(E_{qi}^2 + V_i^2 - 2E_{qi}' V_i \cos(\theta_i - \phi_i)) \frac{1}{x_{di}'} \\
&\quad - V_i^2 (\cos(2\theta_i - 2\phi_i) - 1) \frac{x_{di}' - x_{qi}'}{2x_{di}' x_{qi}'} \\
&\quad + (E_{di}^2 + V_i^2 + 2E_{di}' V_i \sin(\theta_i - \phi_i)) \frac{1}{x_{qi}'} - \frac{V_i^2}{x_{qi}'}] \quad (J.16)
\end{aligned}$$

This is twice the energy term given in Eq.(J.1)-

## J.2. Energy stored in the Transmission Lines

Energy stored in the transmission lines has been given by

$$- \frac{1}{2} \sum_{i=1}^n \sum_{j=1}^n B_{ij} V_i V_j \cos \phi_{ij} \quad (J.17)$$

It will be shown that the energy term given in Eq.(J.17) is half the reactive power loss in the transmission lines.

Power injection at bus  $i$  of a lossless network can be calculated from

$$\begin{aligned}
 P_i + jQ_i &= \bar{V}_i \bar{I}_i^* = V_i e^{j\phi_i} \sum_{j=1}^n (-j B_{ij}) V_j e^{-j\phi_j} \\
 &= \sum_{j=1}^n (-j B_{ij}) V_i V_j e^{j(\phi_i - \phi_j)} \\
 &= - \sum_{j=1}^n j B_{ij} V_i V_j (\cos \phi_{ij} + j \sin \phi_{ij}) \quad (J.18)
 \end{aligned}$$

Hence,

$$Q_i = - \sum_{j=1}^n B_{ij} V_i V_j \cos \phi_{ij} \quad (J.19)$$

In the above expressions  $B_{ij} = \text{Im} [Y_{ij}]$  where  $[Y]$  is the admittance matrix of the transmission network (excluding machine reactances).

The reactive power loss in the transmission network can be given by

$$Q_{rl} = \sum_{i=1}^n Q_i = - \sum_{i=1}^n \sum_{j=1}^n B_{ij} V_i V_j \cos \phi_{ij} \quad (J.20)$$

This is twice the energy term given in (J.17)

Thus, in view of Eqs.(J.16) and (J.20) the total loss in the stationary network (including generator stator windings) is twice the sum of the energy terms given in Eqs.(J.1) and (J.17). The total energy stored is equal to,

$$\frac{1}{2} \sum_{r=1}^L Q_r = \frac{1}{2} \left[ \sum_{i=1}^m Q_{Gi} - \sum_{j=1}^n Q_{Lj} \right] \quad (J.21)$$

where,

$Q_{Gi}$  = reactive power generation at the internal bus of generator  $i$

$Q_{Lj}$  = load at bus  $j$

$L$  = total number of elements in the network including machine reactances.

APPENDIX - K  
DATA FOR 4-MACHINE SYSTEM

Number of machines : 4  
 Number of buses : 6  
 Number of lines : 7  
 Base MVA : 100

Table K.1 : Machine constants

Generator No.	M in p.u sec <sup>2</sup> /rad	$x'_d$ in pu	$x'_q$ in pu	$x_d$ in pu	$T'_{do}$ in sec
1	0.5302	0.004	-	-	-
2	0.0159	0.500	0.950	1.450	8.0
3	0.0106	0.400	0.750	1.150	6.0
4	0.0080	1.0	-	-	-

Table K.2 : Line data

Line No.	From bus	To bus	Line reactance in pu
1	1	5	0.15
2	1	4	0.20
3	4	2	0.50
4	2	3	0.80
5	3	6	0.30
6	6	5	0.40
7	4	6	0.50

Table K.3 : Operating data

Bus No.	Voltage Magnitude (in pu)	Bus angle (in deg.)	Generation		Loads	
			Active power in pu	Reactive power in pu	Active power in pu	Reactive power in pu
1	1.0	0.0	0.30	0.0875	-	-
2	1.0671	5.760	0.30	0.20	-	-
3	1.0263	2.0263	0.20	0.10	-	-
4	1.0048	0.0938	0.10	0.05	0.20	0.10
5	0.9843	-2.6920	-	-	0.30	0.10
6	0.9861	-2.8850	-	-	0.40	0.15

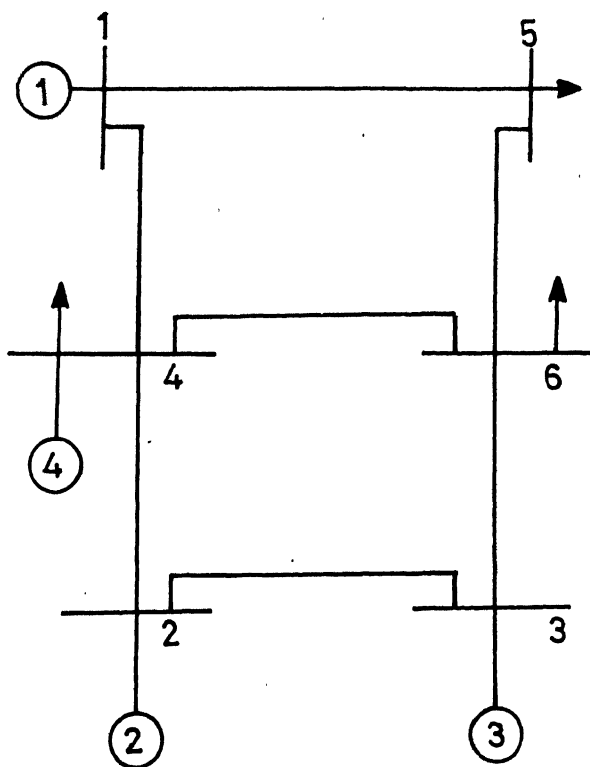


FIG.K.1 SINGLE LINE DIAGRAM OF  
4-MACHINE SYSTEM

## REFERENCES

- [1] M.A. Pai, 'Power System Stability - Analysis by Direct Method of Lyapunov', North-Holland Systems and Control Series, vol.3, 1981.
- [2] P.M. Anderson and A.A. Fouad, 'Power System Control and Stability', Iowa State University Press, Iowa, 1977.
- [3] E.W. Kimbark, 'Power System Stability', vol.I (Elements of Stability Calculations), Wiley, New York, 1948.
- [4] E.W. Kimbark, 'Power System Stability', vol.III (Synchronous Machines), Wiley, New York, 1956.
- [5] W.D. Stevenson, Jr., 'Elements of Power System Analysis', McGraw Hill, 1984.
- [6] S.B. Crary, 'Power System Stability', vol.I (Steady State Stability), Wiley, New York, 1945.
- [7] S.B. Crary, 'Power System Stability', vol.II (Transient Stability), Wiley, New York, 1947.
- [8] 'Electrical Transmission and Distribution Reference Book', Westinghouse Electric Corporation, East Pittsburgh, Pennsylvania, USA, 1950.
- [9] Anjan Bose, 'Application of Direct Methods to Transient Stability Analysis of Power Systems', IEEE Trans. PAS, vol. PAS-103, pp 1629-1636, May 1985.
- [10] F.S. Prabhakar, 'On-line Transient Stability and Security Evaluation using Lyapunov and Pattern Recognition Methods', Ph.D. Thesis, Purdue University, West Lafayette, Indiana, Aug. 1974.
- [11] O. Saito, K. Koizumi, M. Udo, M. Sato, H. Mukai and T. Tsuji, 'Security Monitoring Systems Including Fast Transient Stability Studies', IEEE Trans. PAS, vol. PAS-94, No.5, pp 1789-1805, Sept./Oct. 1975.
- [12] C.L. Gupta and A.H. El-Abiad, 'Transient Security Assessment of Power Systems by Pattern Recognition - A Pragmatic Approach', Proc. IFAC Symposium, pp 359-363, February 1977.

- [13] G.E. Gless, 'Direct Method of Lyapunov Applied to Transient Power System Stability', IEEE Trans., PAS, vol. PAS-85, No.2, pp 159-168, February 1966.
- [14] A.H. El-abiad and K. Nagappan, 'Transient Stability Regions of Multimachine Power Systems', IEEE Trans. PAS, vol.85, pp.169-179, February 1966.
- [15] M. Ribbens-Pavella, 'Critical Survey of Transient Stability Studies of Multimachine Power Systems by Lyapunov's Direct Method', Conference on Circuits and Systems Theory, pp 751-767, Oct. 1971.
- [16] M. Ribbens-Pavella and F.J. Evans, 'Direct Methods in the Study of Dynamics of Large Scale Electric Power Systems - A Survey', IFAC Control Science and Technology, Jan. 1981.
- [17] A.A. Fouad, 'Stability Theory Criteria for Transient Stability', Conference on Systems Engineering for Power Status and Prospects, New Hemisphere, pp 421-450, August 1975.
- [18] M.A. Pai, 'Survey of Practical Direct Methods of Stability Analysis in Power Systems', Electric Machines and Power Systems, vol.9, No.2, 1984.
- [19] P. Varaiya, F.F. Wu and R.L. Chen, 'Direct Methods for Transient Stability Analysis of Power Systems: Recent Results', Proceedings of the IEEE, vol.73, No.12, December 1985.
- [20] J.L. Willems, 'Optimum Lyapunov Functions and Stability Regions for Multimachine Power Systems', Proc. of IEE (London), vol.117, No.3, pp 573-578, March 1970.
- [21] J.L. Willems and J.C. Willems, 'The Application of Lyapunov Methods to the Computation of Transient Stability Regions of Multimachine Power Systems', IEEE Trans. PAS, vol. 89, No.5, pp 795-801, May/June 1970.
- [22] M.A. Pai, M.A. Mohan and J.G. Rao, 'Power System Transient Stability Region using Popov's Method', IEEE Trans. PAS, vol.89, No.5, pp 788-794, May/June 1970.
- [23] M.A. Pai and V. Rai, 'Lyapunov-Popov Stability Analysis of Synchronous-Machine with Flux Decay and Voltage Regulator', Int.Journal of Control, vol.20, No.2, pp 203-212, August 1974.

- [24] H. Sasaki, 'An Approximate Incorporation of Field Flux Decay into Transient Stability Analysis of Multimachine Power Systems by Second Method of Lyapunov', IEEE Trans. PAS, vol.98, pp 473-483, March/April 1979.
- [25] N. Kakimoto, Y. Ohsawa and M. Hayashi, 'Transient Stability Analysis of Multimachine Power Systems by Second Method of Lyapunov', IEEE Trans. PAS, vol.99, No.5, pp 1819-1827, Sept./Oct. 1980.
- [26] N. Kakimoto, Y. Ohnogi, H. Matsuda and H. Shimbuya, 'Transient Stability Analysis of Large Scale Power System by Lyapunov's Direct Method', Paper Presented at IEEE Summer Meeting, California, July 1983.
- [27] F.S. Prabhakar and A.H. El-abiad, 'A Simplified Determination of Transient Stability Regions for Lyapunov Methods', IEEE Trans. PAS, vol.84, pp 672-680, March/April 1975.
- [28] M. Ribbens-Pavella and B. Lemal, 'Fast Determination of Stability Regions for on-line power system Studies', Proc. IEE, vol. 123, pp 689-696, July 1976.
- [29] N. Kakimoto, Y. Ohsawa and M. Hayashi, 'Transient Stability Analysis of Electric Power Systems via Lure type Lyapunov Function - Parts I and II', Trans. of IEE of Japan, vol.98, No.5/6, May/June, 1978.
- [30] T. Athay, R. Podmore and S. Virmani, 'Practical Method for the Direct Analysis of Transient Stability', IEEE Trans. PAS, vol.98, pp 573-584, March/April 1979.
- [31] M. Ribbens-Pavella, T. Grujic Lj, J. Sabatel and A. Bouffiaux, 'Direct Methods for Stability Analysis of Large Scale Power System', IFAC Symposium, New Delhi, Aug. 1979..
- [32] A.A. Fouad and V. Vittal, 'Power System Response to a Large Disturbance Energy Associated with System Separation', IEEE Trans. vol.102, pp 3534-3540, November 1983.
- [33] A.A. Fouad and V. Vittal, 'Critical Energy for Direct Stability Assessment of a Multimachine Power System', Paper presented at IEEE Winter Meeting, Dallas, Texas, Jan./Feb. 1984.
- [34] P.C. Magnusson, 'Transient Energy Method of Calculating Stability', AIEE Trans. vol.66, pp 747-755, 1947.

- [35] P.D. Aylett, 'The Energy Integral Criterion of Transient Stability Limits of Power Systems', Proc. of IEE (London), vol. 105-C, pp 527-536, Sept. 1958.
- [36] C.J. Tavora and O.J.M. Smith, 'Characterization of Equilibrium and Stability in Power Systems', IEEE Trans. PAS, vol. PAS-91, pp 1127-1130, May/June 1972.
- [37] C.J. Tavora and O.J.M. Smith, 'Stability Analysis of Power Systems', IEEE Trans. PAS, vol. PAS-91, pp 1138-1144, May/June 1972.
- [38] M.A. Pai, H.A. Othman, J.H. Chow and J.R. Winkelman, 'Time Scale Energies in Large Power Systems', Paper presented at the 4th IFAC/IFORS Symposium on Large Scale Systems: Theory and Applications held at Zurich, Switzerland, Aug. 26-29, 1986.
- [39] K. Khorasani, M.A. Pai and P.W. Sauer, 'Modal-based Stability Analysis of Power Systems Using Energy Functions', Electric Power and Energy Systems, vol.8, No.1, Jan. 1985.
- [40] J.H. Chow, 'Time Scale Modelling of Dynamic Networks with Applications to Power Systems', Springer-Verlag, New York, 1982.
- [41] J.R. Winkelman, J.H. Chow, B.C. Wheeler, B. Avramovic and P.V. Kokotovic, 'An Analysis of Inter-area Dynamics of Multi-machine Systems', IEEE Trans. PAS, vol. PAS-100, pp 754-763, 1981.
- [42] J.R. Winkelman, J.H. Chow, P.W. Souer and A.K. Behera, 'Direct Power System Transient Stability Analysis with Detailed Machine Models', Paper presented at the 4th IFAC/IFORS Symposium on Large Scale Systems: Theory and Applications held at Zurich, Switzerland, August 26-29, 1986.
- [43] M. Ribbens-Pavella, 'Transient Stability of Multi-machine Power Systems by the Lyapunov's Direct Method', presented at the IEEE Winter Power Meeting, New York, January 1971.
- [44] K. Uemura, J. Matuski, J. Yamada and T. Tsuji, 'Approximation of an Energy Function in Transient Stability Analysis of Power System', Electrical Engineering in Japan, vol. 92, No.6, 1972.

- [45] M.A. Pai and P.G. Murthy, 'On Lyapunov Functions for Power Systems with Transfer Conductances', IEEE Transactions on Automatic Control, vol.AC-18, pp 181-183, April 1973.
- [46] V. Gudar, 'A General Liapunov Function for Multimachine Power Systems with Transfer Conductances', Int.J.Control, vol.21, No.2, pp 333-343, 1975.
- [47] V.E. Henner, 'Comments on [45], Int. J. Control, vol. 23, No.1, pp 143, 1976.
- [48] J.L. Willems, 'Comments on [45], Int. J. Control, vol. 23, No.1, pp 147-148, 1976.
- [49] M.A. Pai and S.D. Varwandkar, 'On the Inclusion of Transfer Conductances in Lyapunov Functions for Multimachine Power Systems', IEEE Trans. on Automatic Control, vol. AC-22, No.6, pp 983-985, Dec. 1977.
- [50] M. El-Guindi and M. Mansour, 'Transient Stability of a Power System by the Lyapunov Method Considering the Transfer Conductances', IEEE Trans. PAS, vol. 101, pp 1088-1094, May 1982.
- [51] M.A. Pai, K.R. Padiyar and C. Radhakrishna, 'Transient Stability Analysis of Multimachine AC/DC Power System via Energy Function Method', IEEE Trans. PAS, vol. 100, pp 5027-5035, December 1981.
- [52] A.R. Bergen and D.J. Hill, 'A Structure Preserving Model for Power System Stability Analysis', IEEE Trans. PAS, vol. 100, pp 25-35, Jan. 1981.
- [53] N. Narasimha Murthy and M.T. Musavi, 'A General Energy Function for Transient Stability Analysis of Power Systems', IEEE Trans. CAS, vol. CAS-31, No.7, pp 637-645, July 1984.
- [54] K.R. Padiyar and H.S.Y. Sastry, 'A Topological Energy Function Analysis of Stability of Power Systems', Jr. of Electric Power and Energy Systems, vol.9, No.1, pp 9-16, Jan. 1987.
- [55] T.V. Cutsem, B. Toumi, Y. Xue and M. Ribbens-Pavella, 'Direct Criteria for Structure Preserving Models of Electric Power Systems', Paper presented at IFAC Symposium on Power Systems and Power Plant Control at Beijing, China, August 12-15, 1986.

- [56] T.V. Cutsem and M. Ribbens-Pavella, 'Structure Preserving Direct Methods for Transient Stability Analysis of Power Systems', Proceedings of 24th Conference on Decision and Control, Ft. Lauderdale, FL. Dec. 1985.
- [57] N. Tsolas, A. Araposthatis and P. Varaiya, 'A Structure Preserving Energy Function for Power System Transient Stability Analysis', IEEE Trans. CAS, vol. CAS-32, No.10, pp 1041-1049, Oct. 1985.
- [58] K.R. Padiyar and H.S.Y. Sastry, 'Direct Stability Analysis of Power Systems with Realistic Generator Models Using Topological Energy Function', paper presented at the IFAC Symposium at Beijing, China, Aug. 12-15, 1986.
- [59] A.A. Fouad and S.E. Stauton, 'Transient Stability of Multimachine Power System Part II : Critical Transient Energy', IEEE Trans. PAS, vol. PAS-100, No.7, pp 3417-3424, July 1981.
- [60] A.N. Michel, A.A. Fouad and V. Vittal, 'Power System Transient Stability Using Individual Machine Energy Functions', IEEE Trans. on Circuits and Systems, vol. CAS-30, No.5, pp 266-276, May 1983.
- [61] A. Fouad, S.E. Stanton, K.R.C. Mamandur and K.C. Kruempel, 'Contingency Analysis Using the Transient Energy Margin Technique', IEEE Trans. on PAS, vol. PAS-101, No.4, pp 757-766, April 1982.
- [62] M. Ribbens-Pavella, P.G. Murthy, J.L. Horward and J.L. Carpentier, 'Transient Stability Index for on-line Stability Assessment and Contingency Evaluation', Electrical Power and Energy Systems, vol.4, No.2, pp 91-99, April 1982.
- [63] P.W. Sauer, K.D. Demaree and M.A. Pai, 'Stability Limited Load Supply and Interchange Capability', IEEE Trans. on Power App. and System, vol. PAS-102, No.11, Nov. 1983.
- [64] M.A. Pai, P.W. Sauer and K.D. Demaru, 'Direct Methods of Stability Analysis in Dynamic Security Assessment', Paper presented at the IFAC World Congress, Budapest, 1984.

- [65] A. Fouad, V. Vittal, M.A. El-kady, C.K. Tang and V.F. Carvalho, 'Dynamic Security Assessment Utilising the Transient Energy Function Method', paper presented at the PICA Conference, IEEE, 1985.
- [66] R. Podmore, 'Power System Dynamic Simulation Program - User's Manual', University of Saskatchewan, Jan. 1974.
- [67] K.R. Padiyar, 'On the Nature of Power Flow Equations in Security Analysis', Electric Machines and Power Systems', No.9, pp 297-306, 1984.
- [68] A.A. Fouad, K.C. Kruempel, V. Vittal, A. Ghafurian, L. Nodehi and J.V. Mitsche, 'Transient Stability Output Analysis', IEEE Summer Power Meeting, 1985.
- [69] H.W. Dommel and N. Sato, 'Fast Transient Stability Solution', IEEE Trans. PAS, vol. PAS-91, pp 1643-1650, July 1972.
- [70] K.R. Padiyar and P. Variya, 'A Network Analogy for Power System Stability Analysis', Preprint, December, 1983.
- [71] H.S.Y. Sastry, 'Applications of Topological Energy Functions for the Direct Stability Evaluation of Power Systems', Ph.D. Thesis, Department of Electrical Engineering, Indian Institute of Technology, Kanpur (India), May 1984.
- [72] M. Ribbens-Pavella, J.L. Howard, B. Lemal, T.P. Nguyen, 'Transient Stability by Scalar Lyapunov Functions: Recent Improvements and Practical Results', University of Liege, Faculty of Applied Science, Report No.67-1977.
- [73] K.D. Demaree, 'Fast Energy Method for Transient Stability Assessment and Maximum Loading of Power Systems', Dept. of Elect.Engg., University of Illinois, Urbana, Illinois, Report No. PAP-RT-83-6, October 1983.
- [74] C. Radhakrishna, 'Stability Studies of AC/DC Power Systems', Ph.D. Thesis, Department of Electrical Engineering, Indian Institute of Technology, Kanpur (India), September 1980.

- [75] S.D. Conte and Carl de Boor, 'Elementary Numerical Analysis - An Algorithmic Approach', Second Edition, McGraw-Hill Kogakusha Publications, pp 287-288, 1972.
- [76] IEEE Committee Report, 'Computer Representation of Excitation Systems', IEEE Trans. PAS, vol. PAS-87, pp 1460-1464, June 1968.
- [77] H.D. Chiang, F.F. Wu, P. Varaiya and C.W. Tan, 'Theory of Potential Energy Boundary Surface', Proceedings of 24th Conference on Decision and Control, Ft. Lauderdale, FL. December 1985.

## CURRICULUM VITAE

1. Candidate's Name : K.K. Ghosh

2. Academic Background :

<u>Degree</u>	<u>Specialisation</u>	<u>Institute</u>	<u>Year</u>
B.E.E.	Electrical Engineering	Jadavpur University Calcutta	1965
M.E.E.	Electrical Engineering (Major: Power Systems)	"	1969

3. Publications :

- \*i) 'Protective Gear Test Bench' (with S.P. Patra, S.K. Basu and S. Choudhuri), Journal of the Institution of Engineers (India), vol.51, pp 155-160, February 1971.
- ii) 'A Novel Structure Preserving Energy Function for Direct Stability Evaluation of Power Systems with Known Modes of Instability' (with K.R. Padiyar), to be published in Electric Machines and Power Systems.

\*Not pertaining to the thesis

## Date Slip

This book is to be returned on the  
date last stamped.

This image shows a full page of primary-ruled paper. It features a central vertical solid line that divides the page into two equal halves. On both sides of this line, there are ten horizontal dotted lines, creating a total of twenty rows for writing practice. The paper is otherwise blank, with no margins or additional markings.

EE- 1987-D-GHO-DIR